

**PHYTOCHEMICAL AND BIOLOGICAL STUDIES ON
LINDERA OXYPHYLLA AND *LITSEA COSTALIS* (NEES)
KOSTERM (LAURACEAE)**

MASOUMEH HOSSEINZADEH

**FACULTY OF SCIENCE
UNIVERSITY OF MALAYA
KUALA LUMPUR**

2013

**PHYTOCHEMICAL AND BIOLOGICAL STUDIES ON
LINDERA OXYPHYLLA AND *LITSEA COSTALIS* (NEES)
KOSTERM (LAURACEAE)**

MASOUMEH HOSSEINZADEH

**THESIS SUBMITTED IN FULFILMENT OF THE
REQUIREMENTS FOR THE DEGREE OF
DOCTOR OF PHILOSOPHY**

**DEPARTMENT OF CHEMISTRY
FACULTY OF SCIENCE
UNIVERSITY OF MALAYA
KUALA LUMPUR**

2013

UNIVERSITI MALAYA

ORIGINAL LITERARY WORK DECLARATION

Name of Candidate: **MASOUMEH HOSSEINZADEH** (I.C/Passport No: **X95385285**)

Registration/Matric No: **SHC090088**

Name of Degree: **DOCTOR OF PHILOSOPHY**

Title of ~~Project Paper/Research Report/Dissertation/Thesis~~ ("this Work"):

**PHYTOCHEMICAL AND BIOLOGICAL STUDIES ON LINDERA
OXYPHYLLA AND LITSEA COSTALIS (NEES) KOSTERM (LAURACEAE)**

Field of Study: **Phytochemistry (Natural product chemistry)**

I do solemnly and sincerely declare that:

- (1) I am the sole author/writer of this Work;
- (2) This Work is original;
- (3) Any use of any work in which copyright exists was done by way of fair dealing and for permitted purposes and any excerpt or extract from, or reference to or reproduction of any copyright work has been disclosed expressly and sufficiently and the title of the Work and its authorship have been acknowledged in this Work;
- (4) I do not have any actual knowledge nor do I ought reasonably to know that the making of this work constitutes an infringement of any copyright work;
- (5) I hereby assign all and every rights in the copyright to this Work to the University of Malaya ("UM"), who henceforth shall be owner of the copyright in this Work and that any reproduction or use in any form or by any means whatsoever is prohibited without the written consent of UM having been first had and obtained;
- (6) I am fully aware that if in the course of making this Work I have infringed any copyright whether intentionally or otherwise, I may be subject to legal action or any other action as may be determined by UM.

Candidate's Signature

Date

Subscribed and solemnly declared before,

Witness's Signature

Date

Name :
Designation:

ABSTRACT

The phytochemical studies on *Lindera oxyphylla* and *Litsea costalis* (Nees) Kosterm from the family Lauraceae were performed. The extraction process was carried out using various solvent such as hexane, dichloromethane and methanol and the separation was conducted using column chromatography followed by preparative TLC or PTLC and finally the structural elucidation of isolated compounds was established on the basis of spectroscopic studies such as UV, IR, CD, OR, 1D and 2D NMR and MS (LC-MS) experiments.

A total of thirty compounds were isolated from *Lindera oxyphylla* and *Litsea costalis* (Nees) Kosterm and these plant species have never been investigated before. From the bark of *Lindera oxyphylla* yielded six compounds which are (+)-onysilin, (+)-pinostrobin, (+)-pinocembrin, flavokawain B, linderone and linderone A is a new compound. Seven compounds were isolated from the leaves of this species and these known compounds are one flavanone, kaempferol, one ketone methylinderone, (+)-laurotetanine, *N*-methylaurotetanine, (+)-norboldine, (+)-10-O-methyl-*N*-methylhernovine and (+)-norisoboldine.

Nine compounds were isolated from the bark of *Litsea costalis* (Nees) Kosterm and five known compounds namely cinnamaldehyde, 2-hydroxy-5-methoxybenzaldehyde, 2, 5-dimethoxybenzaldehyde, bisengenol and (*E*)-4-styrylphenol and four new compounds namely biseugenol A, biseugenol B, biseugenol C and litsin. Eight compounds were isolated from the leaves of this species. These seven known compounds are namely cinnamide, 2, 4-dimethoxybenzamide, 3, 4-dimethoxybenzamide, (+)-pinostrobin, (+)-onysilin, (+)-pinocembrin and 4-allyl-1,2-dimethoxybenzene and one new compound namely costalin.

The DPPH experiments for the isolated compounds from *Lindera oxyphylla*

showed the IC_{50} of **LOB15** was 8.5 $\mu\text{g/mL}$ strong activity, **LOB4** was 78.97 $\mu\text{g/mL}$ low activity, **LOB2** was 41.32 $\mu\text{g/mL}$ low activity, **LOB28** was 157.58 $\mu\text{g/mL}$ and **LOB25** was 149.45 $\mu\text{g/mL}$ both low activity. The IC_{50} for the isolated compounds from *Litsea costalis* (Nees) Kosterm showed that IC_{50} for **LCB17** was 16.34 $\mu\text{g/mL}$ strong activity, **LCB15** was 161.81 $\mu\text{g/mL}$ low activity, **LCB10** was 81.92 $\mu\text{g/mL}$ low activity, **LCB11** was 81.92 $\mu\text{g/mL}$ low activity, **LCB3** was 4.77 $\mu\text{g/mL}$ strong activity, **LCB7** was 73.24 $\mu\text{g/mL}$ low activity, **LCB4** was 26.69 $\mu\text{g/mL}$ strong activity and **LCL7** was 76.45 $\mu\text{g/mL}$ low activity. Ascorbic acid was used as a standard with IC_{50} 4.62 $\mu\text{g/mL}$.

The FRAP experiments for the isolated compounds from *Lindera oxyphylla* showed **LOB15** was 1.0 ± 0.06 , **LOB4** was 0.6 ± 0.01 , **LOB2** was 0.7 ± 0.02 , **LOB28** was 0.5 ± 0.02 and **LOB25** was 0.5 ± 0.03 .

Metal chelating assay for the isolated compounds showed **LOB15** was 33.37 ± 0.1 , **LOB4** was 25.69 ± 0.01 , **LOB2** was 26.11 ± 0.01 , **LOB28** was 13.09 ± 0.006 and **LOB25** was 13.51 ± 0.01 .

The cytotoxic activity were performed using a series of different doses on A549, PC-3, A375, HT-29, CEMSS, WRL-68, HEPG2, Jurkat and MCF-7 cell lines. The EC_{50} for **LOB4** was 79.57 $\mu\text{g/mL}$ for MCF-7 and 30.12 $\mu\text{g/mL}$ for PC-3, **LOB2** showed EC_{50} for PC-3 was 90.13 $\mu\text{g/mL}$, **LOB25** showed EC_{50} for MCF-7 was 96.33 $\mu\text{g/mL}$, **LCB17** was 1.4 ± 0.1 $\mu\text{g/mL}$ for MCF-7, 1.0 ± 0.1 $\mu\text{g/mL}$ for HepG2, 1.32 ± 0.1 $\mu\text{g/mL}$ for HT29 and 1.22 ± 0.1 for Jurkat. **LCB3** was 48 ± 3.05 $\mu\text{g/mL}$ for MCF-7 and 18 ± 2.1 $\mu\text{g/mL}$ for PC3. The EC_{50} for **LCB10** was 81.73 ± 3.7 $\mu\text{g/mL}$ for WRL68, 1.19 ± 0.19 $\mu\text{g/mL}$ for CEMSS and 85.13 ± 7.3 $\mu\text{g/mL}$ for A549.

ABSTRAK

Kajian fitokimia terhadap *Lindera oxyphylla* dan *Litsea costalis* (Nees) Kosterm dari keluarga Lauraceae telah dijalankan. Proses pengekstrakan telah dijalankan menggunakan pelbagai pelarut seperti heksana, diklorometana dan metanol dan proses pemisahan sebatian tulen telah dilakukan menggunakan kaedah kromatografi diikuti oleh TLC atau PTLC dan akhir sekali elusidasi struktur telah dibuat berdasarkan kajian spektroskopi seperti UV, IR, CD, OR, 1D dan 2D NMR dan MS (LC-MS).

Sejumlah 30 sebatian telah dipisahkan dari *Lindera oxyphylla* dan *Litsea costalis* (Nees) Kosterm dan tumbuhan ini belum pernah dikaji sebelum ini. Bahagian kulit dari *Lindera oxyphylla* menghasilkan enam sebatian, (+)-onysilin, (+)-pinostrobin, (+)-pinocembrin, flavokawain B, linderone dan linderone A adalah merupakan sebatian baru. Daripada bahagian daun spesies ini tujuh sebatian telah dipisahkan dan sebatian ini ialah satu flavanon, kaempferol, satu keton methylinderone, (+)-laurotetanine, *N*-metillaurotetanine, (+)-norboldine, (+)-10-O-N-methylhernovine dan (+)-norisoboldine.

Sembilan sebatian telah dipisahkan dari *Litsea costali* (Nees) Kosterm dan lima sebatian ini ialah cinnamaldehyde, 2-hydroxy-5-metoksibenzaldehyde, 2,5-dimetoksibenzaldehyde, bisngenol and (*E*)-4-styrylphenol dan empat daripadanya merupakan sebatian baru dari kumpulan neolignan dan dinamakan sebagai biseugenol A, biseugenol B, biseugenol C, dan litsin. Lapan sebatian telah dipisahkan dari bahagian daun spesies ini dan tujuh sebatian ini adalah cinnamide, 2,4-dimethoxybenzamide, 3,4-dimethoxybenzamide, (+)-pinostrobin, (+)-onysilin, (+)-pinocembrin dan 4-allyl-1,2-dimetoksibenzene dan satu sebatian baru merupakan dari kumpulan kroman dan dinamakan sebagai costalin.

Pemisahan sebatian dari *Lindera oxyphylla* menunjukkan aktiviti antioksidan dengan DPPH. Hasil ujikaji menunjukkan IC₅₀ bagi **LOB15** ialah 8.5 µg/mL tinggi aktiviti, **LOB4** ialah 78.97 µg/mL rendah aktiviti, **LOB2** ialah 41.32 µg/mL rendah aktiviti, **LOB28** ialah 157.58 µg/mL dan **LOB25** ialah 149.45 µg/mL, kedua-duanya menunjukkan rendah aktiviti. Sebatian yang dipisahkan dari *Litsea costalis* (Nees) Kosterm menunjukkan IC₅₀ bagi **LCB17** ialah 16.34 µg/mL tinggi aktiviti, **LCB15** ialah 161.81 µg/mL rendah aktiviti, **LCB10** ialah 81.92 µg/mL rendah aktiviti, **LCB11** ialah 81.92 µg/mL rendah aktiviti, **LCB3** 4.77 µg/mL tinggi aktiviti, **LCB7** ialah 73.24 µg/mL rendah aktiviti, **LCB4** ialah 26.69 µg/mL tinggi aktiviti dan **LCL7** ialah 76.45 µg/mL rendah aktiviti. Asid askorbik digunakan sebagai standard dengan IC₅₀ 4.62 µg/mL.

Ujikaji FRAP untuk sebatian yang dipisahkan dari *Lindera oxyphylla* menunjukkan bahawa penyerapan bagi **LOB15** ialah 1.0 ± 0.06 , **LOB4** ialah 0.6 ± 0.01 , (+)-**LOB2** ialah 0.7 ± 0.02 , **LOB28** ialah 0.5 ± 0.02 dan **LOB25** ialah 0.5 ± 0.03 .

Asai pencelatan logam untuk sebatian yang telah dipisahkan menunjukkan bahawa penyerapan bagi **LOB15** ialah 33.37 ± 0.1 , **LOB4** ialah 25.69 ± 0.01 , **LOB2** ialah 26.11 ± 0.01 , **LOB28** ialah 13.09 ± 0.006 dan **LOB25** ialah 13.51 ± 0.01 .

Kesan sitotoksik aktiviti dalam dos yang berbeza keatas beberapa sel kanser A549, PC-3, A375, HT-29, GEMSS, WRL-68, HEPG2, Jurkat dan MCF-7 telah dijalankan. Keputusan menunjukkan EC₅₀ untuk **LOB4** adalah 79.57 µg/mL merujuk kepada sel MCF-7 dan 30.12 µg/mL untuk PC-3, manakala EC₅₀ untuk **LOB2** kepada sel kanser PC-3 adalah 90.13 µg/mL dan **LOB25** menunjukkan EC₅₀ untuk MCF-7 adalah 96.33 µg/mL, seterusnya untuk **LCB17** adalah 1.4 ± 0.1 µg/mL kepada kanser sel MCF-7, 1.00 ± 0.1 µg/mL untuk HepG2, 1.32 ± 0.1 µg/mL kepada kanser sel HT29 and 1.22 ± 0.1 untuk Jurkat. **LCB3** adalah 48 ± 3.05 µg/mL kepada sel kanser MCF-7

dan 18 ± 2.1 $\mu\text{g/mL}$ kepada sel kanser PC3. Tahap EC_{50} **LCB10** adalah 81.73 ± 3.7 $\mu\text{g/mL}$ kepada sel kanser WRL68, manakala 1.19 ± 0.19 $\mu\text{g/mL}$ kepada sel kanser CEMSS dan 85.13 ± 7.3 $\mu\text{g/mL}$ kepada sel kanser A549.

To

Whom I love and those who love me

ACKNOWLEDGEMENTS

This study would not have been possible without the help and assistance of many people. First and foremost, I would like to express my deepest and sincere gratitude to my supervisor, Professor Datuk Dr. A. Hamid A. Hadi, for his guidance and the continuous support of my study, for his patience, motivation, enthusiasm, and immense knowledge. His guidance helped me throughout this work and writing of this thesis. I am indebted to Allahyarham Associate Professor Dr. Mat Ropi Mukhtar, for his guidance, concern, precious understanding, constant encouragement, kind and support throughout the development of this research project. May his soul rest in peace. It is also a great pleasure and honour to express my thanks to my supervisor Dr. Jamaludin bin Mohamad from ISB and let me worked in his lab. Special thanks to my co-supervisor Dr. Mohammad Ali khalilzadeh from Azad University of Ghaemshahr, Iran for his invaluable guidance throughout this study. I am also thankful to Dr Syam from Department of Pharmacy, University of Malaya for helping me in bioassay.

I wish to express my recognition to all the technical and non-technical staff of the Department of Chemistry, University of Malaya. My deepest appreciation is also dedicated to the Herbarium staffs; Mr. Din, Mr. Teo, Mr. Ujang and Mr. Rafly for their help in sample collection, the LC-MS and NMR staffs; Assoc. Prof. Dr. Azhar Arifin, Ms. Norzalida Zakaria, Mrs. Suwing Eh Vit, Mr. Fateh Ngaliman for NMR services and Mrs. Dara Fiona Mohamad for NMR and UV spectra recording, also, Mr. Mohammad and Hazrina for LC-MS equipment and without their help, this research work could not be completed.

To my colleagues in C-10 lab and C-110 lab I would like to collectively thank the group for providing helpful and critical discussions and I am proud to be one of them. I would like to thank my friends Mr. Mehran, Mr. Arshia, Ms. Joey, Dr. Yasoda,

Mrs. Nadia, Mrs. Faizah, Mrs. Nurul, Ms. Ayu, Mrs. Aziana, Ms. Chan, Mrs. Hanita, Dr Hamid Khaledi, Dr. Key, Ms. Ainnul, Ms Azie, Ms. Afifah, Mrs. Hairin Taha for reading my thesis and others for their kind help, support and friendship. Aside from my lab mates, I would like to thank my friend Mrs. Mona Yaeghoobi for her valuable comments and stimulating suggestions.

This work was supported by a research grant from the University of Malaya (PS265/2010B). I also truly appreciate Ministry of Higher Education, Malaysia for High Impact Research HIR-MOHE (F000009-21001) grant for financial support.

Lastly, I would like to thank my family for all their love and encouragement. My parents deserve special mention for their inspirable support and prayers. Father, in the first place was the person who put the fundamental of my learning character, showing me the joy of intellectual pursuit since I was a child. Mother, is the one who sincerely raised me with her caring and gently love.

Special thanks to my great and respectful brother in law Dr. Ebrahimi and my lovely sister Maliheh, for their financial and moral supports. To my lovely siblings, thanks for being attentive and caring during these often very difficult times.

TABLE OF CONTENTS

ABSTRACT	i
ABSTRAK	iii
ACKNOWLEDGEMENT	vii
LIST OF SCHEMES	xiv
LIST OF FIGURES	xvi
LIST OF TABLES	xxv
LIST OF ABBREVIATIONS	xxx

PART I

CHAPTER 1 : INTRODUCTION

	1
1.0 General	1
1.1 Lauraceae: General Appearance and Morphology	4
1.2 Lauraceae: Distribution and Habitat	6
1.3 Classification of Tribe and Lauraceae Classification	7
1.4 The Genus Lindera	9
Lindera oxyphylla (KL5359)	9
1.5 The Genus Litsea	10
Litsea costalis (Nee) Kosterm (KL5410)	11
1.6 Objectives of study	
13	

CHAPTER 2: GENERAL AND CHEMICAL ASPECTS

2.1 Introduction	14
Sources of natural products	14
2.2 Aromatic Compounds: Phenolics	15
2.2.1. The C ₆ Simple Phenol compounds	16
2.2.2. The C ₆ -C ₁ Phenolic acids and related compounds	17
2.2.3 The C ₆ -C ₂ acetophenones and phenyl acetic acids	17
2.2.4 The C ₆ -C ₃ Cinnamic acid and related compounds	17
2.3 The C ₁₅ Flavonoids	18
2.4 Benzophenones, Xanthones, Stilbens	21
2.5 Lignan and Neolignans	21
2.6 Alkaloids	23
2.6.1 Classification of the Alkaloids	24

2.6.1.1 True Alkaloid	24
2.6.1.2 Pseudo Alkaloid	25
2.6.1.3 Proto Alkaloid	25
2.7 Chemical Constituents of <i>Lindera</i> species	26
2.8 Chemical Constituents of <i>Litsea</i> species	27

CHAPTER 3: RESULTS AND DISCUSSION

PART I

3.0 Introduction	30
3.1 Chemical constituents from bark and leaves <i>Lindera oxyphylla</i>	30
3.1.1 Flavanone LOB4: (+)-Onysilin	33
3.1.2 Flavanone LOB7: (+)-Pinostrobin	40
3.1.3 Chalcone LOB15: FlavokawainB	46
3.1.4 Flavanone LOB2: (+)-Pinocembrin	54
3.1.5 Linderone LOB28: Linderone	59
3.1.6 Linderone LOB25: LinderoneA	69
3.1.7 Linderone LOL34: Methyllinderone	78
3.1.8 Flavonol LOL5: Kaempferol	82
3.1.9 Alkaloid LOL20: (+)-Laurotetanine	88
3.1.10 Alkaloid LOL35: N-Methylaurotetanine	95
3.1.11 Alkaloid LOL50: (+)-Norboldine	99
3.1.12 Alkaloid LOL63: (+)-10-O-Methyl-N-methylhernovine	103
3.1.13 Alkaloid LOL65: (+)-Norisoboldine	106

PART II

3.2 Chemical constituents from bark and leaves <i>Litsea costalis</i> (Nee) Kosterm	110
3.2.1 Aldehyde LCB7: 3',4' Dimethoxycinnamaldehyde	113
3.2.2 Aldehyde LCB11: Salicylaldehyde	121
3.2.3 Benzaldehyde LCB15: 2, 5-Dimethoxybenzaldehyde	129
3.2.4 Neolignan LCB3: Biseugenol A	133
3.2.5 Neolignan LCB9: Biseugenol	142
3.2.6 Oxyneolignan LCB10: Biseugenol B	145
3.2.7 4-allyl-1,2-dimethoxybenzene LCL15	153
3.2.8 Biphenyldrazine LCB17: Biseugenol C	156
Electrochemical investigation	164

3.2.9 Phenolic compound LCB4: Litsin	166
3.2.10 E-4-styryphenol	174
3.2.11 Cinnamide LCL4	178
3.2.12 2, 4 –Dimethoxybenzamide LCL2	183
3.2.13 3, 4 –Dimethoxybenzamide LCL5	190
3.2.14 Flavonoid LCL7: Costalin	193
3.2.15 Flavanone LCL9: (+)-Pinostrobin	206
3.2.16 Flavonol LCL14 (+)-Pinocembrin	206
3.2.17 Flavanone LCL13: (+)-Onysilin	207
3.2.18 Lignan LCL17: Eugenol	208

CHAPTER 4: Bioactivity

4.1 Introduction	213
4.2 Antioxidant: Free radicals and oxidation	214
4.3 Determination of antioxidant activity	215
4.4 DPPH Radical Scavenging Activity Assay	215
4.4.1 Material	216
4.4.2 Preparations of solutions	216
A. Preparation of extracts	216
B. Preparation of Ascorbic	216
C. Preparation of DPPH	217
D. Determination of DPPH activity of compounds	217
E. Determination of percentage of inhibition of DPPH	217
4.5 Ferric Reducing Power Assay (FRAP)	219
4.5.1 Material	219
4.5.2 Preparations of solutions	220
A. Preparation of 1% Potassium Ferricyanide K ₃ [Fe (CN) ₆]	220
B. Preparation of 10% Trichloroacetic acid (TCA)	220
C. Preparation of 0.1% Ferric chloride solution	220
D. Preparation of 0.2 M , buffer solution	220
E. Determination of FRAP Assay	221
4.6 Metal Chelating Activity Assay	222
4.6.1 Material	222
4.6.2 Preparation of solution	222
A. Preparation of 5mM Ferrozine	222

B. Preparation of 2mM Ferrous chloride (FeCl ₂))	222
C. Preparation of standard EDTA	222
D. Determination of metal chelating activity of Compounds	222
E. Determination of percentage of inhibition of Ferrozine	223
4.7 Results and Discussion	224
4.7.1 DPPH Radical Scavenging Activity Assay	224
4.7.2 Antioxidant of lindera Species	226
4.7.3 Antioxidant of litsea Species	226
4.7.4 FRAP (Ferric Reducing Power Assay)	241
4.7.5 Metal Chelating Assay	248
4.8 Anticancer: Cytotoxicity Activity	255
4.8.1 Anti-cancer of Lindera Species	257
4.8.2 Anticancer of Litsea Species	257
4.8.3 Materials & Methods	257
4.8.3.1 Cell culture	257
4.8.3.2 Cellular viability assay	258
4.8.3.3 Statistical analyses	258
4.8.4 Results	259
4.8.4.1 MTT assay costalin LCL7	262
4.8.4.2 Clonogenic assay costalinLCL7	263
4.8.4.3. Quantification of apoptosis (AO/PI) costalinLCL7	264
4.8.4.4 Cell viability study of biseugenol A LCB3and biseugenol BLCB10	266
4.8.4.5 Clonogenic assay biseugenol A LCB3and biseugenol B LCB10	267
4.8.4.6 Quantification of apoptosis biseugenolALC3 and BiseugenolB LCB10	268
4.8.4.7 Quantification of apoptosis (Ao/PI) biseugenolA LCB3and biseugenol B LCB10	269
4.8.4.8 MTT assay Litsin LCB4	270
4.8.4.9 Clonogenic assay Litsin LCB4	270
4.8.4.10 Quantification of apoptosis (AO/PI) Litsin LCB4	271
4.8.4.11 LitsinLCB4-induced caspase-3/7, 8, and 9 Activations	272
4.8.4.12 BC inhibitions TNF- α -induced NF-KB nuclear Trans location	275
4.8.4.13 BC induced caspases activation	277
4.8.4.14 BC up-regulated Bax and suppressed the expression of Bcl2 and	

HSP70 protein	278
4.8.4.15 BC-induced apoptosis in MCF7 cells	279
CHAPTER 5	
Conclusion	282
CHAPTER 6: Experimental	
6.1 Solvent	283
6.2 Instruments	283
6.3 Chromatography	284
6.3.1 Thin Layer Chromatography TLC	284
6.3.2 Column chromatographic	284
6.3.3 High Performance Liquid Chromatography (HPLC)	285
6.4 Plant Materials	285
6.5 Reagents	286
6.5.1 Mayer 's reagent (Potassium mercuric iodide)	286
6.5.2 Dragendorff' s' s reagent (Potassium bismuth iodide)	287
6.6 Extraction and Isolation	287
6.6.1 Extraction and isolation <i>Lindera oxyphylla</i>	287
6.6.2 Extraction and isolation <i>Litsea costalis</i> (Nees) Kosterm	297
6.7 Physical propertion and Spectral Data of Isolated compounds	307
6.7.1 Bark of <i>Lindera oxyphylla</i> (KL 5359)	307
6.7.2 Leaves of <i>Lindera oxyphylla</i> (KL 5359)	310
6.7.3 Bark of <i>Litsea costalis</i> (KL5410)	313
6.7.4 Leaves of <i>Litsea costalis</i> (KL5410)	317
REFERENCE	327
LIST OF PUBLICATIONS	342
APPENDIX	343

LIST OF SCHEMES

Scheme	Page
4.1 Radical-scavenging abilities of DPPH through H-donating agents	215
6.1 Isolation and purification of chemical constituents from plant	296
6.2 Isolation and purification of chemical constituents from N-hexane crude extract of <i>Lindera oxyphylla</i> (bark)	297
6.3 Isolation and purification of chemical constituents from dichloromethane crude extract of <i>Lindera oxyphylla</i> (bark)	298
6.4 Isolation and purification of chemical constituents from methanol crude extract of <i>Lindera oxyphylla</i> (bark)	299
6.5 Isolation and purification of chemical constituents from N-hexane crude extract of <i>Lindera oxyphylla</i> (Laves)	300
6.6 Isolation and purification of chemical constituents from dichloromethane crude extract of <i>Lindera oxyphylla</i> (Leaves)	301
6.7 Isolation and purification of chemical constituents from methanol crude extract of <i>Lindera oxyphylla</i> (Leaves)	302
6.8 Isolation and purification of chemical constituents from n-hexane crude extract of <i>Litsea costalis</i> (bark)	306
6.9 Isolation and purification of chemical constituents from dichloromethane crude extract of <i>Litsea costalis</i> (bark)	307
6.10 Isolation and purification of chemical constituents from methanol crude extract of <i>Litsea costalis</i> (bark)	308
6.11 Isolation and purification of chemical constituents from n-Hexane crude extract of <i>Litsea costalis</i> (Leaves)	309

LIST OF FIGURES

Figure	page
1.1 Drugs isolated from plants	2
1.2 The Leaf and Bark of <i>Lindera oxyphylla</i> (KL 5359)	10
1.3 The Bark and Flowers of <i>Litsea costalis</i>	12
1.4 The Leaf of <i>Litsea costalis</i> (Nees) Kosterm	12
3.1 LC-MS Spectrum of (+) – Onysilin LOB4	33
3.2 ¹ H NMR Spectrum of (+) – Onysilin LOB4	36
3.3 COSY Spectrum of (+) – Onysilin LOB4	37
3.4 ¹³ C NMR / DEPT Spectra of (+) – Onysilin LOB4	38
3.5 HMBC Spectrum of (+) – Onysilin LOB4	39
3.6 LC-MS Spectrum of (+)-pinostrobin LOB7	40
3.7 ¹ H NMR Spectrum of (+)-pinostrobin LOB7	43
3.8 COSY Spectrum of (+)-pinostrobin LOB7	44
3.9 ¹³ C NMR / DEPT Spectra of (+)-pinostrobin LOB7	45
3.10 LC-MS Spectrum of Flavokawain BLOB15	46
3.11 ¹ H NMR Spectrum of Flavokawain BLOB15	49
3.12 Cosy Spectrum of Flavokawain BLOB 15	50
3.13 ¹³ C NMR / DEPT Spectra of Flavokawain BLOB 15	51
3.14 HMQC Spectrum of Flavokawain BLOB15	54
3.15 HMBC Spectrum of Flavokawain BLOB 15	52
3.16 LC-MS Spectrum of (+)-Pinocembrin LOB2	54

3.17	¹ H NMR Spectrum of (+)-Pinocembrin LOB2	57
3.18	¹³ C NMR/ DEPT Spectra of (+)-Pinocembrin LOB2	58
3.19	LC-MAS Spectrum of Linderone LOB28	59
3.20	¹ H NMR Spectrum of Linderone LOB28	62
3.21	COSY Spectrum of Linderone LOB28	63
3.22	¹³ C NMR / DEPT Spectra of Linderone LOB28	64
3.23	HSQC Spectrum of Linderone LOB28	65
3.24	HMBC Spectrum of Linderone LOB28	66
3.25	X-ray Crystallographic Structure monoclinic of LOB28	67
3.26	X-ray Crystallographic Structure Triclinic of LOB28	68
3.27	IR Spectrum of Linderone A LOB25	69
3.28	LC-MS Spectrum of Linderone A LOB25	70
3.29	¹ H NMR Spectrum of LinderoneA LOB25	73
3.30	COSY Spectrum of Linderone A LOB25	74
3.31	¹³ C NMR / DEPT Spectra of Linderone A LOB25	75
3.32	HMQC Spectrum of Linderone A LOB25	76
3.33	HMBC Spectrum of Linderone A LOB25	77
3.34	LC-MS Spectrum of methyllinderone LOL34	78
3.35	¹ H NMR Spectrum of Methyllinderone LOL34	80
3.36	¹³ C NMR / DEPT Spectra of Methyllinderone LOL34	81
3.37	LC-MS Spectrum of kaempferol LOL5	82
3.38	¹ H NMR Spectrum of kaempferol LOL5	85
3.39	COSY Spectrum of kaempferol LOL5	86

3.40	¹³ C NMR Spectrum of kaempferol LOL5	87
3.41	LC-MS Spectrum of (+)-laurotetanine LOL20	88
3.42	¹ H NMR Spectrum of (+)-laurotetanine LOL20	91
3.43	¹³ C-NMR/DEPT Spectra of (+)-laurotetanine LOL20	92
3.44	HMQC Spectrum of (+)-laurotetanine LOL2	93
3.45	HMBC Spectrum of (+)-laurotetanine LOL20	94
3.46	LC-MS Spectrum of <i>N</i> -methyllaurotetanine LOL35	95
3.47	¹ H NMR Spectrum of <i>N</i> -methyllaurotetanine LOL3	97
3.48	¹³ C-NMR/DEPT Spectra of <i>N</i> -methyllaurotetanine LOL35	98
3.49	LC-MS Spectrum of (+)-Norboldine LOL50	99
3.50	¹ H-NMR Spectrum of (+)-Norboldine LOL50	101
3.51	¹³ C-NMR/DEPT Spectra of (+)-Norboldine LOL50	102
3.52	LC-MS Spectrum of (+)-10-O-N-methylhernovine LOL6	103
3.53	¹ H NMR Spectrum of (+)-10-O-N-methylhernovine LOL63	105
3.54	LC-MS Spectrum of (+)-Norisoboldine LOL65	106
3.55	¹ H-NMR Spectrum of (+)-Norisoboldine LOL65	108
3.56	¹³ C-NMR Spectrum of (+)-Norisoboldine LOL65	109
3.57	LC-MS Spectrum of 3',4'- Dimethoxycinnamaldehyde LCB7	113
3.58	¹ H NMR Spectrum of 3',4'-Dimethoxycinnamaldehyde LCB7	116
3.59	COSY Spectrum of 3',4'-Dimethoxycinnamaldehyde LCB7	117
3.60	¹³ C NMR/ DEPT Spectra of 3',4'-Dimethoxycinnamaldehyde LCB7	118
3.61	HMQC Spectrum of 3',4'-Dimethoxycinnamaldehyde LCB7	119
3.62	HMBC Spectrum of 3',4'-Dimethoxycinnamaldehyde LCB7	120
3.63	LC-MS Spectrum of salicylaldehyde LCB11	121

3.64	¹ H NMR Spectrum of salicylaldehyde LCB11	124
3.65	COSY Spectrum of salicylaldehyde LCB11	125
3.66	¹³ C-NMR / DEPT Spectra of salicylaldehyde LCB11	126
3.67	HMQC Spectrum of salicylaldehyde LCB11	127
3.68	HMBC Spectrum of salicylaldehyde LCB11	128
3.69	LC-MS Spectrum of 2,5-Dimethoxybenzaldehyde LCB15	129
3.70	¹ H NMR Spectrum of 2,5-Dimethoxybenzaldehyde LCB15	131
3.71	¹³ C-NMR/ DEPT Spectra of 2,5-Dmethoxybenzaldehyde LCB15	132
3.72	IR Spectrum of biseugenol A LCB3	135
3.73	LC-MS Spectrum of biseugenol A LCB3	134
3.74	¹ H NMR Spectrum of biseugenol A LCB3	137
3.75	COSY Spectrum of biseugenol A LCB	138
3.76	¹³ C-NMR/DEPT Spectra of biseugenol A LCB3	139
3.77	HMQC Spectrum of biseugenol A LCB3	140
3.78	HMBC Spectrum of biseugenol A LCB3	141
3.79	¹ H NMR Spectrum of biseugenol LCB9	144
3.80	IR Spectrum of biseugenol B LCB10	145
3.81:	LC-MS Spectrum of biseugenol B LCB10	146
3.82	¹ H NMR Spectrum of biseugenol B LCB10	148
3.83	COSY Spectrum of biseugenol B LCB10	149
3.84	¹³ C-NMR/DEPT Spectra of biseugenol B LCB10	150
3.85	HMQC Spectrum of biseugenol B LCB10	151
3.86	HMBC Spectrum of biseugenol B LCB10	152
3.87	LC-MS Spectrum of 4-allyl-1,2-d4-allyl-1,2-dimethoxybenzene LCL15	153

3.88	¹ H NMR Spectrum of 4-allyl-1,2-d ₄ -allyl-1,2-dimethoxybenzene LCL15	155
3.89	IR Spectrum of biseugenol CLCB17	156
3.90	LC-MS Spectrum of biseugenol C LCB17	157
3.91	¹ H NMR Spectrum of biseugenol C LCB17	159
3.92	COSY Spectrum of biseugenol CLCB17	160
3.93	¹³ C-NMT/DEPT Spectra of biseugenol CLCB17	161
3.94	HMQC Spectrum of biseugenol CLCB17	162
3.95	HMBC Spectrum of biseugenol C LCB17	163
3.96	(a)Cyclic voltammogram of carbon nanotube paste electrode in 0.1 M phosphate buffer solution (pH 6.0) in the presence of 500 μM biseugenol C at scan rate 50mV ⁻¹ , (b)as in the absence of biseugenol C	164
3.97	Current–pH curve for electrooxidation of 500 μM biseugenol C at carbon Nanotubes paste electrode with a scan rate of 50 mV s ⁻¹ . Inset) influence of pH on cyclic voltammograms of biseugenol C at the surface of the modified electrode, (pH 4.0, 5.0, 6.0, 7.0, 8.0, and 9.0, respectively)	165
3.98	IR Spectrum of Litsin LCB4	166
3.99	LC-MS Spectrum of Litsin LCB4	167
3.100	¹ H NMR Spectrum of Litsin LCB4	169
3.101	COSY Spectrum of Litsin LCB4	170
3.102	¹³ C-NMR/DEPT Spectra of Litsin LCB4	171
3.103	HMQC Spectrum of Litsin LCB4	172
3.104	HMBC Spectrum of Litsin LCB4	173
3.105	LC-MS Spectrum of Stilbene LCB5	174
3.106	¹ H-NMR spectrum of Stilbene LCB5	176
3.107	¹³ C- NMR Spectrum of Stilbene LCB5	177
3.108	LC-MS Spectrum of Cinnamide LCL4	188
3.109	¹ H NMR Spectrum of Cinnamide LCL4	181
3.110	¹³ C-NMR Spectrum of Cinnamide LCL4	182

3.111	LC-MS Spectrum of 2, 4 –Dimethoxybenzamide LCL2	183
3.112	¹ H NMR Spectrum of 2, 4 –Dimethoxybenzamide LCL2	186
3.113	¹³ C-NMR/DEPT Spectra of 2, 4 –Dimethoxybenzamide LCL2	187
3.114	HMQC Spectrum of 2, 4 –Dimethoxybenzamide LCL2	188
3.115	HMBC Spectrum of 2, 4 –Dmethoxybenzamide LCL	189
3.116	LC-MS Spectrum of 3, 4 –Dimethoxybenzamide LCL5	190
3.117	¹ H NMR Spectrum of 3, 4 –Dimethoxybenzamide LCL5	192
3.118	¹³ C-NMR/DEPT Spectra of 3, 4 –Dmethoxybenzamide LCL5	193
3.119	IR Spectrum of Costalin LCL7	194
3.120	LC-MS Spectrum of Costalin LCL7	195
3.121	¹ H NMR Spectrum of Costalin LCL7	198
3.122	COSY Spectrum of Costalin LCL7	199
3.123	¹³ C-NMR/DEPT Spectra of Costalin LCL7	200
3.124	HMQC Spectrum of Costalin LCL7	201
3.125	HMBC Spectrum of Costalin LCL7	202
3.126	NOESY Spectrum of Costalin LCL7	203
3.127	3D Structure of Costalin LCL7	204
3.128	CD structure of Costalin LCL7	205
3.129	LC-MS Spectrum of eugenol LCL17	208
3.130	¹ H NMR Spectrum of eugenol LCL17	211
3.131	¹³ C NMR Spectrum of eugenol LCL17	212
4.1	Graph of concentration (µg/mL) as %inhibition DPPH radical scavaging activity of ascorbic acid	227

4.2	Graph of concentration ($\mu\text{g/mL}$) as %inhibition DPPH radical scavaging activity of flavokawain B	228
4.3	Graph of concentration ($\mu\text{g/mL}$) as %inhibition DPPH radicalscavaging activity of (+) - Onysilin	229
4.4	Graph of concentration ($\mu\text{g/mL}$) as %inhibition DPPH radicalscavaging activity of (+)-Pinocembrin	230
4.5	Graph of concentration ($\mu\text{g/mL}$) as %inhibition DPPH radicalscavaging activity of Linderone	231
4.6	Graph of concentration ($\mu\text{g/mL}$) as %inhibition DPPH radicalscavaging activity of Linderone A	232
4.7	Graph of concentration ($\mu\text{g/mL}$) as %inhibition DPPH radicalscavaging activity of biseugenol C	233
4.8	Graph of concentration ($\mu\text{g/mL}$) as %inhibition DPPH radicalscavaging activity Of 2,5-dimethoxybenzaldehyde	234
4.9	Graph of concentration ($\mu\text{g/mL}$) as %inhibition DPPH radicalscavaging activity of biseugenol B	235
4.10	Graph of concentration ($\mu\text{g/mL}$) as %inhibition DPPH radicalscavaging activity Of 2-hydroxy-5-methoxybenzaldehyde	236
4.11	Graph of concentration ($\mu\text{g/mL}$) as %inhibition DPPH radicalscavaging activity of biseugenol A	237
4.12	Graph of concentration ($\mu\text{g/mL}$) as %inhibition DPPH radicalscavaging activity of Cinnamaldehyde	238
4.13	Graph of concentration ($\mu\text{g/mL}$) as %inhibition DPPH radicalscavaging activity of Litsin	239
4.14	Graph of concentration ($\mu\text{g/mL}$) as %inhibition DPPH radicalscavaging activity of Costalin	240
4.15	Absorbance of BHA standard	245
4.16	Absorbance of flavokawain B	246
4.17	Absorbance of (+)-Pinocembrin	247
4.18	Absorbance of (+)- Onysilin	248

4.19	Absorbance of Linderone	249
4.20	Absorbance of Linderone A	250
4.21	Chelating activity of EDTA	249
4.22	Chelating activity of Flavokawain B	250
4.23	Chelating activity of (+)-Pinocembrin	251
4.24	Chelating activity of (+)-Onysilin	252
4.25	Chelating activity of Linderone	253
4.26	Chelating activity of Linderone A	254
4.27	EC ₅₀ (µg/ml) of five compounds of <i>Lindera oxyphylla</i>	260
4.28	Effect of costalin treatment in the human hepatocellular carcinoma HEPG2 Cells	263
4.29	Comparison of colony formation rate at different concentrations of costalin on HepG2 cells at 24 hr. Data are mean ± SD(n=3)	264
4.30	HepG2 cells stained with AO/PI. Panel (A) shows the green viable HepG2 cells with diffused chromatin as control (Magnification, 20X).	265
4.31	Comparison of colony formation rate using different concentrations of compounds bisugenol A and bisugenol B on HepG2 and PC-3 cell line	268
4.32	Apoptosis quantification of HepG2 and PC-3 cells stained with AO/PI. Panel (A) and (C) show the green viable HepG2 and PC-3 cells	269
4.33	Percentage viability of MCF-7 cells treated with different concentration measured after 48 hours using MTT assay.	270
4.34	Comparison of colony formation rate using different concentrations of <i>Litsin</i> On MCF-7 after 48 hr	271
4.35	MCF-7 cells stained with AO/PI. Panel (A) shows the green viable MCF-7 cells with diffused chromatin as control (Magnification, 20X).	272
4.36	Relative luminescence expression of Caspase 3/7 in the MCF7 cells treated with different concentrations of <i>Litsin</i> .	273
4.37	Relative luminescence expression of caspase 8 in the MCF7 cells treated with	

different concentrations of <i>Litsin</i> .	273
4.38 Relative luminescence expression of Caspase 9 in the MCF7 cells treated with different concentrations of Litsin.	274
4.39 NF-KB fluorescent intensity	276
4.40 NF-kB fluorescent intensity in the nuclei	277
4.41 Active caspases in BC-treated cells	278
4.42 The changes occurred to the MMP and cytochrome c release led us to confirm the role of mitochondria in the apoptosis occurred by BC	279
4.43 MCF7 cells by determining nuclear condensation and fragmentation hallmark for Apoptosis	280
4.44 Quantitative analysis of BC mediated apoptosis parameter.Changes in A) total nuclear intensity, B)cell permeability,C) mitochondrial membrane potential and D) cytochrome localization were all measured simultaneously in MCF7cells.	281
5.1 Submitted structures of chemical constituents from two genera	288
6.1 HPLC spectrum of LCB10 and LCB17	304

LIST OF TABLES

Table	page
1.1 Classification of Lauraceae family	8
2.1 Category of phenolic compounds in plants	16
2.2 Chemical constituents isolated from <i>Lindera</i> species	26
2.3 Chemical constituents isolated from <i>Litsea</i> species	27
3.1 Chemical constituents from the bark of <i>Lindera oxyphylla</i>	31
3.2 Chemical Constituents of leave <i>Lindera oxyphylla</i>	32
3.3 ¹ H NMR (400 MHz) and ¹³ C NMR (100 MHz) spectral data of (+) – onysilin LOB4	35
3.4 ¹ H NMR (400 MHz) and ¹³ C NMR (100 MHz) spectral data of (+)-pinostrobin LOB7	42
3.5 ¹ H NMR (400 MHz) and ¹³ C NMR (100 MHz) spectral data of flavokawain B LOB15	48
3.6 ¹ H NMR (400 MHz) and ¹³ C NMR (100 MHz) spectral data of (+)-pinocembrin LOB2	56
3.7 ¹ H NMR (400 MHz) and ¹³ C NMR (100 MHz) spectral data of linderone LOB28	61
3.8 1D (¹ H and ¹³ C) and 2D(COSY and HMBC) NMR spectral data of linderoneA LOB25	72
3.9 ¹ H NMR (400 MHz) and ¹³ C NMR (100 MHz) spectral data of Methyllinderone LOL34	79
3.10 ¹ H NMR (400 MHz) and ¹³ C NMR (100 MHz) spectral data of kaempferol LOL5	84
3.11 ¹ H NMR (400 MHz) and ¹³ C NMR (100 MHz) spectral data of (+)-laurotetanine LOL20	90
	27

3.12	¹ H NMR (400 MHz) and ¹³ C NMR (100 MHz) spectral data of <i>N</i> -methyl laurotetanine LOL35	96
3.13	¹ H NMR (400 MHz) and ¹³ C NMR (100 MHz) spectral data of (+)-Norboldine LOL50	100
3.14	¹ H NMR (400 MHz) spectral data of (+)-10-O-Methyl- <i>N</i> -methylhernovine LOL63	104
3.15	¹ H NMR (400 MHz) and ¹³ C NMR (100 MHz) spectral data of (+)- Noriso boldine LOL65	107
3.16	Chemical Constituents of Bark <i>Litsea costalis</i>	111
3.17	Chemical Constituents of Leaves <i>Litsea costalis</i>	112
3.18	¹ H NMR (400 MHz) and ¹³ C NMR (100 MHz) spectral data of 3',4'-Dimethoxy cinnamaldehyde LCB7	115
3.19	¹ H NMR (400 MHz) and ¹³ C NMR (100 MHz) spectral data of salicylaldehyde LCB11	123
3.20	¹ H NMR (400 MHz) and ¹³ C NMR (100 MHz) spectral data of 2,5-Dimethoxy benzaldehyde LCB15	130
3.21	1D (¹ H and ¹³ C) and 2D (COSY and HMBC) NMR spectral data of biseugenolA LCB3	136
3.22	1D (¹ H and ¹³ C) and 2D (COSY and HMBC) NMR spectral data of Biseugenol LCB9	143
3.23	1D (¹ H and ¹³ C) and 2D(COSY and HMBC) NMR spectral data of biseugenol B LCB10	146
3.24	1D (¹ H and ¹³ C) and 2D(COSY and HMBC) NMR spectral data of biseugenol C LCB17	158
3.25	1D (¹ H and ¹³ C) and 2D(COSY and HMBC) NMR spectral data of litsin LCB4	168
3.26	¹ H NMR (400 MHz) and ¹³ C NMR (100 MHz) spectral data of stilbene LCB5	175
3.27	¹ H NMR (400 MHz) and ¹³ C NMR (100 MHz) spectral data of cinnamide LCL4	180
3.28	¹ H NMR (400 MHz) and ¹³ C NMR (100 MHz) spectral data of 2, 4 –Dimethoxy benzamide LCL2	185
3.29	¹ H NMR (400 MHz) and ¹³ C NMR (100 MHz) spectral data of 3, 4 –Dimethoxy	

	benzamide LCL5	191
3.30	1D (¹ H and ¹³ C) and 2D(COSY and HMBC) NMR spectral data of costalin LCL7	197
3.31	¹ H NMR (400 MHz) and ¹³ C NMR (100 MHz) spectral data of eugenol LCL17	210
4.1	DPPH and different concentration of standard ascorbic acid	218
4.2	Metal chelating of standard EDTA	223
4.3	Antioxidant of some selected chemicals in species of <i>Lindera</i>	226
4.4	Antioxidant of some selected chemicals in species of <i>Litsea</i>	226
4.5	DPPH radical scavenging activity ascorbic acid	227
4.6	DPPH radical scavenging activity of flavokawain B. LOB15	228
4.7	DPPH radical scavenging activity of (+) - onysilin LOB4	229
4.8	DPPH radical scavenging activity of (+)-pinocembrin LOB2	230
4.9	DPPH radical scavenging activity of linderone LOB28	231
4.10	DPPH radical scavenging activity of linderoneA LOB25	232
4.11	DPPH radical scavenging activity of biseugenolC LCB17	233
4.12	DPPH radical scavenging activity of 2, 5-Dimethoxybenzaldehyde LCB15	234
4.13	DPPH radical scavenging activity of biseugenol B LCB10	235
4.14	DPPH radical scavenging activity of 2-hydroxy-5-methoxybenzaldehyde LCB11	236
4.15	DPPH radical scavenging activity biseugenolA LCB3	237
4.16	DPPH radical scavenging activity of cinnamaldehyde LCB7	238
4.17	DPPH radical scavenging activity of litsin LCB4	239
4.18	DPPH radical scavenging activity of costalin LCL7	240
4.19	FRAP of BHA standard	242

4.20	FRAP of flavokawain B LOB25	243
4.21	FRAP of (+)-pinocembrin LOB2	244
4.22	FRAP of (+)- onysilin LOB4	245
4.23	FRAP of linderone LOB28	246
4.24	FRAP of linderone A LOB25	247
4.25	Metal Chelating Assay of EDTA	249
4.26	Metal Chelating Assay of flavokawain B LOB25	250
4.27	Metal Chelating Assay of (+)-pinocembrin LOB2	251
4.28	Metal Chelating Assay of (+)-onylsilin LOB4	252
4.29	Metal Chelating Assay of linderone LOB28	253
4.30	Metal Chelating Assay of linderone A LOB25	254
4.31	Anticancer of some selected chemicals in species of <i>Lindera</i>	257
4.32	Anticancer of some selected chemicals in species of <i>Litsea</i>	257
4.33	Effect of compounds from <i>Lindera oxyphylla</i> on different cells type expressed as EC ₅₀ values in 24 hours MTT assay	261
4.34	EC ₅₀ values of compounds in different celllines from <i>Litsea costalis</i>	261
4.35	The cloning efficiency (CE) of the LCL7 on HepG2 cell line after 24 hrs	263
4.36	EC ₅₀ values of biseugenol ALCB3 and biseugenol BLCB10 in different cell line	266
4.37	The cloning efficiency (CE) of the biseugenol A LCB3 on HepG2 cells in 48 hrs	267
4.38	The cloning efficiency (CE) of the biseugenol B on PC-3 cells in 48 hrs	268
4.39	The cloning efficiency (CE) of the new compound litsin LCB4 on MCF-7 Cells after 48 hrs	271
5.1	Chemical constituent from <i>Lindera oxyphylla</i> and <i>Litsea costalis</i>	285
6.1	Yield of crude extracted from <i>Lindera oxyphylla</i> and <i>Litsea costalis</i> (Nees)	

Kosterm (Lauraceae)	292
6.2 Chromatography solvent systems and the yield of compounds isolated from <i>Lindera oxyphylla</i> (KL5359)	311
6.3 Chromatography solvent systems and the yield of compounds isolated from <i>Litsea costalis</i> (Nee.)Kosterm (KL5410)	312

LIST OF SYMBOLS AND ABBREVIATIONS

α	Alpha
β	Beta
$\lambda_{(\max)}$	Maximum wave length
δ	Chemical shift
$\nu_{(\max)}$	Frequency
Kg	Kilogram
M	Molar
mM	Milimolar
μM	Micromolar
mg/mL	Milligram per Milliliter
ml	Milliliter
M	Meter
MHz	Mega Hertz
Hz	Hertz
UV	Ultraviolet
IR	Infrared
Ppm	Part per million
eV	Electron Volt
PTLC	Preparative Thin Layer Chromatography
$[\alpha]_D^{25}$	Specific rotation
Aq	Aqueous

conc.	Concentrated
DCM	Dichloromethane (CH ₂ Cl ₂)
DMSO	Dimethylsulphoxide
HPLC	High-performance liquid chromatography
pH	Potency of Hydrogen
TLC	Thin Layer Chromatography
CC	Column Chromatography
NMR	Nuclear Magnetic Resonance
FT-NMR	Fourier Transform Nuclear Magnetic Resonance
Cm ⁻¹	Per centimeter
nm	Nanometer
<i>J</i>	Coupling constant
<i>d</i>	Doublet
<i>Dd</i>	Doublet of doublet
<i>T</i>	Triplet
<i>dt</i>	Doublet of triplet
<i>M</i>	Multiplet
1D-NMR	One Dimensional Nuclear Magnetic Resonance
2D-NMR	Two Dimensional Nuclear Magnetic Resonance
¹ H-NMR	Proton NMR
¹³ C-NMR	13-Carbon NMR
COSY	¹ H - ¹ H Correlation Spectroscopy

DEPT	Distortioness Enhancement by Polarization Transfer
HMQC	Heteronuclear Multiple Quantum Correlation
HSQC	Heteronuclear Single Quantum Correlation
HMBC	Heteronuclear Multiple Bond Correlation
NOESY	Nuclear Overhauser Effect Spectroscopy
LC-MS	Liquid Chromatography-Mass Spectroscopy
MS	Mass Spectroscopy
HRESIMS	High Resolution Electrospray Ionization Mass Spectroscopy
EIMS	Electron Impact Mass Spectroscopy
ESI	Electrospray Ionization
OD	Optical density
m/z	Mass per charge rate (mass of the ion divided by its charge)
DMF	Dimethylformamide
$[M+H]^+$	Pseudo-molecular ion (molecular mass +1)
$[M+Na]^+$	Pseudo-molecular ion (molecular mass +23)
AR	Analytical Reagent Grade
IC ₅₀	Inhibitory Concentration
EC ₅₀	Effect Concentration
LOL	<i>Lindera oxyphylla</i> Leaves
LOB	<i>Lindera oxyphylla</i> Bark
LCL	<i>Litsea costalis</i> Leaves
LCB	<i>Litsea costalis</i> Bark

br	broad
DPPH	1, 1-Diphenyl-2-picryl hydrazyl
FRAP	Ferric reducing antioxidant properties
µg	microgram

INTRODUCTION

1.0 General

Archaeological confirmation indicates humans have used plants to treat and avoid diseases for more than 5000 year (Swerdlow et al ., 2000). Many cultures have a rich history of medicinal plant use dating back thousands of years. Today plant materials are important sources of new drugs. For examples, from 1981-2000, compounds isolated from either plants or microbes have lead to 60% of cancer drugs and 75% of pharmaceuticals for contagious disease (Cragg, 1997; da Rocha et al ., 2001; Newman et al. 2003).

A huge variety of natural products (also called secondary metabolites) are organic compounds such as alkaloids, terpenes, polyphenols and saponins are synthesised exclusively by plants for various purposes (Chew et al., 2009). More than 35,000 plant species have been reported to be used in various mankind around the world for medical purposes (Lewington et al., 1993). Natural products are very important in health care and prevention of diseases. For example, apomorphine **1** was isolated from poppy (*Papaver somniferum*) in 2004 has extensive use in the treatment Parkinson's disease (Chen et al. 2005). Tiotropium bromide **2** was identified from *Atropa belladonna* (Solanaceae) in 2004 was used for the treatment of bronchospasm linked with chronic obstructive pulmonary disease (COPD). Nitisinone **3** (Koumis et al ., 2005) was extracted from plant (*Callistemon citrinus*) in 2002. It had been used clinically in the treatment of hereditary tyrosinaemia type 1 (HT-1) and used to reduced urinary HGA levels in patients with alkaptonuria (Onojafe et al., 2005). Galantamine **4** was isolated from *Galanthus nivalis* in 2001 and was used traditionally in Bulgaria, Iran and Turkey for neurological conditions and poliomyelitis in children (Berkov et al., 2009; Howes et al 2003). Arteether **5** was isolated from *Artemisia annua* (Asteraceae) in 2000 and it has been developed artemisinin, a sesquiterpene lactone

(Dewick, et al., 2009; van Agtmael et al ., 1999).

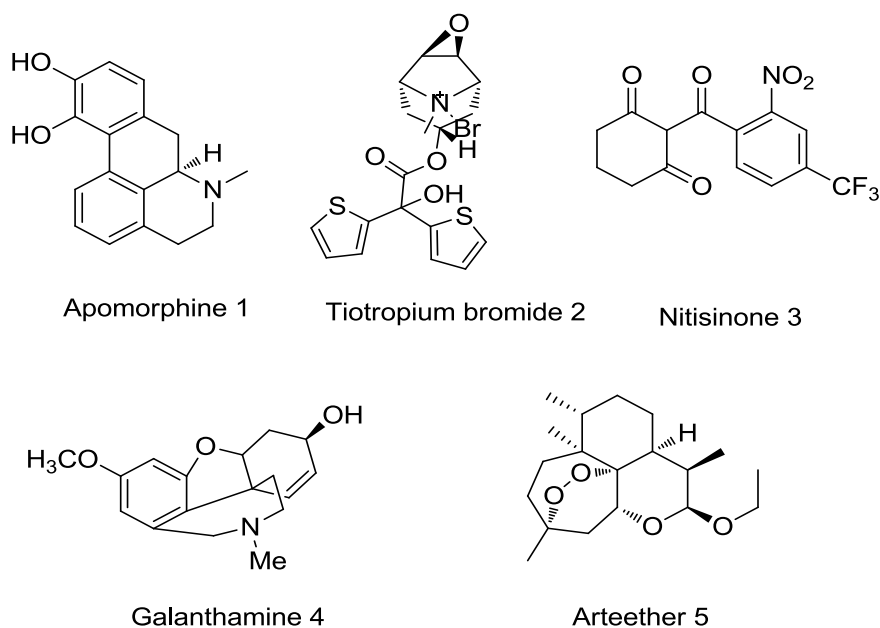


Figure 1.1: Drugs isolated from plants.

Herbal medicines role an important ingredient in preparations linked to human culture since early time. In 1993, studies conducted by the World Health Organization (WHO) reported 80% of the world's population rely on traditional medicine. In other words, despite the advances of modern medicine, the practice of traditional medicine persists 90% comes either directly or indirectly from plant sources (Benowitz et al., 1996). Forty-seven percentage of the anticancer drugs in the market come from natural products (Newman et al., 2007).

Malaysia is one of the richest and oldest rain forests in the world. It may be attributed to the warm and nearly uniform which is suitable for the growth of the tropical rain forest. Malaysia is considered as a stable region and this has made possible for their persistence over 50 million years ago (Keng.,1978) . The flora of Malaysia is very rich and is conservatively estimated to number contain 15,000 species of flowering plants and more than 1,000 species of ferns. Malaysia, widely recognized as one of the

centres of biological diversity, is richly endowed with plants, animals and microbial genetic resources. If exploited and managed wisely, these genetic resources could provide renewable useful products for not only the present but also the future generation (Soepadmo et al., 1999).

In Malaysia, the practice of traditional medicine is still common among various ethnic groups, Malay, Chinese and Indian. This traditional medicine knowledge has been passed on through many generations (Ali et al., 1999).

In the last decades, many different types of natural products had been isolated, which possess different types of biological activities. Some of the diverse classes of natural products, acetogenins, alkaloids, biflavonoids, coumarins, terpenoids and xanthonoids were isolated from the family of Annonaceae, Apocynaceae, Guttiferae, Meliaceae, Rubiaceae, Rutaceae, Verbenaceae (Rahmani et al., 2001).

The flowering plants and in particular the tree species have received comprehensive studies through the Tree Flora of Malaya project and on-going Tree Flora of Sabah and Sarawak project. After the completion of the Tree Flora of Malaya, a total of more than 2830 tree species were documented and of these 746 species or 26.4% of the total are found to be endemic to Peninsular Malaysia. For the Peninsular Malaysia the number of non-tree species which comprise shrubs, herbs, parasites, epiphytes, saprophytes, climbers and others may be more than that of trees, but their taxonomy and diversity remain uncertain because there is no similar efforts to study their taxonomy, distribution and endemism like that of tree species (Zakri et al., 2000).

Recently, there is a trend that people are turning towards natural products as remedy. One of the main reason stems from the fact that modern pharmaceuticals frequently utilize chemicals and synthetic drugs that may have adverse effect on human's health. Additionally, some these drugs have so far away failed to cure certain

chronic disease, e.g. hypertension, cancer, HIV. Herbal plants suppose have less side affect but they are unusual for disease avoidance and healing. The medicinal value of plants is found in roots, leaves or other plants parts. Their efficiency and attractiveness depend on new research achievements and knowledge of traditional treatment, ethnic beliefs and the availability of plant materials (Bhakuni et al., 1978).

Natural products (secondary metabolites) and their derivatives (including antibiotics) characterize more than 50% of all drugs used in the world. Higher plants contribute less than 25 % of the total drugs and about 100 drugs nowadays earn from natural products in USA. Some known example of plant derived medicines are strychnine, ziconotide, codeine, colchicine, atropine, reserpine and digoxin. Important new anticancer drugs such as taxol and vincristine have been developed from plants. The international consumer market for herbs and botanicals is estimated at about USD 18 billion, which is just under half of the total market for supplements (including minerals, vitamins, homoeopathic products and sport supplements), estimated more than USD 50 billion (Bhakuni et al., 1981).

Plant materials are not only use as drugs but many of them can be used as chemical models or templates for the design, synthesis and semi-synthesis of novel substances for treating human diseases.

1.1 Lauraceae: General Appearance and Morphology

Most of the species are evergreen, tough intermittent in flowering and in the development of new leaves. The colors of new leaves vary from nearly white to pink, purple, red or brown. The leaves are simple, spiral, alternate, opposite, subopposite or whorled, entire, leathery, without stipules; usually with numerous gland dots, and often aromatic when crushed; secondary veins pinnate; sometimes with only one pair of veins

(trinerved) as in *Cinnamomum*, occasionally with more than one pair but basal pair enhanced so that the leaf base appeared trinerved. The leaves of some species have domatias in the axils of the nerves, inhabited by mites.

The bark is usually smooth, rarely fissured, scaly or dippled, often covered with large lenticels, grey-brown to reddish-brown. The inner bark is usually very thick, granular, mottled or laminated, often with strong aromatic smell, yellow, orange-brown, pinkish or reddish. Sapwood is pale yellow to pale brown with satiny lustre when freshly cut. Terminal bud naked or covered with bud scales which sometimes appear like small leaves.

The flowers are protogynous, often with a complex flowering system to prevent inbreeding. The flowers are pollinated chiefly by flies and beetles which are attracted by the smell emitted from the flowers. Their flowers are small, regular, greenish white or yellow, fragrant or with rancid smell with 6 petals in two rows (4 tepals in 2 rows in *Neolitsea*); tepals equal or outer whorl smaller, perianth tube either reciduous or persistent appearing as a cup at the base of the fruit or completely enclosing the fruit.

The fruits of this family are small to large one-seeded berry, sometimes enveloped by the accrescent perianth tube or the perianth persisting and clasping the base of the fruit. In some genera perianth lobes dropping but the tube developing into a shallow or deep cup at base of fruit or perianth absent or the perianth lobes spreading or reflexed in fruit. Fruit stalk enlarging and becoming highly coloured in some species of *Alseodaphne* and *Dehaasia*.

The seed without albumen, with thin testa. Cotyledons are very large, flat convex, pressed against each other. The fruit are eaten by monkeys, squirrels, bats, musangs and birds. However, some of the species are not touch by these animals. Wood of Lauraceae is soft to moderately hard, light to moderately heavy to varying from 350-880 kg/nr' air dry. Grain straight or slightly interlocked, texture moderately fine and

even. Sapwood usually is a distinctly lighter shade than the heartwood. The heartwood is yellow-white (*Beilschmiedia*), yellow brown or red-brown in most species of *Cinnamomum*, *Cryptocarya* and *Endiandra*, olive green in species of *Litsea*, *Actinodaphne*, *Alseodaphne*, *Notaphoebe*, *Phoebe*, and dark olive green-brown in *Dehaasia* (Wood et al., 1958).

The family of Lauraceae provided many useful economic products. Most of the economically important species other than sources of excellent wood are spices or flavoring agent. For example avocado (*Persea*) is one of important tropical fruit (Bannister et al. 2012; Okuda et al., 2003).

1.2 Lauraceae: Distribution and Habitat

Lauraceae is one of the major families of plants. Lauraceae or Laurel family is known as “*Medang*” or “*Tejur*” in Malay, comprises a group of flowering plants included in the order Laurales; The family consists about 55 genera and over 2500 (perhaps as many as 4000) species world-wide and about 16 genera and 213 species were found in Malaysia. The tree of Lauraceae are usually evergreen, shrubs, and without buttresses.

Ecology of Lauraceae is dependent on type of the lands, whether lowlands or highlands. In the lowlands, Lauraceae are typically small trees except for a few species which may reach 30 m tall. In the highlands, Lauraceae like Fagaceae, becoming more abundant reaches the top layer of the forest, which lies at 1200-1600 m. such as Oak-Laurel Forest which is a feature of the mountains of tropical Asia from Himalayas to New Guinea (Corner et al., 1988).

1.3 Classification of Tribe and Lauraceae Classification

There are many primitive and archaic features, which characterize the Lauraceae family. The determination is dependent on a combination of characters. Scheme 1.1 illustrated the classification proposed by (Keng et al ., 1978). There are over 30 genera, mainly tropical and sub-tropical Asia and America, about 16 are found in Malaysia. This classification is according to Malayan seed plants .

The classification of Lauraceae included 63 genera, mainly in Southeast Asia and Latin America that can be illustrated in the list below:

Kingdom: Plantae

Divison: Magnoliophyta

Class: Magnoliopsida

Order: Laurales

Family: Lauraceae (Wilson., 2010)

Genera:

1. *Actinodaphne*
2. *Adenodaphne*
3. *Aiouea*
4. *Alseodaphne*
5. *Anaueria*
6. *Aniba*
7. *Apollonias*
8. *Aspidostemon*
9. *Beilschmiedia*
10. *Brassiodendron*
11. *Caryodaphnops*
12. *Cassytha*
13. *Chlorocardium*
14. *Cinnadenia*
15. *Cinnamomum*
16. *Cryptocarya*
17. *Dahlgrenodendron*
18. *Dehaasia*
19. *Dicypellium*
20. *Dodecadenia*
21. *Endiandra*
22. *Endlicheria*
23. *Eusideroxylon*
24. *Gamanthera*
25. *Hexapora*
26. *Hypodaphnis*
27. *Iteadaphne*
28. *Kubitzkia*
29. *Laurus*
30. *Licaria*
31. *Lindera*
32. *Litsea*
33. *Machilus*
34. *Mezilaurus*
35. *Mochinnodaphne*
36. *Mutisiopersea*
37. *Nectandra*
38. *Nocinnamomum*
39. *Neolitsea*
40. *Nothaphoebe*
41. *ocotea*
42. *Paraia*
43. *Parasassaras*
44. *Persea*
45. *Phoebe*
46. *Phyllostemonodaphne*
47. *Pleurothyrium*
48. *Potameia*
49. *Potoxylon*
50. *Povedadaphne*
51. *Ravensara*
52. *Rhodostemonodaphne*
53. *Sassafras*
54. *Sextonia*
55. *Sinosassafras*
56. *Syndiclis*
57. *Triadodaphne*
58. *Umbellularia*
59. *Urbanodendron*
60. *Williamodendron*
61. *Yushunia*
62. *Clinostemon*
63. *Cryptocarya*

Table 1.1: Classification of Lauraceae Family

1.4 The Genus *Lindera*

Lindera is a genus of evergreen trees belongs to the Lauraceae family. The genus of *Lindera* includes about 80-100 species of flowering plants in the family Lauraceae (Durtsche), mostly located in eastern Asia and eastern North America (Suzuki et al. 1971) and can be seen as shrubs and small trees. The examples of *Lindera* species are *L. aggregata*, *L. reticulosa*, *L. chienii*, *L. benzoin*, *L. obtusiloba*, *L. lucida*, *L. melissifolia*, *L. wrayi*, *L. akoensis*, *L. angustifolia*, *L. communis*, *L. doniana*, *L. erythrocarpa*, *L. flavinervia*, *L. floribunda*, *L. glauca*, *L. gracilipes*, *L. guangxiensis*, *L. kariensis*, *L. kwangtungensis*, *L. latifolia*, *L. limprichtii*, *L. longipedunculata*, *L. metcalfiana*, *L. monghaiensis*, *L. motuoensis*, *L. oxyphylla*, *L. nacusua*, *L. neesiana*, *L. praecox*, *L. prattii*, *L. pulcherrima*, *L. reflexa*, *L. robusta*, *L. rubronervia*, *L. strychnifolia*, *L. supracostata*, *L. thomsonii*, *L. tienchuanensis*, *L. tonkinensis*, *L. umbellata* and *L. villipes*. The leaves can be either deciduous or evergreen depending on species, and are alternate, entire or three-lobed, and strongly spicy-aromatic. The flowers are small, yellowish, with six tepals arranged in a star shape. The fruit is small red, purple or black drupe containing a single seed.

***Lindera oxyphylla* (KL 5359)**

Lindera oxyphylla (KL 5359) was collected at Hutan Simpan Ulu Muda, Baling, Kedah. It is a medium size tree up to 30 m tall, 80 cm girth. Bark is brown, smooth reticulately fissured to cracked. The inner barks are reddish brown. Leaves are alternate simple, thinly coriaceous, lanceolate apex acuminate acute.

Base cuneate, 7.5-15.0 x 3-5 cm shining dark green above, glaucous below, young leaves pinkish brown secondary nerves 7-11 pairs, raised below faint. Tertiary nerves and reticulations visible beneath faint above. Petioles 1-1.5 cm long, in flowers cence in axillary olusters of umbellules or on the leaf less twigs flower buds rusty brown tomentose opening greenish, silky hairy.



Figure 1.2: The Leaf and Bark of *Lindera oxyphylla* (KL 5359)

1.5 The Genus *Litsea*

The genus *Litsea evergreen* belonging to the large family Lauraceae comprises nearly 200 to 400 species, which are spreaded abundant throughout tropical and subtropical Asia, North and South America. In Malaysia, it's found widely in Penang, Perak, Pahang, Selangor, Negeri Sembilan and Johor. *Litsea* is represented by 72 species and mostly growing in the south and south western parts of Malaysia (Institute of Botany., 1982). In Indonesia, it's represented about 22 species (Henry et al., 1999).

The species that can be found in Peninsular Malaysia are *L. johorensis*, *L. trunciflora*, *L. magnifica*, *L. tomentosa*, *L. grandis*, *L. artocarpifolia*, *L. firma*, *L. gracilis*, *L. amara*, *L. polyantha*, *L. wrayi*, *L. cordata*, *L. glabrifolia*, *L. angulata*, *L. quercina*, *L. perakensis*, *L. machilifolia*, *L. panamonja*, *L. robusta* and also *L. costalis*.

Litsea species are normally trees or shrubs. The leaves are usually alternate or

opposite or sub-opposite. The wood of *Litsea* is soft to moderately hard and the color generally grey. The seeds of *Litsea* contain oils and are used for burning and soap-making. The flowers are shortly pedicelled or sessile. The perianth tube in males was small or none while in females it is funnel shaped and have 6 lobes. The fruits were globose ovoid, ellipsoid or cylindric on the perianth tube enlarged in a cup, usually large and often thick (Ridley et al., 1924).

***Litsea costalis* (Nees) Kosterm (KL 5410)**

Litsea costalis was collected from Hutan Simpan Piah, Lasah, Sg. Siput and Perak. It is a medium size tree up to 3 m tall, 6 cm girth. Bark is dark grey, inner bark yellow green, smooth reticulately fissured to crack. Leaves spirally simple, Thinly coriaceous, from elliptic oblong to oblong obovate in Apex minutely tipped base narrowed acute, 26.5-57cm x 15-23 cm dark green above, glaucous below, margin entire, midrib sunken above, secondary nerves 8-12 pairs, tertiary nerves and reticulations faint on both surfaces, petioles up to 4.5 cm long, in flowers cence in axillary, terminal racemes flowers yellowish green to creamy white .



Figure 1.3: The Bark and Flowers of *Litsea costalis* (Nees) Kosterm



Figure 1.4: The Leaf of *Litsea costalis* (Nees) Kosterm

1.6 Objectives of study

The objectives of the study are:

1. To extract and isolate the chemical constituents from the leaves and stem barks of *Lindera oxyphylla* and *Litsea costalis* (Nees) Kosterm using n-hexane, dichloromethane and methanol as solvents.
2. To elucidate the structure of isolated compounds using spectroscopic methods such as UV, IR, MS, 1D-NMR (^1H , ^{13}C , DEPT, NOE) and 2D NMR (COSY, NOESY, HMQC, HMBC).
3. To study the biological activities such as antioxidant (DPPH, FRAP, FIC) and anti cancer activities for selected compounds on various cancer cell lines, A375 human melanoma, HT-29 colon adenocarcinoma, MCF-7 human breast adenocarcinoma , WRL-68 normal hepatic cells, A549 non-small cell lung cancer and PC-3 prostate adenocarcinoma, MDA-MA231 human breast adenocarcinoma, CEM-ss *flagelliforme* tuber on human T4 lymphoblastoid, HepG2 Hepatocellular carcinoma human, CCD841 human normal colonic cell line and Jurkat which are an immortalized line of T lymphocyte cells that are used to study acute T cell leukemia.

GENERAL CHEMICAL ASPECTS

2.1 Introduction

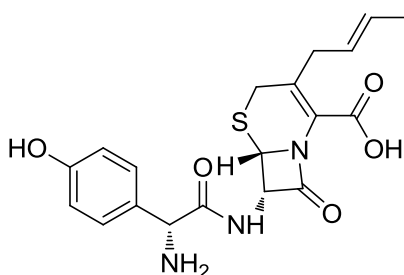
Plants have been explored by chemists for their chemical compounds of their medicinal value. The studies have been aimed on compounds that are of the pharmaceutical interest in the scope of medicinal importance. Plants play an important role as medicine to human.

Lauraceous plants consists non-alkaloid (e.g. carbohydrates, lipids, amino acids and proteins, polyphenol, essential oils, terpenes and aromatic compounds) and alkaloid constituents and studies have been made on it (Fischer et al. 1999; Kochummen, 1997).

Sources of Natural Products.

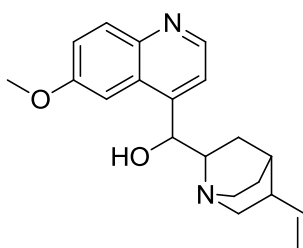
Natural products are derived from four classic sources (Dewick, 2009):

- Microbial sources : For example, Cefprozil



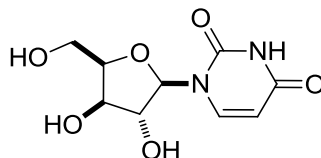
Cefprozil (Cephalosporin)

- Plant Sources: Several important drugs such as: Quinine



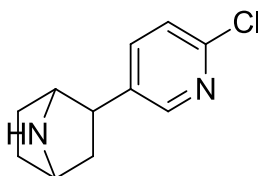
Quinine

- Marine Sources: first time separated in 1950 such as spongouridine



Spongouridine

- Animal Sources: Epibatidine, obtained from the skin of an Ecuadorian poison frog



Epibatidine

2.2 Aromatic Compounds: Phenolics

Phenolic compounds are the compounds that have one or more hydroxyl groups attached directly to the aromatic ring. The natural phenolic compounds are derived from the pentose phosphate, shikimate and phenylpropanoid pathways in plants (Randhir et al., 2004).

The phenolic compounds can be classified in a number of ways:

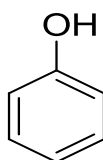
- Harborne and Simmonds have classified these compounds into groups based on the number of carbons in the molecule (Table 2.1) (Barton., 1999).
- Swain and Bate-Smith category these compounds in common and less common .
- Ribereau-Gayon has classified phenolic compounds into three families

Table 2.1: Category of phenolic compounds in plants.

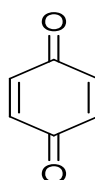
Number of C- atoms	Basic skeleton	Families of Phenols
6	C ₆	Simple phenol 8 and benzoquinone 9
7	C ₆ -C ₁	Gallic acid 10 and protocatechuic acid 11
8	C ₆ -C ₂	2-Hydroxyacetophenone 12
9	C ₆ -C ₃	Cinnamic acids 13 and isocoumarins 14
15	C ₁₅	Kaemferol 15 , quercetin 16 and myricetin 17
15	C ₁₅	Isoflavonoid 18 and neoflavonoid 19
15	C ₁₅	epicatechin 20 and 3'-O-methylepicatechin 21
15	C ₁₅	Flavanone 22
15	C ₁₅	Flavanol 23
15	C ₁₅	Chalcones 24 and dihydrochalcone 25
15	C ₁₅	Aurones 26
13,14	C ₆ -C ₁ -C ₆ , C ₆ -C ₂ -C ₆	Benzophenone 27 , xanthone 28 and stilbens 29
N	Lignans, neolignans	(+)-Pinoresinol 30 and (+)-sesamin 31

2.2.1 The C₆ simple phenol compounds.

Phenols **8** and benzoquinones **9** are phenolic compounds consisting of a hydroxyl functional group (-OH) attached to an aromatic hydrocarbon group.



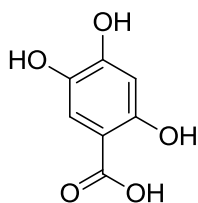
8



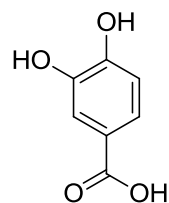
9

2.2.2 The C₆-C₁ phenolic acids and related compounds

The C₆-C₁ phenolic acid usually designates phenols that possess one carboxylic acid functionality (Robbins et al., 2003; Haig et al., 2000). Phenolic acid can be found in many plants especially in dried fruits.



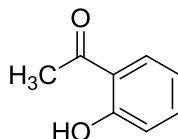
Gallic acid **10**



Protocatechuic acid **11**

2.2.3 The C₆-C₂ acetophenones and phenyl acetic acids

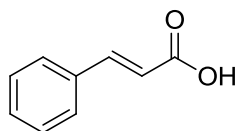
The C₆-C₂ phenolic compounds consist of C₂ side chain such as acetophenone (Lamola et al., 1967) and phenyl acetic acid (Amir et al., 2004). Another is 2-hydroxyacetophenone **12** (Dakternieks et al., 1998).



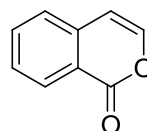
12

2.2.4 The C₆-C₃ Cinnamic acids and related compounds

This group includes cinnamic acid **13** (Beavis et al., 1989) and isocoumarin **14**.



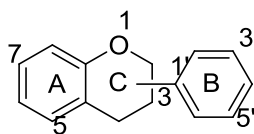
13



14

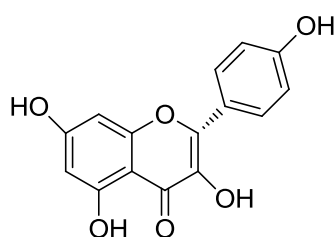
2.3 The C₁₅ Flavonoids.

Flavonoid compounds are the main group of plant phenolics and they can be found in all part of plants such as fruit, flower, leaves, root and stem (Henning et al., 2004; Mulder et al., 2005). The name of flavonoid was derived from Latin word flavus which means yellow. Flavonoids have small molecular weight consisting of fifteen carbon atoms, arranged in a C₆–C₃–C₆ configuration. Essentially the structure of flavonoid consists of two aromatic rings A and B, joined by a 3-carbon bridge, usually in the form of a heterocyclic ring (Bohm et al., 1998; Merke et al., 2000). The aromatic ring A is derived from the acetate/malonate pathway, while ring B is derived from phenylalanine through the shikimate pathway.

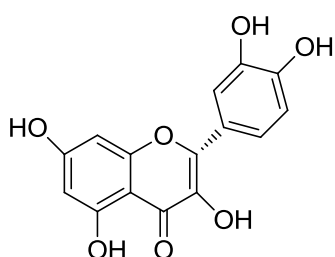


Flavonoid

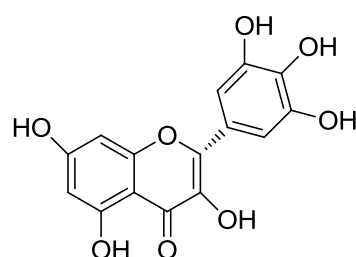
Depending on the degree of oxidation of the central ring C, they can be subdivided into several classes : flavones, flavonols, flavanones, isoflavones, flavans, flavanols, and anthocyanins (Pietta et al., 2000). The pyran ring can be opened (chalcones) and recyclized into a furan ring (aurones) (Pharmacognosie et al., 1999). The most widely distributed flavones in nature are kaemferol (5, 7, 4' - trihydroxyflavone) **15**, quercetin (5, 7, 3', 4' -tetrahydroxyflavone) **16** and myricetin (5, 7, 3', 4', 5' -pentahydroxy flavone **17**.



15

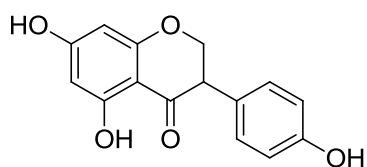


16

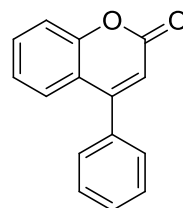


17

Isoflavonoid (Graham et al., 1991) is flavonoid with aromatic ring at position C-3, for example 5, 7, 4'-trihydroxyisoflavone **18**. When aromatic ring attached at position C-4 in the flavonoid skeleton, this compound is called neoflavonoid, for example 4-phenylcoumarins **19**.

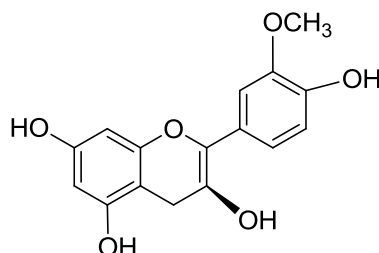
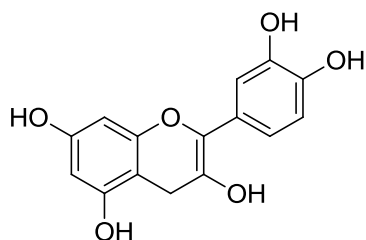


18

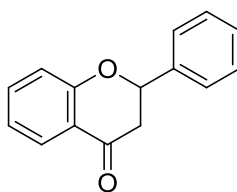


19

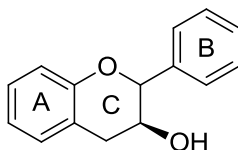
Flavonol (Li et al., 1997) has a hydroxyl group at position C-3 and a double bond at C-2. They are present in a wide variety of fruits and vegetables, for examples epicatechin **20** and 3'-*O*-methylepicatechin **21**.



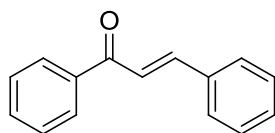
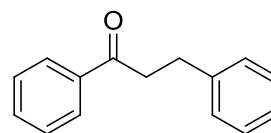
Flavanone **22** (Fabre et al., 2001) has carbonyl group at position C-4 and it can form various derivatives including hydroxyl and methoxyl groups.

**22**

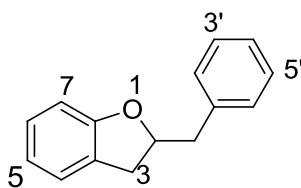
Flavanol **23** (Schroeter et al., 2006) has hydroxyl group at position C-3 and there is no double bond in ring C.

**23**

Chalcone **24** (Napoli et al., 1990) and dihydrochalcone **25** (Horowitz et al., 1963) have a linear C₃-chain connecting the two rings. The C₃-chain of chalcone contains a double bond whereas the C₃-chain of dihydrochalcones is saturated.

**24****25**

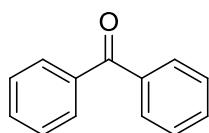
Aurone **26** (Ono et al., 2006) has furan ring in the molecule.



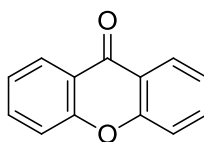
26

2.4 Benzophenones, xanthenes, stilbenes

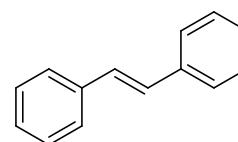
Benzophenone **27** (Dorman et al., 1994) and xanthone **28** (Qin et al., 2010) have C₆-C₁-C₆ and stilbene **29** (Tao et al., 2001) has C₆-C₂-C₆.



27



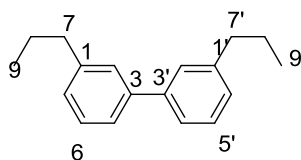
28



29

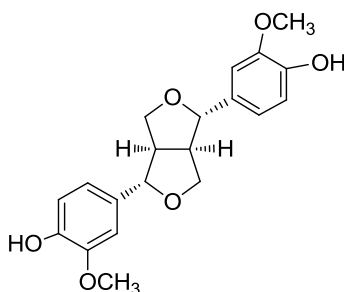
2.5 Lignan and Neolignans

In 1927 Robinson (Proc et al., 1927) found that a common feature of many natural products have a C₆-C₃ unit (propylbenzene skeleton) which perhaps derived from cinnamyl units. Haworth (Rep et al., 1936) suggested the class of compounds derived from two C₆-C₃ units and has β, β'-linked which could be called lignans. Lignans are a class of secondary metabolites produced by oxidative dimerization of two phenylpropanoid units consist of two phenylpropane (C₆-C₃) units, lignans show huge structural diversity (Mohan et al., 2012). The nomenclature of the diverse range of structures classified as lignans depended largely on slight names and if necessary the correct numbering derived from the systematic name. For example, 3, 3' –neolignan **30**.

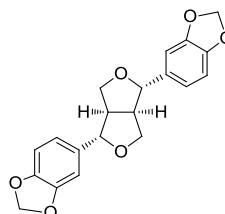


30

Lignans are dimers or oligomers that product from the coupling of monolignols; *p*-coumaryl alcohol, sinapyl alcohol and coniferyl alcohol, with coniferyl alcohol being the most common monolignol used in lignan biosynthesis. Lignans are nearby in ferns, angiosperms and gymnosperms. They are localized in woody stems and in seeds and play a role as insect deterrents. Some of these compounds have medicinal properties.



31



32

The monolignol radicals, in this example derived from *p*-coumaryl alcohol, are generated enzymatically by activated cell-wall bound peroxidases, which eliminate the proton on the para-hydroxyl-group of the phenol. Most lignans are optically active, and typically only one enantiomer is found in a given species. Examples of lignans include (+)-pinoresinol **31** (Katayama et al., 1992) and (+)-sesamin **32** (Orito et al., 1991).

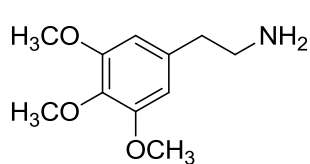
As the range of lignoids and their plant sources has widened so the distinction between lignans and neolignans has become less significant. Thus the neolignans were long - identified as more typical of plants of the family Lauraceae, but in recent years they have been isolated from the *Piperaceae* (Jensen et al., 1993), *Magnoliaceae* (Li et al., 2005), *Brassica fruticulosa* (Cutillo et al., 2003) and *Callicarpa japonica* Thunb (Ono et al., 2009) and other plants.

2.6 Alkaloids

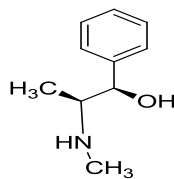
Alkaloids are among the first natural products to be isolated from medicinal plants. When they were first obtained from plant material in the early years of the 19th century, it was found that they were nitrogen containing bases which formed salts with acids. For this reason, they were known as the vegetable alkalis or alkaloids (Thomson et al., 1993). The alkaloids have ability to be in the form of salts and make complex with metal ions and it helped their isolation and recognition in the period of time before chromatography techniques. The word alkaloid has been firstly drawn from the word ‘vegetable alkali’ and was used to express the basicity or alkalinity of a number of initial alkaloidal segregations. And also, the word of alkaloid meant simply, alkali like (Middle English *alcaly*, from Medieval Latin *alkali*, from Arabic “*alqaliy* = ashes of stalwart, from *qualey*, to fry) (Cave et al., 1987). Name ‘alkaloid’ derives from the word ‘alkaline’, which means a water soluble base (Cordell et al., 1989).

An “alkaloid” is a substance with nitrogen in the molecule, connected to at least two carbon atoms and must have at least one ring, but not necessarily heterocyclic. Alkaloids are grouped in three main categories based on knowledge and speculation about their biogenesis (Lee et al., 2000). It has been estimated that in excess of 6000 compounds with the alkaloid-like properties are known, comprises the largest single class of secondary plant substance (Schiff et al., 1991).

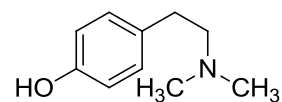
The majority of the alkaloids are heterocyclic (compound containing a closed ring of atoms of which at least one is not a carbon atom) in nature. But there can be in other types like mescaline **33**, ephedrine **34** and hordenine **35** that are non-cyclic. These are often known as ‘protoalkaloids’.



33



34



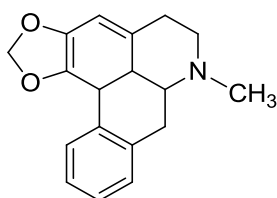
35

2.6.1 Classification of the Alkaloids

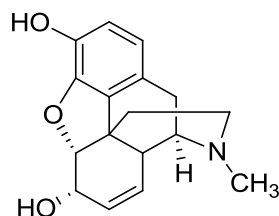
Alkaloids have been classified to three main groups by Hegnauer which based on speculation of biogenetic pathways (Cordell et al., 1981) .

2.6.1.1 True Alkaloid

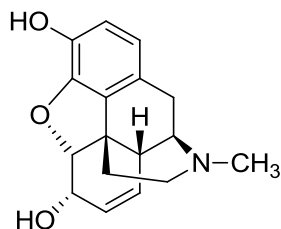
The compounds which the nitrogen-containing heterocyclic system is derived from a biogenetic amine and produced by decarboxylation from amino acid were named true alkaloids. They are usually found as salts in plant such as liriodenine **36** (Buchanan et al., 1960), codeine **37** (Sindrup et al., 1995) and morphine **38** (Cordell et al., 1981).



36



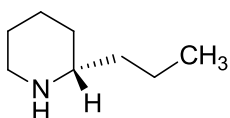
37



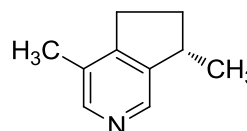
38

2.6.1.2 Pseudo Alkaloid

Pseudo alkaloids are in fact unrelated to amino acid (Schmidt et al., 2003). The pseudo alkaloids are nitrogen-containing molecules but they have carbon skeletons derived from monoterpenes, other acetate derivatives and aliphatic polyketo acids such as coniine **39**. It is also known as heterocyclic containing nitrogen and derived from terpenoids such as actinidine **40**.



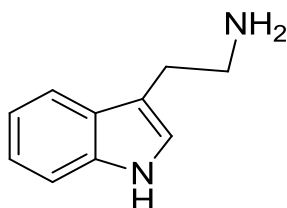
39



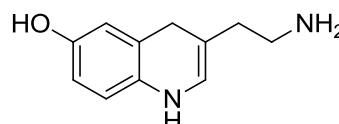
40

2.6.1.3 Proto Alkaloids

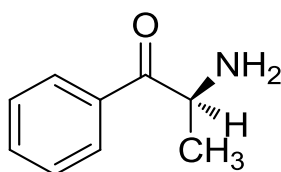
These compounds like true alkaloids, that derived from amino acid or biogenic amines but they do not contain any heterocyclic system (Piettre et al., 1990). They are represented in nature by biogenic amine themselves and their methylated derivatives such as serotonin **41**. They are derived also from amino acid such as serotonin **42** and cathinone **43**.



41



42



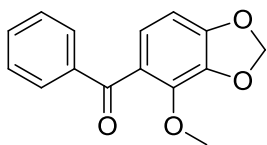
43

2.7 Chemical Constituents of *Lindera* Species

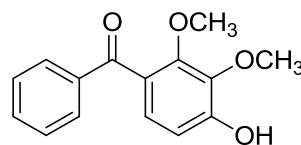
Table 2.2 showed the list of some selected compounds from *Lindera* species. All of these compounds have never been found in *Lindera oxyphylla*.

Table 2.2: Chemical constituents isolated from *Lindera* species

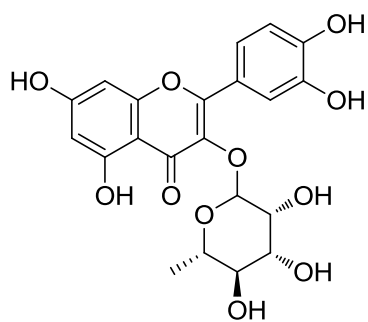
NO.	<i>Lindera</i> species	Type of Compounds	Examples	Ref.
1	<i>Lindera fruticosa</i>	Phenolic compound	2-methoxy-3, 4-methylene dioxycyclohexenone 44	(Song et al., 2006)
2	<i>Lindera fruticosa</i>	Benzophenone	2, 3-dimethoxy-4-hydroxy benzophenone 45	(Song t al., 2007)
3	<i>Lindera aggregata</i>	Flovonoid	quercetin-3-O-L-rhamnoside 46	(Xiao et al., 2011)
4	<i>Lindera Obtusiloba blume</i>	Lignan	pluviatilol 47	(Kwon et al., 1999)
5	<i>Lindera chunii</i>	Alkaloid	lindechunine B 48	(Zhang et al., 2002)



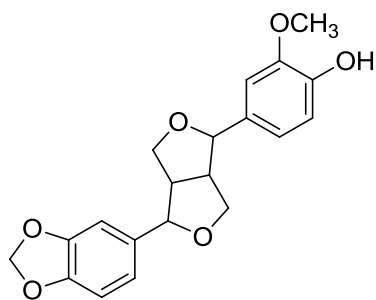
44



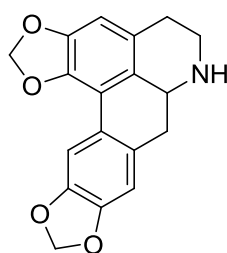
45



46



47



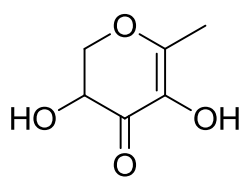
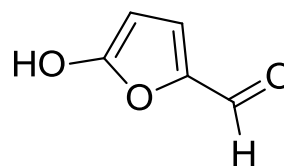
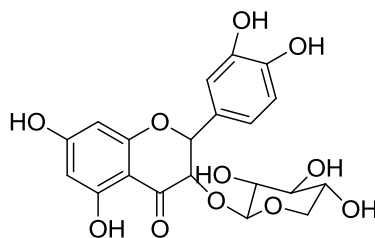
48

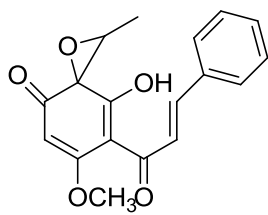
2.8 Chemical Constituents of *Litsea* Species.

Listed some selected chemicals of *Litsea* species, here again no investigation has been found on *Litsea costalis* (Table 2.3).

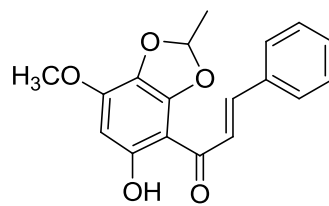
Table 2.3: Chemical constituents isolated from *Litsea* species

NO.	<i>Litsea</i> species	Type of Compounds	Examples	Ref.
1	<i>Litsea decanensis gamble</i>	Heterocyclic compound	3,5-dihydroxy-6-methyl-2H-pyran-4(3H)-one 49 and 5-hydroxyfuran-2-carbaldehyde 50	(Kumara et al., 2000)
2	<i>Twelve Litsea and neolitsea</i>	Flavonoid	2(3,4-dihydroxy phenyl)-5,7-dihydroxy-3-(((2 <i>S</i> ,4 <i>S</i> ,5 <i>R</i>)-3,4,5-trihydroxy tetrahydro-2H-pyran-2-yl)oxy)hroman-4-one 51	(Tsai et al., 2011)
3	<i>Litsea rubescens</i> and <i>Litsea pedunculata</i>	Flavonoid	Litseaone A 52 Litseaone B 53	(Li et al., 2011)
4	<i>Litsea pedunculata</i>	Lignan	Aryltetralone 54	(Wang et al., 2009)
5	<i>Litsea glutinosa</i>	Alkaloid	Aporphine 55	(Yang et al., 2005)
6	<i>Litsea lancifolia</i>	Alkaloid	Bisbenzylisoquinoline 56	(Sulaiman et al., 2011)

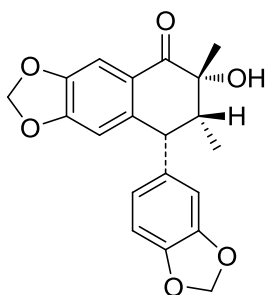
**49****50****51**



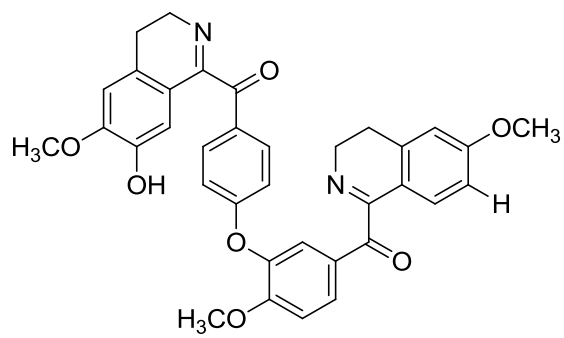
52



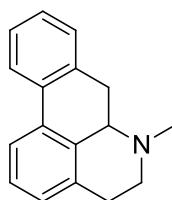
53



54



55



56

RESULTS AND DISCUSSION

3.0 Introduction

In recent years, chemists are interested in isolation of natural compounds from plants due to their pharmacological activities, they can be used as a source of therapeutics. In this course of studies the plants from the family Lauraceae, namely *Lindera oxyphylla* and *Litsea costalis* have been studied for their chemical constituents.

The cold extraction with n-hexane, followed by dichloromethane and methanol has been used for extracting the natural compounds from the bark and also the leaves. The isolation of the pure compounds from crude extract was carried out using chromatographic technique such as column chromatography (CC), preparative thin layer chromatography (PTLC) and higher performance liquid chromatography (HPLC). The structural elucidation was established through spectroscopic methods such as UV, IR, MS, 1D (^1H -NMR and ^{13}C -NMR, DEPT) and 2D-NMR (COSY, HMQC, HSQC, HMBC and NOESY), as well as X-ray reflection technique. The known compounds were identified by comparison their spectroscopic data with the literature data.

3.1 Chemical constituents from bark and leaves of *Lindera oxyphylla*

The bark and leaves of *Lindera oxyphylla* were investigated for their chemical constituents. The plant sample was soaked with n-hexane followed by dichloromethane and methanol to extract its compounds. The compounds from crude n-hexane, dichloromethane and methanol extracts were separated using chromatographic technique and the structural elucidation of isolated compounds were done using spectroscopic method. A total of six compounds were isolated from the bark of *Lindera oxyphylla* and those compounds were (+)-onysilin **LOB4** and linderone **LOB28** which

were isolated from n-hexane extract, (+)-pinostrobin **LOB7**, flavokawain B **LOB15** and linderone A **LOB25** were isolated from dichloromethane extract and (+)-pinocembrin **LOB2** was isolated from methanol extract. A total of seven compounds were isolated from the leaves and those compounds were 1-methylinderone **LOL34** which was isolated from n-hexane extract, (+)-laurotetanine **LOL20**, *N*-methyllaurotetanine **LOL35**, (+)-norboldine **LOL50**, (+)-*N*-methylhernovine **LOL63** and (+)-norisoboldine **LOL65** which were isolated from dichloromethane extract and kaempferol **LOL5** isolated from methanol extract. The percentage yields of the isolated compounds are shown in Table 3.1 and Table 3.2.

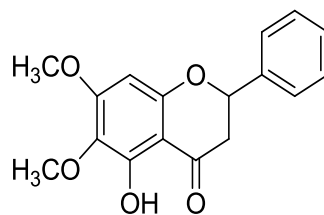
Table 3.1: Chemical constituents from the bark of *Lindera oxyphylla*

Compounds	Types	Part	%Yield
(<i>S</i>)-5-hydroxy-6,7-dimethoxy-2-phenylchroman-4-one, (+)-onysilin LOB4	Flavanone	bark	0.04
(<i>E</i>)-2-(1-hydroxy-3-phenylallylidene)-4,5-dimethoxycyclopent-4-ene-1,3-dione LOB28	Linderone	bark	0.7
(<i>E</i>)-1-(2-hydroxy-4,6-dimethoxyphenyl)-3-phenylprop-2-en-1-one, flavokawain B LOB15	Chalcone	bark	0.5
2-cinnamoyl-3-hydroxy-4,5-dimethoxycyclopenta-2,4-dienone LOB25	Linderone A	bark	1.0
5,7-dihydroxy-2(<i>S</i>)-phenyl chroman-4H-one, (+)-pinocembrin LOB2	Flavanone	bark	0.5
5-Hydroxy-7-methoxy-2-phenyl chroman-4H-one, (+)-pinostrobin LOB7	Flavanone	Bark	0.5

Table 3.2: Chemical Constituents of leaves *Lindera oxyphylla*

Compounds	Types	Part	%Yield
(<i>E</i>)-2-(1-methoxy-3-phenylprop-2-en-1-ylidene)-4, 5-dimethoxycyclopent-4-ene-1,3-dione LOL34	Methylinderone	Leaf	0.1
3, 5, 7-trihydroxy-2-(4-hydroxyphenyl)-4H-chromen-4-one (Kaempferol) LOL5	Flavanone	Leaf	0.01
(+)-Laurotetanine LOL20	Alkaloid	Leaf	0.05
N-methylaurotetanine LOL35	Alkaloid	Leaf	0.25
(+)-Norboldine LOL50	Alkaloid	Leaf	0.05
(+)-N-methylhernovine LOL63	Alkaloid	Leaf	0.05
(+)-Norisoboldine LOL65	Alkaloid	Leaf	0.25

3.1.1 Flavanone LOB4: (+) – Onysilin



LOB4

Flavanone **LOB4**, (+)-Onysilin with IUPAC name [(2*S*)-5-hydroxy -6, 7-dimethoxy-2-phenyl chroman-4*H*-one] (Garó et al., 1996) was isolated as yellow amorphous solid with $[\alpha]_D^{25} = +3.1$ (2.00×10^{-4} g/100 mL, MeOH). In the UV spectrum, absorption maxima were observed at λ_{\max} (MeOH) nm (log ϵ) 293 (4.00) and 349 (1.43) which indicated the existence of the conjugated double bond system. Its IR spectrum showed absorption bands at ν_{\max} 3446 cm^{-1} due to hydroxyl group and 1644 cm^{-1} for conjugated carbonyl group. The LC-MS (positive mode) spectrum showed an intense pseudomolecular ion peak, $[M+H]^+$ at m/z 301.0824 corresponding to the molecular formula of $C_{17}H_{16}O_5$ (Chantrapromma et al., 1997).

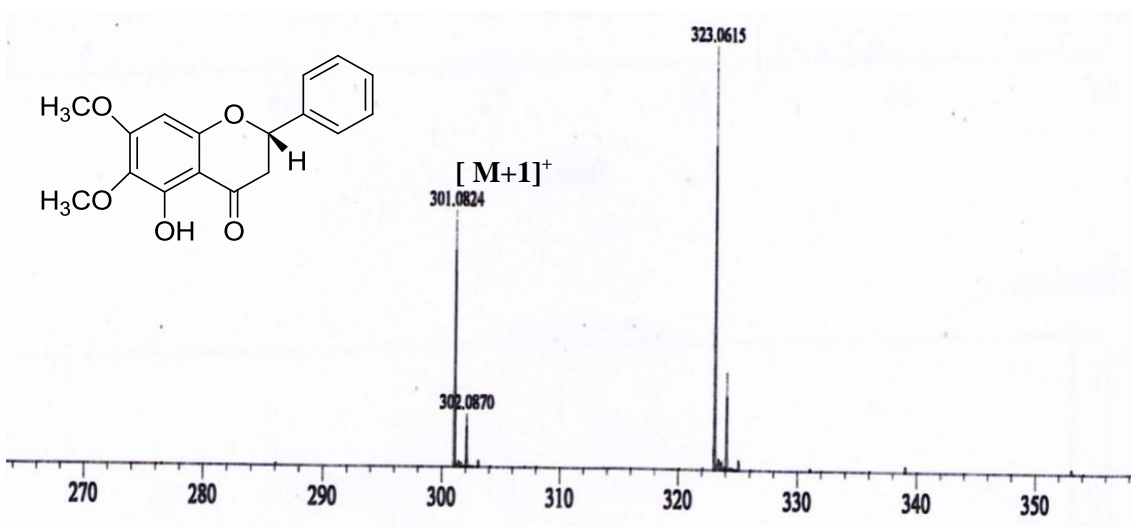


Figure 3.1: LC-MS Spectrum of (+) – Onysilin **LOB4**

The ^1H NMR spectrum (Table 3.3, Figure 3.2) exhibited two methoxyl groups at δ 3.83 and 3.87 as a singlet corresponding to C₇-OMe and C₆-OMe, respectively. The C-8 proton was observed as a singlet at δ 6.02 and sp^3 methine group at C-2 appeared at δ 5.41 as doublet of doublet. Two up field signals appeared as doublet of doublet at δ 2.83 and 3.19 and these signals belong to methylene group at H-3 $_{\alpha}$ and H-3 $_{\beta}$ and the two methyl group were not equivalent. Furthermore one singlet signal appeared at δ 11.76 was assigned to OH group and this OH group formed hydrogen bond with carbonyl group at C-4. The aromatic protons gave a multiplet between δ 7.31 and 7.44 attributed to H2', H3', H4', H5' and H6'. The above observations were supported by COSY (Table 3.3, Figure 3.3) spectrum which showed cross peaks between H-2/H-3 $_{\alpha}$, H-2/H-3 $_{\beta}$, and H-3 $_{\alpha}$ /H-3 $_{\beta}$. The ^{13}C NMR and DEPT spectra (Table 3.3, Figure 3.4) established the resonances of seventeen carbon signals including two methyl signals at δ 61.9 for C₆-OCH₃ and δ 56.1 for C₇-OCH₃, one sp^3 methylene at δ 43.3 for C-3, seven methines resonated at δ 79.5 for sp^3 C-2, δ 91.6 (C-8), δ 126.9 (C-2', C-6'), δ 128.9 (C-3', C-4', C-5') and seven quaternary carbon signals at δ 196.3 (C-4), δ 154.9 (C-8a), δ 103.1 (C-4a), δ 150.4 (C-5), δ 130.5 (C-6), δ 160.9 (C-7) and δ 138.2 (C-1') consistent with the proposed structure (Kamperdick et al., 2002).

In the HMBC spectrum (Table 3.3, Figure 3.5) the cross-peaks were observed between H-2 to C-1', C-2', C-6', H-3 $_{\alpha}$ to C-4, H-3 $_{\beta}$ to C-4, H-3 to C-2, C-1', H-8 to C-7, C-4, C-6, C-4a, 6-OMe to C-7, 7-OMe to C-6, OH to C-5, C-4a, C-6, H-Ar to C-Ar, C-1'.

Finally, by comparison of the spectroscopic data obtained with the data from literature values, it was deduced that compound **LBO4** was (+)-onysilin (Mukhtar et al., 2000; Sulaiman et al., 2003), which existed widely among the family of Annonaceae, Monimiaceae, and Lauraceae (Achenbach et al., 1982; Fischer et al., 1999).

Table 3.3: ^1H NMR (400 MHz) and ^{13}C NMR (100 MHz) spectral data of (+) – onysilin **LOB4**

Position	^1H -NMR(δ , J in Hz)	^{13}C -NMR(δ)
1	-	-
2	5.41(1H, <i>dd</i> , 13.4, 3.5)	79.5
3	2.83 (1H, <i>dd</i> , 17.3, 3.1, H_{α} -3) 3.19 (1H, <i>dd</i> , 17.3, 13.5, H_{β} -3)	43.3
4	-	196.3
4a	-	103.1
5	-	158.6
6	-	130.5
7	-	160.9
8	6.05 (1H, <i>s</i> , H-8)	91.6
8a	-	154.9
1'	-	138.2
2', 6'	7.31-7.44 (2H, <i>m</i>)	126.9
3',4',5'	7.31-7.44 (3H, <i>m</i>)	128.9
6-OCH ₃	3.87 (3H, <i>s</i>)	61.9
7-OCH ₃	3.83 (3H, <i>s</i>)	56.1
5-OH	11.76 (1H, <i>s</i>)	-

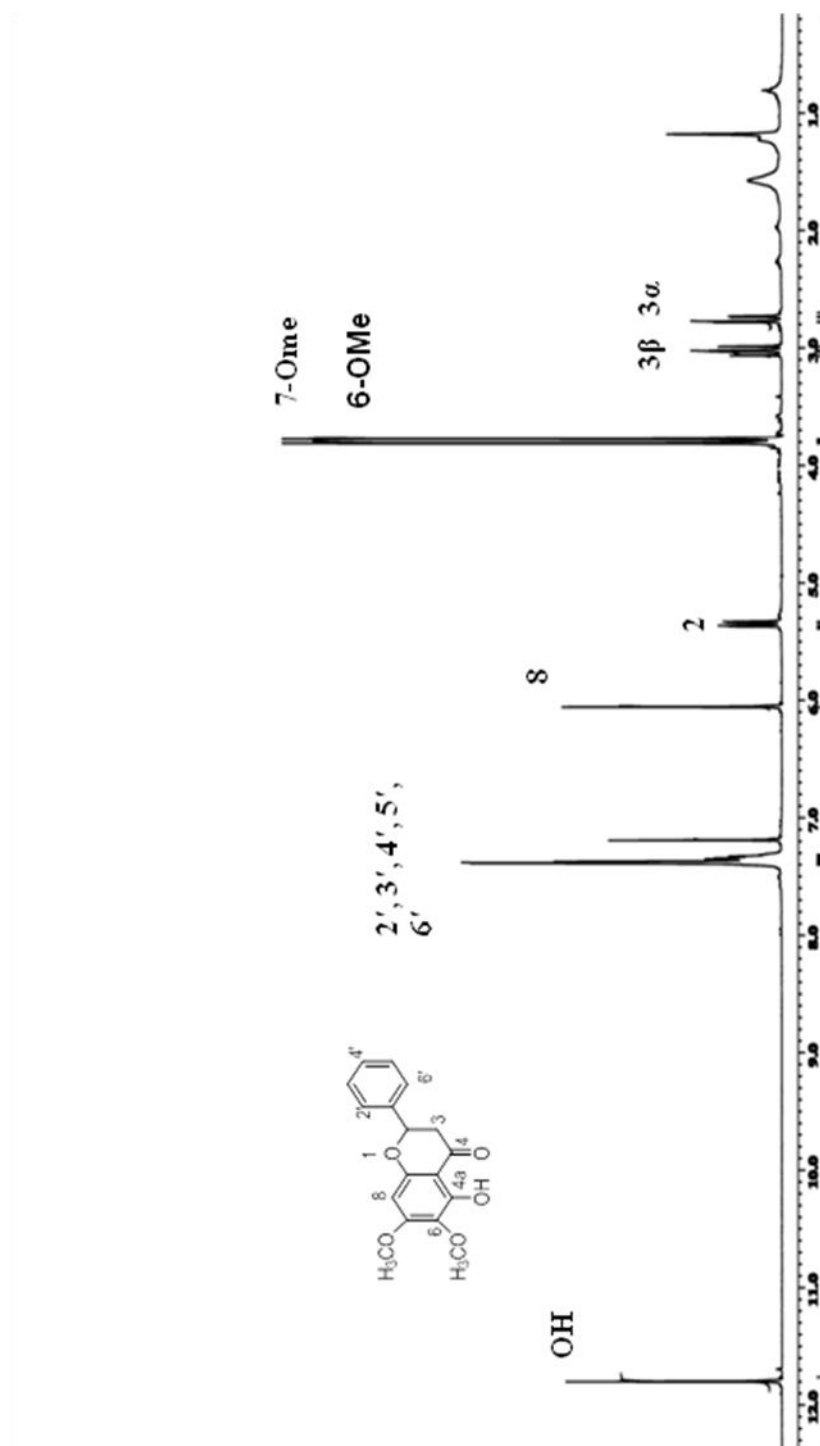


Figure 3.2: ^1H -NMR spectrum of (+) – Onysilin LOB4

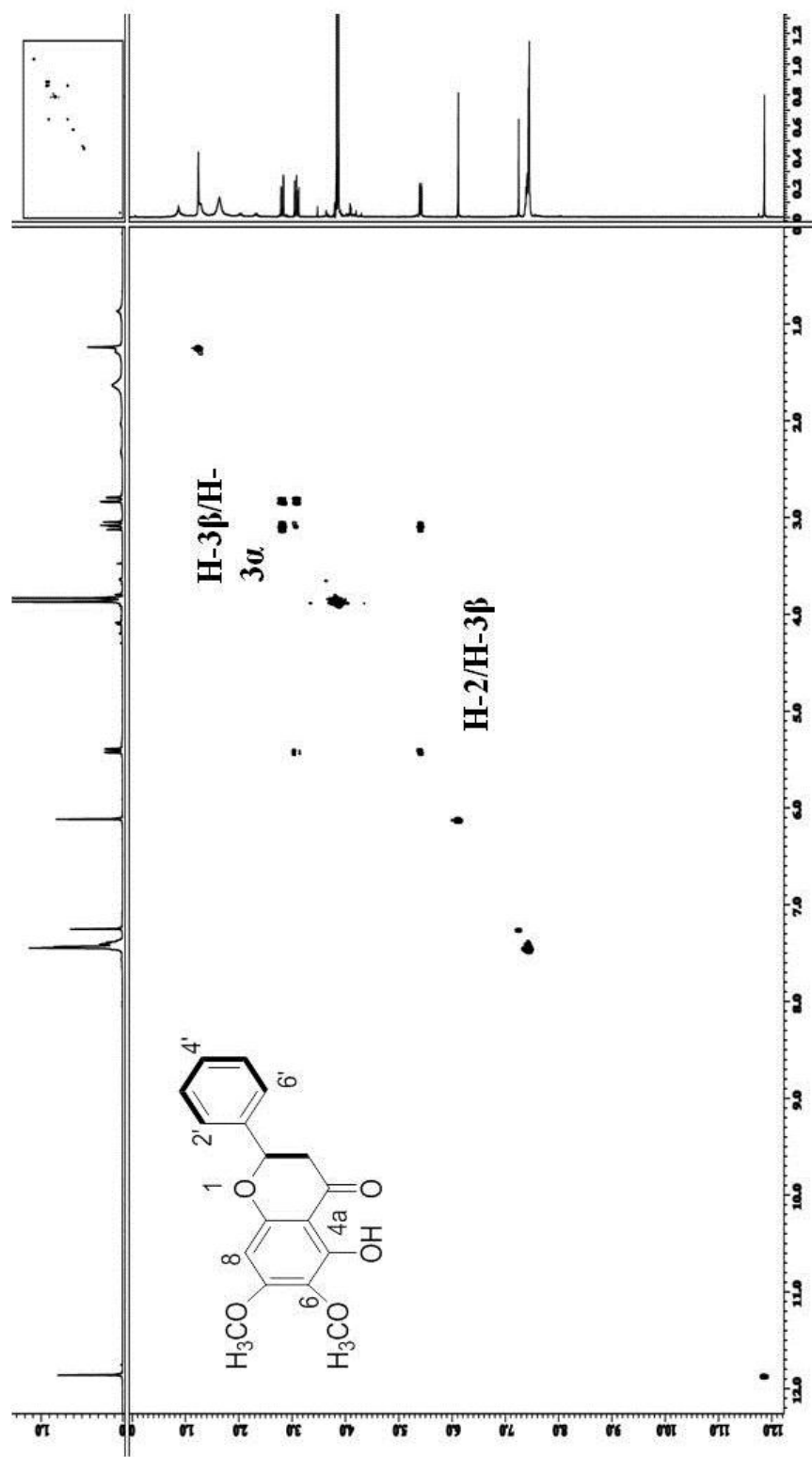


Figure 3.3. COSY spectrum of (+) – Onysilin LOB4

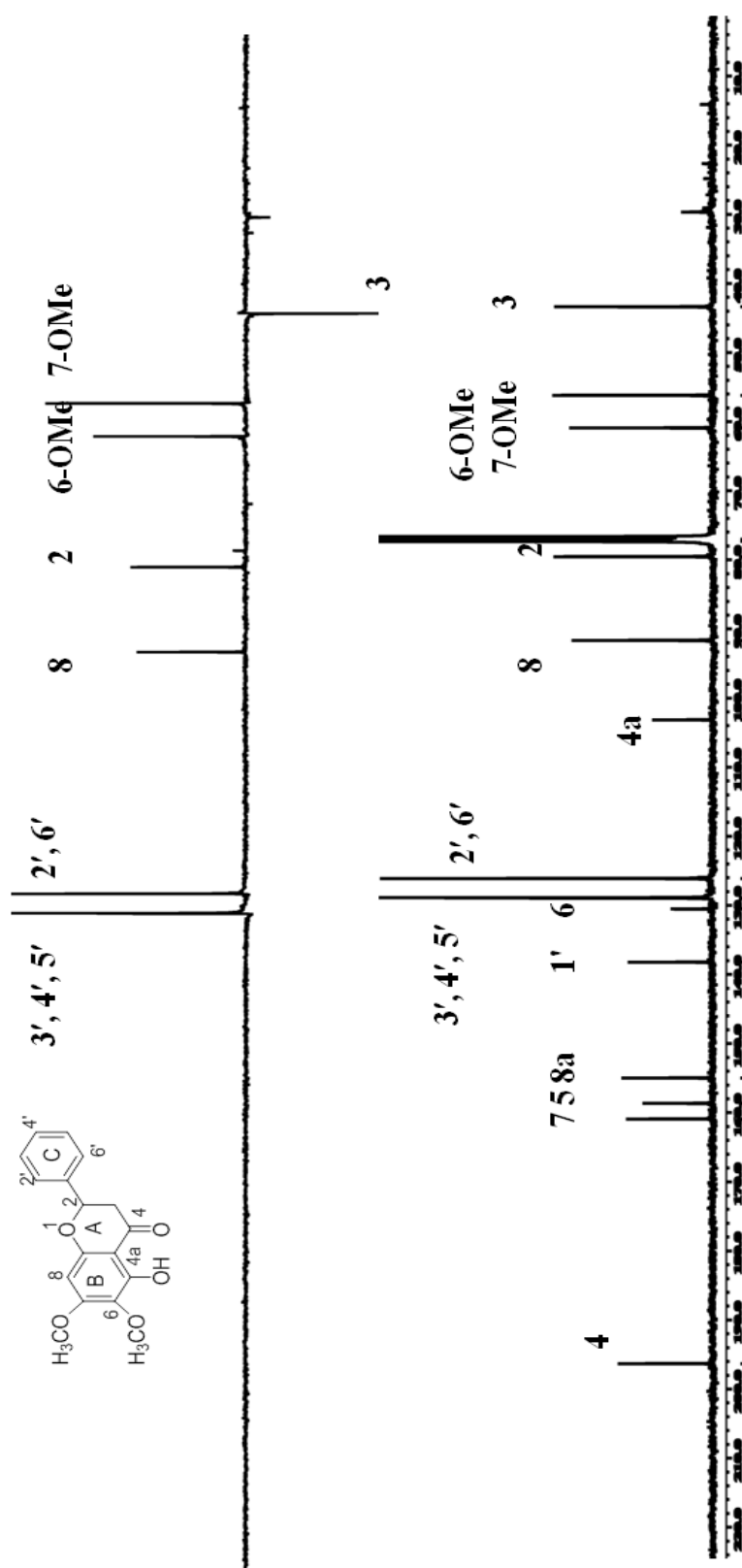


Figure 3.4: ^{13}C NMR / DEPT spectra of (+) – Onysilin LOB4

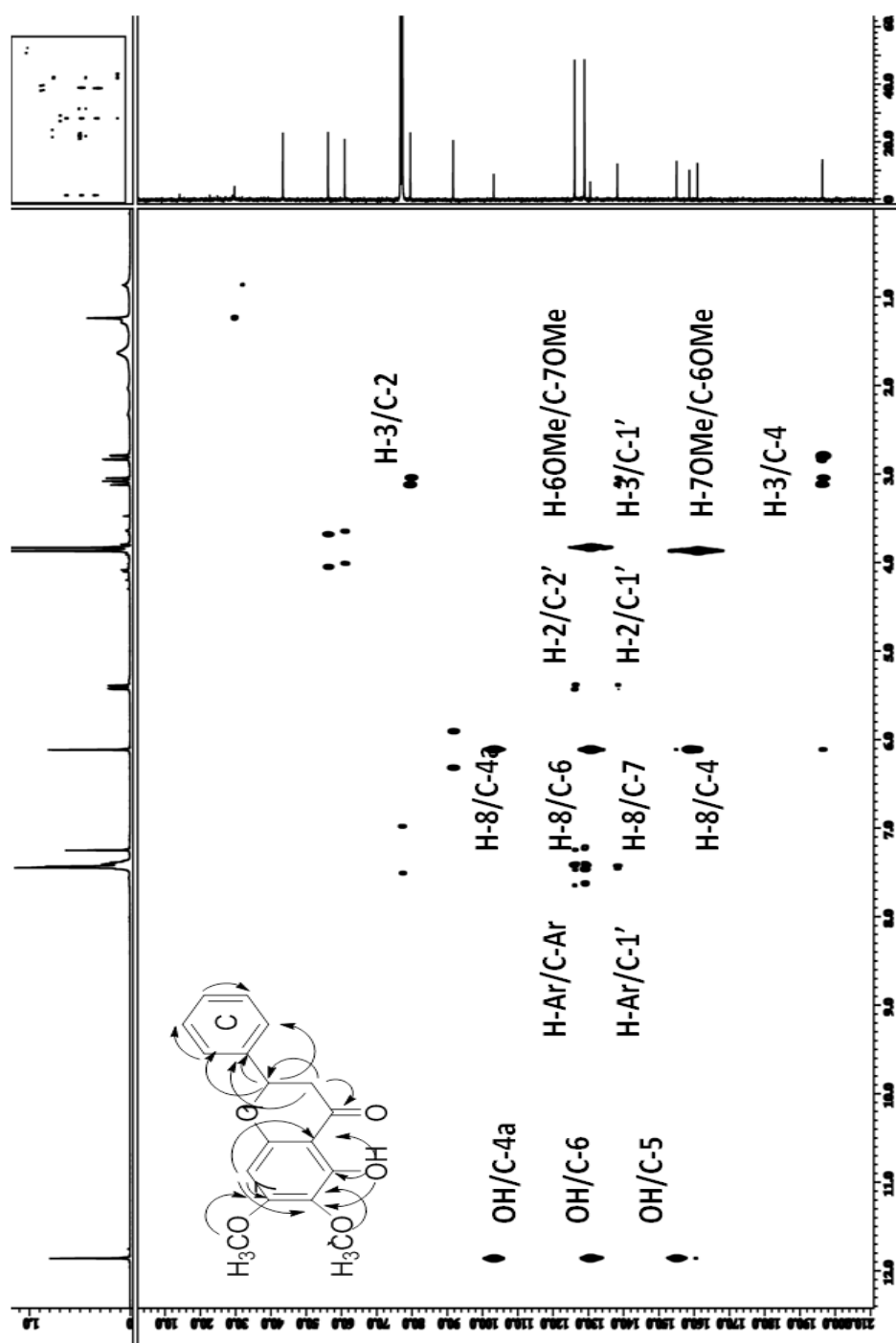
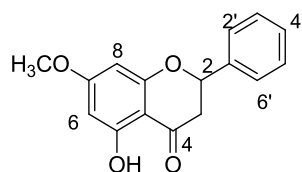


Figure 3.5: HMBC spectrum of (+) – Onyslin LOB4

3.1.2 Flavanone LOB7: (+)-Pinostrobin



LOB7

Flavanone **LOB7**: (+)-pinostrobin with IUPAC name [(*S*)-5-hydroxy - 7-methoxy-2-phenyl chroman-4H-one) (Garo et al., 1996) was isolated as yellow amorphous solid with $[\alpha]_D^{25} = +1.52$ (2.00×10^{-4} g/100 mL, MeOH). The structure of compound **LOB7** has the same skeleton and substituents with compound **LOB4** except the lack of methoxyl group at C-6 and the spectroscopic data will also be the same except the lack of one methoxyl group. In the UV spectrum, absorption maxima were observed at λ_{\max} (MeOH) nm (log ϵ) 306 (1.273) and 223 (2.316) (Jayaprakasam et al. 1999) which indicated the existence of the conjugated double bond system. Its IR spectrum showed absorption bands at ν_{\max} 3429 cm^{-1} due to hydroxyl group, 1642 cm^{-1} assigned for conjugated carbonyl group. The LC-MS (positive mode) spectrum showed an intense pseudomolecular ion peak, $[M+H]^+$ at m/z 271.088 corresponding to the molecular formula of $C_{16}H_{14}O_4$ (Cuong et al., 1996).

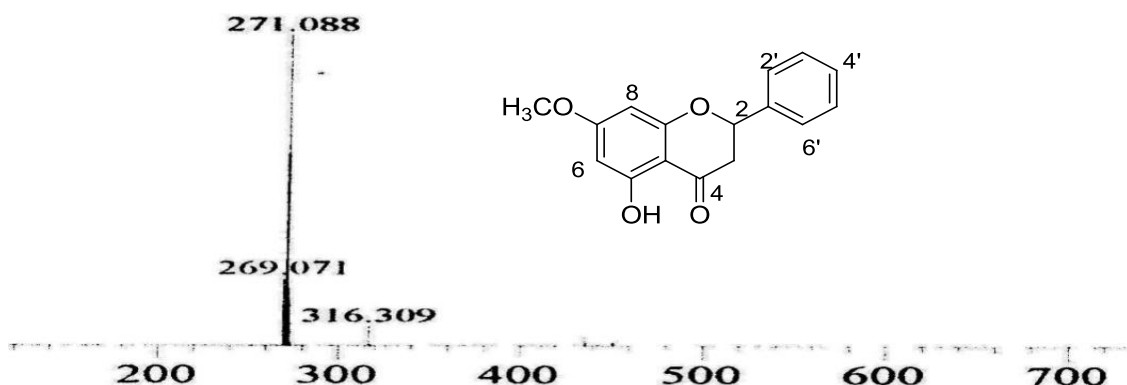


Figure 3.6: LC-MS Spectrum of (+)-pinostrobin **LOB7**

The ^1H NMR spectrum of (Table 3.4, Figure 3.7) exhibited one group methoxyl signal at δ 3.88 which was positioned at C-7. A two proton singlet at δ 6.15 was observed in the spectrum, confirming that H-6 and H-8 were unsubstituted. The downfield signal appeared as doublet and doublet at δ 5.42 was assigned to H-2 and two up filed signals appeared as doublet and doublet at δ 2.81 and 3.11 was assigned to H-3 α and H-3 β respectively. Furthermore one downfield signal appeared as singlet at δ 11.68 was assigned to OH group. The aromatic protons gave a multiplet signal between δ 7.38 and 7.49 attributed to H-2', H-3', H-4', H-5' and H-6'. The above observations were reinforced by COSY (Table 3.4, Figure 3.8) experiment which displayed correlations of H-2/H-3 α , H-3 β and H-3 α /H-3 β (Kulmagambetova et al., 2003; Tran et al., 2011).

The ^{13}C NMR and DEPT spectra (Table 3.4, Figure 3.9) established the resonances of sixteen carbons; one methoxyl appeared at δ 55.7 (C-7 -OCH₃), one methylene at δ 43.4 (C-3), eight methines at δ 79.3 (C-2), 94.3 (C-8), 95.2 (C-6), 126.2 (C-2',6') and 128.9 (C-3',4',5') and six quaternary carbons at δ 162.9 (C-8a), 102.1(C-4a), 164.2 (C-5), 168.0 (C-7), 138.5 (C-1') and 195.8 (C-4) consistent with the proposed structure.

Based on the spectroscopic data of **LOB7** and comparison with the literature values, it was confirmed that compound **LOB7** was (+)-pinostrobin (Kulmagambetova et al., 2002; Passador et al., 1997) .

Table 3.4 ^1H NMR (400 MHz) and ^{13}C NMR (100 MHz) spectral data of (+)-pinostrobin **LOB7**

Position	^1H -NMR(δ , J in Hz)	^{13}C -NMR δ_{c}
1	-	-
2	5.42 (1H, <i>dd</i> , 13, 3.2)	79.3
3	2.81 (2H, <i>dd</i> , 17.2, 3.4, H-3 α) 3.11 (2H, <i>dd</i> , 17.4, 13, H-3 β)	43.4
4	-	195.8
4a	-	102.8
5	-	164.2
6	6.15 (1H, <i>s</i>)	95.2
7	-	168.0
8	6.15 (1H, <i>s</i>)	94.3
8a	-	162.9
1'	-	138.5
2', 6'	7.38, 7.49 (2H, <i>m</i>)	126.2
3', 4', 5'	7.38, 7.49 (3H, <i>m</i>)	128.9
7-OCH ₃	3.88 (3H, <i>s</i>)	55.7
OH	11.86 (1H, <i>s</i>)	-

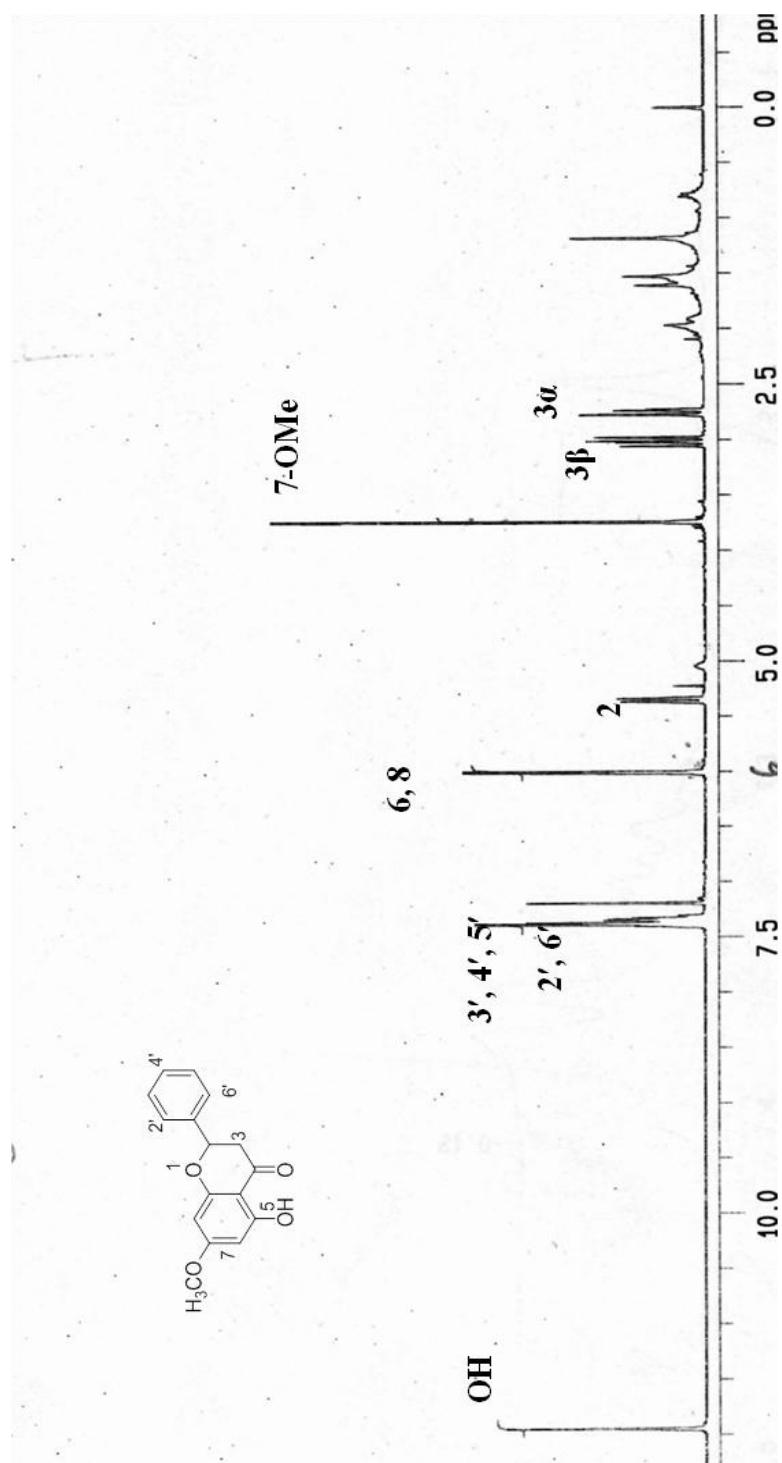


Figure 3.7: ^1H NMR spectrum of (+)-pinostrobin LOB7

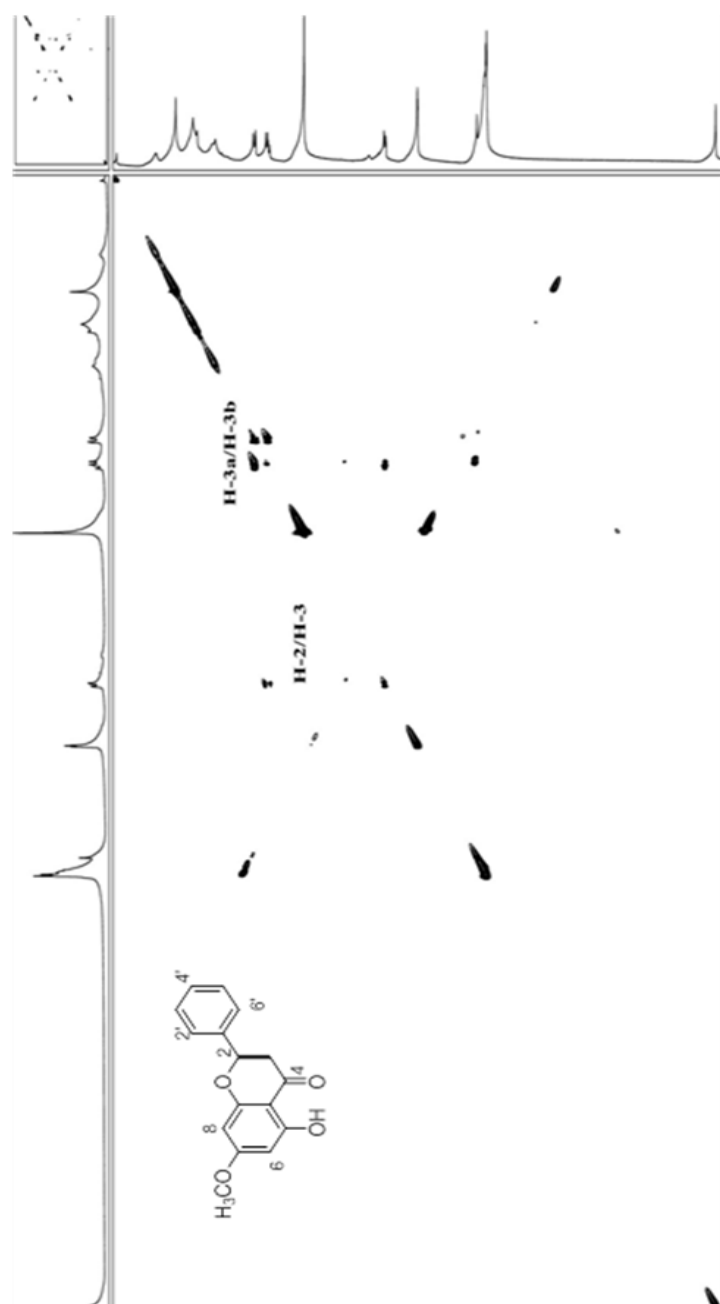


Figure 3.8: COSY spectrum of (+)-pinostrobin LOB7

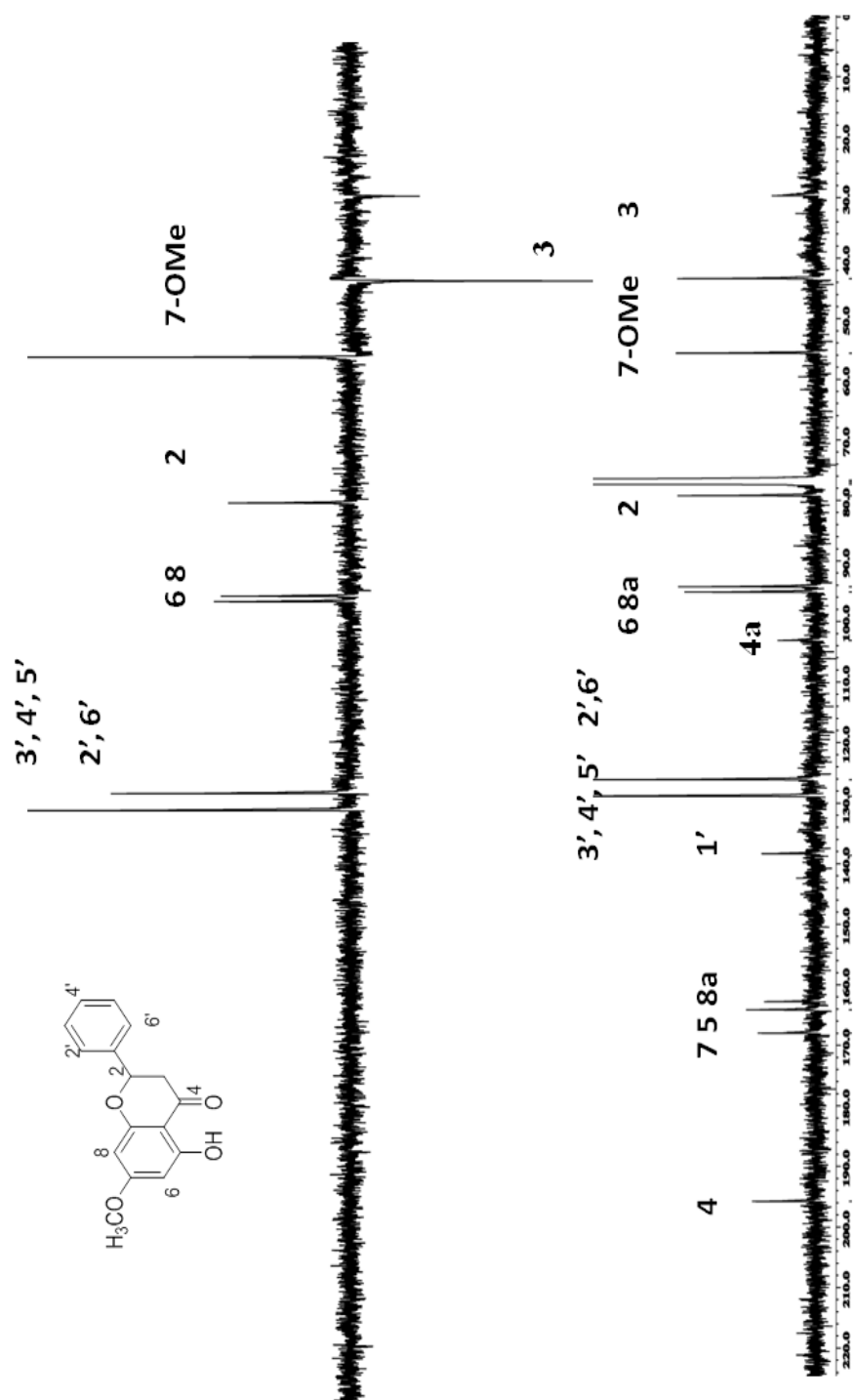
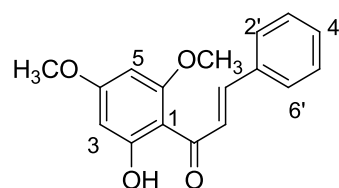


Figure 3.9: ^{13}C NMR / DEPT spectra of (+)-pinostrobin **LOB7**

3.1.3 Chalcone LOB15: Flavokawain B



LOB15

Flavonoid **LOB15**, Flavokawain B with IUPAC name (*E*)-1-(2-hydroxy-4, 6-dimethoxyphenyl)-3-phenylprop-2-en-1-one was afforded as a red ctystal with $[\alpha]_D^{25} = +12.3$ (2.00 $\times 10^{-4}$ g/100 mL, MeOH). In the UV spectrum, absorption maxima, λ_{\max} (MeOH) nm (log ϵ) at 241 (1.297) and 336 (1.860) indicated the presence of conjugated double bond system. Its IR spectrum showed absorption bands at ν_{\max} 3436 cm^{-1} for hydroxyl group and 1634 cm^{-1} for conjugated carbonyl group. The ESIMS (negative mode) spectrum showed an intense pseudomolecular ion peak, $[\text{M}-\text{H}]^+$ at m/z 283.7380 corresponding to the molecular formula of $\text{C}_{17}\text{H}_{16}\text{O}_4$.

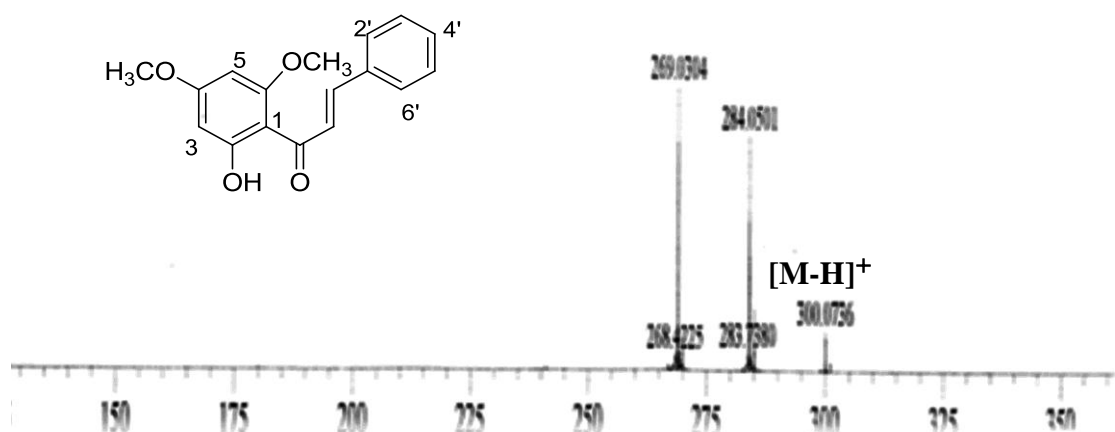


Figure 3.10: LC-MS Spectrum of Flavokawain B **LOB15**

The ^1H NMR spectrum (Table 3.5, Figure 3.11) exhibited two distinct methoxyl signals at δ 3.84 and δ 3.91 which were most probably positioned at H-4 and H-6. A one proton singlet appeared at δ 6.09 was assigned to H-5 proton and a one proton signal at δ 6.91 was observed which belongs to H-3. Two downfield signals appeared as doublet of doublet at δ 8.14 and δ 7.87 assigned to H- α and H- β respectively. The aromatic protons gave a multiplet signal between δ 7.38 and δ 7.43 attributed to H-3', H-4', H-5' and δ 7.62-7.65 attributed H-2' and H-6'. The above observations were reinforced by COSY (Table 3.5, Figure 3.12) experiment which displayed correlations of H- α /H- β and H-Ar/H-Ar.

The ^{13}C NMR and DEPT spectra (Table 3.5, Figure 3.13) established the total of seventeen carbon resonances; two methoxyls at δ 57.1 (C-4) and δ 62.5 (C-6), nine methines at δ 93.9 (C-3), 93.9 (C-5), 144.5 (C- α), 129.7 (C- β), 130.5 (C-2', C-6') and 131.4 (C-3', 4', 5'). Six quaternary carbons appeared at δ 105.4 (C-1), 152.1 (C-2), 164.2 (C-4), 159.5 (C-6), 136.5 (C-1') and 193.5 (C- γ) consistent with the structure proposed (Koorbanally et al., 2003).

HSQC spectrum (Table 3.5, Figure 3.14) showed the connectivity between proton and carbon: H- α /C- α , H- β /C- β , H-3/C-3, H-5/C-5, H-Ar/C-Ar, H-4'/C-4', H-4OMe/C-4OMe, H-6OMe/C-6OMe.

In the HMBC spectrum (Table 3.5, Figure 3.16) the cross-peaks were observed between H- α to C- γ , C-1', H- β to C- α , C-1', C- γ , H-2' to C-3', C-4', C- α , H-3' to C-2', C-4', H-4' to C-3', C-6' and H-5' to C-6', H-3 to C-1, C-4, C-2, H-5 to C-1, C-4, C-6, H-4 OMe to C-4OMe and H-6-OMe to C-6-OMe.

Comparison of the empirical data with the literature values of the known compound, it was confirmed that compound **LOB15** was flavokawain B, chalcone.

Table 3.5: ^1H NMR (400 MHz) and ^{13}C NMR (100 MHz) spectral data of flavokawain B
LOB15

Position	^1H -NMR(δ , J in Hz)	^{13}C -NMR(δc)
1	-	105.4
2	-	152.1
3	6.91 (1H, <i>s</i>)	93.9
4	-	164.2
5	6.09 (1H, <i>s</i>)	93.9
6	-	159.5
1'	-	136.5
3',4',5'	7.38-7.43 (3H, <i>m</i>)	131.7
2',6'	7.62-7.65 (2H, <i>m</i>)	130.7
β	7.87(1H, <i>d</i> ,15.2)	129.7
α	8.14 (1H, <i>d</i> ,15.6)	144.5
γ	-	193.5
4-OMe	3.84 (3H, <i>s</i>)	57.1
6-OMe	3.91(3H, <i>s</i>)	62.5
OH	11.96 (1H, <i>s</i>)	-

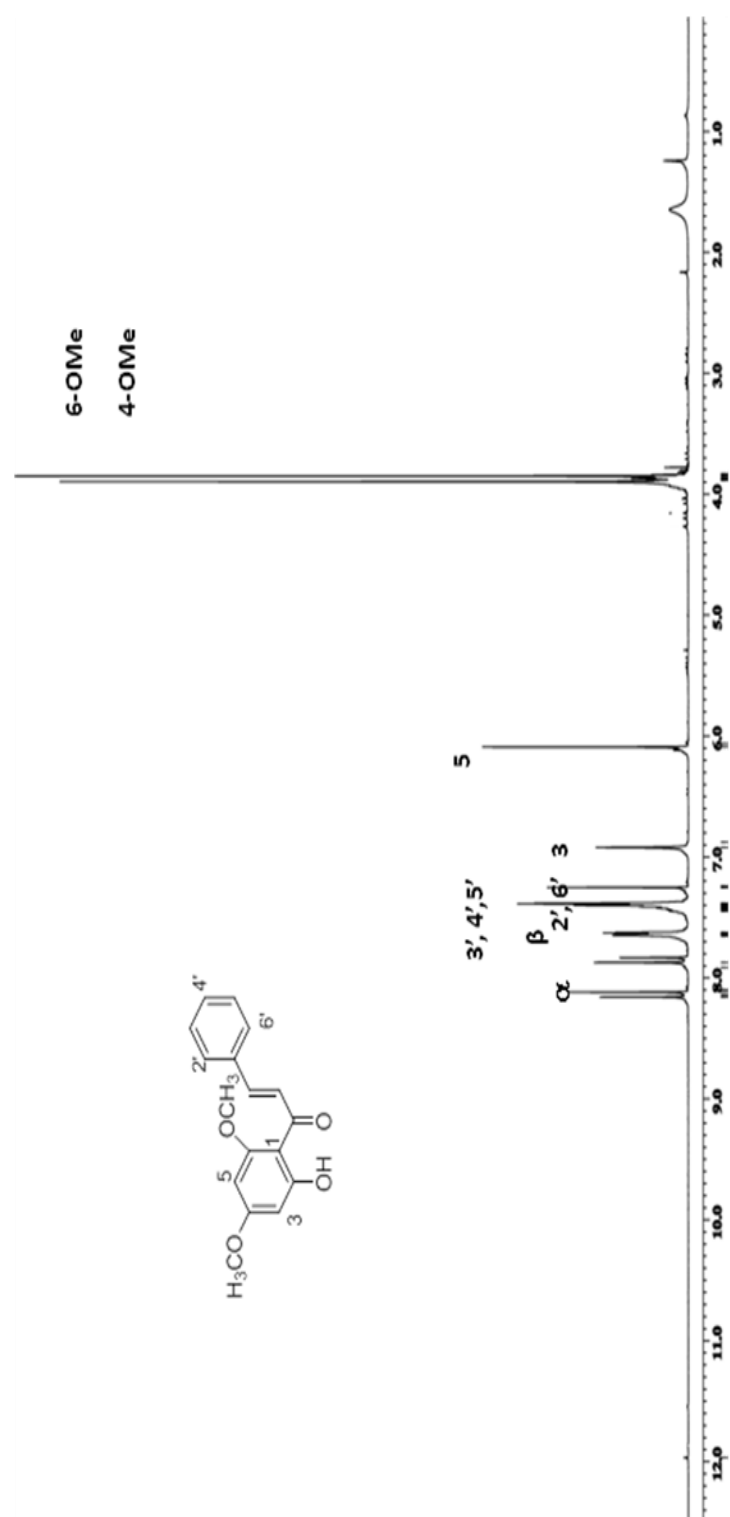


Figure 3.11. ^1H NMR spectrum of Flavokawain B L OB15

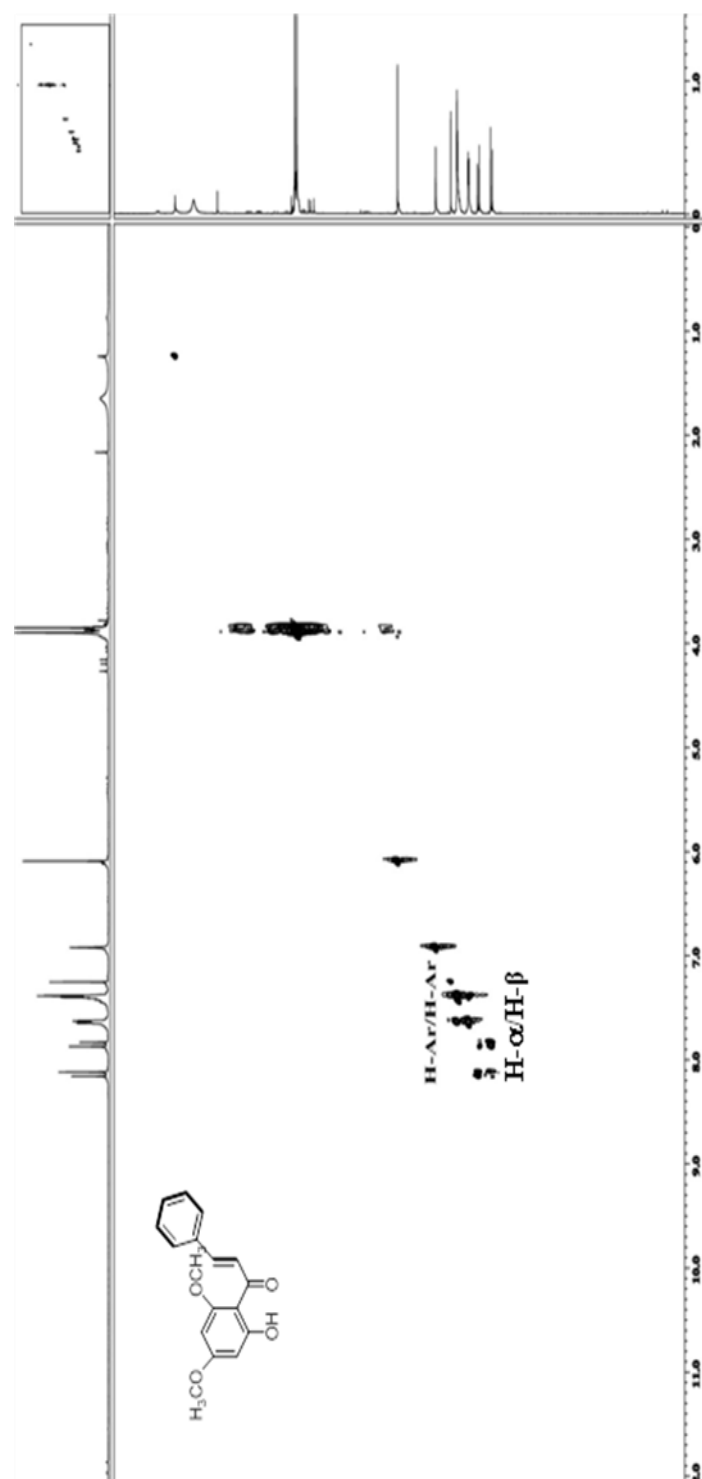


Figure 3.12: Cossy spectrum of flavokawain B LOB 15

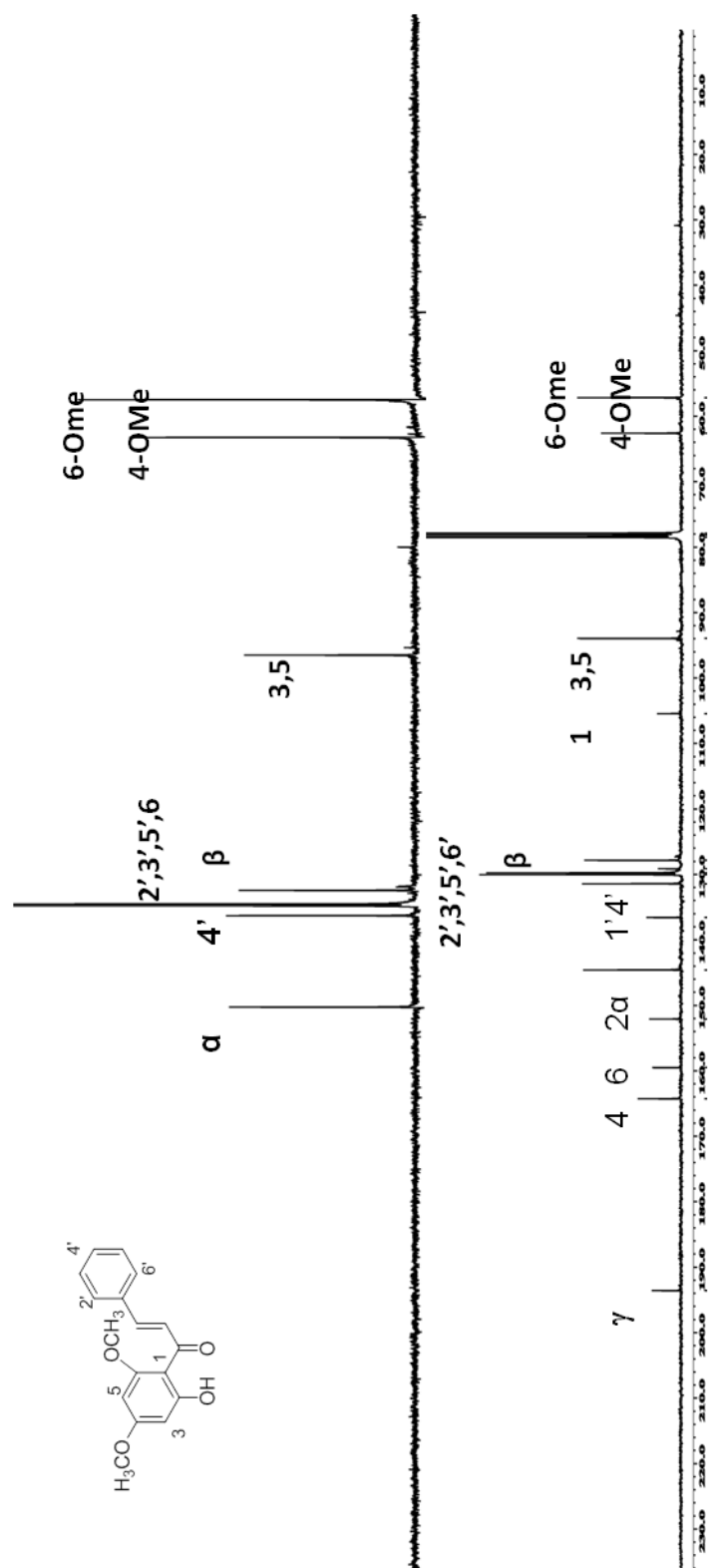


Figure 3.13. ^{13}C NMR / DEPT spectrum of flavokawain B **LOB 15**

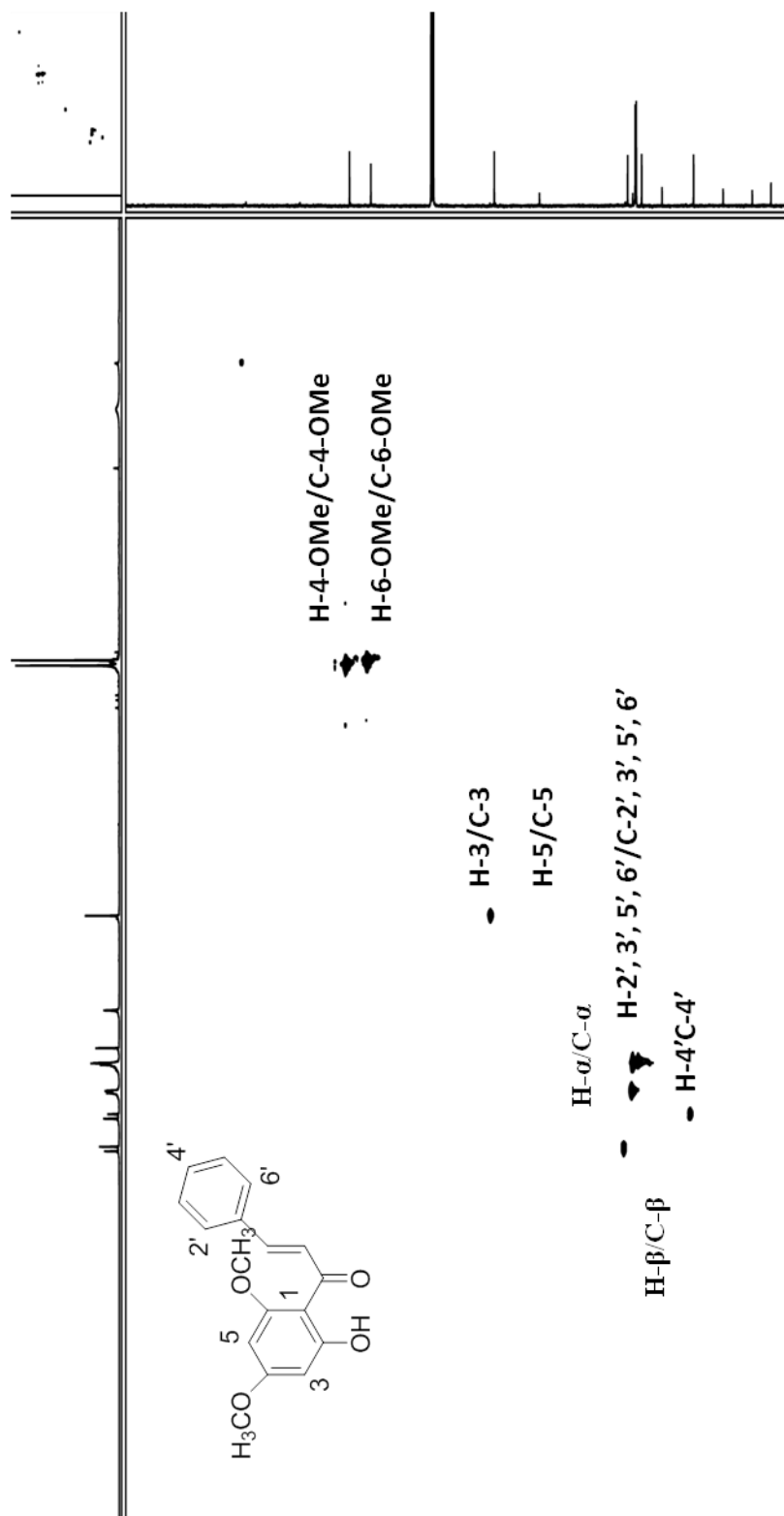


Figure 3.14: HMQC spectrum of flavokawain B **LOB15**

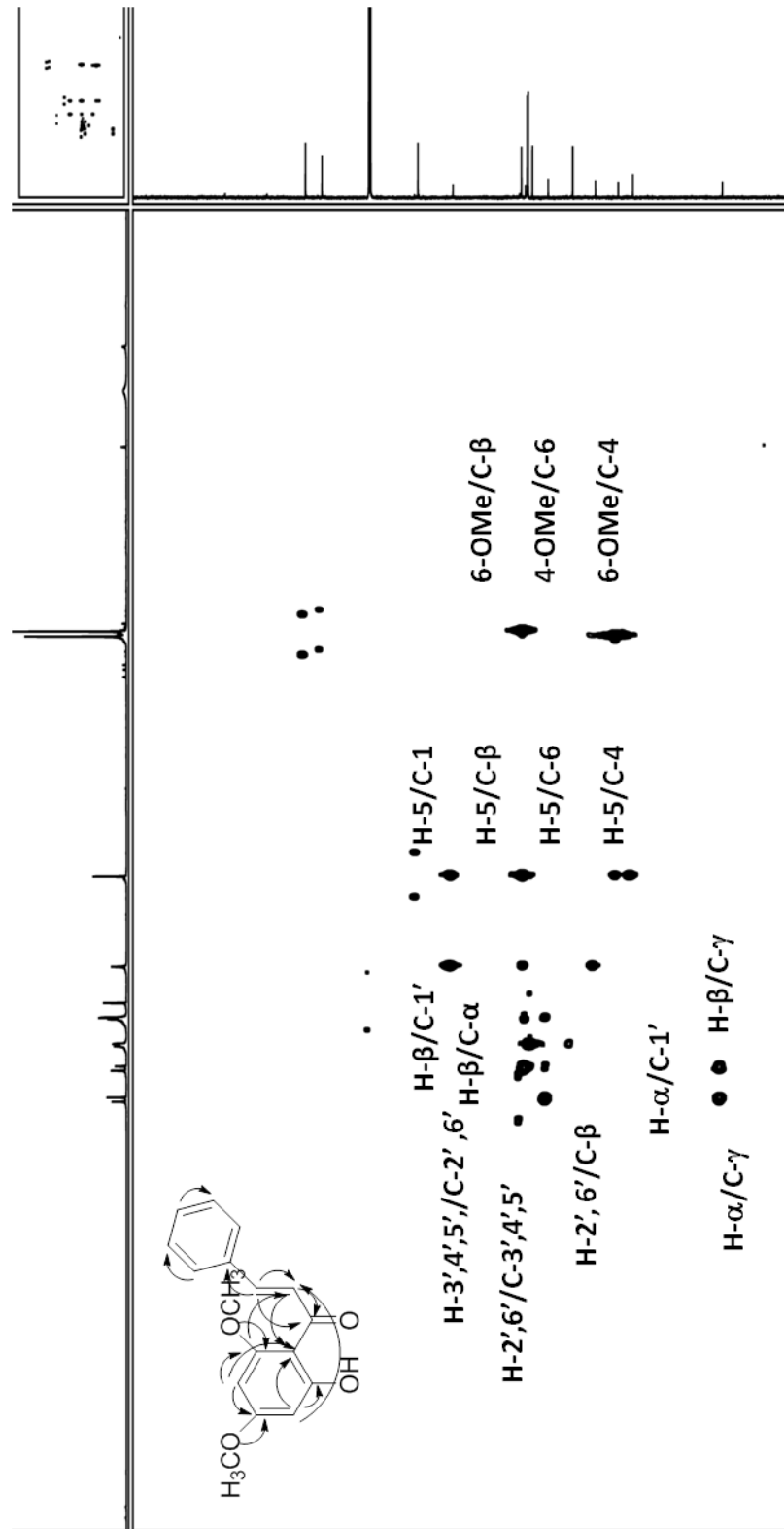
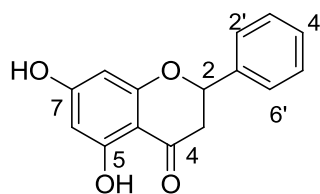


Figure 3.15: HMBC spectrum of flavokawain BLOB 15

3.1.4 Flavanone LOB2: (+)-Pinocembrin



LOB2

Flavonoid **LOB2**, (+)-pinocembrin with IUPAC name 5, 7-dihydroxy -2(S)-phenyl chroman-4H-one was afforded as a yellow amorphous solid with $[\alpha]_D^{25} = +2.81$ (2.00×10^{-4} g/100 mL, MeOH). The structure of **LOB2** has the same skeleton with **LOB4** and **LOB7** which have been discussed before. In the UV spectrum, the absorption maxima at λ_{\max} (MeOH) nm (log ϵ) 241 (1.519) and 290 (2.783) (Jayaprakasam et al., 1999). Its IR spectrum showed absorption bands at ν_{\max} 3417 cm^{-1} for hydroxyl group and 1640 cm^{-1} assigned for chelated α, β unsaturated carbonyl. The molecular formula of **LOB2** was established as $\text{C}_{15}\text{H}_{12}\text{O}_4$ on the basis of ESI-MS (negative mode): m/z 255.0475 $[\text{M} - \text{H}]^-$. MS/MS: m/z (relative abundance) 256.07 (Neacsu et al., 2007).

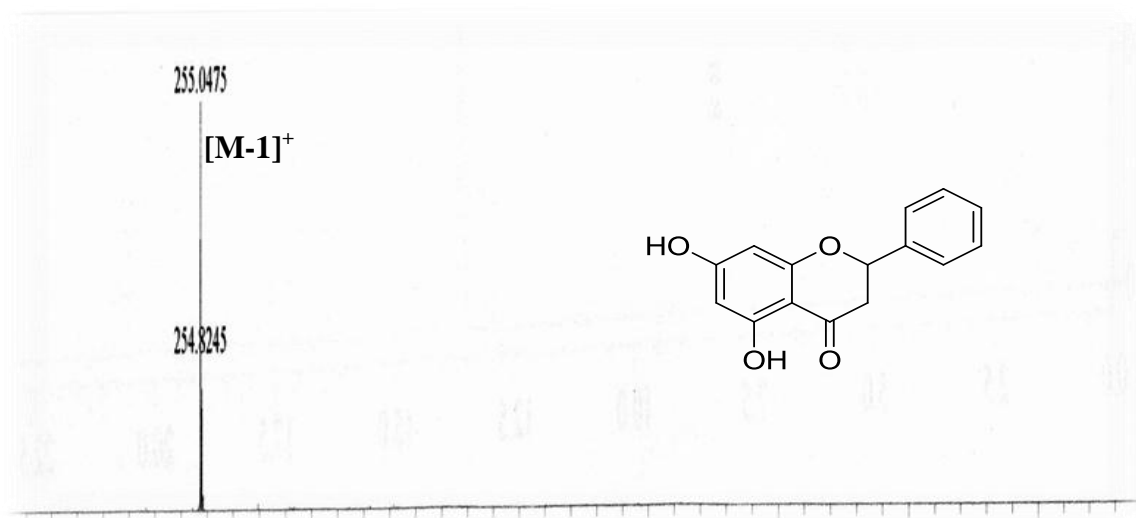


Figure 3.16: LC-MS Spectrum of (+)-Pinocembrin **LOB2**

The ^1H NMR spectrum (Table 3.6, Figure 3.17) and ^{13}C NMR spectrum (Table 3.6, Figure 3.18) assembled the data for compound **LOB7** except the hydroxyl group at C-7 appeared at δ 11.8 as a singlet which was overlapped with OH group at C-5 in the ^1H NMR and the C-7 resonated at δ 165.7 in ^{13}C NMR.

Based on the spectroscopic data of **LOB2** and comparison with the literature values, it was confirmed that compound **LOB2** was (+)-pinocembrin (Bick et al., 1972; Geogina N et al., 2009; Yenjai et al., 2009).

Table 3.6: ^1H NMR (400 MHz) and ^{13}C NMR (100 MHz) spectral data of (+)-Pinocembrin
LOB2

Position	^1H -NMR(δ , J in Hz)	^{13}C -NMR (δc)
1	-	-
2	5.33 (1H, <i>dd</i> , 13.6, 3.5)	79.0
3	2.62 (1H, <i>dd</i> , 17.4, 3.2, H-3 α) 3.01(1H, <i>dd</i> , 17.3, 13.5, H-3 β)	43.2
4	-	195.6
4a	-	102.8
5	-	164.2
6	5.33 (1H, <i>d</i> , 2.2)	96.8
7	-	165.7
8	5.94 (1H, <i>d</i> , 2.2)	95.6
8a	-	163.0
1'	-	138.3
2',6'	7.31-7.45 (2H, <i>m</i>)	126.2
3',4',5'	7.31-7.45(3H, <i>m</i>)	128.8
5-OH	11.81(1H, <i>s</i>)	-
7-OH	11.81(1H, <i>s</i>)	-

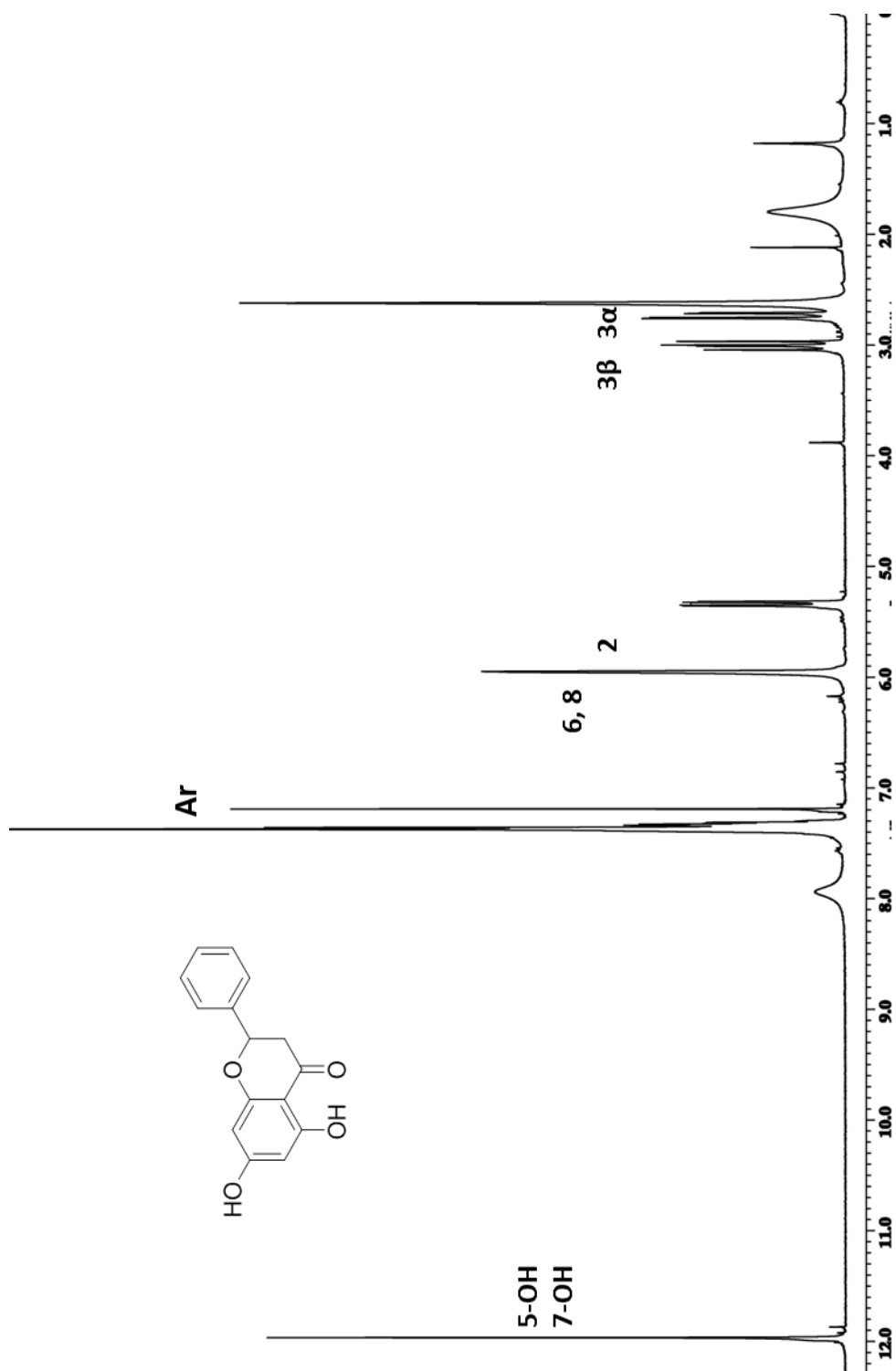


Figure 3.17: ¹H NMR spectrum of (+)-Pinocembrin **LOB2**

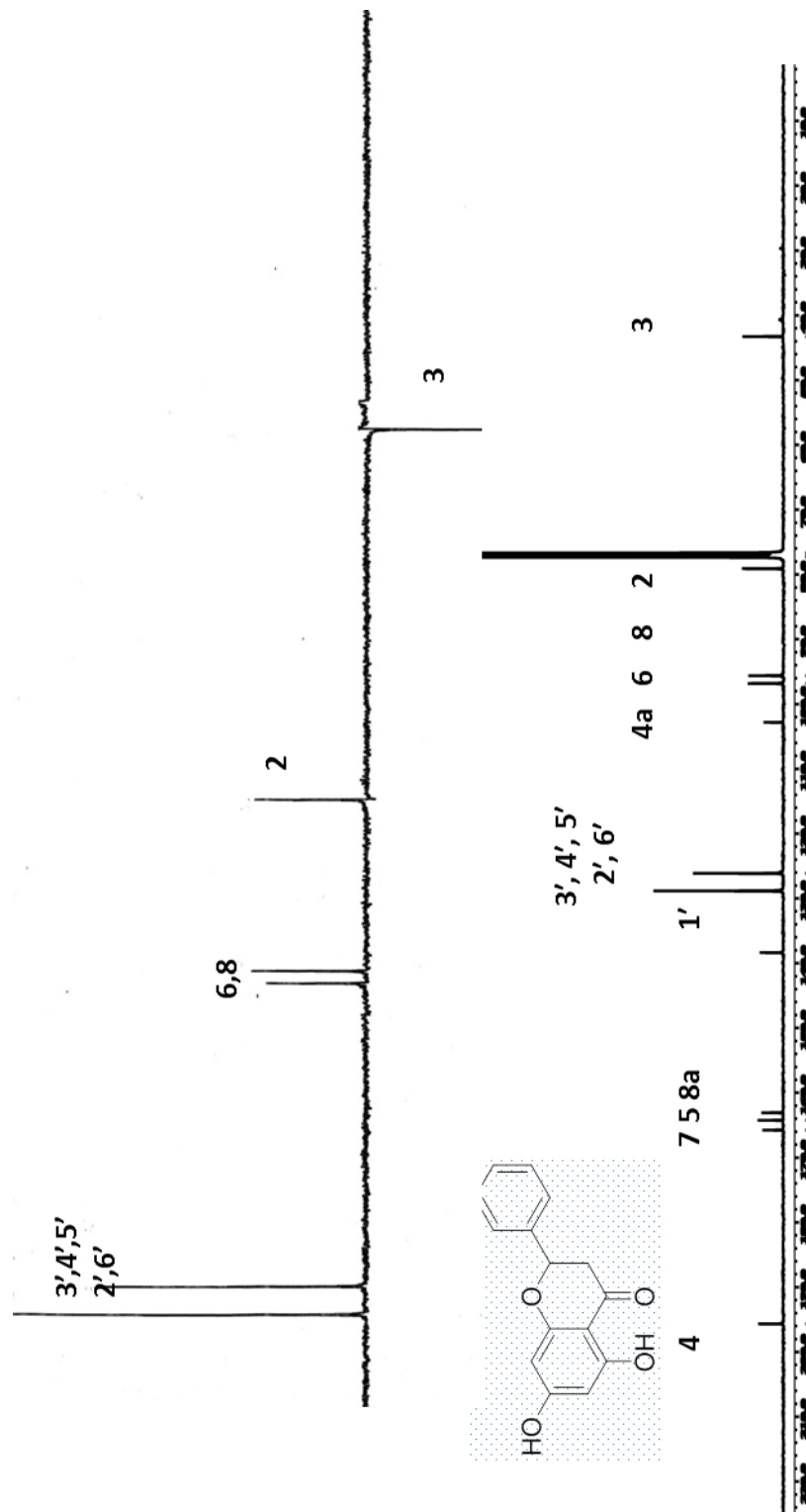
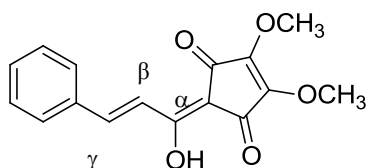


Figure 3.18: ^{13}C NMR/DEPT spectrum of (+)-Pinocembrin LOB2

3.1 .5 Linderone LOB28: Linderone



LOB28

Linderone **LOB28** with IUPAC name (*E*)-2-(1-hydroxy-3-phenylprop-2-en-1-ylidene)-4,5-dimethoxycyclopent-4-ene-1,3-dione was afforded as a yellow crystal with m.p 92 °C (Oh et al., 2005). In UV spectrum, absorption maxima was observed at λ_{\max} (MeOH) nm (log ϵ) 246 (1.529) and 364 (1.631). Its IR spectrum showed absorption bands at ν_{\max} 3435 cm^{-1} assigned for hydroxyl group and 1632 cm^{-1} for conjugated carbonyl groups. The LC-MS (positive mode) spectrum showed an intense pseudomolecular ion peak, $[\text{M}+\text{H}]^+$ at m/z 287.0677 corresponding to the molecular formula of $\text{C}_{16}\text{H}_{14}\text{O}_5$.

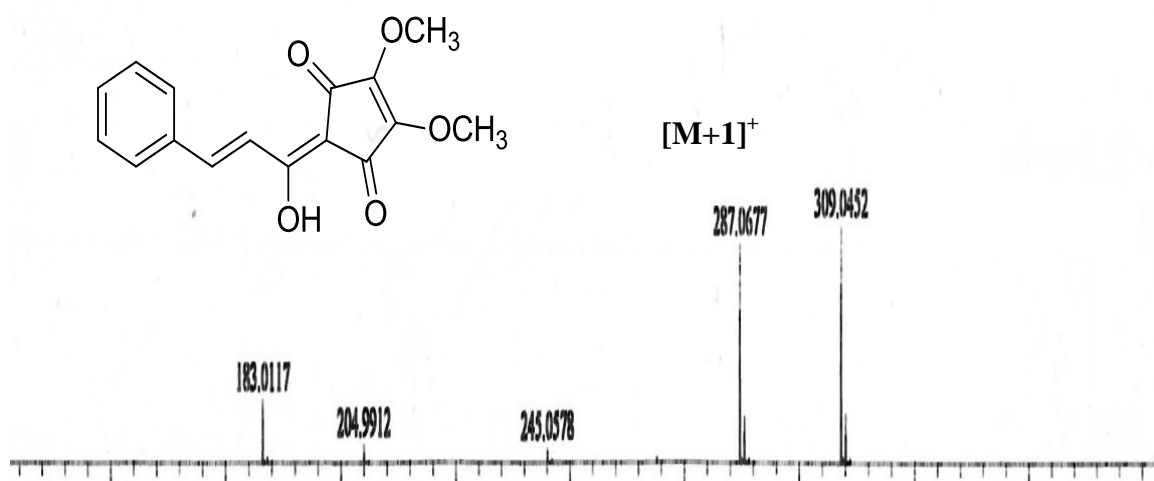


Figure 3.19: LC-MS Spectrum of Linderone **LOB28**

The ^1H NMR spectrum of linderone **LOB28** (Table 3.7, Figure 3.20) exhibited two distinct methoxyl signals at δ 3.91 and δ 4.08 which were most probably positioned at C-4 and C-5. The aromatic protons gave a three signal at δ 7.41 (H-3', H-5'), 7.61 attributed to (H-2', 6') and 7.72 belongs to H-4'. One signal appeared as a singlet at δ 11.51 was assigned for OH group. The above observations were reinforced by COSY (Table 3.7, Figure 3.21) experiment which displayed correlations of H-3'/H-4', H-5'/H-6'.

The ^{13}C NMR and DEPT spectra (Table 3.7, Figure 3.22) established the total of sixteen carbon signals; two methoxyls at δ 60.0 (C-4) and δ 59.9 (C-5). Seven methines at δ 117.7 (C- β), 141.5 (C- γ), 128.9 (C-3'), 128.9 (C-5'), 128.5 (C-2'), 128.5 (C-6') and 130.4 (C-4'), seven quaternary carbons resonated at δ 193.3 (C-1), 101.8 (C-2), 184.8 (C-3), 148.2 (C-4), 145.3 (C-5), 164.6 (C- α) and 135.0 (C-1').

In HSQC (Table 3.7, Figure 3.23) spectrum showed the correlation between hydrogen and carbon such as H-2'/C-2', H-6'/C-6', H-3'/C-3', H-4'/C-4', H-5'/C-5', H-4/C-4OMe and H-5/C-5OMe (Hiok-Huang et al. 1990).

In the HMBC spectrum (Table 3.7, Figure 3.24) the cross-peak were observed between H-2' to C-3', H-2' to C-4', C-1', H-6' to C-5', H-6' to C-4', H-4' to C-3', C-5', H-4OMe to C-4OMe, H-5OMe/C-5OMe.

Based on the spectroscopic data of **LOB28** and comparison with the literature values, it was confirmed that compound **LOB28** was (*E*)-2-(1-hydroxy-3-phenylprop-2-en-1-ylidene)-4,5-dimethoxycyclopent-4-ene-1,3-dione or linderone (Haibo Tan et al. 2011). The structure of compound **LOB28** was also confirmed by x-ray crystallography and this x-ray structure was the first time reported (see Figures 3.25 and 3.26).

Table 3.7: ^1H NMR (400 MHz) and ^{13}C NMR (100 MHz) spectral data of linderone **LOB28**

Position	^1H -NMR(δJ in Hz)	^{13}C -NMR (δc)
1	-	193.3
2	-	101.8
3	-	184.8
4	-	148.2
5	-	145.3
α	-	164.6
β	-	117.7
γ	-	141.5
1'	-	135.0
2',6'	7.61(2H, <i>m</i>)	128.5
3',5'	7.41(2H, <i>m</i>)	128.9
4'	7.41(1H, <i>m</i>)	130.4
4-OMe	3.91(3H, <i>s</i>)	60.0
5-OMe	4.08 (3H, <i>s</i>)	59.9
OH	11.51(1H, <i>s</i>)	-

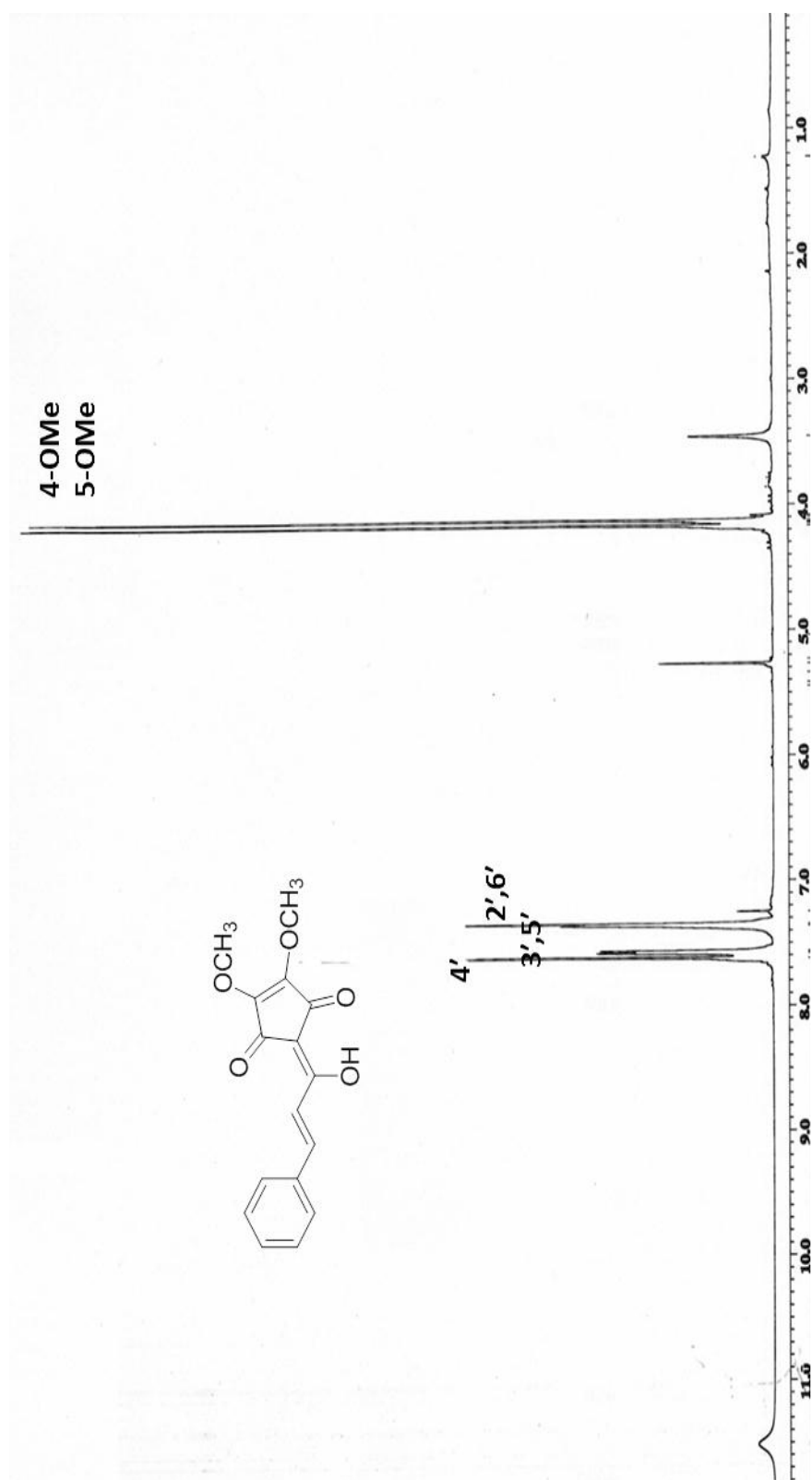


Figure 3.20: ^1H -NMR spectrum of Linderone LOB28

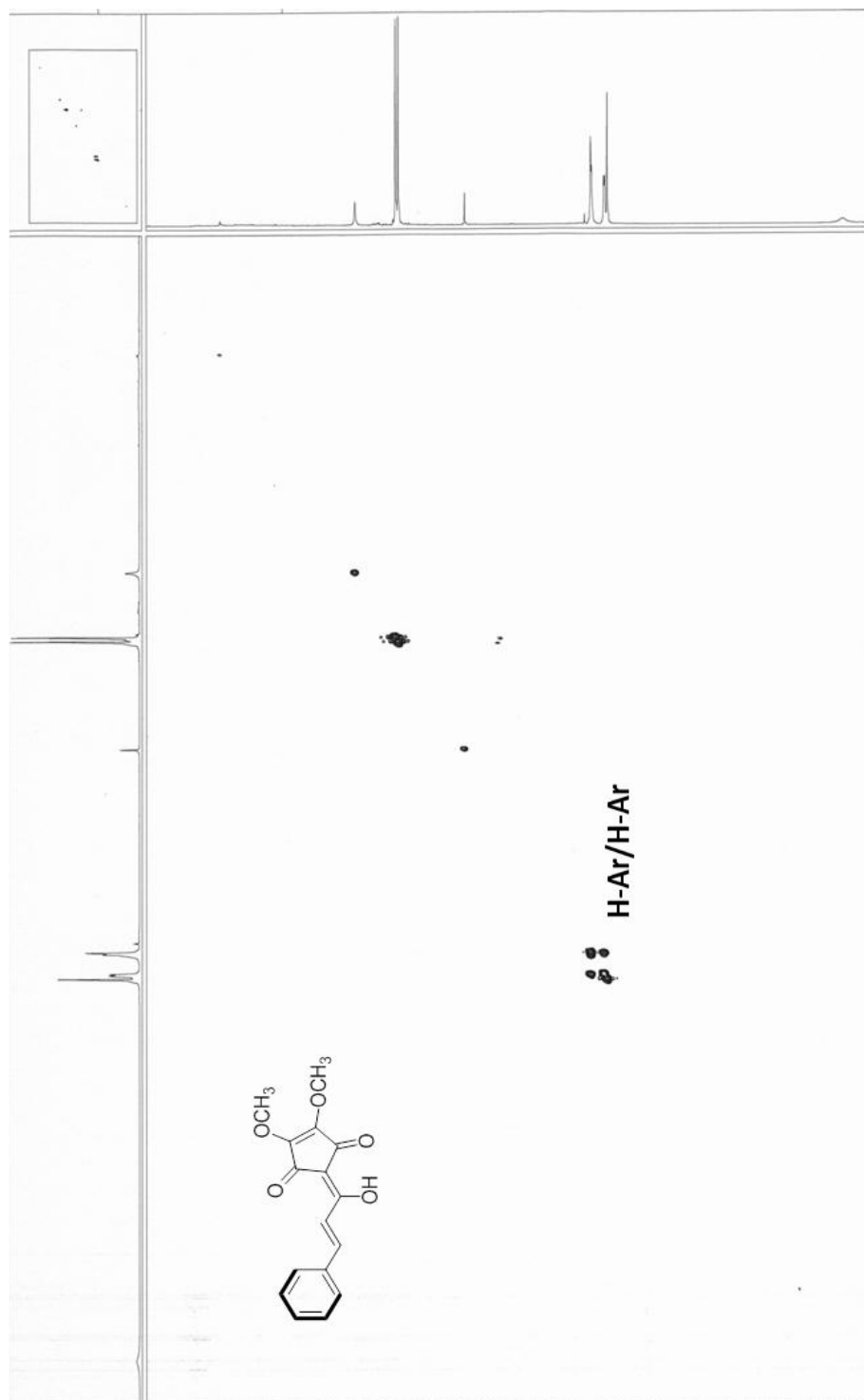


Figure 3.21: COSY spectrum of Linderone LOB28

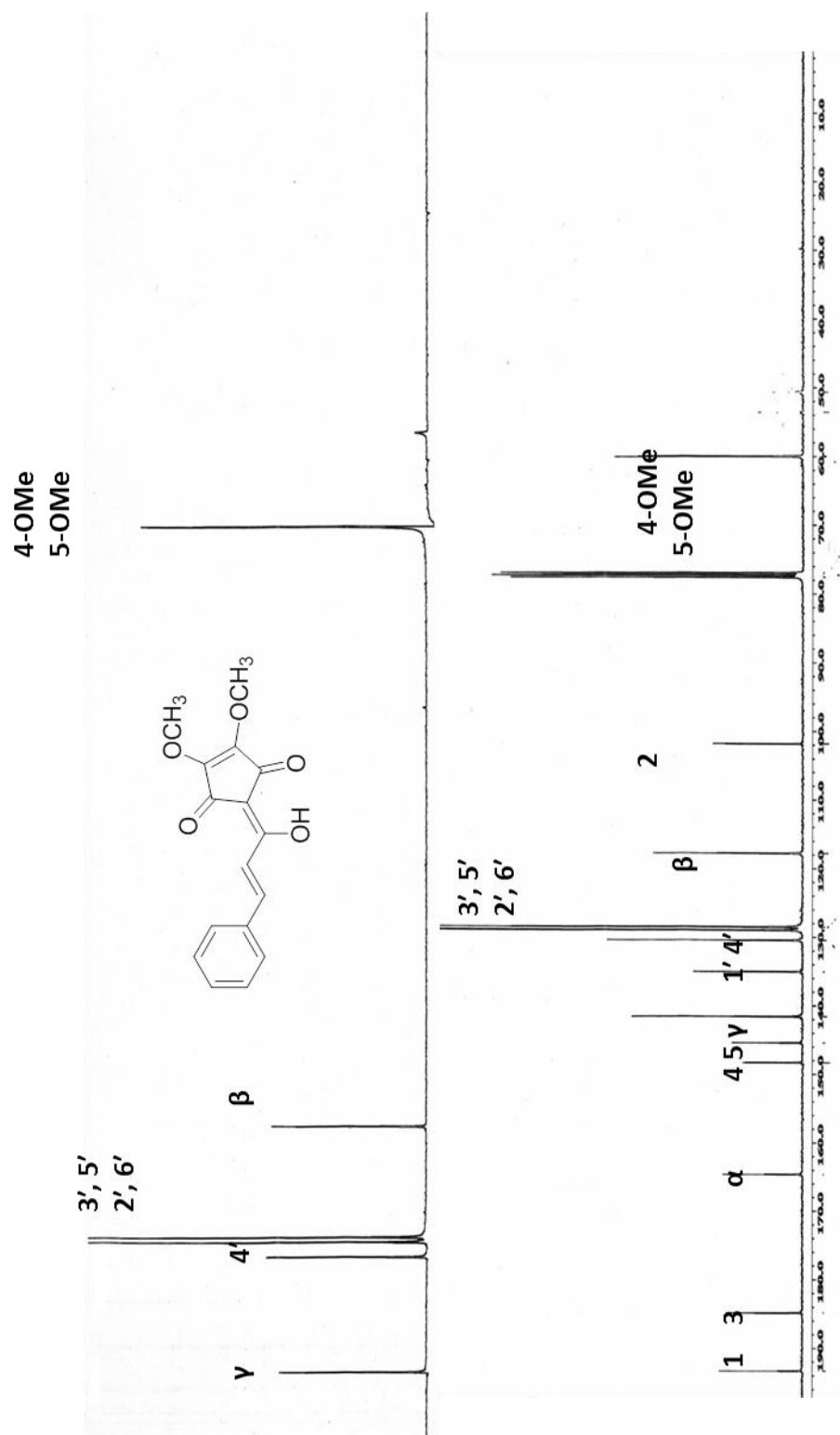


Figure 3.22: ^{13}C NMR/DEPT spectrum of Linderone LOB28

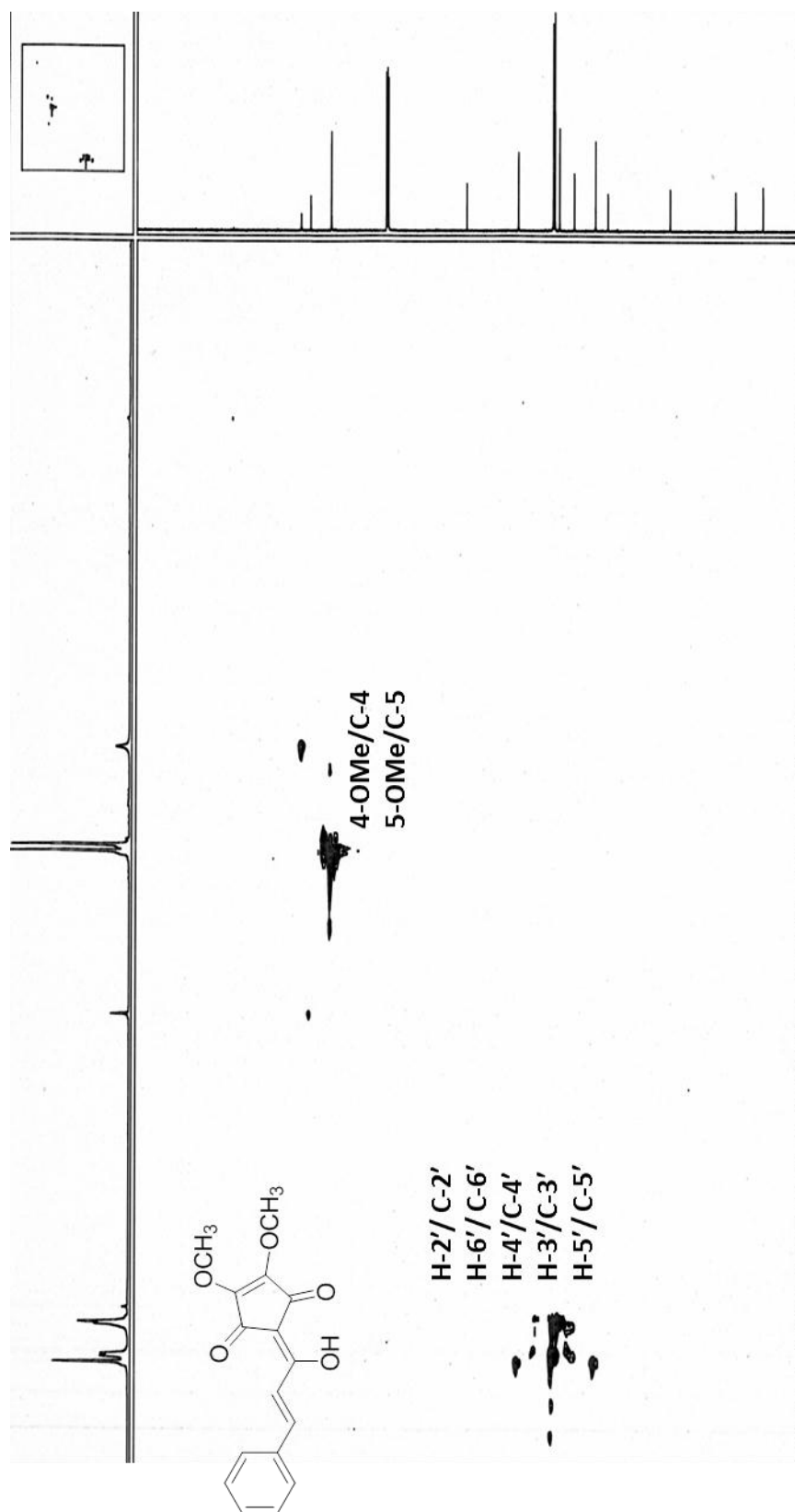


Figure 3.23: HSQC spectrum of Linderone **LOB28**

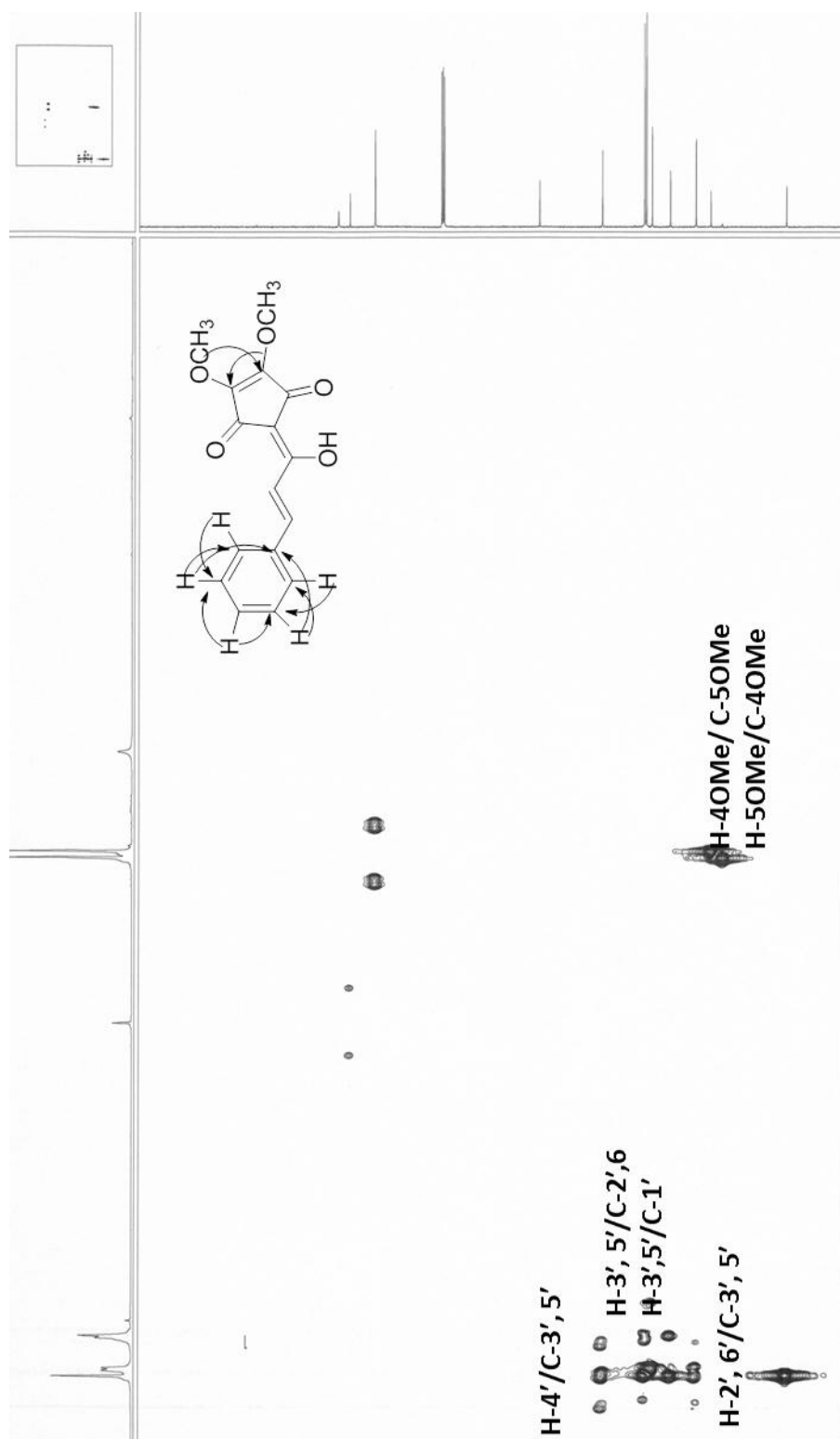


Figure 3.24: HMBC spectrum of Linderone LOB28

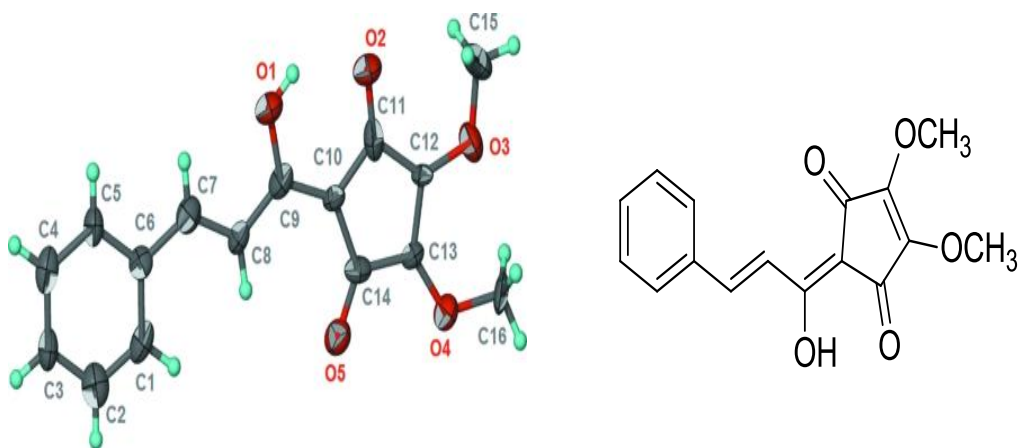


Figure 3.25: X-ray Crystallographic Structure monoclinic of **LOB28**
(Hosseinzadeh, et al., 2011)

Empirical formula	$C_{16}H_{14}O_5$
Formula weight	$M_r = 286.27$
Crystal system	Monoclinic
Space group	$P 2_1/c$
a (Å)	7.3195 (5) Å
b (Å)	9.8635 (7) Å
c (Å)	18.6724 (11) Å
β (°)	96.586 (6)°
Volume (Å ³)	1339.17 (15) Å ³
Z value	4
Calculated density, D_{calc} (Mg/m ³)	1.420 Mg m ⁻³
Absorption coefficient, μ (mm ⁻¹)	0.71073 Å
Crystal size (mm)	0.20 × 0.20 × 0.10 mm
Cell determination, 2θ range (°)	Cell parameters from 4706 reflections

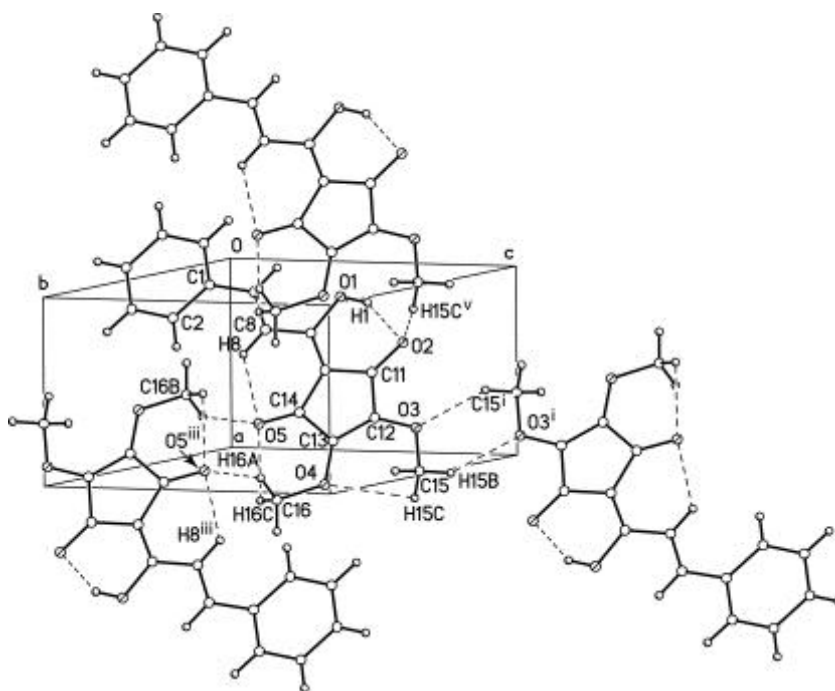
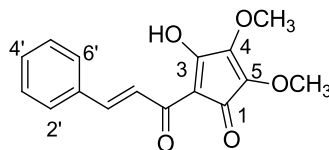


Figure 3.26: X-ray Crystallographic Structure Triclinic of **LOB28**
(Hosseinzadeh, et al., 2011)

Empirical formula	$C_{16}H_{14}O_5$
Formula weight	$M_r = 286.27$
Crystal system	Triclinic
Space group	$P 2_1/c$
a (Å)	5.4055 (2) Å
b (Å)	11.2731 (3) Å
c (Å)	11.6441 (3) Å
α (°)	72.070 (1)°
β (°)	83.088 (1)°
γ (°)	77.760 (1)°
Volume (Å ³)	77.760 (1)°
Z value	2
Calculated density, D_{calc} (Mg/m ³)	1.444 Mg m ⁻³
Absorption coefficient, μ (mm ⁻¹)	0.71073 Å
Crystal size (mm)	0.26 × 0.19 × 0.11 mm
Cell determination, 2θ range (°)	Cell parameters from 2073 reflections

3.1.6 Linderone LOB25: Linderone A



LOB 25

Linderone A **LOB25** with IUPAC name 2-cinnamoyl-3-hydroxy-4,5-dimethoxycyclopenta-2,4-dienone was afforded as a yellow amorphous solid. The UV spectrum showed the absorption peak at λ_{\max} (MeOH) nm (log ϵ) 246 (1.291) and 309 (1.580) indicated the presence of conjugated carbon-carbon double bond and carbonyl group. Its IR spectrum showed absorption bands at ν_{\max} 3431 hydroxyl group, 1639, carbonyl group. The LC-MS (positive mode) spectrum showed an intense pseudomolecular ion peak, $[M+H]^+$ at m/z 287.0677 corresponding to the molecular formula of $C_{16}H_{14}O_5$.

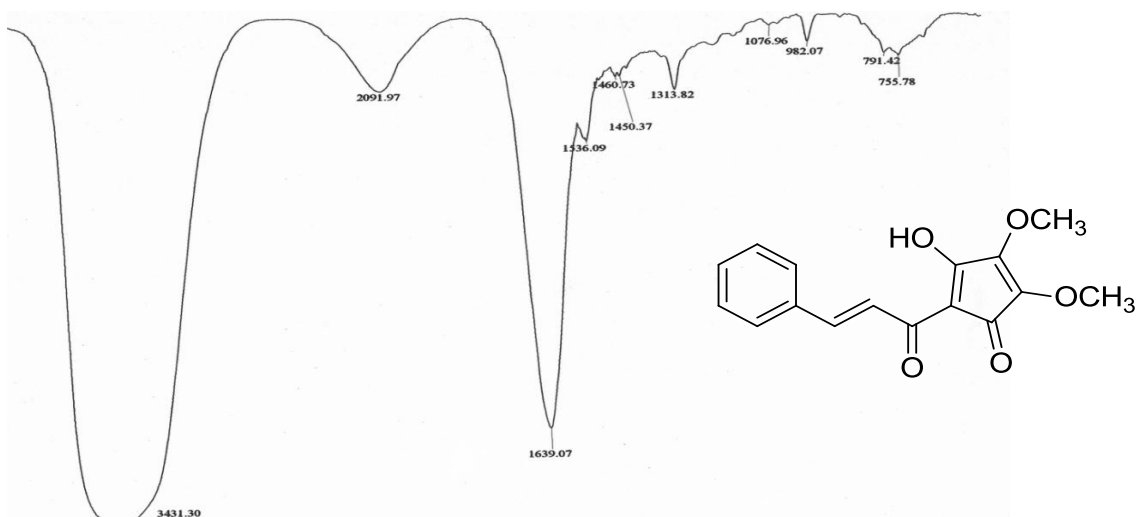


Figure 3.27: IR Spectrum of Linderone A **LOB25**

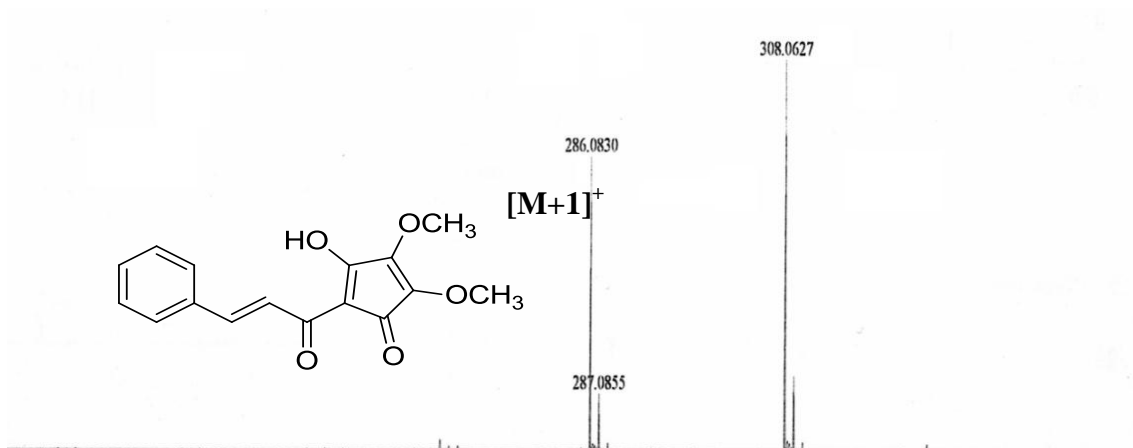


Figure 3.28: LC-MS Spectrum of Linderone A LOB25

The ^1H NMR spectrum (Table 3.8, Figure 3.29) exhibited one signal appeared as singlet at δ 4.15 corresponding to two methoxyl groups positioned at C-4 and C-5. A peak at δ 7.25 was observed as a doublet which was assigned for H- β and at δ 8.04 for H- γ . The aromatic protons gave a doublet signal δ 7.57 attributed to H-2' and H-6' and multiplate signal at δ 7.55 for H-3', H-5' and one signal appeared as singlet at δ 7.41 corresponding for H-4'. The above observations were reinforced by COSY (Table 3.8, Figure 3.30) experiment which displayed correlations of H- β /H- γ and H-2'/H-3', H-3'/H-4', H-4'/H-5', H-5'/H-6'.

The ^{13}C NMR and DEPT spectra (Table 3.8, Figure 3.31) established the resonances of seventeen carbons; two methoxyls at δ 60.1 corresponding to methyl group at C-4 and C-5. Seven sp^2 methines appeared at δ 120.2 (C- β), 136.7 (C- γ), 128.1 (C-3'), 128.1 (C-5'), 129.1 (C-2'), 129.1 (C-6') and 130.0 (C-4'). seven quaternary carbons resonated at δ 97.1 (C-2), 187.8 (C-3), 145.1 (C-4), 145.1 (C-5) and 135.2 (C-1') and two carbonyl signals appeared at δ 191.5 (C-1) and 153.4 (C- α).

The HMQC spectrum (Table 3.8, Figure 3.32) showed the correlation between hydrogen to their respective carbon atoms; H- γ /C- γ , H- β /C- β , H-2'/C-2', H-3'/C-3', H-

4'/ C-4', H-5'/ C-5' and H-6/ C-6'.

In the HMBC spectrum (Table 3.8, Figure 3.33) the cross-peak were observed between H-2' to C-4', C-3', H- γ to C- α , C-1', H- β to C- α , H-3' to C-4', C-2', H-4OMe to C-4-OMe and H-5OMe to C-5-OMe.

Based on the spectroscopic data of **LOB25**, it was confirmed that compound **LOB25** is a new compound and has never been reported before. This compound named as 2-cinnamoyl-3-hydroxy-4,5-dimethoxycyclopenta-2, 4-dienone or linderone A.

Table 3.8: 1D (^1H and ^{13}C) and 2D (COSY and HMBC) NMR spectral data of Linderone A LOB25

Position	^1H -NMR(δ , J in Hz)	^{13}C -NMR(δc)	COSY	HMQC	HMBC
1	-	191.5	-	-	-
2	-	97.1	-	-	-
3	-	187.8	-	-	-
4	-	145.1	-	-	-
5	-	145.1	-	-	-
α	-	153.4	-	-	-
β	7.25 (1H, d , 17.7)	120.2	H- γ	H- β	α
γ	8.04 (1H, d , 17.7)	136.7	H- β	H- γ	1', α
1'	-	135.2	-	-	-
2',6'	7.57 (2H, m)	129.1	H-3',5'	H-2',6'	4', γ
3',5'	7.55 (2H, m)	128.1	H-2',6',4'	H-3',5'	4'
4'	7.41 (H, m)	130.0	H-3',5'	H-4'	-
4-OMe	4.15 (3H, s)	60.1	H-OMe	H-4OMe	5-OMe
5-OMe	4.15 (3H, s)	60.1	H-OMe	H-5OMe	4-OMe

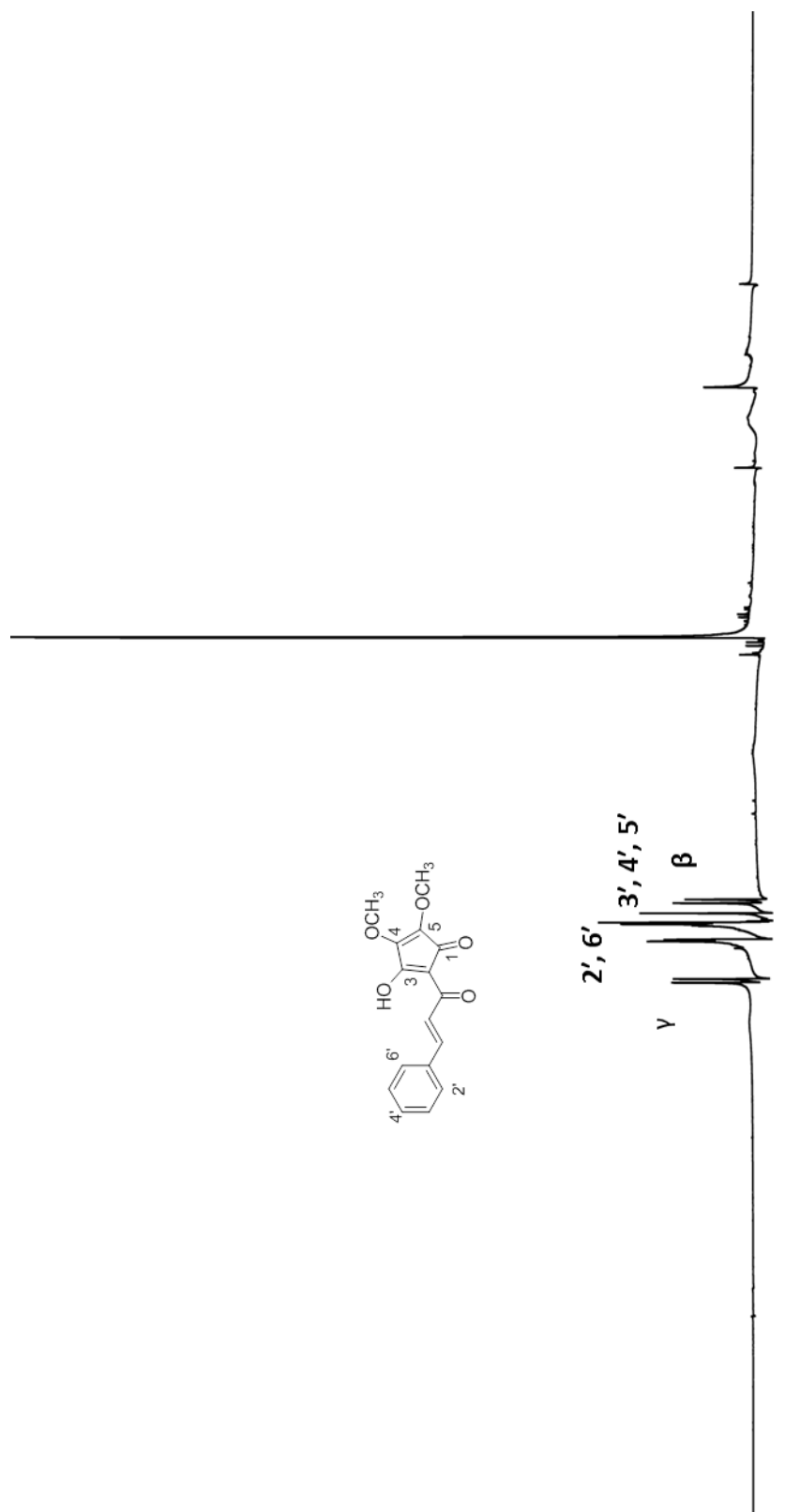


Figure 3.29: ^1H -NMR spectrum of Linderone A LOB25

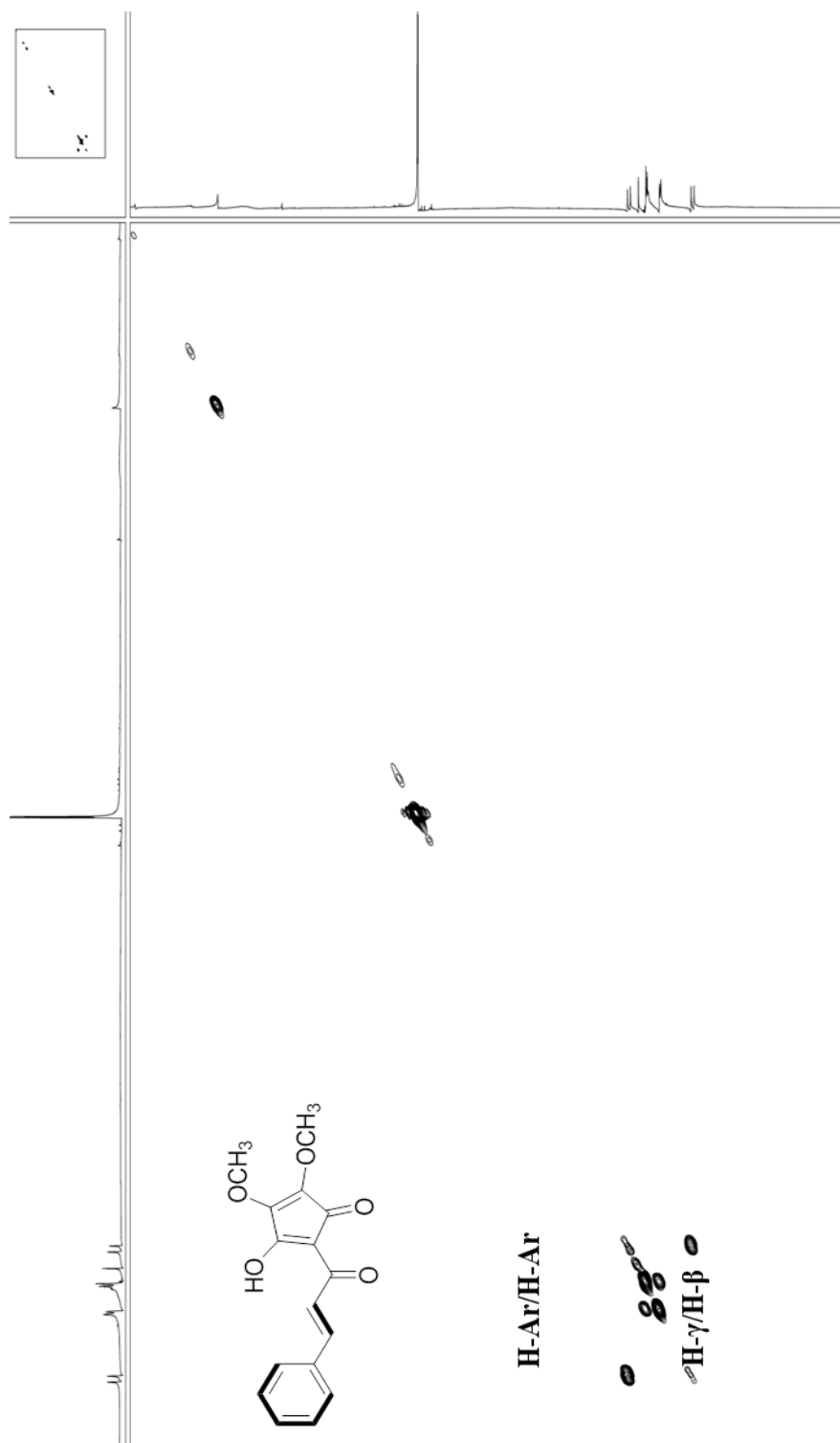


Figure 3.30: COSY spectrum of Linderone A LOB25

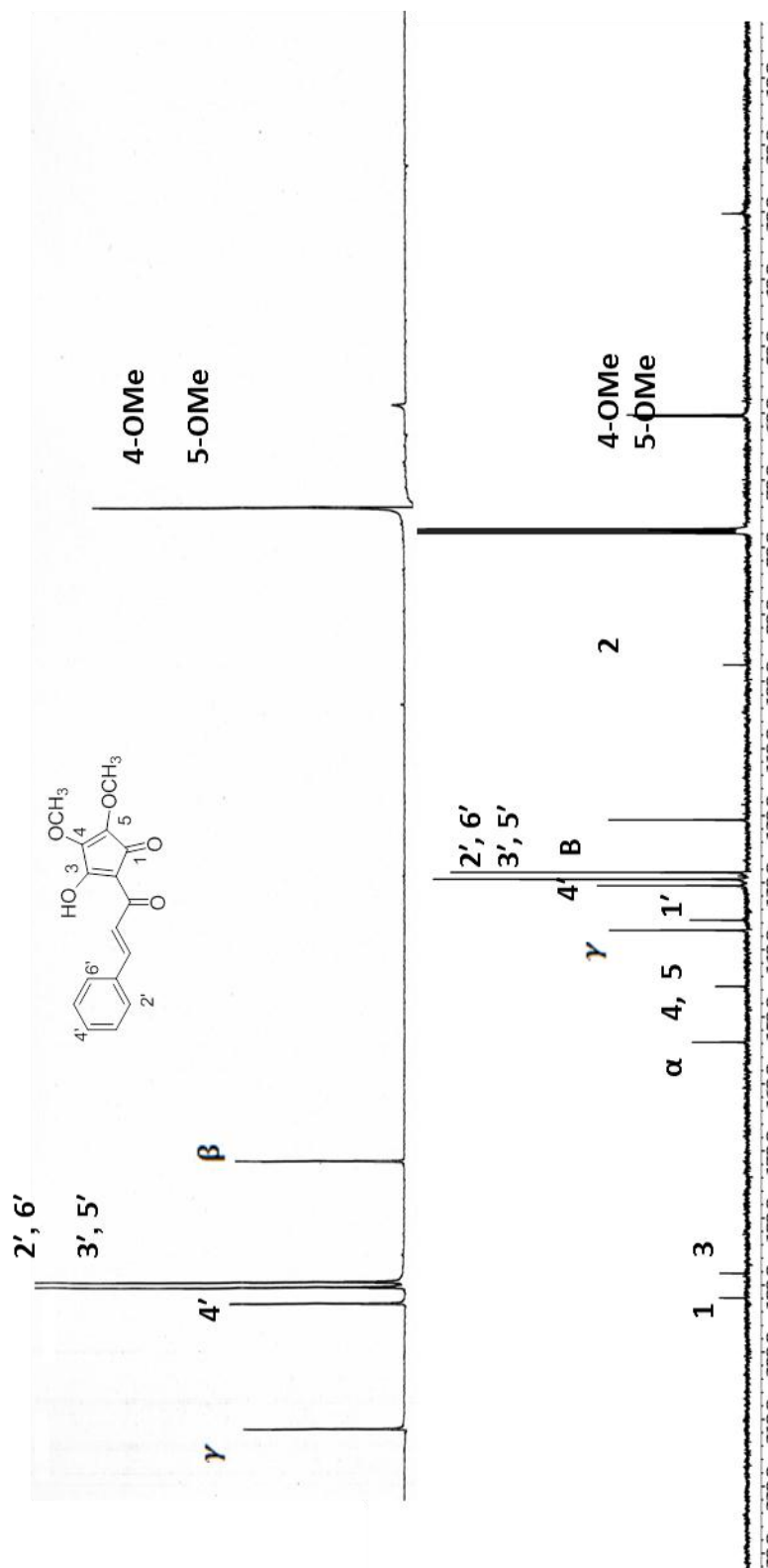


Figure 3.31: ^{13}C NMR / DEPT spectrum of linderone A LOB25

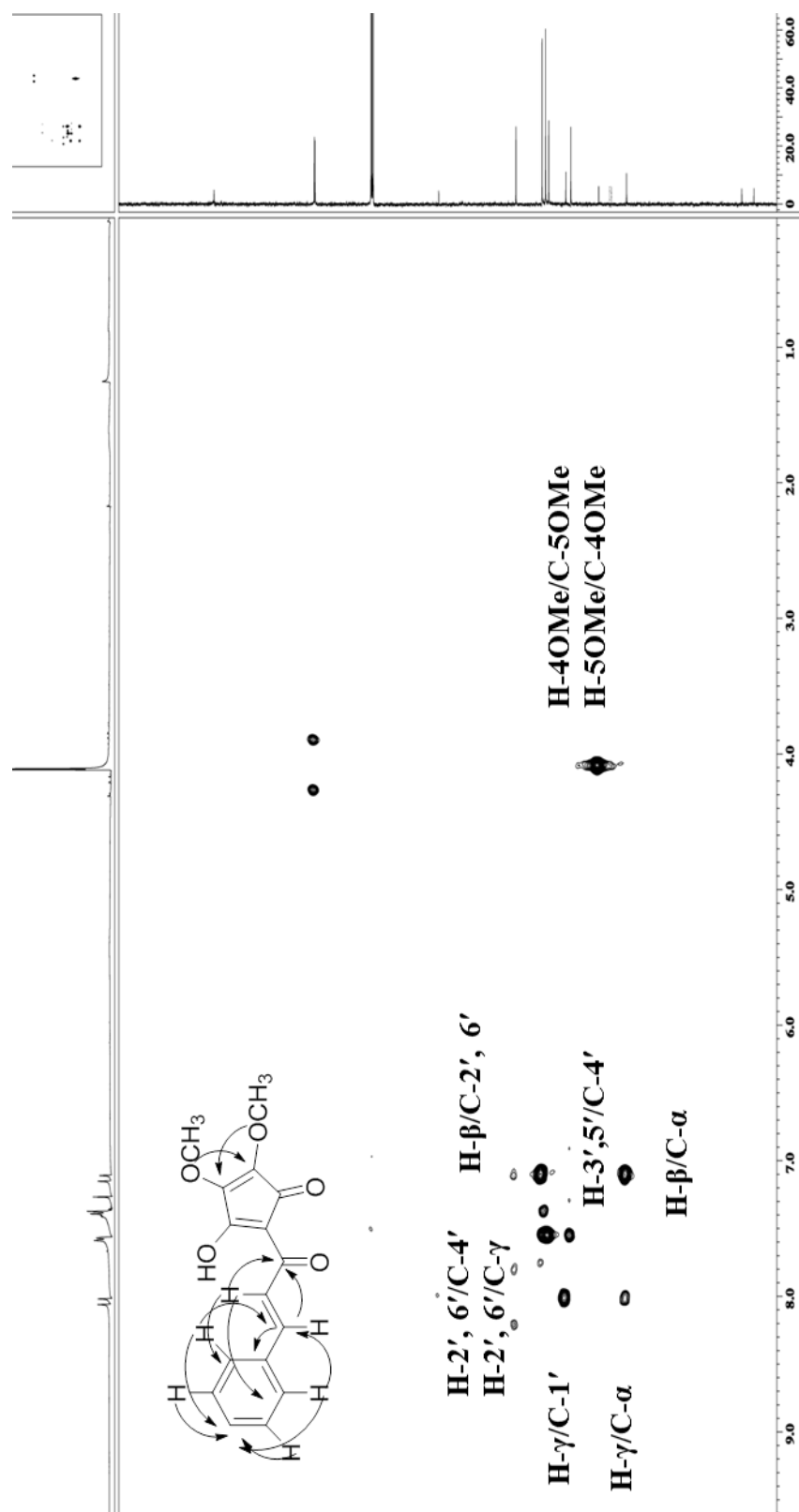


Figure 3.33: HMBC spectrum of Linderone A LOB25

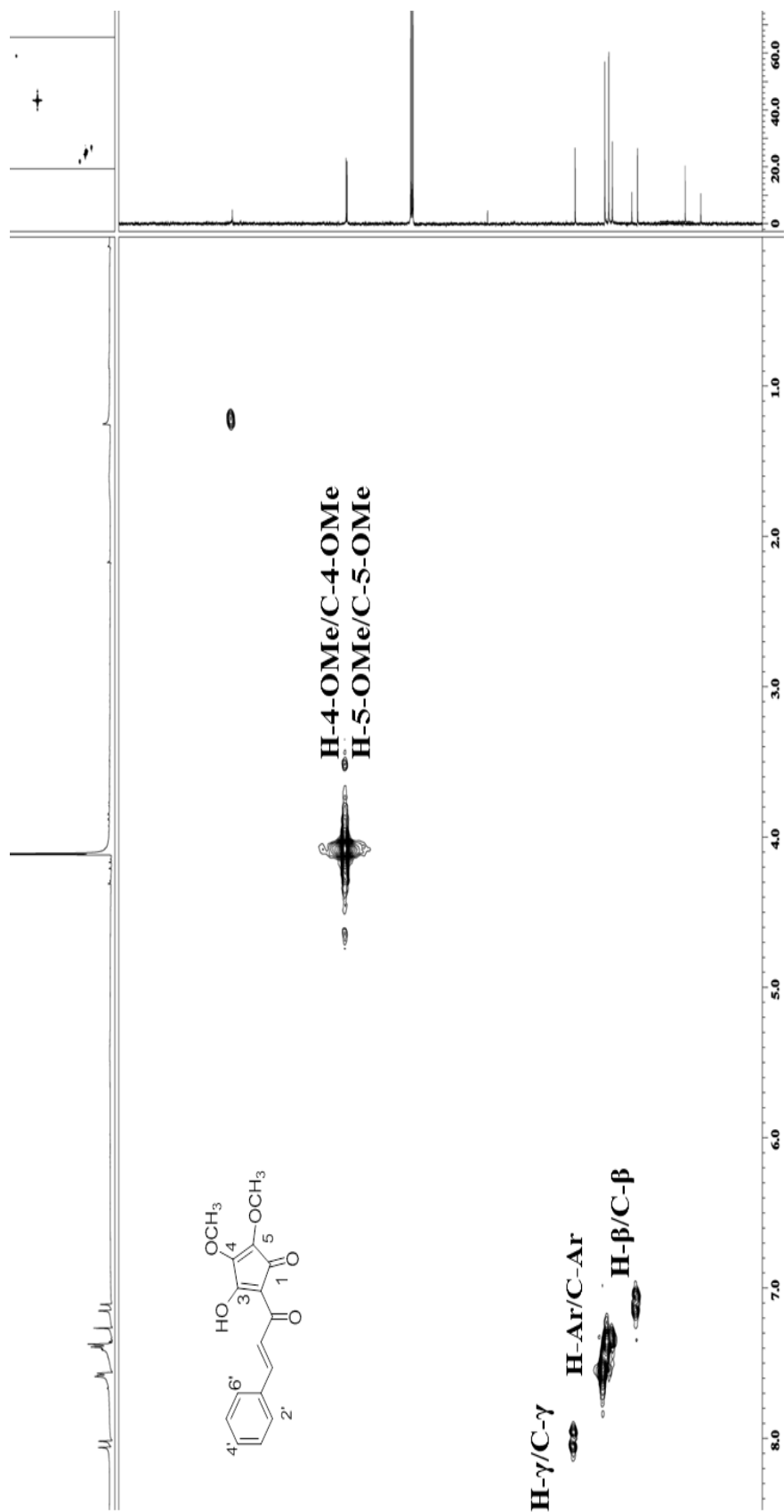
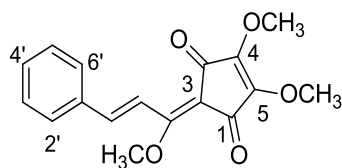


Figure 3.32: HMQC spectrum of Linderone A LOB25

3.1.7 Linderone **LOL34**: Methyllinderone



LOL34

Linderone **LOL34** with IUPAC name (*E*)-2-(1-methoxy-3-phenylprop-2-en-1-ylidene)-4, 5-dimethoxycyclopent-4-ene-1, 3-dione was isolated as a yellow amorphous solid. The UV spectrum exhibited absorption maxima at λ_{\max} (MeOH) nm (log ϵ) 241 (0.908) and 357 (1.158). Its IR spectrum showed absorption bands at ν_{\max} 1702 cm^{-1} indicated the presence of carbonyl group. The LC-MS (positive mode) spectrum showed an intense pseudomolecular ion peak, $[\text{M}]^+$ at m/z 300.88 corresponding to the molecular formula of $\text{C}_{17}\text{H}_{16}\text{O}_5$ (Oh et al., 2005).

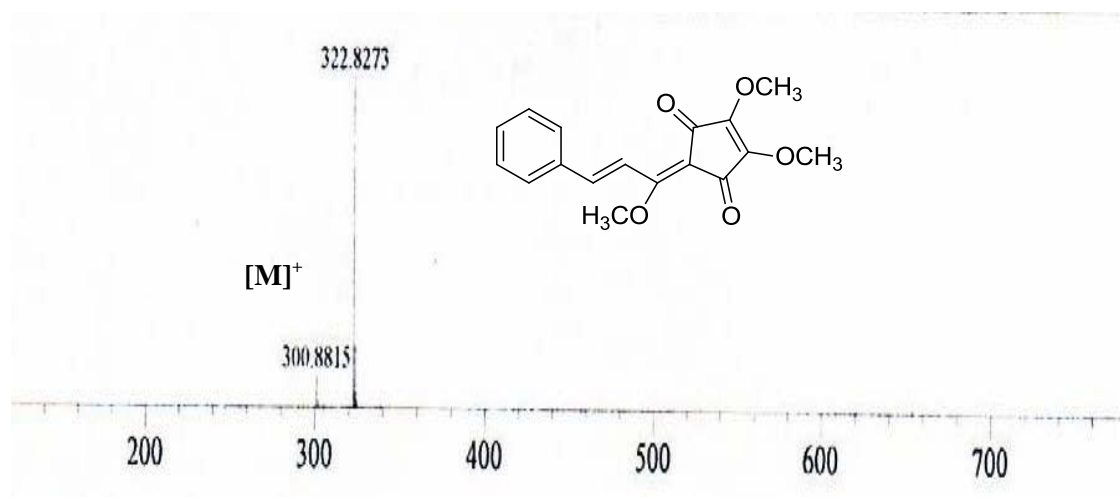


Figure 3.34: LC-MS Spectrum of methyllinderone **LOL34**

The ^1H NMR (Table 3.9, Figure 3.35), ^{13}C -NMR, COSY, HMQC and HMBC spectra showed the same pattern with that of linderone **LOB28** except for the

hydroxyl group in **LOB28** was replaced by methoxyl group in **LOL34**. The methoxyl group at C- α appeared at δ 4.32 in ^1H -NMR and δ 64.4 in ^{13}C -NMR (Table 3.9, Figure 3.36) (oh et al ., 2005).Based on the spectroscopic data of **LOL34** and comparison with the literature values, it was confirmed that compound **LOL34** was (*E*)-2-(1-methoxy-3-phenylprop-2-en-1-ylidene)-4, 5-dimethoxycyclopent-4-ene-1, 3-dione or methyllinderone.

Table 3.9: ^1H NMR (400 MHz) and ^{13}C NMR (100 MHz) spectral data of Methyllinderone **LOL34**

Position	^1H -NMR(δ , <i>J</i> in Hz)	^{13}C -NMR (δC)
1	-	188.7
2	-	110.1
3	-	185.9
4	-	150.2
5	-	148.4
α	-	165.3
β	7.52 (1H, <i>d</i> , 17.5)	120.2
γ	7.95 (1H, <i>d</i> , 15.8)	142.5
1'	-	135.7
2',6'	7.58 (2H, <i>m</i>)	129.1
3',5'	7.52 (2H, <i>m</i>)	128.5
4'	7.52 (H, <i>m</i>)	131.4
4,5-OMe	4.21(3H, <i>s</i>)	60.0
α -OMe	4.32 (3H, <i>s</i>)	64.4

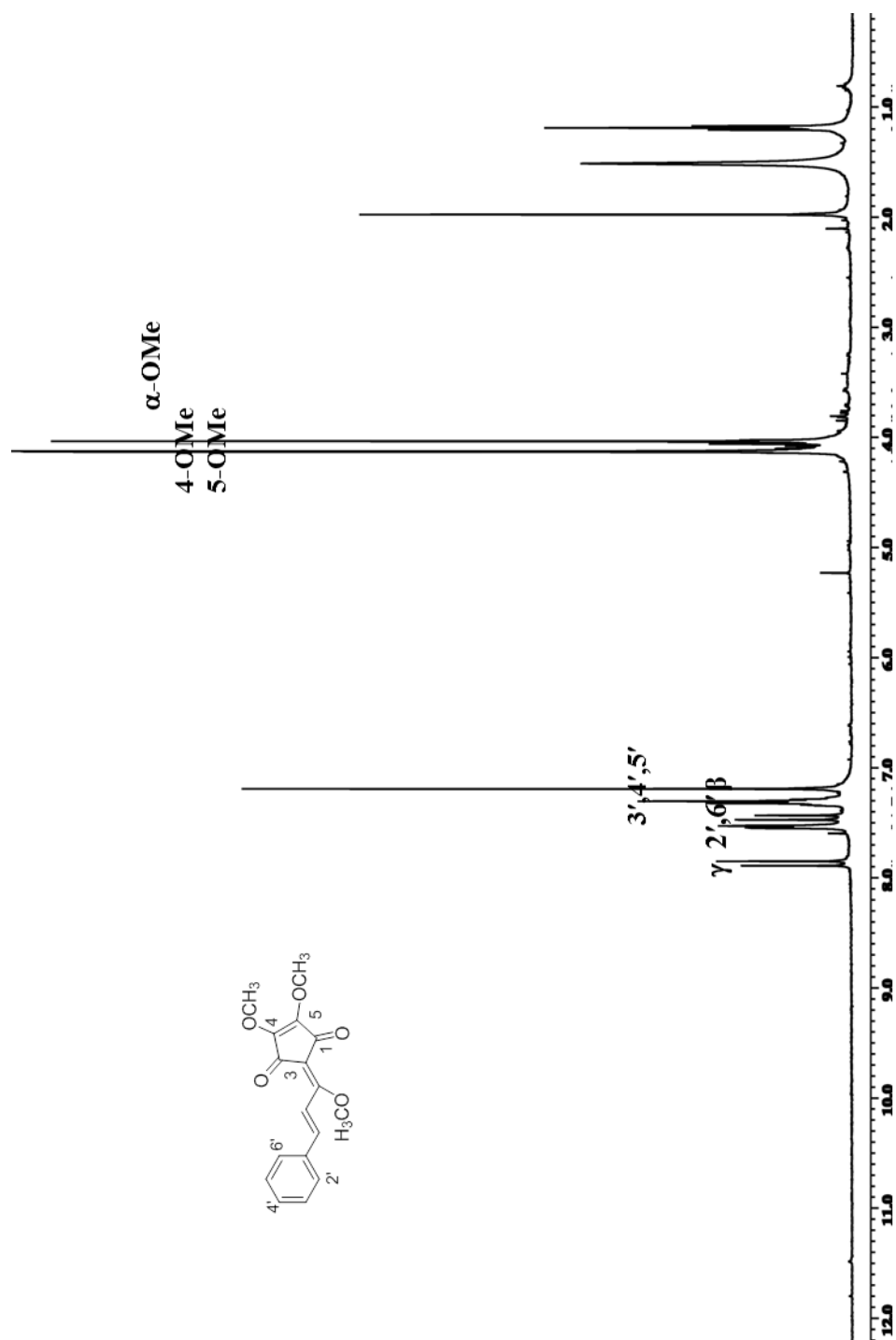


Figure 3.35: ^1H NMR spectrum of Methylinderone LOL34

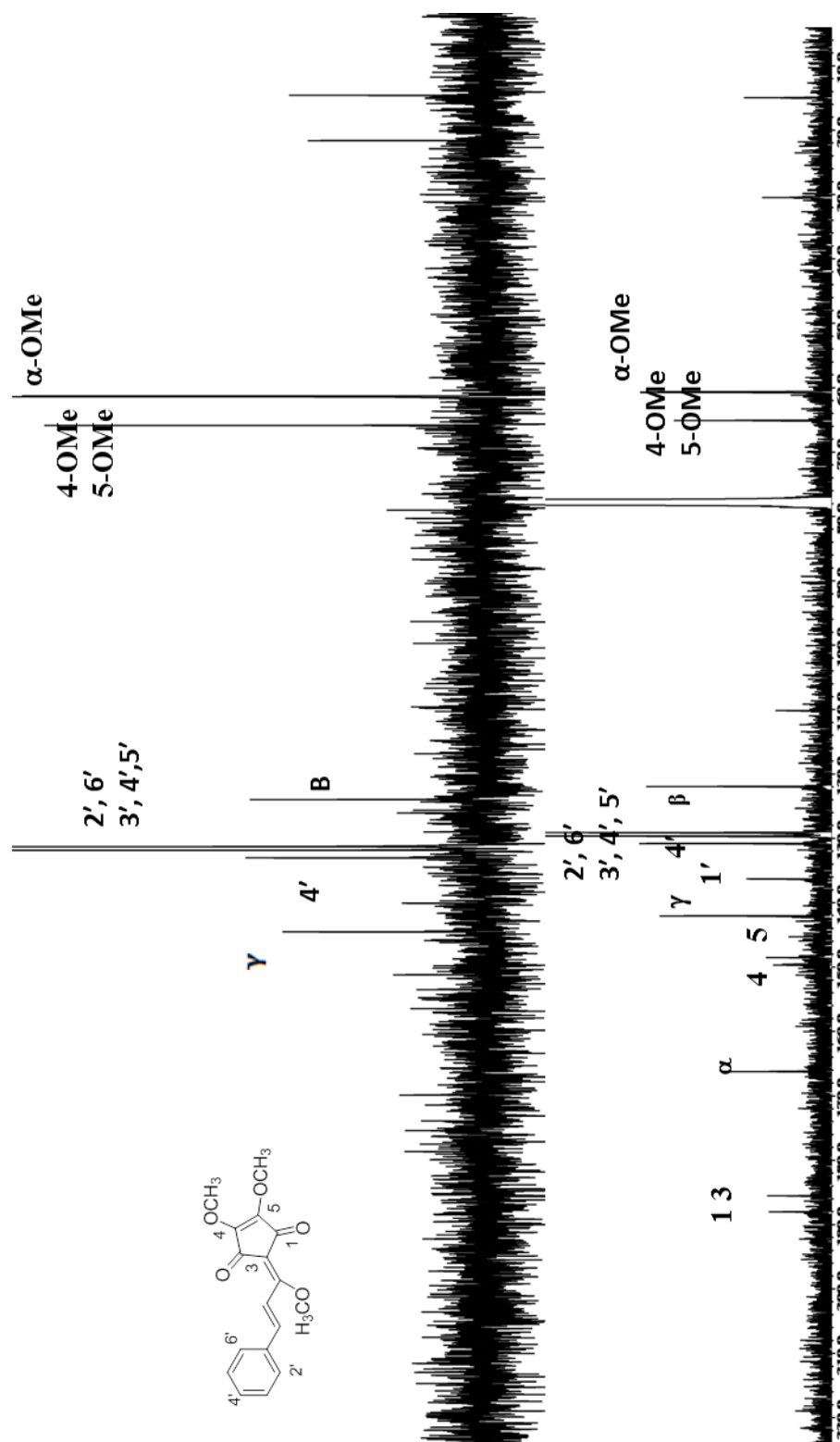
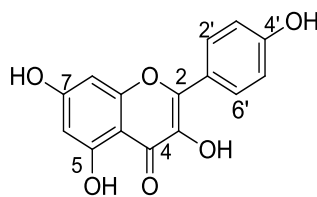


Figure 3.36: ¹³C NMR / DEPT spectrum of Methylinderone LOL34

3.1.8 Flavonol LOL5: Kaempferol



LOL5

Flavonol **LOL5** with IUPAC name 3, 5, 7-trihydroxy-2-(4-hydroxy phenyl)-4H-chromen-4-one) was afforded as pale yellow amorphous solid. The UV spectrum exhibited absorption maxima at λ_{\max} (MeOH) nm (log ϵ) 253 (0.434) and 364(0.616). The IR spectrum showed absorption bands at ν_{\max} 3431 cm^{-1} indicated the presence of hydroxyl group and 1646 cm^{-1} for carbonyl group stretching. The LC-MS (negative mode) spectrum showed an intense pseudomolecular ion peak, $[\text{M}-1]^+$ at m/z 285.04 corresponding to the molecular formula of $\text{C}_{15}\text{H}_{10}\text{O}_6$.

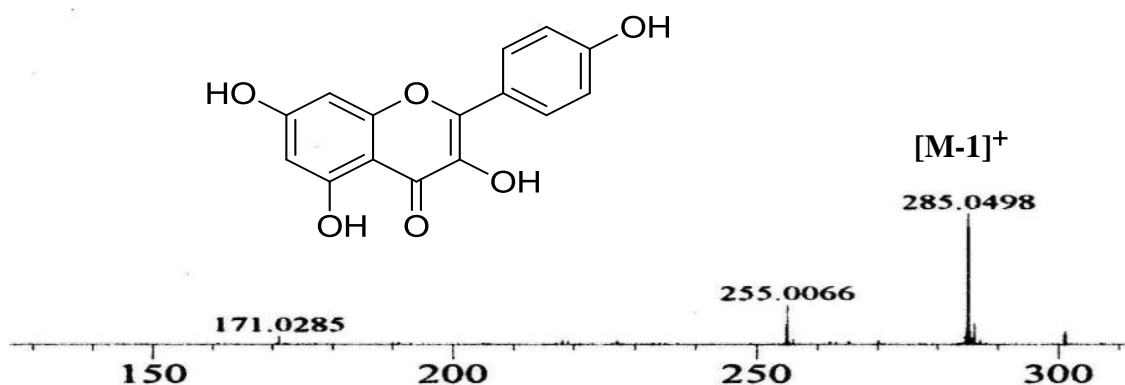


Figure 3.37: LC-MS Spectrum of Kaempferol **LOL5**

The ^1H NMR spectrum (Table 3.10, Figure 3.38) showed a one proton singlet at δ 6.15 which was assigned for aromatic proton at H-6 and one proton singlet δ 6.41 for aromatic proton at H-8. Furthermore, the peak with two protons at δ 6.91 appeared as doublet of doublet was assigned to H-2' and H-6'. Another doublet of doublet peak with two protons at δ 8.00 was assigned for H-5' and H-3'. The COSY spectrum (Table 3.10, Figure 3.39) showed the proton-proton correlation for H-2'/H-3' and H-5'/H-6'.

The ^{13}C NMR spectrum (Table 3.10, Figure 3.40) established the resonances of fifteen carbon atoms. Six sp^2 methines appeared at δ 92.1 (C-6), 95.3 (C-8), 114.2 (C-3', 5'), 131.8 (2',6') and nine quaternary carbons resonated at δ 110.4 (C-4a), 125.5 (C-1'), 135.4 (C-3), 142.7 (C-2), 142.7 (C-4'), 152.1 (C-8a), 155.8 (C-5), 161.2 (C-7) and 198.5 (C-4).

Based on the spectroscopic data of **LOL5** and comparison with the literature values, it was confirmed that compound **LOL5** was kaemferol (Kim et al., 2006; Rao et al., 2009).

Table 3.10: ^1H NMR (400 MHz) and ^{13}C NMR (100 MHz) spectral data of Kaempferol **L0L5**

Position	^1H -NMR(δJ in Hz)	^{13}C -NMR (δc)
1	-	-
2	-	142.7
3	-	135.4
4	-	198.5
4a	-	110.4
5	-	155.8
6	6.15 (1H, <i>s</i>)	92.1
7	-	161.2
8	6.41(1H, <i>s</i>)	95.3
8a	-	152.1
1'	-	125.5
2',6'	8.00 (2H, <i>dd</i> , 8.5)	131.8
3',5'	6.91(2H, <i>dd</i> , 8.6)	114.2
4'	-	142.7

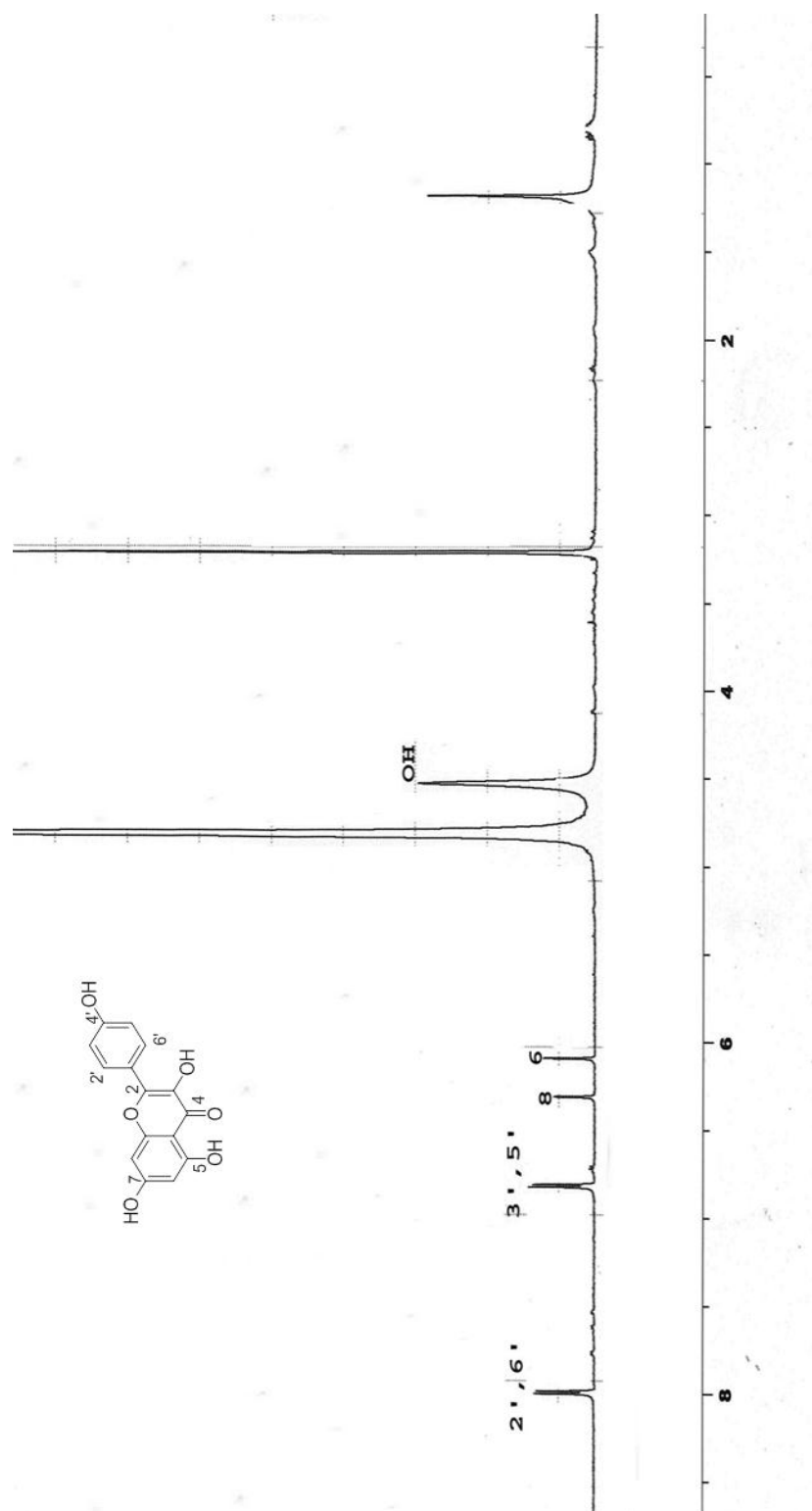


Figure 3.38: ^1H NMR spectrum of Kaempferol LOL5

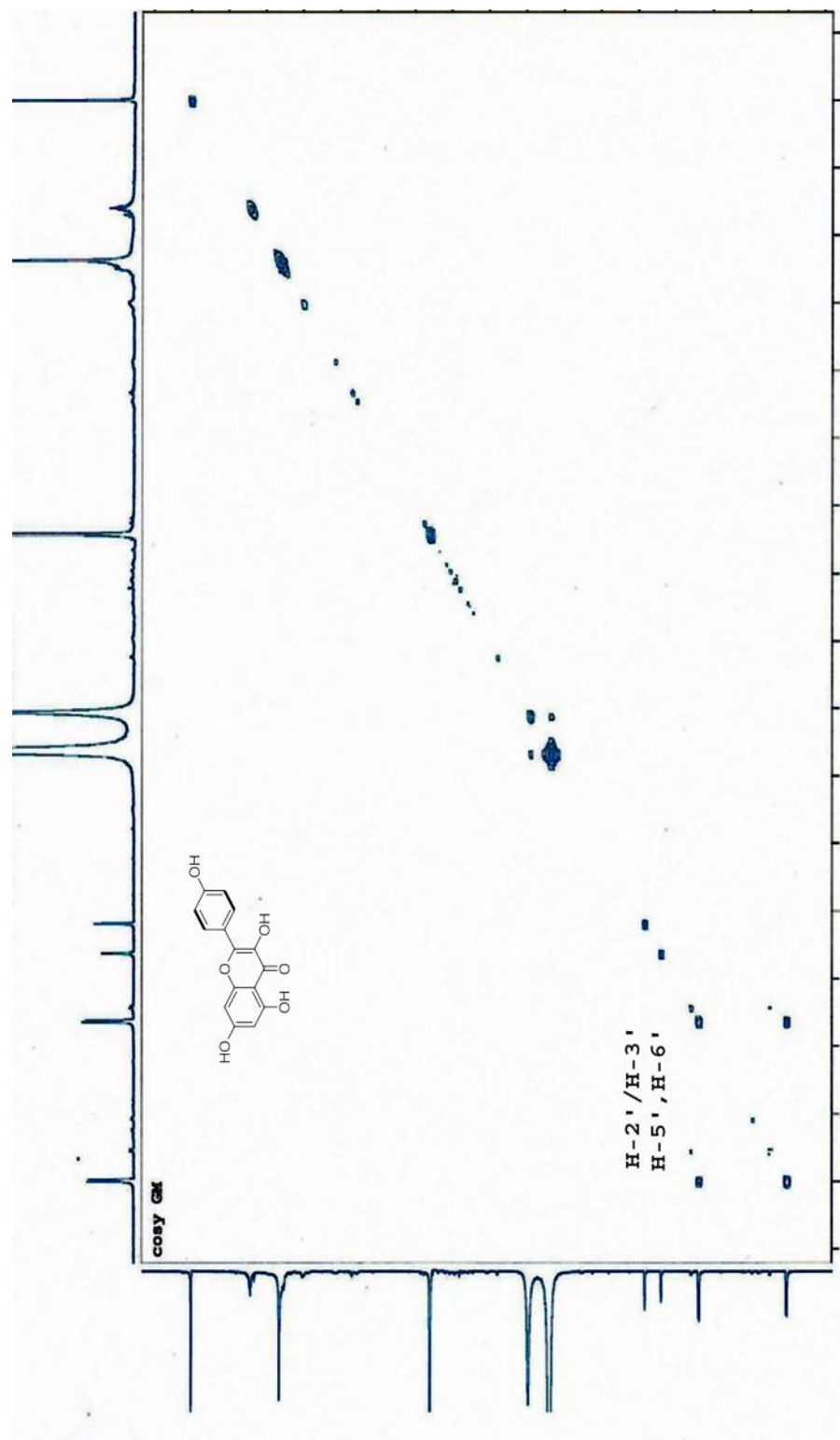


Figure 3.39: COSY spectrum of Kaempferol **L0L5**

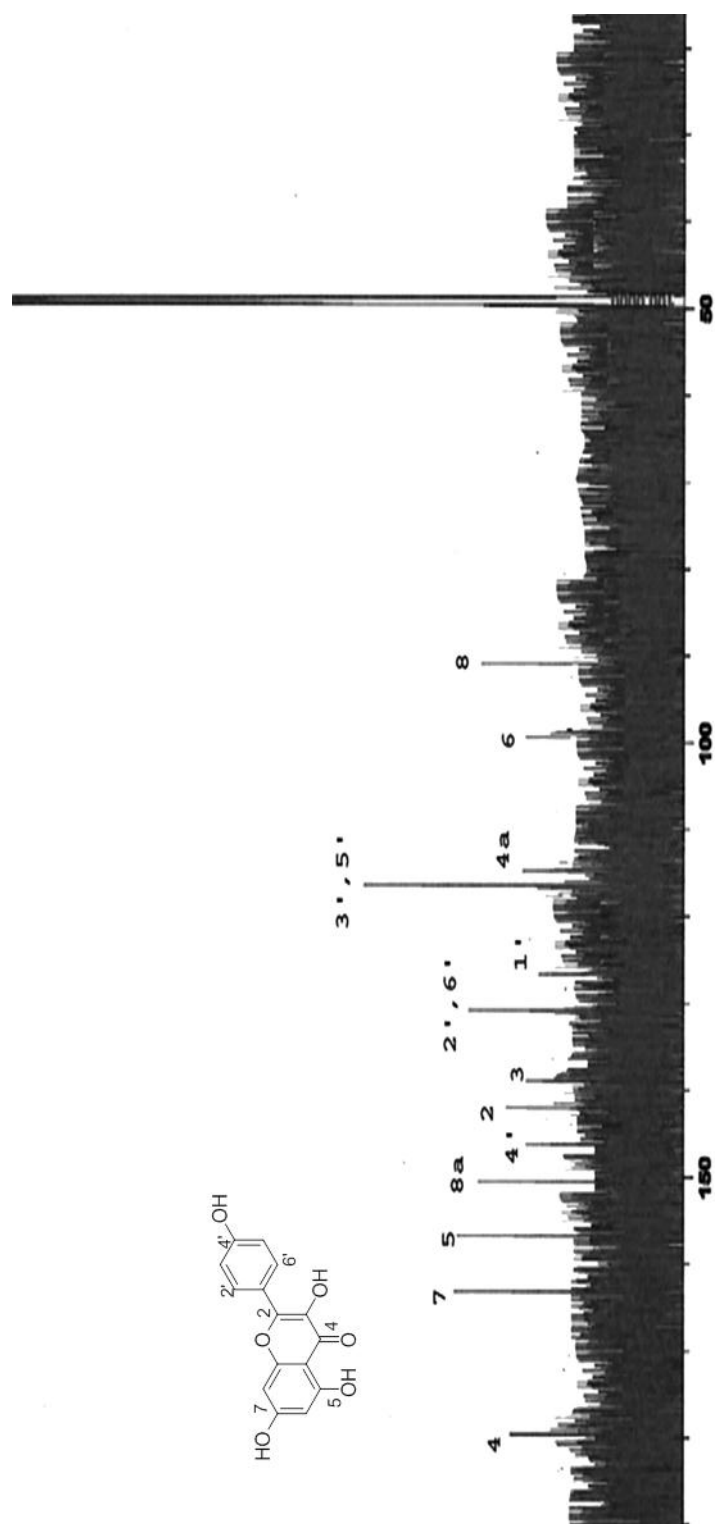
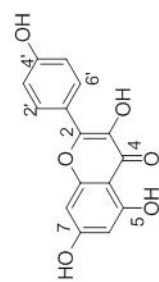
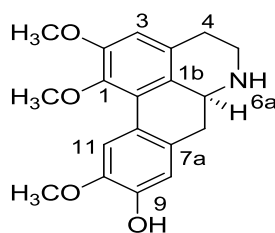


Figure 3.40: ^{13}C - NMR spectrum data of Kaempferol LOL5

3.1.9 Alkaloid LOL20: (+)-laurotetanine



LOL 20

Alkaloid **LOL20** laurotetanine with IUPAC name 4H-dibenzoquinolin-9-ol, 5, 6, 6a,7-tetrahydro-1,2,10-trimethoxy with $[\alpha]_D^{25} = +29.4^\circ$ (2.00×10^{-4} g/100 mL, MeOH) was afforded as a dark brown amorphous solid (Govindachari et al., 1977). The UV spectrum showed absorptions at λ_{\max} (MeOH) nm (log ϵ), 217 (2.345) and 242 (3.098) nm thus suggesting a 1, 2, 9, 10-tetrasubstituted aporphine skeleton. The IR spectrum showed absorption peak at 3429 cm^{-1} indicated presence of NH group and also hydroxyl group (Guinaudeau et al., 1994). The LC-MS spectrum showed an intense pseudomolecular ion peak, $[M+H]^+$ at m/z 328.1566 corresponding to the molecular formula of $C_{19}H_{21}NO_4$.

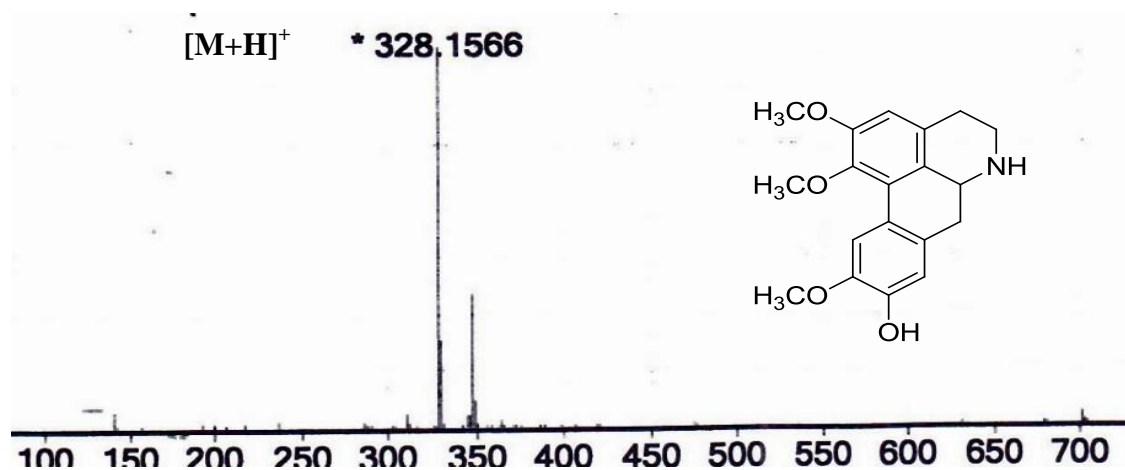


Figure 3.41: LC-MS Spectrum of (+)-laurotetanine **LOL20**

The ^1H -NMR spectrum of **LOL20** (Table 3.11, Figure 3.42) exhibited three distinct methoxyl groups which were observed as singlets at δ 3.64, δ 3.87 and δ 3.89 corresponding to $\text{C}_1\text{-OMe}$, $\text{C}_2\text{-OMe}$ and $\text{C}_{10}\text{-OMe}$ respectively. Seven aliphatic protons were observed at a high field region between δ 2.71- 3.81 corresponding to H-4, H-5, H-6a and H-7. One proton singlet observed at δ 6.57 which was assigned to H-3 confirming the substitutions at C-1 and C-2. Furthermore, the singlet at δ 6.77 was attributed to H-8. This value is typical of that 9, 10-substitution pattern (Guinaudeau et al., 1975; Johns et al., 1970). It was clear that, the low field signal of H-11 at δ 8.06 suggested that C-10 was substituted by a methoxyl group.

The ^{13}C -NMR and DEPT spectra (Table 3.11, Figure 3.43) established the resonances of nineteen carbons three methoxyls resonated at δ 60.2 (C-1), 56.1 (C-2) and 55.9 (C-10) , three methylenes at δ 29.0 (C-4), 43.1 (C-5) and 36.5 (C-7), four methines at δ 110.8 (C-3), 53.7 (C-6a), 113.9 (C-8) and 111.3 (C-11) and nine quaternary carbons at δ 144.3 (C-1), 152.2 (C-2) , 129.0 (C-3a), 126.8 (C-1a), 127.4 (C-1b), 124.0 (C-11a), 129.7 (C-7a), 144.9 (C-10) and 145.3 (C-9).

The HMQC spectrum (Table 3.11, Figure 3.44) showed the connectivity between proton and carbon: H-3/C-3, H-4/C-4, H-7/C-7, H-6a/C-6a, H-5/C-5, H-8/C-8, H-1OMe/C-1OMe, H-2OMe/C-2OMe, H-10OMe/C-10OMe and H-11/C-11.

In the HMBC spectrum (Table 3.11, Figure 3.45) the cross-peaks were observed between H-3 to C-4, C-1b, C-1, C-2, H-4 to C6a, C1b, H-5 to C-6a, C-3a, H-7 to C-6a, C-8, C-1b, C-11, H-8 to C-10, C-11a, C-7, H-11 to C-7a, C-9, 10- OCH_3 to C-10, 2- OCH_3 to C-2 and 1- OCH_3 /C-1.

The structural elucidation was completed by the help of the 2D experiment. according to comparison of the spectroscopic data obtained with the literature values, it was confirmed that alkaloid **LOL20** was laurotetanine (Mukhtar et al., 2003).

Table 3.11: ^1H NMR (400 MHz) and ^{13}C NMR (100 MHz) spectral data of (+)-laurotetanine **LOL20**

Position	^1H -NMR(δJ in Hz)	^{13}C -NMR (δc)
1	-	144.3
1a	-	126.8
1b	-	127.4
2	-	152.2
3	6.57(1H, <i>s</i>)	110.8
3a	-	129.0
4	2.74 (2H, <i>dd</i> , 13.6, 4.6)	29.0
5	3.01 (2H, <i>dd</i> , 12.9, 4.1) 3.6, <i>m</i>	43.1
6a	3.80 (1H, <i>dd</i> , 4.4, 13.2)	53.7
7	2.64 (2H, <i>d</i> , 13.6)	36.5
7a	-	129.7
8	6.77 (1H, <i>s</i>)	113.9
9	-	145.3
10	-	144.9
11	8.06 (1H, <i>s</i>)	111.3
11a	-	124.0
1-OCH ₃	3.64 (3H, <i>s</i>)	60.2
2-OCH ₃	3.86 (3H, <i>s</i>)	56.1
10-OCH ₃	3.87(3H, <i>s</i>)	55.9

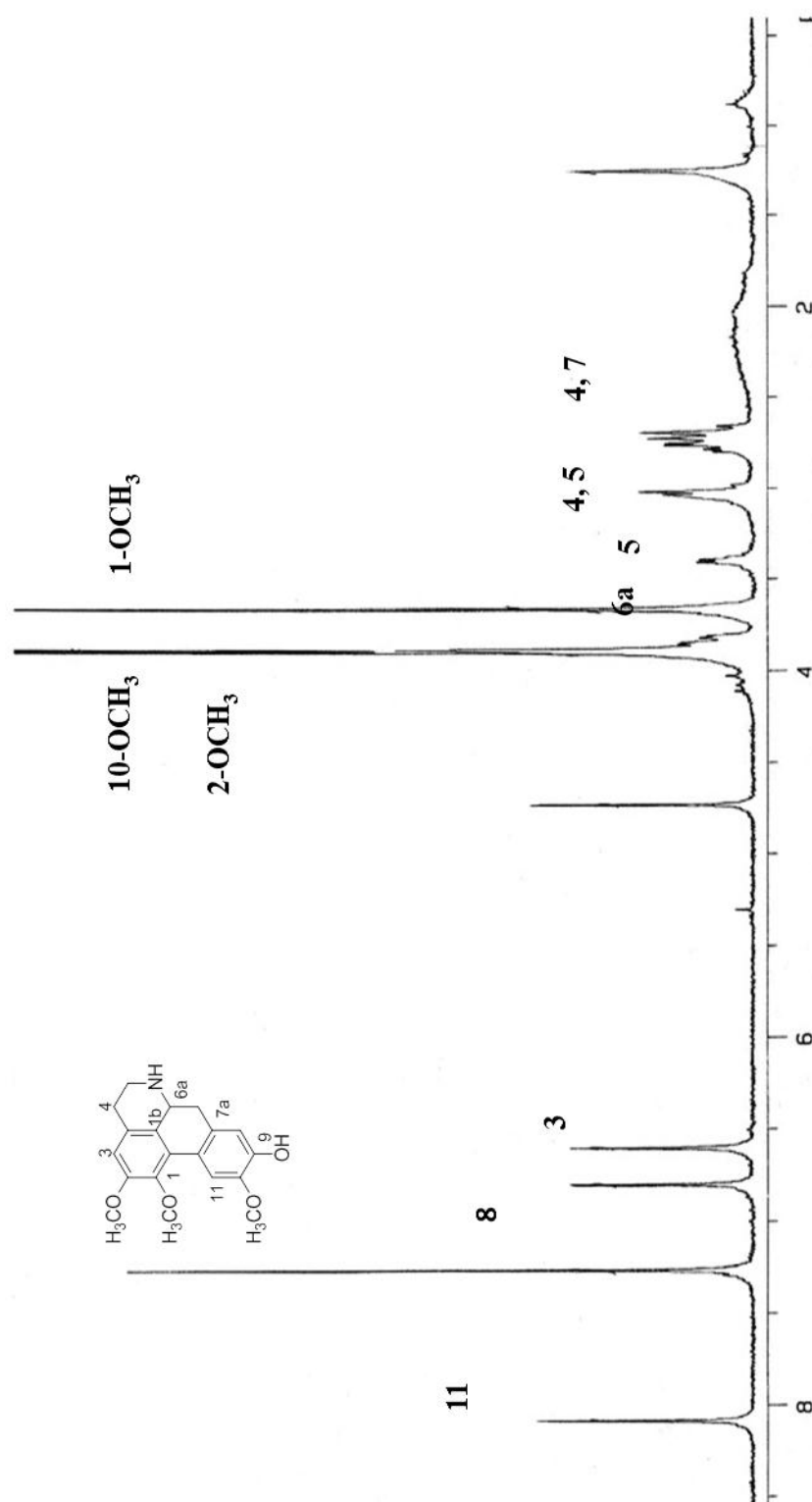


Figure 3.42: ^1H -NMR spectrum of (+)-laurotetanine LOL20

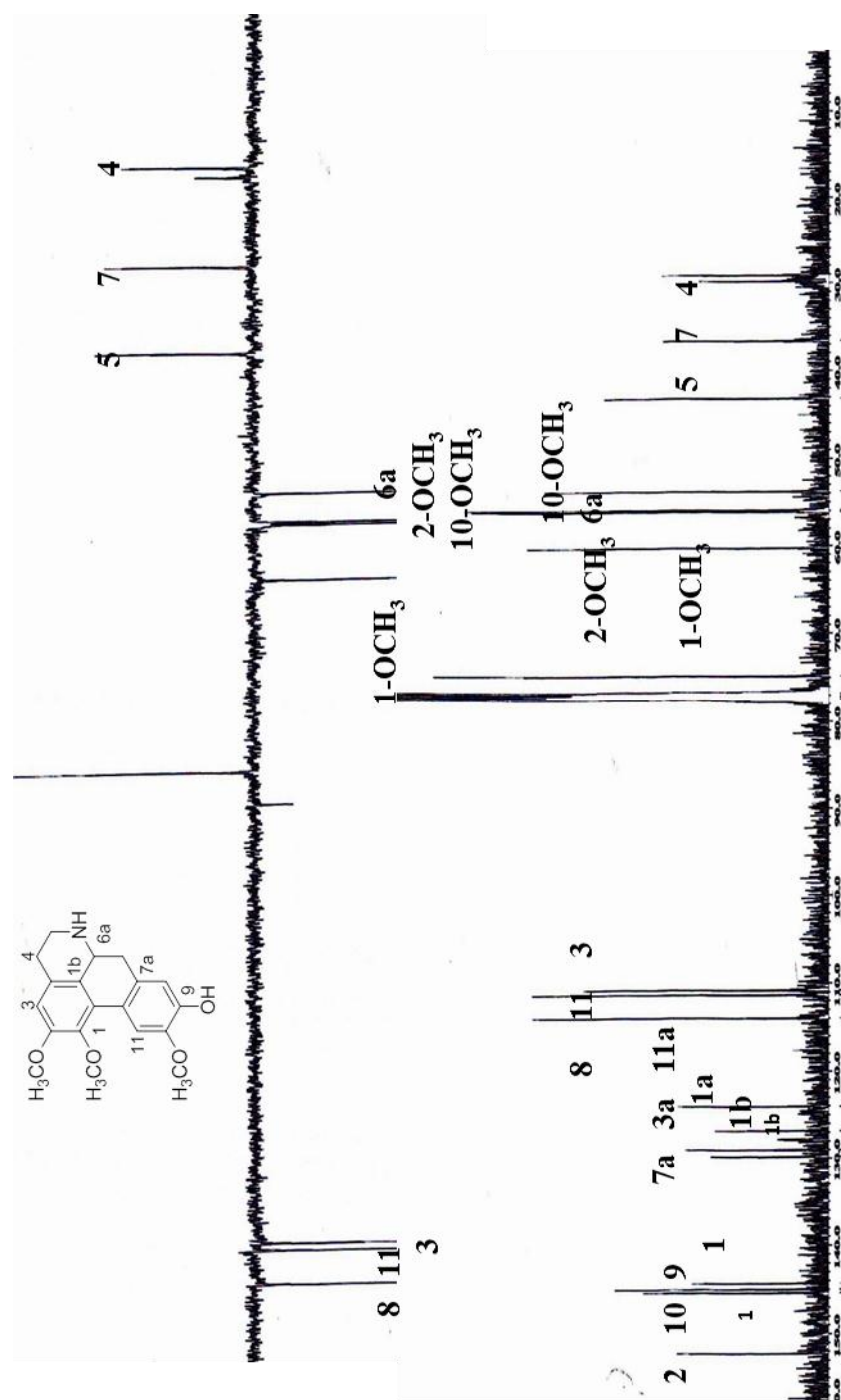


Figure 3.43: ^{13}C NMR/DEPT spectrum of (+)-laurotetanine LOL20

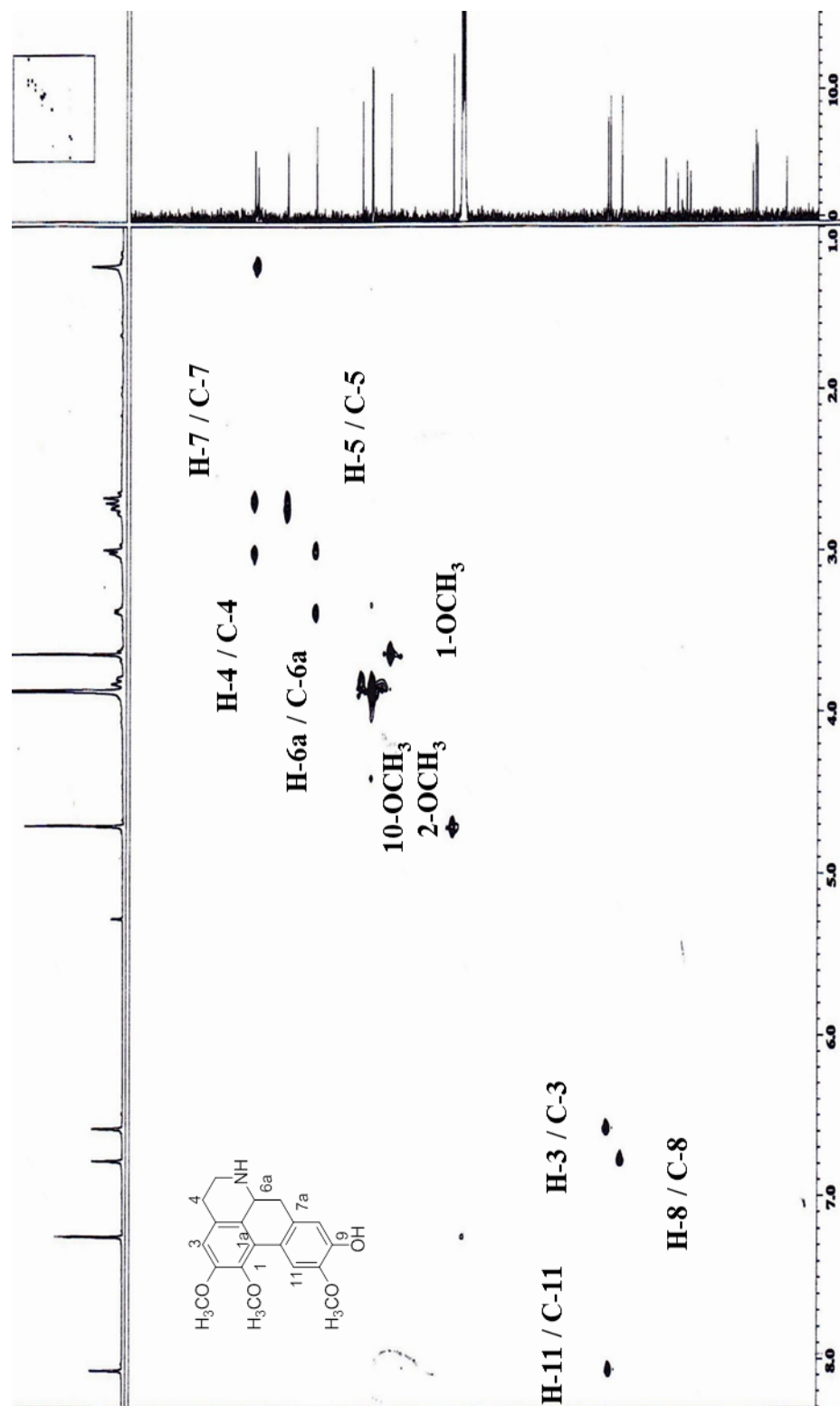
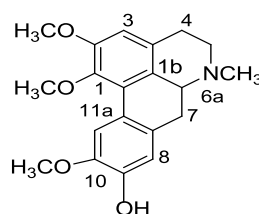


Figure 3.44: HMQC spectrum of (+)-laurotetanine LOL20

3.1.10 Alkaloid **LOL35**: *N*-Methyllaurotetanine



LOL 35

Alkaloid **LOL35** *N*-methyllaurotetanine with $[\alpha]_D^{25} = +15.0$ (2.00×10^{-4} g/100 mL, MeOH) was isolated as a brown amorphous solid and its UV spectrum showed absorptions at λ_{\max} (MeOH) nm (log ϵ) 222 (2.098), 280 (1.987) and 320 (3.564) nm (Goodwin et al., 1958) indicated the aporphine substituted at positions C-1, C-2, C-9 and C-10 (Shamma et al., 1964). The IR spectrum showed a broad band of hydroxyl absorption at 3391 cm^{-1} . The LC-MS revealed the presence a pseudomolecular ion peak, $[M]^+$ at m/z 401.1625 consistent with the molecular formula of $\text{C}_{24}\text{H}_{35}\text{NO}_4$.

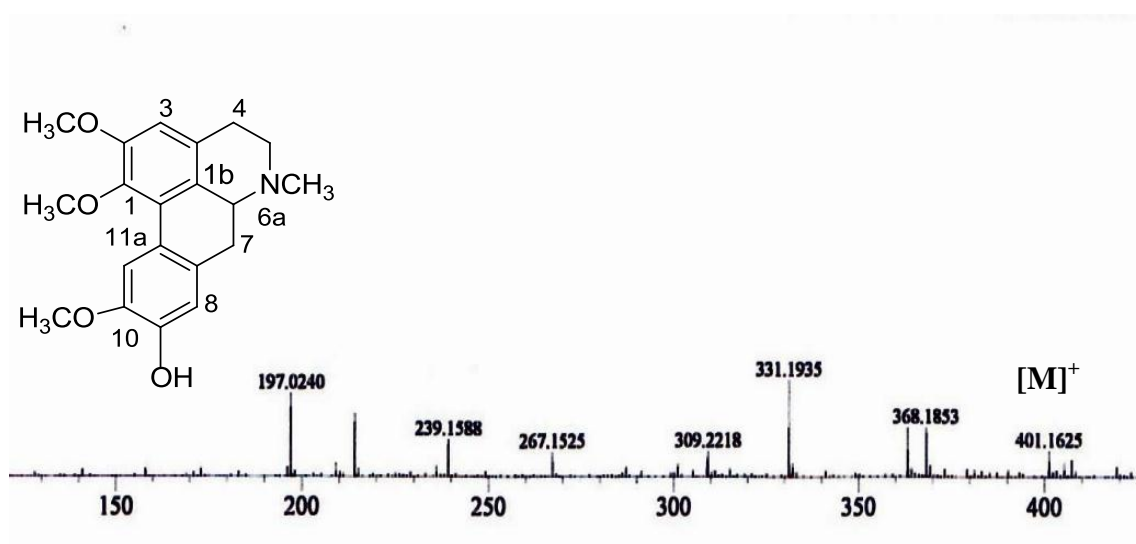


Figure 3.46: LC-MS Spectrum of *N*-methyllaurotetanine **LOL35**

The ^1H and ^{13}C NMR spectrum (Table 3.12, Figure 3.47) of **LOL35** have similar structure as (+)-laurotetanine **LOL20** except that compound **LOL35** has *N*-methyl substitution (Wu et al. 1980).

Based on the spectroscopic data of **LOL35** and comparison with the literature values, it was confirmed that compound **LOL35** was known *N*-methyllaurotetanine.

Table 3.12: ^1H NMR (400 MHz) and ^{13}C NMR (100 MHz) spectral data of *N*-methyl laurotetanine **LOL35**

Position	^1H -NMR(δJ in Hz)	^{13}C -NMR (δc)
1	-	144.2
1a	-	127.1
1b	-	127.2
2	-	152.1
3	6.58 (1H, s)	110.3
3a	-	128.9
4	2.68 (2H, <i>d</i> , 3.6, 3.1)	29.2
5	2.51 (2H, <i>d</i> , 3.6, 3.0 (<i>dd</i> , 5.9, 11.9)	53.3
6a	2.99 (1H, <i>m</i>).2.6 (2H, <i>d</i> , 3.2)	62.6
7	2.95 (2H, <i>d</i> , 2.12)	34.3
7a	-	130.1
8	6.82 (1H, s)	113.9
9	-	144.8
10	-	145.3
11	8.06 (1H, s)	111.2
11a	-	124.0
1-OMe	3.65 (3H, s)	60.2
2-OMe	3.88 (3H, s)	55.8
10- OMe	3.90 (3H, s)	56.1
N-CH ₃	2.54 (3H, s)	44.0

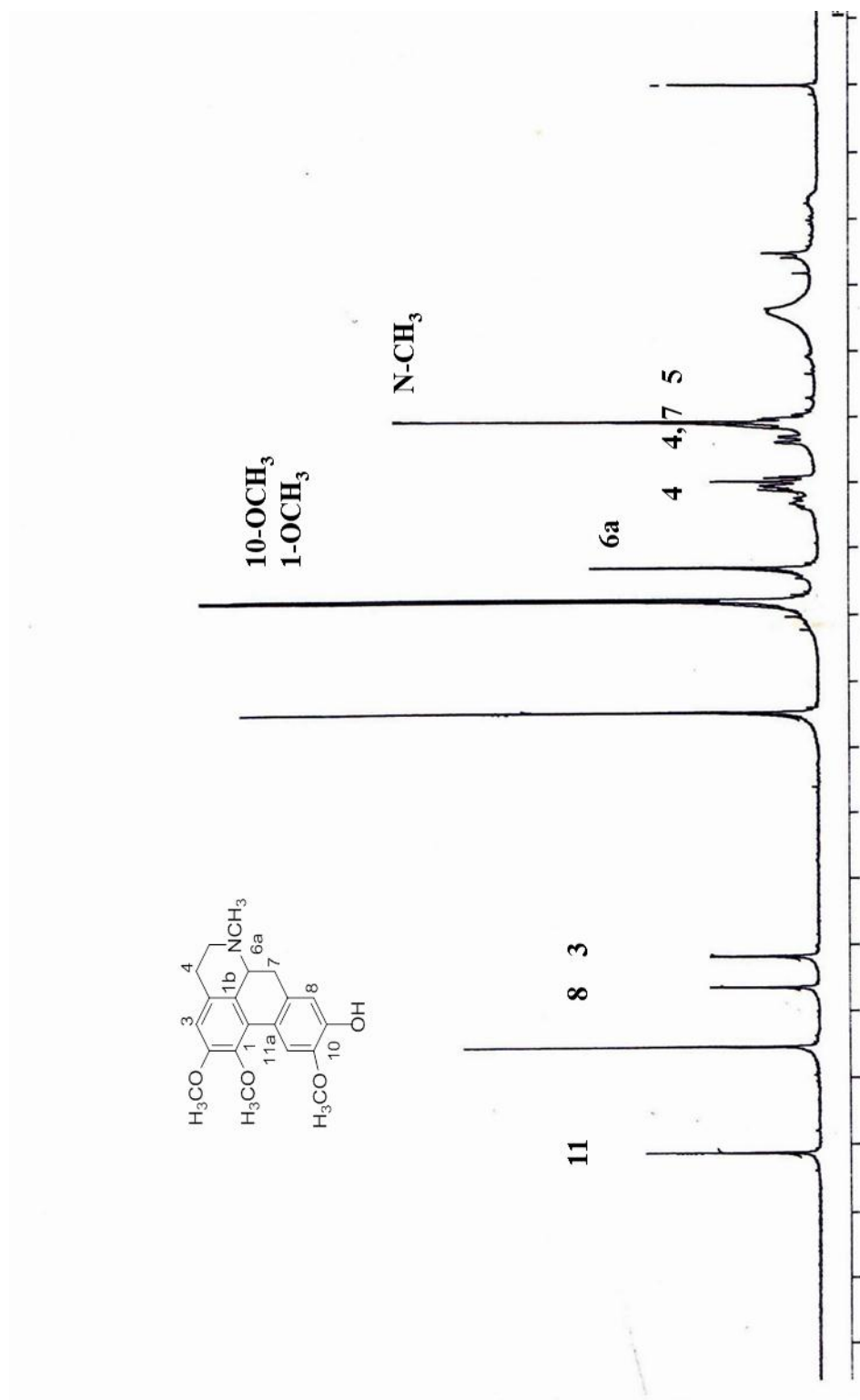


Figure 3.47: ^1H -NMR spectrum of *N*-methyl-laurotetanine **LOL35**

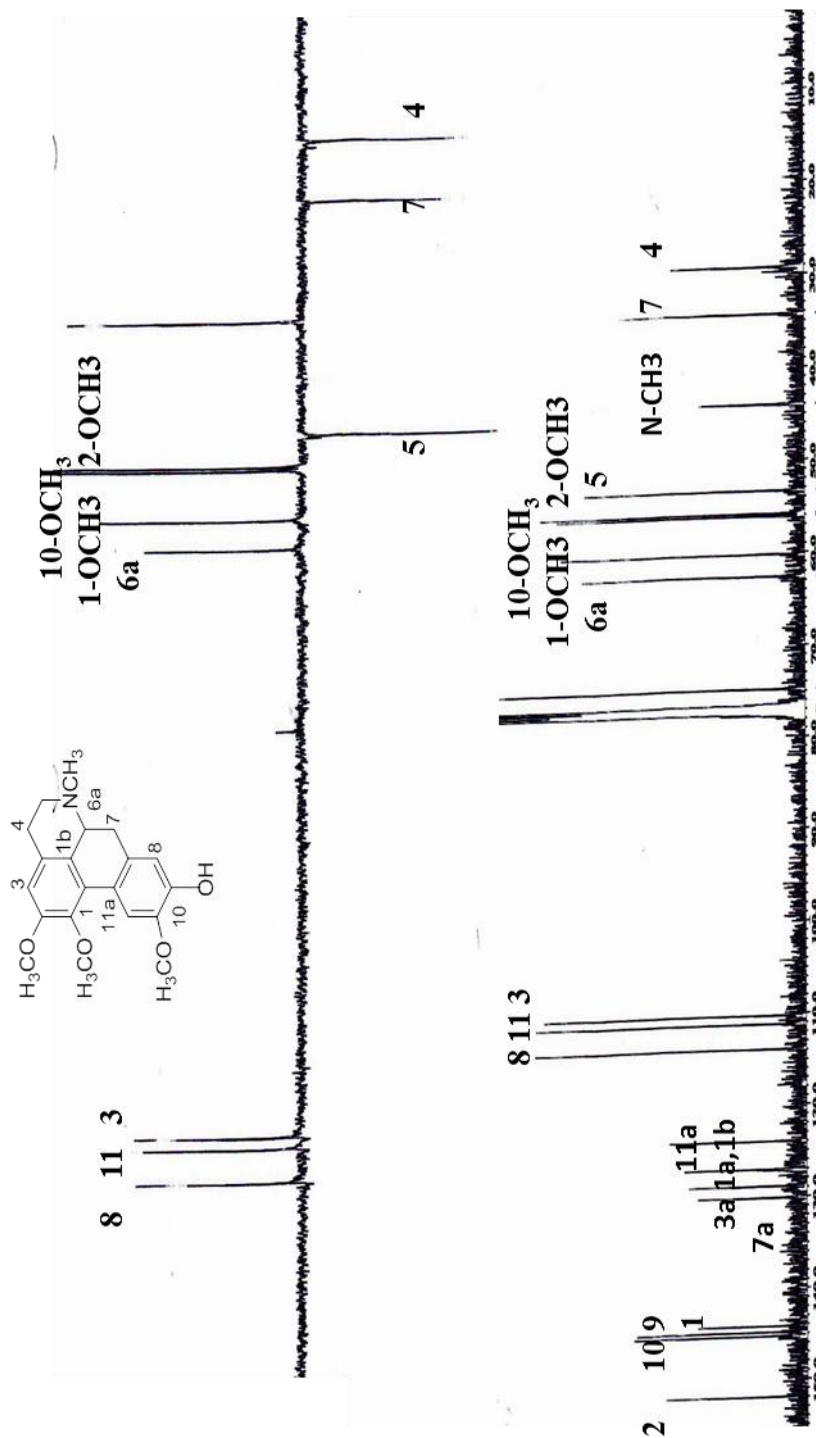
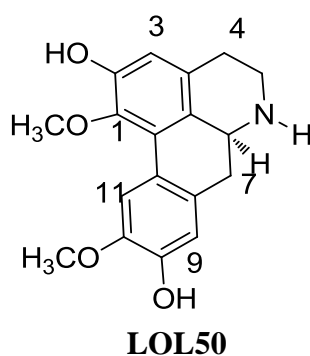


Figure 3.48: ¹³C NMR/DEPT spectrum of *N*-methyl-laurotetanine LOL35

3.1.11 Alkaloid **LOL50**: (+)-Norboldine



Alkaloid **LOL50**, Norboldine with $[\alpha]_D^{25} = +9.87$ (2.00×10^{-4} g/100 mL, MeOH), was isolated as a brown amorphous solid (Pachler et al., 1965). The UV spectrum showed absorptions λ_{\max} (MeOH) nm (log ϵ) at 276 (3.765) and 317 (2.987) nm (Sangster et al., 1965). The IR spectrum showed broad band at 3432 cm^{-1} due to the presence of OH and NH functional groups. The LC-MS revealed a pseudomolecular ion peak, $[M+H]^+$ at m/z 314.1397 suggesting a molecular formula of $C_{18}H_{19}NO_4$ (Guinaudeau et al., 1994).

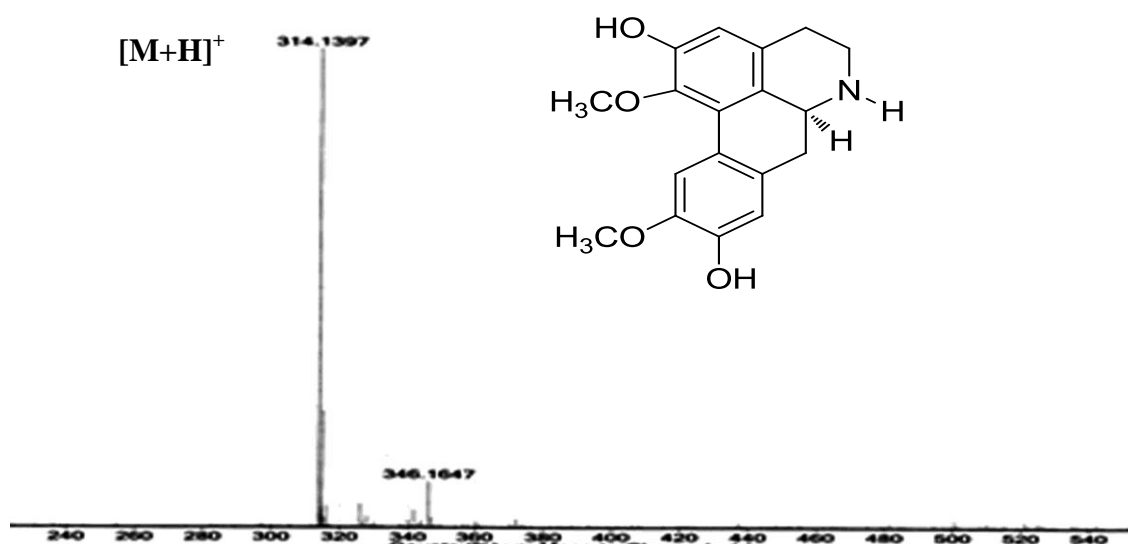


Figure 3.49: LC-MS Spectrum of (+)-norboldine **LOL50**

The ^1H and ^{13}C NMR spectra (Table 3.13, Figure 3.50) and (Table 3.13, Figure 3.51) of compound **LOL50** have the same pattern as **LOL20** except that the C-2 in **LOL50** bearing the OH group (Weber et al., 1986).

Based on the spectroscopic data of **LOL50** and comparison with the literature values, it was confirmed that compound **LOL50** was (+)- norboldine.

Table 3.13: ^1H NMR (400 MHz) and ^{13}C NMR (100 MHz) spectral data of (+) - Norboldine **LOL50**

Position	^1H -NMR(δ , J in Hz)	^{13}C -NMR (δc)
1	-	148.1
1a	-	125.6
1b	-	128.0
2	-	141.9
3	6.58 (1H, s)	113.7
3a	-	130.2
4	2.68 (1H, m , H_α)	29.0
	2.91(1H, m , H_β)	
5	2.94 (1H, m , H_α)	43.3
	3.29 (1H, m , H_β)	
6a	3.72 (1H, dd , 4.2, 13.1)	53.8
7	2.60 (2H, m)	36.7
7a	-	130.1
8	6.74 (1H, s)	114.1
9	-	145.1
10	-	145.6
11	7.84 (1H, s)	110.2
11a	-	123.7
1-OCH ₃	3.29 (3H, s)	60.4
10-OCH ₃	3.72 (3H, s)	56.2

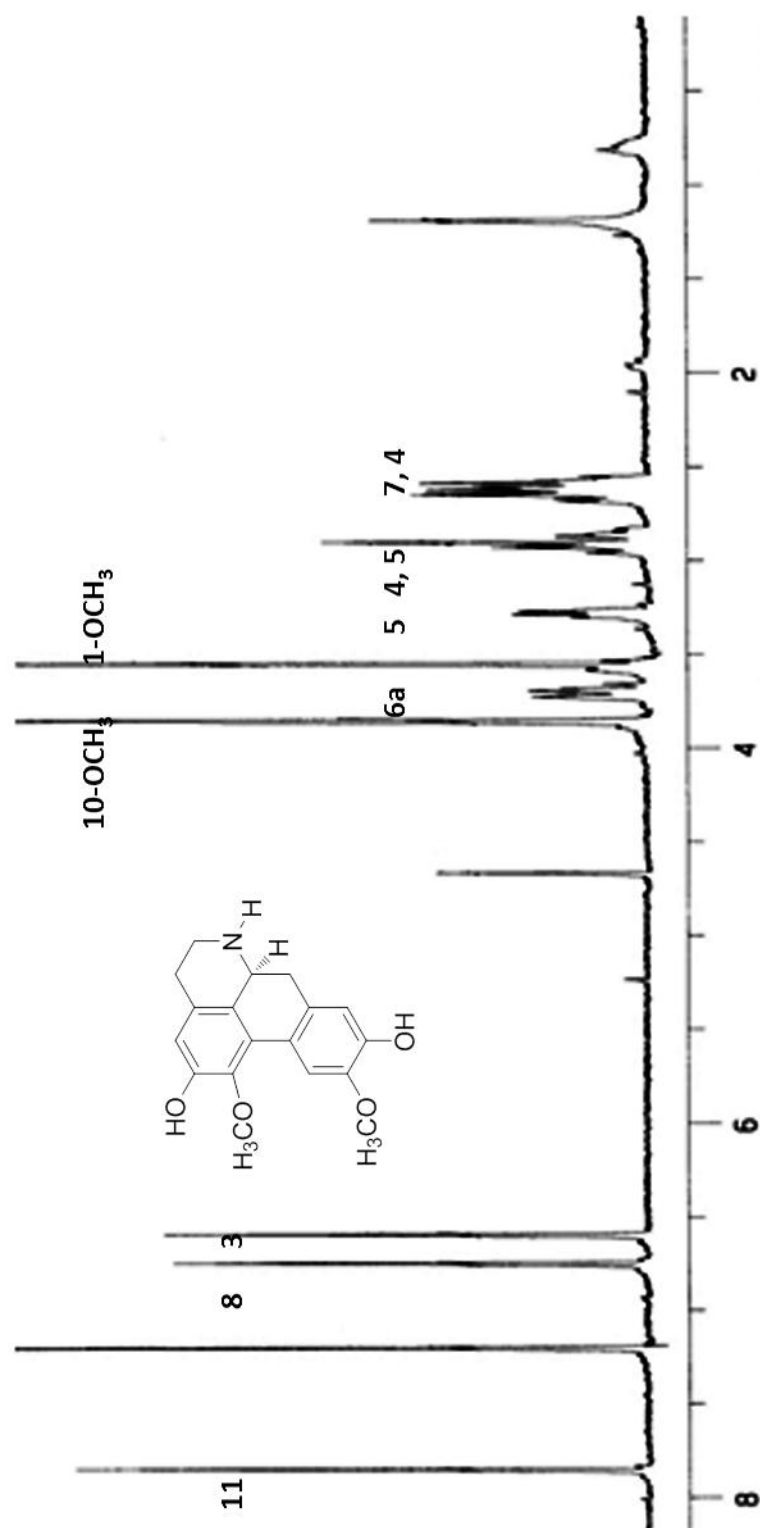


Figure 3.50: ^1H -NMR spectrum of norboldine LOL50

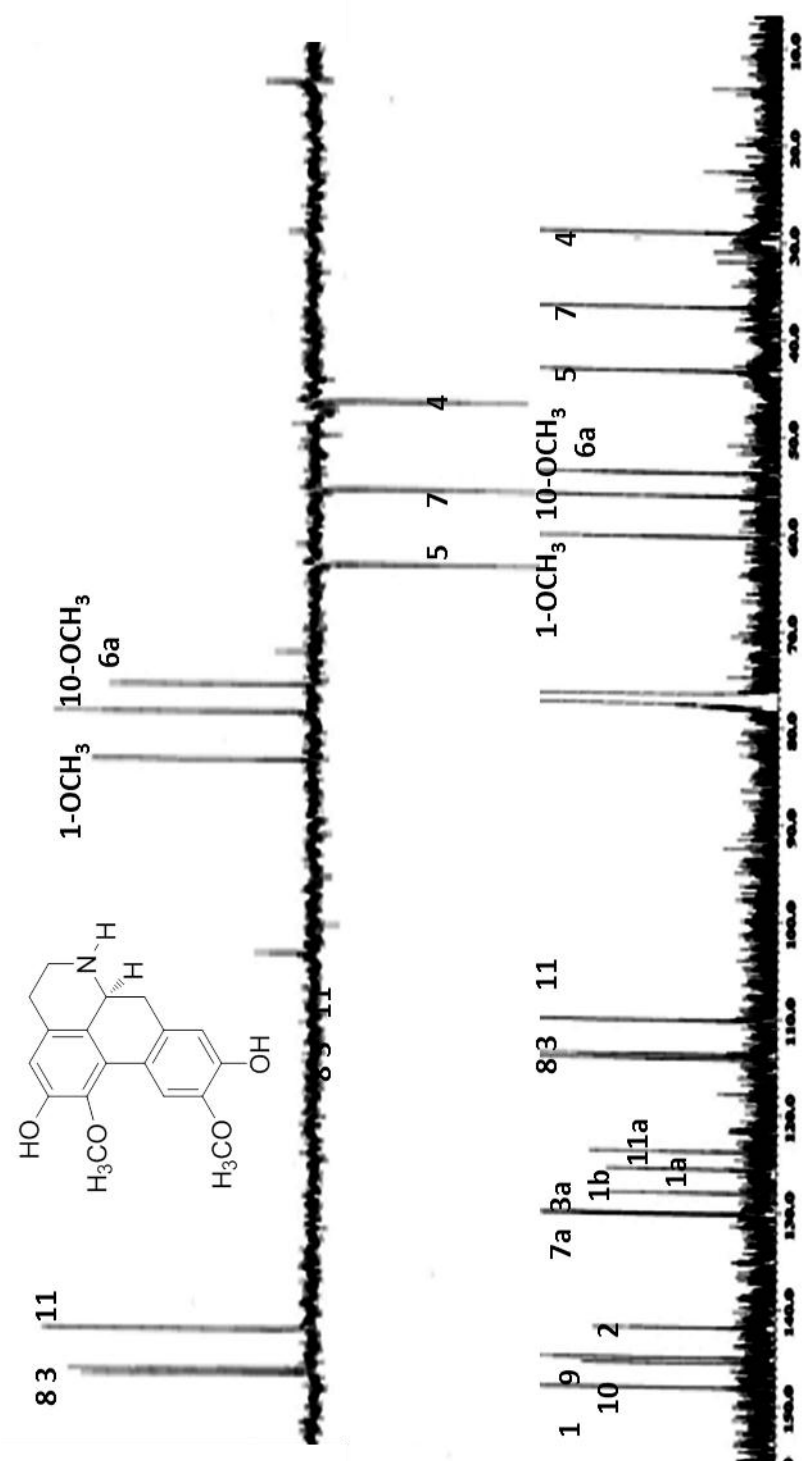
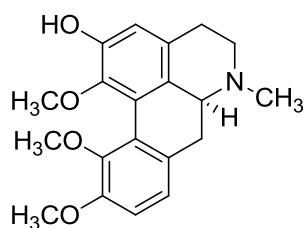


Figure 3.51: ^{13}C -NMR/DEPT spectrum of norboldine LOL50

3.1.12 Alkaloid LOL63: (+)-10-O-Methyl-N-methylhernovine



LOL63

Alkaloid **LOL63**, (+)-10-O-Methyl-N-methylhernovine with $[\alpha]_D^{25} = +4.50$ (2.00×10^{-4} g/100mL, MeOH) was afforded as a brownish amorphous powder (Buchanan, et al., 2007). The UV spectrum showed absorptions at λ_{\max} (MeOH) nm (log ϵ) 244 (1.65) and 276 (2.76) nm, a characteristic values for 1, 2, 10, 11-tetrasubstituted aporphine. The IR spectrum showed absorption peak at 3390 cm^{-1} indicated the presence of hydroxyl group in the structure (Guinaudeau et al., 1994). The LC-MS spectrum showed an intense pseudomolecular ion peak at m/z 328.20 $[M+H]^+$ corresponding to the molecular formula of $C_{19}H_{21}NO_4$.

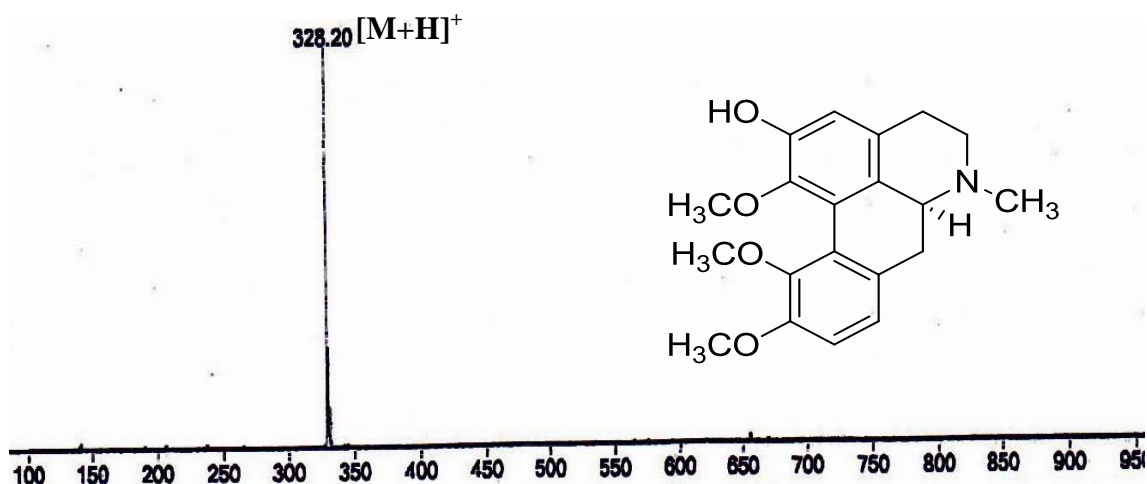


Figure 3.52: LC-MS Spectrum of (+)-10-O-Methyl-N-methylhernovine **LOL63**

The $^1\text{H-NMR}$ spectra (Table 3.14, Figure 3.53) exhibited the same spectra pattern with compound **LOL50** except the position C-11 in **LOL63** was substituted with methoxyl group and C-9 was unsubstituted.

Based on the spectroscopic data of **LOL63** and comparison with the literature

values, it was confirmed that compound **LOL63** was (+)-O10-N-methylhernovine (Shamma et al., 1964).

Table 3.14: ^1H NMR (400 MHz) spectral data of (+)-10-O-Methyl-N-methylhernovine **LOL63**

Position	^1H -NMR(δ , J in Hz)
1	-
1a	-
1b	-
2	-
3	6.66 (1H, <i>s</i>)
3a	-
4	2.68 (2H, <i>dd</i> , 14.0, 4.1)
5	2.82 (2H, <i>dd</i> , 12.0, 4.1) 3.42(2H, <i>m</i>)
6a	3.58 (1H, <i>dd</i> , 4.4, 13.4)
7	2.70 (2H, <i>d</i> , 13.2)
7a	-
8	7.45(1H, <i>d</i> , 7.8)
9	6.80(1H, <i>d</i> , 7.8)
10	-
11	-
11a	-
1-OCH ₃	3.58 (3H, <i>s</i>)
10-OCH ₃	3.85 (3H, <i>s</i>)
11-OCH ₃	3.85 (3H, <i>s</i>)

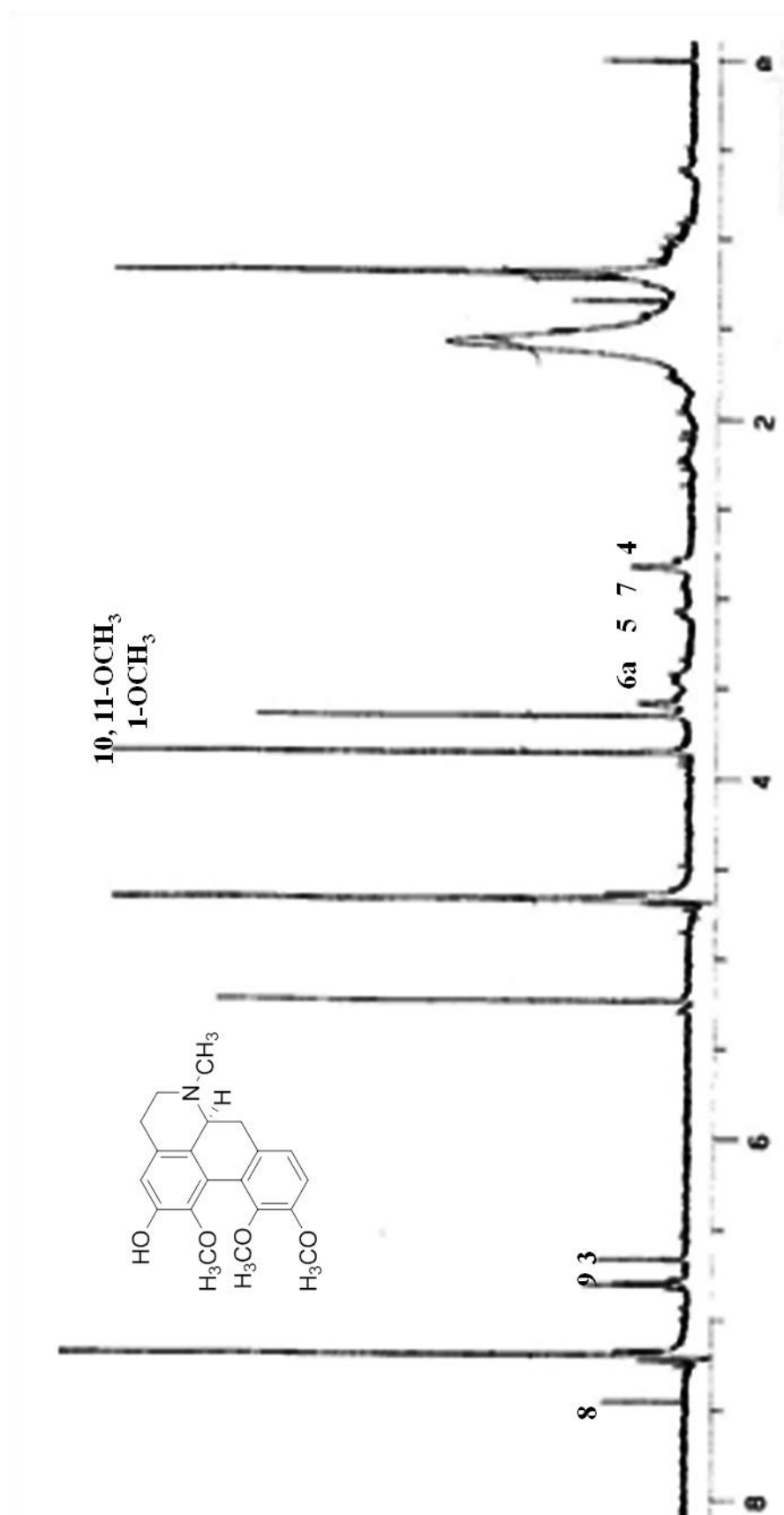
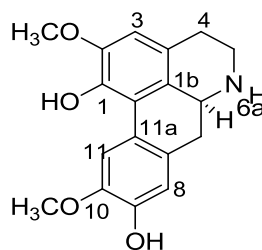


Figure 3.53: ^1H -NMR spectrum of (+)-10-O-Methyl-N-methylhernovine Lol63

3.1.13 Alkaloid LOL65: (+)-Norisoboldine



LOL 65

Alkaloid **LOL65**, (+)-norisoboldine with $[\alpha]_D^{25} = +11.52$ (2.00×10^{-4} g/100 mL, MeOH) was afforded as a brown amorphous solid. The UV spectrum showed absorptions at λ_{\max} (MeOH) nm (log ϵ) 241 (1.87), 250 (1.98) and 270 (2.98) nm, a characteristic values for 1, 2, 9, 10-tetrasubstituted aporphine. The IR spectrum showed absorption peak at 3436 cm^{-1} indicated the presence of hydroxyl group in the structure (Guinaudeau et al., 1994). The LC-MS spectrum showed an intense pseudomolecular ion peak $[M+H]^+$ at m/z 314.1399 corresponding to the molecular formula of $C_{18}H_{19}NO_4$.

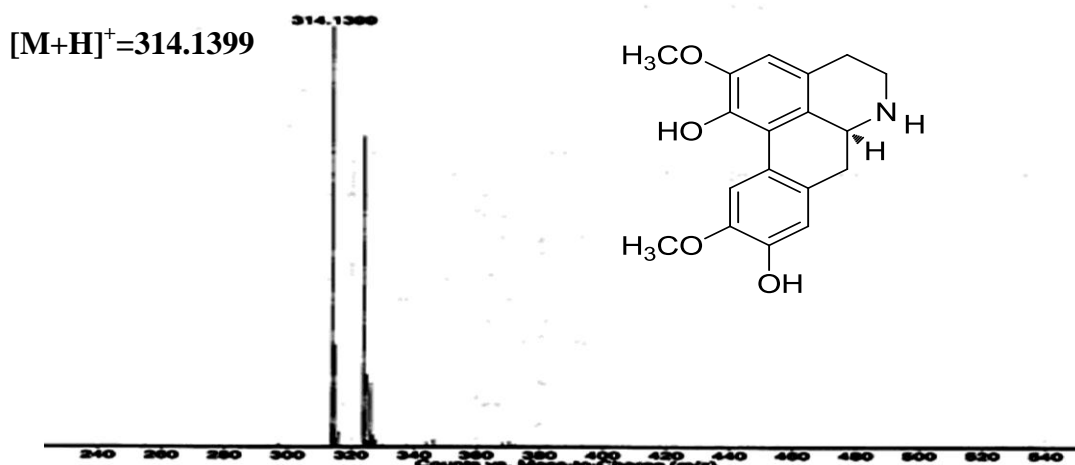


Figure 3.54: LC-MS Spectrum of (+)- Norisoboldine LOL65

The ^1H and ^{13}C NMR spectra (Table 3.15, Figure 3.55) of **LOL65** shared the same characteristics with that of **LOL50** but the only difference was the substitution

pattern at ring A. The position C-1 and C-2 in **LOL50** were substituted with methoxyl and hydroxyl group, respectively, where as in **LOB65** these positions were substituted with hydroxyl and methoxyl group, respectively.

Based on the spectroscopic data of **LOL65** and comparison with the literature values, it was confirmed that compound **LOL65** was (+)-norisoboldine (Marsaioli et al., 1979)

Table 3.15: ^1H NMR (400 MHz) and ^{13}C NMR (100 MHz) spectral data of (+)- Norisoboldine **LOL65**

Position	^1H -NMR(δJ in H_2)	^{13}C -NMR (δc)
1	-	148.0
1a	-	124.9
1b	-	128.1
2	-	142.0
3	6.53(1H, <i>s</i>)	113.2
3a	-	130.6
4	2.68 (1H, <i>m</i> , $\text{H}\alpha$) 2.90 (1H, <i>m</i> , $\text{H}\beta$)	30.1
5	2.85 (1H, <i>m</i> , $\text{H}\alpha$) 3.25 (1H, <i>m</i> , $\text{H}\beta$)	43.6
6a	3.70 (1H, <i>dd</i> , 4.7, 13.6)	54.0
7	2.85 (2H, <i>m</i>)	36.1
7a	-	130.0
8	6.7 9 (1H, <i>s</i>)	114.1
9	-	145.6
10	-	145.9
11	7.98 (1H, <i>s</i>)	111.4
11a	-	124.0
2-OCH ₃	3.88 (3H, <i>s</i>)	60.4
10-OCH ₃	3.90 (3H, <i>s</i>)	57.0

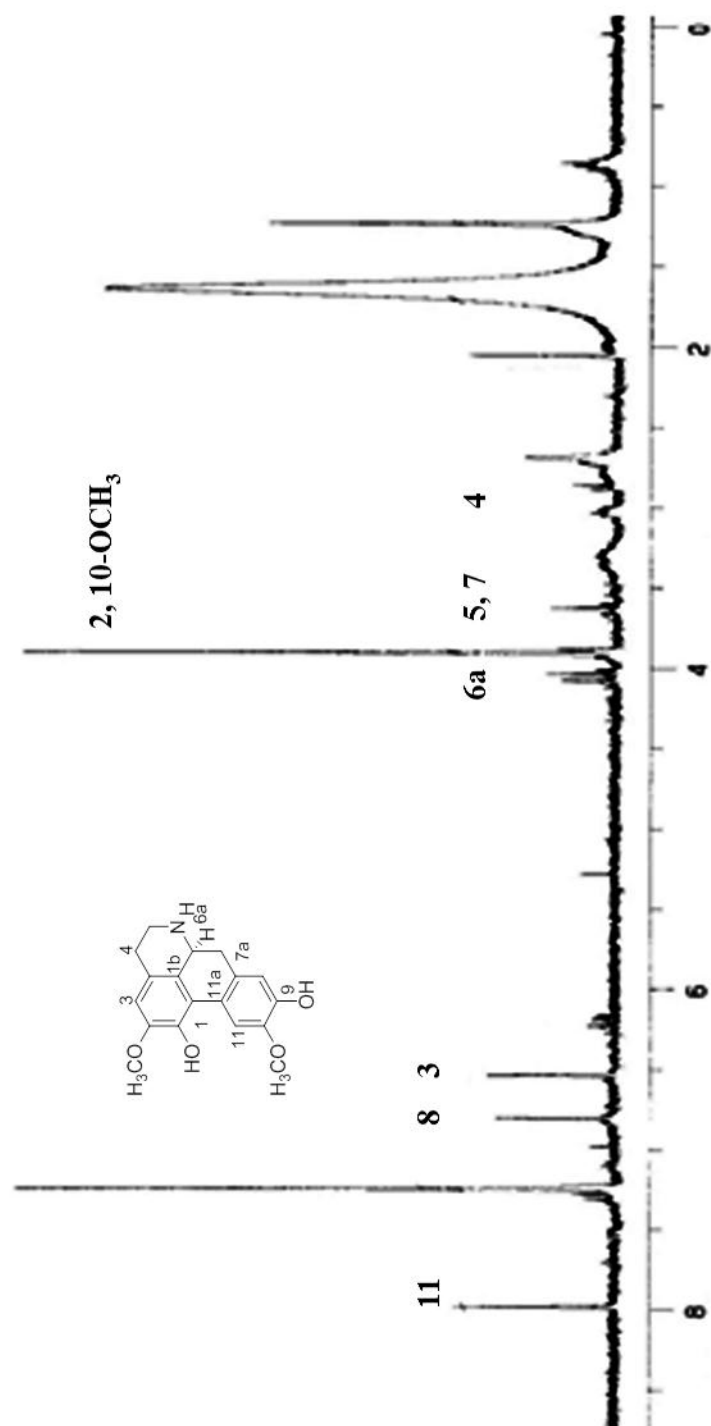


Figure 3.55: ^1H NMR Spectrum of (+)-norisoboldine LOL65

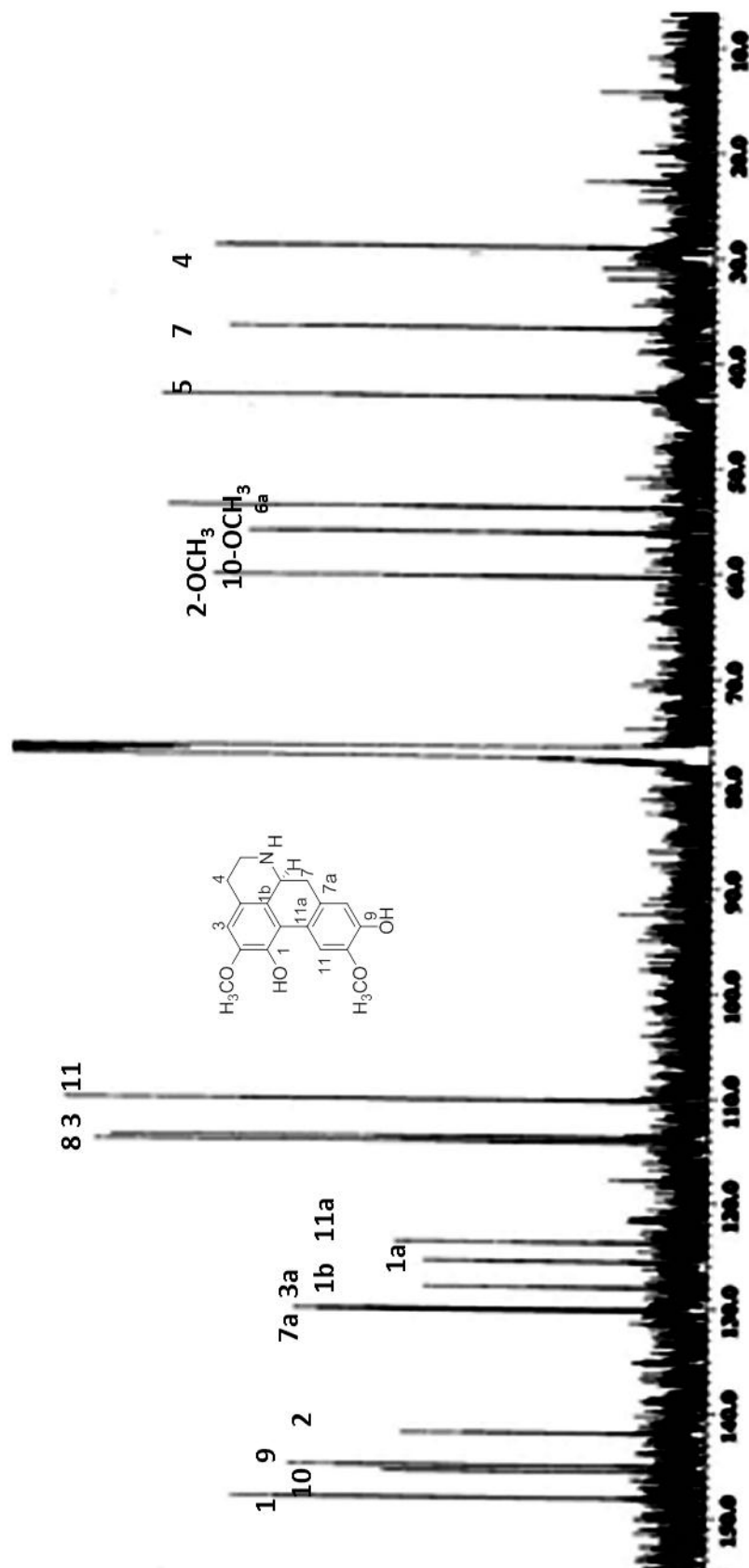


Figure 3.56: ¹³C-NMR spectrum of (+)-norisoboldine LOL65

3.2 Chemical constituents from bark and leaves *Litsea costalis* (Nee) Kosterm

The extraction, isolation, purification and structural elucidation of the compounds from the bark and leaves of *Litsea costalis* have been performed and the procedure used was the same with the compounds isolated from *Lindera oxyphylla*. Eight compounds were isolated from the bark of *Litsea costalis* and these compounds are 3,4-dimethoxycinnamaldehyde **LCB7**, 2-hydroxy-5-methoxybenzaldehyde **LCB11**, 2, 5-dimethoxybenzaldehyde **LCB15**, 4,4'-diallyl-5,5'-dimethoxy-[1,1'-biphenyl]-2,2'-diol **LCB3**, 4,4'-diallyl-6,6'-dimethoxy-[1,1'-biphenyl]-2,2'-diol **LCB9**, 2,2'-oxybis(4-allyl-1-methoxybenzene) **LCB10**, 1,2-bis(5-allyl-2-methoxyphenyl)hydrazine **LCB17**, (*E*)-4(4-hydroxy-1,1-dimethoxybut-2-en-1-yl) benzene-1, 2-diol **LCB4** and (*E*)-4-styrylphenol **LCB58**. Seven compounds were isolated from the leaves of *Litsea costalis* and these compounds are cinnamide **LCL4**, 2,4-dimethoxybenzamide **LCL2**, 3,4-dimethoxybenzamide **LCL5**, 2*S*,4*S*-2-(3',4'-methylenedioxyphenyl)-5,7-dimethoxychroman-4-ol **LCL7**, (+)-pinostrobin **LCL9**, (+)-onysilin **LCL13**, (+)-pinocembrin **LCL14**, 4-allyl-1,2-dimethoxybenzene **LCL15** and 4-allyl - 2methoxyphenol **LCL17**. The percentage yields of the isolated compounds were shown in (Table 3.16 and 3.17).

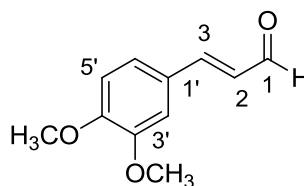
Table 3.16: Chemical Constituents of Bark *Litsea Costalis*

Compounds	Types	%Yield
3, 4-Dimethoxycinnamaldehyde LCB7	Aldehyde	0.35
2-Hydroxy-5-methoxybenzaldehyde LCB11	Aldehyde	0.04
2, 5-Dimethoxybenzaldehyde LCB15	Aldehyde	0. 1
4,4'-Diallyl-5,5'-dimethoxy-[1,1'-biphenyl]- 2,2'-diol LCB3	Neolignan	0.05
4,4'-Diallyl-5,5'-dimethoxy-[1,1'-biphenyl]- 2,2'-diol LCB9	Neolignan	0.05
2,2'-Oxybis(4-allyl-1-methoxybenzene LCB10	Biphenyl ether Lignan	30
1,2-Bis(5-allyl-2-methoxyphenyl)hydrazine LCB17	Phenyl hydrazine	30
(<i>E</i>)-4(4-hydroxy-1, 1-dimethoxybut-2-en-1-yl) benzene-1, 2-diol LCB4	Phenolic compound	0.05
(<i>E</i>)-4-styrylphenol LCB58	Stilbene	2.5

Table3.17: Chemical Constituents of Leaves *Litsea costalis*

Compounds	Types	%Yield
3, 4-Dimethoxycinnamaldehyde LCL4	Aldehyde	0.6
2,4- Dimethoxybenzamide LCL2	Amide	0.3
3,4- Dimethox benzamide LCL5	Amide	2.33
2S,4S-2-(3',4'-methylenedioxyphenyl)-5,7-dimethoxychroman-4-ol LCL7	Flavonoid	2.5
(+)-Pinostrobin LCL9	Flavonoid	1.0
(+)- Onysilin LCL13	Flavonoid	2.5
(+)-Pinocembrin LCL14	Flavonoid	1.5
4-allyl-1,2-dimethoxybenzene LCL15	Lignan	1.5
4-allyl-2-methoxyphenol LCL17	Lignan	1.5

3.2.1 Aldehyde LCB7: 3', 4'-Dimethoxycinnamaldehyde



LCB 7

Compound **LCB7**, 3', 4'-Dimethoxycinnamaldehyde was obtained as brown oil. The UV spectrum showed absorption bands at λ_{\max} (MeOH) nm (log ϵ) 306 (1.847) and 326 (1.876) nm indicating a highly unsaturated chromophoric system. The IR spectrum showed the presence of conjugated carbonyl at ν_{\max} 1668 cm^{-1} and C-H stretching of aldehyde group at ν_{\max} 2848 cm^{-1} . The LC-MS spectrum showed an intense pseudomolecular ion peak, $[\text{M}-\text{H}]^+$ at m/z 191.0499 corresponding to the molecular formula of $\text{C}_{11}\text{H}_{12}\text{O}_3$.

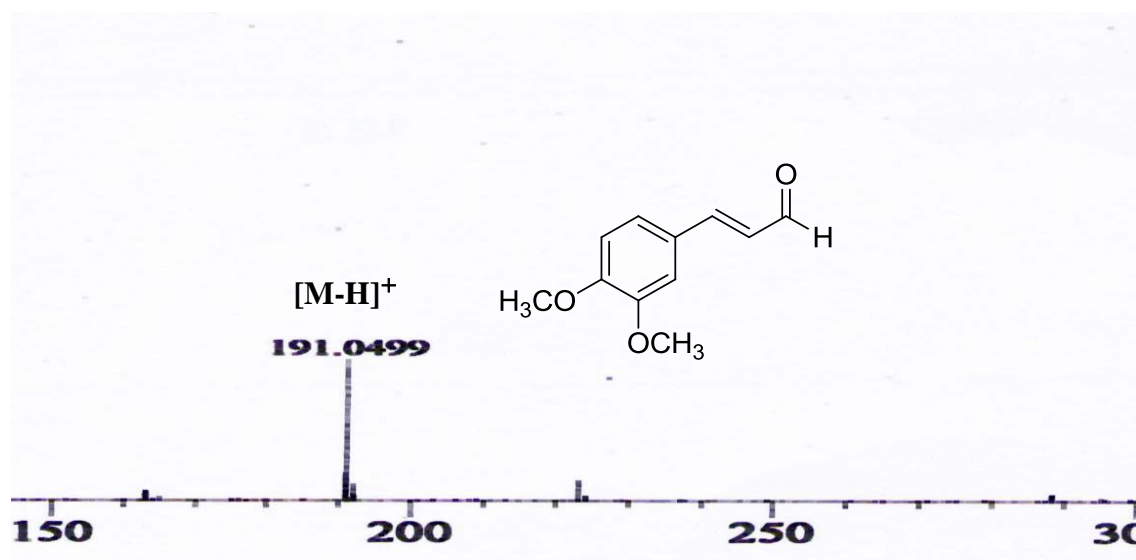


Figure 3.57: LC-MS Spectrum of 3',4'-Dimethoxycinnamaldehyde **LCB7**

The ^1H -NMR spectrum (Table 3.18, Figure 3.58) showed the existence of an aldehyde group at δ 9.65. A peak at δ 3.95 appeared as a singlet with six protons were assigned for two methoxyls at positions C-3' and C-4'. The aromatic proton at C-5' was resonated at δ 6.97 as a doublet and the peak at δ 7.24 appeared as doublet of doublet with J values of 7.8 and 1.8 Hz belongs to proton at C-6' due to meta coupling with H-2'. The aromatic proton at position C-2' was resonated at δ 7.06 as doublet with J value 1.8 Hz due to meta coupling with H-6'. The COSY spectrum (Table 3.18, Figure 3.59) showed the correlations of H-2/H-3 and H-6'/H-5'.

The ^{13}C -NMR and DEPT spectra (Table 3.18, Figure 3.60) showed 10 carbon signals consist of one carbonyl group, five methine groups and four quaternary carbons. The carbonyl group resonated at δ 193.5 and two methoxyls resonated at δ 56.1 (C-3' and C-4'). Five methines were observed at δ 127.2 (C-2), 152.1 (C-3), 109.4 (C-2'), 111.7 (C-5') and 124.6 (C-6'), and four quaternary carbons resonated at δ 193.5 (C-1), 127.4 (C-1'), 147.8 (C-3') and 149.5 (C-4'). The HMQC data was tabulated in (Table 3.18, Figure 3. 61) which showed the connectivity between proton to their respective and carbon atoms: H-2'/C-2', H-6'/C-6', H-3/C-3, H-2/C-2, H-5'/C-5', H-4'OMe/C-4'OMe and H-3'OMe/C-3'OMe and the HMBC spectrum (Table 3.18, Figure 3.62) showed the cross-peak between H-1 to C-2, H-3 to C-2', C-6', C-1', C-1, H-6' to C-2', C-4', H-2' to C-6', C-4', C-3', H-5' to C-2, C-3', H-3',4'OMe to C-3', 4'OMe.

Based on the spectroscopic data of **LCB7** and comparison with the literature values (Herath et al., 1998), it was confirmed that compound **LCB7** was 3', 4'-dimethoxycinnamaldehyde (Banwell et al., 2004).

Table 3.18: ^1H NMR (400 MHz) and ^{13}C NMR (100 MHz) spectral data of 3',4'-Dimethoxy Cinnamaldehyde **LCB7**

Position	^1H -NMR(δ , J in Hz)	^{13}C -NMR (δc)
1	9.65 (1H, d , 7.7)	193.5
2	6.63 (1H, dd , 15.8, 7.7)	127.2
3	7.45 (1H, d , 16.0)	152.1
1'	-	127.2
2'	7.06 (1H, d , 1.8)	109.4
3'	-	147.8
4'	-	149.5
5'	6.97(1H, d , 7.8)	111.7
6'	6.90 (1H, dd , 7.8, 1.8)	124.2
3'-OMe	3.95 (1H, s)	56.1
4'-OMe	3.95 (1H, s)	56.1

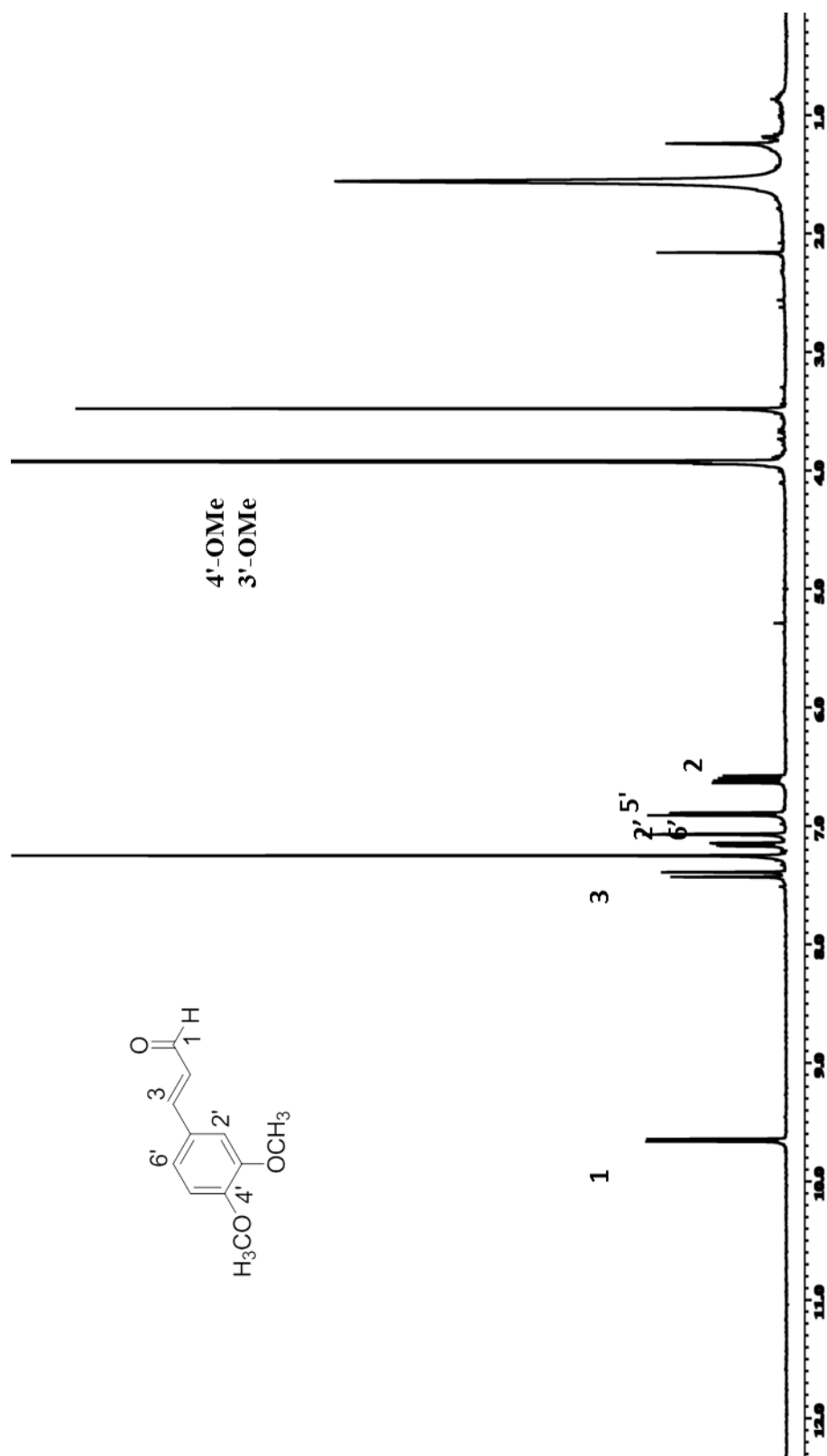


Figure 3.58: ^1H NMR spectrum of 3', 4'-dimethoxycinnamaldehyde **LCB7**

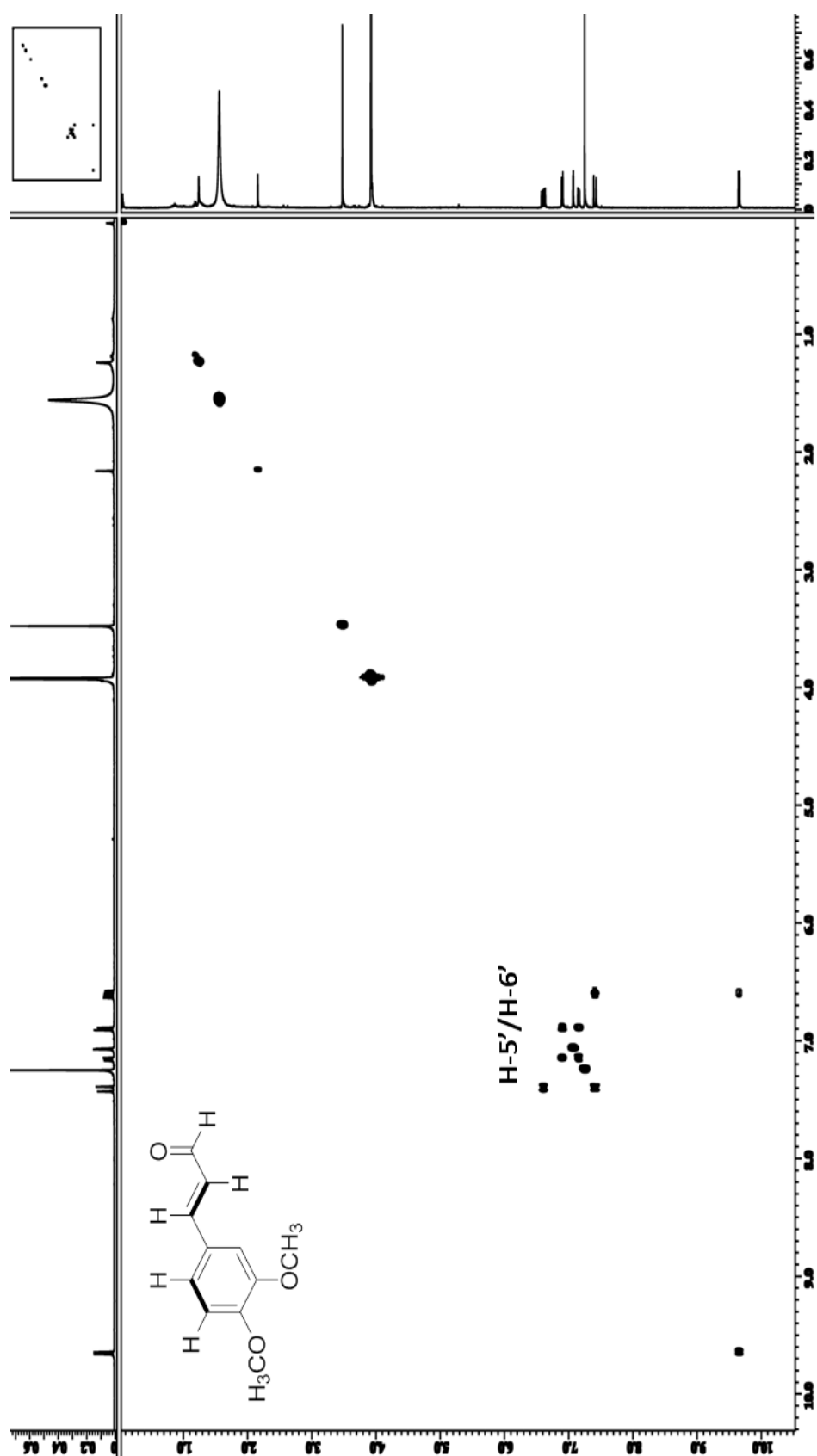


Figure 3.59: COSY spectrum of 3', 4'-dimethoxycinnamaldehyde LCB7

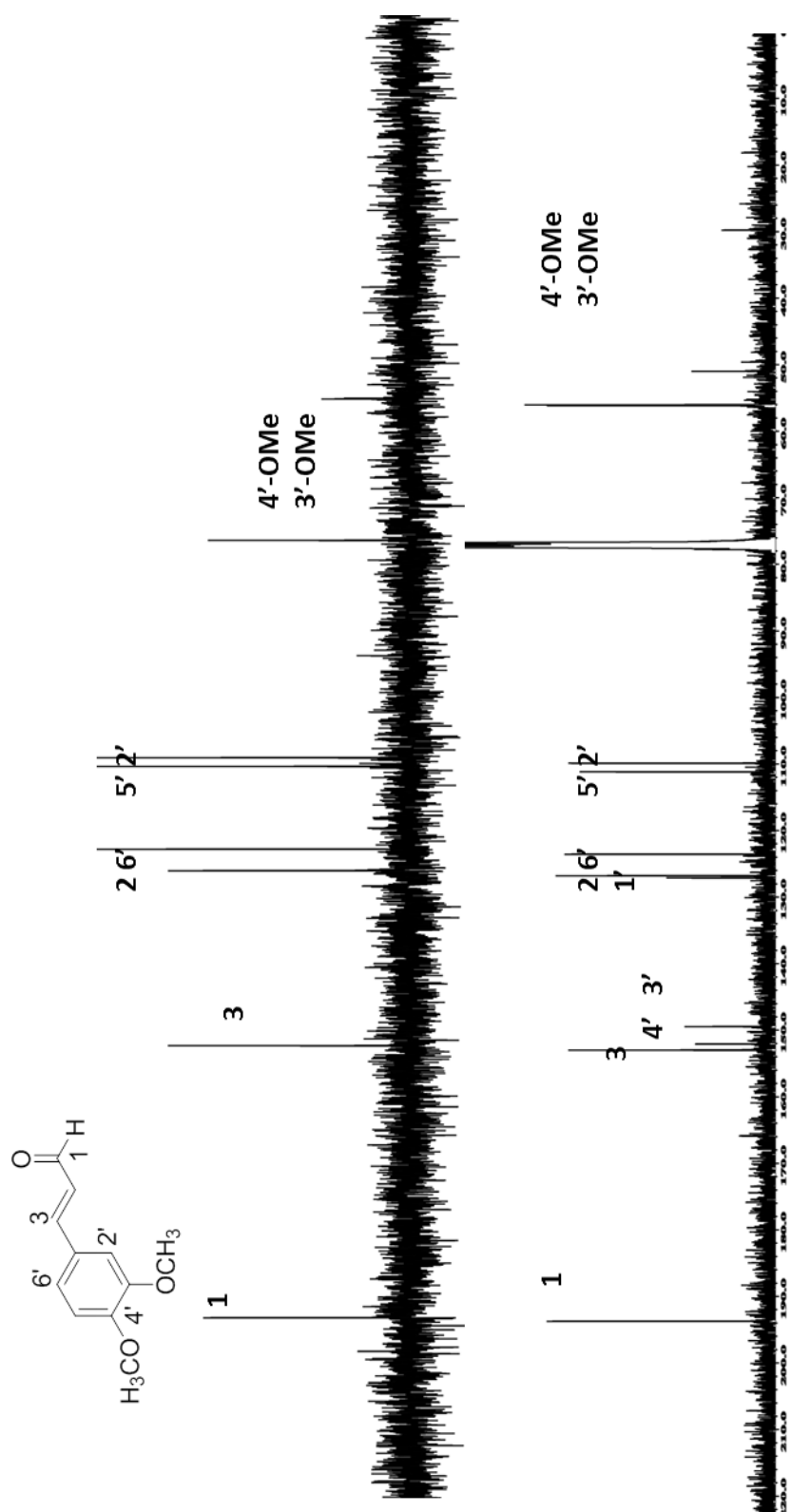


Figure 3.60: ¹³C NMR/ DEPT spectrum of 3', 4'-dimethoxycinnamaldehyde LCB7

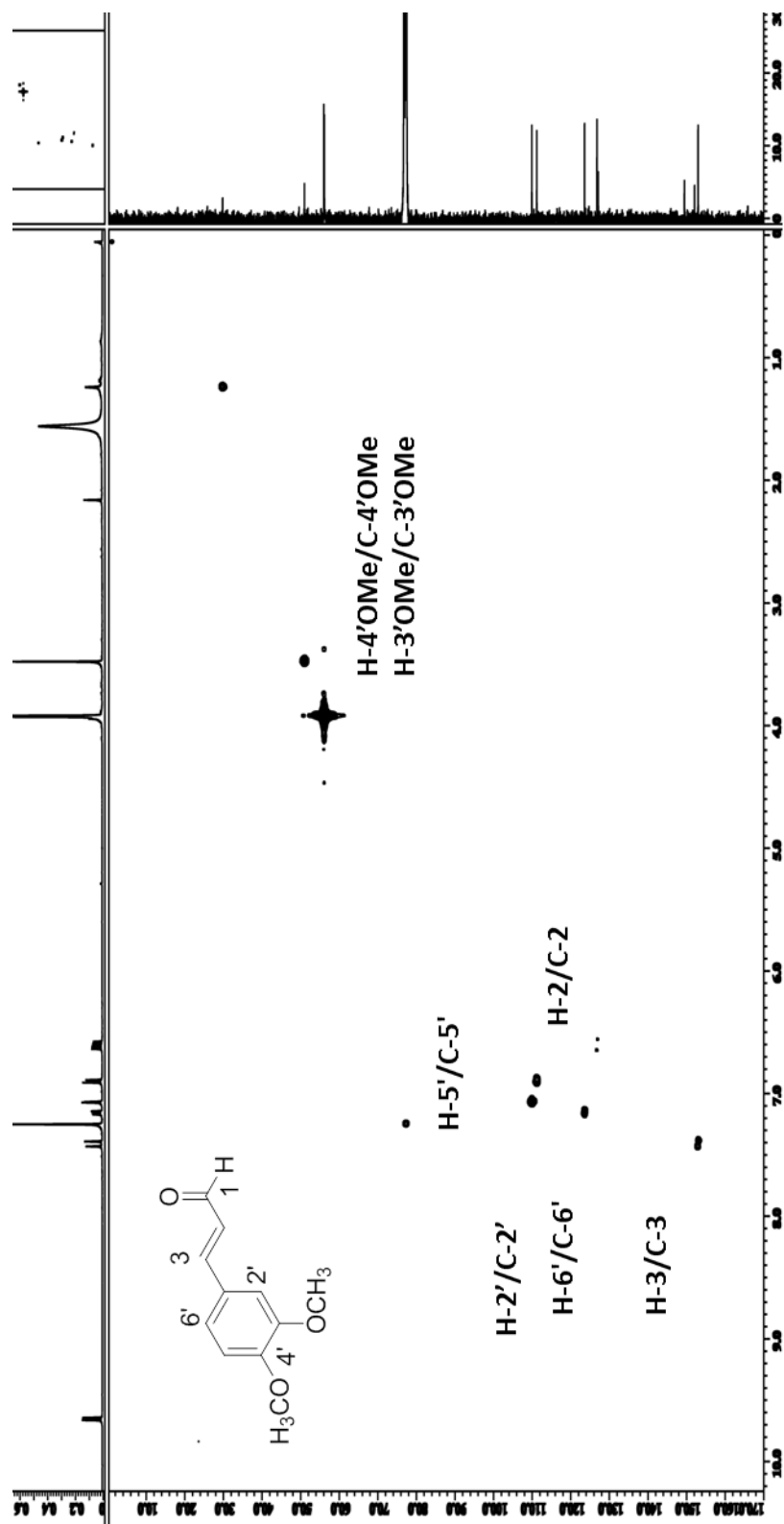


Figure 3.61: HMQC spectrum of 3', 4'-dimethoxycinnamaldehyde LCB7

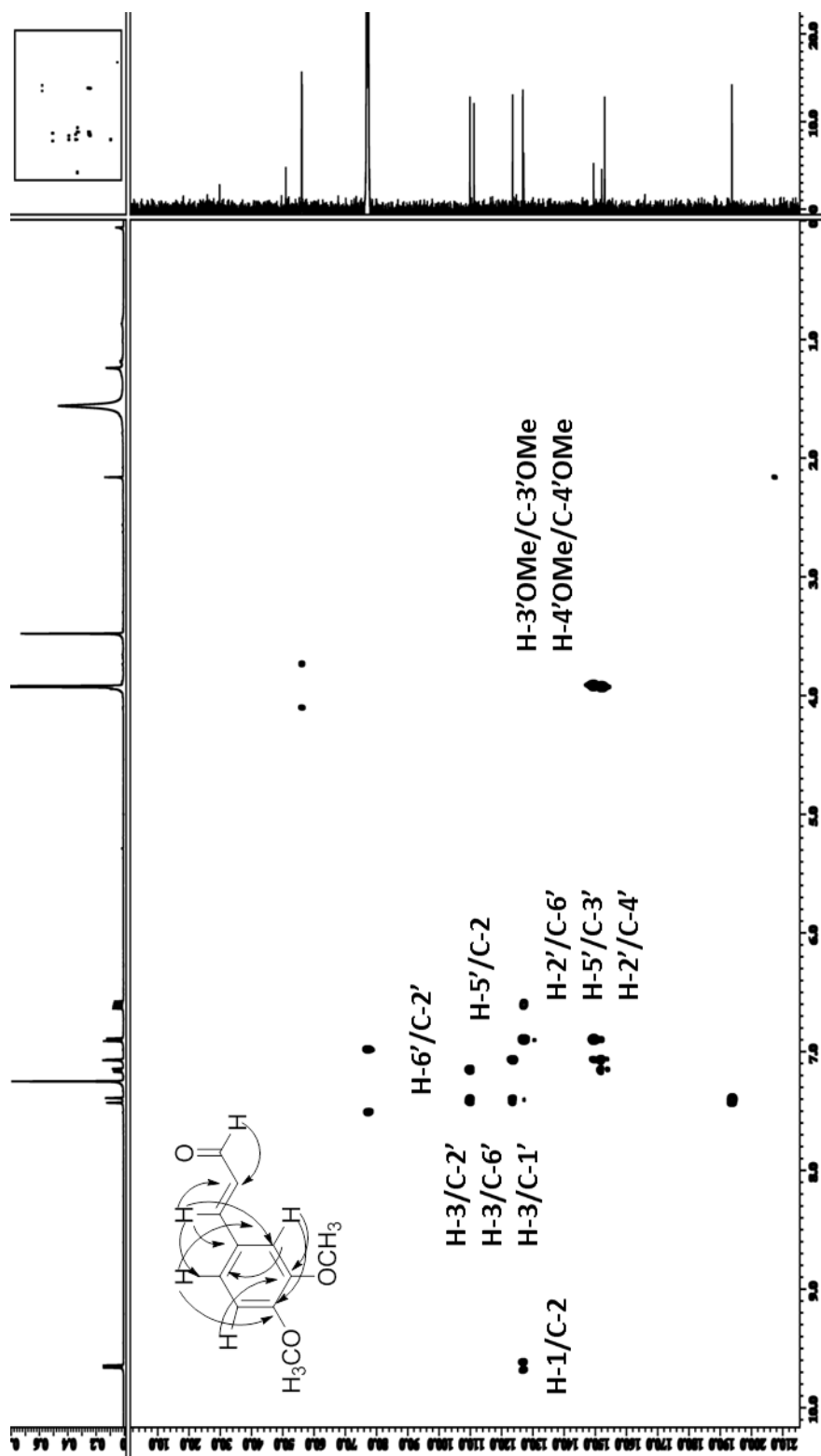
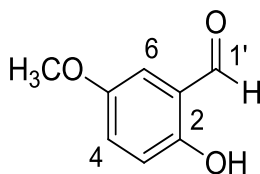


Figure 3.62: HMBC spectrum of 3', 4'-dimethoxycinnamaldehyde LCB7

3.2.2 Aldehyde LCB11: Salicylaldehyde



LCB11

Compound **LCB11**, 2-hydroxy-5-methoxybenzaldehyde was obtained as light yellow amorphous solid. The IR spectrum showed the presence of hydroxyl group at ν_{\max} 3431 cm^{-1} and aldehyde group at 1669 cm^{-1} . The UV spectrum showed absorption bands at λ_{\max} (MeOH) nm (log ϵ) 306 (1.845) and 231(1.723) nm. The LC-MS spectrum displayed pseudomolecular ion peak, $[\text{M}+\text{H}]^+$ at m/z 153.0504 corresponding to the molecular formula of $\text{C}_8\text{H}_8\text{O}_3$.

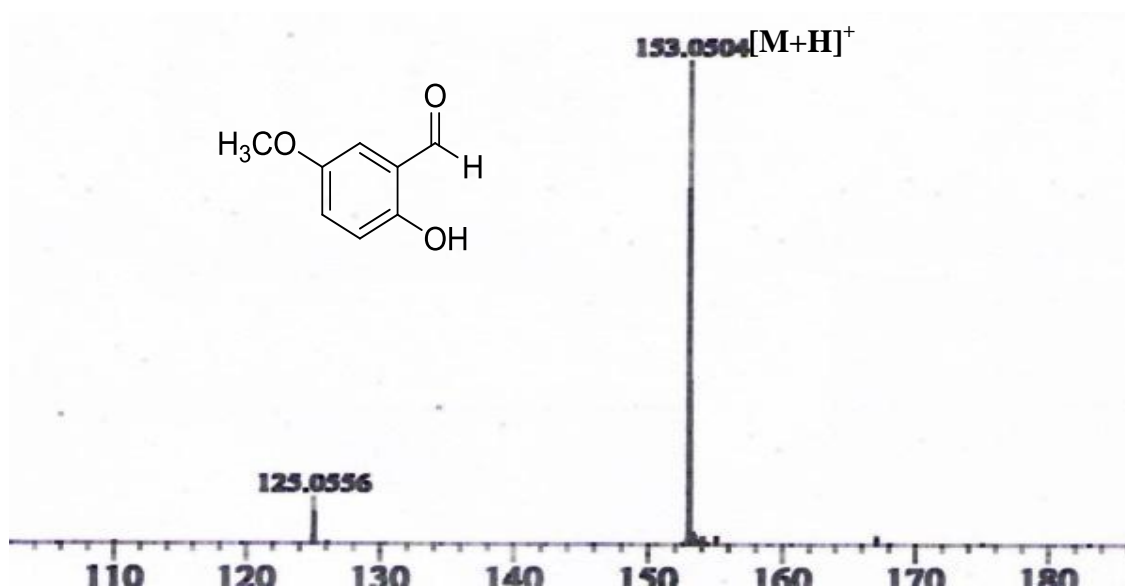


Figure 3.63: LC-MS Spectrum of salicylaldehyde **LCB11**

¹H-NMR spectrum (Table 3.19, Figure 3.64) showed the existence of an aldehyde group which resonated at δ 9.61 as a singlet, one methoxy group was observed at δ 3.95 as a singlet and a broad one proton peak appeared at δ 6.21 which was assigned for a hydroxyl group position at C-2. The aromatic protons were observed at δ 7.05 (C-3), δ 7.40 (C-6) and δ 7.41 (C-4). The COSY (Table 3.19, Figure 3.65) showed only one proton-proton connectivity which displayed correlations of H-4/H-3 (Wang et al., 2000).

¹³C NMR and DEPT spectra (Table 3.19, Figure 3.66) showed 8 carbon signals of which three signals were due to the methine groups, one carbonyl, one methoxy group and three quaternary carbons. The methoxyl group was observed at δ 56.2 (C-5), carbonyl group was resonated at δ 191.0, three methines were resonated at δ 108.8 (C-3), 114.4 (C-4) and 127.6 (C-6). Three quaternary carbon were observed at δ 129.9 (C-1), 151.7 (C-2) and 147.2 (C-5).

The HMQC and HMBC data were tabulated in (Table 3.19, Figure 3.67 and 3.68), respectively (Alarcón et al., 1994).

Based on the spectroscopic data of **LCB11** and comparison with the literature values, it was confirmed that compound **LCB11** was salicylaldehyde (Chang et al., 1998).

Table 3.19: ^1H NMR (400 MHz) and ^{13}C NMR (100 MHz) spectral data of salicylaldehyde LCB11

Position	^1H -NMR(δ , J in Hz)	^{13}C -NMR(δc)
1	-	129.9
2	-	151.8
3	7.05 (1H, <i>d</i> , 8.2)	108.8
4	7.40(1H, <i>dd</i> , 8.2 ,1.8)	127.6
5	-	147.2
6	7.43 (1H, <i>d</i> , 1.8)	114.4
1'	9.65 (1H, <i>s</i>)	191.0
2-OMe	3.95 (3H, <i>s</i>)	56.2
OH	6.21(1H, <i>s</i>)	-

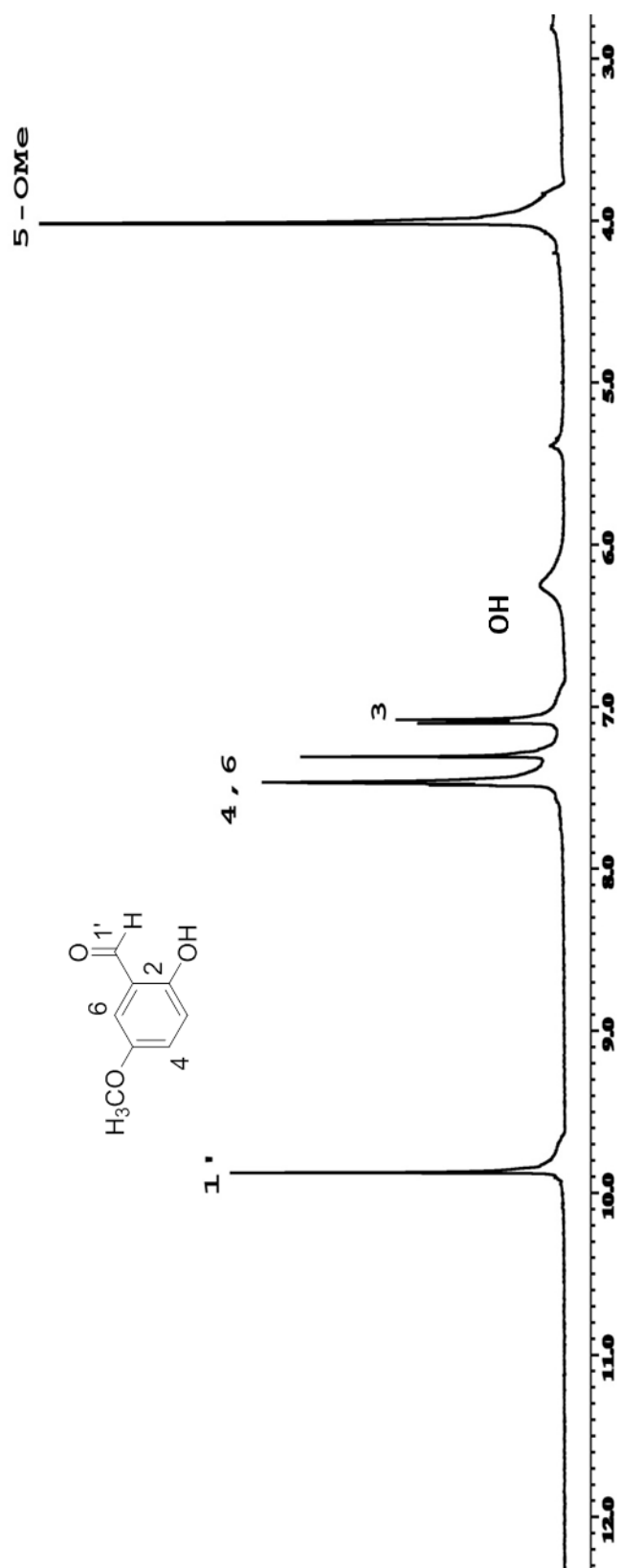


Figure 3.64: ^1H NMR spectrum of salicylaldehyde LCB11

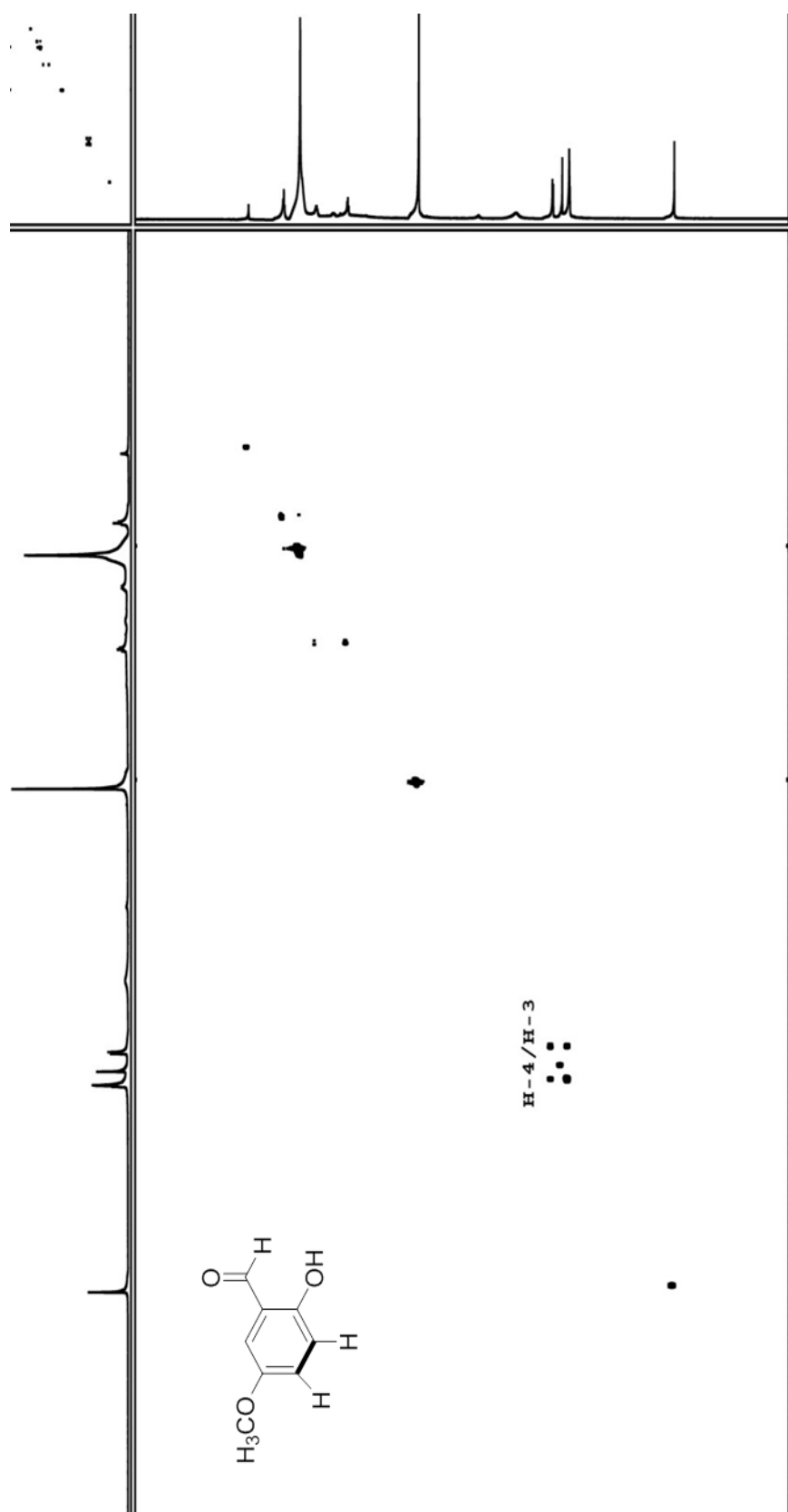


Figure 3.65: COSY spectrum of salicylaldehyde LCB11

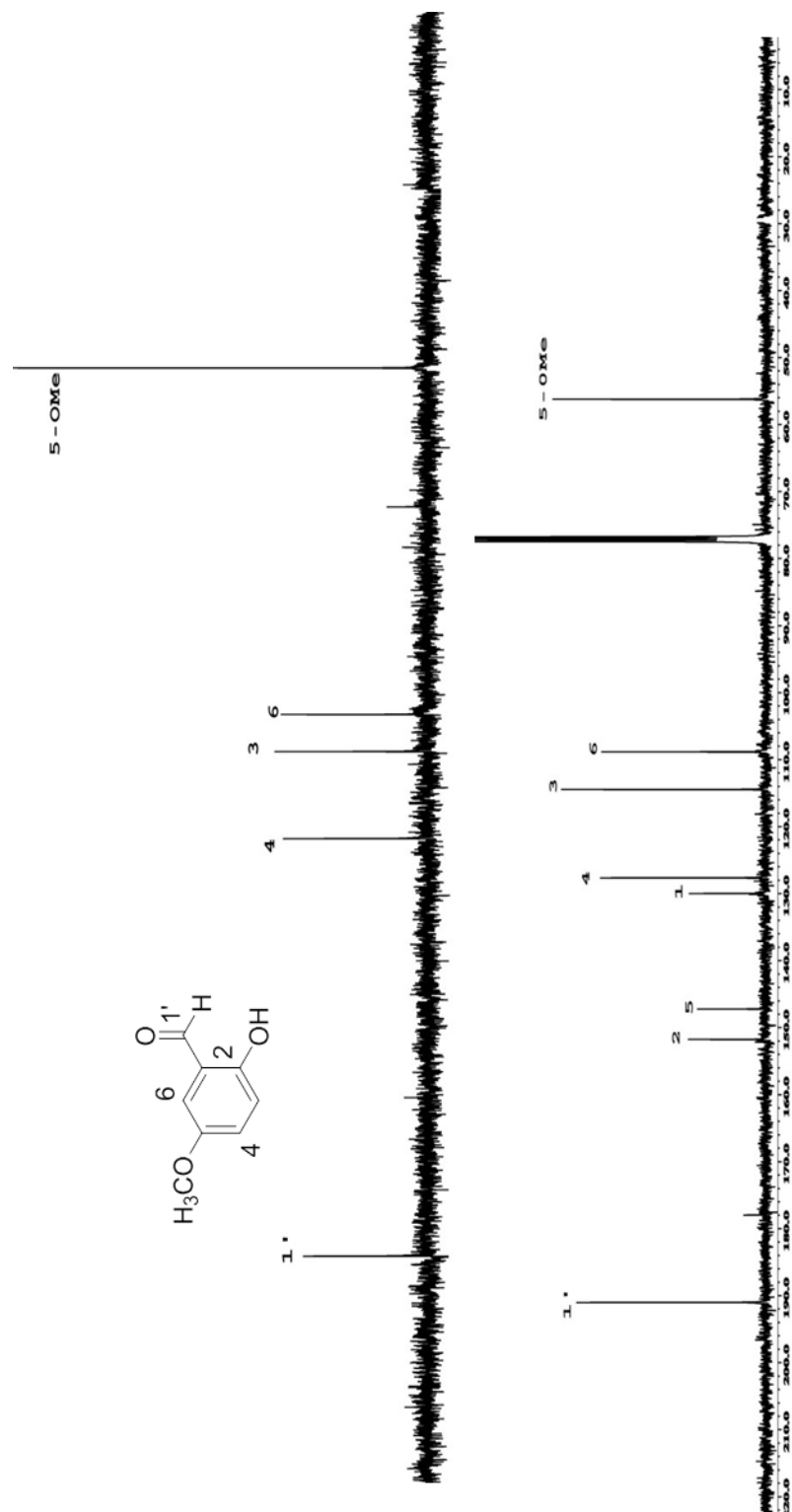


Figure 3.66: ^{13}C -NMR / DEPT spectrum of salicylaldehyde LCB11

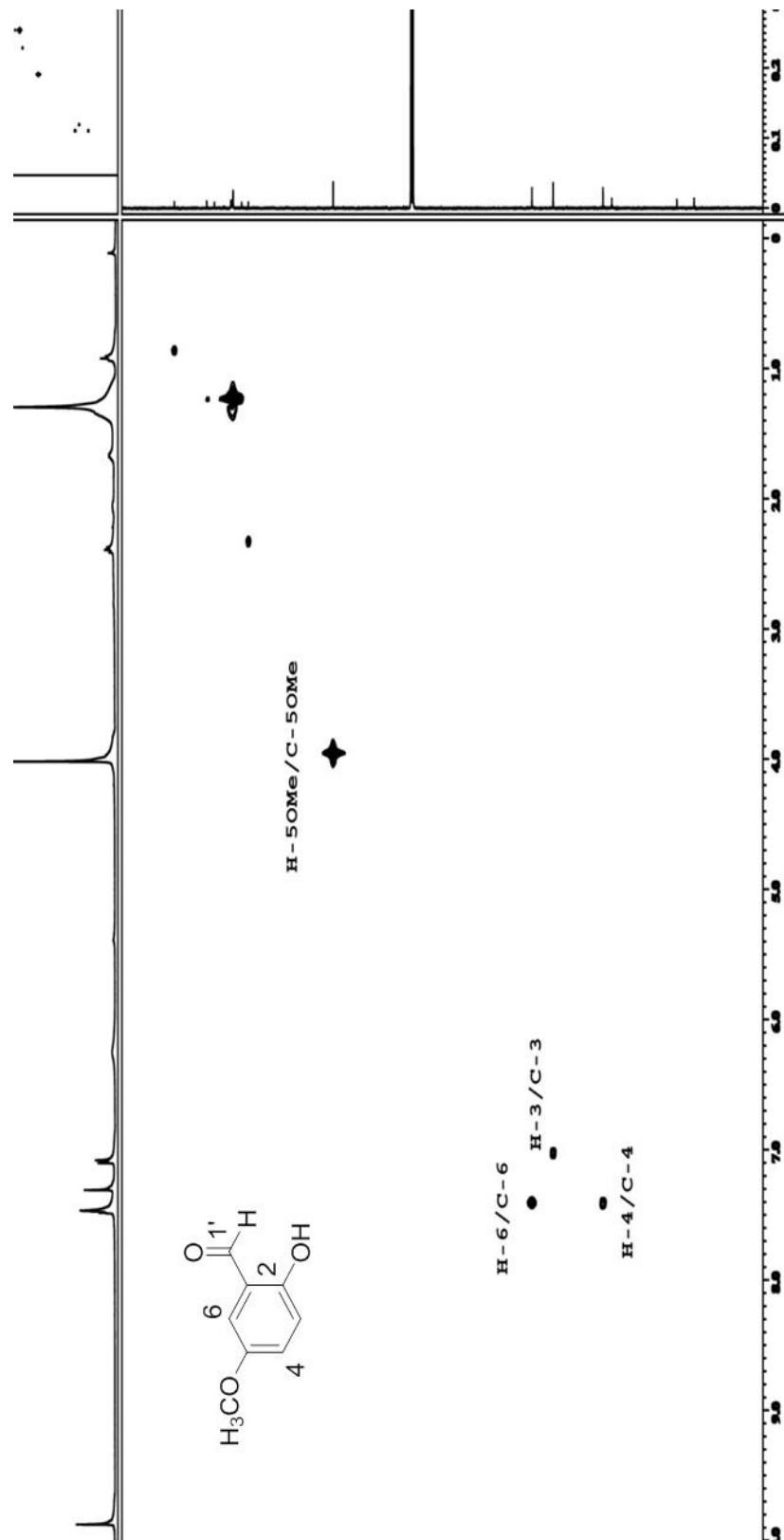


Figure 3.67: HMQC spectrum of salicylaldehyde LCB11

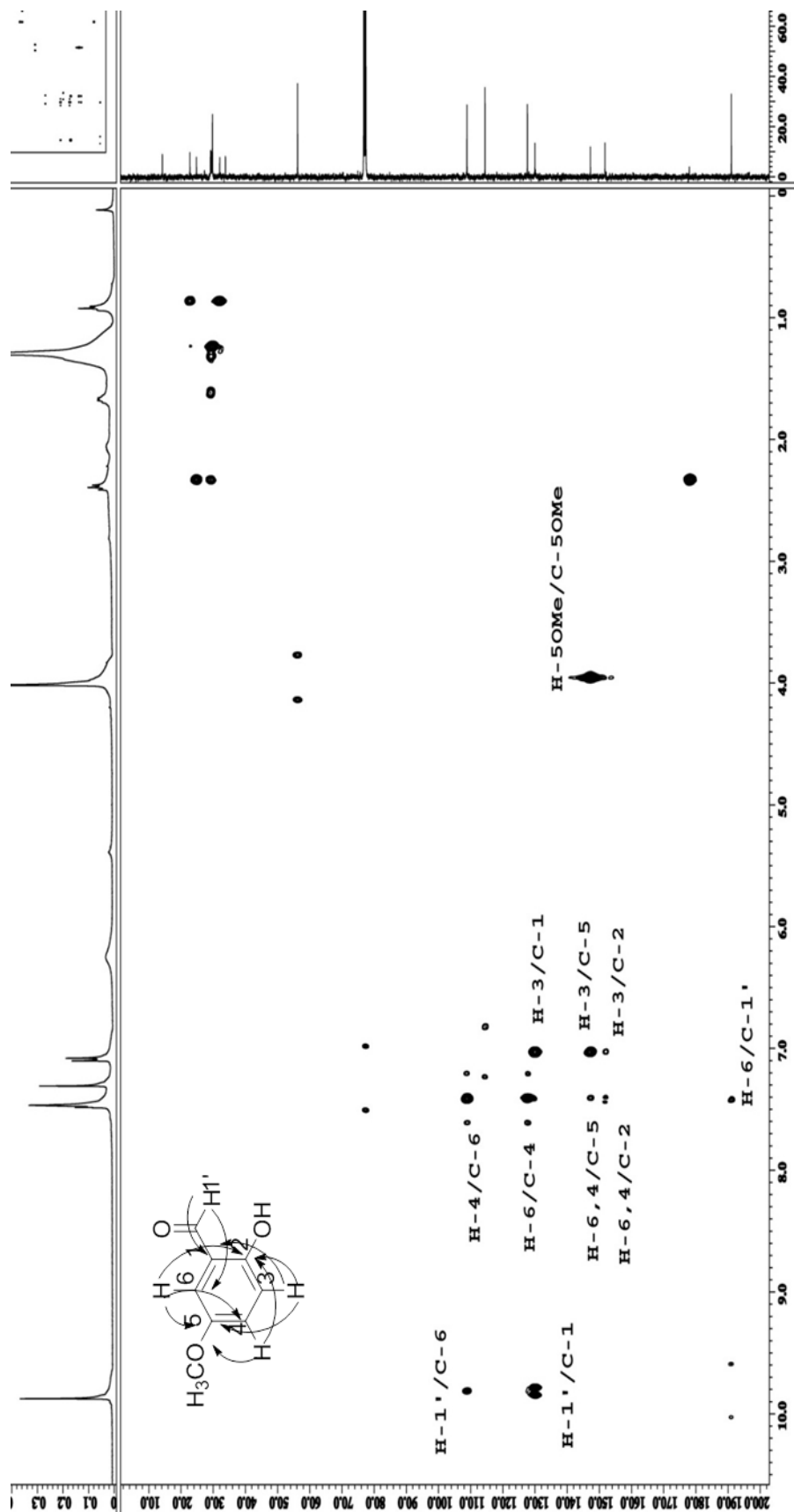
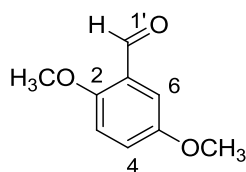


Figure 3.68: HMBC spectrum of salicylaldehyde LCB11

3.2.3 Benzaldehyde LCB15: 2, 5-Dimethoxybenzaldehyde



LCB 15

Compound **LCB15** 2, 5-dimethoxybenzaldehyde was obtained as light yellow solid . The IR spectrum showed the absorption peak at 2848 cm^{-1} which assigned for C-H stretching of CHO group and 1669 cm^{-1} indicated the presence of C=O . The UV spectrum showed absorption bands at λ_{max} (MeOH) nm (log ϵ) 306 (2.703) and 234 (2.531) nm indicating the presence of conjugated carbonyl group. The LC-MS spectrum displayed pseudomolecular ion peak $[M+H]^+$ at m/z 167.064, gave molecular formula of $\text{C}_9\text{H}_{10}\text{O}_3$.

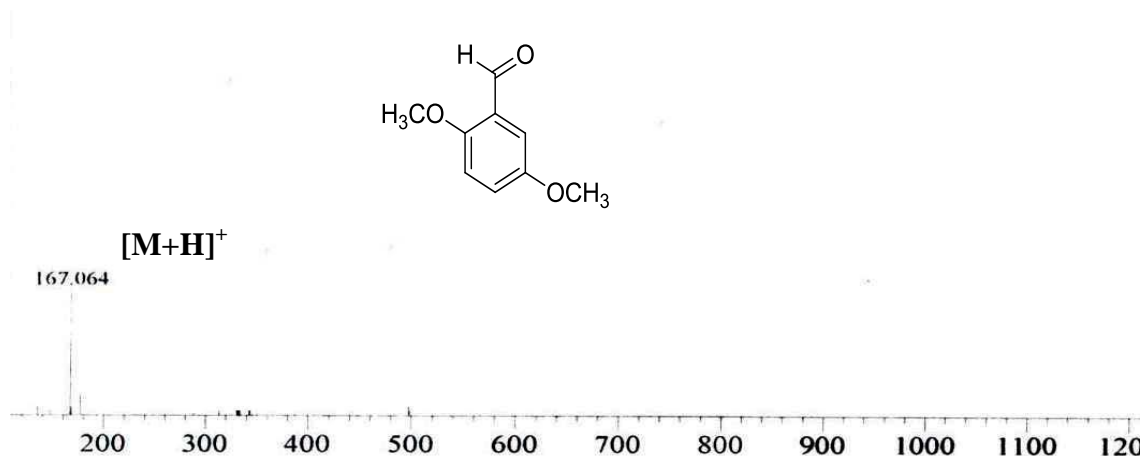


Figure 3.69: LC-MS Spectrum of 2, 5-Dimethoxybenzaldehyde **LCB15**

The ^1H and ^{13}C - NMR spectra (Table 3.20, Figure 3.70) and (Table 3.20, Figure 3.71) of **LCB15** resembled the spectra assignments of **LCB11** and the only difference was the substitution at position C-2 in **LCB15** that was substituted with methoxyl instead of hydroxyl group. Based on the spectroscopic data of **LCB15** and comparison with the literature values, it was confirmed that compound **LCB15** was 2, 5-dimethoxybenzaldehyde (Chang et al., 1998) (Natiello et al., 1983).

Table 3.20: ^1H NMR (400 MHz) and ^{13}C NMR (100 MHz) spectral data of 2,5-dimethoxy benzaldehyde **LCB15**

Position	^1H -NMR(δ , J in Hz)	^{13}C -NMR (δ c)
1	-	129.5
2	-	152.8
3	7.05 (1H, <i>d</i> , 8.8)	108.8
4	7.44 (1H, <i>dd</i> , 8.8, 1.2)	127.6
5	-	147.6
6	7.43 (1H, <i>s</i>)	114.4
1'	9.65 (1H, <i>s</i>)	191.0
2,5-OMe	3.95 (6H, <i>s</i>)	56.2

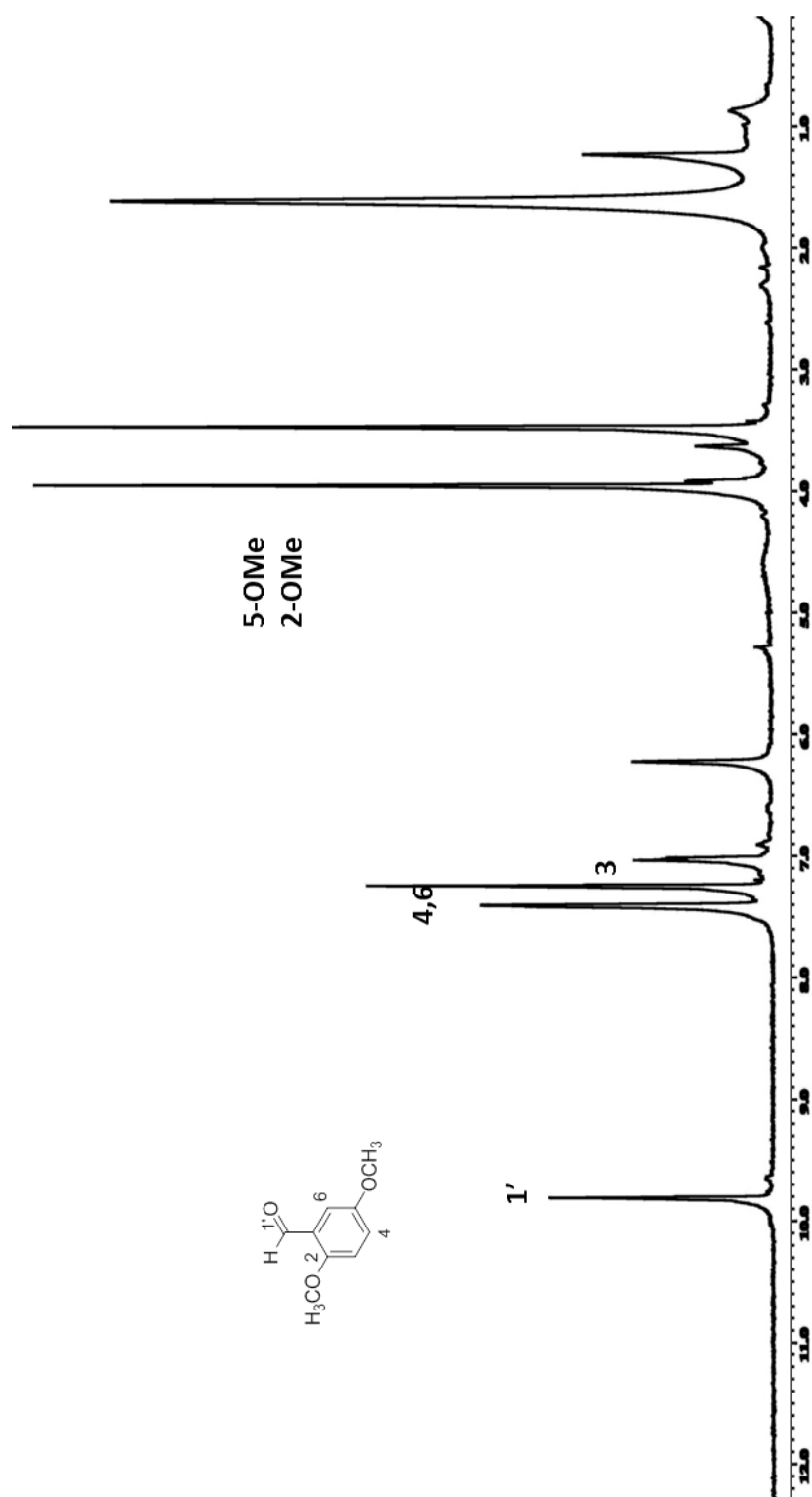


Figure 3.70: ^1H NMR spectrum of 2,5-dimethoxybenzaldehyde LCB15

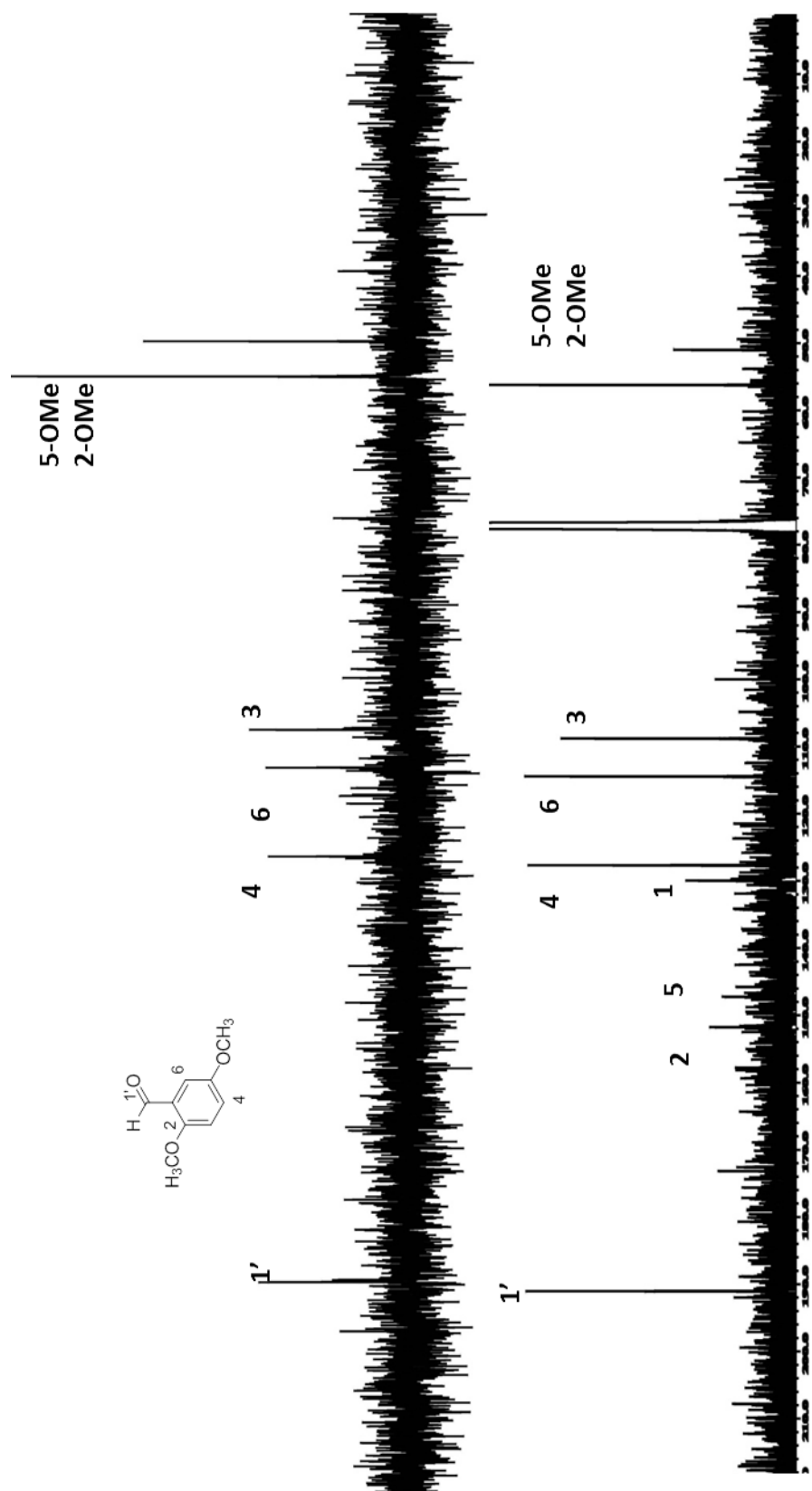
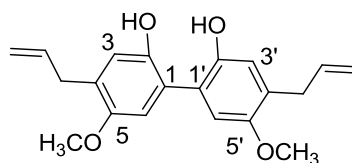


Figure 3.71: ^{13}C -NMR/DEPT spectrum of 2, 5-dimethoxybenzaldehyde LCB15

3.2.4 Neolignan LCB3: Biseugenol A



LCB 3

Neolignan **LCB3** with IUPAC name of 4, 4'-diallyl-5, 5'-dimethoxy-(1, 1'-biphenyl)-2, 2'-diol was afforded as brown oil. The UV spectrum showed absorptions at λ_{max} (MeOH) nm (log ϵ) 247 (3.121), 291 (2.214) and 306 (1.462). The IR spectrum showed absorptions at 3427 cm^{-1} due to the stretching of O-H, and 1642 cm^{-1} indicated the existing of C=C group in the structure. LC-MS (negative mode) showed the pseudomolecular ion peak at m/z 325.1394 corresponding to the molecular formula of $\text{C}_{20}\text{H}_{22}\text{O}_4$.

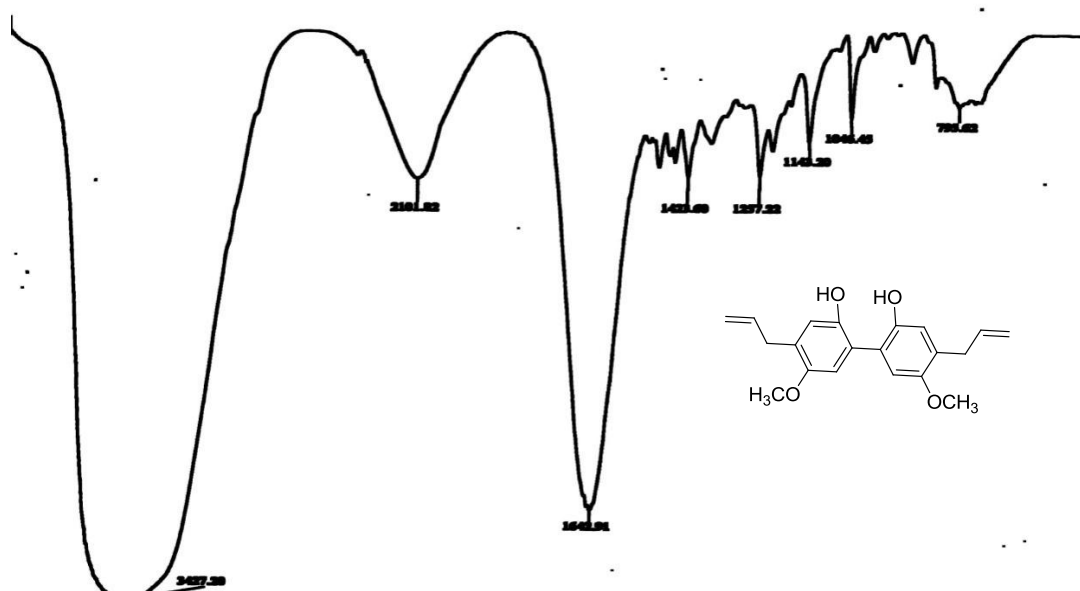


Figure 3.72: IR Spectrum of biseugenol A **LCB3**

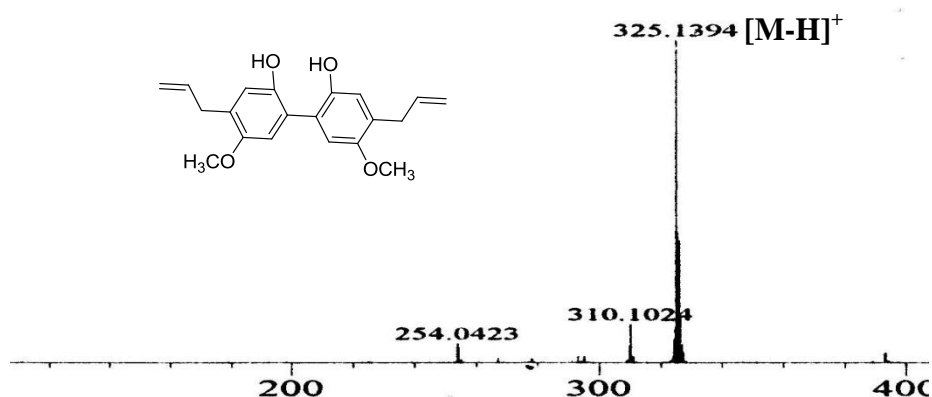


Figure 3.73: LC-MS spectrum of biseugenol A LCB3

The ^1H -NMR (Table 3.21, Figure 3.74) analysis exhibited the presence of two methoxyl groups which resonated at δ 3.81 as a singlet and these methoxyl groups were positioned at C-5 and C-5'. The two hydroxyl group were observed at δ 5.91 as a singlet. Two sp^3 methylene groups were resonated at δ 3.34 which was at lower field due to the deshielding effect of carbon-carbon double bond. Two sp^2 methylene protons in the allyl groups were observed at δ 5.04 appeared as a doublet of doublet and the sp^2 methine groups were resonated at δ 5.95 as a multiplet. The aromatic proton peaks were observed at δ 6.73 (C-3) and δ 6.74 (C-6) (Nam et al., 1992). The COSY spectrum (Table 3.21, Figure 3.75) displayed only the correlations of H- γ /H- β , H- α /H- β .

The ^{13}C NMR and DEPT spectra (Table 3.21, Figure 3.76) showed 20 carbon signals which consist of two methoxyls, four methylenes, six methines and eight quaternary carbons. The two methoxyls were observed at δ 56.1 as a singlet and these methoxyls positioned at C-5 and C-5'. Two sp^3 methylenes were resonated at δ 39.9 (C- α , α') and two sp^2 methylene peaks appeared at δ 115.7 (C- γ , γ'). Two methines in the allyl group were observed at 137.6 (C- β , β') and four aromatic protons appeared at δ 123.1 (C-3, 3') and 110.6 (C-6, 6'). Eight quaternary carbon peaks appeared at δ

124.4(C-1, 1'), 140.8 (C-2, 2'), 147.2 (C-5, 5') and 131.9 (C-4,4') (Delogu et al., 2004; Fujisawa et al., 1999; Suarez et al., 1983). The HMQC spectrum (Table 3.21, Figure 3.77) showed the connectivity between proton and carbon: H- β / C- β , H- γ /C- γ , H- α /C- α , H-3/ C-3 , H-6/C-6 and H-OCH₃/C-OCH₃ (Kawanishi et al., 1981).

The HMBC spectrum (Table 3.21, Figure 3.78) the cross-peaks were observed between H- α to C-6,6', C- γ , γ' , C-3,3', C-4,4', C- β , β' ; OH to C-3,3', C-2,2', C-5,5'; OCH₃ to C-5,5'; H-3 to C- α , C-6,6', C-2,2', C-3,3' ; H-6 to C- α , α' , C-3,3', C-2,2', C-4,4', C-5,5'; H- β to C-4,4' , C- α , α' and H- γ to C- α , C- β .

Based on the observed data it is confirmed that the compound **LCB3** was 4, 4'-diallyl-5, 5'-dimethoxy-[1, 1'-biphenyl]-2, 2'-diol **LCB3** and this compound is a new neolignan and has never been isolated from any plant species before. We named this compound as **biseugenol A**. The structure of biseugenol A has the similar skeleton with biseugenol which has been reported before and the different was only the position of hydroxyl and methoxyl groups attached to the ring.

Table 3.21: 1D (^1H and ^{13}C) and 2D (COSY, HMQC and HMBC) NMR spectra data of bis Eugenol A **LCB3**

Position	^1H -NMR(δ , J in Hz)	^{13}C -NMR (δc)	COSY	HMQC	HMBC
1,1'	-	124.4	-	-	-
2,2'	-	140.8	-	-	-
3,3'	6.73 (2H, <i>s</i>)	123.1	-	H-3/C-3	6,3,2, α
4,4'	-	131.9	-	-	-
5,5'	-	147.2	-	-	-
6,6'	6.74 (2H, <i>s</i>)	110.6	-	H-6/C-6	2,3,4,5, α
α	3.3 (4H, <i>d</i> , 6.7)	39.9	H- α /H- β	H- α /C- α	4,6, β , γ ,3
β	5.91-5.95 (2H, <i>m</i>)	137.6	H- γ /H- β	H- β /C- β	4, α
γ	5.04 (4H, <i>dd</i> , 17,1, 13.4)	115.7	-	H- γ /C- γ	α , β
5-OMe	3.81(6H, <i>s</i>)	56.1	-	H-OMe/C-5OMe	5
2-OH	5.91(1H, <i>s</i>)	-	-	-	5,3,2

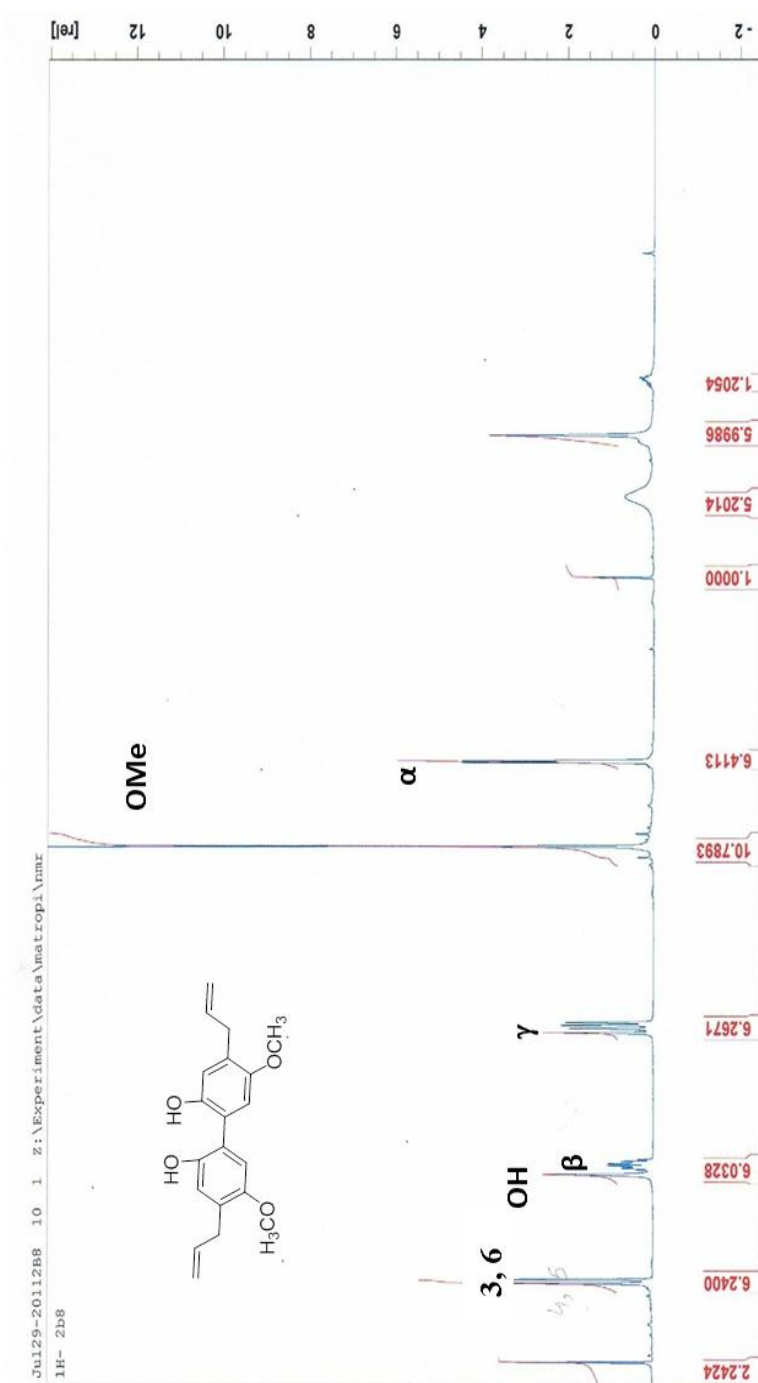


Figure 3.74: ^1H NMR spectrum of bisphenol A LCB3

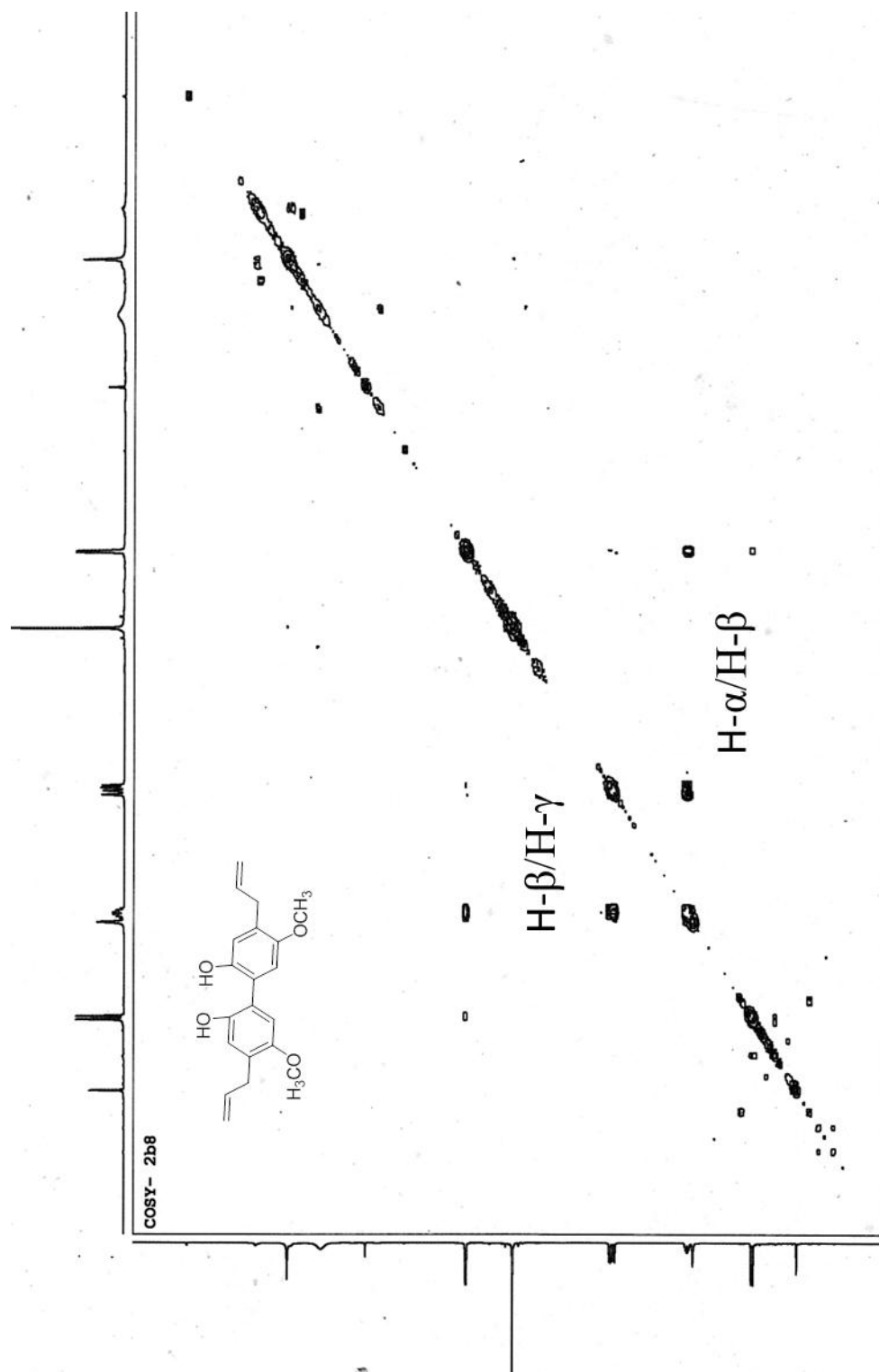


Figure 3.75: COSY spectrum of bisugenol ALCB3

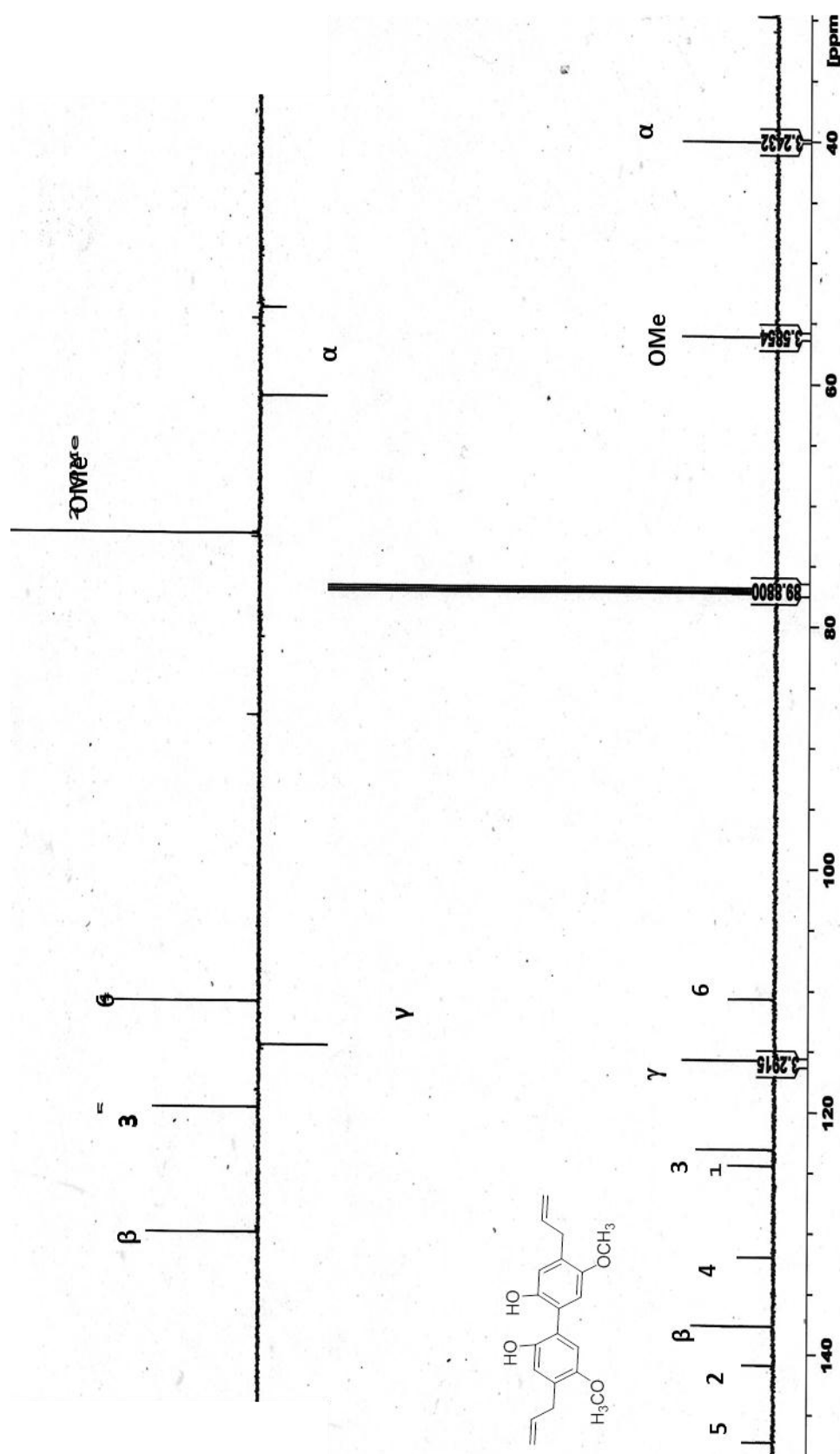


Figure 3.76: ^{13}C NMR/DEPT spectrum of bisphenol A LCB3

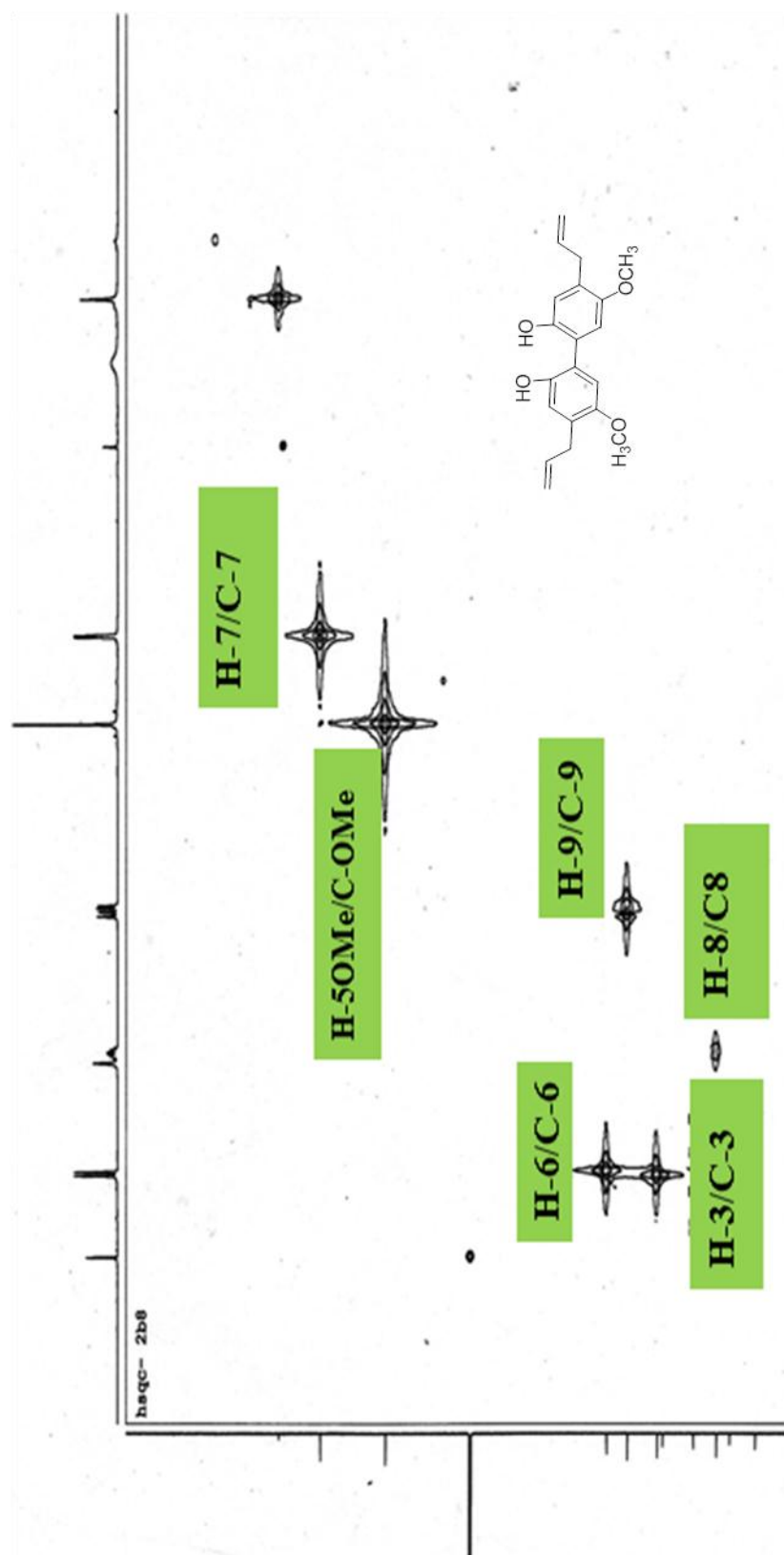


Figure 3.77: HSQC spectrum of bisugenol A LCB3

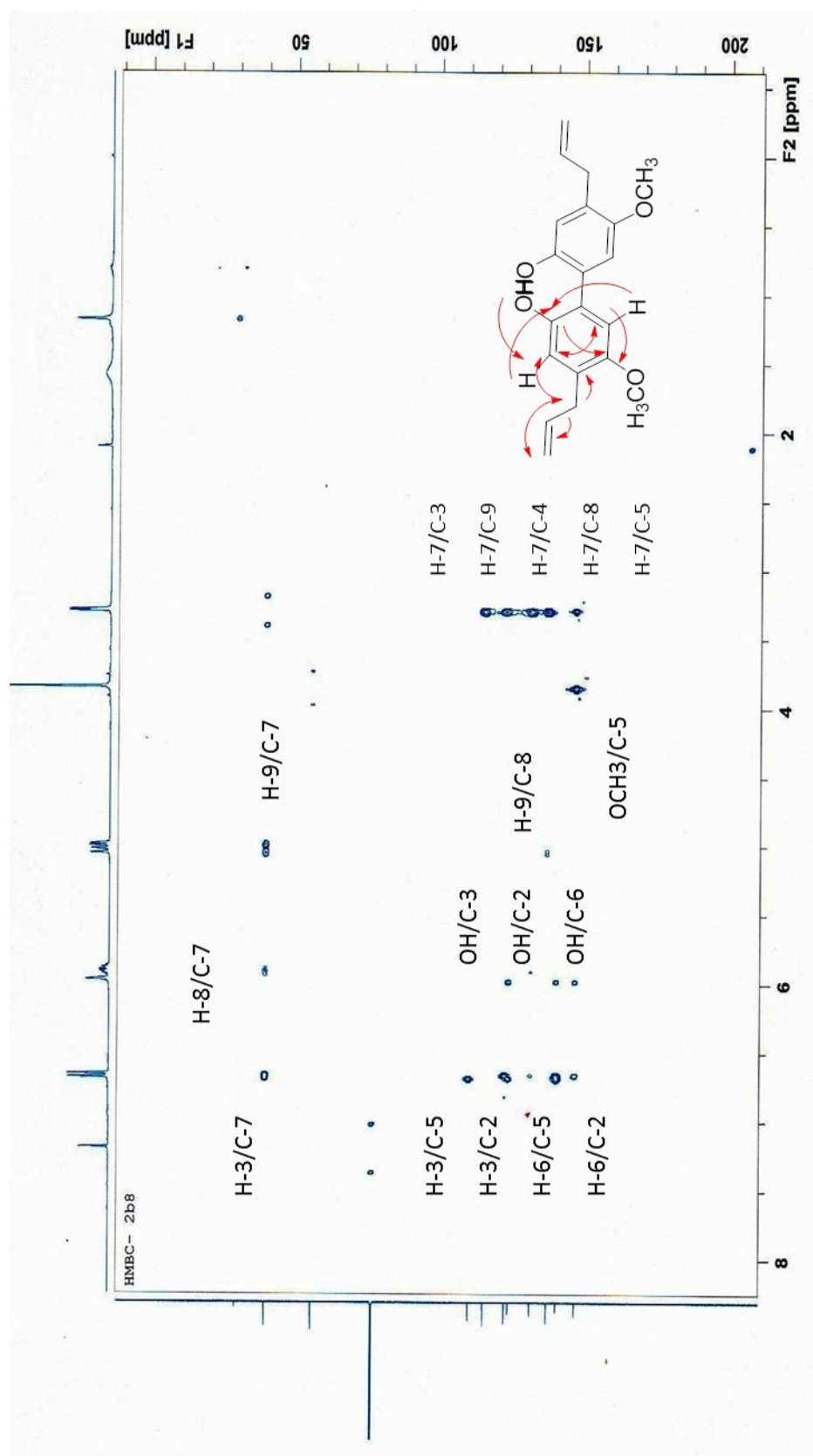
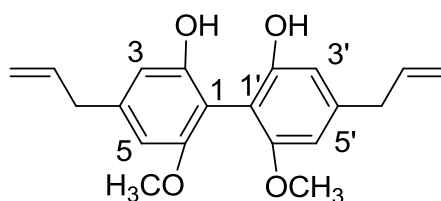


Figure 3.78: HMBC spectrum of bisugenol A LCB3

3.2.5 Neolignan **LCB9**: Biseugenol



LCB9

Neolignan **LCB9** with IUPAC name of 4, 4'-diallyl-6, 6'-dimethoxy-[1, 1'-biphenyl]-2, 2'-diol was afforded as brown oil. the same Biseugenol A just different in the HMBC spectrum. The HMBC spectrum (Table 3.22, Figure 3.79) the cross-peaks were observed between H- α /C-6,6', C- γ , γ' , C-3,3', C-4,4', C- β , β' ; OH/C-3,3', C-2,2', C-5,5'; OCH₃/C-5,5'; H-3/C- α , C-6,6', C-2,2', C-3,3'; H-6/C- α , α' , C-3,3', C-2,2', C-4,4', C-5,5'; H- β / C-4,4' , C- α , α' and H- γ /C- α , C- β .

Table 3.22: 1D (^1H and ^{13}C) and 2D (COSY, HMQC and HMBC) NMR spectra data of biseugenol **LCB9**

Position	^1H -NMR(δ , J in Hz)	^{13}C -NMR (δc)	COSY	HMQC	HMBC
1,1'	-	124.4	-	-	-
2,2'	-	140.8	-	-	-
3,3'	6.73 (2H, s)	123.1	-	H-3/C-3	6,3,2, α
4,4'	-	131.9	-	-	-
5,5'	6.74 (2H, s)	110.6	-	H-5/C-5	-
6,6'	-	142.2	-	-	2,3,4,5, α
α	3.3 (4H, d , 6.7)	39.9	H- α /H- β	H- α /C- α	4,5, β , γ ,3
β	5.91-5.95 (2H, m)	137.6	H- γ /H- β	H- β /C- β	4, α
γ	5.04 (4H, dd , 17,1, 13.4)	115.7	-	H- γ /C- γ	α , β
6-OMe	3.81(6H, s)	56.1	-	H-OMe/C-6OMe	5
2-OH	5.91(1H, s)	-	-	-	5,3,2

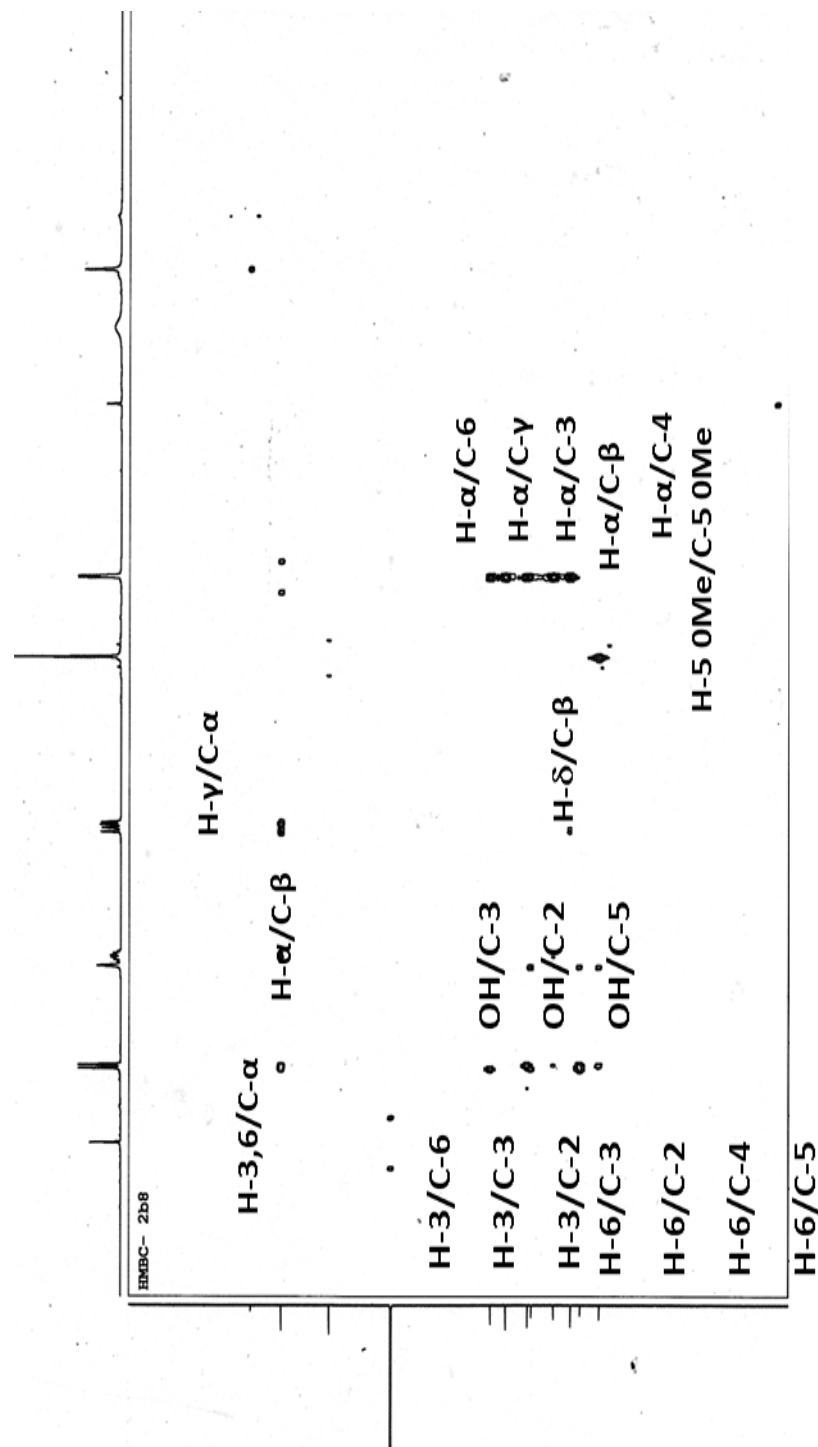
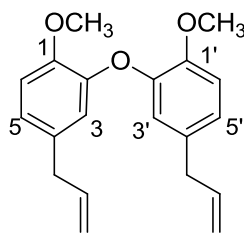


Figure 3.79: HMBC spectrum of biseugenol LCB7

3.2.6 Oxyneolignan LCB 10: Biseugenol B



LCB10

Compound **LCB10** with IUPAC name 2, 2'-oxybis (4-allyl-1-methoxybenzene) was afforded as yellow brown oil. The UV spectrum showed absorptions at λ_{\max} (MeOH) nm (log ϵ) 278 (2.337) and 239 (2.767) indicating the presence of unsaturated carbon-carbon bond. The IR spectrum showed an absorption peak at 1591 cm^{-1} assigned for the aromatic characteristics and allyl group was absorbed at 1638 cm^{-1} (Iio et al., 1982). LC-MS showed the pseudomolecular ion peak $[M-1]^-$ at m/z 309.20 corresponding to the molecular formula of $\text{C}_{20}\text{H}_{22}\text{O}_3$.

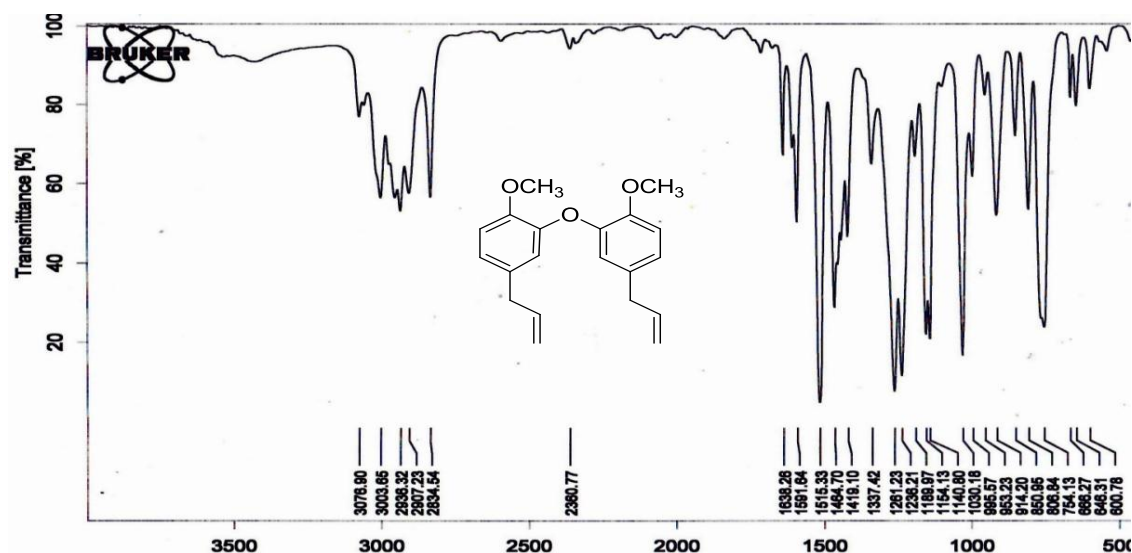


Figure 3.80: IR Spectrum biseugenol B LCB10

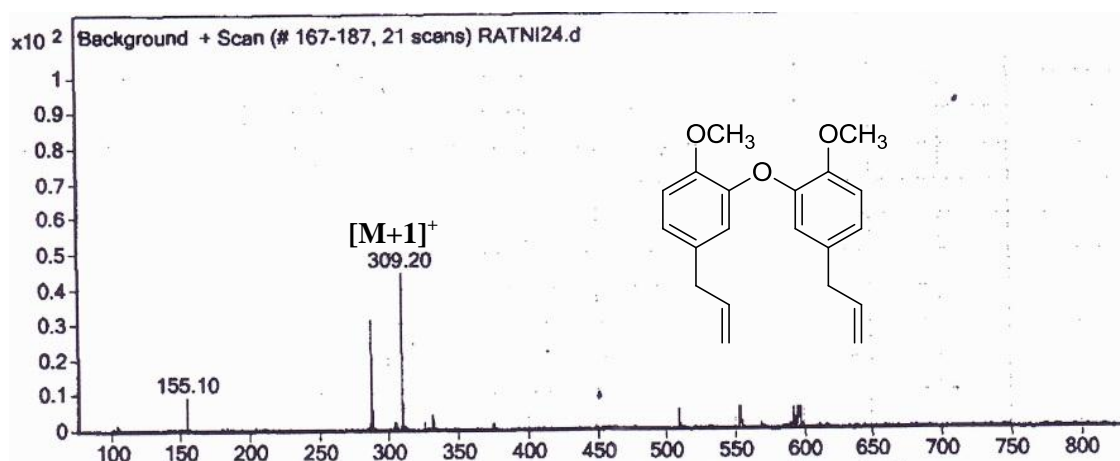


Figure 3.81: LC-MS spectrum of biseugenol B LCB10

The ^1H -NMR spectrum (Table 3.23, Figure 3.82) exhibited two methoxyls resonated at δ 3.81 as a singlet and these methoxyls positioned at C-1 and C-1'. One sp^3 methylene group was observed at δ 3.31 as a doublet and sp^2 methylene group was resonated at δ 5.05 as a doublet of doublet. The sp^2 methine was observed at δ 5.04 as a multiplet. The aromatic protons were resonated at δ 6.81 (C-5), δ 6.31 (C-6) and δ 6.72 (C-3). The above observations were reinforced by COSY (Table 3.23, Figure 3.83) experiment which displayed correlations of H-5/H-6, H- α /H- β and H- β /H- γ .

The ^{13}C NMR and DEPT spectrum (Table 3.23, Figure 3.84) established 20 carbon signals which consist of two methoxyls, two sp^2 methylene, two sp^3 methylene, eight methines and six quaternary carbons. The two methoxyl groups positioned at C-1 and C-1' were resonated at δ 56.0. Two sp^3 methylenes were observed at δ 39.8 (C- α , α'), two sp^2 methylenes appeared at δ 115.6 (C- γ , γ'). Two methines in allyl group were observed at δ 137.7 (C- β , β') and six aromatic protons appeared at δ 111.3 (C-6, 6'), 111.9 (C-3, 3') and 120.4 (C-5, 5'). Six quaternary carbons were resonated at δ 132.7 (C-4, 4'), 148.9 (C-1, 1') and 147.4 (C-2, 2'). HMQC spectrum (Table 3.23, Figure 3.85) showed the connectivity between proton and carbon: H- β /C- β , H- γ /C- γ , H- α /C- α , H-3/C-3, H-5/C-5, H-6/C-6 and H-OMe/C-OCH₃). In the HMBC spectrum (Table 3.23, Figure 3.86) the cross-peaks were observed between H-3 to C-6, C-5, C-2, C- α , H-6 to

C-2, H-5 to C-4, C-5, C-2, C- α , H- α to C-5, C- γ , C- β , C-4, C-3, H- β to C-4, /C- α , H-OMe to C-2, H- γ to C- β (Kwak et al., 2008).

Based on the observed spectral data of **LCB10** it was confirmed that compound **LCB10** was 2, 2' -oxybis (4-allyl-1-methoxybenzene). This is a new compound and has never been reported before. This compound has the same skeleton with eugenol and related to compound **LCB3**. This compound was named as biseugenol B.

Table 3.23. 1D (^1H and ^{13}C) and 2D (COSY, HMQC and HMBC) NMR spectra data of biseugenol B **LCB10**

Position	^1H -NMR(δ , J in Hz)	^{13}C -NMR (δc)	COSY	HMQC	HMBC
1,1'	-	148.9	-	-	-
2,2'	-	147.4	-	-	-
3,3'	6.72(2H, s)	111.9	-	H-3/C-3	2,5,6, α
4,4'	-	132.7	-	-	-
5,5'	6.81(2H, d , 7.9)	120.4	H-5/H-6	H-5/C-5	2,4,5, α
6,6'	6.31 (2H, d , 7.9)	111.3	H-6/H-5	H-6/C-6	2
α	3.31(4H, d , 6.8)	39.8	β	-	$\beta,\gamma,3,5,4$
β	5.09 (2H, m)	137.7	γ	H- β /C- β	4, α
γ	5.01-5.09(4H, dd , 17.1, 12.4)	115.6	-	H- γ /C- γ	B, α
1-OMe	3.81(3H, s)	56.0	-	H-OMe/C-1OMe	2

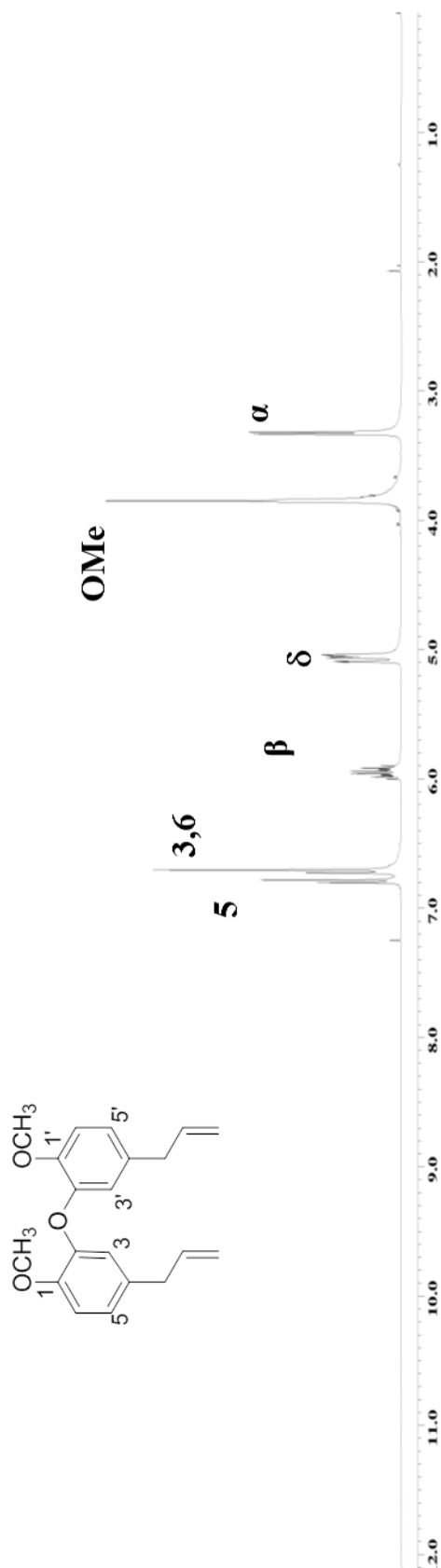


Figure 3.82: ¹H-NMR spectrum of bisugenol B LCB10

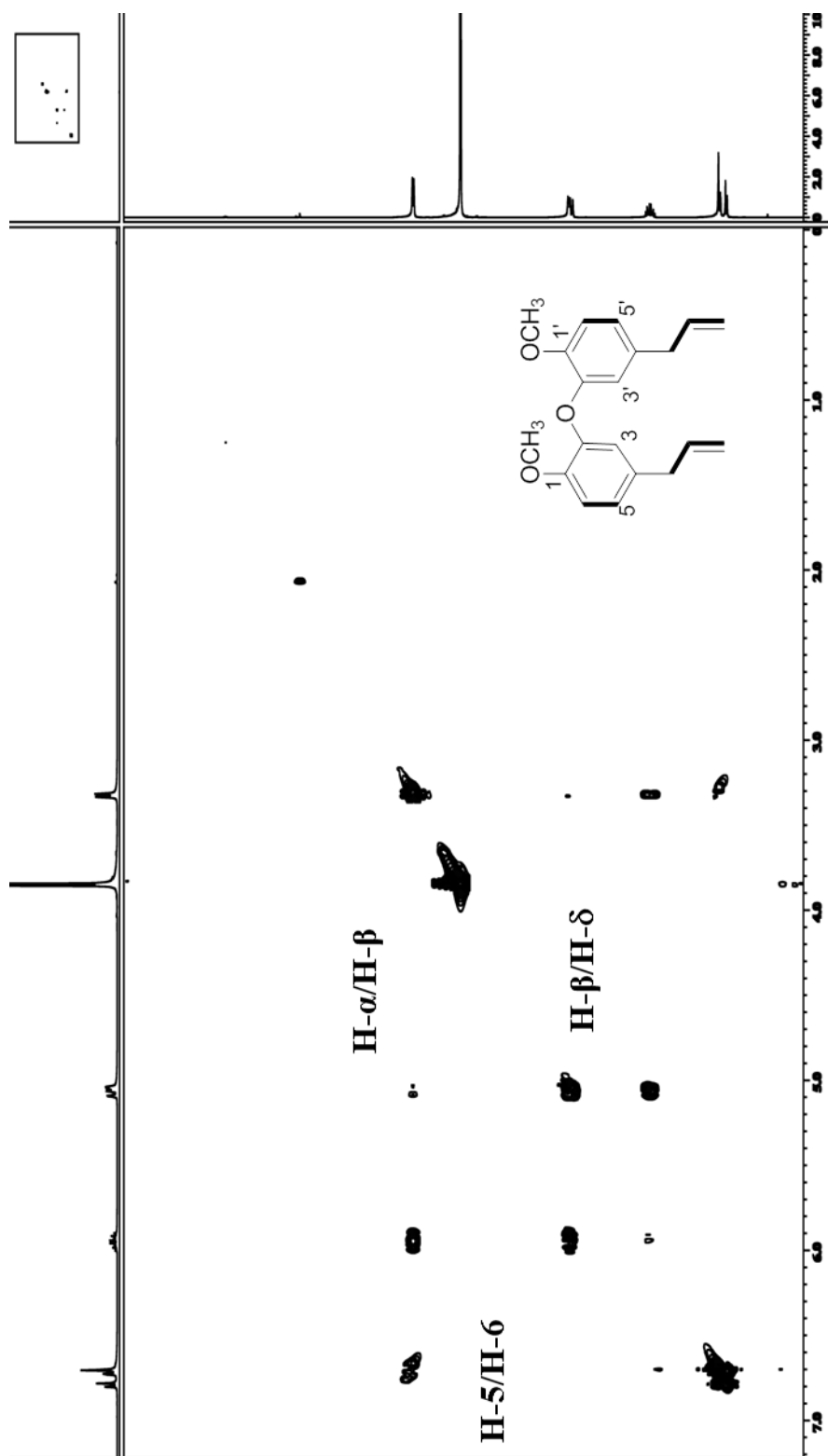


Figure 3.83: COSY spectrum of bisphenol B LCB10

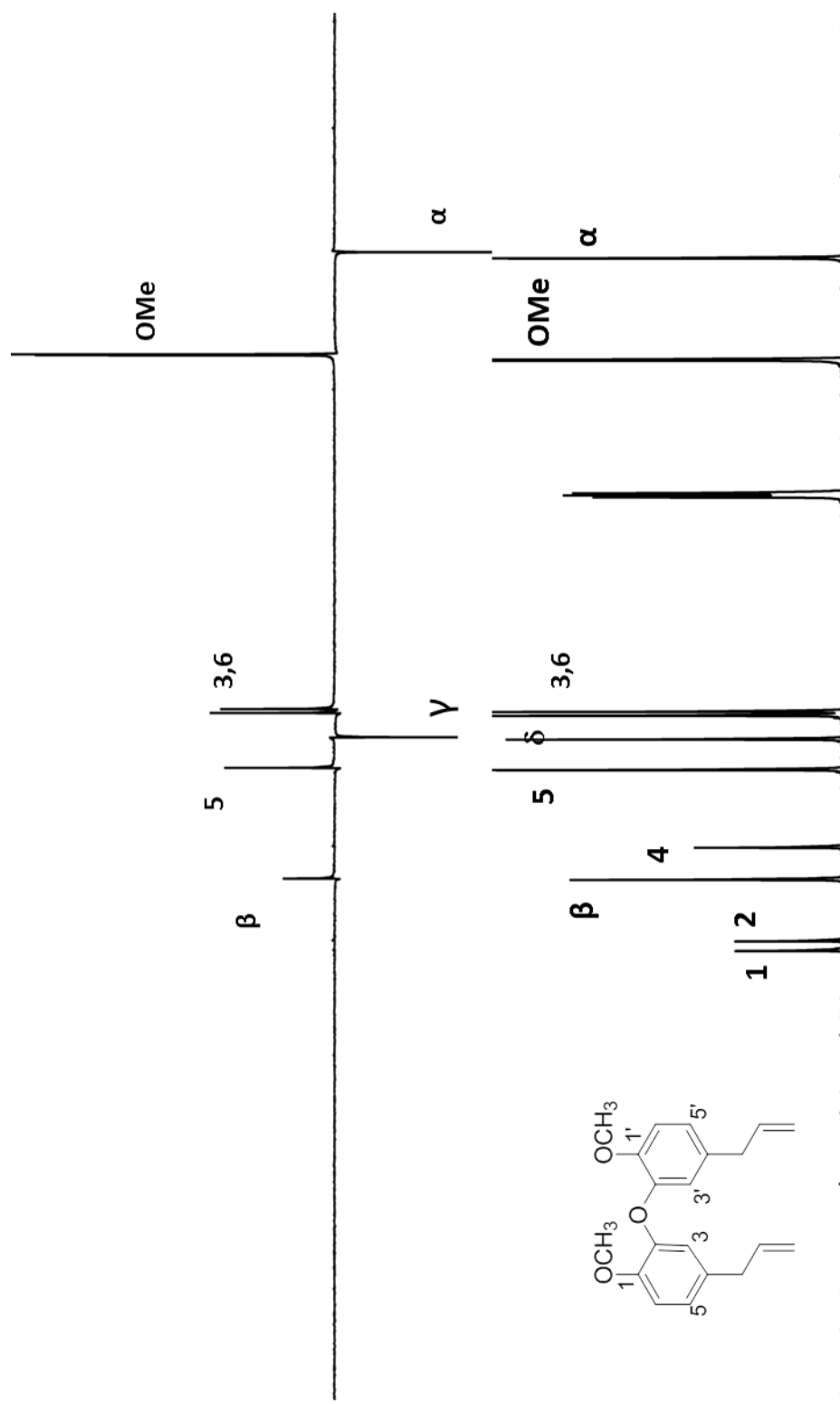


Figure 3.84: ^{13}C -NMR/DEPT spectrum of bisugenol B LCB10

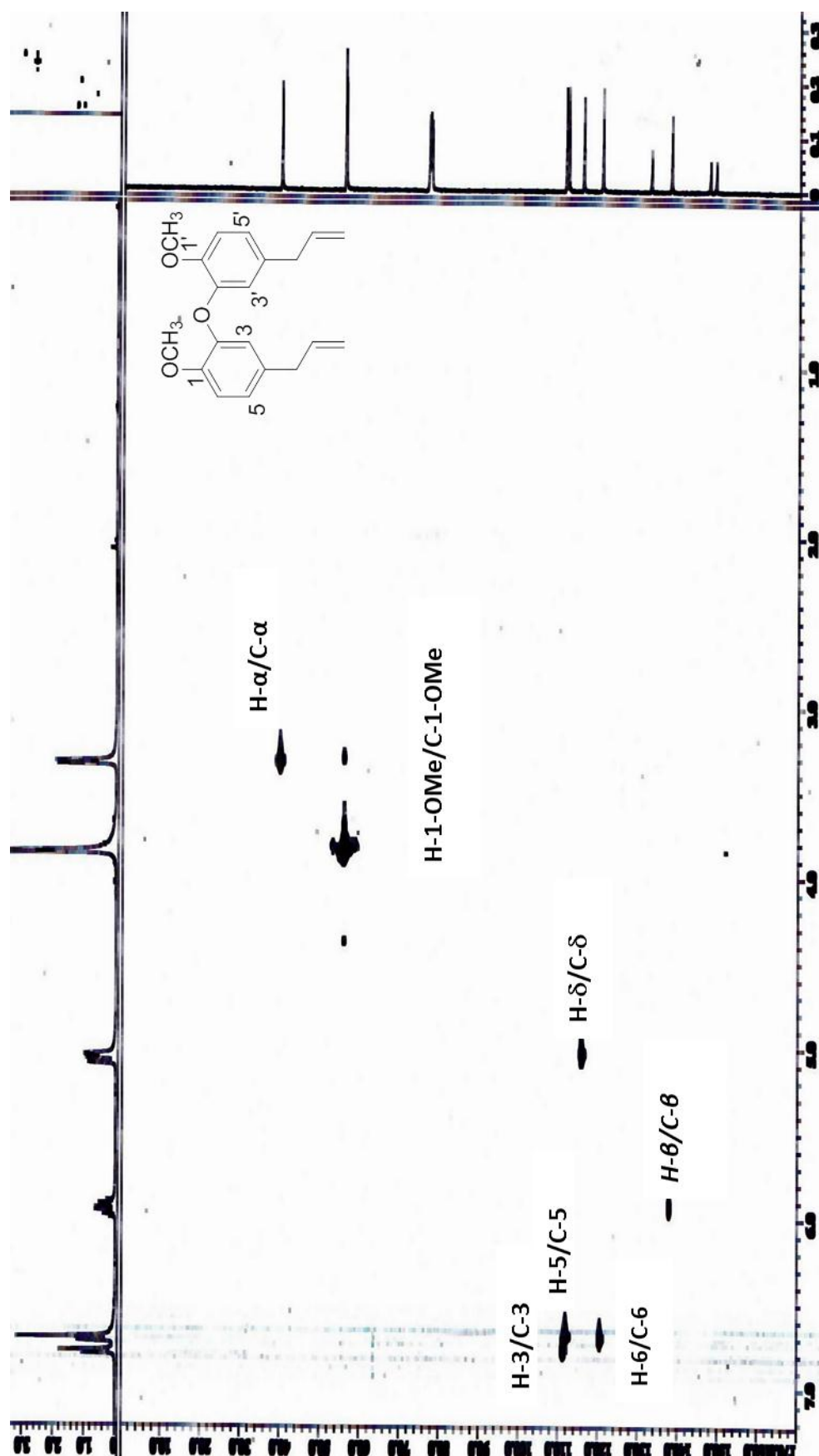


Figure 3.85: HMQC spectrum of bisugenol B LCB10

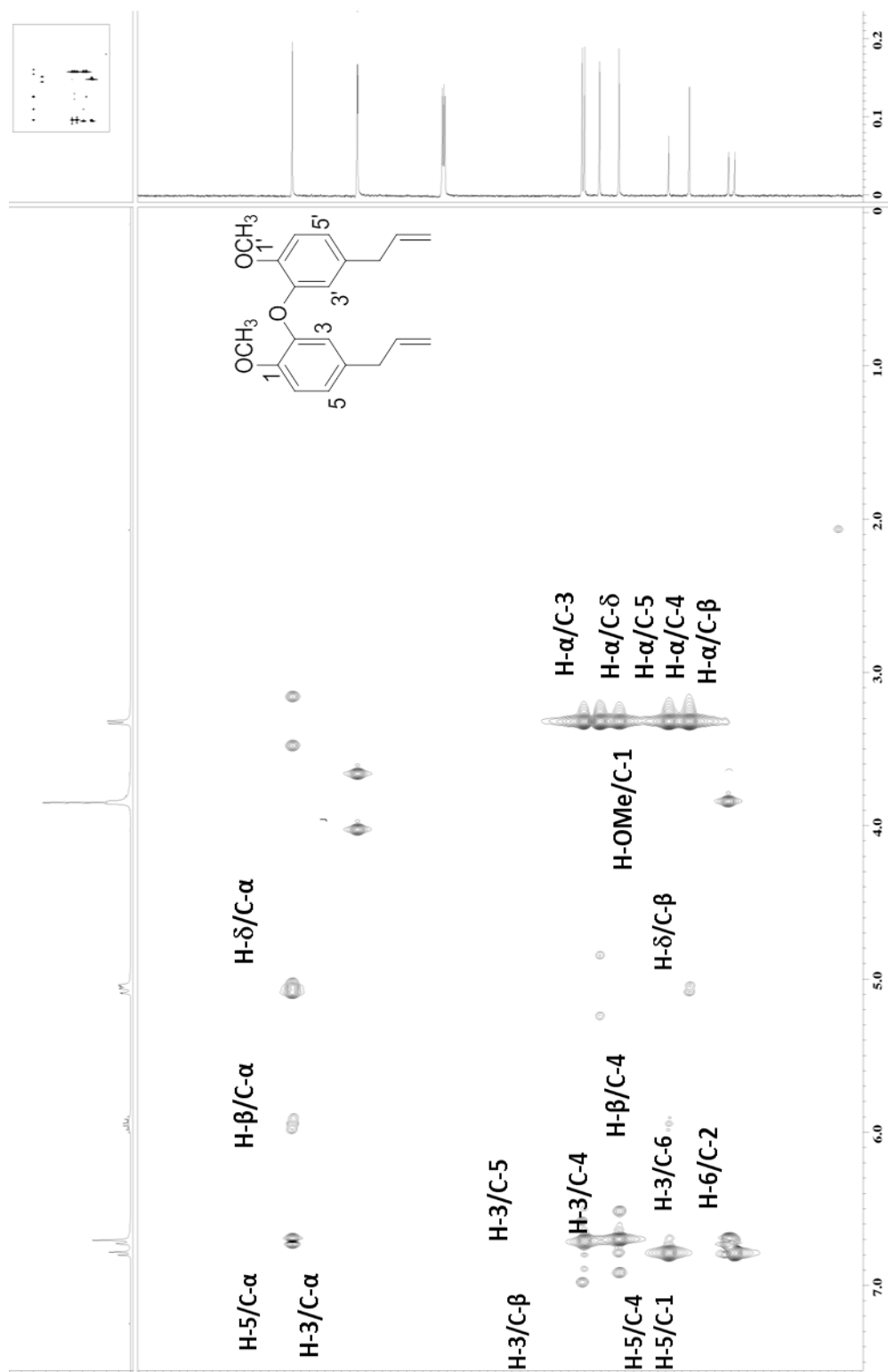
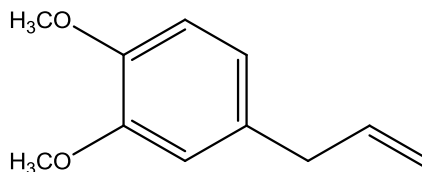


Figure 3.86: HMBC spectrum of bisphenol B LCB10

3.2.7 4-Allyl-1,2-dimethoxybenzene



LCL15

Compound **LCL15** with IUPAC name 4-allyl-1,2-dimethoxy benzene was afforded as yellow brown oil. The UV spectrum showed absorptions at λ_{max} (MeOH) nm (log ϵ) 278 (2.337) and 239 (2.767) indicating the presence of unsaturated carbon-carbon bond. The IR spectrum showed an absorption peak at 1591 cm^{-1} assigned for the aromatic characteristics and allyl group was absorbed at 1638 cm^{-1} (Iio et al., 1982). LC-MS showed the pseudomolecular ion peak $[M - H]^-$ ion peak at m/z 177.084 corresponding to the molecular formula of $\text{C}_{11}\text{H}_{14}\text{O}_2$.

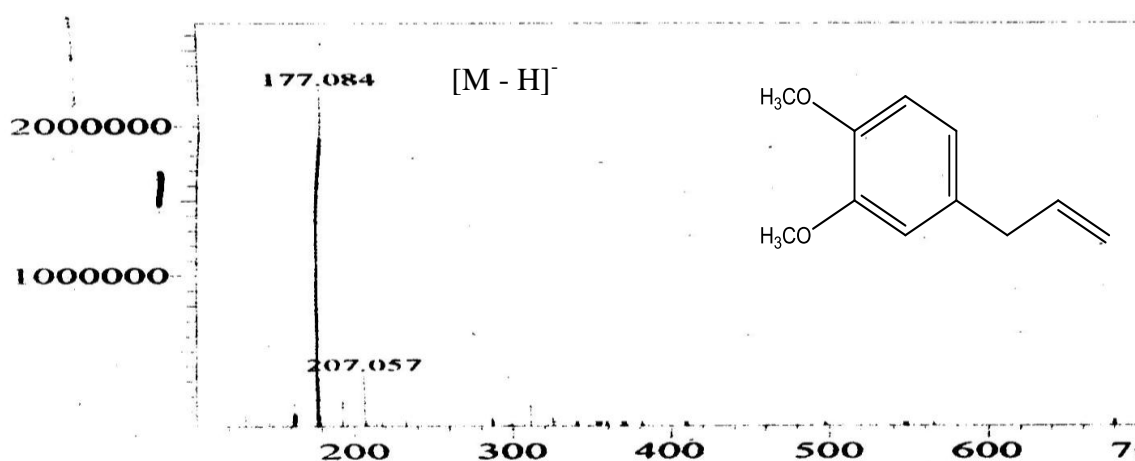


Figure 3.87: LC-MAS Spectrum of 4-allyl-1,2-dimethoxybenzene **LCL15**

The ^1H NMR spectra of **LCB15** showed the presence of 1, 2, 4-trisubstituted benzene. The presence of one C_3 units and two methoxyl groups suggesting that **LCB15** is a lignan. The ^1H NMR spectrum of **LCL15** showed sets of ABX-type hydrogen aromatic signals, [δ 6.72 (1H, d, $J=2.0\text{Hz}$, H-3), δ 6.81 (1H, d, $J=7.93$, H-5) and 6.73 (1H, d, $J=7.93$, H-6)], an allyl group, [δ 3.31 (2H, d, $J=6.84\text{ Hz}$, H-7), 5.04 (1H, d, $J=10.4\text{ Hz}$, Ha-9), 5.08 (1H, d, $J=17.2\text{ Hz}$, Hb-9) and 5.95 (1H, ddt, $J=17.2, 10.4, 6.8\text{ Hz}$, H-8)] and two methoxy groups, [δ 3.81, 3H, s] (Figure 3.88).

Based on the observed data it was confirmed that **LCL15** was 4-allyl-1,2-dimethoxybenzene and it was a simple aromatic compound.

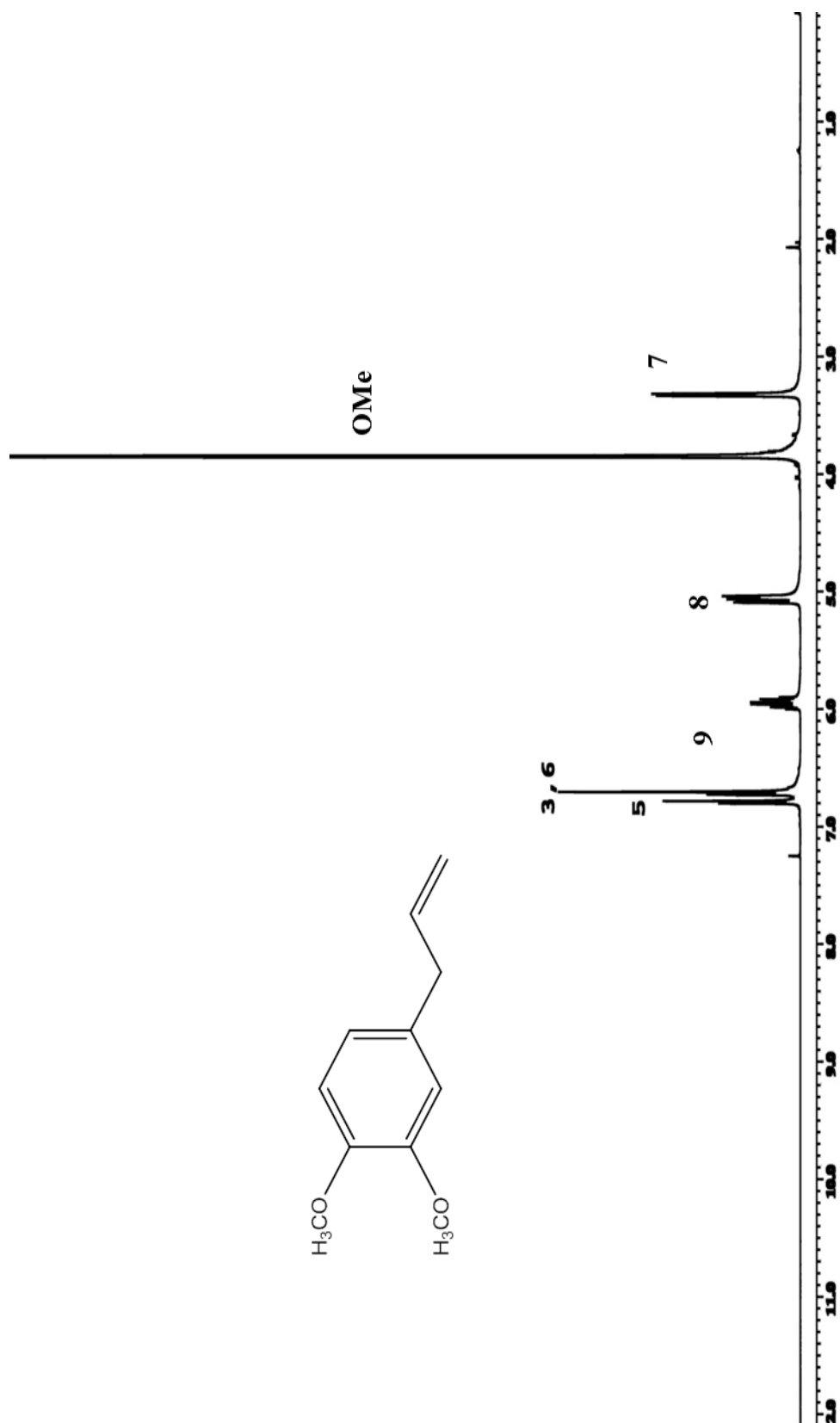
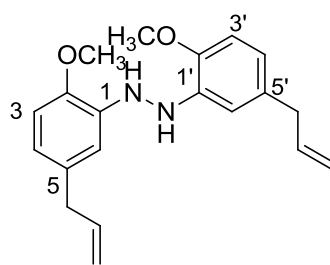


Figure 3.88: ¹H-NMR spectrum of 4-allyl-1,2-dimethoxybenzene LCL15

3.2.8 Biphenylhydrazine LCB17: Biseugenol C



LCB 17

Compound **LCB17** with IUPAC name 1, 2-bis (5-allyl-2-methoxyphenyl) hydrazine was afforded as yellow oil . The UV spectrum showed absorptions at λ_{\max} (MeOH) nm (log ϵ) 225 (2.413) and 239 (2.763) indicating the presence of unsaturated carbon-carbon bond. The IR spectrum showed absorption peak at 3517 cm^{-1} indicated the existing of NH, 1638 cm^{-1} for olefinic SP bond and 1513 cm^{-1} assigned for the aromatic characteristics. LC-MS showed the pseudomolecular ion peak $[M+Na]^+$ at m/z 348.8434 and molecular ion peak $[M]^+$ at m/z 324.7967 corresponding to the molecular formula of $C_{20}H_{24}N_2O_2$.

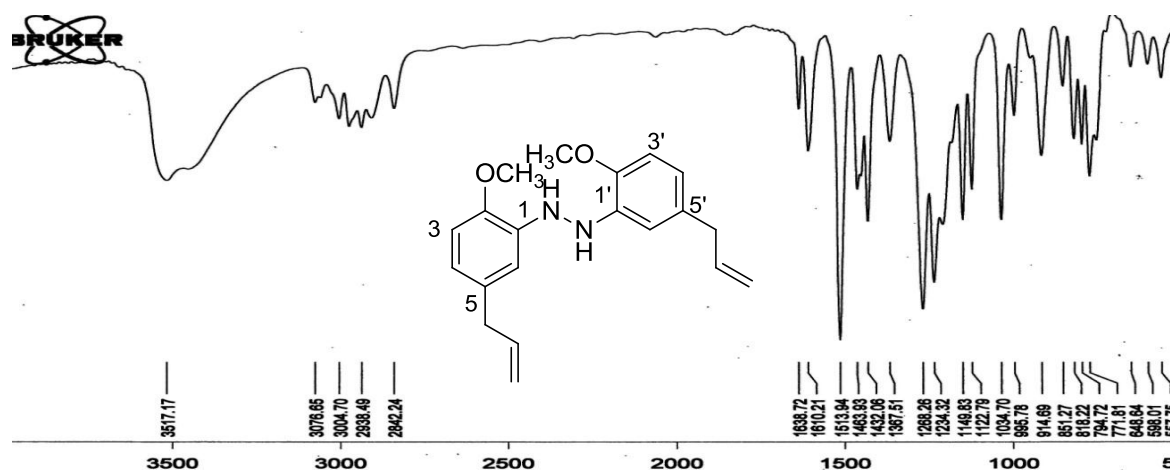


Figure 3.89: IR Spectrum of biseugenol C LCB17

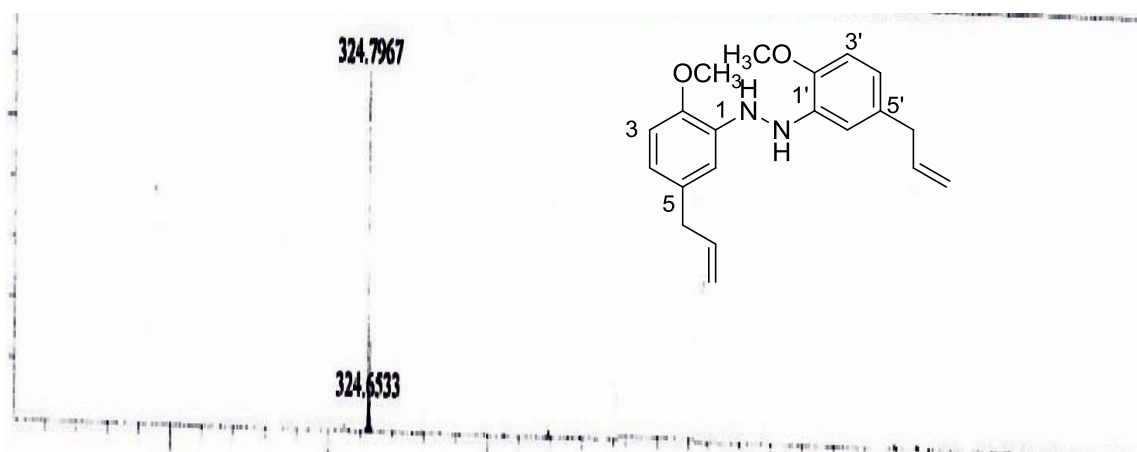


Figure 3.90: LC-MS Spectrum of bis-eugenol C LCB17

The ^1H -NMR spectrum (Table 3.24, Figure 3.91) exhibited two methoxyls resonated at δ 3.81 as a singlet and these methoxyls positioned at C-6 and C-6'. One sp^3 methylene group was observed at δ 3.31 as a doublet and sp^2 methylene group was resonated at δ 5.05 as a doublet of doublet. The sp^2 methine was observed at δ 5.95 as a multiplet. The aromatic protons were resonated at δ 6.73 (C-3 and C-4) and δ 6.89 (C-5). The above observations were reinforced by COSY (Table 3.24, Figure 3.92) experiment which displayed correlations of H- γ /H- β , H- α /H- β , H-4/H-5 and H-3/H-4.

The ^{13}C NMR and DEPT spectra (Table 3.24, Figure 3.93) established 20 carbon signals which consist of two methoxyls, two sp^2 methylene, two sp^3 methylene, eight methines and six quaternary carbons. The two methoxyl groups positioned at C-6 and C-6' were resonated at δ 55.9. Two sp^3 methylenes were observed at δ 39.8 (C- α , C- α'), two sp^2 methylenes appeared at δ 115.5 (C- γ , C- γ'). Two methines in allyl group were observed at δ 137.8 (C- β , C- β') and six aromatic protons appeared at δ 111.2 (C-3, C-3'), 114.2 (C-5, C-5'), 121.1 (C-4, C-4'). Six quaternary SP carbons were resonated at δ 143.8 (C-1, C-1'), 131.9 (C-2, C-2') and 146.4 (C-6, C-6'). HMQC spectrum (Table 3.24, Figure 3.94) showed the connectivity between proton and carbon: H- β /C- β , H- γ /C- γ , H- α /C- α , H-3/C-3, H-4/C-4 and H-5/C-5.

In the HMBC spectrum (Table 3.24, Figure 3.95) the cross-peaks were observed between H- α to C-3, C- β , C- γ , C-4, C-2; OMe to C-6,6'; H- β to C-2, C- α ; NH to C-5, C-1, C-6; H- γ to C- α , C- β ; H-4 to C-3, C-2, C-6; H-3 to C-4, C-2, C-1, C-6; H-5 to C-2, C-1, C-6. Based on the observed spectral data of **LCB17** it was confirmed that compound **LCB17** was 1, 1'-bis (2-allyl-6-methoxyphenyl) hydrazine. This is a new compound and has never been reported before. Compound LCB17 was named as biseugenol C. The structure of this compound has similarity with biseugenol.

Table 3.24: 1D (^1H and ^{13}C) and 2D (COSY, HMQC and HMBC) NMR spectra data biseugenol C **LCB17**

Position	^1H -NMR(δ , J in Hz)	^{13}C -NMR (δc)	COSY	HMQC	HMBC
1,1'	-	143.8	-	-	-
2,2'	-	131.9	-	-	-
3,3'	6.73 (2H, <i>d</i> , 8.0)	111.2	H-3/H-4	H-3/C-3	1,2,4,6
4,4'	6.73 (2H, <i>m</i>)	121.1	H-4/H-5,3	H-4/C-4	3,6,2
5,5'	-	146.4	H-5/H-4	H-5/C-5	1,2,6
6,6'	6.89 (2H, <i>m</i> , 8.2)-	114.2	-	-	-
α , α'	3.31(4H, <i>d</i> , 7.1)	39.8	H- α /H- β	H- α /C- α	2,3,4, γ , β
β , β'	5.95 (2H, <i>m</i>)	137.8	H- β /H- α	H- β /C- β	2, α
γ , γ'	5.05 (4H, <i>dd</i> , 14.8, 12.4)	115.5	-	-	α , β
6,6'OMe	3.81 (6H, <i>s</i>)	55.9	-	-	6
NH	5.51(1H, <i>s</i>)	-	-	-	1,5,6

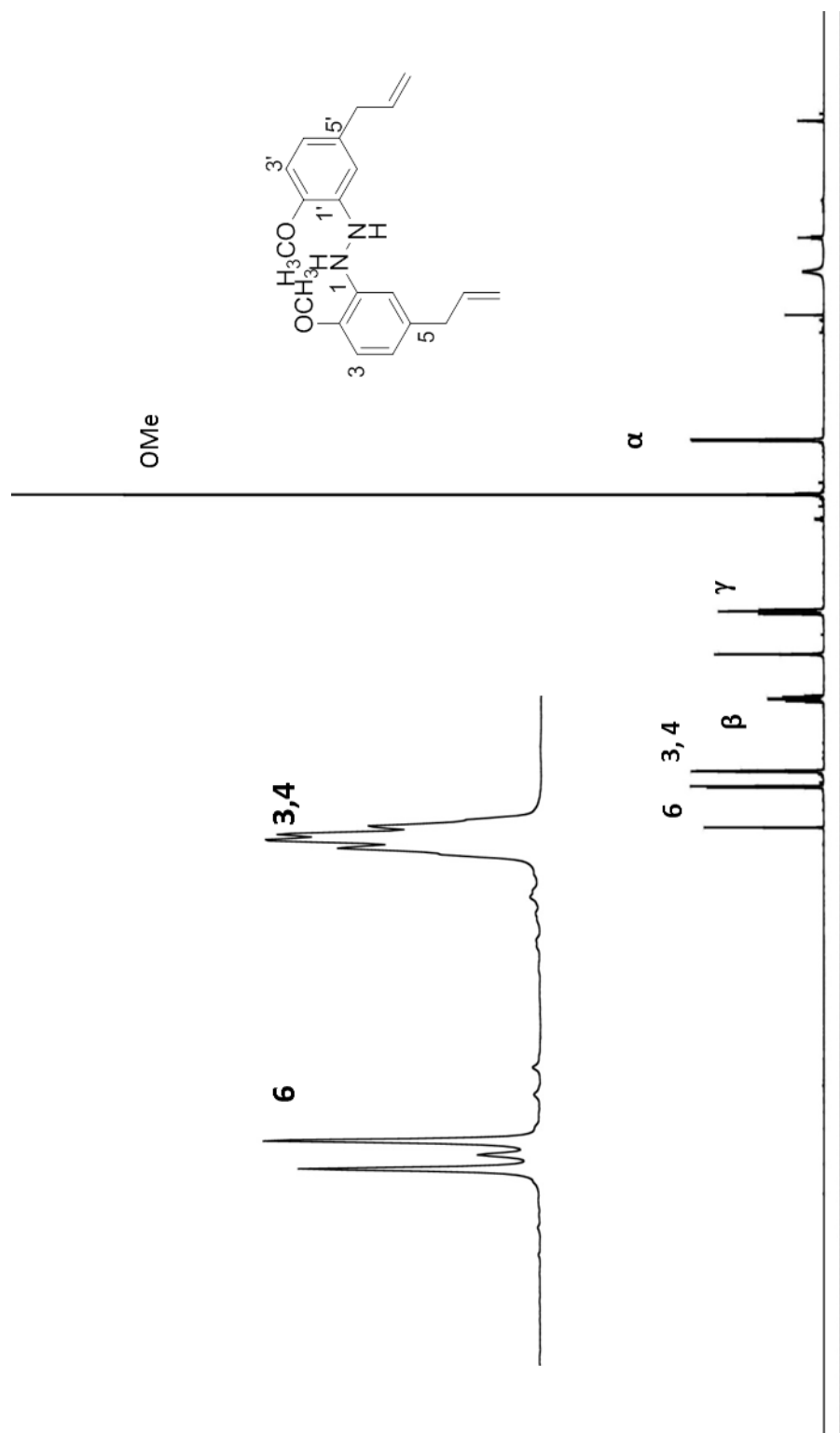


Figure 3.91: ^1H -NMR spectrum of bisphenol C LCB17

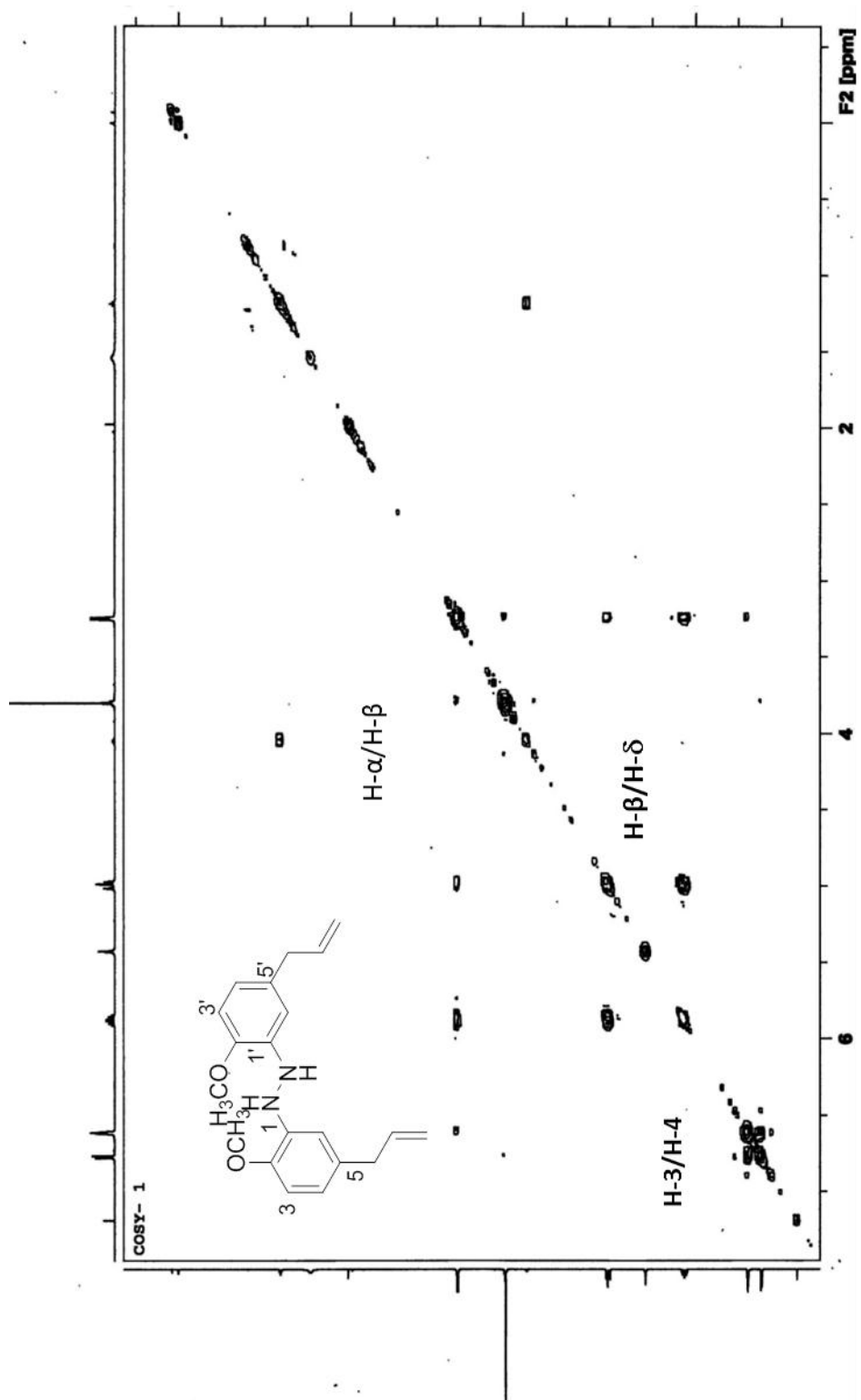


Figure 3.92: COSY spectrum of bisugenol C LCB17

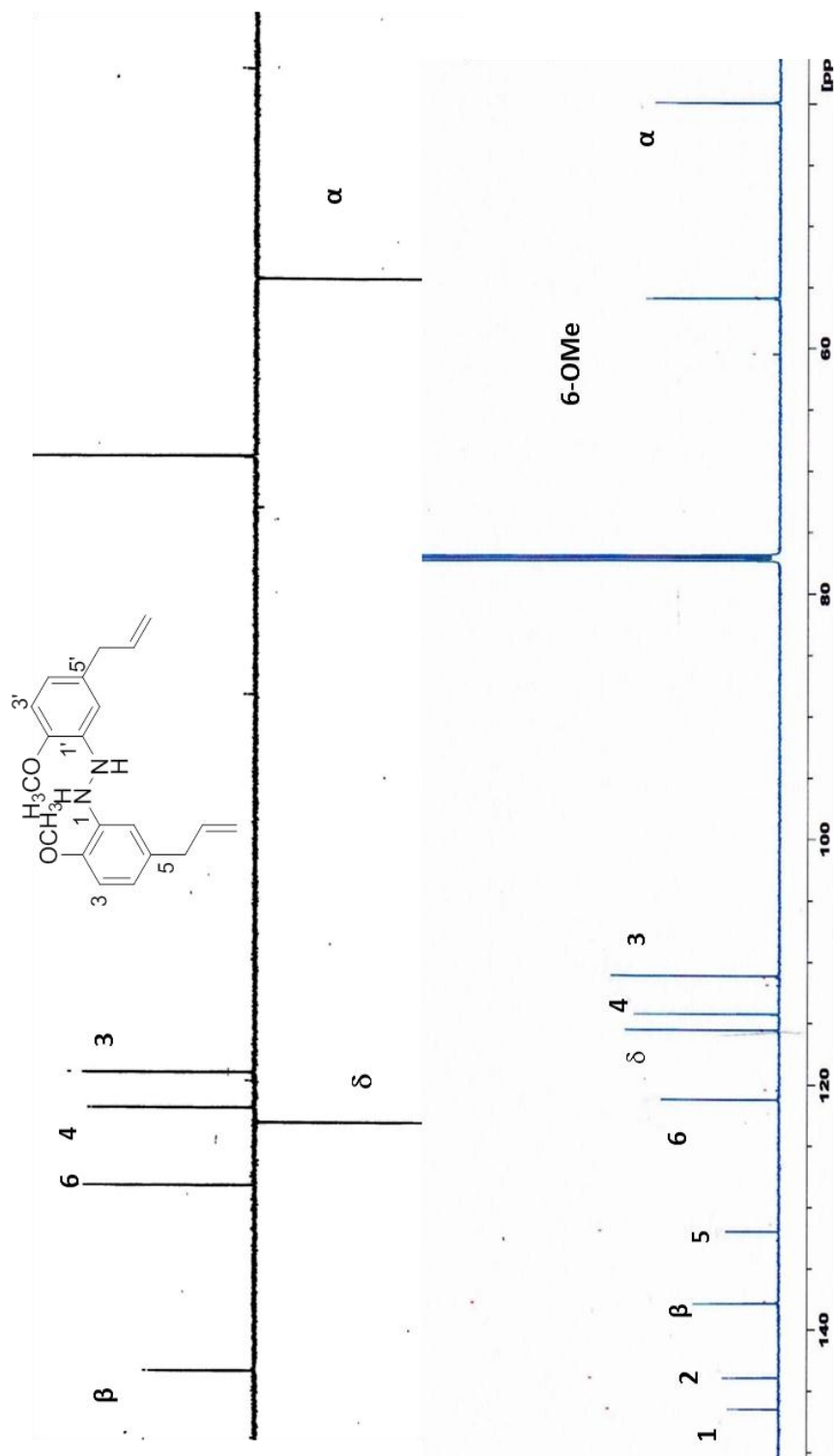


Figure 3. 93: ^{13}C -NMR/DEPT spectrum of bisugenol C LCB17

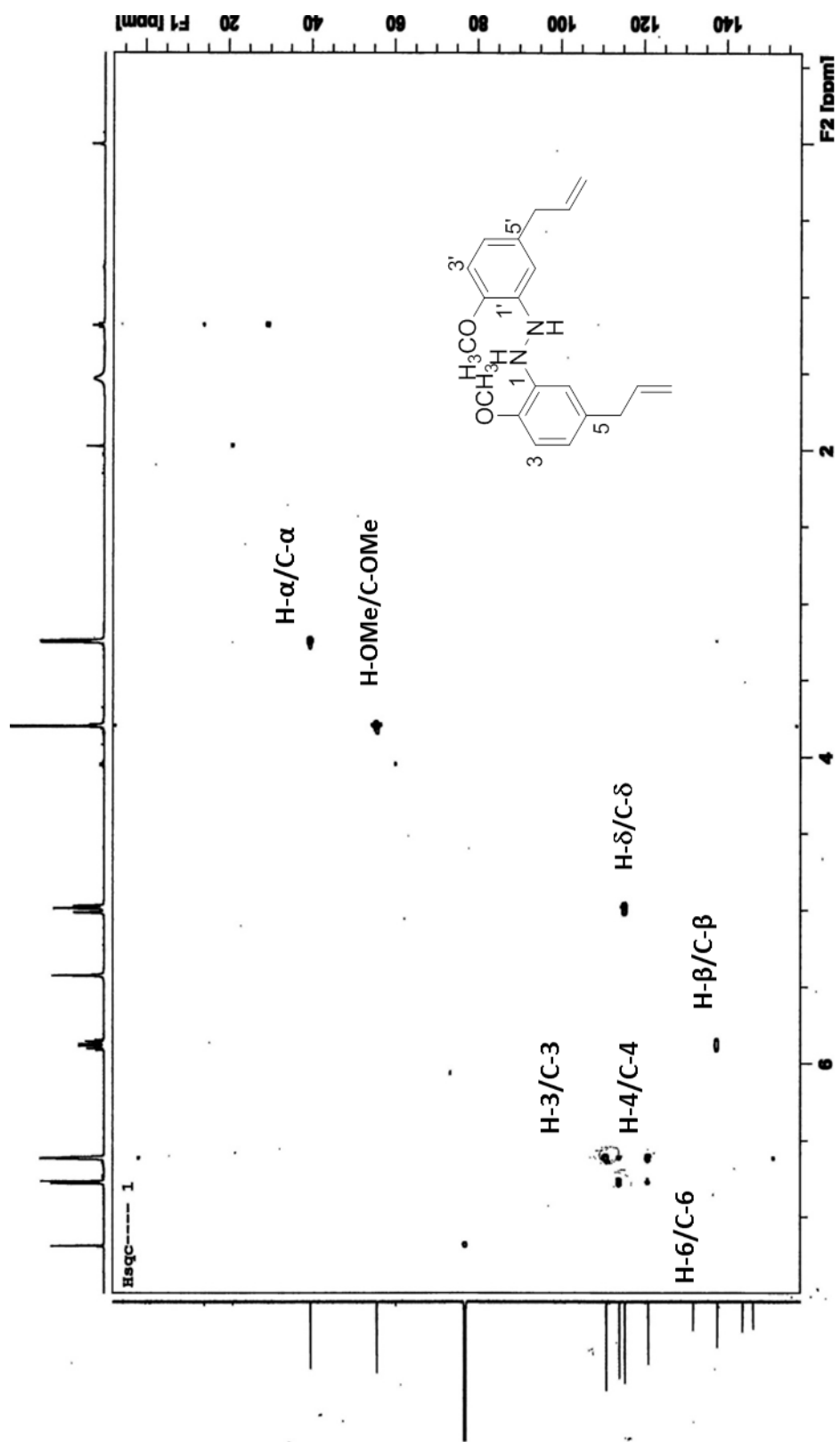


Figure 3.94: HMQC spectrum of bisugenol CLCB17

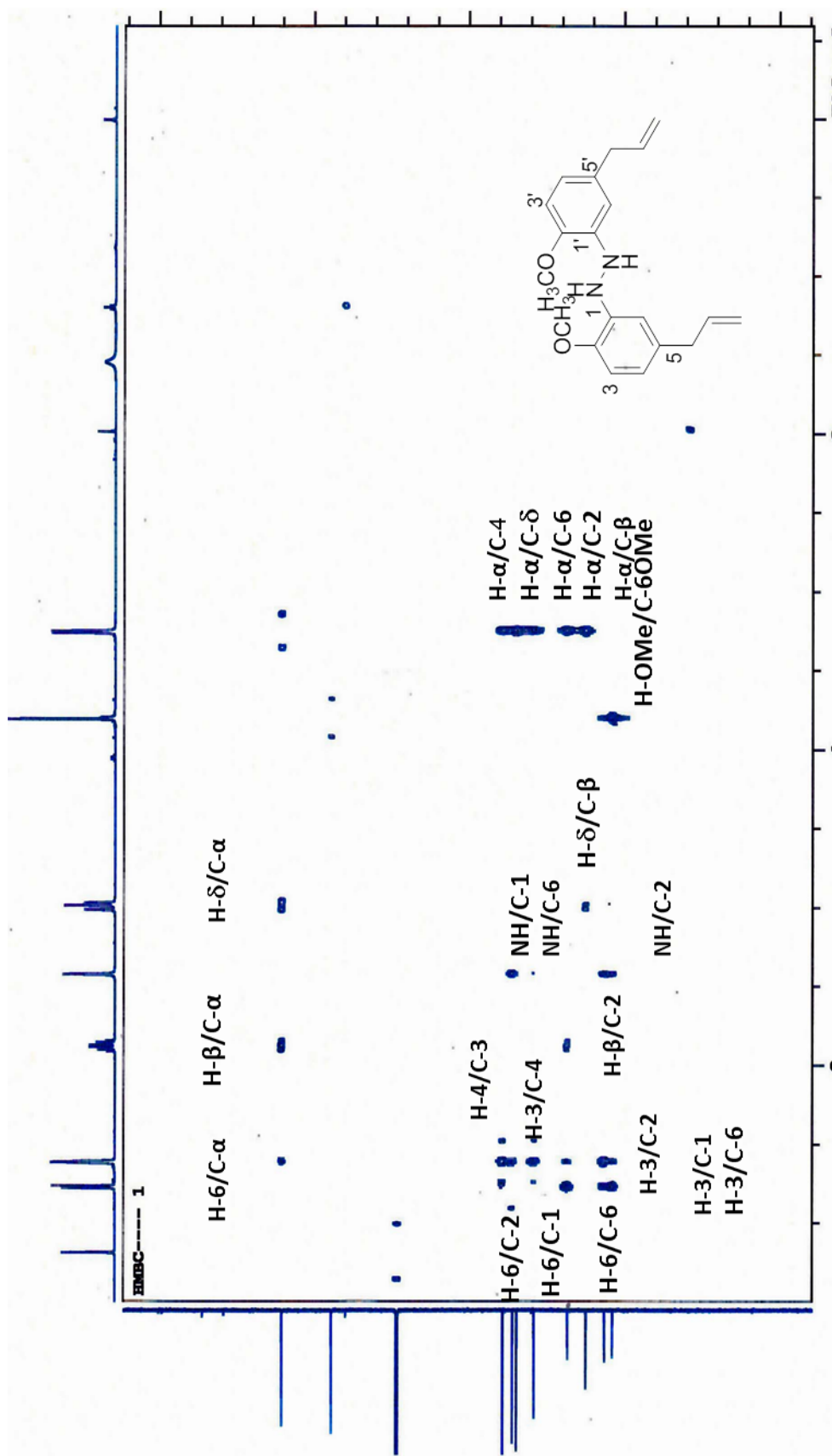


Figure 3.95: HMBC spectrum of bisegenol C LCB17

Electrochemical investigation

As the biseugenol C as a phenylhydrazine-derivative is electrochemical active and soluble in aqueous solutions. For the electrochemical investigation of biseugenol C we used a carbon nanotubes paste electrode in the presence of 500 μM above compound in phosphate buffer solution (pH 6.0). As (Figure 3.96) shows, the cyclic voltammogram of biseugenol C exhibits an anodic and cathodic peak at the forward and reverse scans of the potential related to the oxidation and reduction of the NH-NH bond in biseugenol C, respectively (Beitollahi et al., 2008).

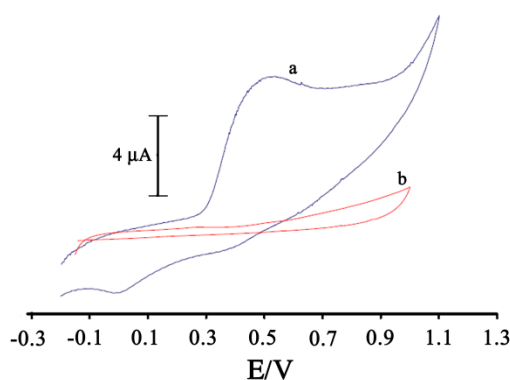


Figure 3.96: (a) Cyclic voltammogram of carbon nanotube paste electrode in 0.1 M phosphate buffer solution (pH 6.0) in the presence of 500 biseugenol C at scan rate 50 mV s^{-1} , (b) as a) in the absence of biseugenol C.

A pair of reversible peaks observed at $E_{\text{pa}}=0.5 \text{ V}$ and $E_{\text{pc}}=0.0 \text{ V}$. The half-wave potential ($E_{1/2}$) and ΔE_p were 0.5 and 0.25 V, respectively. The peak separation potential, $\Delta E_p (= E_{\text{pa}}-E_{\text{pc}})$, is greater than the $(59/n) \text{ mV}$ expected for a reversible system, which indicates a quasi-reversible behavior for the mediator in an aqueous medium. In addition, the effect of the scan rate of the potential on the electrochemical properties of the biseugenol C was studied in phosphate buffer solution by cyclic voltammetry. The plots of the anodic and cathodic peak currents were linearly dependent on the square root of scan rate ($v^{1/2}$) (Not shown). This behavior indicates that the nature of the redox process is diffusion controlled (Afzali et al. 2011; Ensafi and Kanim et al. 2010). Double potential step chronoamperometry was used with

carbon nanotubes paste electrode to determine the diffusion coefficient of biseugenol C .We have determined the diffusion coefficient, D , of biseugenol C using the Cottrell equation (Bard et al., 2001; Ensafi et al., 2011) .

$$I = nFAD^{1/2} C_b \pi^{-1/2} t^{-1/2} \quad (1)$$

According above equation we calculated a diffusion coefficient of $7.5 \times 10^{-6} \text{ cm}^2 \text{ s}^{-1}$ for this compound. In addition, the effect of pH on biseugenol C peak potential and peak current was investigated by cyclic voltammetry using 0.1 mol L^{-1} buffer solutions at pH levels ranging from 4.0 to 9.0 with a scan rate of 50 mV s^{-1} (Figure.3.97). The results showed that the slope of E vs. pH was 67.1 mV pH^{-1} over a pH range of 4.0 to 9.0, which is very close to the anticipated Nernstian value of 59.2 mV for a two electron and two-proton process. Results suggest oxidation of NH-NH group to N=N in biseugenol C with two electron and two-proton that can be confirm for structure of this compound.

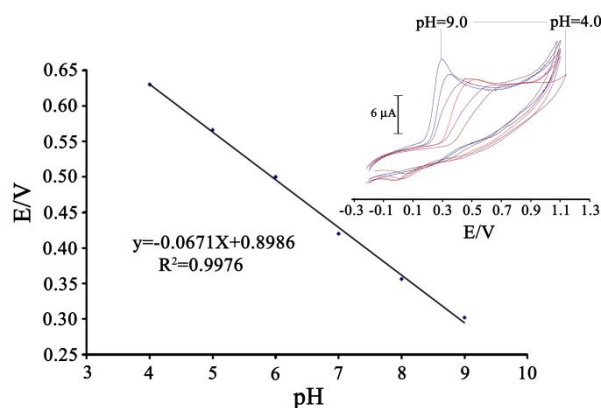
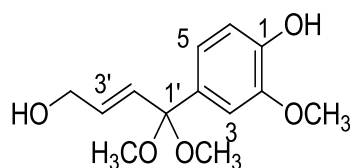


Figure 3.97: Current–pH curve for electrooxidation of $500 \mu\text{M}$ biseugenol C at carbon nanotubes paste electrode with a scan rate of 50 mV s^{-1} . Inset influence of pH on cyclic voltammograms of biseugenol C at the surface of the modified electrode, (pH 4.0, 5.0, 6.0, 7.0, 8.0, and 9.0).

3.2.9 Phenolic Compound LCB4: Litsin



LCB4

Compound **LCB4** with IUPAC name (E)-4-(4'-hydroxy-1',1'-dimethoxybut-2'-en-1-yl)benzene-1,2-diol was afforded as white amorphous solid with $[\alpha]_D^{25} = + 2.93$ (2.00×10^{-4} g/100 mL, MeOH). The UV spectrum showed absorptions at λ_{\max} (MeOH) nm (log ϵ) 261 (2.486) and 223 (2.202) indicating the presence of unsaturated carbon-carbon bond. The IR spectrum showed absorption peak at 3434 cm^{-1} indicated the existing of hydroxyl group and 1640 cm^{-1} assigned for the alkene group. LC-MS showed the molecular ion peak $[M^+]$ at m/z 240.72 corresponding to the molecular formula of $\text{C}_{12}\text{H}_{16}\text{O}_5$.

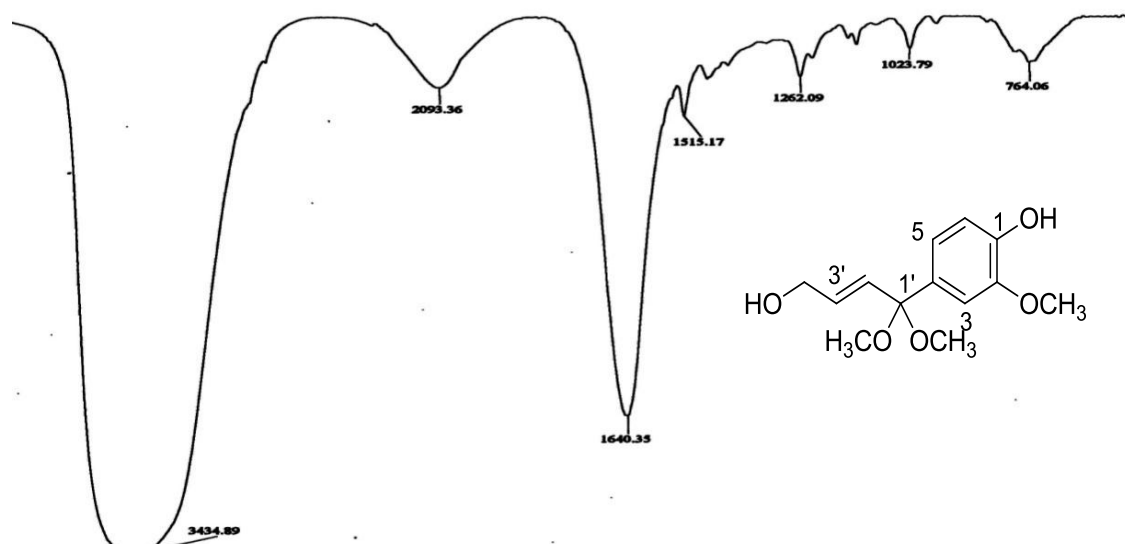


Figure 3.98: IR Spectrum of litsin **LCB4**

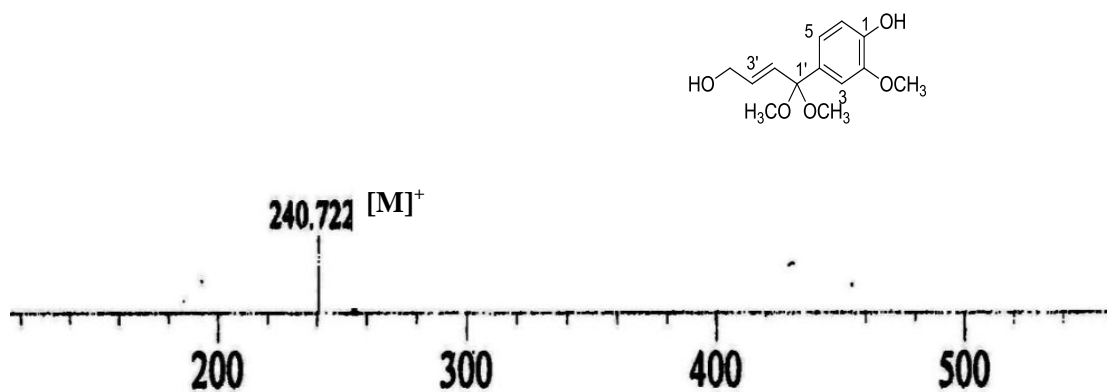


Figure 3.99: LC-MS Spectrum of litsin **LCB4**

The ^1H -NMR spectrum (Table 3.25, Figure 3.100) displayed two methoxyl peaks at δ 3.88 as singlet and these methoxyl groups were positioned at C-1', one sp^3 methylene was resonated further downfield as a doublet at δ 4.32 assigned to H-4'. One multiplet peak observed at δ 6.22 assigned to H-3' and one doublet peak at δ 6.56 assigned to H-2'. The aromatic protons were resonated at δ 6.94 as a doublet of doublet and was assigned for H-5, δ 6.90 as a doublet assigned to H-6 and δ 6.93 as a doublet assigned to H-3. The COSY (Table 3.25, Figure 3.101) experiment which displayed correlations of H-5/H-6, H-2'/H-3' and H-3'/H-4'.

The ^{13}C -NMR and DEPT spectrum (Table 3.25, Figure 3.102) showed 12 carbon signals in the molecule which consist of one sp^3 methylene at δ 63.9 (C-4'), four quaternary carbon exhibited at δ 114.0 (C-4), δ 129.7 (C-1') and δ 148.6 (C-1, C-2) and three aromatic methines at δ 107.8 (C-5), δ 110.6 (C-6) and δ 119.7 (C-3). The sp^2 methines were observed at δ 132.2 (C-2') and δ 126.3 (C-3') and two methoxyl groups appeared at δ 55.9 (C-1'). HMQC spectrum (Table 3.25, Figure 3.103) showed the connectivity between proton and carbon: H-3/C-3, H-5/C-5, H-6/C-6, H-2'/C-2' and two H-OMe/C-OMe. In the HMBC spectrum (Table 3.25, Figure 3.104), the cross-peaks were observed between H-5/C-1, C-2, C-3, C-6; H-OMe/C-2, H-3/C-1, C-6, C-

2; H-6/C-1, C-1', C-2 ; H-2'/C-4', C-3'; H-4'/C-3' and C-2'.

Based on the observed spectral data, it was confirmed that **LCB4** was litsin.

Table 3.25: 1D (^1H and ^{13}C) and 2D (COSY, HMQC and HMBC) NMR spectra data of litsin

LCB4

Position	^1H -NMR(δ , J in Hz)	^{13}C -NMR(δc)	COSY	HMQC	HMBC
1	-	148.6	-	-	-
2	-	148.6	-	-	-
3	6.93 (1H, <i>d</i> , 1.7)	119.7	-	H-3/C-3	1,2,6
4	-	114.1	-	-	-
5	6.94(1H, <i>dd</i> , 8.0, 2.1)	107.8	H-5/H-6	H-5/H-5	6,3,1,2
6	6.90 (1H, <i>d</i> , 8.0)	110.6	H-6/H-5	H-6/C-6	1',1,2
1'	-	129.7	-	1'-OMe/C1'-OMe	-
2'	6.56 (1H, <i>d</i> , 15.3)	132.2	-	-	4',3'
3'	6.22 (1H, <i>m</i>)	126.3	-	-	
4'	4.32 (2H, <i>d</i> , 6.6)	63.9	-	H-4'/C-4'	3',2'
OMe	3.88(9H, <i>s</i>)	55.9	-	-	2-OH

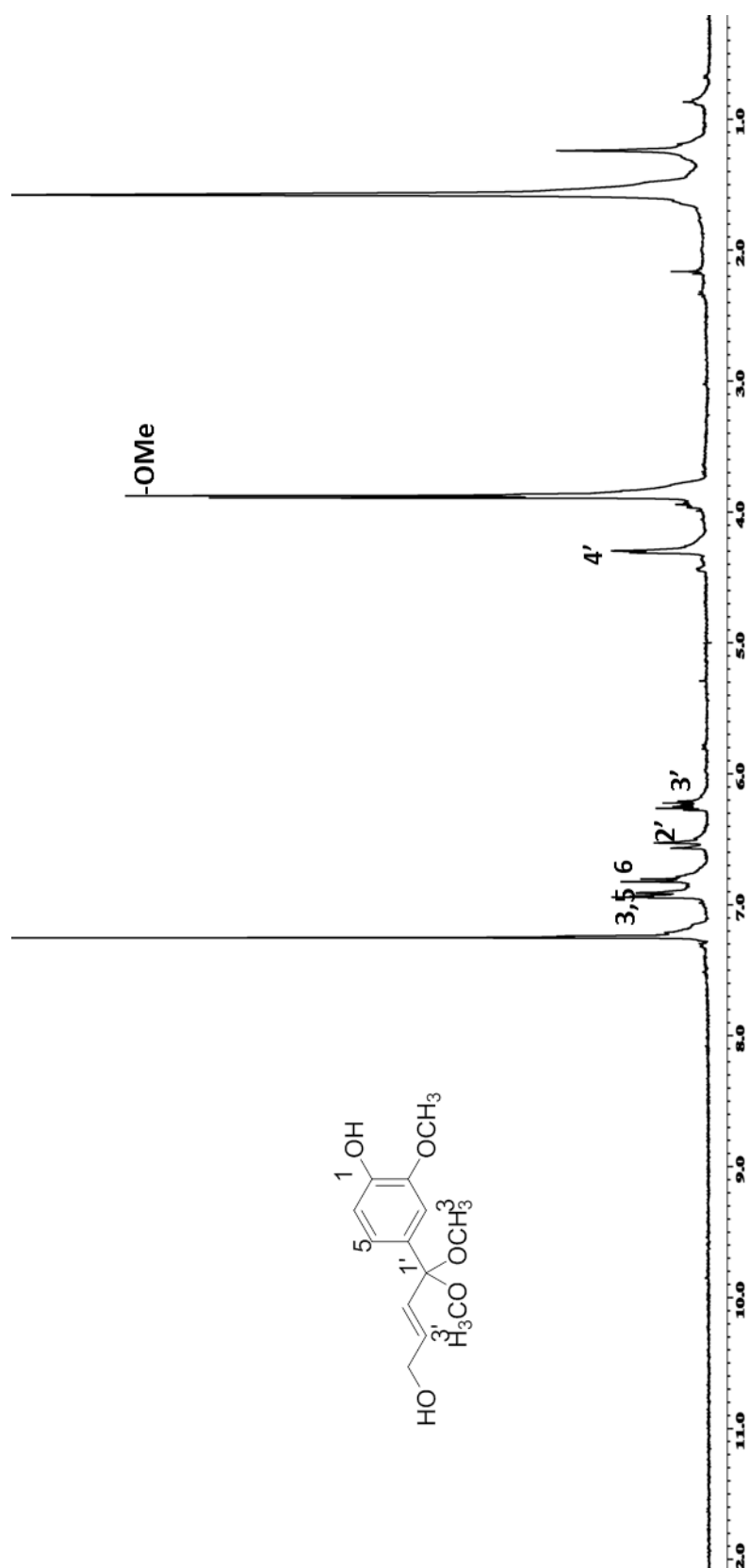


Figure 3.100: ¹H-NMR spectrum of litsin LCB4

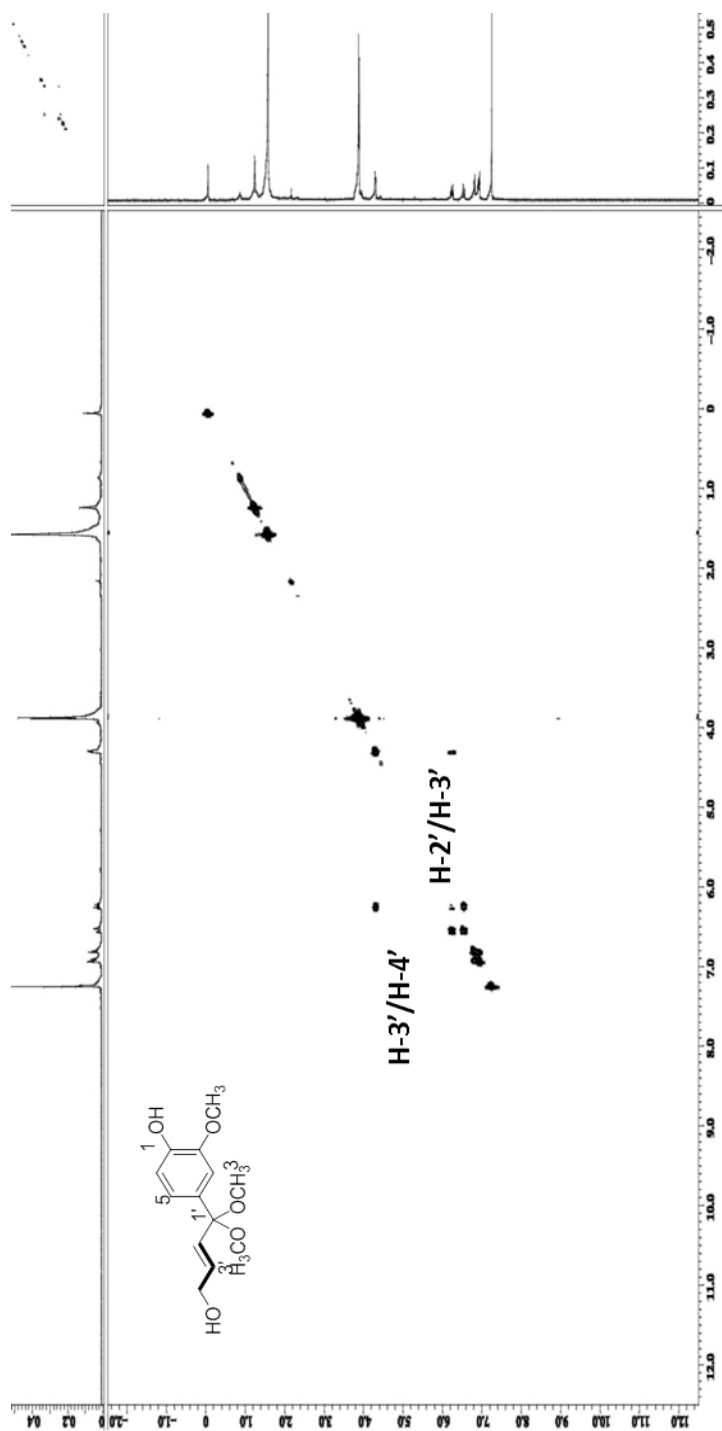


Figure 3.101: COSY spectrum of litesin LCB4

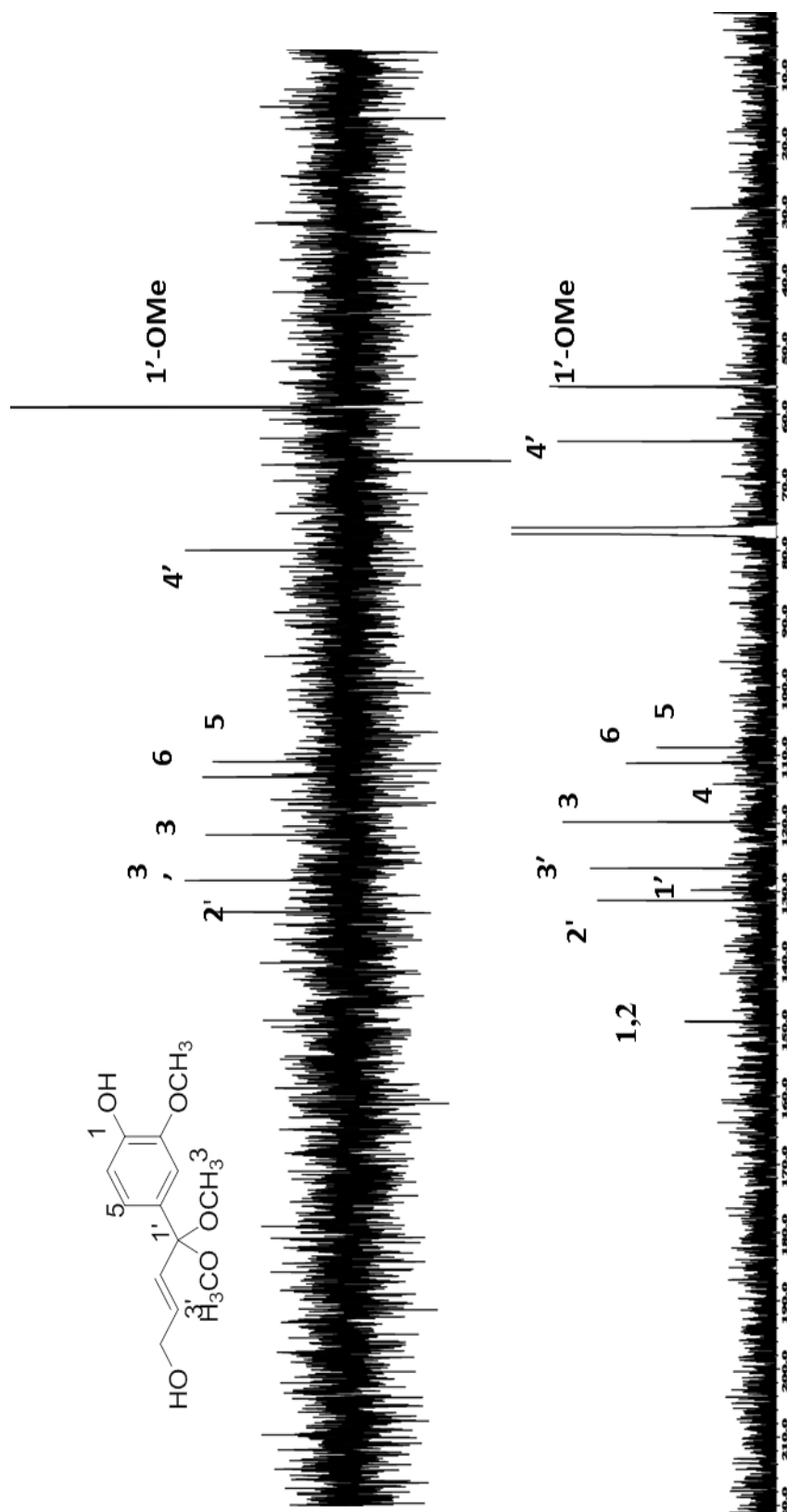


Figure 3.102: ^{13}C -NMR/DEPT spectrum of litsin LCB4

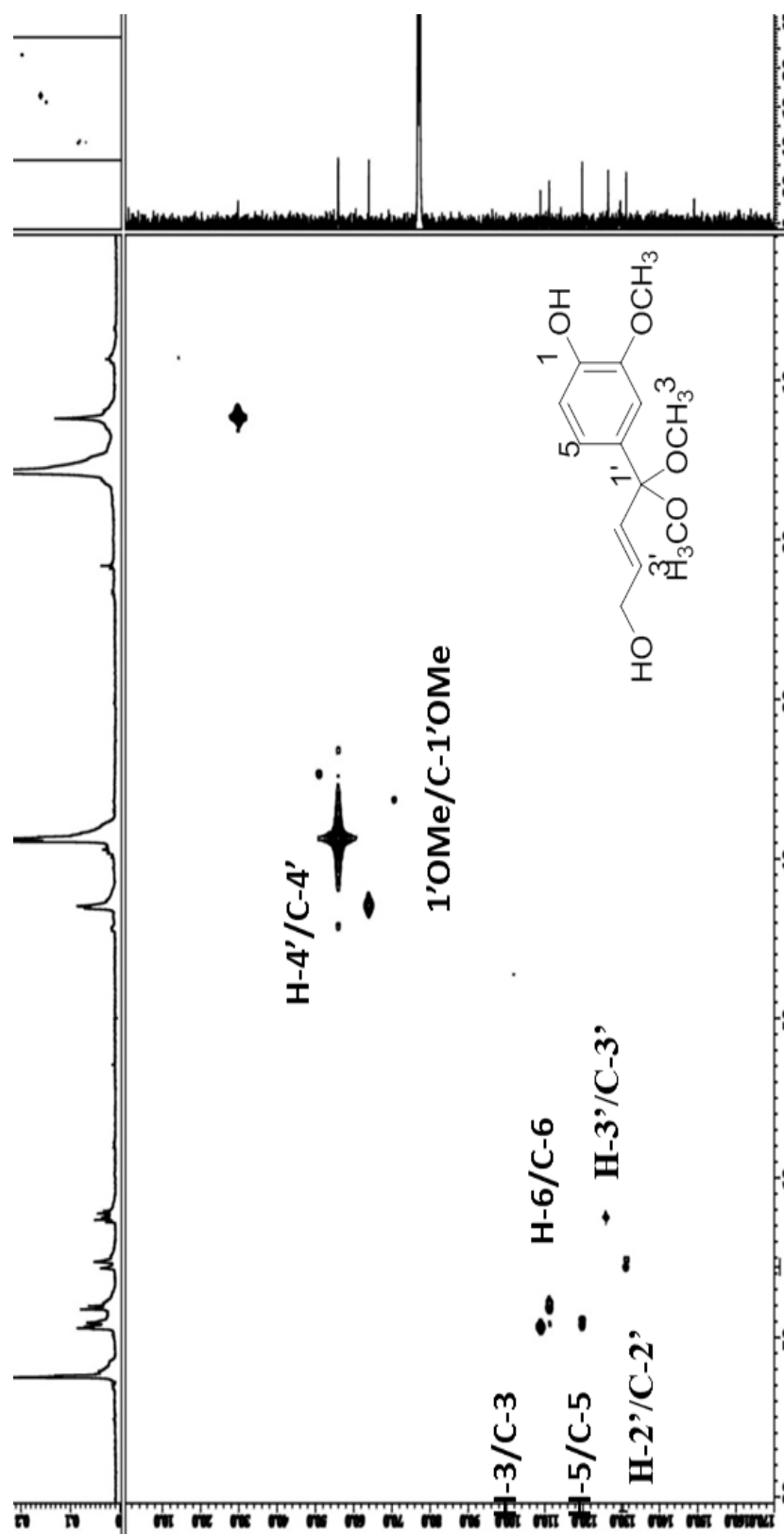


Figure 3. 103: HMQC spectrum of litsin **LCB4**

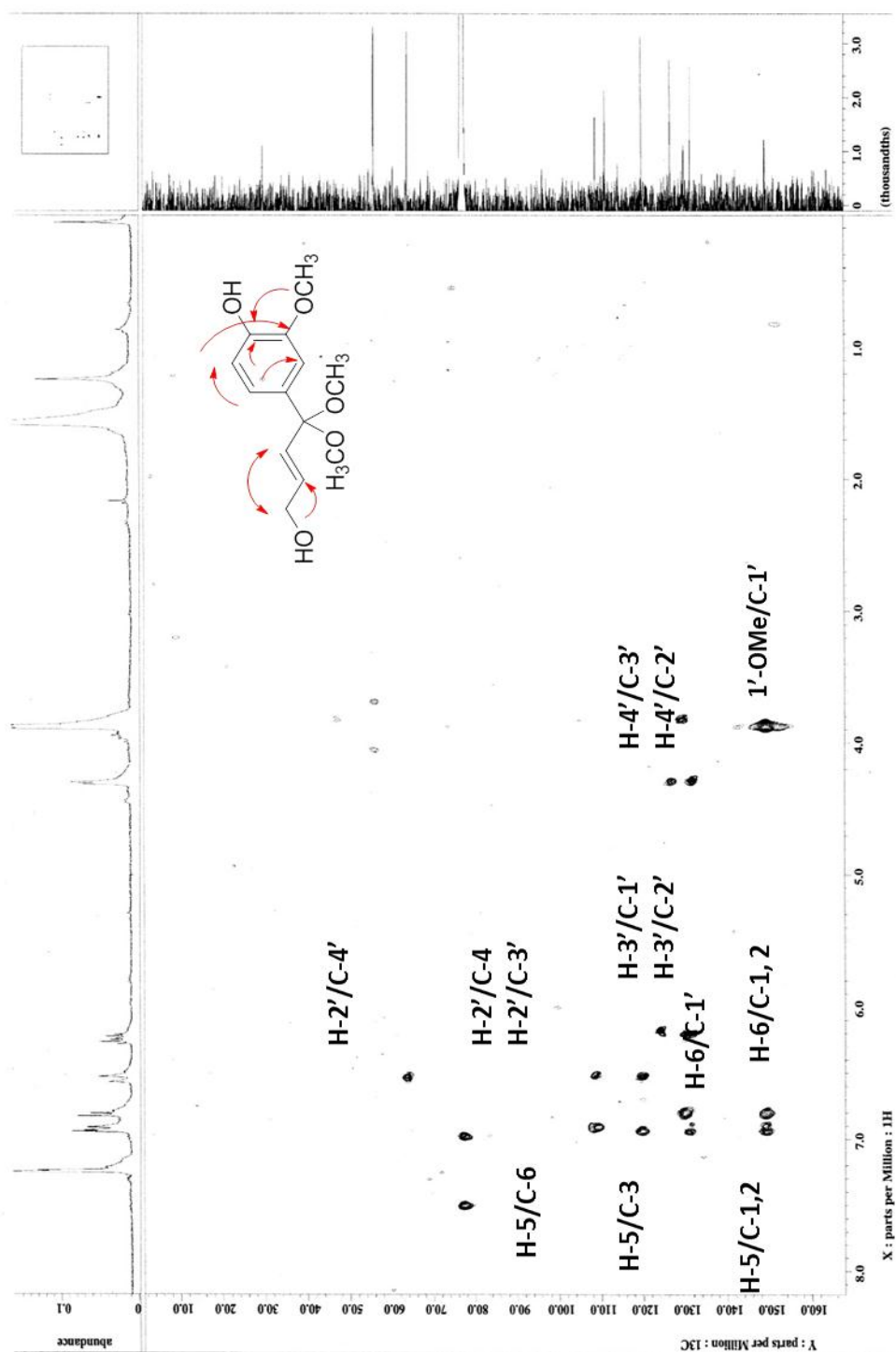
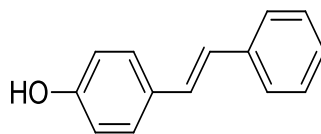


Figure 3.104: HMBC spectrum of litsin LCB4

3.2.10 *E*-4-styrylphenol LCB5



LCB5

(*E*)-4-Styrylphenol **LCB5** was afforded as a brown amorphous solid with $[\alpha]_D^{27} = -22.8$ (2×10^{-4} g/100 mL, MeOH). In the UV spectrum absorption maxima were observed at λ_{\max} (MeOH) nm (log ϵ) 306 (0.418) and 213 (0.424) which indicated the existence of the conjugated system. Its IR spectrum showed absorption bands at ν_{\max} 3425 cm^{-1} (hydroxyl), 1643 cm^{-1} (C=C). The LCMS (positive mode) spectrum showed an intense pseudomolecular ion peak, $[M+1]^+$ at m/z 196.0295 which was associated the molecular formula of $\text{C}_{14}\text{H}_{12}\text{O}$.

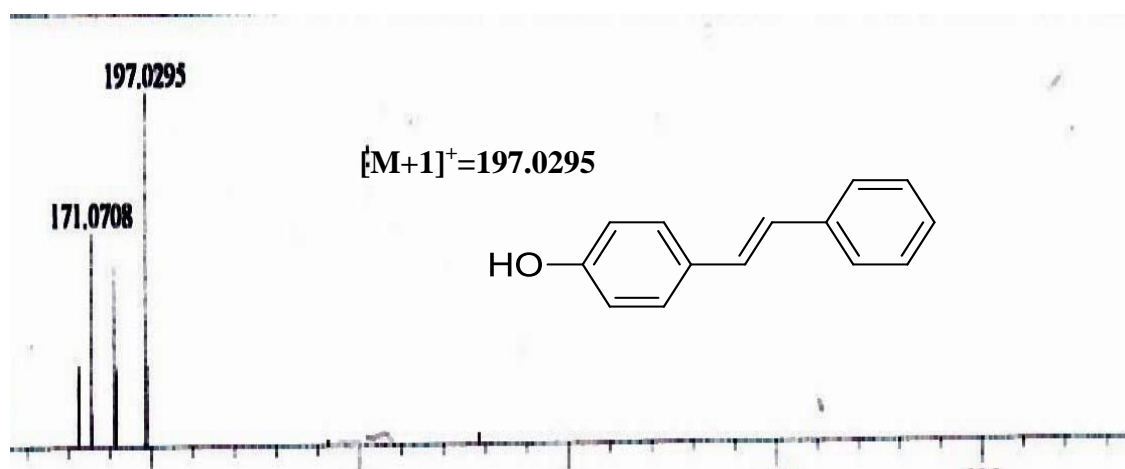


Figure 3.105: LC-MS Spectrum of stilbene **LCB5**

The ^1H -NMR spectrum of *E*-4-styrylphenol (Table 3.26 , Figure 3.106) showed the presence of two protons peak at δ 8.15 appeared as a doublet which was assigned for H- 2' and H-6', the doublet signal appeared as a doublet at δ 7.80 was assigned to H-1'', H-2''. One doublet peak with two protons at δ 7.42 was assigned to H-2 and H-6, one doublet of doublet peak at δ 7.60 was assigned to H-4', one doublet peak resonated at δ 7.70 was assigned to H-3'and H-5' and one doublet appeared at δ 7.50 belongs to H-3,

H-5. The above observations were reinforced by COSY (Table 3.26, Figure 3.107) spectrum showed cross peaks between H-2', 6'/H-3',5', H-1''/H-2'' and H-2,6/H-3,5 (Sako et al., 2004).

The ^{13}C -NMR spectrum (Table 3.26, Figure 3.108) of 4-hydroxystilbene revealed a total of 14 carbon atoms in the molecule. Three quaternary carbons exhibited at δ 154.8 (C-4), 138.2 (C-1') and δ 134.9 (C-1) and eleven sp^2 methines resonated at δ 132.8 (C-1''), 130.5 (C-2''), 110.6 (C-3', C-5'), 132.2 (C-2,H-6), 129.7 (C-3',5'), 110.6 (C-4') and 122.1 (C-3,C-5).

Based on the spectroscopic data of **LCB5** and comparison with the literature values, it was confirmed that compound **LCB5** was (*E*)-4-styrylphenol.

Table 3.26: ^1H NMR (400 MHz) and ^{13}C NMR (100 MHz) spectral data of stilbene **LCB5**

Position	^1H -NMR(δ , J in Hz)	^{13}C -NMR (δc)
1	-	134.9
2,6	7.42 (2H, <i>d</i> , 7.7)	128.9
3,5	7.50 (2H, <i>d</i> , 7.0)	122.1
4	-	154.8
1'	-	138.2
2',6'	8.15 (2H, <i>d</i> , 7.7)	132.2
3',5'	7.70 (2H, <i>dd</i> , 7.9)	129.7
4'	7.60 (1H, <i>dd</i> , 7.1)	110.6
1''	7.80 (1H, <i>d</i> , 16.8)	132.8
2''	7.80 (1H, <i>d</i> , 16.8)	130.5

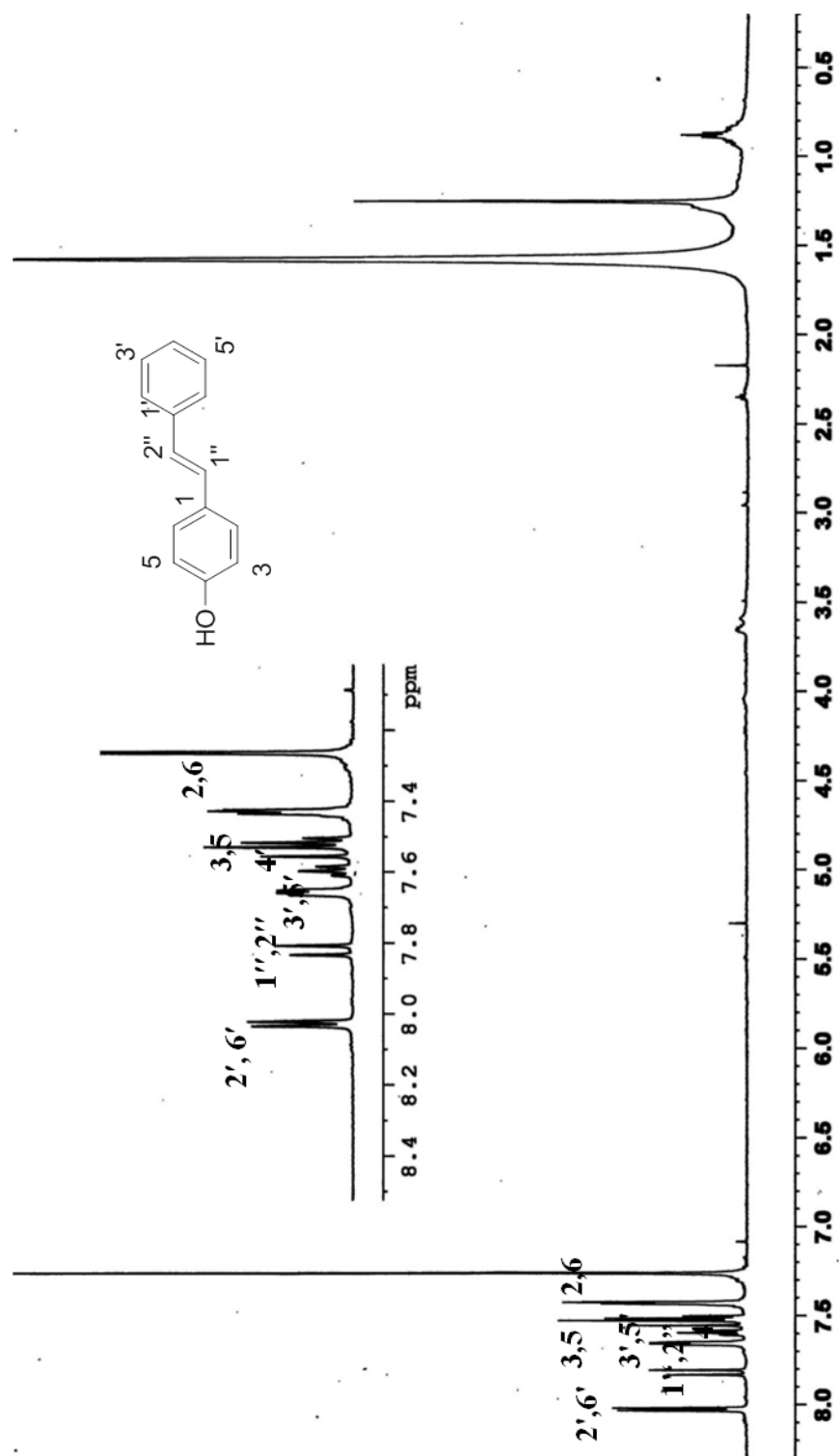


Figure 3.106: ^1H -NMR spectrum of stilbene LCB5

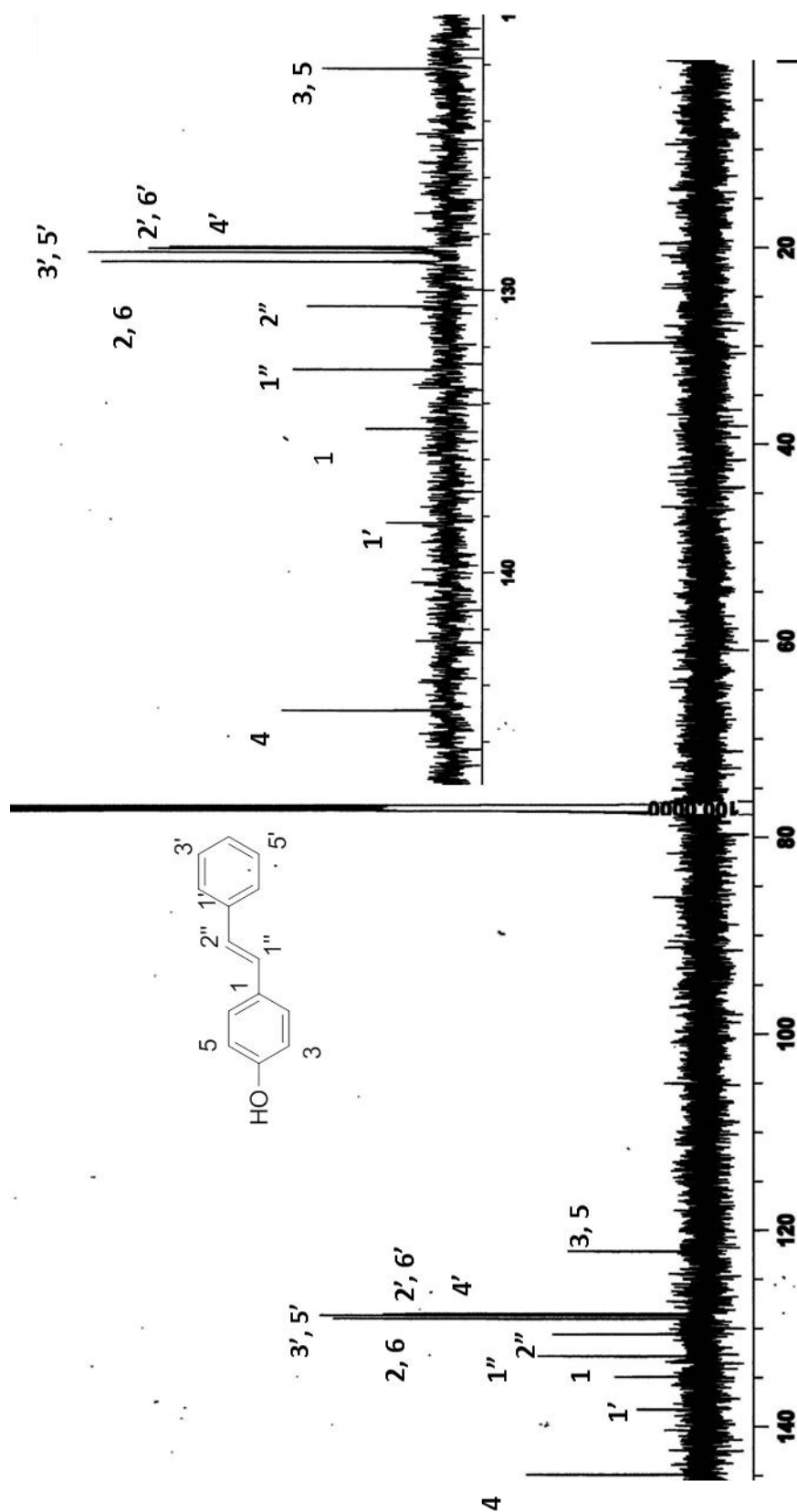
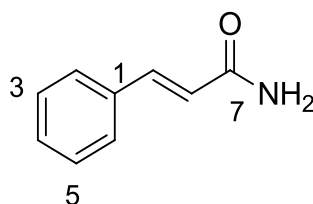


Figure 3.107: ^{13}C -NMR spectrum of stilbene LCB5

3.2.11 Cinnamide LCL4



LCL4

Compound **LCL4**, cinnamide was afforded as a colorless crystalline needle (Zhang et al., 2010). The UV spectrum showed the absorption bands at λ_{max} (MeOH) nm (log ϵ) at 223 (1.204) and 278 (0.875) nm. The IR spectrum of this amide showed absorption peaks at 3353 cm^{-1} and 1669 cm^{-1} indicated the presence of N-H group and amide carbonyl stretching vibrations, respectively (Balasubraman et al., 2004) The LC-MS spectrum was relatively simple with a molecular ion peak, observed at m/z 148.30 $[\text{M}+\text{H}]^+$ suggesting a molecular formula of $\text{C}_9\text{H}_9\text{NO}$.

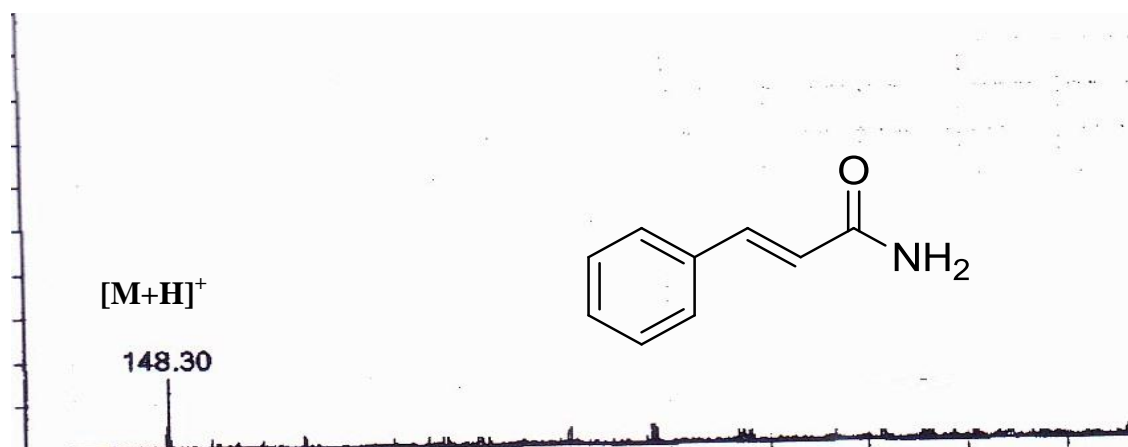


Figure 3.108: LC-MS Spectrum of cinnamide **LCL4**

The ^1H -NMR spectrum (Table 3.27, Figure 3.109) showed five aromatic proton signals appeared at δ 7.49 (C-2, C-6), δ 7.36 (C-3, C-5) and δ 7.24 (C-4). The NH_2 group was resonated at δ 5.5 as a broad singlet.

The ^{13}C -NMR spectrum showed only a total of 9 carbon signals (Table 3.27, Figure 3.110) which consist of seven sp^2 methines and two quaternary carbon. There are 2 overlapping carbons appeared at the same chemical shift which has equivalent environment in the aromatic ring. These signals appeared at δ 134.4 (C-1), δ 128.10 (C-2, C-6), δ 129.0 (C-3, C-5) and δ 130.2 (C-4). The carbonyl amide group was resonated at δ 168.4 (C-7). The signals appeared at δ 119.5 was assigned to C-8 and at δ 142.2 for C-9.

Based on the spectroscopic data of **LCL4** and comparison with the literature values, it was confirmed that compound **LCL4** was cinnamide.

Table 3.27: ^1H NMR (400 MHz) and ^{13}C NMR (100 MHz) spectral data of cinnamide **LCL4**

Position	^1H -NMR(δ , J in Hz)	^{13}C -NMR (δc)
1	-	134.4
2	7.49 (1H, <i>dd</i> , 9.3, 3.9)	128.1
3	7.36 (1H, <i>dd</i> , 15.6, 7.5)	129.0
4	7.24, (1H, <i>m</i>)	130.2
5	7.36 (1H, <i>dd</i> , 15.6, 7.5)	129.0
6	7.49 (1H, <i>dd</i> , 9.3, 3.9)	128.1
7	-	168.4
8	6.45 (1H, <i>d</i> , 15.6)	119.5
9	7.65 (1H, <i>d</i> , 15.6)	142.2
NH ₂	5.5 (br, <i>s</i>)	-

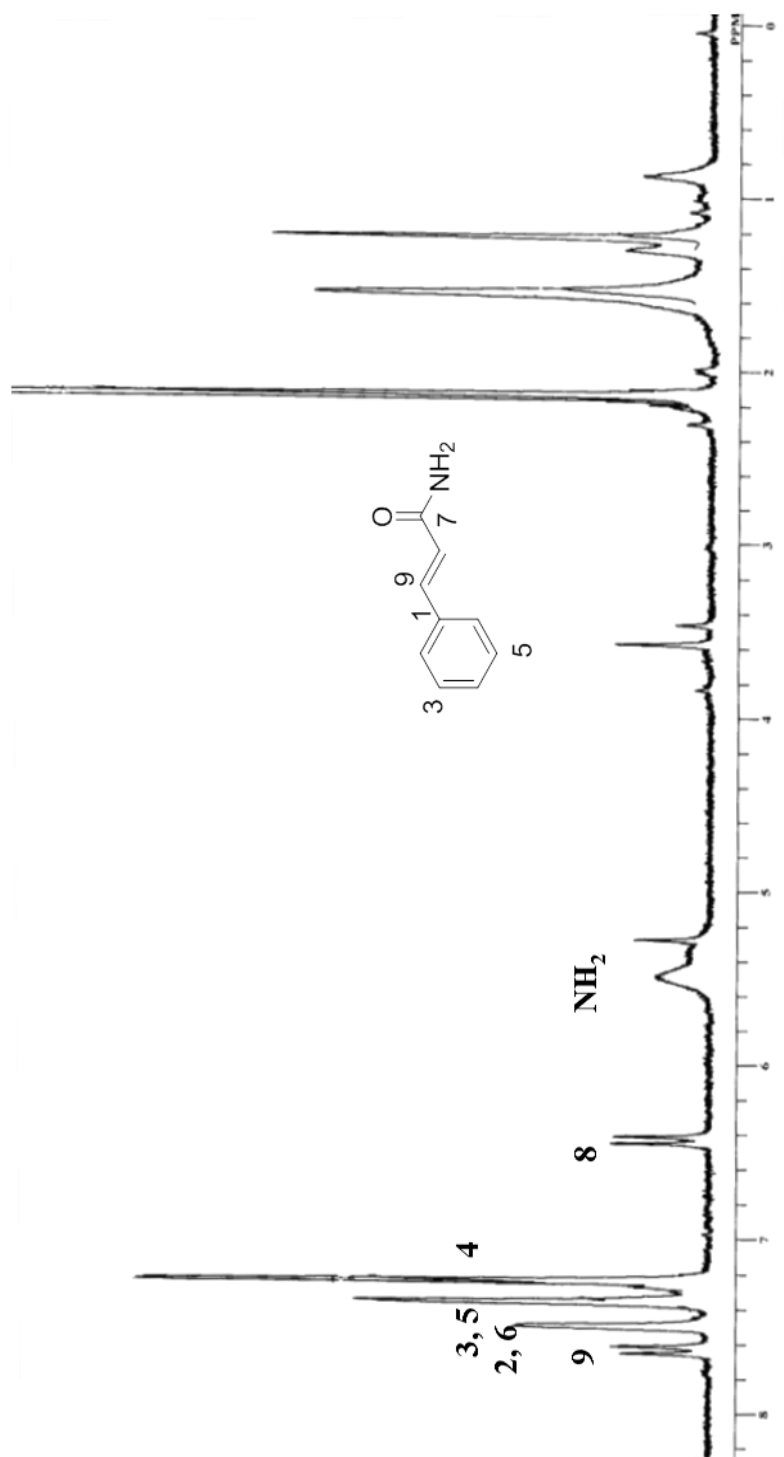


Figure 3.109: ^1H -NMR spectrum of cinnamide LCL4

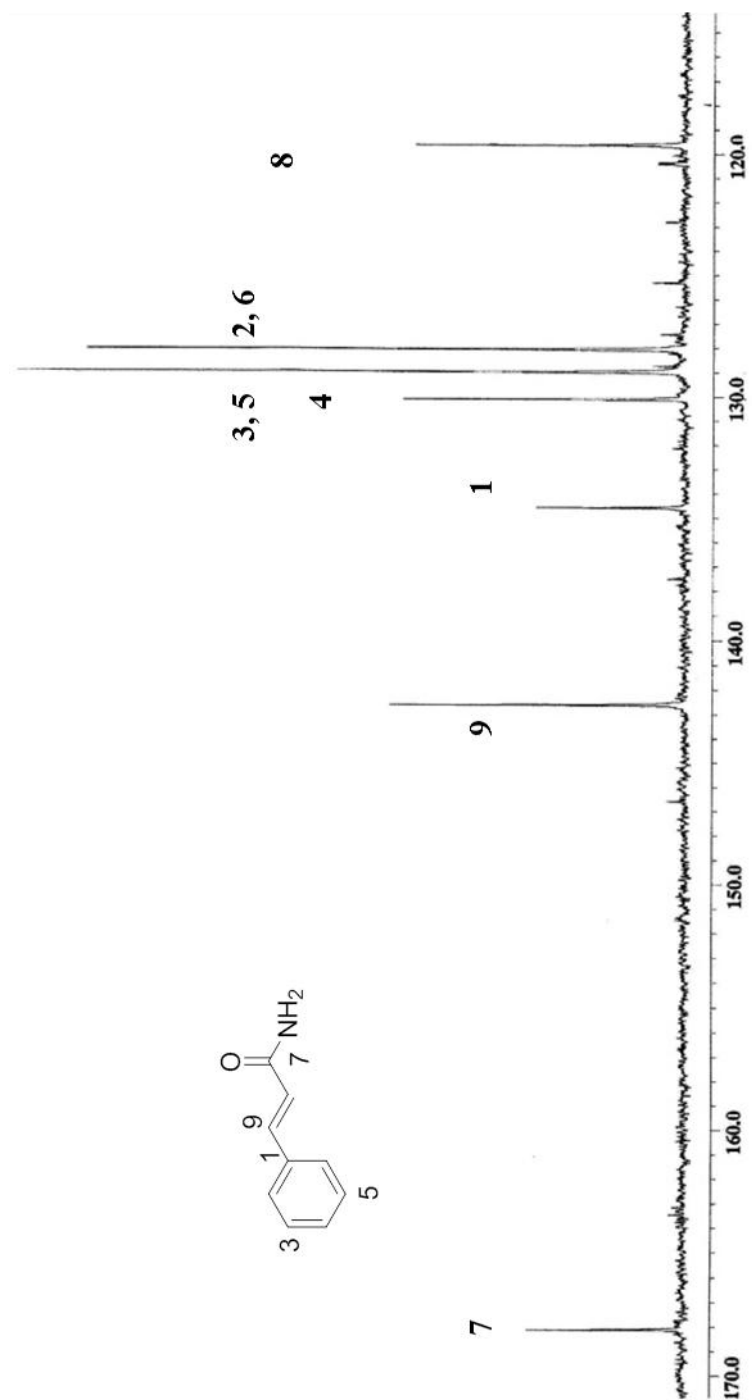
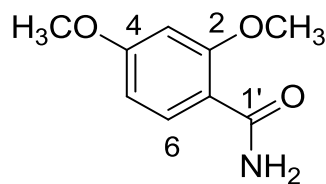


Figure 3.110: ^{13}C -NMR spectrum of cinnamide LCL4

3. 2.12 2, 4 –Dimethoxybenzamide LCL2



LCL2

Compound **LCL2**, 2, 4–dimethoxybenzamide was obtained as brown oil. The IR spectrum showed the absorption peak at 3448 cm^{-1} indicated the presence of NH_2 group and 1607 cm^{-1} showed amide carbonyl stretching vibrations. The UV spectrum showed absorption bands at λ_{max} (MeOH) nm (log ϵ) 261 (2.474) and 258 (2.486) nm. The LC-MS spectrum displayed the ion peak $[\text{M}]^+$ at m/z 181.044 which gave a molecular formula of $\text{C}_9\text{H}_{11}\text{NO}_3$.

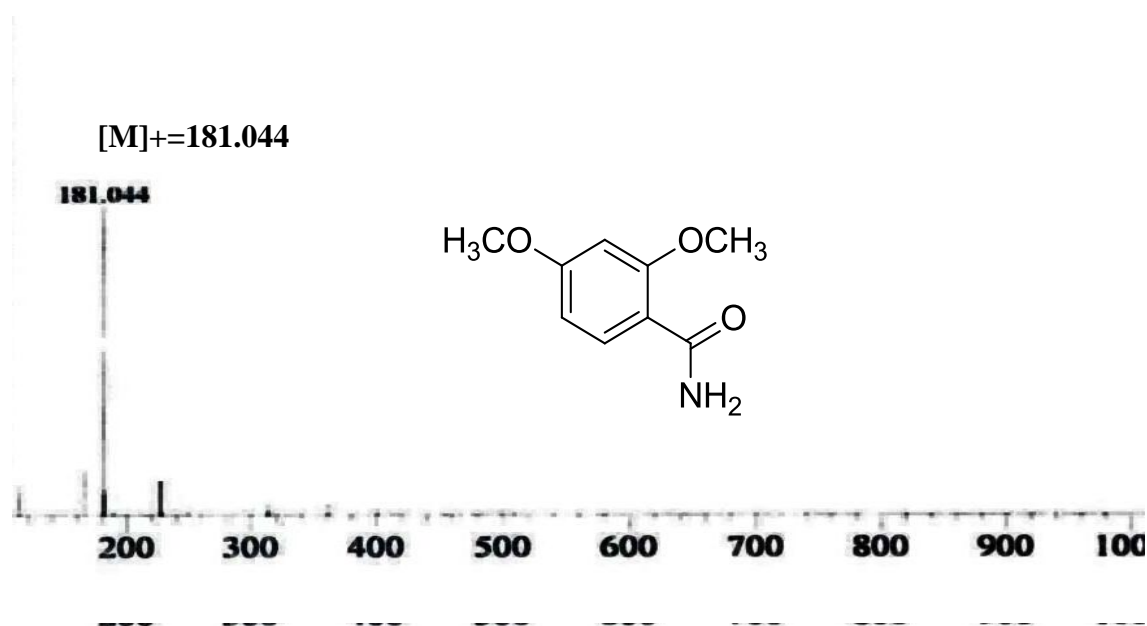


Figure 3.111: LC-MS spectrum of 2, 4 –dimethoxy benzamide **LCL2**

The ^1H -NMR spectrum (Table 3.28, Figure 3.112) showed there aromatic proton signals appeared at δ 6.82 (H-3, *d*), δ 7.49 (H-5, *s*) and δ 7.58 (H-6, *d*) and two methoxyl groups were resonated at δ 3.90 as a singlet. The NH_2 amide group was resonated at δ 3.10 as abroad peak.

The ^{13}C -NMR spectrum (Table 3.28, Figure 3.114) showed a total of nine carbon signals which consist of six aromatic carbon, two carbon methoxyls and one carbonyl amide. The aromatic carbons were resonated at δ 112.2 (C-3), δ 114.3(C-6) and δ 124.5 (C-5), δ 150.7 (C-4), δ 146.37 (C-1) and δ 122.1(C-2). The carbonyl amide was resonated at δ 169.0 (C-1'). Two methoxyl groups were resonated at δ 56.1 (Schnyder et al., 2001).

HMQC spectrum (Table 3.28, Figure 3.115) showed the connectivity between proton and carbon: H-3/C-3, H-5/C-5, H-6/C-6 and H-OMe/C-OMe.

In the HMBC spectrum (Table 3.28, Figure 3.116) the cross-peak were observed between H-6/C-2, C-1, C-4, H-3/C-4, C-5, C-1', H-5/C-3, C-4, C-1', H-OMe/C-1,C4.

Based on the spectroscopic data of **LCL2** and comparison with the literature values, it was confirmed that compound **LCL 2** was 2, 4 –dimethoxybenzamide (Zhang et al. , 2006).

Table 3.28: ^1H NMR (400 MHz) and ^{13}C NMR (100 MHz) spectral data of 2, 4 –dimethoxy benzamide **LCL2**

Position	^1H -NMR(δ , J in Hz)	^{13}C -NMR (δc)
1	-	146.3
2	-	122.1
3	6.82 (1H, <i>d</i> , 8.0 Hz, H-6)	112.2
4	-	150.7
5	7.45 (1H, <i>s</i> , H-5)	124.5
6	7.58 (1H, <i>d</i> , 1.9 Hz, H-3)	114.3
1'	-	169,0
2,4-OMe	3.95 (6H, <i>s</i>)	56.2
NH ₂	3.10 (2H, br <i>s</i>)	-

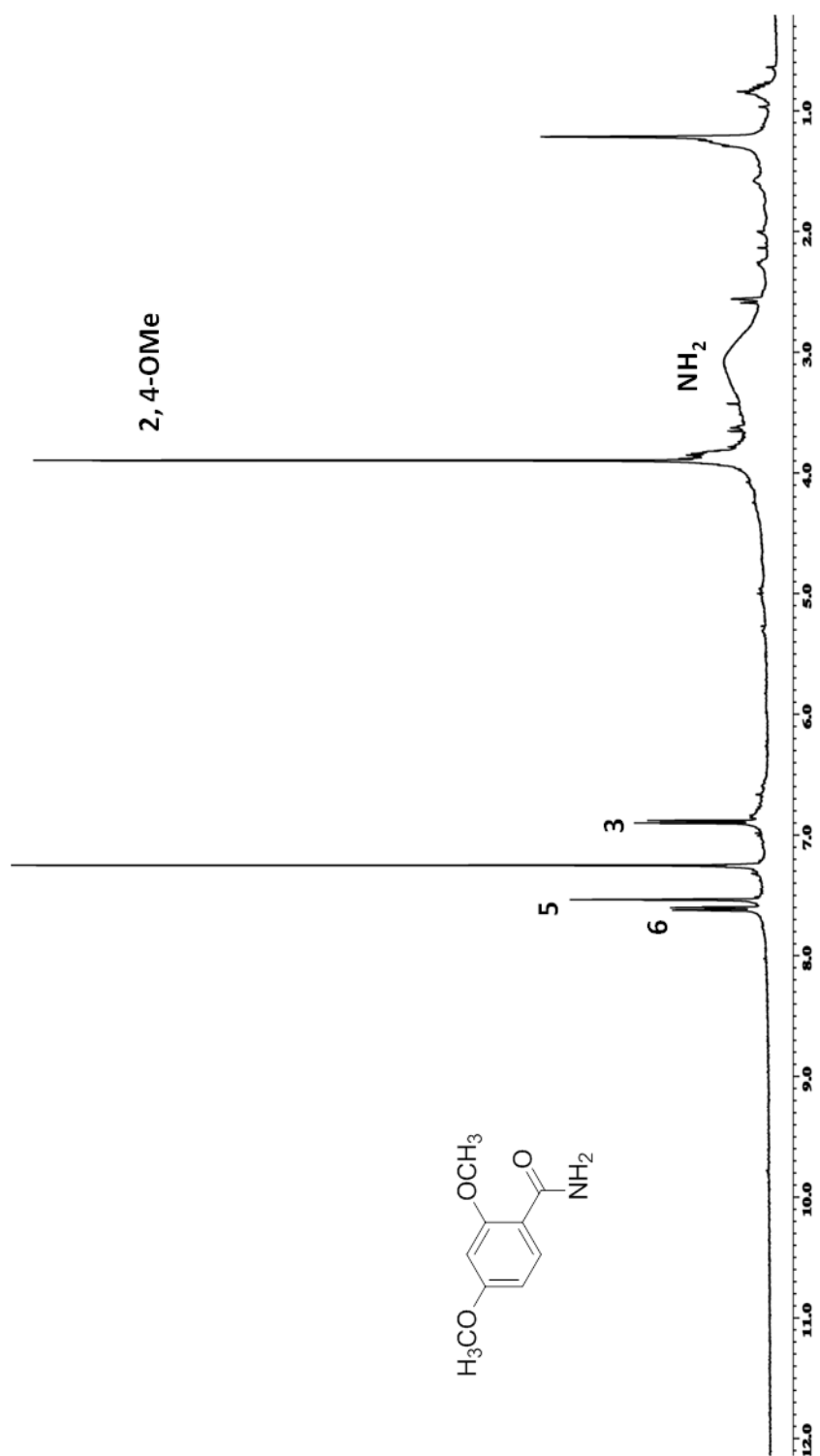


Figure 3.112. ¹H-NMR spectrum of 2,4-dimethoxybenzamide LCL2

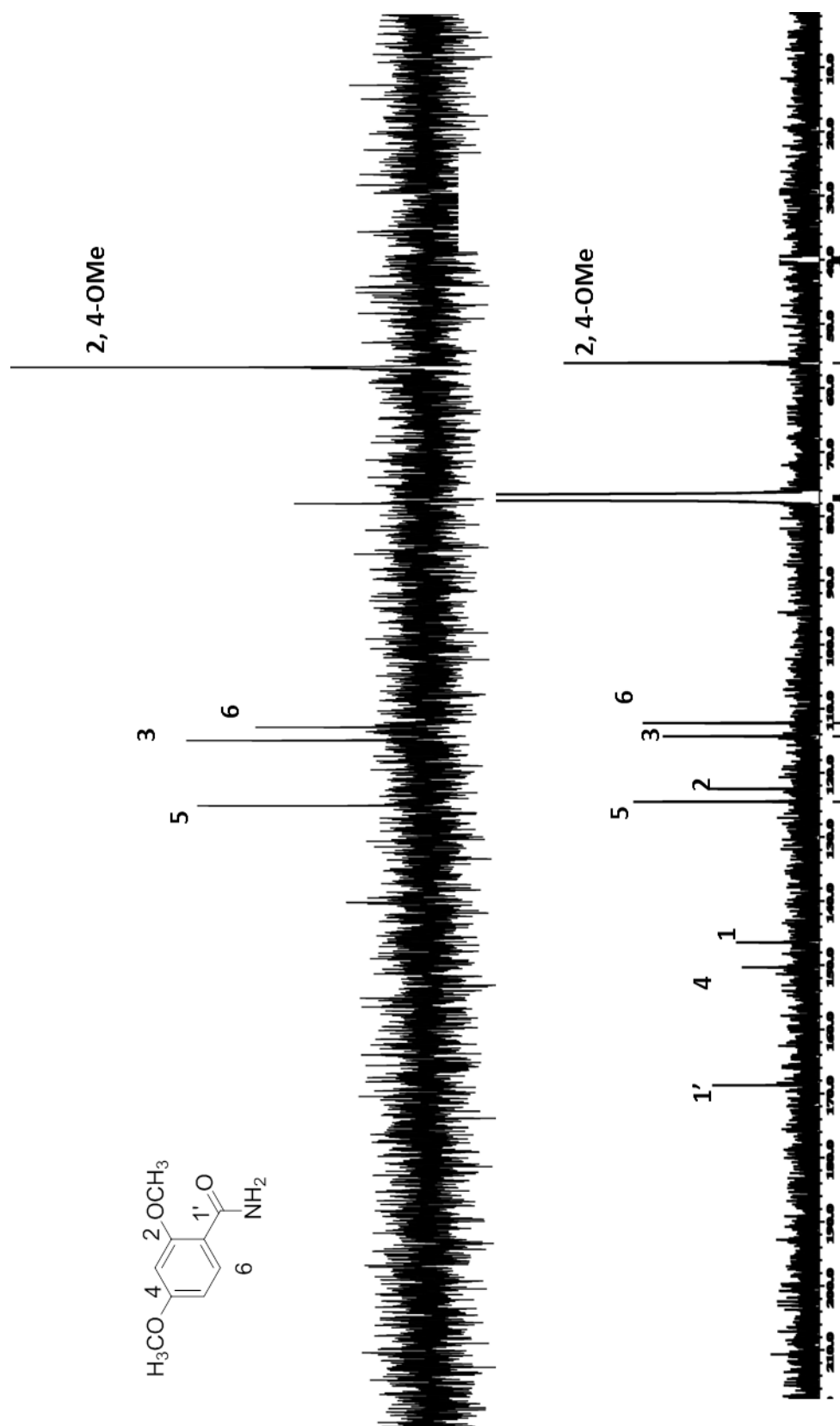


Figure 3. 113: ¹³C-NMR/DEPT spectrum of 2, 4 –dimethoxy benzamide LCL2

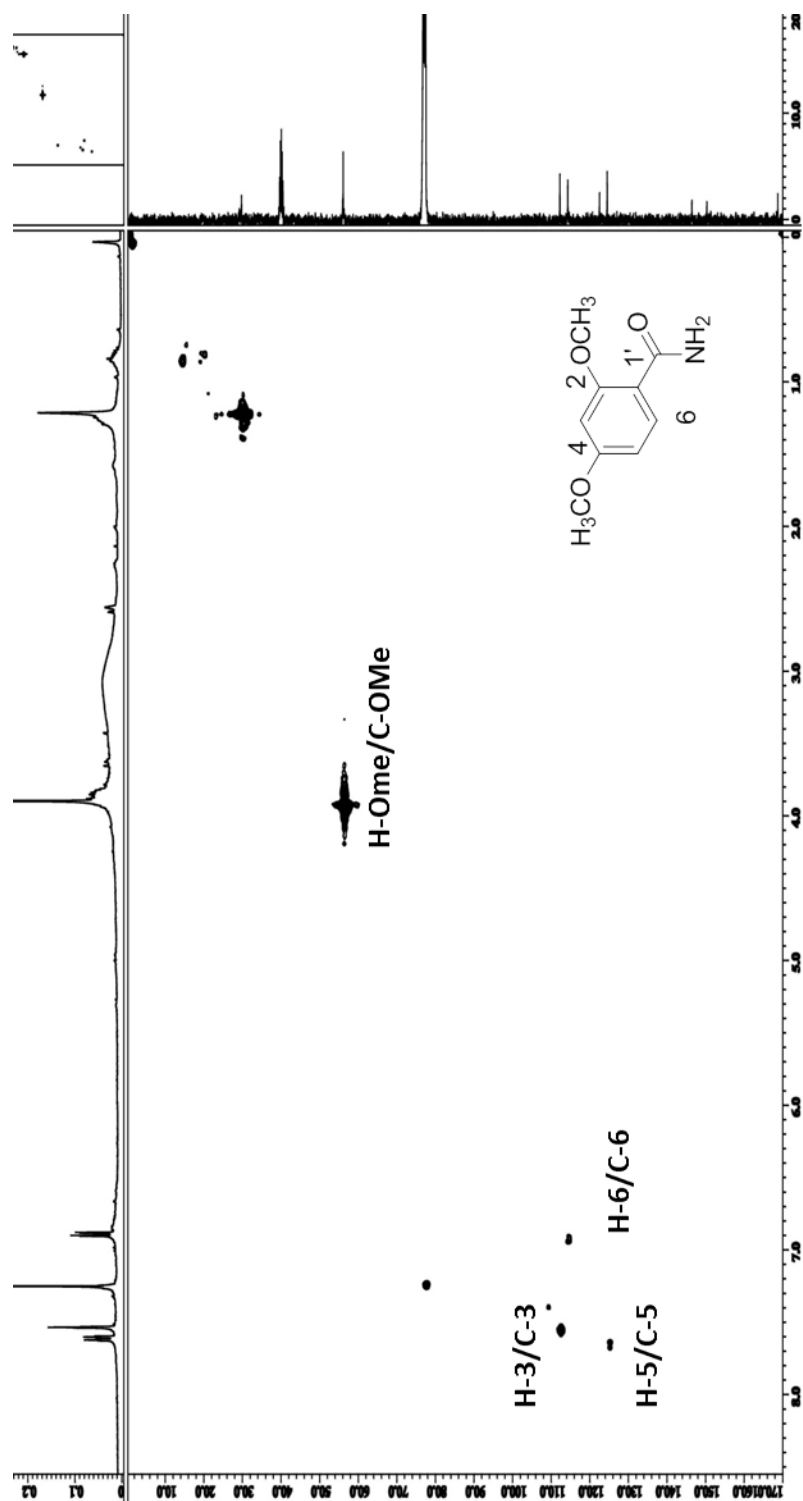


Figure 3.114: HMQC spectrum of 2, 4 -dimethoxybenzamide **LCL2**

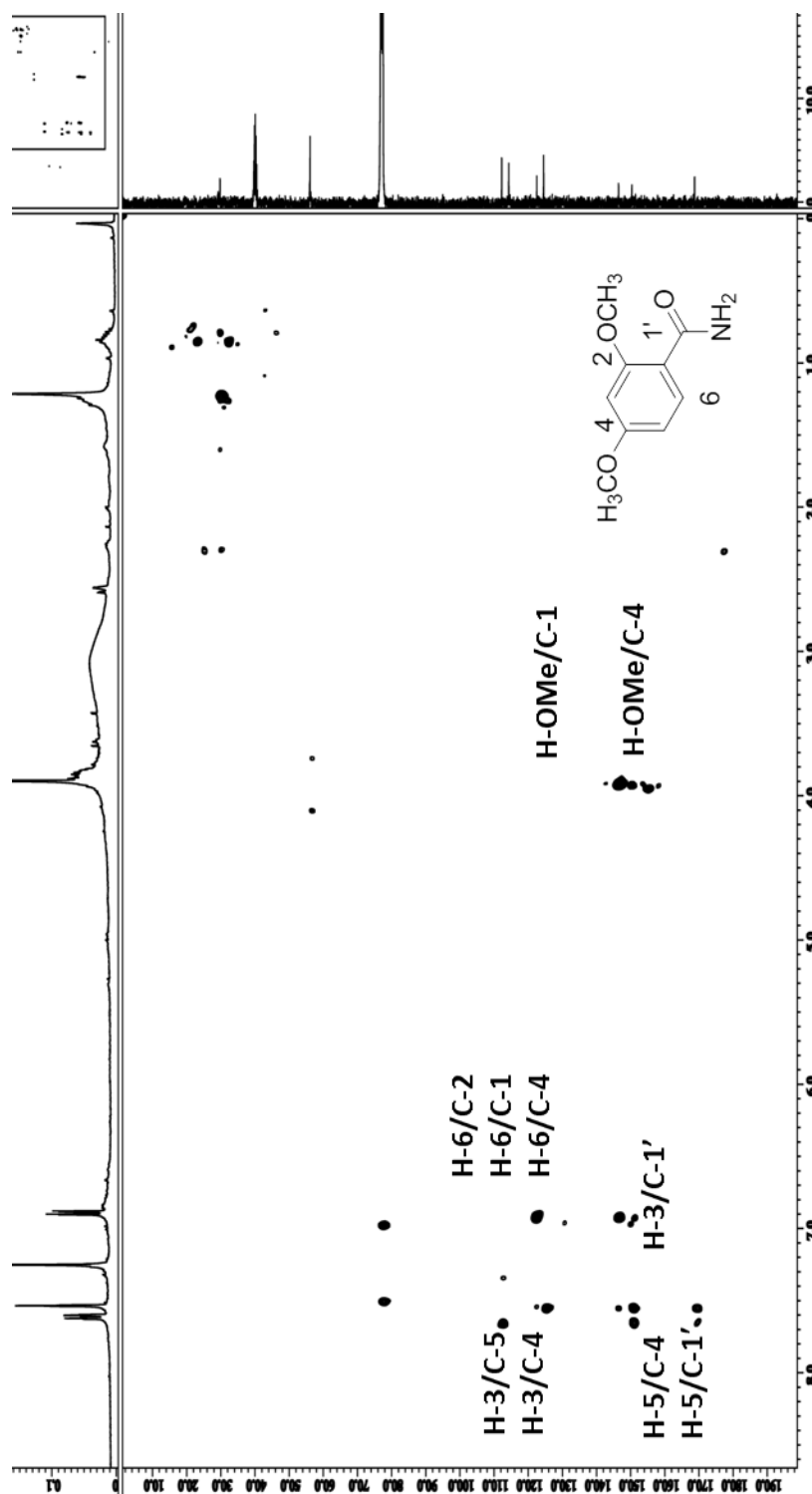
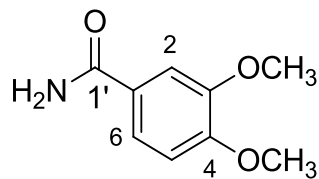


Figure 3.115: HMBC spectrum of 2, 4 –dimethoxybenzamide LCL2

3.2.13 3,4-Dimethoxybenzamide LCL5



LCL5

Compound **LCL5**, 3, 4 –Dimethoxy benzamide was obtained brown oil. The IR spectrum of at 3448 cm^{-1} indicated the presence of NH_2 group and 1607 cm^{-1} showed amide carbonyl stretching vibrations,. The UV spectrum showed absorption bands at λ_{max} (MeOH) nm (log ϵ), 261 (2.474) and 258 (2.486) nm. The LC-MS spectrum displayed ion peak $[\text{M}]^+$ at m/z 181.044, gave molecular formula of $\text{C}_9\text{H}_{11}\text{NO}_3$.

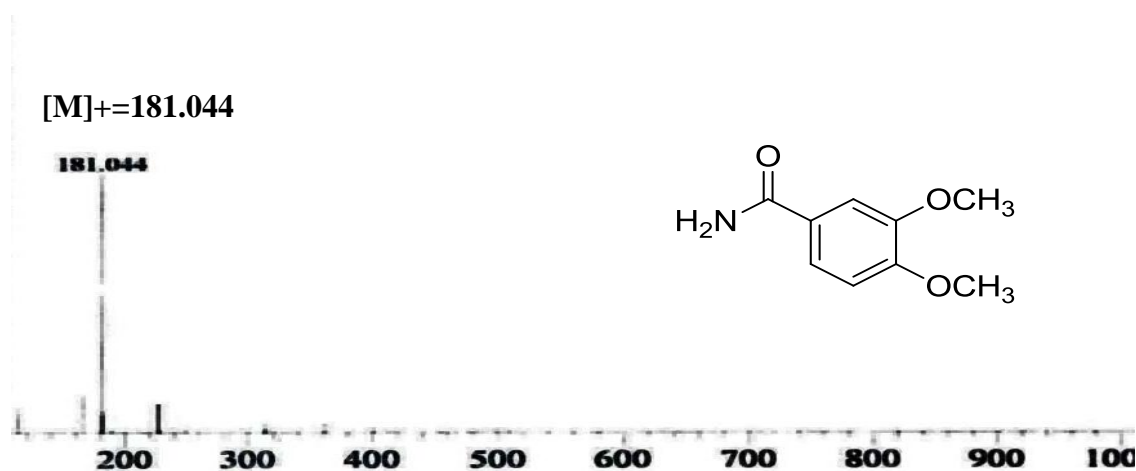


Figure 3.116: LC-MS Spectrum of 3, 4 –dimethoxy benzamide **LCL5**

The ^1H and ^{13}C NMR spectra (Table 3.29, Figure 3.117) and (Table 3.28 , Figure 3.118) exhibited the same spectra pattern with compound **LCL2** except the position C-3 in **LCL5** was substituted with methoxyl group and C-2 was unsubstituted (Van Daele et al., 1991). The aromatic proton at C-5 appeared at δ 6.90 as a doublet, the C-6 proton resonated at δ 7.57 as a doublet and the C-2 proton signal appeared at δ 7.58.

Based on the spectroscopic data of **LCL5** and comparison with the literature values, it was confirmed that compound **LCL5** was 3,4-dimethoxybenzamide.

Table 3.29: ^1H NMR (400 MHz) and ^{13}C NMR (100 MHz) spectral data of 3, 4 –dimethoxy benzamide **LCL5**

Position	^1H -NMR(δ , J in H_2)	^{13}C -NMR (δc)
1	-	112.9
2	7.58 (1H, d , 1.9 , H-2)	116.6
3	-	143.1
4	-	148.6
5	6.90 (1H, d , 8.0, H-5)	114.9
6	7.57 (1H, d , 8.0 , H-6)	123.8
1'	-	167.1
3,4-OMe	3.96 (6H, s)	52.1
NH ₂	6.15 (2H, $br s$)	-

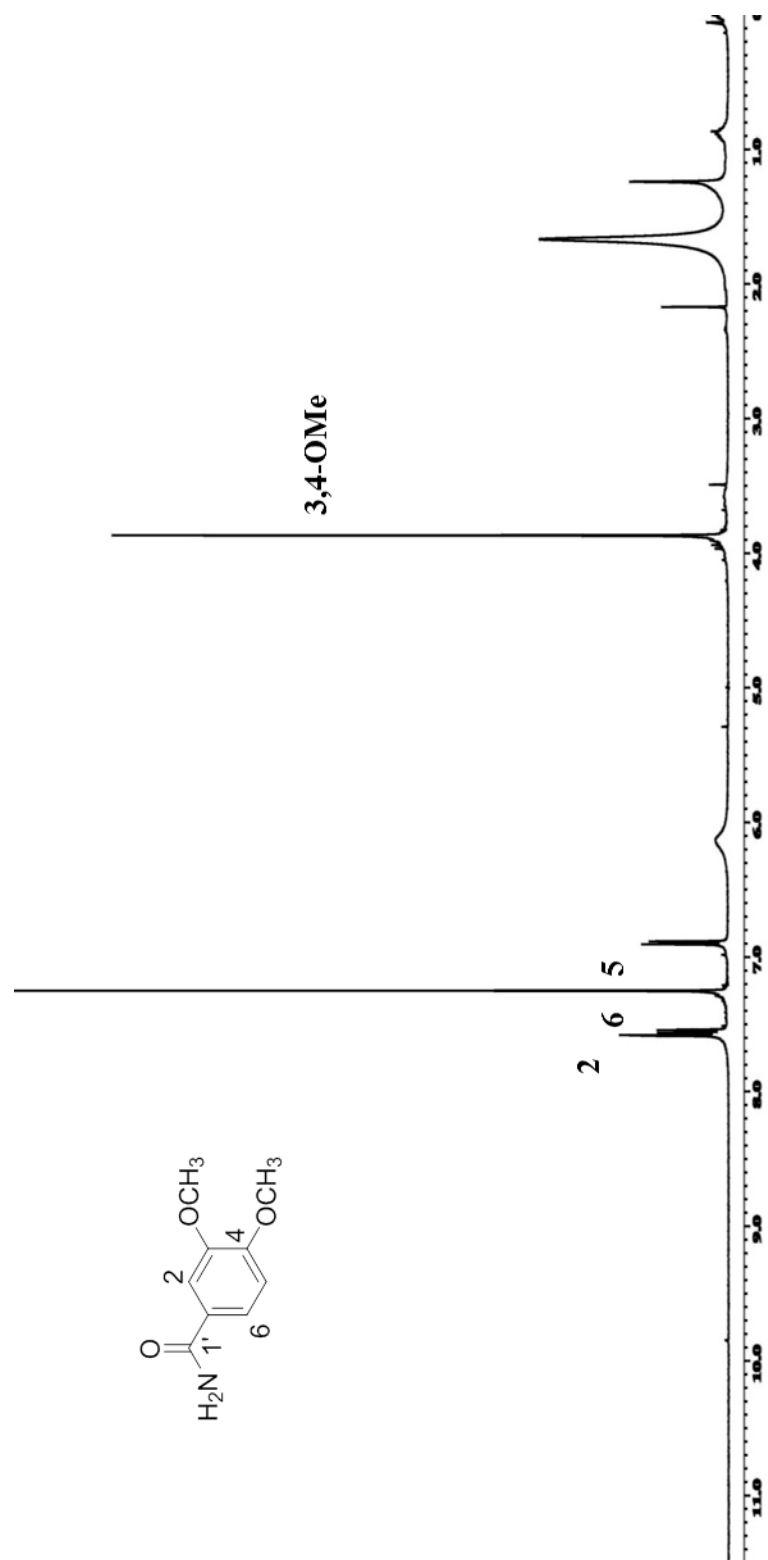


Figure 3.117 ¹H NMR spectrum of 3, 4 –dimethoxybenzamide LCL5

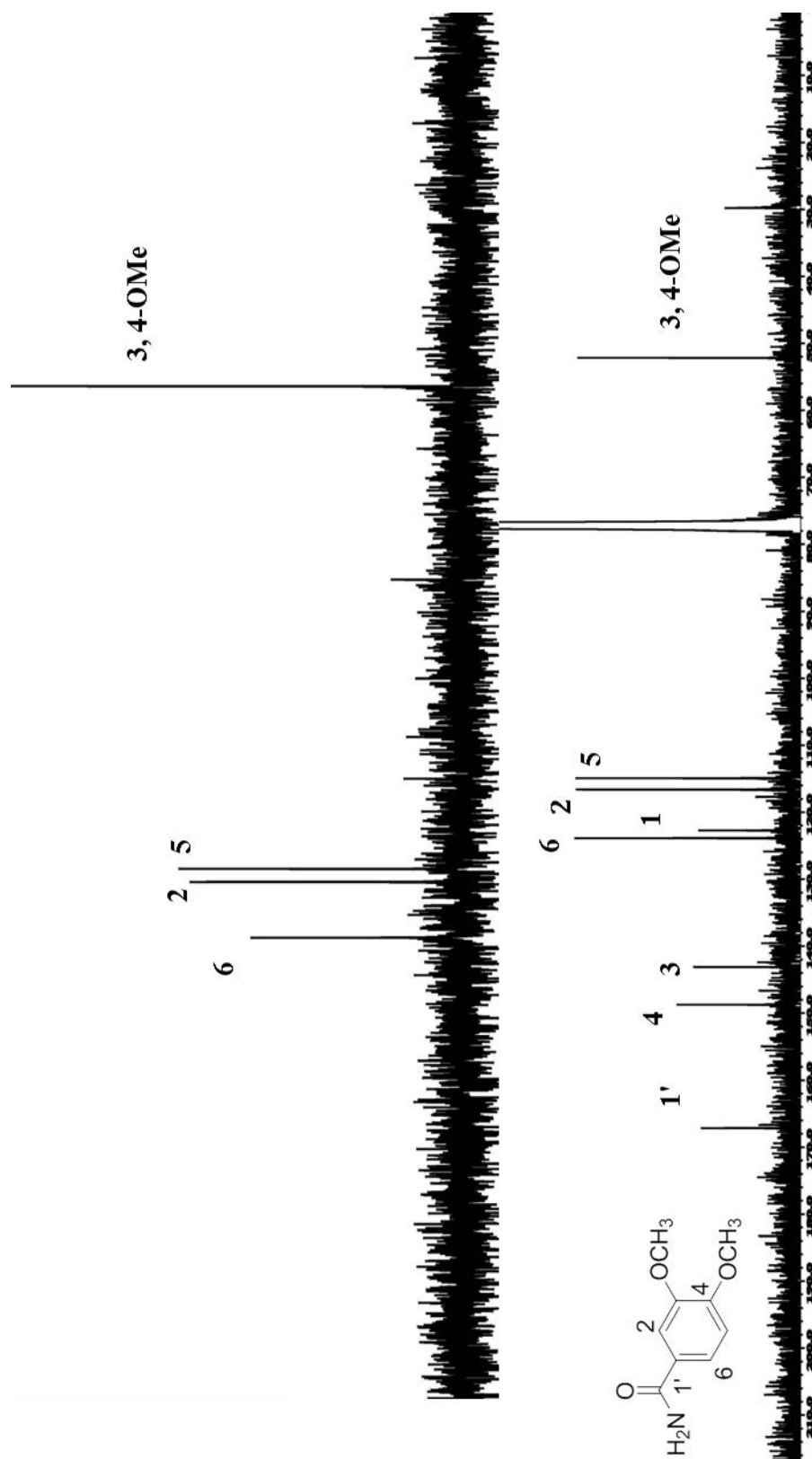
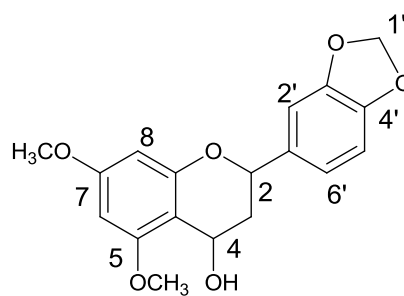


Figure 3.118: ^{13}C -NMR/DEPT spectrum of 3, 4 –dimethoxybenzamide LCL5

3.2.14 Flavonoid LCL7: Costalin



LCL7

Compound **LCL7** with IUPAC name (2*S*, 4*S*)-5,7-dimethoxy-3', 4'-methylenedioxyflavanone was obtained as white amorphous solid. $[\alpha]_D^{25} = +12.1$ (2.00×10^{-4} g/100 mL, MeOH). In the UV spectrum absorption maxima were observed at λ_{\max} nm (log ϵ) 293 (4.00) and 349 (1.433) which suggested a flavan type of the compound (Jayaprakasam et al., 1999). The IR spectrum of **LCL7** indicated the presence of hydroxyl (3392 cm^{-1}) and aromatic rings (1600 and 1454 cm^{-1}). The LC-MS spectrum showed pseudomolecular ion peak $[M+1]^+$ at m/z 331.0867 and $[M+Na]^+$ peak at m/z 353.0665 corresponding to the molecular formula of $C_{18}H_{18}O_6$.

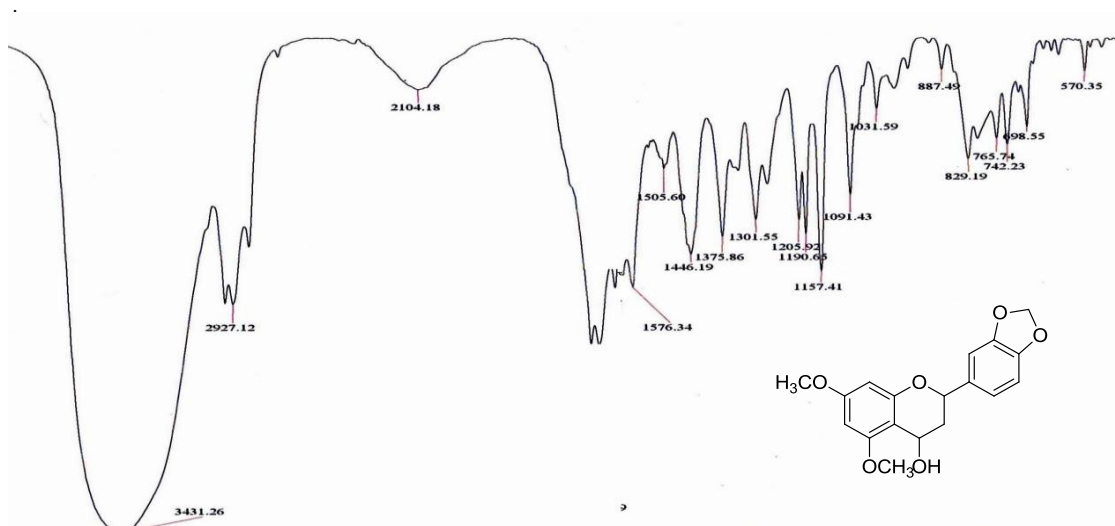


Figure 3.119: IR Spectrum of costalin **LCL7**

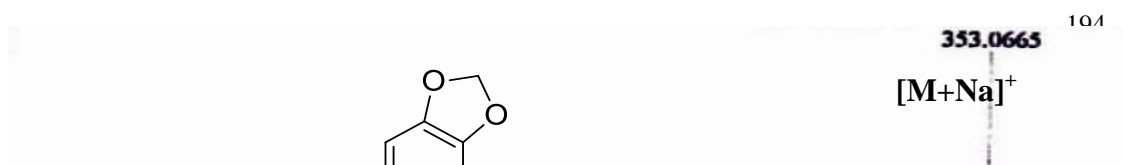


Figure 3.120: LC-MS Spectrum of costalin **LCL7**

Nine proton signals were observed in the ^1H -NMR spectrum (Table 3.30, Figure 3 .121) and eighteen carbon signals were observed in the ^{13}C -NMR spectrum (Table 3.30, Figure 3 .122). The type of groups present were sorted by the DEPT experiment which showed the presence of two methoxyls, two methylenes, seven methines and seven quaternary carbons. The ^1H NMR spectrum showed three sets of doublet triplet at δ 4.91(1H, dt $J=14.6$, 6.3 Hz, H-2), δ 2.88 (2H, m, H-3) and δ 4.24 (1H, dt, $J=14.0$, 6.1Hz, H-4) of ring-C of a Flavanone moiety. It also showed signals for two methoxyl groups at δ 3.76 and δ 3.78 which were assigned for C-5 and C-7 positions, respectively, as they showed 3J correlation with these carbons at δ 155.2 and δ 159.7 in the HMBC spectrum. The meta-coupled doublets at δ 6.10 (1H, d , $J=2.3$ Hz, H-8) and δ 6.16 (1H, d , $J=2.6$ Hz, H-6), which correlated to carbons at δ 93.3 and δ 92.3, respectively, in the HSQC spectrum (Table 3.29, Figure 3 .124) which were assigned to H-6 and H-8 of ring-A respectively. A sharp two-proton singlet at δ 5.96, correlation with the carbon at δ 101.2 in the HSQC spectrum of **LCL7** indicated a methylenedioxy group. HMBC (Table 3.30, Figure 3 .125) experiments also confirmed the ring-B have a methylenedioxy group between C-3' (δ 148.0) and C-4' (δ 147.4) positions. The ^1H

NMR spectrum also exhibited a typical AMX spectrum at δ 7.03 (1H, *d*, $J=1.3$ Hz, H-2'), δ 6.94 (1H, *d*, $J=8.1$ Hz, H-5') and δ 6.83 (1H, *dd*, $J=8.1, 1.3$ Hz, H-6') corresponding to three aromatic protons of ring-B (Mukherjee et al., 1994). The proton positioned at C-2 has connectivity with C-2', C-6' and C-1' and also it has correlation to C-3 and C-4 position. On the basis of these observations the methylenedioxy group at δ 5.96 was found to be located between C-3' and C-4' positions. The connectivity also observed between H-3 at δ 2.88 with C-2, C-4 and C-4a. H-4 at δ 4.24 has correlation with C-2, C-3 and C-4a. The configuration at C-2 and C-4 were found to be *S* as it showed in CD and in the NOESY (Table 3.29, Figure 3.126 and 3.128) spectrum the H-2 at δ 4.91 can see H-4 at δ 4.24. Thus, the structure of compound **LCL7** was established as (2*S*, 4*S*) – 5, -dimethoxy-3', 4'-methylenedioxyflavanone. This is the first time that flavonoid has hydroxyl group at the C-4 position has been isolated from leaves plant (Reddy et al., 2003).

Based on the observed data it was confirmed that the compound **LCL7** was (2*S*, 4*S*) – 5, -dimethoxy-3', 4'-methylenedioxyflavanone. This is a new compound and has never been reported before and this compound was named as **costalin**.

Table3.30: 1D (^1H and ^{13}C) and 2D (COSY, HMQC and HMBC) NMR spectra data of costalin **LCL7**

Position	^1H -NMR(δ , J in Hz)	^{13}C -NMR (δc)	COSY	HMBC	NOESY
1	-	-	-	-	-
2	4.91 (1H, dt, 14.6, 6.3)	78.5		1',2',6',3,4	H-4, H-3
3	2.88 (2H, <i>m</i>)	28.2	H-3/H-4	2,4,4a,	H-2, H-4
4	4.24 (1H, dt, 14.0, 6.1)	66.5	H-4/H-3	2,3,4a	H-2, H-3
4a	-	100.2	-	-	-
5	-	155.2	-	-	-
6	6.18 (1H, d, 2.6)	93.3	-	4a,5,8	-
7	-	159.7	-	-	-
8	6.10 (1H, <i>d</i> , 2.3)	92.3	-	4a,6,8a	-
8a	-	159.3	-	-	-
1'	-	132.2	-	-	-
2'	7.03 (1H, <i>d</i> , 1.3)	119.8	-	2,3',4',6'	-
3'	-	148.0	-	-	-
4'	-	147.4	-	-	-
5'	6.94 (1H, <i>d</i> , 8.1)	107.2	H-5'/H-6'	4',1',3'	-
6'	6.83 (1H, <i>dd</i> , 8.1, 1.3)	108.4	H-6'/H-5'	2'	-
1''	5.96 (2H, <i>s</i>)	101.2	-	3',4'	-
5-OCH ₃	3.76 (3H, <i>s</i>)	55.4	-	7	-
7-OCH ₃	3. 78 (3H, <i>s</i>)	55.5	-	5	-

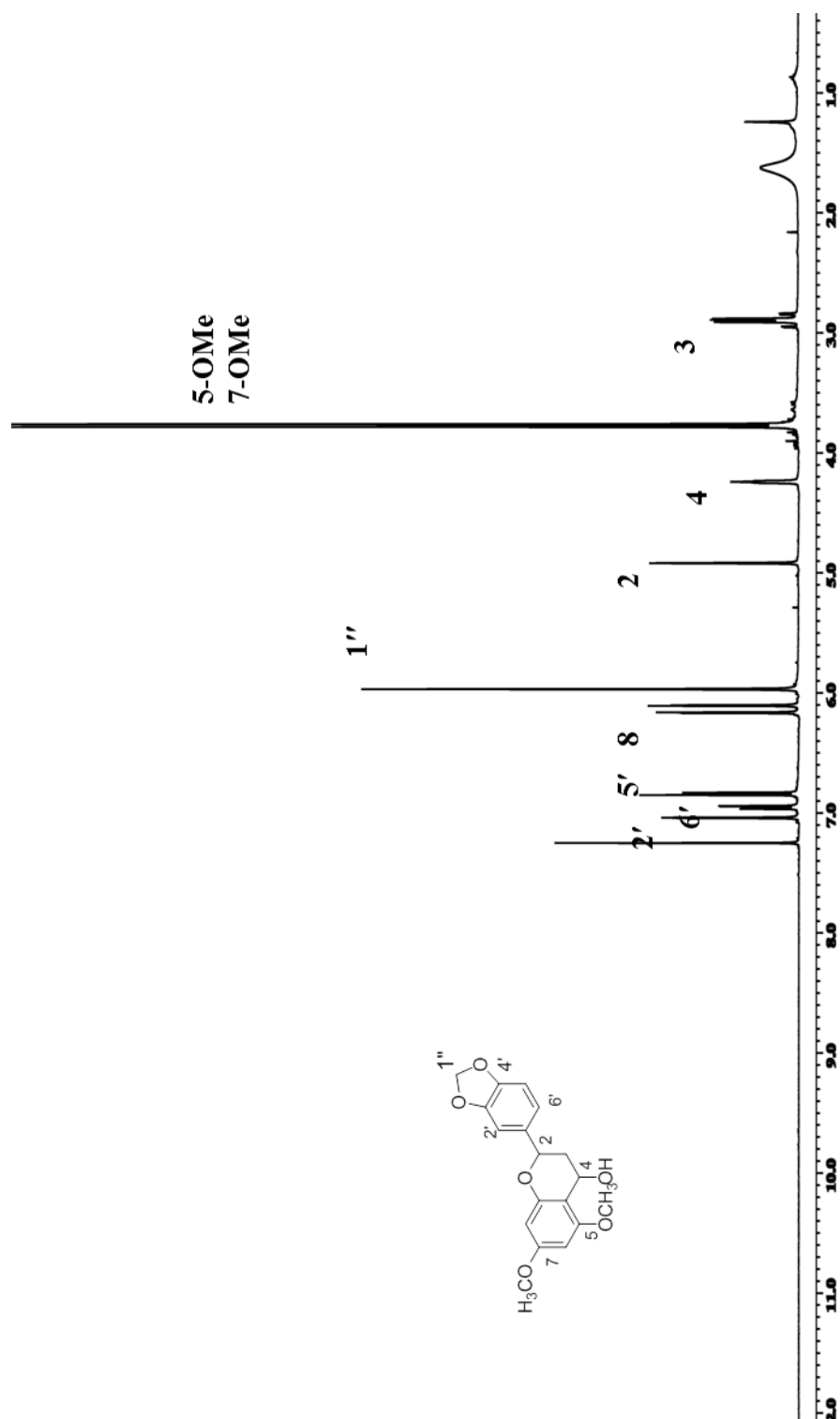
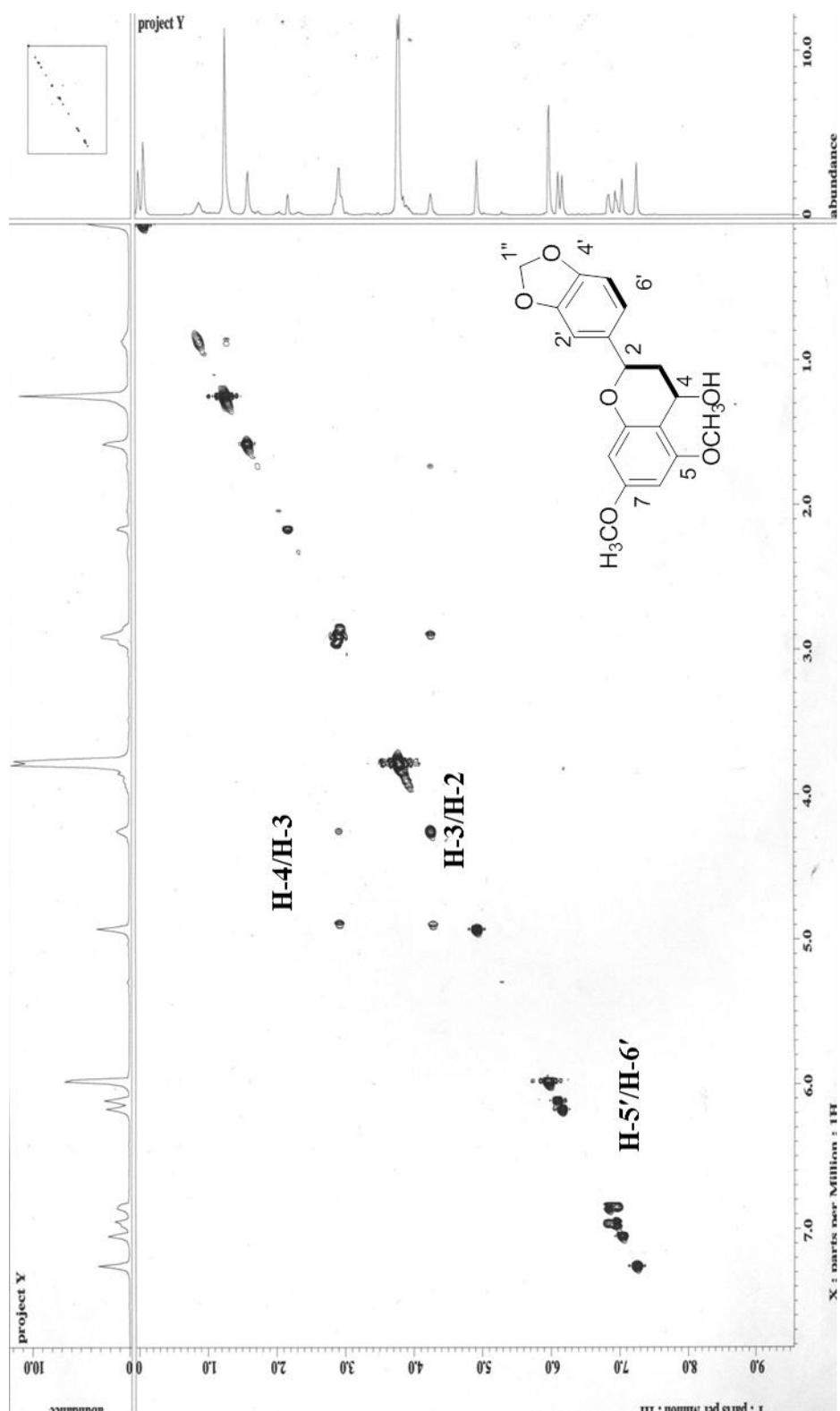


Figure 3.121: ^1H NMR spectrum of costalin LCL7



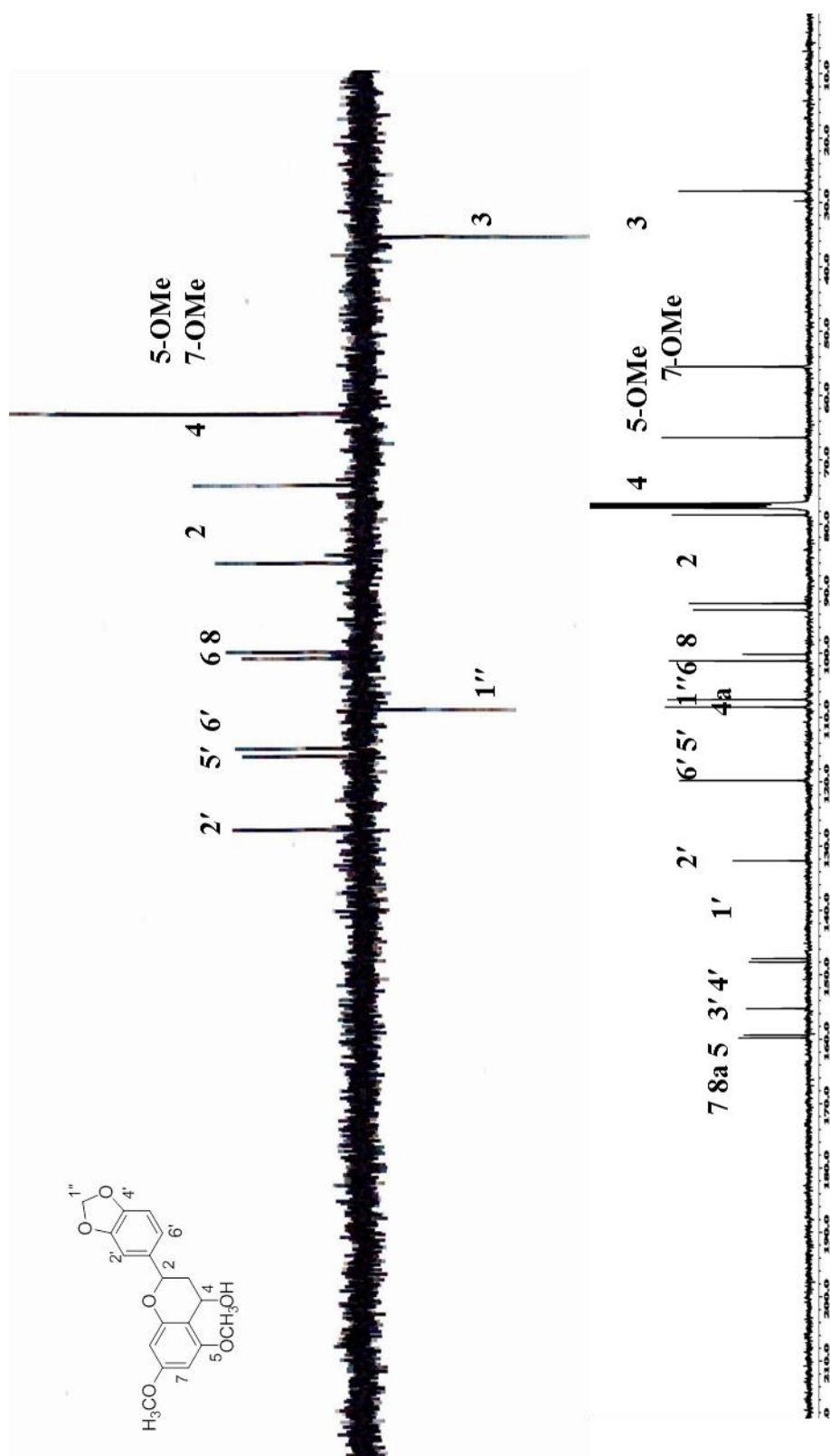


Figure 3.123: ¹³C-NMR/DEPT spectrum of Costalin LCL7

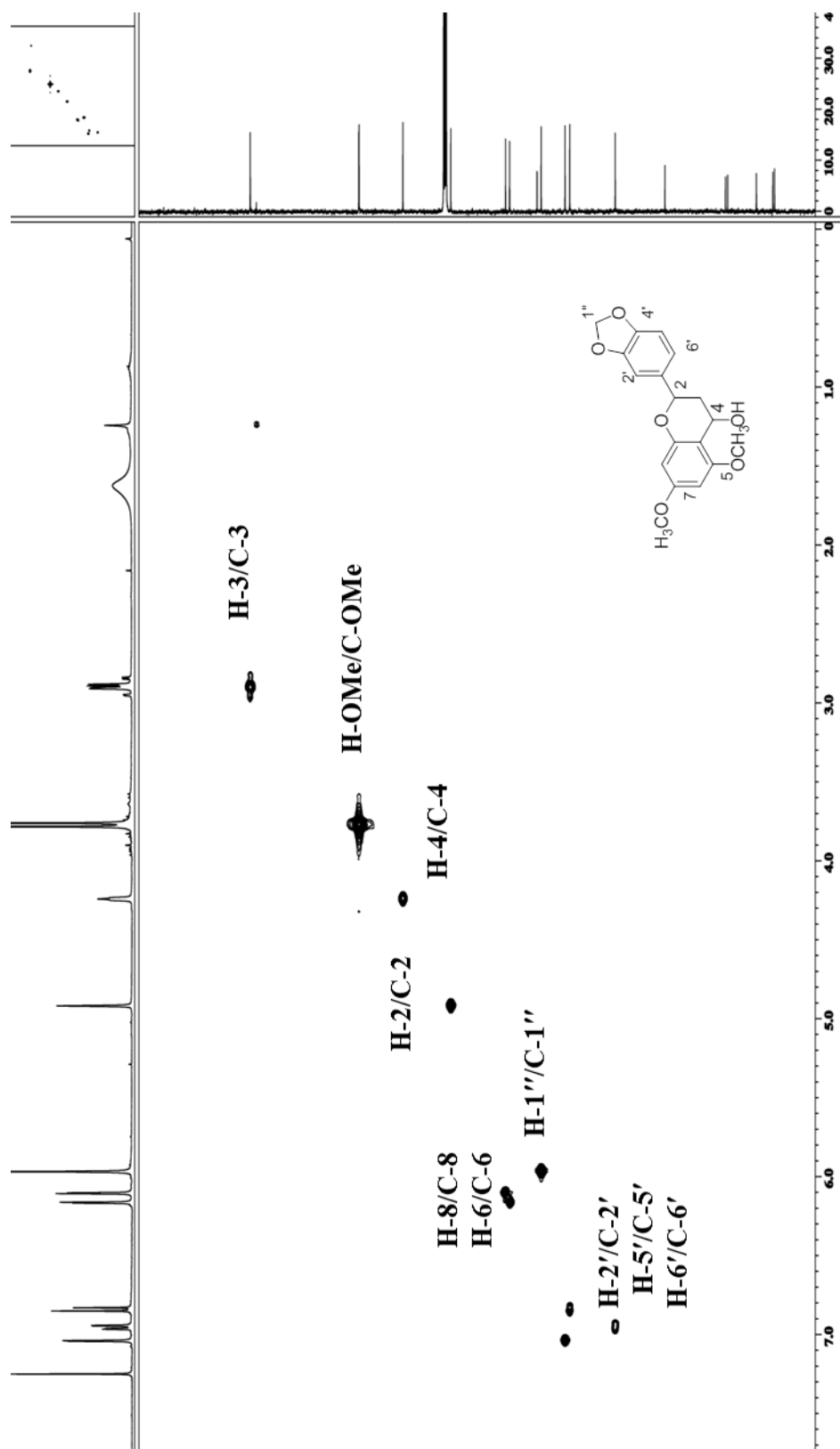


Figure 3.124: HMQC spectrum of costalin LCL7

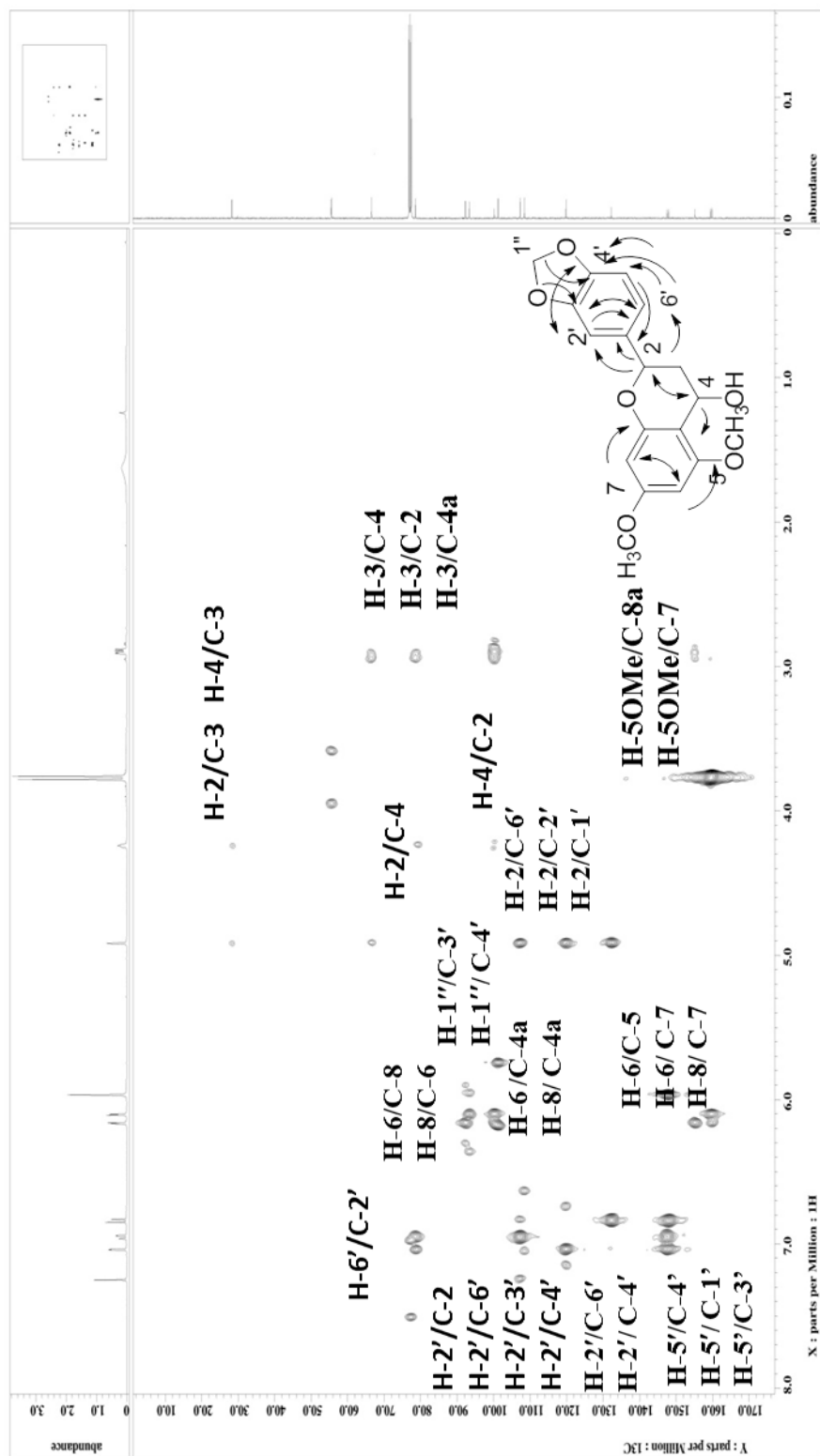


Figure 3.125: HMBC spectrum of costalin LCL7

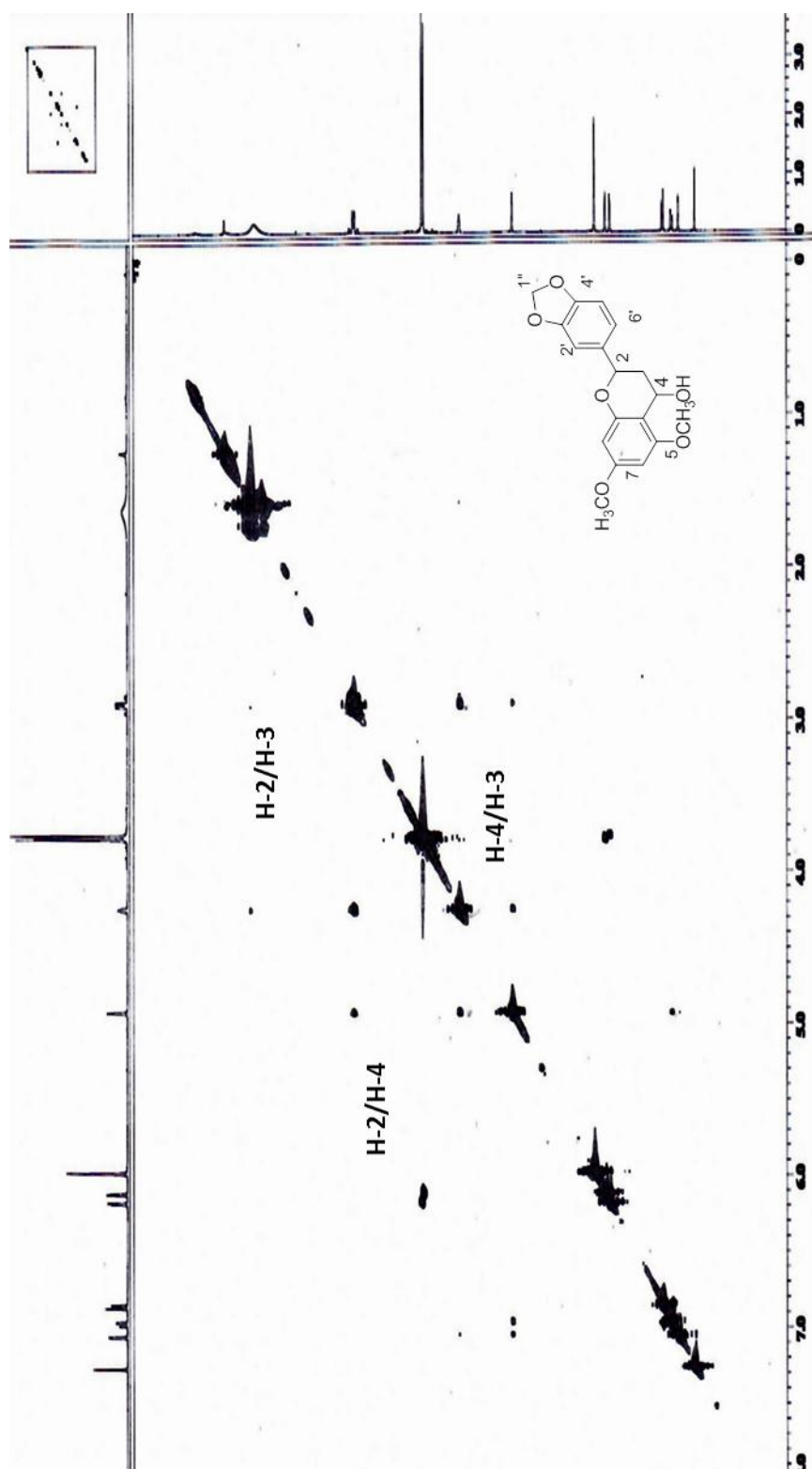


Figure 3.126: NOESY spectrum of costalin LCL7

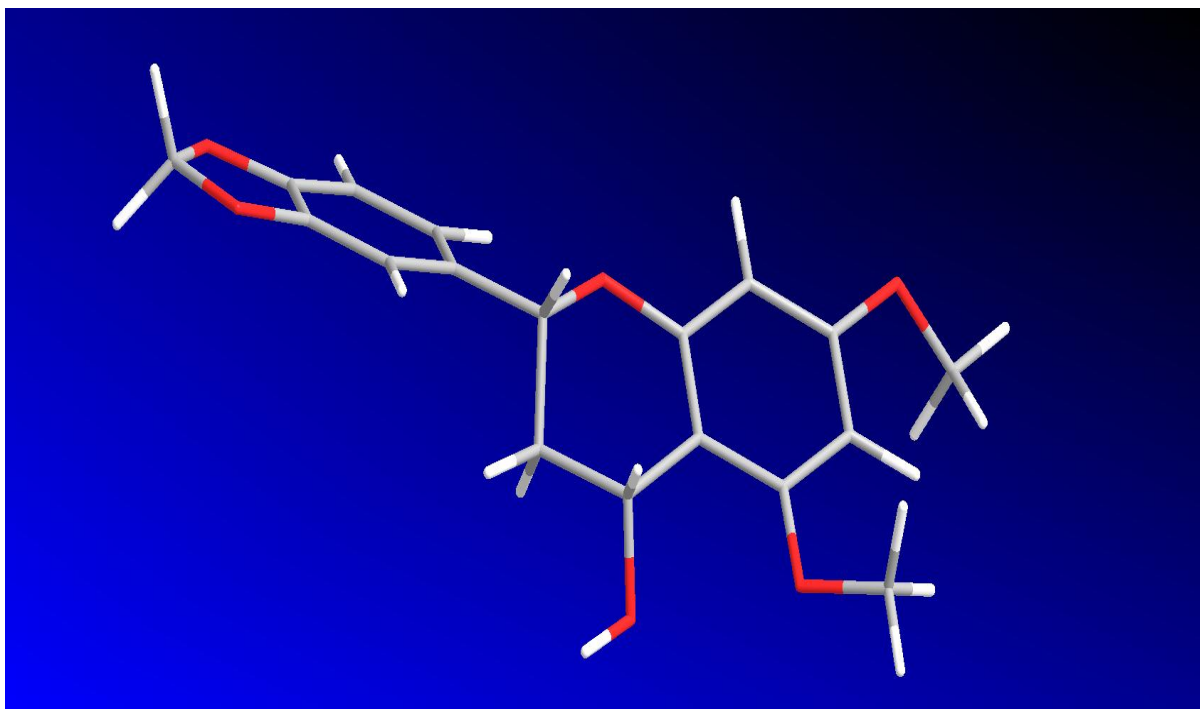


Figure 3.127: 3D Structure of costalin **LCL7**

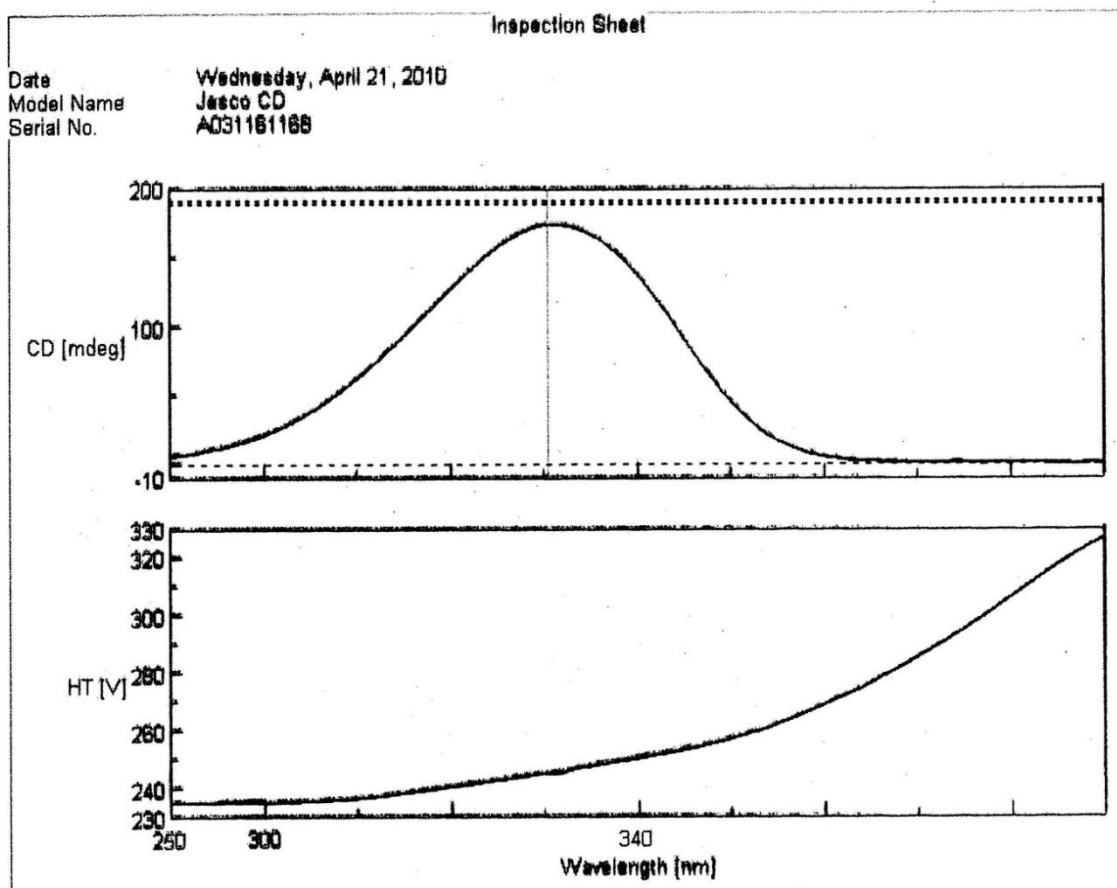
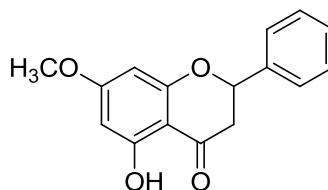


Figure 3.128: CD Structure of Costalin LCL

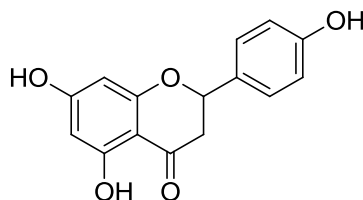
3.2.15 Flavanone **LCL9**: (+)- pinostrobin



LCL9

Flavanone **LCL9**: (+)-pinostrobin with IUPAC name [(*S*)-5-hydroxy - 7-dimethoxy-2-phenyl chroman-4H-one. was afforded as a yellow amorphous solid with $[\alpha]_D^{25} = +1.52$ (2.00 $\times 10^{-4}$ g/100 mL, MeOH). The UV spectrum, absorption maxima were observed at λ_{\max} (MeOH) nm (log ϵ) 306 (1.273) and 223 (2.316). Its IR spectrum showed absorption bands at ν_{\max} 3429 cm^{-1} assigned for bonded hydroxyl, 1642 cm^{-1} assigned for carbonyl group. The LC-MS (positive mode) spectrum showed an intense pseudomolecular ion peak, $[M+H]^+$ at m/z 271.088 corresponding to the molecular formula of $\text{C}_{16}\text{H}_{14}\text{O}_4$. ^1H -NMR and ^{13}C -NMR data were assemble to **LCL9**. In fact **LCL9** is **LOB7** and has been discussed in Section 3.1.2. (Please refer to page 40-45).

3.2.16 Flavonol **LCL14**: (+)-Pinocembrin

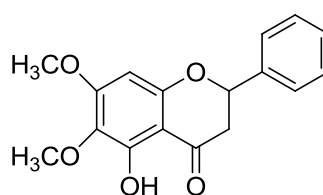


LCL14

Flavonoid **LCL14**, (+)-Pinocembrin, was afforded as a yellow amorphous solid with $[\alpha]_D^{25} = +2.81$ (2.00 $\times 10^{-4}$ g/100 mL, MeOH). In the UV spectrum, the absorption maxima at λ_{\max} (MeOH) nm (log ϵ) 241 (1.519) and 290 (2.783). Its IR spectrum

showed absorption bands at ν_{\max} 3417 cm^{-1} for bonded hydroxyl and 1640 cm^{-1} assigned for chelated α,β unsaturated carbonyl. The molecular formula of **LCL14** was established as $\text{C}_{15}\text{H}_{12}\text{O}_4$ on the basis of ESI-MS (negative mode): m/z 255.0475 $[\text{M} - \text{H}]^-$. MS/MS: m/z (relative abundance) 256.07. ^1H -NMR and ^{13}C -NMR data were assemble to **LCL14**. In fact **LCL14** is **LOB2** and has been discussed in Section 3.1.4. (Please refer to page 54-58).

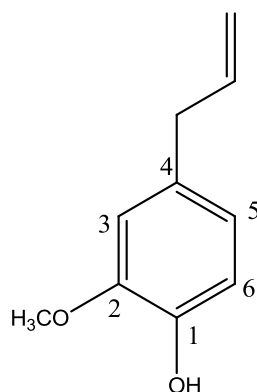
3.2.17 Flavanone LCL13: (+)-Onysilin



LCL13

Flavanone **LCL13**, (+)-Onysilin with IUPAC name [(2*S*)-5-hydroxy -6, 7-dimethoxy-2-phenyl chroman-4-one] was afforded as a yellow amorphous solid with $[\alpha]_D^{25} = +3.1$ ($2.00 \times 10^{-4} \text{g}/100 \text{mL}$, MeOH). In the UV spectrum, absorption maxima were observed at λ_{\max} (MeOH) nm (log ϵ) 293 (4.00) and 349 (1.43) which indicated the existence of the conjugated double bond system. Its IR spectrum showed absorption bands at ν_{\max} 3446 cm^{-1} assigned for bonded hydroxyl group and 1644 cm^{-1} for carbonyl group. The ESIMS (positive mode) spectrum showed an intense pseudomolecular ion peak, $[\text{M} + \text{H}]^+$ at m/z 301.0824 corresponding to the molecular formula of $\text{C}_{17}\text{H}_{16}\text{O}_5$. ^1H -NMR and ^{13}C -NMR data were assembled to **LCL13**. In fact **LCL13** is **LOB4** and has been discussed in Section 3.1.1. (Please refer to page 35-39).

3.2.18 Lignan LCL17: Eugenol



LCL17

Compound **LCL17** with IUPAC name 4-allyl-2methoxyphenol was afforded as yellow oil . The UV spectrum showed absorptions at λ_{max} (MeOH) nm (log ϵ) 225 (2.413) and 239 (2.763) indicating the presence of unsaturated carbon-carbon bond. The IR spectrum showed absorption peak at 3517 cm^{-1} indicated the existing of OH, 1638 cm^{-1} for olefenic SP bond and 1513 cm^{-1} assigned for the aromatic characteristics. LC-MS showed the pseudomolecular ion peak $[M+1]^+$ at m/z 165.0855 and molecular ion peak corresponding to the molecular formula of $\text{C}_{10}\text{H}_{12}\text{O}_2$.

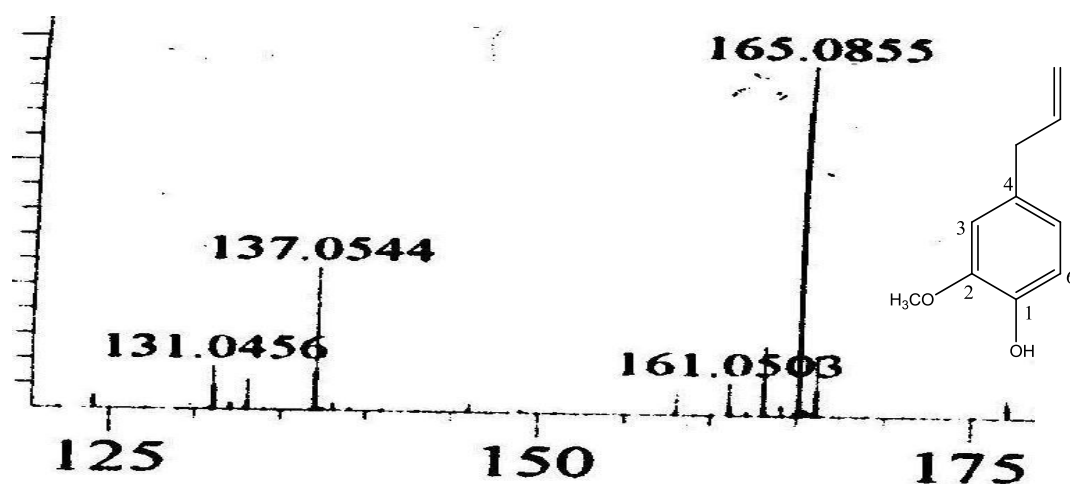


Figure 3.129: LC-MS Spectrum of eugenol **LCL17**

The ^1H -NMR spectrum (Table 3.31, Figure 3.130) exhibited one methoxyls resonated at δ 3.81 as a singlet and these methoxyls positioned at C-2. One sp^3 methylene group was observed at δ 3.31 as a doublet and sp^2 methylene group was resonated at δ 5.05 as a doublet of doublet. The sp^2 methine was observed at δ 5.95 as a multiplet. The aromatic proton were resonated at δ 6.69-6.71 (H-3 and H-5) and δ 6.85-6.86 (C-6) .

The ^{13}C NMR spectrum (Table 3.31, Figure 3.131) established 10 carbon signals which consist of one methoxyl, sp^2 methylene, sp^3 methylene, four methines and three quaternary carbons. The one methoxyl group positioned at C-2 was resonated at δ 55.9. sp^3 methylenes was observed at δ 39.8 (C- α), sp^2 methylenes appeared at δ 115.5 (C- γ). Methines in allyl group were observed at δ 137.8 (C- β) and three aromatic protons appeared at δ 111.2 (C-3), δ 114.2 (C-5), δ 121.1 (C-6). Three quaternary SP carbons were resonated at δ 143.8 (C-1), δ 131.9 (C-4) and δ 146.4 (C-2).

Based on the observed spectral data of **LCL17** it was confirmed that compound **LCL17** was eugenol.

Table 3.31: ^1H NMR (400 MHz) and ^{13}C NMR (100 MHz) spectral data of eugenol **LCL17**

Position	^1H -NMR(δ , J in Hz)	^{13}C -NMR(δc)
1	-	143.8
2	-	131.9
3	6.69-6.71 (H, m)	111.2
4	-	121.1
5	6.69-6.71 (H, m)	114.2
6	6.85-6.86(1H, d , 8.1)	146.4
α	3.31(2H, d , 7.1)	39.8
β	5.95 (H, m)	137.8
γ	5.05 (2H, dd , 14.8, 12.4)	115.5
^tOMe	3.81 (3H, s)	55.9

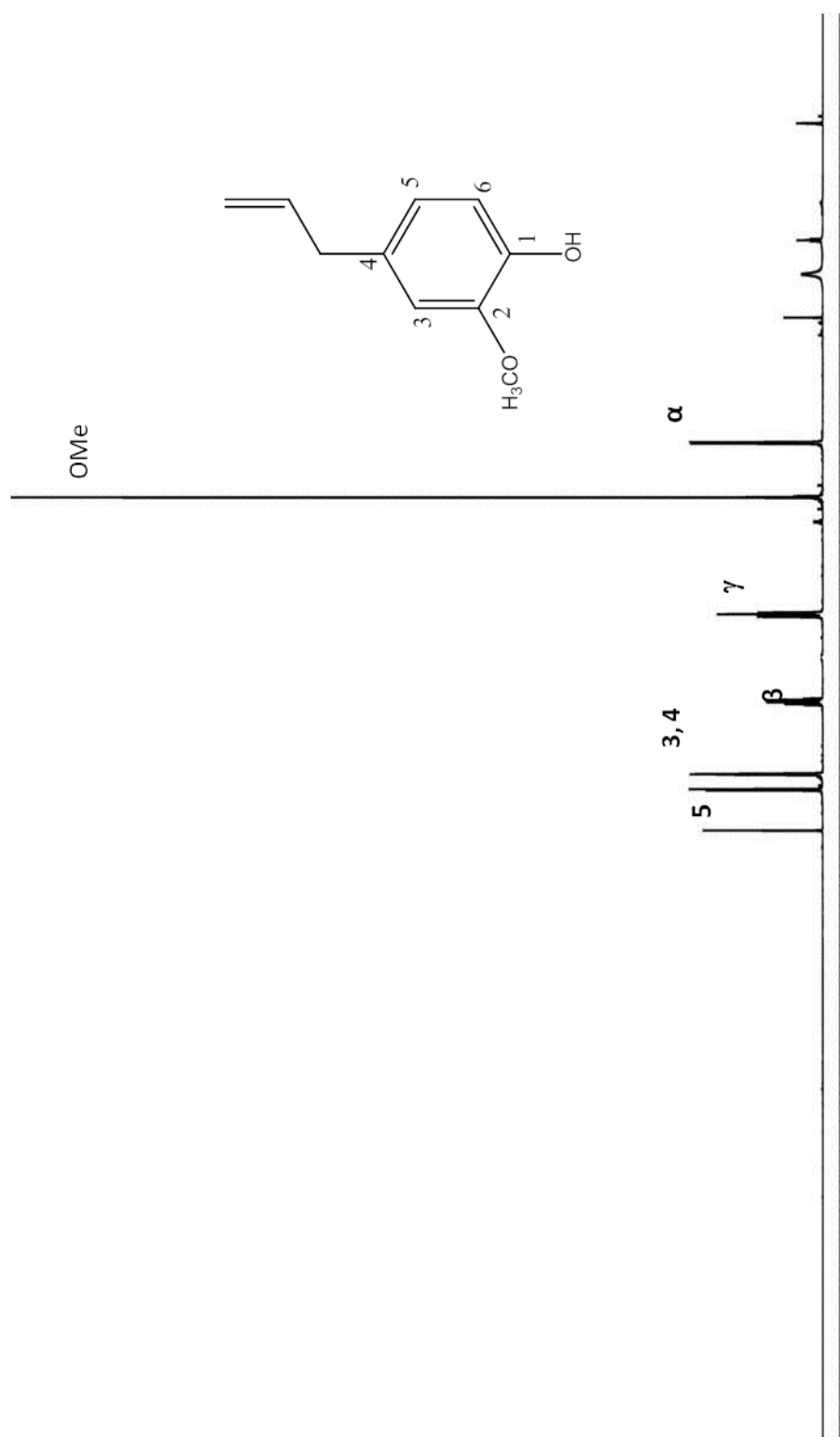


Figure 3.130: ^1H -NMR spectrum of eugenol

BIOACTIVITY

4.1 Introduction

This chapter is about antioxidant and anticancer activities of some isolated compounds. The compounds were first isolated from plants followed by antioxidant assay by several methods such as free radical scavenging activity by means of DPPH, Ferric Reducing Assay (FRAP) and Metal Chelating Assay.

Free radicals are produced during oxidation process of damaging cells caused by diseases and these free radical scan contain one electron or more unpaired electrons. Examples of free radicals are hydroxyl (OH^\cdot), superoxide (O_2^\cdot), nitric oxide (NO^\cdot) and peroxy (RO_2^\cdot). Antioxidants have ability to delay or prevent the oxidation of molecules. Antioxidant activity of plants function in several methods including free radical scavenging (DPPH), metal ion chelating (FIC) and FRAP performing as a substrate to absorb radicals such as superoxide and hydroxide. There are three mechanisms to determine antioxidant activity of a plant extract based on hydrogen atom transfer (HAT) reactions and electron transfer (ET) (Huang et al., 2005). 1,1'-Diphenyl- 2-picryl hydrazyl radical scavenging assay (DPPH) is one of a few stable and commercially available organic nitrogen radicals and has a UV-Vis absorption maximum at 517 nm (Miliauskas et al., 2004). Polyphenolic compounds, such as flavonoids, phenolic acids and lignans in plants have been reported to have multiple biological effects, including antioxidant activity and anticancer (Kähkönen MP et al., 1999). Phenolic compounds are natural antioxidants in the plants showed their antioxidant activity in several ways (Bombardelli et al., 1993) .

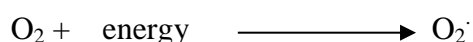
Radical scavenging activity toward either reactive species such as OH^\cdot , O_2^\cdot functioning *via* hydrogen atom exchange or electron donation (Niki et al., 2000). Phenolic compounds exhibit a wide range of bioactivly substances, such as anti-

allergenic, anti-atherogenic (Benavente et al., 1997), anti-inflammatory (Manach et al., 2005), anti-microbial (Middleton et al., 2000), antioxidant, anti-thrombotic (Heim et al., 2002), cardioprotective and vasodilatory effects (Cook.N.C, Samman, S. 1996).

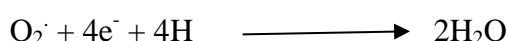
4.2 Antioxidant: Free radicals and oxidation

A free radical has high-energy and can be defined as any element or compound that needs an electron to fill an unfilled molecular valence orbital. They often “attack” and remove electrons from the molecule in closest proximity which can be neutral, positively or negatively charged (Hughes et al., 1999). This mechanism indicates the oxidized molecule a free radical and may initiate a chain reaction which can pursue stability from a nearby molecule without discrimination.

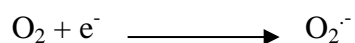
Oxygen can become a reactive molecule when oxygen is exposed to a source of high energy, the energy is transferred to form singlet oxygen (Ardestani et al., 2007).



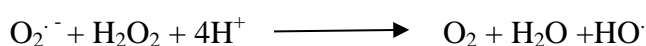
Normally, over 95% of the oxygen reduced to H₂O by the electron transport system in the mitochondria:



When molecule oxygen is reduced by one electron, formation superoxide radical:



After this added second electron at physiologic pH the formation two products of hydrogen peroxide (H₂O₂) and hydroxyl radical:



The formation of HO^\cdot from H_2O_2 is catalyzed by transition metals, mostly iron and copper. $\text{O}_2^{\cdot-}$, H_2O_2 and HO^\cdot are known as reactive oxygen species (ROS) and are continuously produced by aerobically growing cells (Castro et al., 2001).

4.3 Determination of antioxidant activity

We evaluated by using three different methods:

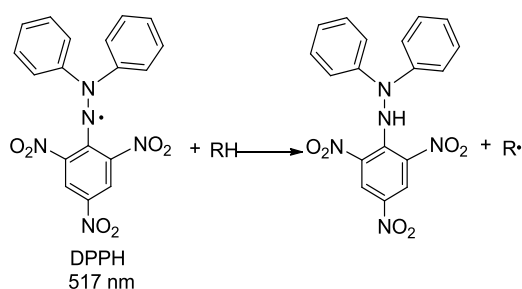
- i) 1,1-diphenyl-2-picrylhydrazyl (DPPH) Radical Scavenging Activity Assay
- ii) Ferric Reducing Power Assay (FRAP)
- iii) Metal Chelating Assay

4.4 DPPH Radical Scavenging Activity Assay

The DPPH radical scavenging activity assay is an assay that can determine the activity of antioxidants to directly react with DPPH stable free radical by observing its absorbance at 517 nm with a spectrophotometer. The DPPH radical is a stable nitrogen centered free radical. Purple coloured 1, 1-diphenyl-2-picrylhydrazyl (DPPH), a stable free radical which reduced to α, α' -diphenyl- β -picrylhydrazine. DPPH was observed yellow in colour if reacts with antioxidant. The decolorization of purple colour indicated the potential of antioxidants of the samples. When the more decolorization of purple colour occurred, the antioxidant concentration of the sample was higher.

The DPPH radical scavenging activity was used in the screening of the antioxidant properties of pure compounds and plant extracts. This method is simple and can be determined by using single read spectrophotometer. However, the disadvantage of the DPPH activity scavenging assay is the use of non physiologically relevant free radicals which resembled to free radicals that involved in the oxidation process in biological system (Adedapo et al., 2008) (Miller et al., 2000). The relative radical-scavenging abilities of phenolic compounds through their properties as electron- or H-

donating agents DPPH is discredited in (scheme 4.1).



Scheme 4.1: Radical-scavenging abilities of DPPH through H-donating agents

4.4.1 Material

DPPH (1,1'diphenyl-2-picrylhydrazyl), trichloroacetic acid, sodium phosphate monobasic, and sodium phosphate dibasic were purchased from Sigma Chemical Co. (St. Louis, MO, USA). Ferric chloride, methanol and water (HPLC) were purchased from Chemolab Supplies (Kuala Lumpur, Malaysia). An ELISA reader (Sunrise, Switzerland) and UV-vis spectrophotometer-1700 (Shimadzu, Japan) were used for absorbance determinations.

4.4.2 Preparations of solutions

A. Preparation of compounds

1.00 mg/mL concentration of compounds in methanol were prepared by dissolving 1.00 mg of compound in 1.00 mL methanol (Ranilla et al., 2010).

B. Preparation of Ascorbic acid.

Ascorbic acid was used as the positive standard reference in DPPH radical scavenging assay. Ascorbic acid standard, DPPH, and methanol were prepared as shown in (Table 4.1). Ascorbic acid was prepared at the concentration of 1000 µg /mL. 1.00 mg of ascorbic acid was dissolved in 1.00 mL methanol. The stock solution was

kept in flask which was wrapped in aluminium foil.

C. Preparation of DPPH

A stock of DPPH in methanol was prepared at the concentration at 60 μ M by dissolving 0.0024 g of DPPH stock in 100 mL methanol. The stock solution was kept in flask which was wrapped in aluminium foil (Ranilla et al., 2010).

D. Determination of DPPH activity of compounds.

The scavenging activity of all compound and ascorbic acid were tested at different concentrations (1000 μ g/mL, 500 μ g/mL, 250 μ g/mL, 125 μ g/mL, 62.5 μ g/mL, and 31.25 μ g/mL). Reaction mixtures containing DPPH and compounds or ascorbic were prepared according to Table 4.1.

Assay was run by mixing 1250 μ L of 60 μ M DPPH solution with 250 μ L of each crude compounds at various concentrations (31.25 to 1000 μ g/ml) in 96-well microplate. This reaction can tolerate to stand at 25 $^{\circ}$ C for 30 min. After 30 min incubation in darkness, the absorbance at 517 nm was measured by using ELISA reader (Sunrise, Switzerland).

E. Determination of percentage of inhibition of DPPH.

DPPH Scavenging effect activity was calculated by using the following formula:

$$\text{DPPH Scavenging effect (\%)} = \frac{A_0(\text{Control}) - A_1(\text{Sample})}{A_0(\text{Control})} \times 100$$

Where;

A_0 control = absorbance value of control

A_1 sample = absorbance value of sample

Percentage inhibition for each sample for the active extract was calculated by using the

above formula. A graph of percentage of inhibition against concentration was plotted in order to IC_{50} value can be determined. The IC_{50} value was the concentration (in $\mu\text{g/mL}$) at which 50% of DPPH radicals were inhibited.

The entire test was performed in triplicate and results were expressed as mean \pm standard deviation (SD).

Table 4.1: DPPH and different concentration of standard ascorbic acid

Concentration of compounds ($\mu\text{g/mL}$)	Volume of methanol (μL)	Volume of compounds (μL)	Volume of DPPH solution (μL)
1000.0	0.0	250.0	1250.0
500.0	500.0	250.0	1250.0
250.0	750.0	250.0	1250.0
125.0	875.0	250.0	1250.0
62.5	937.5	250.0	1250.0
31.25	968.75	250.0	1250.0
Control	250.00	-	1250.0

4.5 Ferric Reducing Power Assay (FRAP)

The Reducing Power Assay was one of the mechanism actions of antioxidants and it can be used to measure the electron-donating ability of antioxidants using the potassium ferricyanide reduction method. The ferric ion or ferricyanide complex was reduced by the antioxidants to the ferrous form and Perl's Prussian blue complex was observed. Fe(III) reduction was often used as an indicator of electron-donating activity and it can be strongly correlated with other antioxidant properties (Ozsoy et al., 2008).

The yellow colour of the test solution can change to various blue and green colours depending on the reducing power potential of each extract. The reductions that present in the compounds caused the Fe^{3+} /Ferricyanide complex to be reduced to ferrous ion, Fe^{2+} . When the Perl's Prussian blue was formed in the reaction mixture, it indicated the presence of Fe^{2+} . The more intense of blue colour showed the higher reducing power capability of the compounds and the increase of OD reading (700 nm) indicated the greater reducing power of the extract. Reducing power can evaluate the ability of extract to reduce from Fe^{3+} to Fe^{2+} (Chang, et al., 2007).

4.5.1 Material

Potassium ferricyanide $\text{K}_3[\text{Fe}(\text{CN})_6]$, trichloroacetic acid, ferric chloride solution, sodium phosphate from Sigma Chemical Co. (St. Louis, MO, USA). methanol and water (HPLC) were purchased from Chemolab Supplies (Kuala Lumpur, Malaysia). An ELISA reader (Sunrise, Switzerland) and UV-vis spectrophotometer-1700 (Shimadzu, Japan) were used for absorbance determination.

4.5.2 Preparations of solutions

A. Preparation of 1% Potassium Ferricyanide $K_3 [Fe (CN)_6]$

A stock of potassium ferricyanide was prepared at the concentration of 10 mg/mL. 0.6 g of potassium ferricyanide stock was dissolved in 60 mL distilled water. The stock solution was kept in flask wrapped with aluminium foil (Yu et al., 2008).

B. Preparation of 10% Trichloroacetic acid (TCA)

A stock of trichloroacetic acid was prepared at the concentration of 100 mg/mL. 6 g of trichloroacetic acid stock was dissolved in 60 mL distilled water. The stock solution was kept in flask wrapped with aluminium foil.

C. Preparation of 0.1% Ferric chloride solution

A stock of ferric chloride solution was prepared at the concentration of 1 mg/mL. 0.01 g of ferric chloride was dissolved in 10 mL distilled water. The stock solution was kept in flask wrapped with aluminium foil.

D. Preparation of 0.2 M , buffer solution

Sodium phosphate buffer were prepared according to published method (Dawson et al. 1986).

D.1 Preparation of 0.4 M sodium phosphate monobasic (NaH_2PO_4) stock solution

To prepare 250 mL of 0.4 M stock solution, 12 g of sodium phosphate monobasic (MW=119.98 g/mole) was dissolved in 250 mL distilled water. The stock was kept in a flask prior to prepare 0.2 M sodium phosphate buffer.

D.2 Preparation of 0.4 M sodium phosphate dibasic (Na_2HPO_4) stock solution

To prepare 250 mL of 0.4 M stock solution, 14.2 g of sodium phosphate dibasic (MW=141.96 g/mole) was dissolved in 250 mL distilled water. The stock was kept in a flask prior to prepare 0.2 M sodium phosphate buffer.

To prepare 500 mL of 0.2 M sodium phosphate buffer solution (pH = 6.6), approximately 93.75 mL of sodium phosphate dibasic (Na_2HPO_4) stock solution was mixed with 156.25 mL of sodium phosphate monobasic (NaH_2PO_4) stock solution and it was diluted to 500 mL with distilled water. This solution can be stored in the refrigerator for several months.

E. Determination of FRAP Assay

Generally, different amount of compounds were dissolved in 1 mL methanol and were vortexed until it mixed completely. 0.5 mL of prepared compounds was then added to 0.5 mL of 0.2 M Phosphate buffer (pH 6.6) and 0.5 mL of 1% (W/V) potassium ferricyanide. The mixtures were incubated in water bath at 50°C for 20 min. After incubation, 0.5 ml of 10% trichloroacetic acid (TCA) solution was added to each mixture and then centrifuged at 3000 rpm for approximately 10 minutes. The supernatant (0.5 mL) was mixed with 0.5 mL of distilled water and 0.1 mL of freshly prepared 0.1% ferric chloride solution. The absorbance was measured at 700 nm using UV spectrophotometer (Shimadzu, Japan). The BHA at different concentrations (16.62-1000 $\mu\text{g/mL}$) was used as standard reference. Methanol was used as blank. All the tests were carried out triplicates and results were expressed as mean \pm standard deviation (SD).

4.6 Metal Chelating Activity Assay

The chelating activity of compounds was determined according to the method of (Dinis et al., 1994). The purpose of this assay is to evaluate the ability of compounds extract from plant to chelate ferrous ion and preventing the formation of ferrozine – Fe^{2+} complex.

4.6.1 Material

Ferrozine, EDTA, ferric chloride from Sigma Chemical Co. (St. Louis, MO, USA). methanol and water (HPLC) were purchased from Chemolab Supplies (Kuala Lumpur, Malaysia). An ELISA reader (Sunrise, Switzerland) and UV-vis spectrophotometer-1700 (Shimadzu, Japan) were used for absorbance determinations.

4.6.2 Preparation of solution

A. Preparation of 5mM Ferrozine

0.0246 g ferrozine stock was dissolved in 10 mL deionized water. The stock was kept in flask wrapped with aluminium foil.

B. Preparation of 2mM Ferrous chloride (FeCl_2)

0.004 g of FeCl_2 stock was dissolved in 10 mL deionized water. The stock was kept in flask wrapped with aluminium foil.

C. Preparation of standard EDTA

Ethylenediamine tetraacetic acid (EDTA) was used as positive reference standard in this assay. The tested compound was carried out in different concentration of (62.5 -1000 $\mu\text{g/mL}$) followed by treatment with ferric chloride (FeCl_3) and ferrozine respectively in centrifuge tubes according to (Table 4.2) .

D. Determination of metal chelating activity of compounds

Compounds in different concentration of (62.5 -1000 $\mu\text{g/mL}$) was treated with 0.05 ml ferric chloride (FeCl_3 2 mM) and 0.2 ml ferrozine (5mM) respectively in centrifuge tubes according to (Table 4.2).

The reaction mixture was shaken and left incubated in the room temperature for 10 minutes. 1 ml of mixture was divided into 3 cuvettes each. The absorbance was measured at 562 nm. Methanol is used as balank. All compounds were tested in triplicates and the readings were averaged out

E. Determination of percentage of inhibition of ferrozine

The percentage of metal chelating effect of ferrozine Fe^{2+} complex formation was calculated using the formula below.

$$\text{Metal chelating effect (\%)} = \frac{\text{Abs control} - \text{Abs sample}}{\text{Abs control}} \times 100$$

Where;

Abs control=absorbance reading of control

Abs sample= absorbance reading of sample

Table4.2:Metal chelating of standard EDTA

Concentration of EDTA and compound(mg/mL)	Volume of methanol (mL)	Volume of FeCl_2 mM(mL)	Volume of ferrozine 5mM(mL)
1000	0	0.05	0.2
500	500	0.05	0.2
250	750	0.05	0.2
125	875	0.05	0.2
62.5	937.5	0.05	0.2
Control	1000	0.05	0.2

4.7 Results and Discussion

4.7.1 DPPH Radical Scavenging Activity Assay

The percentage inhibition against DPPH radical of ascorbic acid (compound 1), (Table 4.5, Figure 4.1) at 1000 $\mu\text{g/mL}$ showed the inhibition activity range between 83.98 ± 0.001 to 95.68 ± 0.003 at concentration of $31.5\mu\text{g/mL}$ and IC_{50} value was determined as $4.62 \mu\text{g/mL}$. The percentage inhibition of flavokawain B **LOB15** (compound 2) against DPPH radical showed inhibition activity ranging between $28.66 \pm 0.004\%$ to $92.68 \pm 0.002\%$ at concentration of $62.5 \mu\text{g/mL}$ and $\text{IC}_{50} = 8.5 \mu\text{g/mL}$ (Table 4.6, Figure 4.2). The percentage inhibition of (+)-onysilin **LOB4** (compound 3) against DPPH radical showed the inhibition activity ranging between 19.03 ± 0.02 to 64.15 ± 0.006 and $\text{IC}_{50} = 78.97 \mu\text{g/mL}$ (Table 4.7, Figure 4.3). The percentage inhibition of (+)-pinocembrin **LOB2** (compound 4) against DPPH showed the inhibition activity ranging between 25.14 ± 0.004 to 66.86 ± 0.02 and $\text{IC}_{50} = 41.32 \mu\text{g/mL}$ (Table 4.8, Figure 4.4). The percentage inhibition of linderone **LOB28** (compound 5) against DPPH radical showed the inhibition activity between 8.94 ± 0.02 to 52.88 ± 0.04 and $\text{IC}_{50} = 157.58 \mu\text{g/mL}$ (Table 4.9, Figure 4.5). The percentage inhibition of Linderone A **LOB25** (compound 6) against DPPH radical showed the inhibition activity ranging between 20.43 ± 0.007 to 55.76 ± 0.002 and $\text{IC}_{50} = 149.45 \mu\text{g/mL}$ (Table 4.10, Figure 4.6). The percentage inhibition of biseugenol C **LCB17** (compound 7) against DPPH radical showed the inhibition activity ranging between 38.47 ± 0.01 to 81.96 ± 0.01 and $\text{IC}_{50} = 16.34 \mu\text{g/mL}$ (Table 4.11, Figure 4.7). The percentage inhibition of 2, 5-dimethoxybenzaldehyde **LCB15** (compound 8) against DPPH radical showed the inhibition activity ranging between 8.75 ± 0.01 to 51.5 ± 0.01 $\text{IC}_{50} = 161.81 \mu\text{g/mL}$ (Table 4.12, Figure 4.8). The percentage inhibition of biseugenol B **LCB10** (compound 9) against DPPH radical showed the inhibition activity ranging between 12.15 ± 0.03 to 59.72 ± 0.03 and $\text{IC}_{50} = 81.92 \mu\text{g/mL}$ (Table 4.13, Figure 4.9). The percentage

inhibition of 2-hydroxy-5-methoxybenzaldehyde **LCB11** (compound 10) against DPPH radical showed the inhibition activity ranging between 3.93 ± 0.03 to 84.46 ± 0.003 $IC_{50} = 81.92 \mu\text{g/mL}$ (Table 4.14, Figure 4.10). The percentage inhibition of biseugenol A **LCB3** (compound 11) against DPPH radical showed the inhibition activity ranging between 54.52 ± 0.01 to 72.86 ± 0.01 and $IC_{50} = 4.77 \mu\text{g/mL}$ (Table 4.15, Figure 4.11). The percentage inhibition of 3, 4-dimethoxycinnamaldehyde **LCB7** (compound 12) against DPPH radical showed the inhibition activity range between 7.63 ± 0.01 to 65.27 ± 0.02 and $IC_{50} = 73.24 \mu\text{g/mL}$ (Table 4.16, Figure 4.12). The percentage inhibition of Litsin **LCB4** (compound 13) against DPPH radical showed the inhibition activity ranging between 16.45 ± 0.02 to 93.3 ± 0.003 and $IC_{50} = 26.69 \mu\text{g/mL}$ (Table 4.17, Figure 4.13). The percentage inhibition of Costalin **LCL7** (compound 14) against DPPH radical showed the inhibition activity ranging between 14.75 ± 0.003 to 69.75 ± 0.01 and $IC_{50} = 76.45$ (Table 4.18, Figure 4.14).

The results showed that biseugenol A **LCB3** with $IC_{50} = 4.77 \mu\text{g/mL}$, C **LCB17** $IC_{50} = 16.34 \mu\text{g/mL}$ and flavokawain B **LOB15** $IC_{50} = 8.5 \mu\text{g/mL}$ demonstrated very good radical scavenging activity using DPPH method compared to ascorbic acid with $IC_{50} = 4.62 \mu\text{g/mL}$. Biseugenol A showed comparable activity to that of ascorbic acid, thus it is suitable as a potential antioxidant.

The ability of neolignan and phenyl hydrazine to be better radical scavenger could be due to OH and NH groups to attached to the ring system. our results obtained from DPPH test validated some of previous studies on neolignan as antioxidant (Woo, S. L et al., 2004). Generally Flavonoid has better antioxidant activity than their corresponding chalcones in vitro antioxidant assays because of their strong capacity to donate electrons or hydrogen atoms.

4.7.2 Antioxidant of *Lindera* Species

From our literature review we have listed in (Table 4.3) some selected antioxidant preperitise of *Lindera* species, here again no investigation has been found on *Lindera oxyphylla*.

Table 4.3: Antioxidant of some selected chemicals in species of *Lindera*

No.	<i>Lindera</i> species	Antioxidant	RF
1	<i>Lindera pulcherrima</i> (Nee) Benth	Essential oil	(Joshi et al. 2012)
2	<i>Lindera strychnifolia</i>	Extracts	(Yan, Peng, et al. 2011)
3	<i>Lindera angustifolia</i> Chen	Alkaloids	(Zhao et al. 2006)

4.7.3 Antioxidant of *Litsea* Species

From our literature review we have listed in Table 4.4 some selected antioxidant preperitise of *Litsea* species, here again no investigation has been found on *Litsea costalis*.

Table 4.4: Antioxidant of some selected chemicals in species of *Litsea*

No.	<i>Litsea</i> species	Antioxidant	RF
1	<i>Litsea coreana</i> L	Loying tea	(Zhang et al 2000)
2	<i>Litsea monopetala</i>	Phenolic compounds	(Arfan et al. 2008)
3	<i>Litsea akoensis</i>	Essential oil	(Ho et al. 2011)
4	<i>Litsea cubeba</i>	Methanol extract	(Hwang et al. 2005)
5	<i>Litsea japonica</i>	Ethanol extract	(Yoon et al. 2010)

Table 4.5: DPPH radical scavenging activity **Ascorbic acid**

Concentration of Ascorbic acid ($\mu\text{g/mL}$)	Ascorbic acid at 517 nm			% Inhibition	STDV	Mean \pm SD	IC ₅₀ ($\mu\text{g/mL}$)
	1	2	3				
31.25	0.078	0.079	0.076	83.98	0.001	0.08 \pm 0.001	4.62
62.5	0.069	0.075	0.082	84.59	0.006	0.07 \pm 0.004	
125	0.06	0.054	0.05	88.91	0.005	0.05 \pm 0.003	
250	0.048	0.032	0.036	92.19	0.008	0.04 \pm 0.009	
500	0.034	0.028	0.025	94.04	0.004	0.03 \pm 0.003	
1000	0.027	0.02	0.017	95.68	0.005	0.02 \pm 0.003	

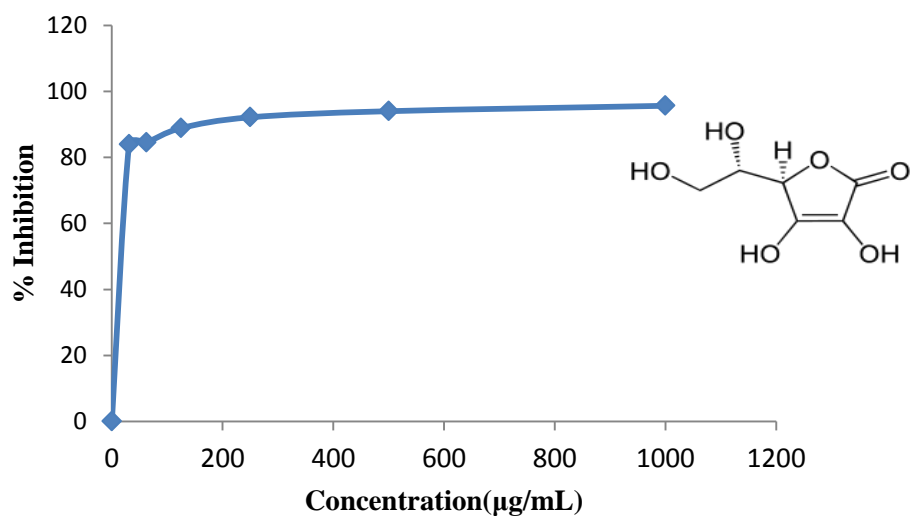
**Figure 4.1:** Graph of concentration ($\mu\text{g/mL}$) as % inhibition DPPH radical scavenging activity of Ascorbic Acid.

Table 4.6: DPPH radical scavenging activity of flavokawain B LOB15

Concentration of compound ($\mu\text{g/mL}$)	<u>Absorbance at 517 nm</u>			% Inhibition	STDV	Mean \pm SD	IC ₅₀ ($\mu\text{g/mL}$)
	1	2	3				
31.25	0.691	0.684	0.686	28.66	0.004	0.687 ± 0.002	
62.5	0.332	0.346	0.34	64.79	0.007	0.339 ± 0.004	8.5
125	0.165	0.148	0.159	0.009	82.3	0.157 ± 0.005	
250	0.087	0.072	0.078	91.1	0.007	0.079 ± 0.004	
500	0.07	0.065	0.068	92.45	0.002	0.07 ± 0.001	
1000	0.068	0.065	0.064	92.68	0.002	0.06 ± 0.001	

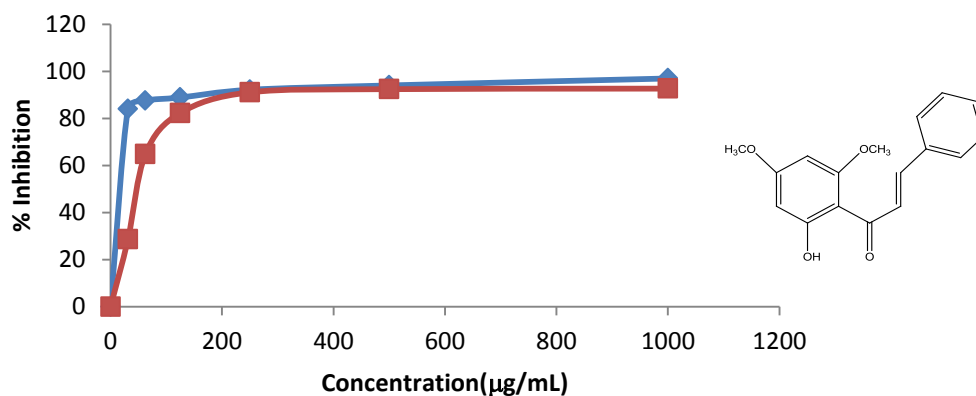
**Figure 4.2:** Graph of concentration ($\mu\text{g/mL}$) as % inhibition DPPH radical scavenging activity of Flavokawain B LOB15.

Table 4.7: DPPH radical scavenging activity of (+) -Onysilin **LOB4**

Concentration of compound ($\mu\text{g/mL}$)	Absorbance at 517 nm			% Inhibition	STDV	Mean \pm SD	IC ₅₀ ($\mu\text{g/mL}$)
	1	2	3				
31.25	0.67	0.7	0.670	19.03	0.02	0.7 ± 0.01	
62.5	0.551	0.550	0.587	34.19	0.05	0.6 ± 0.03	
125	0.486	0.420	0.443	47.23	0.03	0.4 ± 0.02	
250	0.465	0.412	0.413	49.47	0.03	0.4 ± 0.01	
500	0.423	0.398	0.387	52.76	0.003	0.4 ± 0.001	78.97
1000	0.320	0.307	0.288	64.15	0.006	0.3 ± 0.004	

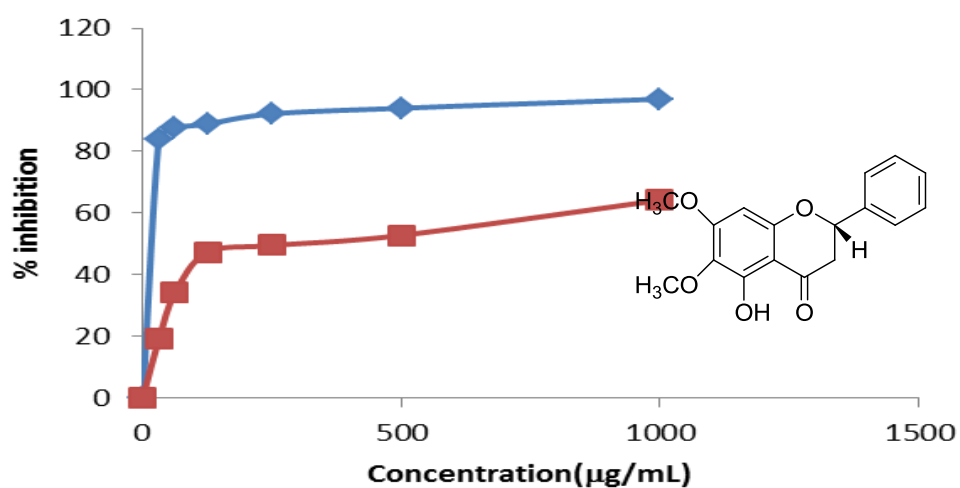


Figure 4.3: Graph of concentration ($\mu\text{g/mL}$) as % inhibition DPPH radical scavenging activity of (+)-Onysilin **LOB4**

Table 4.8: DPPH radical scavenging activity of (+)-Pinocembrin **LOB2**

Concentration of compound ($\mu\text{g/mL}$)	<u>Absorbance at 517 nm</u>			% Inhibition	STDV	Mean \pm SD	IC ₅₀ ($\mu\text{g/mL}$)
	1	2	3				
31.25	0.620	0.687	0.604	25.14	0.04	0.6 ± 0.02	
62.5	0.550	0.560	0.565	34.43	0.008	0.5 ± 0.004	
125	0.473	0.490	0.489	43.12	0.01	0.5 ± 0.005	
250	0.412	0.426	0.430	50.41	0.01	0.4 ± 0.005	41.32
500	0.324	0.312	0.350	61.45	0.02	0.3 ± 0.01	
1000	0.301	0.256	0.289	66.86	0.02	0.3 ± 0.01	

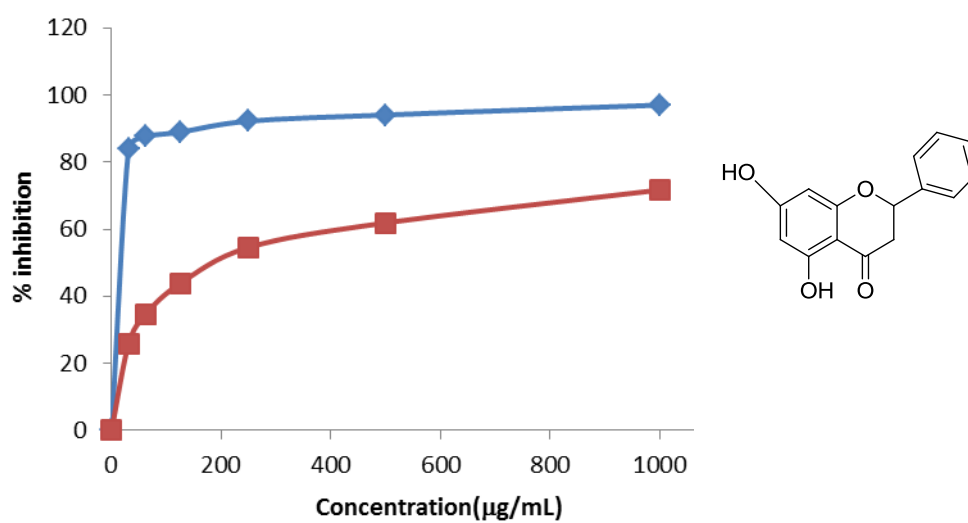
**Figure 4. 4:** Graph of concentration ($\mu\text{g/mL}$) as % inhibition DPPH radical scavenging activity of (+)-pinocembrin **LOB2**

Table 4.9: DPPH radical scavenging activity of Linderone **LOB28**

Concentration of compound ($\mu\text{g/mL}$)	<u>Absorbance at 517 nm</u>			% Inhibition	STDV	Mean \pm SD	IC ₅₀ ($\mu\text{g/mL}$)
	1	2	3				
31.25	0.970	0.923	0.950	8.94	0.02	0.9 ± 0.01	
62.5	0.868	0.819	0.83	19.23	0.02	0.8 ± 0.01	
125	0.815	0.771	0.8	23.26	0.02	0.8 ± 0.01	
250	0.742	0.667	0.752	30.76	0.05	0.7 ± 0.03	
500	0.604	0.597	0.611	41.92	0.007	0.6 ± 0.004	
1000	0.450	0.521	0.5	52.88	0.04	0.5 ± 0.02	157.58

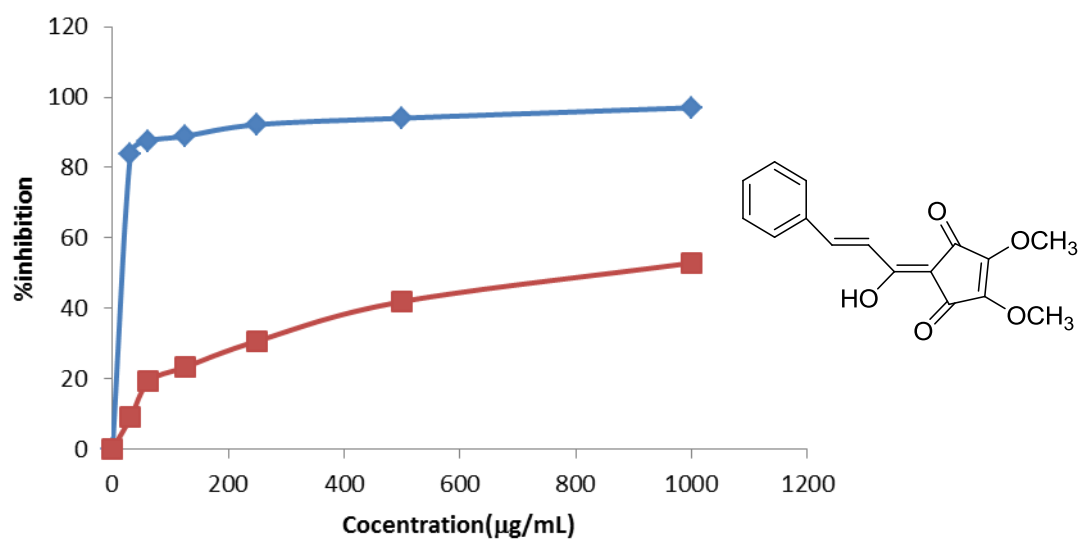
**Figure 4.5:** Graph of concentration ($\mu\text{g/mL}$) as % inhibition DPPH radical scavenging activity of Linderone **LOB28**.

Table 4.10: DPPH radical scavenging activity of Linderone A **LOB25**

Concentration of compound ($\mu\text{g/mL}$)	Absorbance at 517 nm			% Inhibition	STDV	Mean \pm SD	IC ₅₀ ($\mu\text{g/mL}$)
	1	2	3				
31.25	0.549	0.537	0.550	20.43	0.007	0.5 ± 0.004	
62.5	0.485	0.536	0.568	22.77	0.004	0.5 ± 0.02	
125	0.431	0.451	0.448	35.32	0.01	0.4 ± 0.006	
250	0.35	0.414	0.389	43.94	0.03	0.4 ± 0.02	
500	0.311	0.387	0.379	47.59	0.03	0.4 ± 0.02	
1000	0.278	0.308	0.324	55.76	0.02	0.3 ± 0.01	149.45

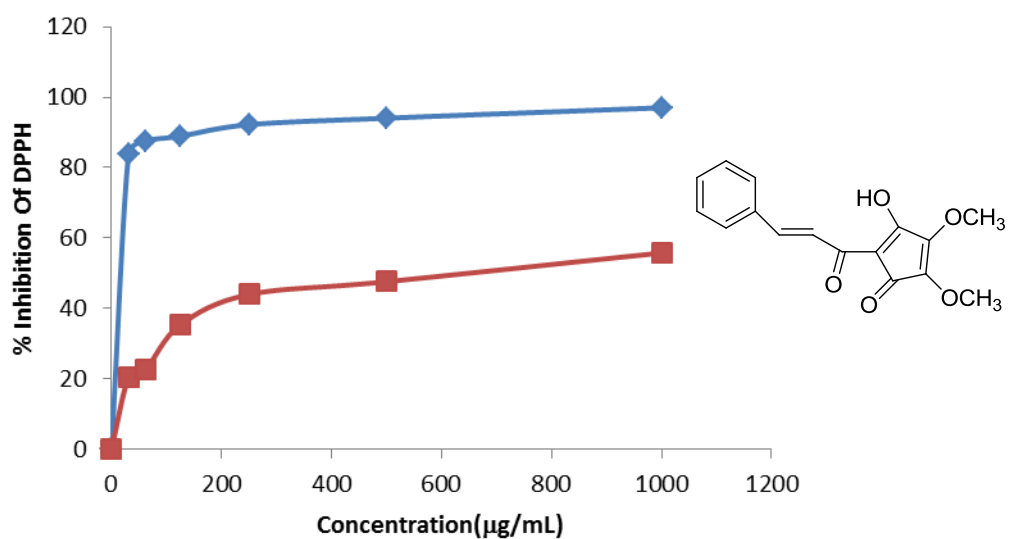


Figure 4. 6: Graph of concentration ($\mu\text{g/mL}$) as % inhibition DPPH radical scavenging activity of Linderone A **LOB25**.

Table 4.11: DPPH radical scavenging activity of biseugenol C LCB17

Concentration of compound ($\mu\text{g/mL}$)	<u>Absorbance at 517 nm</u>			% Inhibition	STDV	Mean \pm SD	IC ₅₀ ($\mu\text{g/mL}$)
	1	2	3				
31.25	0.322	0.299	0.301	38.47	0.011	0.3 ± 0.007	
62.5	0.223	0.282	0.253	49.49	0.03	0.3 ± 0.02	
125	0.180	0.170	0.195	63.72	0.01	0.2 ± 0.007	16.34
250	0.221	0.125	0.187	64.52	0.05	0.2 ± 0.03	
500	0.118	0.105	0.11	77.95	0.006	0.1 ± 0.004	
1000	0.09	0.08	0.101	81.96	0.01	0.1 ± 0.006	

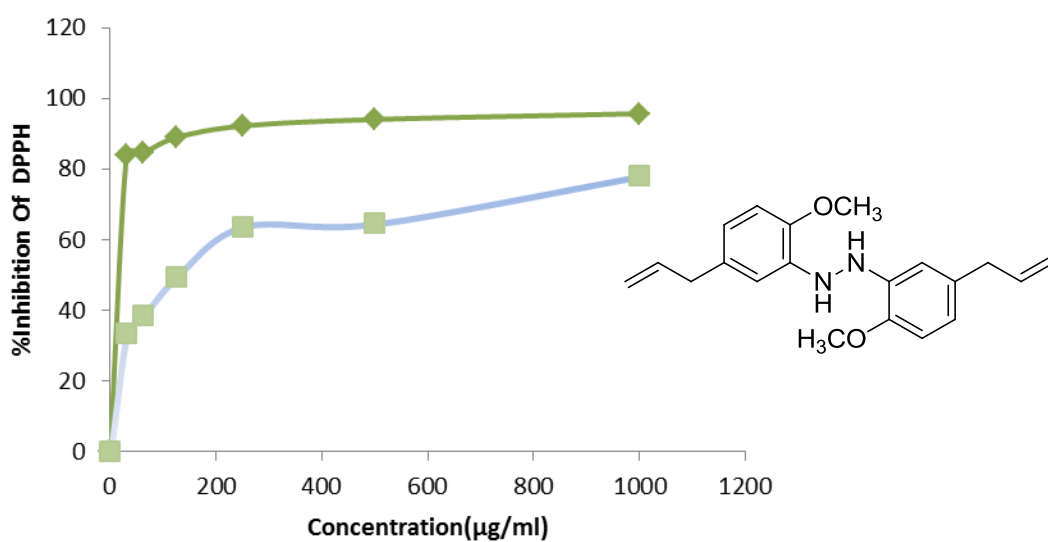
**Figure 4.7: Graph of concentration ($\mu\text{g/mL}$) as % inhibition DPPH radical scavenging activity of Biseugenol C LCB17.**

Table 4.12: DPPH radical scavenging activity of 2, 5-Dimethoxybenzaldehyde **LCB15**

Concentration of compound ($\mu\text{g/mL}$)	Absorbance at 517 nm			% Inhibition	STD V	Mean \pm SD	IC ₅₀ ($\mu\text{g/mL}$)
	1	2	3				
31.25	0.355	0.368	0.373	8.75	0.01	0.365 \pm 0.005	
62.5	0.309	0.397	0.345	12.5	0.04	0.350 \pm 0.03	
125	0.272	0.299	0.354	23	0.04	0.308 \pm 0.02	
250	0.250	0.280	0.291	31.75	0.02	0.273 \pm 0.01	
500	0.233	0.243	0.225	41.75	0.009	0.233 \pm 0.005	
1000	0.202	0.198	0.183	51.5	0.01	0.194 \pm 0.006	161.81

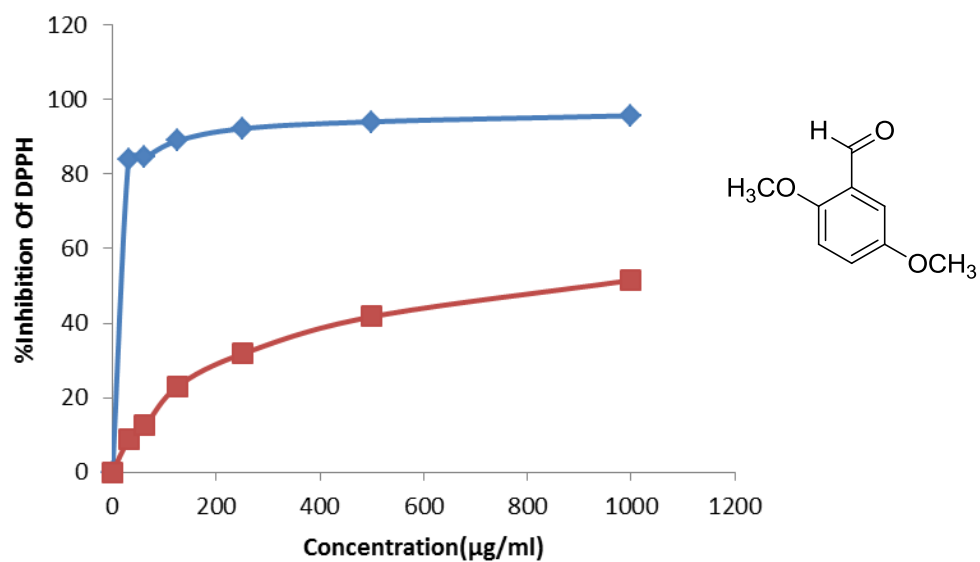
**Figure 4. 8:** Graph of concentration ($\mu\text{g/mL}$) as % inhibition DPPH radical scavenging activity of 2,5-Dimethoxybenzaldehyde **LCB15**.

Table 4.13: DPPH radical scavenging activity of biseugenol B LCB10

Concentration of compound ($\mu\text{g/mL}$)	Absorbance at 517 nm			% Inhibition	STDV	Mean \pm SD	IC ₅₀ ($\mu\text{g/mL}$)
	1	2	3				
31.25	0.480	0.538	0.50	12.15	0.03	0.5 \pm 0.02	
62.5	0.481	0.520	0.490	13.71	0.02	0.5 \pm 0.01	
125	0.513	0.427	0.453	19.44	0.04	0.5 \pm 0.02	
250	0.404	0.427	0.411	28.12	0.01	0.4 \pm 0.007	
500	0.299	0.250	0.301	50.86	0.03	0.3 \pm 0.02	81.92
1000	0.253	0.245	0.199	59.72	0.03	0.2 \pm 0.02	

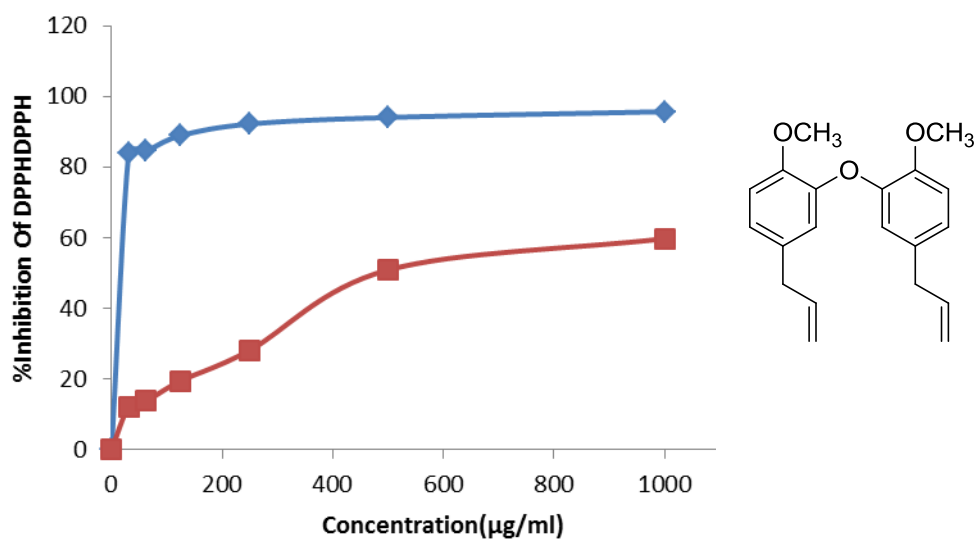
**Figure 4.9:** Graph of concentration ($\mu\text{g/mL}$) as % inhibition DPPH radical scavenging activity of Biseugenol B LCB10.

Table 4.14: DPPH radical scavenging activity of 2-hydroxy-5-methoxybenzaldehyde LCB11

Concentration of compound ($\mu\text{g/mL}$)	Absorbance at 517 nm			% Inhibition	STDV	Mean \pm SD	IC ₅₀ ($\mu\text{g/mL}$)
	1	2	3				
31.25	0.517	0.586	0.551	3.93	0.03	0.6 ± 0.02	
62.5	0.520	0.510	0.515	10.11	0.005	0.5 ± 0.003	
125	0.465	0.394	0.429	25.11	0.03	0.4 ± 0.02	
250	0.394	0.389	0.385	32.11	0.03	0.4 ± 0.01	
500	0.295	0.226	0.245	55.49	0.03	0.2 ± 0.02	81.92
1000	0.088	0.086	0.093	84.46	0.003	0.09 ± 0.002	

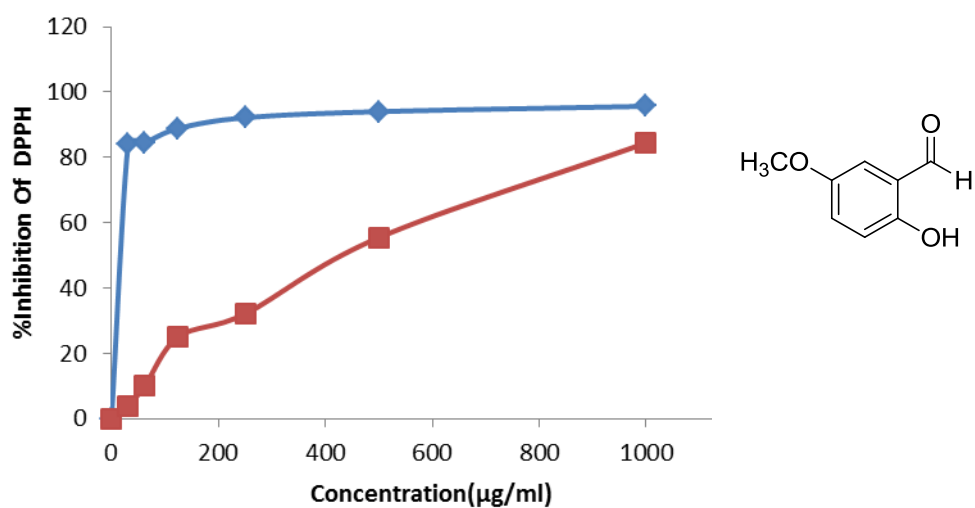


Figure 4.10: Graph of concentration ($\mu\text{g/mL}$) as % inhibition DPPH radical scavenging activity of 2-hydroxy-5-dimethoxybenzaldehyde LCB11.

Table 4.15: DPPH radical scavenging activity of biseugenol A **LCB3**

Concentration of compound ($\mu\text{g/mL}$)	Absorbance at 517 nm			% Inhibition	STDV	Mean \pm SD	IC ₅₀ ($\mu\text{g/mL}$)
	1	2	3				
31.25	0.177	0.198	0.185	54.52	0.01	0.2 \pm 0.006	4.77
62.5	0.160	0.163	0.159	60.88	0.002	0.2 \pm 0.001	
125	0.133	0.145	0.150	64.54	0.01	0.1 \pm 0.007	
250	0.142	0.140	0.138	65.77	0.002	0.1 \pm 0.001	
500	0.117	0.128	0.112	70.9	0.008	0.1 \pm 0.004	
1000	0.122	0.102	0.111	72.86	0.01	0.1 \pm 0.006	

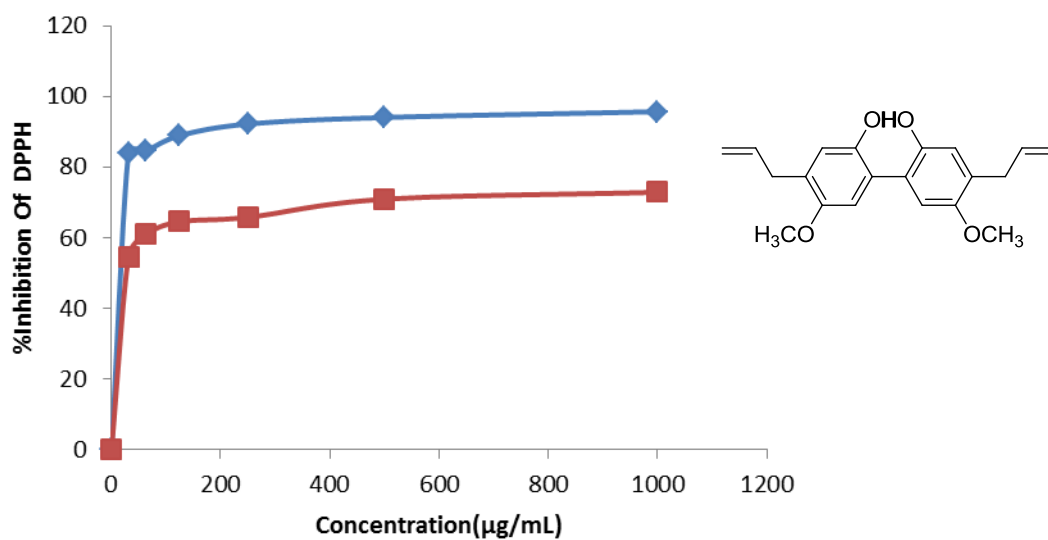


Figure 4.11: Graph of concentration ($\mu\text{g/mL}$) as % inhibition DPPH radical scavenging activity of Biseugenol A **LCB3**.

Table 4.16: DPPH radical scavenging activity of Cinnamaldehyde **LCB7**

Concentration of compound ($\mu\text{g/mL}$)	<u>Absorbance at 517 nm</u>			% Inhibition	STDV	Mean \pm SD	IC ₅₀ ($\mu\text{g/mL}$)
	1	2	3				
31.25	0.375	0.379	0.371	7.63	0.01	0.4 \pm 0.006	
62.5	0.398	0.321	0.354	12.06	0.004	0.4 \pm 0.002	
125	0.331	0.336	0.325	18.71	0.005	0.3 \pm 0.003	
250	0.3	0.245	0.286	31.77	0.03	0.3 \pm 0.02	
500	0.173	0.188	0.165	56.89	0.01	0.2 \pm 0.007	73.24
1000	0.154	0.148	0.122	65.27	0.02	0.1 \pm 0.01	

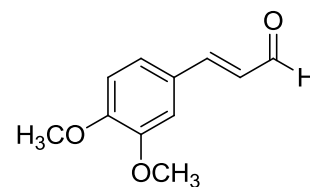
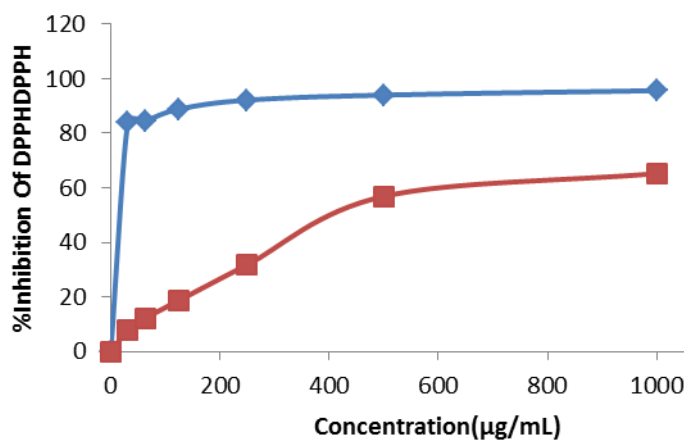
**Figure 4.12:** Graph of concentration ($\mu\text{g/mL}$) as % inhibition DPPH radical scavenging activity of Cinnamaldehyde **LCB7**.

Table 4.17: DPPH radical scavenging activity of Litsin **LCB4**

Concentration of compound ($\mu\text{g/mL}$)	<u>Absorbance at 517 nm</u>			% Inhibition	STDV	Mean \pm SD	IC ₅₀ ($\mu\text{g/mL}$)
	1	2	3				
31.25	0.887	0.864	0.853	16.45	0.02	0.9 \pm 0.01	
62.5	0.756	0.763	0.745	26.79	0.009	0.7 \pm 0.005	
125	0.517	0.590	0.555	46.21	0.04	0.5 \pm 0.02	
250	0.229	0.211	0.239	78.05	0.01	0.2 \pm 0.008	26.69
500	0.087	0.108	0.093	90.67	0.01	0.1 \pm 0.006	
1000	0.068	0.067	0.073	93.30	0.003	0.07 \pm 0.002	

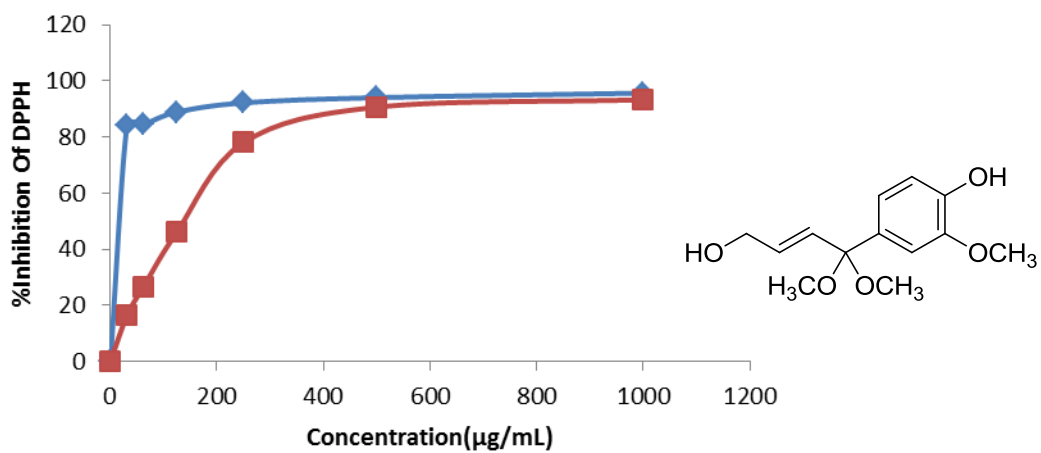
**Figure 4.13:** Graph of concentration ($\mu\text{g/mL}$) as % inhibition DPPH radical scavenging activity of Litsin **LCB4**.

Table 4.18: DPPH radical scavenging activity of Costalin **LCL7**

Concentration of compound ($\mu\text{g/mL}$)	<u>Absorbance at 517 nm</u>			% Inhibition	STDV	Mean \pm SD	IC ₅₀ ($\mu\text{g/mL}$)
	1	2	3				
31.25	0.367	0.311	0.345	14.75	0.003	0.3 \pm 0.02	
62.5	0.321	0.301	0.298	23.5	0.01	0.3 \pm 0.007	
125	0.258	0.273	0.296	31.25	0.02	0.3 \pm 0.01	
250	0.211	0.198	0.235	46.5	0.02	0.2 \pm 0.01	
500	0.188	0.176	0.184	54.5	0.006	0.2 \pm 0.003	76.45
1000	0.109	0.121	0.134	69.75	0.01	0.1 \pm 0.007	

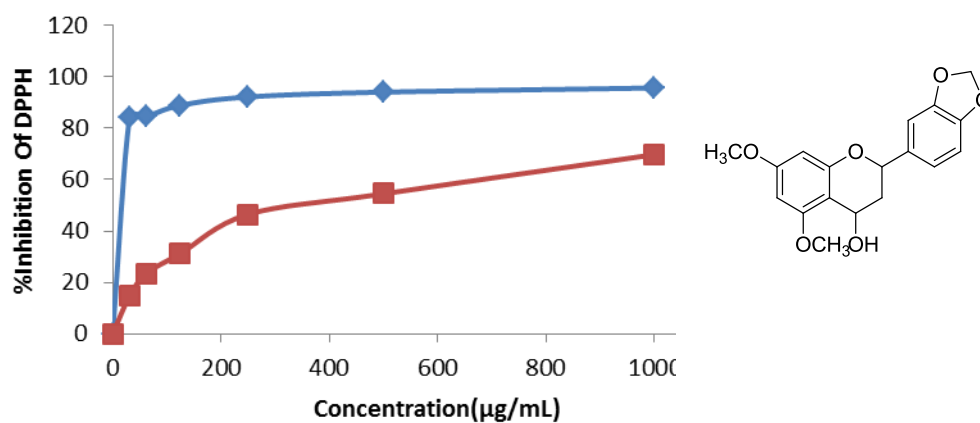


Figure 4.14: Graph of concentration ($\mu\text{g/mL}$) as % inhibition DPPH radical scavenging activity of Costalin **LCL7**.

4.7.4 FRAP (Ferric Reducing Power Assay)

The antioxidant activities of compounds from *Lindera oxyphylla* and *Litsea costalis* were determined by using reducing power assay. The reaction mixtures turned from yellow to green and Perl's Prussian blue complex and it depending on the reducing power of each compounds used. The absorbance reading at 700 nm was taken. This assay was carried out in triplicates and average reading was recorded.

BHA (compound 1) (Table 4. 19, Figure 4. 15) showed the absorbance 1.0 ± 0.05 at concentration of 1000 $\mu\text{g/mL}$. Flavokawain B **LOB15** (compound 2) ,(Table 4.20, Figure 4. 16) showed the absorbance 1.0 ± 0.06 at concentration of 1000 $\mu\text{g/mL}$. (+)-Pinocembrin **LOB2** (compound 3), (Table 4.21, Figure 4.17) showed the absorbance 0.7 ± 0.02 at concentration of 1000 $\mu\text{g/mL}$. (+)-Onysilin **LOB4** (compound 4), (Table 4.22, Figure 4.18) showed the absorbance 0.6 ± 0.01 at concentration of 1000 $\mu\text{g/mL}$. Linderone **LOB28** (compound 5) ,(Table 4.23, Figure 4. 19) showed the absorbance 0.6 ± 0.02 at concentration of 1000 $\mu\text{g/mL}$. Linderone A **LOB25** (compound 6), (Table 4.24 , Figure 4.20) showed the absorbance 0.6 ± 0.03 at concentration of 1000 $\mu\text{g/mL}$.

The results showed that flavokawain B **LOB15** the absorbance 1.0 ± 0.06 , demonstrated very good FRAP method compared to BHA showed the absorbance 1.0 ± 0.05

Flavonoid has better antioxidant activity than their corresponding chalcones in vitro antioxidant assays because of their strong capacity to donate electrons or hydrogen atoms.

Table 4.19: FRAP of **BHA** standard

Concentration of BHA ($\mu\text{g/mL}$)	Absorbance at 700 nm			STDV	Mean \pm SD
	1	2	3		
15.62	0.594	0.733	0.662	0.069	0.7 ± 0.04
31.25	0.645	0.687	0.728	0.041	0.7 ± 0.02
62.5	0.689	0.723	0.786	0.05	0.7 ± 0.03
125	0.754	0.826	0.787	0.036	0.8 ± 0.02
250	0.865	0.898	0.923	0.03	0.9 ± 0.02
500	1.083	0.925	0.987	0.08	1.0 ± 0.05
1000	1.11	1.16	0.987	0.09	1.0 ± 0.05

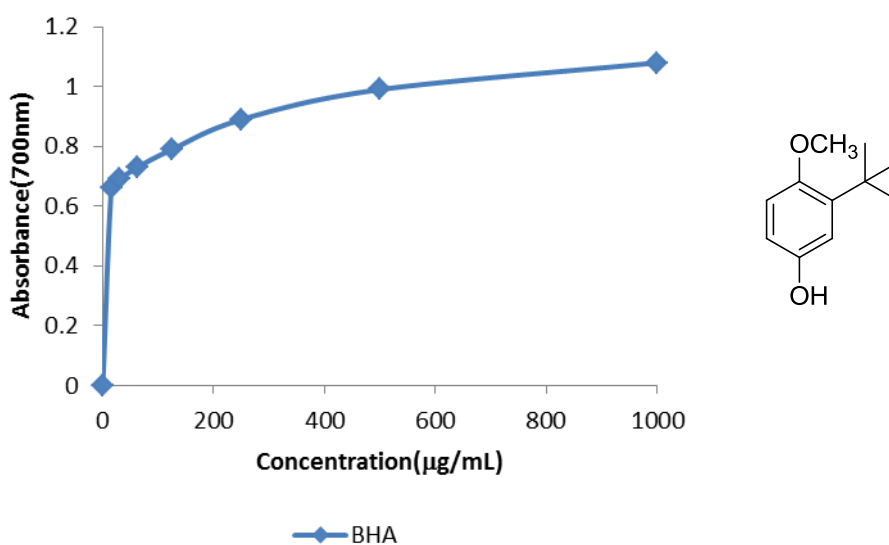


Figure 4.15: Absorbance of BHA standard

Table 4.20: FRAP of flavokawain B LOB25

Concentration of compound ($\mu\text{g/mL}$)	Absorbance at 700 nm			STDV	Mean \pm SD
	1	2	3		
15.62	0.401	0.398	0.415	0.01	0.4 ± 0.005
31.25	0.446	0.414	0.422	0.017	0.4 ± 0.01
62.5	0.468	0.419	0.453	0.025	0.4 ± 0.01
125	0.541	0.655	0.648	0.063	0.6 ± 0.04
250	0.795	0.757	0.762	0.02	0.8 ± 0.01
500	0.798	0.812	0.856	0.03	0.8 ± 0.01
1000	1.121	0.978	0.912	0.1	1.0 ± 0.06

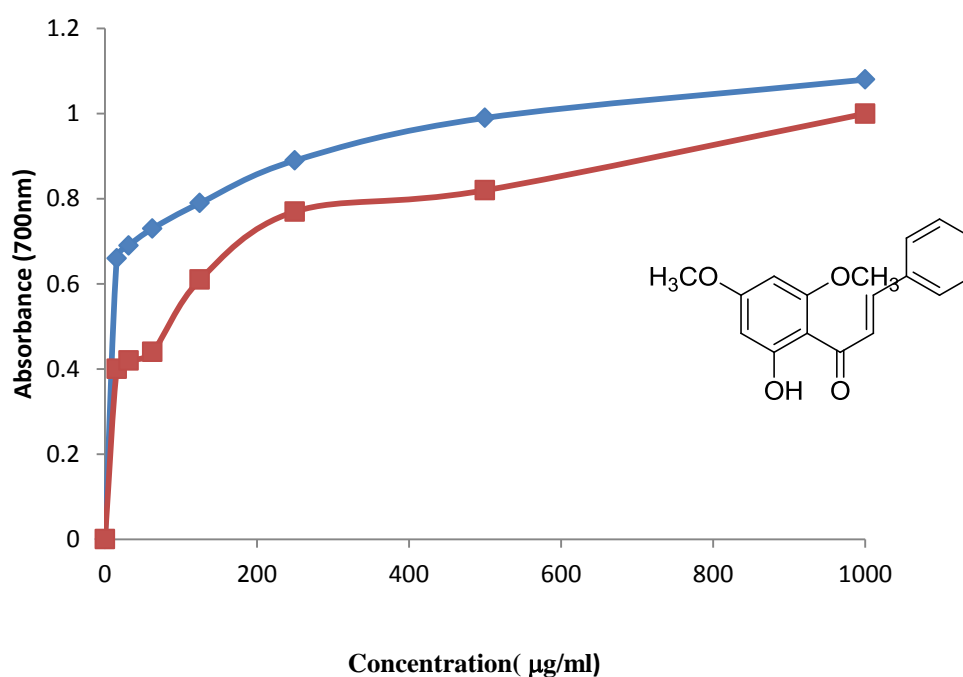
**Figure 4.16:** Absorbance of flavokawain B LOB25

Table 4.21: FRAP of (+)-Pinocembrin **LOB2**

Concentration of compound ($\mu\text{g/mL}$)	Absorbance at 700 nm			STDV	Mean \pm SD
	1	2	3		
15.62	0.312	0.345	0.338	0.03	0.3 ± 0.01
31.25	0.380	0.326	0.373	0.03	0.3 ± 0.02
62.5	0.450	0.383	0.401	0.03	0.4 ± 0.02
125	0.527	0.424	0.498	0.05	0.5 ± 0.03
250	0.504	0.521	0.513	0.008	0.5 ± 0.005
500	0.564	0.589	0.612	0.024	0.6 ± 0.01
1000	0.645	0.678	0.713	0.03	0.7 ± 0.02

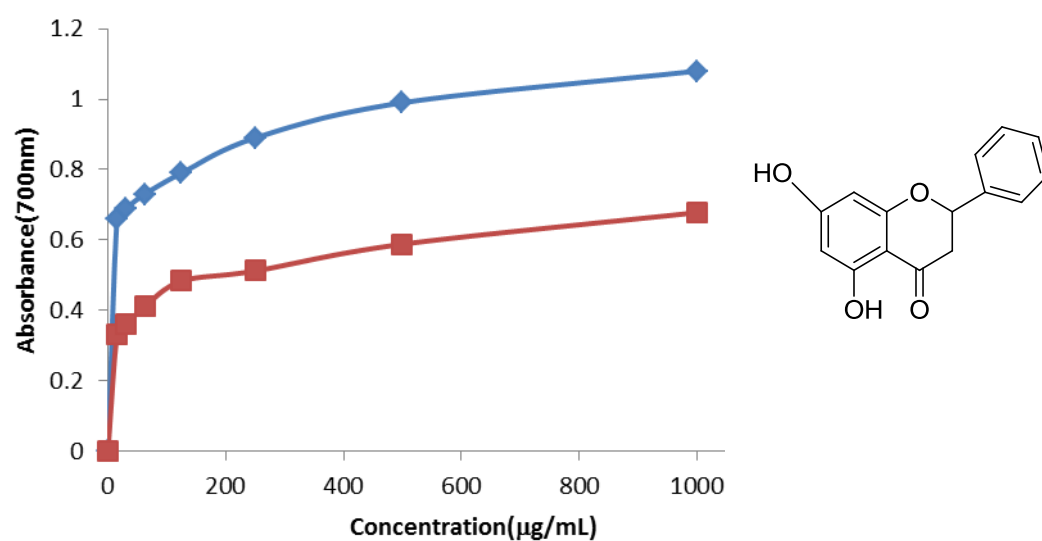


Figure 4.17: Absorbance of (+)-Pinocembrin **LOB2**

Table 4.22: FRAP of (+)- Onysilin LOB4

Concentration of compound ($\mu\text{g/mL}$)	Absorbance at 700 nm			STDV	Mean \pm SD
	1	2	3		
15.52	0.310	0.324	0.335	0.01	0.323 ± 0.001
31.25	0.3	0.352	0.343	0.02	0.335 ± 0.012
61.5	0.352	0.365	0.378	0.01	0.365 ± 0.008
125	0.405	0.432	0.478	0.02	0.438 ± 0.02
250	0.425	0.453	0.489	0.03	0.455 ± 0.02
500	0.463	0.502	0.545	0.02	0.56 ± 0.02
1000	0.523	0.547	0.669	0.02	0.6 ± 0.01

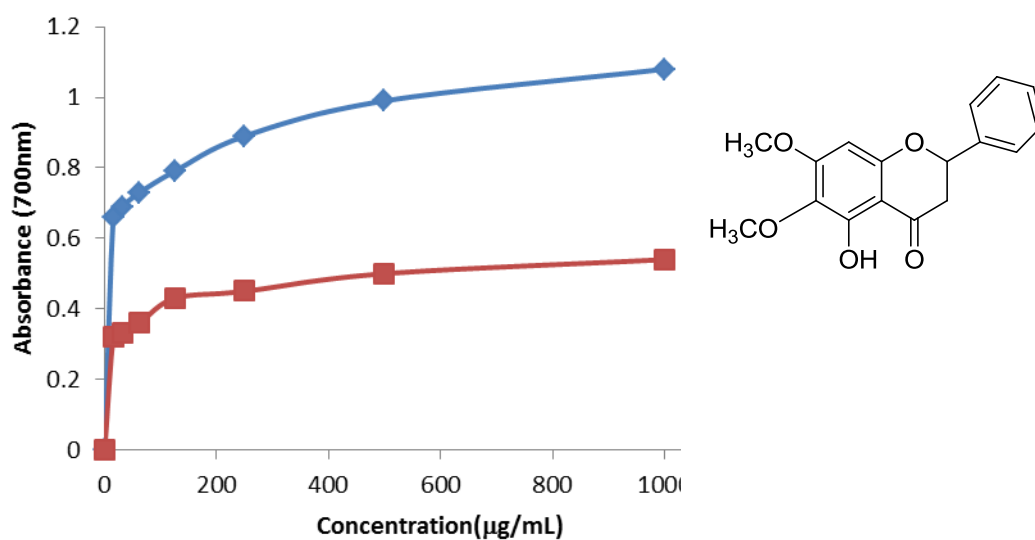


Figure 4.18: Absorbance of (+)- Onysilin LOB4

Table 4.23: FRAP of Linderone **LOB28**

Concentration of compound ($\mu\text{g/mL}$)	Absorbance at 700 nm			STDV	Mean \pm SD
	1	2	3		
15.62	0.3	0.301	0.312	0.01	0.304 ± 0.005
31.25	0.345	0.325	0.333	0.006	0.334 ± 0.003
62.5	0.375	0.320	0.355	0.03	0.35 ± 0.016
125	0.387	0.372	0.385	0.008	0.381 ± 0.005
250	0.419	0.369	0.401	0.02	0.396 ± 0.014
500	0.462	0.491	0.555	0.05	0.502 ± 0.027
1000	0.534	0.564	0.601	0.03	0.566 ± 0.02

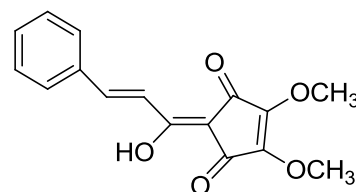
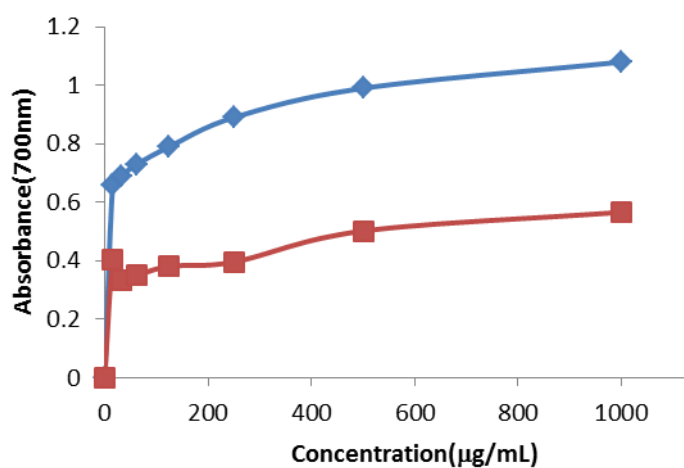
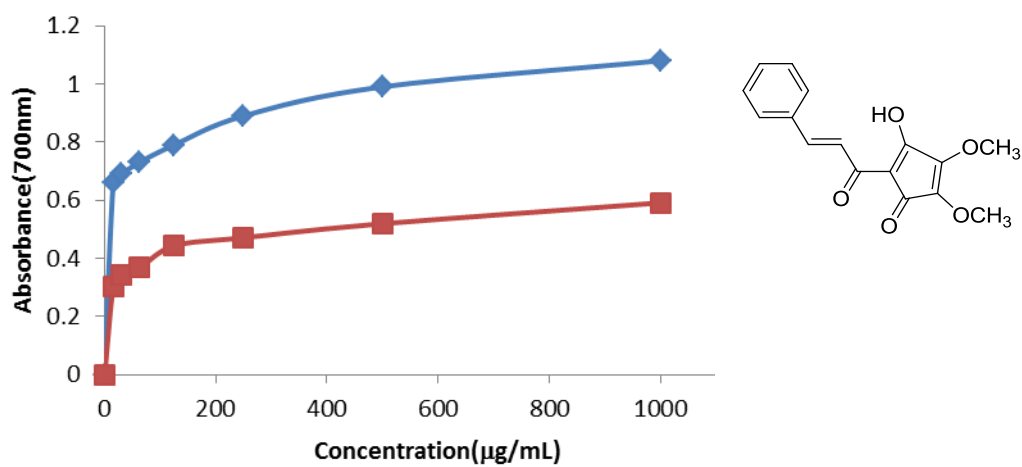
**Figure 4.19:** Absorbance of Linderone **LOB28**

Table 4.24: FRAP of Linderone A LOB25

Concentration of compound ($\mu\text{g/mL}$)	<u>Absorbance at 700 nm</u>			STDV	Mean \pm SD
	1	2	3		
15.62	0.3	0.301	0.312	0.01	0.304 ± 0.005
31.25	0.350	0.341	0.338	0.006	0.343 ± 0.003
62.5	0.363	0.355	0.383	0.01	0.367 ± 0.008
125	0.401	0.447	0.483	0.04	0.443 ± 0.02
250	0.437	0.478	0.498	0.03	0.471 ± 0.02
500	0.474	0.494	0.589	0.06	0.519 ± 0.03
1000	0.543	0.598	0.634	0.04	0.591 ± 0.03

**Figure 4. 20: Absorbance of Linderone A LOB25**

4.7.5 Metal Chelating Assay

The antioxidant activities of compounds from *Lindera oxyphylla* and *Litsea costalis* were determined using metal chelating assay. It was based on the chelating effect of Fe^{2+} ions by ferrozine reagent. Antioxidant from the test samples disturbed the formation of ferrozine- Fe^{2+} complexes. The colour intensity of the reaction mixtures reduced. As the concentration of the samples and standard increased, the metal chelating activity increased. This assay was also carried out in triplicates and the average reading was recorded.

Ethylenediaminetetraacetic acid (EDTA) was used as the standard in the metal chelating assay. At the concentration 1000 $\mu\text{g/mL}$ of EDTA (Table 4.25, Figure 4.21) the chelating activity was 99.08 ± 0.007 . All of the tested compounds showed chelating activity less than 50% when it was tested at various concentrations of 61.5-1000 $\mu\text{g/mL}$. The chelating activity for flavokawain B **LOB15** (Table 4.26, Figure 4.22), (+)-pinocembrin **LOB2** (Table 4.27, Figure 4.23), (+)-onysilin **LOB4** (Table 4.28, Figure 4.24), linderone **LOB28** (Table 4.29, Figure 4.25) and linderone A **LOB25** (Table 4.30, Figure 4.26) were 33.37 ± 0.01 , 26.11 ± 0.01 , $25.69 \pm 0.01\%$, 13.09 ± 0.006 and 13.51 ± 0.01 , respectively.

In this study, the purple colour of reaction solutions did not change much in the presence of all compounds and their percentages of metal ion chelating effect were lower than the standard control EDTA. EDTA is a strong metal chelator (Gülçin, Berasvili & Gepdiremen, 2005), hence, it was used as standard metal chelator agent in this study.

Table 4.25: Metal Chelating Assay of EDTA

Concentration EDTA ($\mu\text{g/mL}$)	Absorbance at 517 nm			Metal chelate effect (%)	STDV	Mean \pm SD
	1	2	3			
62.5	0.141	0.094	0.107	95.26	0.02	0.114 \pm 0.01
125	0.055	0.062	0.06	97.54	0.003	0.06 \pm 0.002
250	0.063	0.053	0.047	97.75	0.008	0.05 \pm 0.005
500	0.043	0.031	0.049	98.29	0.009	0.041 \pm 0.005
1000	0.034	0.011	0.021	99.08	0.01	0.022 \pm 0.007

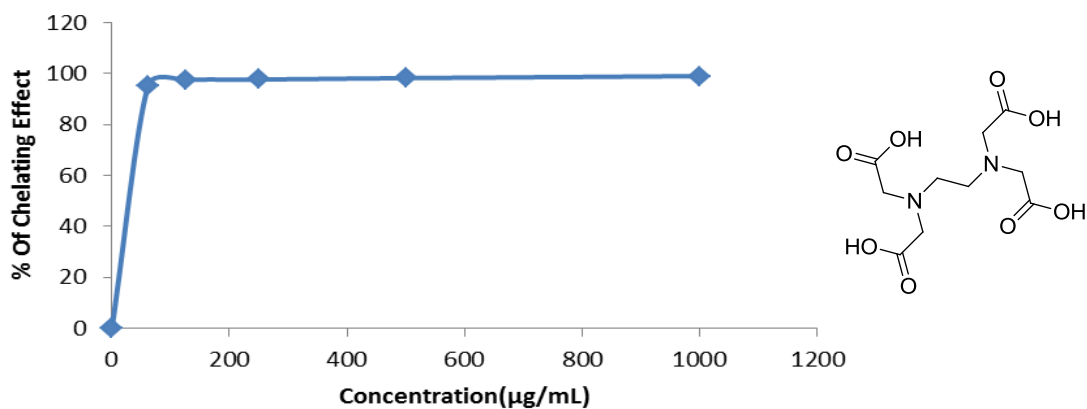
**Figure 4.21: % Chelating activity of EDTA**

Table 4.26: Metal Chelating Assay of flavokawain B **LOB15**

Concentration of compound ($\mu\text{g/mL}$)	<u>Absorbance at 517 nm</u>			Metal chelate effect (%)	STDV	Mean \pm SD
	1	2	3			
125	2.279	2.288	2.301	4.2	0.01	2.289 ± 0.006
250	2.109	2.123	2.112	11.25	0.007	2.114 ± 0.004
500	2.098	1.897	1.965	16.87	0.1	1.986 ± 0.06
1000	1.43	1.567	1.765	33.37	0.2	1.587 ± 0.1

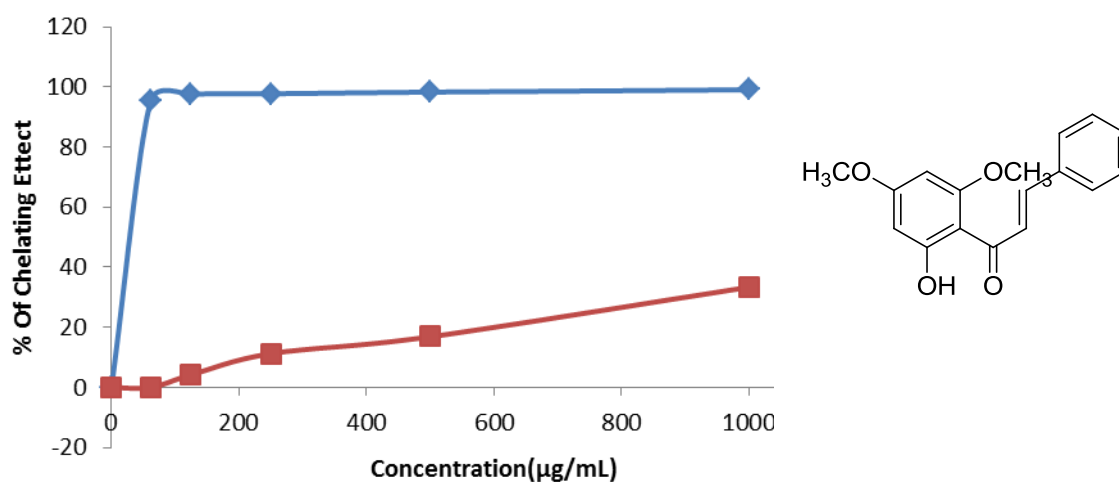
**Figure 4.22:** % Chelating activity of flavokawain B **LOB15**

Table 4.27: Metal Chelating Assay of (+)-Pinocenbrin LOB2

Concentration of compound ($\mu\text{g/mL}$)	Absorbance at 517 nm			Metal chelate effect (%)	STDV	Mean \pm SD
	1	2	3			
125	2.345	2.232	2.211	3.4	0.07	2.262 \pm 0.04
250	2.243	2.257	2.276	10.7	0.02	2.258 \pm 0.01
500	2.234	2.211	2.225	20.56	0.01	2.223 \pm 0.007
1000	2.163	2.139	2.129	26.11	0.02	2.142 \pm 0.01

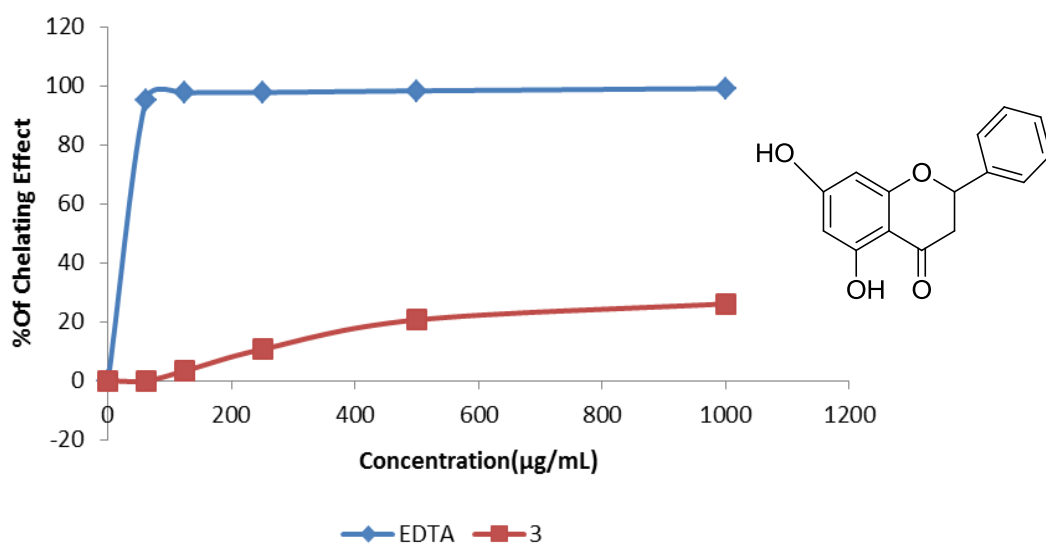
**Figure 4.23: % Chelating activity of (+)-Pinocenbrin LOB2**

Table 4.28: Metal Chelating Assay of (+)-Onysilin **LOB4**

Concentration of compound ($\mu\text{g/mL}$)	<u>Absorbance at 517 nm</u>			Metal chelate effect (%)	STDV	Mean \pm SD
	1	2	3			
125	2.332	2.289	2.291	5.03	0.02	2.301 ± 0.01
250	2.253	2.278	2.229	10.07	0.02	2.253 ± 0.01
500	2.247	2.217	2.223	20.02	0.01	2.229 ± 0.009
1000	2.187	2.153	2.142	25.69	0.02	2.16 ± 0.01

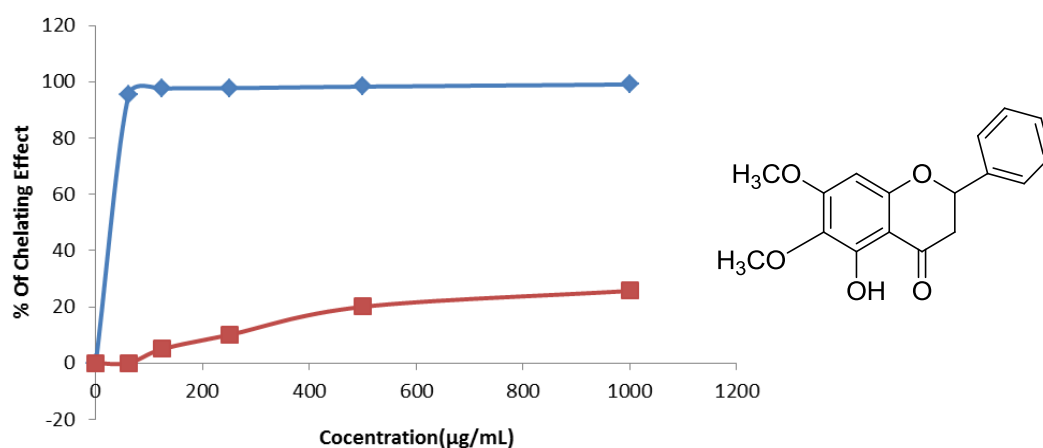
**Figure 4.24:** % Chelating activity of (+)-Onysilin **LOB4**

Table 4.29: Metal Chelating Assay of Linderone LOB28

Concentration of compound ($\mu\text{g/mL}$)	<u>Absorbance at 517 nm</u>			Metal chelate effect (%)	STDV	Mean \pm SD
	1	2	3			
125	2.323	2.309	2.287	3.19	0.01	2.366 \pm 0.01
250	2.253	2.294	2.268	4.65	0.02	2.271 \pm 0.01
500	2.189	2.162	2.148	9.06	0.02	2.166 \pm 0.01
1000	2.065	2.039	2.084	13.51	0.02	2.062 \pm 0.01

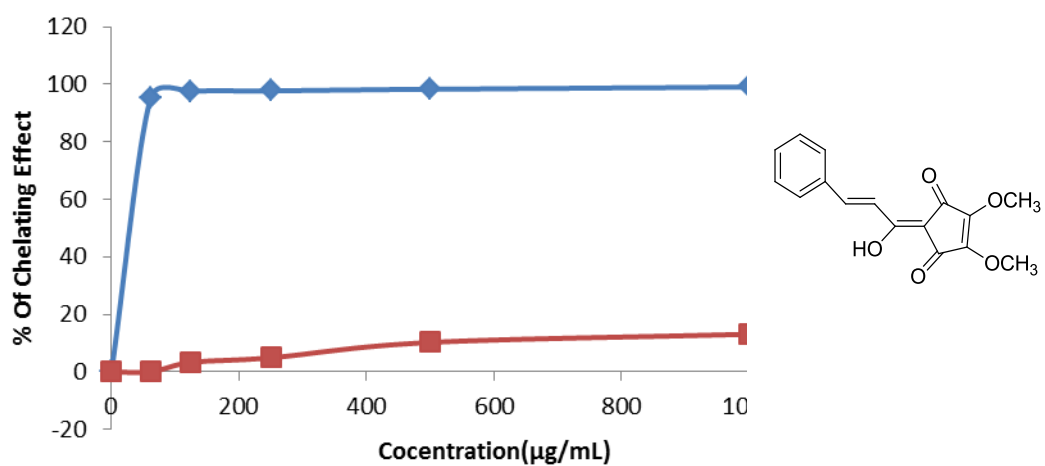
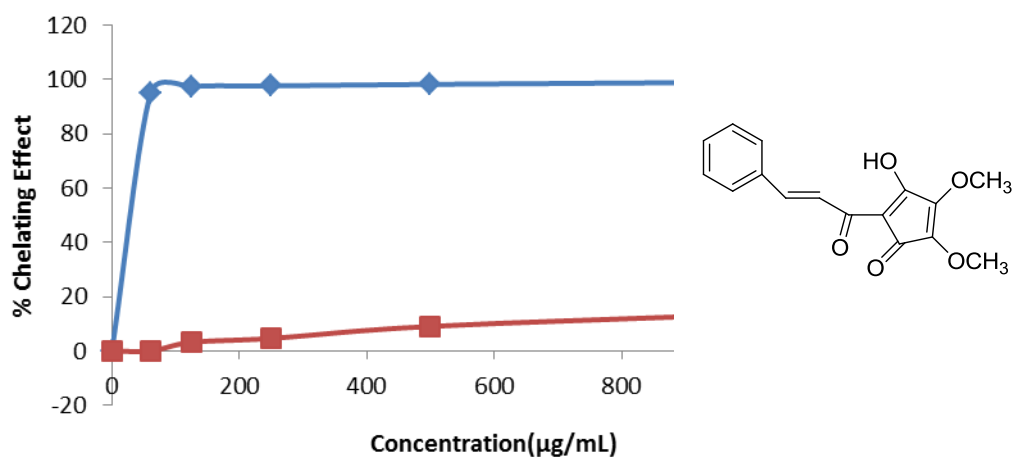


Figure 4. 25: % Chelating activity of Linderone LOB28

Table 4.30: Metal Chelating Assay of Linderone A LOB25

Concentration of compound ($\mu\text{g/mL}$)	Absorbance at 517 nm			Metal chelate effect (%)	STDV	Mean \pm SD
	1	2	3			
125	2.302	2.312	2.297	3.31	0.008	2.303 \pm 0.004
250	2.278	2.256	2.263	4.91	0.01	2.265 \pm 0.006
500	2.165	2.142	2.109	10.24	0.03	2.138 \pm 0.02
1000	2.065	2.087	2.074	13.09	0.01	2.075 \pm 0.006

**Figure 4. 26: % Chelating activity of Linderone A LOB2**

4.8 Anticancer: Cytotoxicity Activity

Cancer is a wide group of several diseases. In cancer, cells divide and grow wildly, and invade nearby parts cells of the body. The cancer may also spread to more distant parts of the body through the lymphatic system or blood stream. do not all tumors are cancerous. Benign tumors do not grow uncontrollably, do not invade neighboring tissues, and do not spread throughout the body. Cancer is the second leading cause of death among children between the ages of one to fourteen and it is also responsible for 25% of all deaths today (Jemal et al. 2005). There were 10.9 million new cancer cases diagnosed in USA and 6.7 million deaths in 2002 (Tan et al., 2006). Seventy-seven percent of all the cancers diagnosed were observed in people aged 55 years or older ("Cancer facts and figures," 2002). These figures show that the death toll from cancer is going to increase with the aging of US population. In spite of the availability of a large number of anticancer drugs and various chemotherapy options, there is still an acute need for less toxic and more potent cancer drugs and continues be the concern. Cancer can be detected in a number of ways, counting the presence of certain signs and symptoms, screening tests, or medical imaging. Once a possible cancer is detected it is diagnosed by microscopic examination of a tissue sample. Cancer is usually treated with chemotherapy, radiation therapy and surgery. The risks of surviving the disease vary greatly by the type and location of the cancer and the extent of disease at the start of treatment. While cancer can affect people of all ages, and a few types of cancer are more showed in children, the risk of developing cancer generally increases with age. In 2007, cancer produced about 13% of all human deaths worldwide (7.9 million). Rates are growing as more people live to an old age and as mass lifestyle changes occur in the developing world (Jemal et al. 2011). Most of the drugs available are not selective to cancer cells and affect normal cells as well leading to severe side effects. However, these drugs are now the most effective means to fight cancer. The aim

of research in cancer drug development is to find new drugs that are specific to cancer cells, or to develop a method that alters the nature of the drug administered such that it acts only on the target cells and not the regular normal functioning cells, thereby reducing the side effects.

Several anticancer agents available in the market today derive from natural sources. One of the earliest compounds isolated as an anticancer agent was podophyllotoxin, a compound obtained from *Podophyllum peltatum* (Sweeney) in 1944 (Imbert et al., 1998). It was initially used therapeutically as a purgative and in the treatment of venereal warts (Kaplan et al., 1942). Later, in 1974, it was shown that it acts as an anticancer agent by binding irreversibly to tubulin (Wilson et al., 1974). Etoposide and teniposide, the modified analogs of podophyllotoxin, can cause cell death by inhibition of topoisomerase II, thus preventing the cleavage of the enzyme- DNA complex and arresting the cell growth (Srivastava et al. 2005). Both these analogs are currently used in the treatment of various cancers (Odwyer et al., 1985).

Bioassays are crucial for the successful isolation of active compounds from various natural sources. The usual method for isolation of active components is the bioassay guided fractionation. Several bioassays are available to evaluate different types of bioactivities of different types of compounds. The assays can be chosen based on the nature and the type of activity that is desired to isolate. An ideal bioassay would be highly sensitive to small amounts of active material, selective to the specific bioactivity, cost effective and easy to run and maintain (Rahman et al., 2003).

4.8.1 Anti cancer of *Lindera* Species

From our literature review we have listed in Table 4.31 some selected anticancer properties of *Lindera species*, and no investigation on cancer has been found on *Lindera oxyphylla*.

Table 4.31: Anticancer activity of some selected species of *Lindera*

No.	<i>Lindera</i> species	Type of compound	Cell lines	Refrence
1	<i>Lindera ommunis</i>	sesquiterpenoids	HepG2	(Deng et al., 2011)
2	<i>Lindera trychnifolia</i>	LinerolideA-F	RAW264.7	(Sumiokaet al., 2011)
3	<i>Lindera trychnifolia</i>	phenolic compound	HepG2	(Yan et al., 2011)

4.8.2 Anticancer of *Litsea* Species

From our literature review we have listed in Table 4.32 some selected anticancer properties of *Litsea* species, no investigation on cancer has been found on *Litsea costalis*.

Table 4.32: Anticancer activity of some selected species of *Litsea*

No.	<i>Litsea</i> species	Type of compound	Cell lines	Refrence
1	<i>Litsea cubeba</i>	The leaf and fruit oils	A549	(Ho et al., 2010)
2	<i>Litsea coreanalevl</i>	Green tea	AGS and HT-29	(Xin & Yan-fei, 2008)
3	<i>Litsea akoensis</i>	Compounds	P-388, KB16, A549 and HT-29	(Chen, Lai-Yaun, Duh, & Tsai, 1998)

4.8.3 Materials and Methods

4.8.3.1 Cell culture

All the cells that used in this study were obtained from American Type Cell Collection (ATCC) and maintained in a 37°C incubator with 5% CO₂ saturation cell line A375 human melanoma, HT-29 human colon adenocarcinoma cells and WRL-68 normal hepatic cells were maintained in Dulbecco's modified Eagle's medium

(DMEM). Whereas A549 non-small cell lung cancer cells and PC3 prostate adenocarcinoma cells were maintained in RPMI medium. Both medium were supplemented with 10% fetus calf serum (FCS), 100 units/mL penicillin, and 0.1 mg/mL streptomycin.

4.8.3.2 Cellular viability assay

Different cell types from above were used to determine the inhibitory effect of compounds on cell growth using the MTT assay. This colorimetric assay is based on the conversion of the yellow tetrazolium bromide (MTT) to the purple formazan derivatives by mitochondrial succinate dehydrogenase in viable cells. The MTT assay was modified as described by (Cheah et al., 2011) and (Friedman et al., 2009). Briefly, cells were seeded at a density of 1×10^5 cells/mL in a 96-well plate and incubated for 24 hours at 37°C, 5% CO₂. Next day, cells were treated with the compounds and incubated for another 24 hours. After 24 hours, MTT solution at 2 mg/mL was added for 1 hour. Absorbance at 570 nm were measured and recorded. Results were expressed as a percentage of control giving percentage cell viability after 24 hours exposure to test agent. The potency of cell growth inhibition for each test agent was expressed as an EC₅₀ value, defined as the concentration that caused a 50% loss of cell growth. Viability was defined as the ratio (expressed as a percentage) of absorbance of treated cells to untreated cells.

4.8.3.3 Statistical Analyses

Each experiment was performed at least three times. Results are expressed as the mean value \pm standard deviation (SD). Log EC₅₀ calculations were performed using the built-in algorithms for dose-response curves with variable slope using Graphpad Prism software (version 4.0; GraphPad Software Inc., San Diego, CA). A fixed maximum value of the dose-response curve was set to the maximum obtained value for each drug.

4.8.4 Results

To evaluate the cytotoxic activity, compound was tested with a series of different doses on MTT, (Figures 4.27). After 24 hours, cell viability was determined by the MTT assay. Test agents induced cell cytotoxicity in a concentration dependent manner. These dose titration curves allowed determination of EC_{50} for the test agents towards different cell lines (Tables 4.33 and Table 4.34).

In Table 4.33 showed mild cytotoxicity of selected compounds against various cancer cell lines; MCF-7 was 79.57 $\mu\text{g/mL}$ for flavokawain B LOB15 , PC3 was 30.12 $\mu\text{g/mL}$, A549 was 65.03 $\mu\text{g/mL}$ and MCF-7 was 47.67 $\mu\text{g/mL}$ for (+)-Onysilin LOB4, PC-3 was 90.13 $\mu\text{g/mL}$ for (+)-pinocembrin LOB2 and MCF-7 was 96.33 $\mu\text{g/mL}$ for LOB25 . This results showed that cytotoxic activity of the isolated compounds from *Lindera oxyphylla* have moderate activity These results also indicate that cell lines differ in their sensitivity to the same test agent, which may be determined by multiple cell type-specific signalling cascades and transcription factor activities.

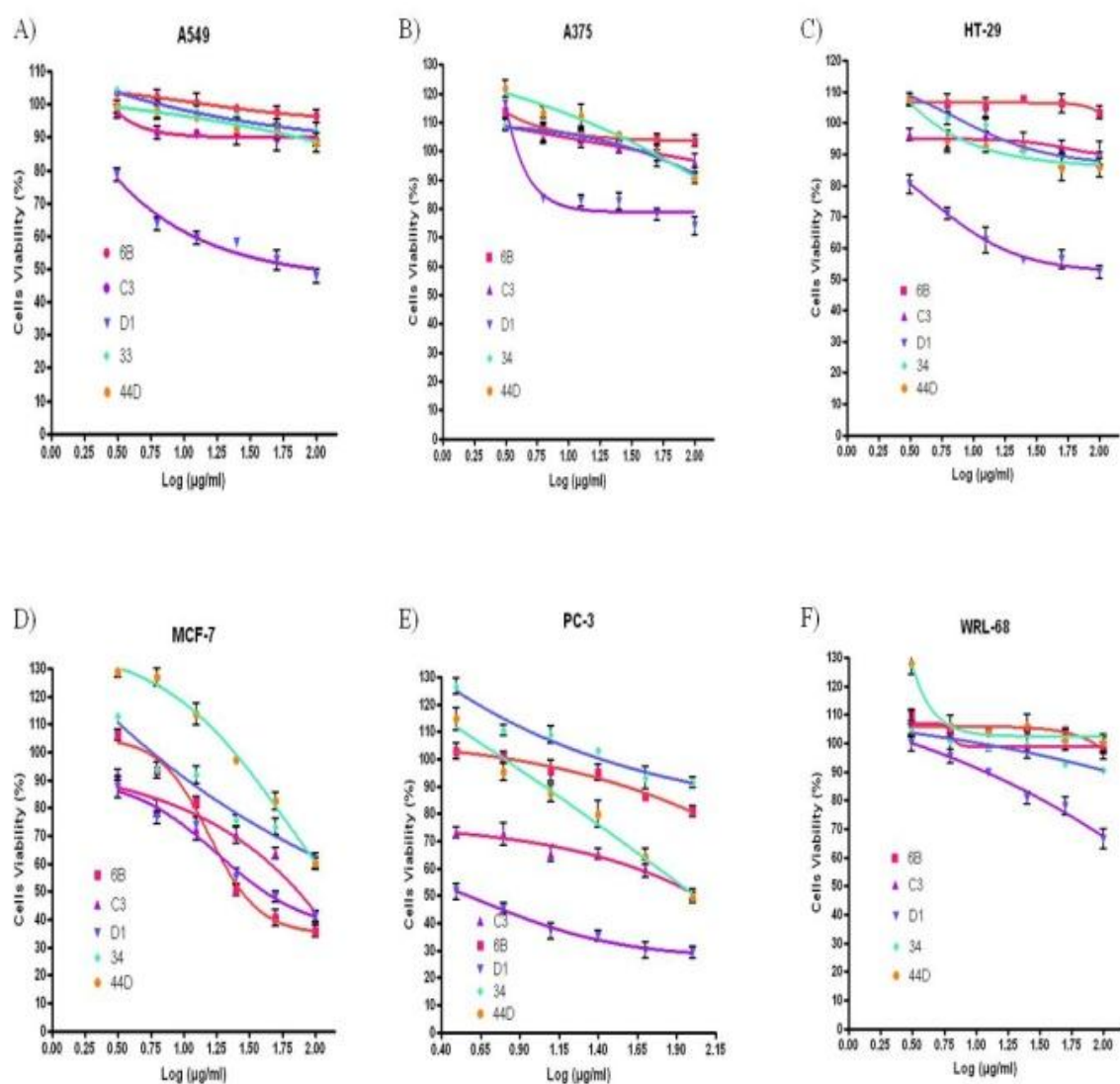


Figure 4.27: EC_{50} ($\mu\text{g/ml}$) of five compounds of *Lindera oxyphylla*

Table 4.33: Effect of compounds from *Lindera oxyphylla* on different cells type expressed as EC₅₀ values in 24 hours using MTT assay.

Cell lines	LOB15 EC ₅₀ (µg/mL)	LOB25 EC ₅₀ (µg/mL)	LOB4 EC ₅₀ (µg/mL)	LOB28 EC ₅₀ (µg/mL)	LOB2 EC ₅₀ (µg/mL)
A549	>100	>100	65.03	>100	>100
A375	>100	>100	>100	>100	>100
WRL-68	>100	>100	>100	>100	>100
PC-3	>100	>100	30.12	>100	90.13
HT-29	>100	>100	>100	>100	>100
MCF-7	79.57	96.33	47.67	>100	>100

Table 4.34: EC₅₀ values of compounds in different cell lines from *Litsea costalis*.

Cell lines	LCB3 IC ₅₀ µg/mL	LCB10 IC ₅₀ µg/mL	LCB4 IC ₅₀ µg/mL	LCB17 IC ₅₀ µg/mL	LCL7 IC ₅₀ µg/mL
WRL68	>100	81.73 ± 3.7	>100	>100	-
MCF-7	48 ± 3.05	>100	34. 65± 0.1	1.4 ± 0.1	-
.MDA-MB231	>100	>100	>100	>100	-
CEMSS	>100	>100	>100	>100	-
PC3	>100	1.19 ± 0.19	>100	>100	-
HepG2	18± 2.1	>100	>100	1.00± 0.1	10±1
HT29	>100	>100	>100	1.32± 0.1	-
CCD841	>100	>100	>100	>100	-
Jurkat	>100	>100	>100	1.22± 0.1	-
A549	>100	85.13 ± 7.3	>100	>100	-

In Table 4.34 the selected compounds showed mild cytotoxicity against various cancer cell lines. In MCF-7 EC_{50} values was 48 ± 3.05 and HepG2 was 18 ± 2.1 for biseugenol A **LCB3**, WRL68 was 81.73 ± 3.7 , PC3 was 1.19 ± 0.19 and A549 was 85.13 ± 7.3 for biseugenol B **LCB10**, MCF-7 was 34.65 ± 0.1 for Litsin **LCB4**, MCF-7 was 1.4 ± 0.1 , HepG2 was 1.00 ± 0.1 , HT29 was 1.32 ± 0.1 and Jurkat was 1.22 ± 0.1 for biseugenol C **LCB17**.

In addition of HepG2 test showed (Figure 4.28) for costalin **LCL7**, Other tests like clonogenic assay and quantification of apoptosis (AO/PI) were also carried out.

4.8.4.1 MTT assay costalin **LCL7**

MTT assay was used to determine the cytotoxicity of costalin against human hepatocellular liver carcinoma cell line (HepG2). This assay served as an index used to determine cytotoxicity of compound to stimulate or inhibit cell viability and growth by detecting the reduction of tetrazolium salt to blue formazan by mitochondrial enzyme activity of succinate dehydrogenase in living cells. HepG2 cell lines were treated with different concentrations of the compound for 24, 48, 72h, and the cells viability were measured by MTT assay. The costalin was found to inhibit the growth of HepG2 cells in a dose-dependent manner with IC_{50} of 10 ± 1 , 8.5 ± 1 and $6.5 \pm 1 \mu\text{g/mL}$ for 24, 48 and 72 hours, respectively (Figure 4.28).

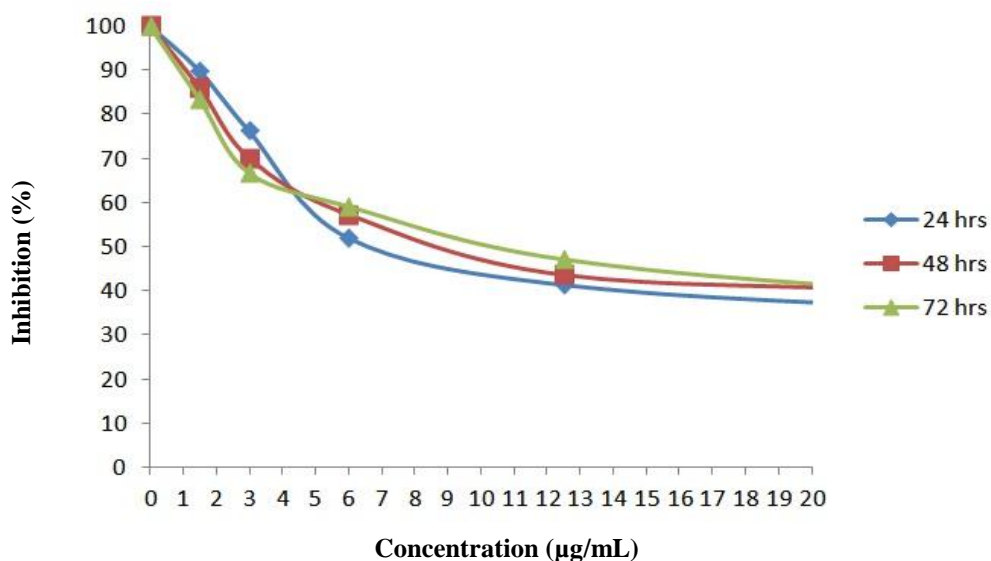


Figure 4.28 : Effects of costalin **LCL7** treatment in the human hepatocellular carcinoma HepG2 cells.

4.8.4.2 Clonogenic assay costalin **LCL7**

To further evaluate the antitumor potential of costalin, we used clonogenic assay to elucidate the effects of costalin on the growth of HepG2 cells. Costalin treated HepG2 cells inhibited the clonogenic growth of HepG2 cells at concentrations of 6.5, 10 and 16 µg/mL by 28%, 54% and 98%, respectively, in comparison with untreated cells as control (Table 4.35). The clonogenic efficiency (CE) of HepG2 cells at the dosage of 6.5, 10 and 16 µg/mL was reduced to 7, 4 and 0 (µg/mL), respectively, as compared to the untreated control cells. Clonogenicity of HepG2 cells were reduced in a dose-dependent manner after treatment with costaline and no viable colony was observed at concentration higher than 16 µg/mL. This result indicated that costalin was able to inhibit HepG2 cell proliferations (Figure 4.29 and Table 4.35).

Table 4.35: The cloning efficiency (CE) of the costalin **LCL7** on HepG2 cell line after 24 hrs.

Compound	Concentrations ($\mu\text{g/mL}$)	No. of Cells	Total viable colony numbers before treatment	Number of Apoptotic Colonies	Death of clonogenic cells (%)	Clonogenic efficiency (%)
(Control)	-	5×10^3	500	5 ± 1.5	1	9
Costalin	6.5	5×10^3	500	137 ± 12	28	7
Costalin	10	5×10^3	500	266 ± 15	54	4
Costalin	16	5×10^3	500	500 ± 12	-	0

CE*: clonogenic efficiency; $^{*}\text{IC}_{50}$

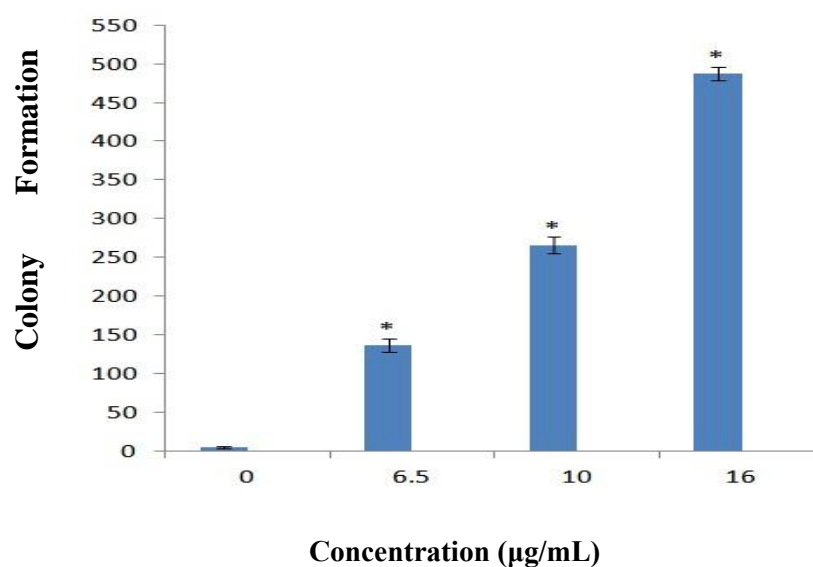


Figure 4.29: Comparison of colony formation rates at different concentrations of costalin **LCL7** on HepG2 cells at 24 hr. Data are mean \pm SD (n = 3).

4.8.4.3 Quantification of apoptosis (AO/PI) costalin **LCL7**

The percentages of viable, apoptotic and necrotic cells were determined in more than 200 cells. Acridine orange (AO) and propidium iodide (PI) are intercalating nucleic acid specific fluorochromes which emit a green and orange fluorescence, respectively, when they are bound to DNA. Of the two, only AO can cross the plasma membrane of

viable and early apoptotic cells. Viewed by fluorescence microscopy, viable cells appear to have a green nucleus with intact structure while apoptotic cells exhibit a bright-green nucleus showing condensation of chromatin as dense green areas. Late apoptotic cells and necrotic cells will stain with both AO and PI. Comparatively, PI produces the highest intensity emission. Hence, late apoptotic cells exhibited an orange nucleus showing condensation of chromatin whilst necrotic cells display an orange nucleus with intact structure (Figure 4.30). This assay provides a useful quantitative evaluation and was done three times ($n = 3$).

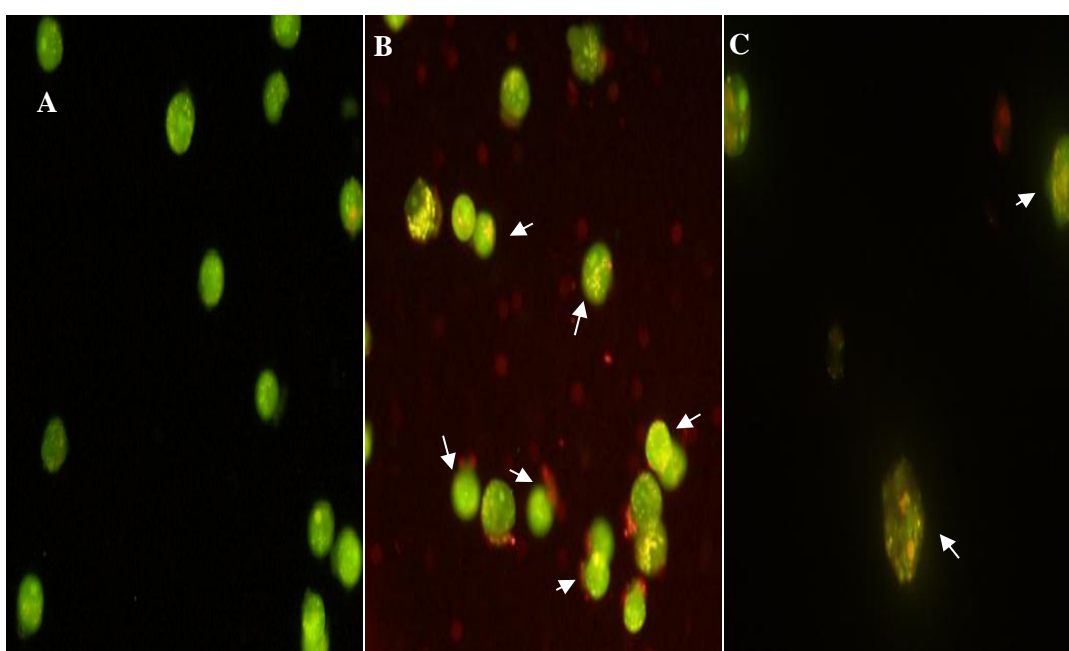


Figure 4.30: HepG2 cells stained with AO/PI. Panel (A) shows the green viable HepG2 cells with diffused chromatin as control (Magnification, 20X).

^ In addition of MTT test for biseugenol A LCB3 and biseugenol B LCB10 other tests like clonogenic assay and quantification of apoptosis (AO/PI) were also carried out.

4.8.4.4 Cell viability study of biseugenol A LCB3 and biseugenol B LCB10

The IC₅₀ values of biseugenol A **LCB3** and biseugenol B **LCB10** were shown in (Table 4.36). Cell viability was analysed using the MTT assay, measuring metabolic activity. In cells with normal metabolism, a tetrazolium salt is converted to formazan, measurable by change in absorbance. Among the three compounds, biseugenol B **LCB10** exhibited the most significant anti-cancer effects, but it was interesting to note that only in PC3 cell lines that is showed very potent cytotoxicity effect. All other cell lines except WRL68 (IC₅₀: 81.73 ± 3.7 µg/ml) and A549 (IC₅₀: 85.13± 7.3 µg/ml) had no effect until 100 µg/ml.

On the other hand we found that biseugenol A **LCB3** was only significantly active on HepG2 cells as there was no sign of toxicity by this compound in other tested cell lines. Considering these data, biseugenol B **LCB10** shown to have high level of significance to be exploited in the molecular level for development as a lead compound in the anti-cancer drug discovery against prostate cancer.

Table 4.36. EC₅₀ values of biseugenol A **LCB3** and biseugenol B **LCB10** in different cell lines.

Cell Line	biseugenol A LCB3 (µg/mL)	biseugenol B LCB10 (µg/mL)
WRL68	>100	81.73±3.7
MCF7	48±3.05	>100
MDA-MB-231	>100	>100
CEMSS	>100	>100
PC-3	>100	1.19±0.19
HepG2	18±2.1	>100
HT29	>100	>100
CCD841	>100	>100
Jurkat	>100	>100
A549	>100	85.13±7.3

4.8.4.5 Clonogenic assay biseugenol A LCB3 and biseugenol B LCB10

In order to evaluate the ability of the biseugenol A **LCB3** and biseugenol B **LCB10** to inhibit the growth of HepG2 cells, cells were treated with increasing amounts of compounds. The number of colony-forming cells was reduced in a concentration-dependent manner. The cloning efficiency (CE) of biseugenol A **LCB3** on HepG2 cells at the dosage of 26, 36 and 50 µg/mL was 0.073, 0.044 and 0.00, respectively, but CE of untreated HepG2 cells (as control) was 0.098. The cloning efficiency (CE) of biseugenol B **LCB10** on PC-3 at the dosage of 1.19, 3 and 5 µg/mL was 0.046, 0.025 and 0.00, respectively, but CE of untreated PC-3 cells (as control) was 0.097 (Table 4.37 and Table 4.38) and (Figure 4.31). No viable colony could be observed at dosage of 50 and 5 µg/mL for HepG2 and PC-3, respectively which indicated the inhibition of proliferation activity of HepG2 and PC-3 cells *in vitro* condition. This result was consistent with the result of MTT assay.

Table 4.37. The cloning efficiency (CE) of the biseugenol A **LCB3** on HepG2 cells in 48 hrs.

Compound	Concentration (µg/mL)	Number of Cells/Plate	Total viable colony number before treatment	Number of Apoptotic Colonies (size of 50-200 µm)	CE*
Untreated HepG2 (Control)	-	5×10 ³	500	10	0.098
biseugenol A	18 (µg/mL)*	5×10 ³	500	190	0.062
biseugenol A	36 (µg/mL)	5×10 ³	500	290	0.042
biseugenol A	50 (µg/mL)	5×10 ³	500	500	0

CE*: clonogenic efficiency; *IC₅₀

Table 4.38. The cloning efficiency (CE) of the biseugenol B **LCB10** on PC-3 cells in 48 hrs.

Compound	Concentration (µg/mL)	Number of Cells/Plate	Total viable colony number before treatment	Number of Apoptotic Colonies (size of 50-200 µm)	CE*
Untreated PC-3 (Control)	-	5×10 ³	500	12	0.097
biseugenol B	1.19 (µg/mL)*	5×10 ³	500	270	0.046
biseugenol B	3 (µg/mL)	5×10 ³	500	375	0.025
biseugenol B	5 (µg/mL)	5×10 ³	500	500	0

CE*: clonogenic efficiency; *IC₅₀

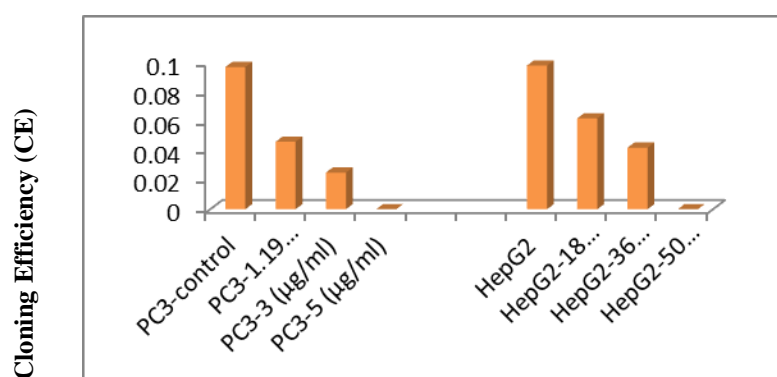


Figure 4.31: Comparison of colony formation rate using different concentrations of compounds biseugenol A **LCB3** and biseugenol B **LCB10** on HepG2 and PC-3 cell lines respectively in 48 hrs.

4.8.4.6. Quantification of apoptosis biseugenol A **LCB3** and biseugenol B **LCB10**

Apoptosis was quantified using propidium iodide (PI) and acridine-orange (AO) double staining and examined under fluorescence microscope (Lieca, Germany) attached with Q-Floro Software. Briefly, treatment was carried out in a 25 ml culture flask. Cells were plated at a concentration of 1×10⁶ cell/mL and treated with IC₅₀ of 26 µg/mL. Flasks were incubated in an atmosphere of 5% CO₂ at 37°C for 48 hrs. Harvested cells were washed, stained with fluorescent dyes and observed under a UV-fluorescence microscope within 30 min before the fluorescence color starts to fade.

4.8.4.7 Quantification of apoptosis (AO/PI) biseugenol A LCB3 and biseugenol B LCB10

The percentages of viable, apoptotic and necrotic cells were determined in more than 200 cells. Acridine orange (AO) and propidium iodide (PI) are intercalating nucleic acid specific fluorochromes which emit a green and orange fluorescence, respectively, when they are bound to DNA. Of the two, only AO can cross the plasma membrane of viable and early apoptotic cells. Viewed by fluorescence microscopy, viable cells appear to have a green nucleus with intact structure while apoptotic cells exhibit a bright green nucleus showing condensation of chromatin as dense green areas. Late apoptotic cells and necrotic cells will stain with both AO and PI. Comparatively, PI produces the highest intensity emission. Hence, late apoptotic cells exhibited an orange nucleus showing condensation of chromatin. On the other hand necrotic cells display an orange nucleus with intact structure. This assay provides a useful quantitative evaluation and was done in triplicates ($n = 3$) (Figure 4.32).

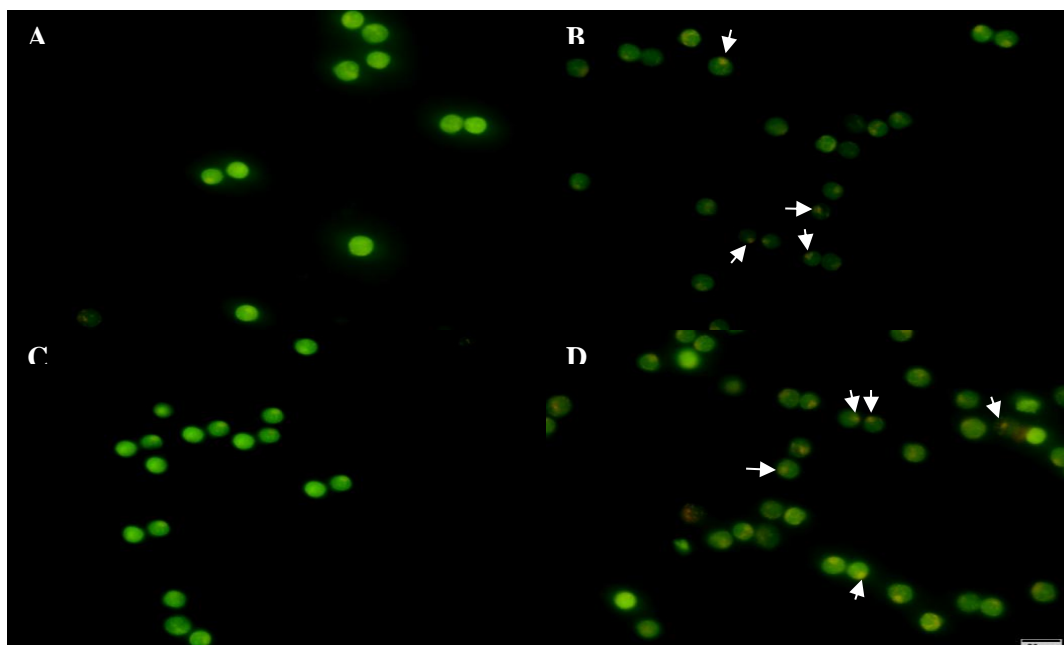


Figure 4.32 : Apoptosis quantification of HepG2 and PC-3 cells stained with AO/PI. Panel (A) and (C) show the green viable HepG2 and PC-3 cells,

In addition of MCF-7 test for Litsin **LCB4**, other tests like clonogenic assay and quantification of apoptosis (AO/PI) were also carried out.

4.8.4.8 MTT assay Litsin **LCB4**

MTT assay was used to determine the Litsin **LCB4** cytotoxicity against MCF-7. This assay served as an index used to determine cytotoxicity of compound to stimulate or inhibit cell viability and growth by detecting the reduction of tetrazolium salt to blue formazan by mitochondrial enzyme activity of succinate dehydrogenase in living cells. MCF-7 cell lines were treated with different concentrations of Litsin **LCB4** 1 for 48 h, and the cells viability were measured by MTT assay. The compound was found to inhibit the growth of MCF-7 cells in a dose-dependent manner with IC_{50} of 17 ± 1 $\mu\text{g/mL}$ (Fig 4.33).

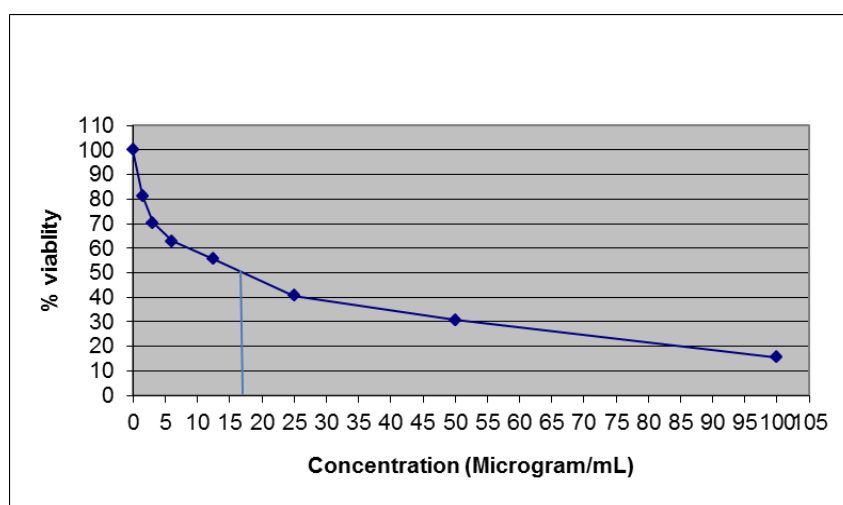


Figure.4.33: Percentage viability of MCF-7 cells treated with different concentration meagured after 48 hours using MTT assay.

4.8.4.9 Clonogenic assay Litsin **LCB4**

In order to evaluate the ability of the compound inhibit growth of MCF-7 cells, cells were treated with increasing amounts of compound. The number of colony-forming cells was reduced in a concentration-dependent manner by the compound. The cloning efficiency (CE) of MCF-7 at the dosage of 17, 35 and 45 $\mu\text{g/mL}$ was 0.056, 0.024 and 0.00 respectively and CE of untreated MCF-7 cells was 0.098 as control. No

viable colony could be observed at the dosage of 50 µg/mL, which indicated compound can pronounced inhibit the proliferation of MCF-7cell (Table 4.38). This result is consistent with the result of MTT assay.

Table.4.39: The cloning efficiency (CE) of the new compound Litsin **LCB4** on MCF-7 cells after 48 hrs.

Compound	Concentration (µg/mL)	Number of Cells/Plate	Total viable colony number before treatment	Number of Apoptotic Colonies (size of 50-200 µm)	CE*
Untreated MCF-7 (Control)	-	5×10 ³	500	10	0.098
Litsin	17 (µg/mL)*	5×10 ³	500	220	0.056
Litsin	35 (µg/mL)	5×10 ³	500	380	0.024
Litsin	45 (µg/ml)	5×10 ³	500	500	0

CE*: clonogenic efficiency; *IC₅₀

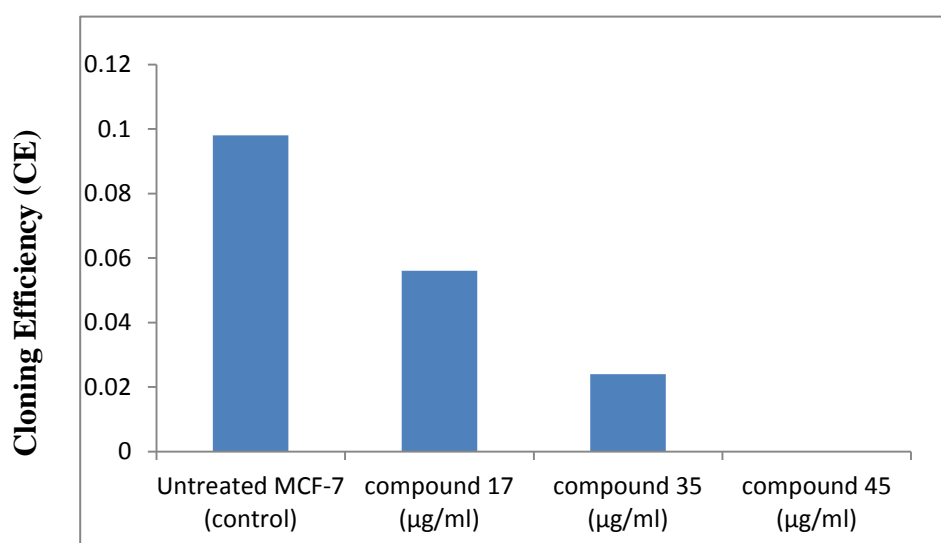


Figure.4.34: Comparison of colony formation rate using different concentrations of Litsin **LCB4** on MCF-7 after 48 hr.

4.8.4.10 Quantification of apoptosis (AO/PI) Litsin **LCB4**

The percentages of viable, apoptotic and necrotic cells were determined in more than 200 cells. Acridine orange (AO) and propidium iodide (PI) are intercalating nucleic acid specific fluorochromes which emit a green and orange fluorescence, respectively,

when they are bound to DNA. Of the two, only AO can cross the plasma membrane of viable and early apoptotic cells. Viewed by fluorescence microscopy, viable cells appear to have a green nucleus with intact structure while apoptotic cells exhibit a bright green nucleus showing condensation of chromatin as dense green areas. Late apoptotic cells and necrotic cells will stain with both AO and PI. Comparatively, PI produces the highest intensity emission. Hence, late apoptotic cells exhibited an orange nucleus showing condensation of chromatin. On the other hand necrotic cells display an orange nucleus with intact structure. This assay provides a useful quantitative evaluation and was done in triplicates ($n = 3$) (Figure 4.36).

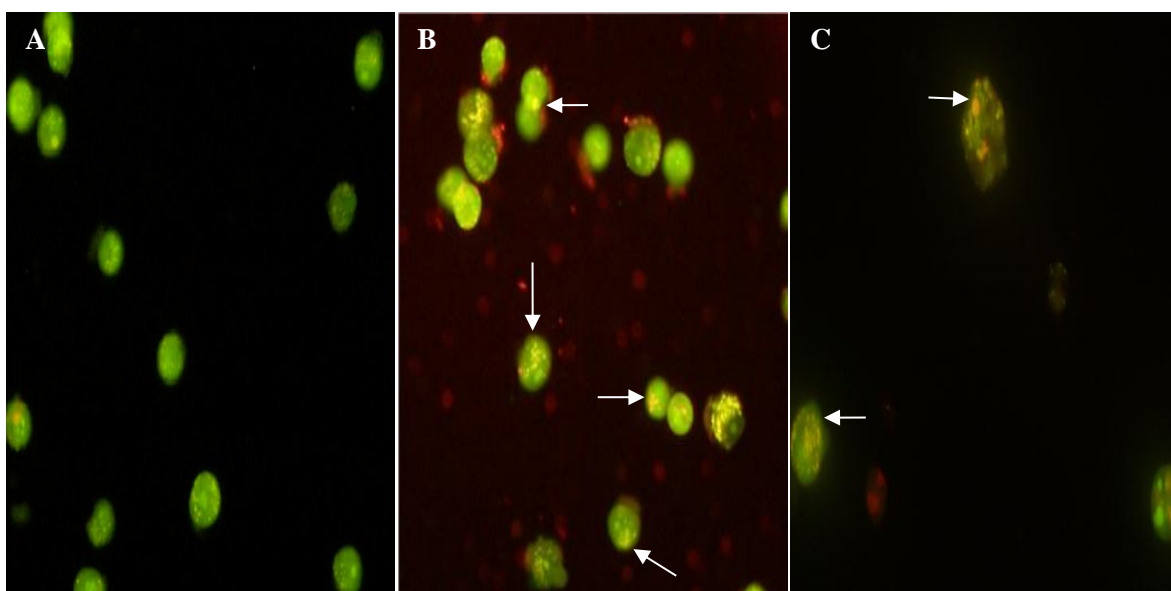


Figure 4.35: MCF-7 cells stained with AO/PI. Panel (A) shows the green viable MCF-7 cells with diffused chromatin as control (Magnification, 20X).

4.8.4.11 Litsin LCB4-induced caspase-3/7, 8, and 9 activations

An activation of caspases (aspartate specific cysteine protease) is one of the biochemical changes during apoptosis. All the levels of caspase-3/7, 8 and 9 induced by Litsin **LCB4** treatment were markedly increased (2–6 folds) as compared to the untreated group. High level of caspase 3/7, 8 and 9 was found at 24 ($p < 0.01$), 48($p < 0.05$) and 24($p < 0.01$) hours, respectively. However, low level of caspase 3/7, 8 and 9

was found at 6 ($p < 0.05$), 3 ($p < 0.01$) and 6 ($p < 0.01$) hrs (Figure 4.36, 4.37, 4.38), respectively. These results indicate that apoptosis induced by litsin was mediated via caspase activations.

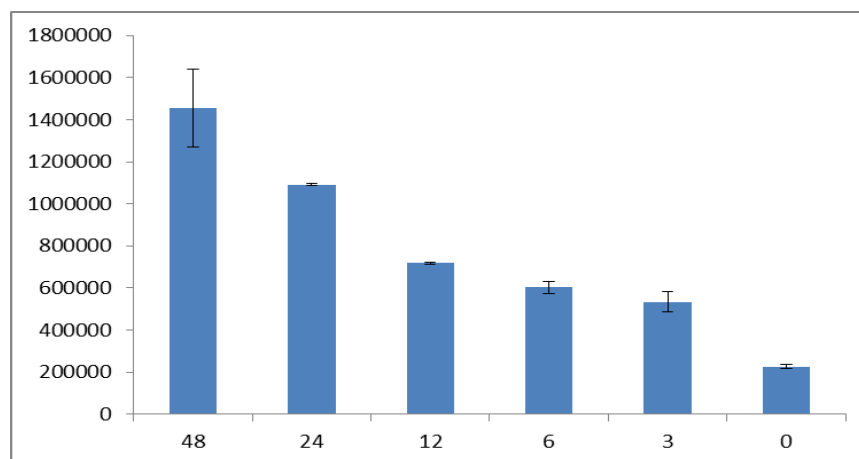


Figure 4.36. Relative luminescence expression of Caspase 3/7 in the MCF7 cells treated with different concentrations of Litsin **LCB4**.

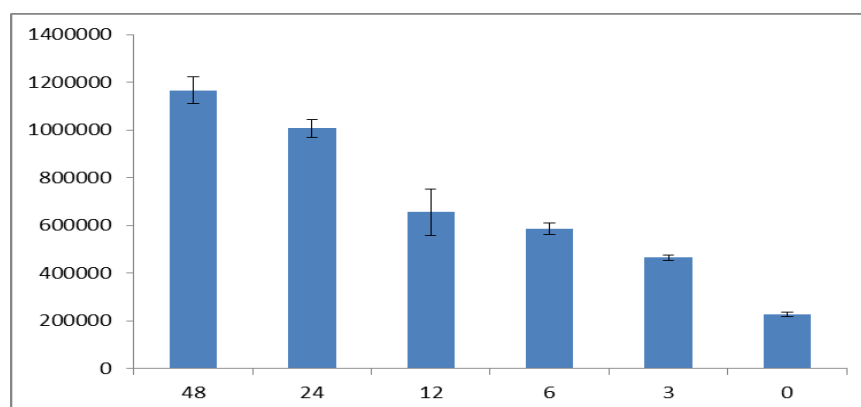


Figure.4.37. Relative luminescence expression of caspase 8 in the MCF7 cells treated with different concentrations of Litsin **LCB4**.

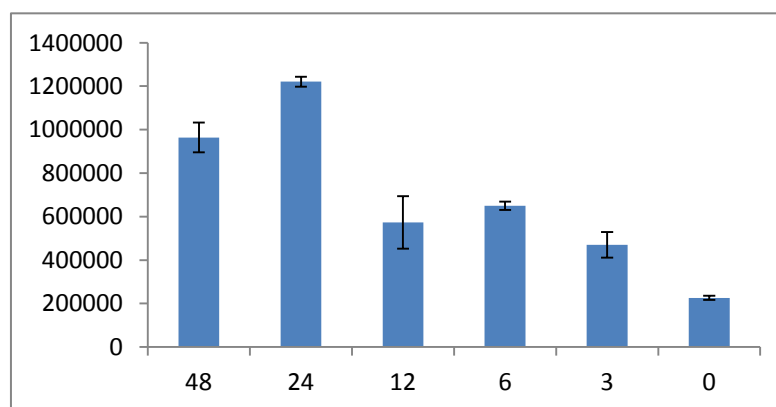


Figure 4.38. Relative luminescence expression of Caspase 9 in the MCF7 cells treated with different concentrations of Litsin **LCB4**.

In the intrinsic pathway, the release of cytochrome from the mitochondria into the cytosol is fundamental to apoptosome formation and downstream caspase activation. The release of cytochrome c and the activation of caspase 3/7, 9 and 8 by Litsin **LCB4** at different time clearly showed that the apoptosis happened are through this pathway. There are evidences that members of the Bcl2 protein family are key mediators of cytochrome c release in the context of apoptotic stimuli (Kluck et al., 1997) (Green, 2006). Many lines of evidence established that activation of caspase is a central mechanism of apoptosis (Vaux and Kobmeyer et al., 1999). The treatment with Litsin **LCB4** on MCF7 cells activated the caspases 3/7, 8 and 9. Caspase 9 is found in the intermembrane space of mitochondria, and released in a Bcl2-inhibitable fashion upon induction of permeability transition in isolated mitochondria and upon apoptosis induction in cells. The released caspase 9 is then activate post-mitochondrial caspases including caspase 3 and 7, the disassembly of the cell occurs in what is known as the execution phase of apoptosis (Li et al., 2010) (Susin et al., 1999). Even though, caspase 8 activation was found both upstream and downstream of mitochondria, it is closely involved with apoptosis signaling through the extrinsic pathway (Jin et al., 2009). Besides, in many instance caspase 8 may interlinked to mitochondrial pathways by cleavage of Bcl2 family member Bid to tBid (Gu et al., 2005).

In addition of Anticancer test for Biseugenol C, other tests like BC inhibits TNF- α -induced NF- κ B nuclear translocation, induced caspases activation were also carried out.

4.8.4.12 BC inhibits TNF- α -induced NF- κ B nuclear translocation

The role of BC in the inhibition of activated NF- κ B induced by the inflammatory cytokine, TNF- α using Alexa Fluor 488-conjugated anti-NF- κ B antibody was investigated. In control cells (Fig. 4.39), high NF- κ B fluorescent intensity was found in cytoplasm but faintly in nuclei, which indicated that there was no NF- κ B activation at the non-stimulated condition. Meanwhile, TNF- α alone stimulated cell significantly increased the NF- κ B fluorescent intensity in the nuclei. BC exhibited significant inhibitory effects on the activation of NF- κ B (Fig. 4.40). In the cells treated with curcumin, a known inhibitor of NF- κ B activation, it was observed that significant inhibition of TNF- α -induced NF- κ B nuclear translocation as evidenced by low nuclear NF- κ B-related fluorescence intensity (Fig. 4.40). In parallel, the morphological changes of NF- κ B translocation indicated by immunofluorescence staining (Fig. 4.40) showed an inhibitory effect of BC on TNF- α -induced NF- κ B translocation in a dose-dependent manner with a strong inhibition at 2 and 3 μ g/ml concentration of BC.

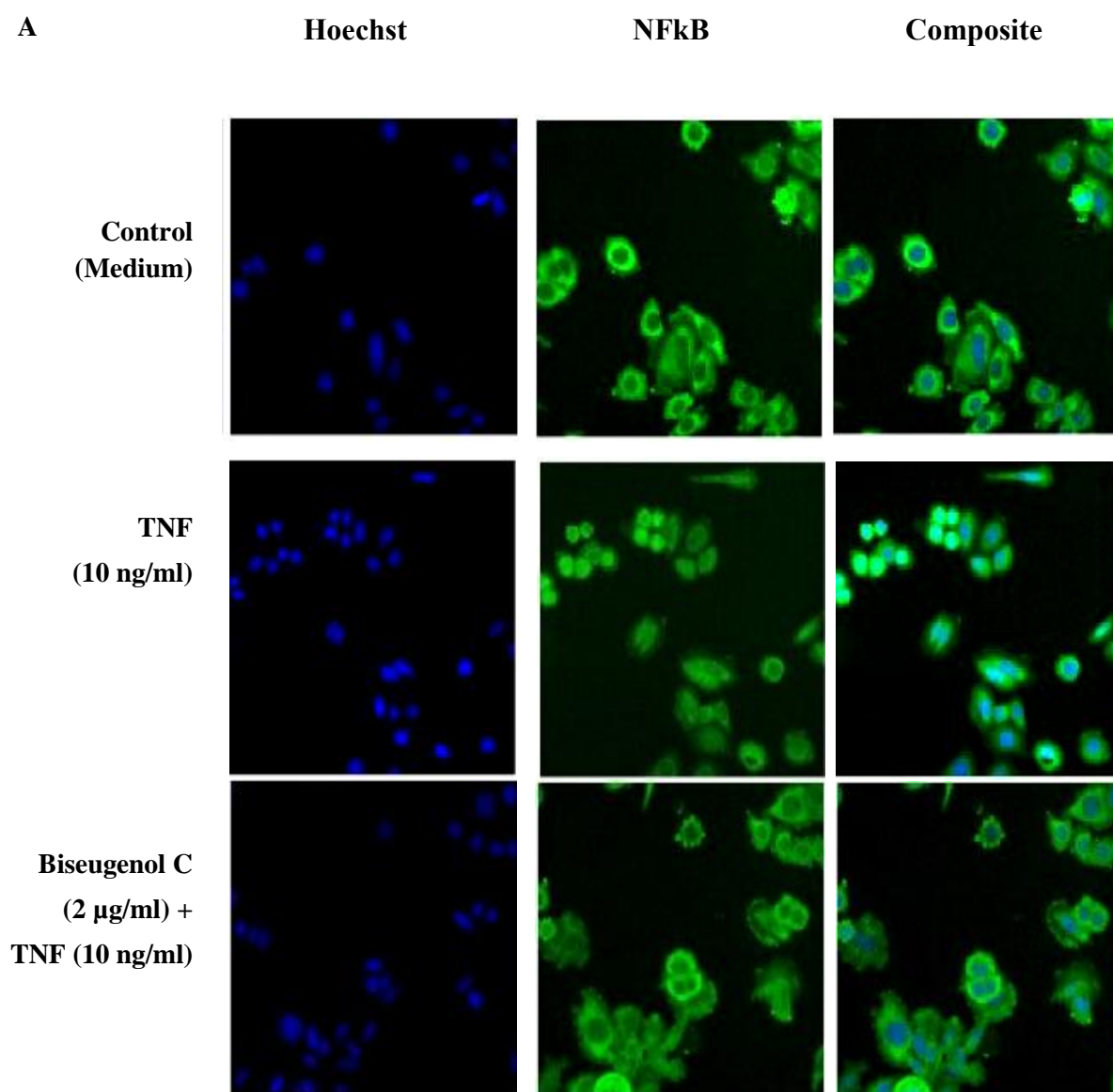


Figure 4.39: NF-kB fluorescent intensity

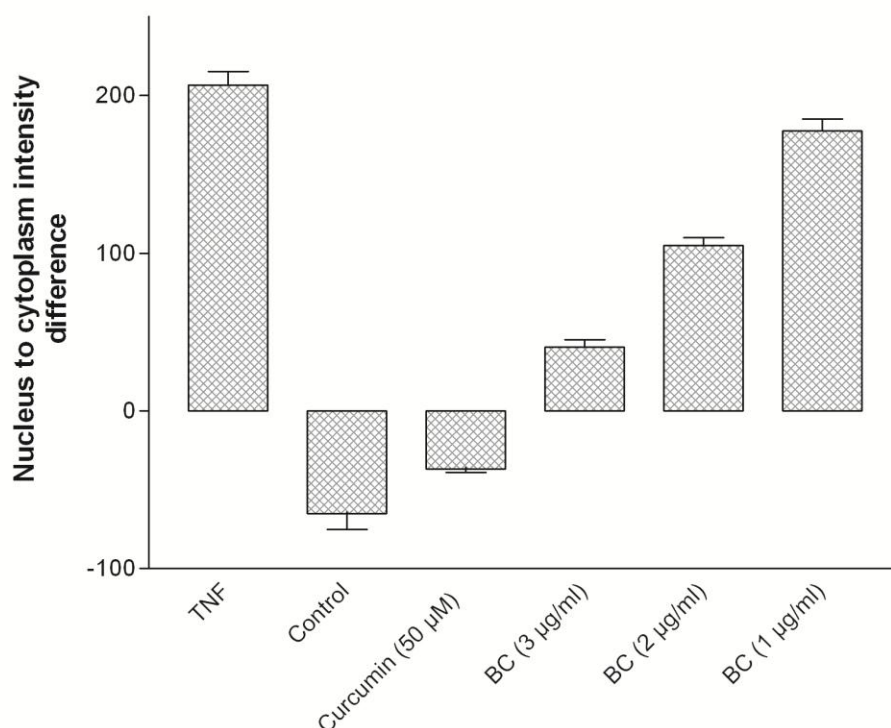


Figure 4.40: NF-kB fluorescent intensity in the nuclei

4.8.4.13 BC induced caspases activation

To determine whether caspases are involved in apoptosis induction by BC, the protein levels of active caspases in BC-treated cells were evaluated. Activation of both the caspases were found to be time-dependent (Figure 4.41). Caspase-8 activity was significantly elevated at the 6 hour of treatment and progressed to a maximal level (2.5-fold over vehicle control) after 24 hours of incubation (Fig. 4.41). The same pattern of caspase expressions were observed for caspase-9. Cell permeable-specific inhibitors of caspase-8 (z-IETD-FMK) and caspase-9 (z-LEHD-FMK) were added into BC treatment to determine whether the activation of caspase-8 and -9 by BC can be blocked by these inhibitors. The results obtained were clearly showed the activation of caspase-8 and -9 by BC in MCF-7 cells.

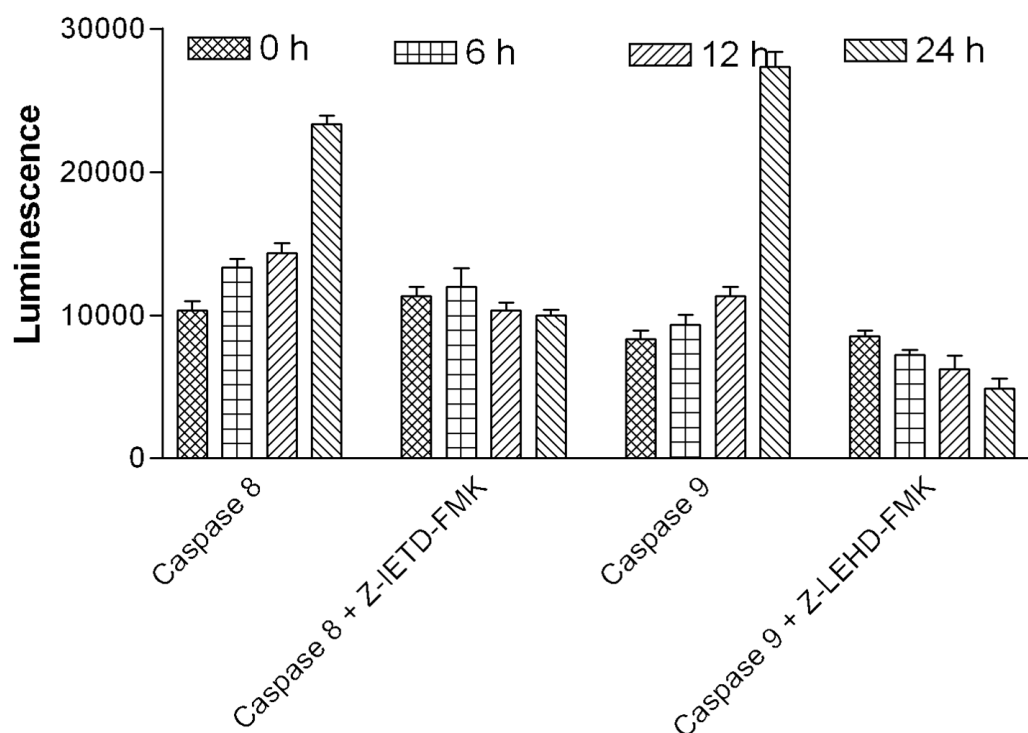


Figure 4.41: active caspases in BC-treated cells

4.8.4.14 BC up-regulated Bax and suppressed the expression of Bcl2 and HSP70 protein

The changes occurred to the MMP and cytochrome c release led us to confirm the role of mitochondria in the apoptosis occurred by BC at protein level using western blot analysis. Exposure of MCF7 cells to BC increased the pro-apoptotic protein, Bax and decreased the expression of anti-apoptotic, Bcl2 protein. Further, the expression of HSP70 did down regulated in a concentration-depended manner (Figure 4.42).

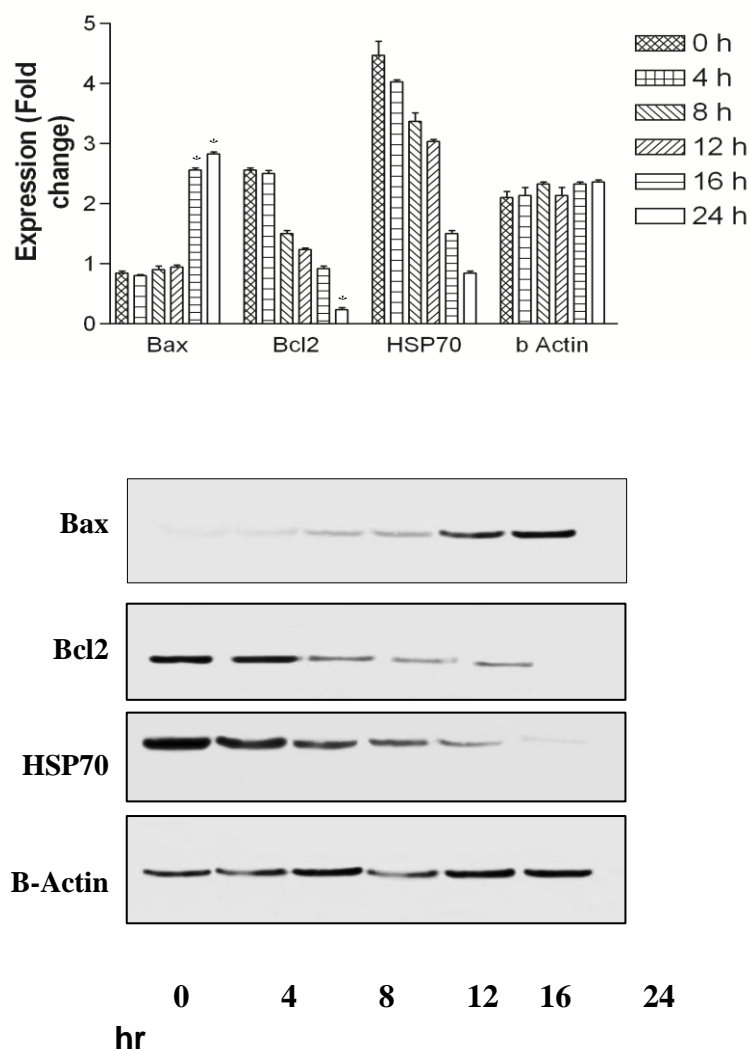


Figure 4.42: The changes occurred to the MMP and cytochrome c release led us to confirm the role of mitochondria in the apoptosis occurred by BC

4.8.4.15 BC-induced apoptosis in MCF7 cells

To confirm the presence of apoptosis, we examined nuclear morphological changes of MCF7 cells by determining nuclear condensation and fragmentation hallmark for apoptosis (Fig.4.43). Hoechst 33342 staining showed that a part of the cells displayed nuclear condensation at 24 h after BC treatment. The nuclear intensity which is directly corresponding to apoptotic chromatin changes: blebbing, fragmentation and condensation where quantitated in (Figure 4.44) Meanwhile, concurrent increase in the cell permeability also was observed.

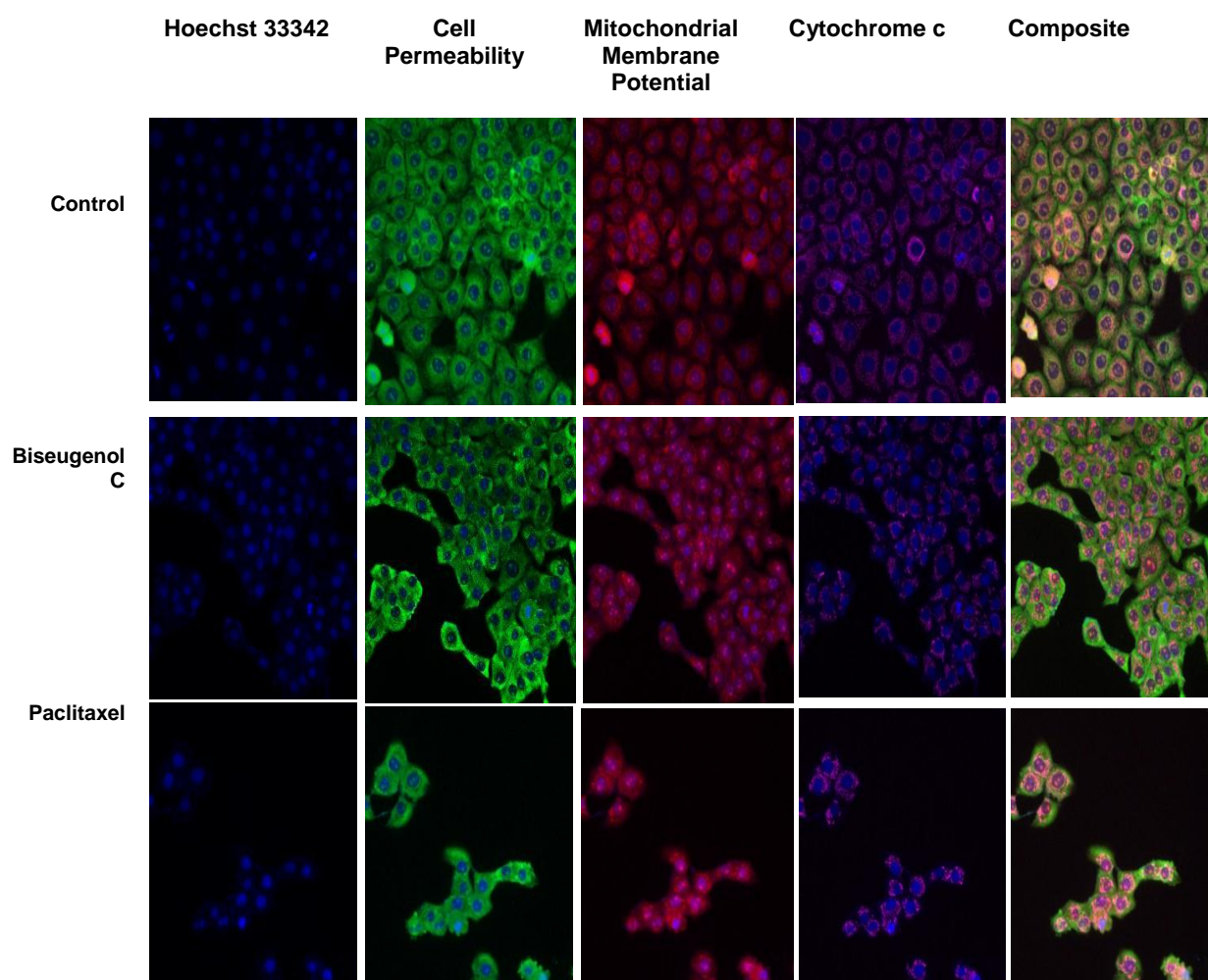


Figure 4.43: MCF7 cells by determining nuclear condensation and fragmentation
hallmarkforapoptosis

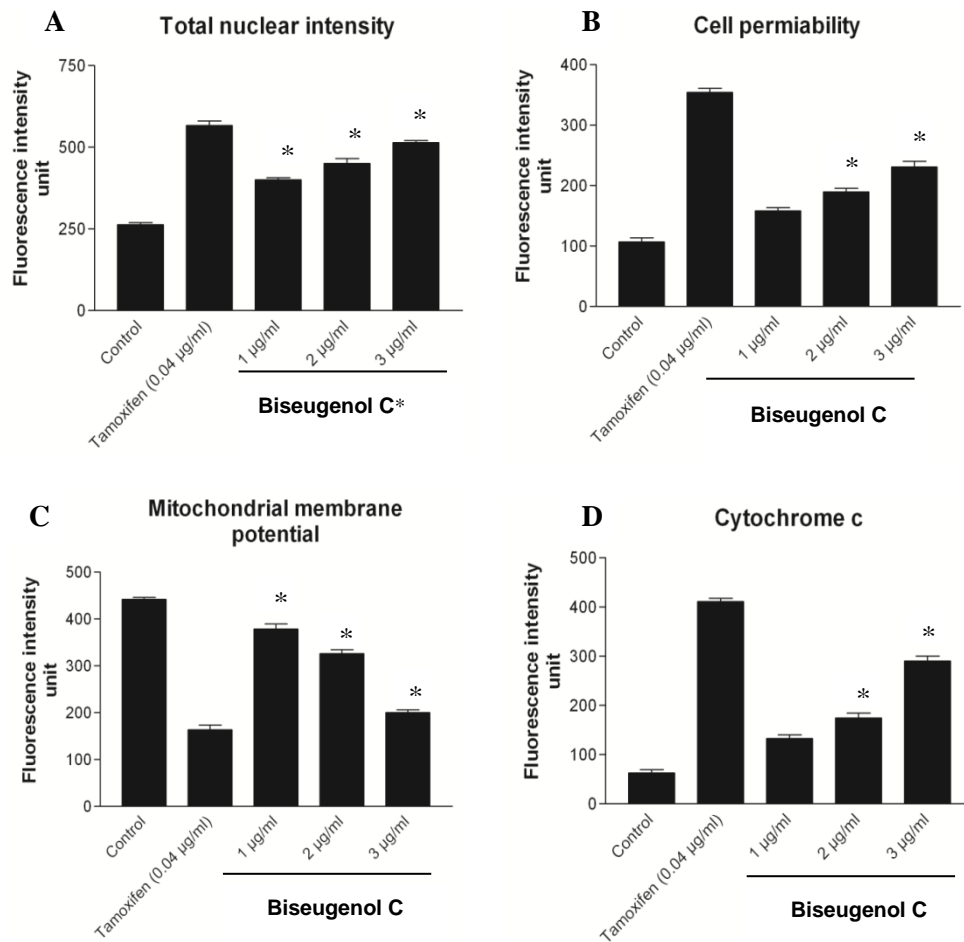


Figure 4.44: Quantitative analysis of BC mediated apoptosis parameter. Changes in A) total nuclear intensity, B) cell permeability, C) mitochondrial membrane potential and D) cytochrome c localization were all measured simultaneously in MCF7 cells.

CONCLUSION

Two species from family Lauraceae have been studied for their chemical constituents. They were *Lindera oxyphylla* (KL 5359) and *Litsea costalis* (Nees) Kosterm (KL 5410). Phytochemical studies of these two species from Lauraceae led to the isolation and structural elucidation of alkaloids, flavonoids, linderone, phenolic compounds, neolignan, oxyneolignan, aldehyde and benzamide as shown in (Table 5.1). Structural elucidation was established through several spectroscopic methods, notably UV, IR, MS (HRMS, GCMS, and LCMS), and 1D, 2D-NMR (^1H -NMR, ^{13}C NMR, COSY, DEPT, HMQC, HMBC, NOESY, and single crystal X-ray diffraction analysis. The bark of *lindera oxyphylla* yielded three flavanones, namely (+)-onysilin **LOB4**, (+)- pinostrobin **LOB7** and (+)-pinocenbrin **LOB2**; one chalcone, namely flavokawain B **LOB15** and two ketones, namely, 2-cinnamoyl-3-hydroxy-4,5-dimethoxycyclopenta-2,4-dienone or linderone **A LOB25** which is a new compound and known (*E*)-2-(1-hydroxy-3-phenylallylidene)-4,5-dimethoxycyclopent-4-ene-1,3-dione or linderone **LOB28**. Seven compounds have been isolated from the leaves of this species and these compounds were one flavanone, namely kaempferol **LOL34** and a ketone, (*E*)-4,5-dimethoxy-2-(1-methoxy-3-phenylallylidene)cyclopent-4-ene-1,3-dione or methylinderone **LOL18**, and five aporphine alkaloids, namely (+)-laurotetanine **LOL20**, *N*-methyllaurotetanine **LOL35**, (+)-norboldine **LOL50**, (+)-10-O-methylhernovine **LOL63** and (+)-norisoboldine **LOL65**. nine compounds have been isolated from the bark of *Litsea costalis* (Nees) Kosterm and these compounds were 3, 4-dimethoxycinnamaldehyde **LCB7**, 2-hydroxy-5-methoxybenzaldehyde **LCB11**, 2, 5-dimethoxybenzaldehyde **LCB15**, 4,4'-diallyl-6,6'-dimethoxy-[1,1'-biphenyl]-2,2'-diol **LCB9**, 4,4'-diallyl-5,5'-dimethoxy-[1,1'-biphenyl]-2,2'-diol **LCB3** which is a new compound and belongs to neolignin group of compound and

named biseugenol A, 2, 2'-oxybis (4-allyl-1-methoxybenzene) **LBC10** which is a new from lignan group of compound and named biseugenol B, 1,2-bis (5-allyl-2-methoxyphenyl)hydrazine **LCB17** which is a new compound and named as biseugenol C, (*E*)-4(4-hydroxy-1, 1-dimethoxybut-2-en-1-yl) benzene-1, 2-diol **LCB4** which is also a new compound and named litsin and (*E*)-4-styrylphenol **LCB58**. eight compounds have been isolated from the leaves of this species and these compounds were cinnamide **LCL4**, 2,4-dimethoxybenzamide **LCL2**, 3,4-dimethoxybenzamide **LCL5**, 4-allyl-1, 2-dimethoxybenzane **LCL15**, 2*S*,4*S*-2-(3',4'-methylenedioxyphenyl)-5,7-dimethoxy chroman -4-ol **LCL7** which is a new compound which belongs to chroman group of compound and named costalin, (+)- pinostrobin **LCL9**, (+)-onysilin **LCL13** and (+)-pinocenbrin **LCL14**.

These constituents showed interesting biological bioactivities such as antioxidant and cytotoxicity activities. The results showed the IC₅₀ values for DPPH assay from compounds of *Lindera oxyphylla*, flavokawain B **LOB15** (+)-onysilin **LOB4** was, (+)-pinocenbrin **LOB2**, linderone **LOB28** and linderone **ALOB25** were 8.5, 78.97, 41.32, 157.58 and 149.45 µg/mL, respectively.

The IC₅₀ for DPPH assay for compounds from *Litsea costalis* (Nees) Kosterm showed that IC₅₀ for biseugenol C **LCB17** was 16.34 µg/mL, 2,5-dimethoxybenzaldehyde **LCB15** was 161.81 µg/mL, biseugenol B **LCB10** was 81.92 µg/mL, 2-hydroxy-5-methoxy benzaldehyde **LCB11** was 81.92 µg/mL, biseugenol A **LCB3** was 4.77 µg/mL, 3,4-dimethoxycinnamaldehyde **LCB7** was 73.24 µg/mL, litsin **LCB4** was 26.69 µg/mL and costalin **LCL7** was 76.45 µg/mL. Ascorbic acid was used as positive control and exluted value IC₅₀ of 4.62 µg/mL.

The **FRAP** experiments for the isolated compounds from *Lindera oxyphylla* showed that the absorbance of flavokawain B **LOB15** was 1.0 ± 0.06, (+)-onysilin **LOB4** was 0.7 ± 0.02, (+)-pinocenbrin **LOB2** was 0.6 ± 0.01, linderone **LOB28** was

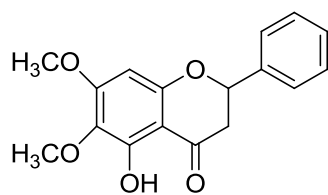
0.5 ± 0.02 and linderone A **LOB25** was 0.5 ± 0.03 .

Metal Chelating assay for the isolated compounds showed that the Inhibition % of *Lindera oxyphylla*, flavokawain B **LOB15** was 25.69 ± 0.01 , (+)-Onysilin **LOB4** was 26.11 ± 0.01 , (+)-pinocenbrin **LOB2** was 33.37 ± 0.01 , linderone **LOB28** was 13.09 ± 0.006 and linderone A **LOB25** was 13.51 ± 0.01 .

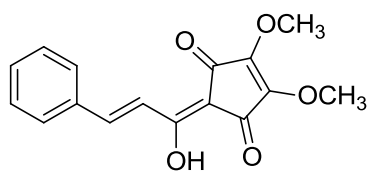
The **Anti Cancer** study showed mild cytotoxicity against various cancer cell lines; MCF-7 was $79.57 \mu\text{g/mL}$ for flavokawain B **LOB15**, PC3 was 30.12 , A549 was 65.03 and MCF-7 was 47.67 for (+)-onysilin **LOB4**, PC-3 was 90.13 for (+)-pinocenbrin **LOB2** and MCF-7 was 96.33 for **LOB25**. These constituents showed interesting biological bioactivities such as antioxidant and cytotoxicity activities *Litsea costalis*; **Anti Cancer**: showed mild cytotoxicity against various cancer cell lines; MCF-7 was 48 ± 3.05 and HEPG2 was 18 ± 2.1 for biseugenol A **LCB3**, WRL68 was 81.73 ± 3.7 , PC3 was 1.19 ± 0.19 and A549 was 85.13 ± 7.3 for , biseugenol B **LCB10**, MCF-7 was 34.65 ± 0.1 for Litsin **LCB4**, MCF-7 was 1.4 ± 0.1 , HEPG2 was 1.00 ± 0.1 , HT29 was 1.32 ± 0.1 and Jurkat was 1.22 ± 0.1 for biseugenol C **LCB17**.

Table 5.1: Chemical constituent from *Lindera oxyphylla* and *Litsea costalis*

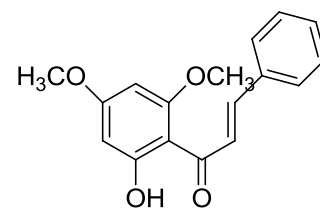
Species	Part of Plants	Remark	Types of skeleton
<i>Lindera oxyphylla</i> (KL 5359)	Bark	(+)-Onysilin 4	Flavanone
		Linderone 28	Linderone
		Flavokawain B 15	Chalcone
		Linderone A 25	Linderone
		(+)-Pinocenbrin 2	Flavanone
		(+)-pinostrobin 7	Flavanone
	Leaves	Methyl Linderone 34	Linderone
		Kaempferol 5	Flavonol
		(+)- laurotetanine 20	aporphine
		N-Methylaurotetanine 35	aporphine
		(+)- norboldine 50	aporphine
		(+)-10-O-N-methylhernovine 63	aporphine
		(+)- norisoboldine 65	aporphine
<i>Litsea costalis</i> (KL 5410)	Bark	3, 4-dimethoxycinnamaldehyde 7	Aldehyde
		2-hydroxy-5-methoxy benzaldehyde 11	Aldehyde
		2, 5-dimethoxybenzaldehyde 15	Aldehyde
		4,4'-diallyl-6,6'-dimethoxy-[1,1'-biphenyl] -2,2'-diol (biseugenol) 9	neolignan
		4,4'-diallyl-5,5'-dimethoxy-[1,1'-biphenyl] -2,2'-diol (biseugenol A) 3	neolignan
		2,2'-oxybis(4-allyl-1-methoxy benzene) (biseugenol B) 10	Oxyneolignan
		1,2-bis(5-allyl-2-methoxyphenyl) hydrazine (biseugenol C) 17	Hydrazine
		(E)-4(4-hydroxy-1, 1-dimethoxybut-2-en-1-yl) benzene-1, 2-diol (Litsin) 4	Phenolic Compound
		4-Hydroxystibene 58	Stilbene
		Cinnamide 4	Amide
	Leaves	2,4-dimethoxybenzamide 2	Benzamide
		3,4- dimethoxybenzamide 5	Benzamide
		2S,4S-2-(3',4'-methylenedioxyphenyl)-5,7-dimethoxychroman-4-ol (Costalin) 7	Flavonoid
		(+)-Pinocenbrin 9	Flavanone
		4-allyl-1,2-dimethoxybenzane 15	Lignan
		(+)-Pinostrobin 14	Flavonoid
		(+)-Onysilin 13	Flavonoid
		4-allyl-2methoxyphenol 17	Lignan



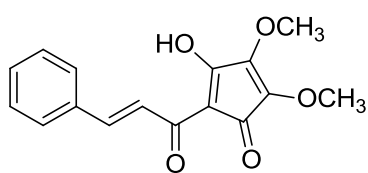
LOB4



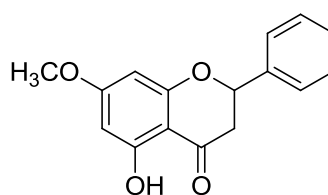
LOB28



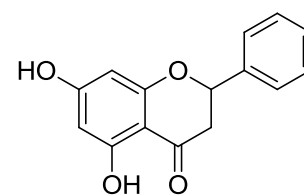
LOB15



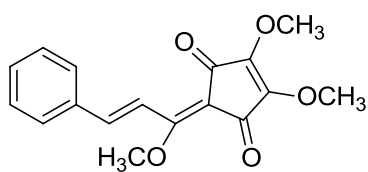
LOB25



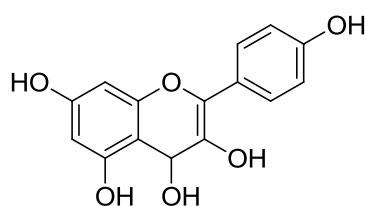
LOB2



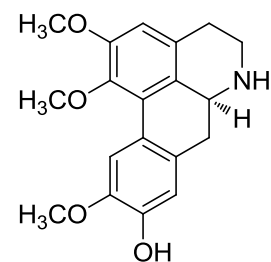
LOB7



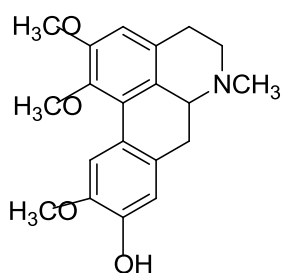
LOL34



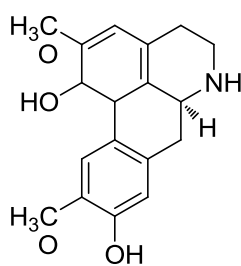
LOL5



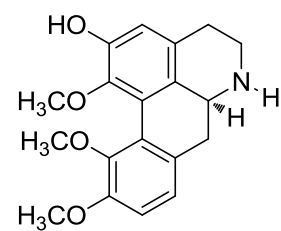
LOL20



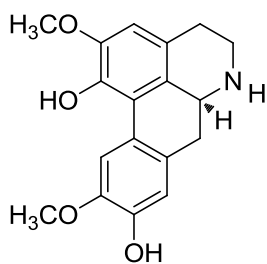
LOL35



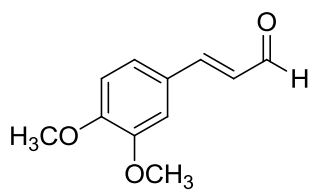
LOL50



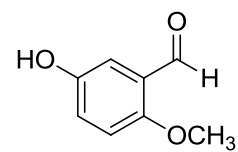
LOL63



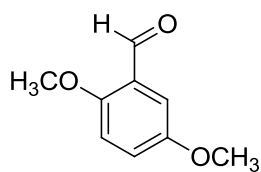
LOL65



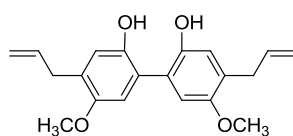
LCB7



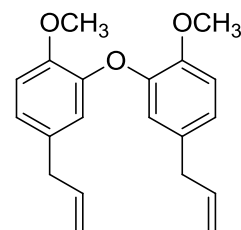
LCB11



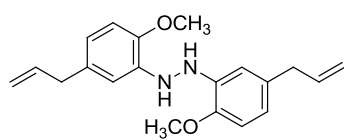
LCB15



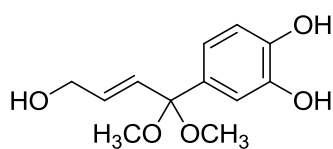
LCB3



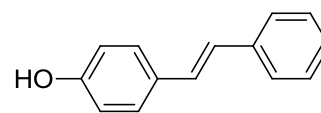
LCB10



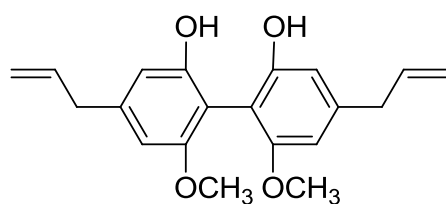
LCB17



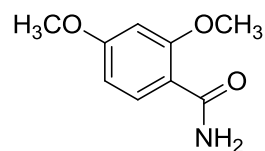
LCB4



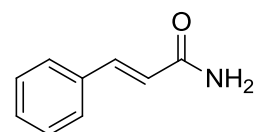
LCB58



LCB9



LCL4



LCL2

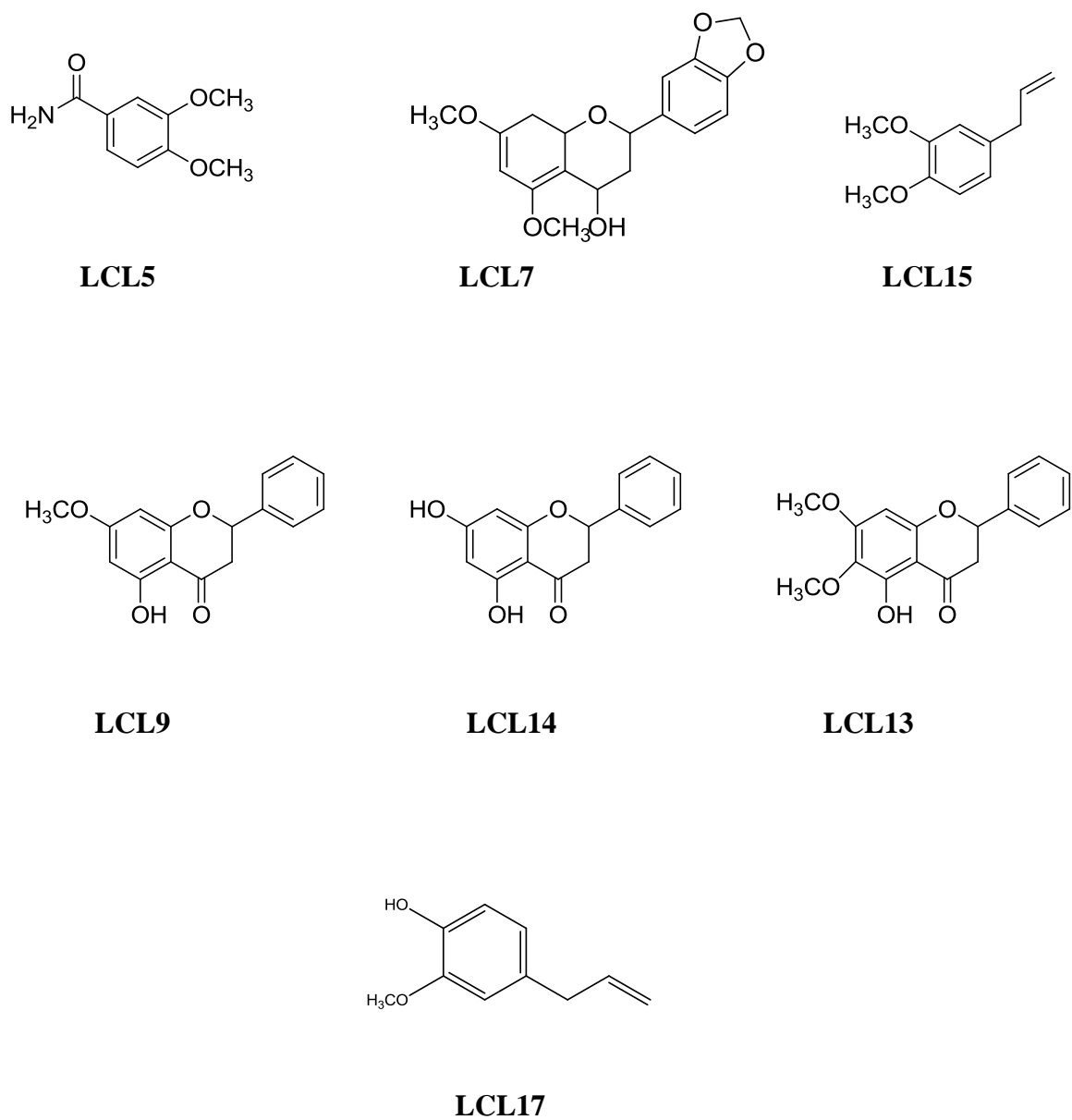


Figure 5.1: Submitted structures of chemical constituents from two genera

EXPERIMENTAL

6.1 Solvents

Industrial grade solvents were used for extraction and these solvents were distilled twice before use. Analytical grade solvents were used for chromatographic separation of the compounds. HPLC grade solvent were used for high performance liquid chromatography analysis.

Chemicals used for antioxidant assay were DPPH (1,1' diphenyl-2-picrylhydrazyl), trichloroacetic acid, sodium phosphate monobasic, sodium phosphate dibasic, ascorbic acid, potassium ferricyanide, ferrozine and ethylenediamine tetraacetic acid were purchased from Sigma Chemical Co. (St. Louis, MO, USA). Ferric chloride and methanol were purchased from Chemolab Supplies (Kuala Lumpur, Malaysia).

6.2 Instruments

Melting points were taken on hot stage Gallen Kamp melting point apparatus and uncorrected.

Compact hot plate stirrer with a Ceran top plate of 135x135mm and heating from 40-400 °C. The brushless DC motor enables precise speed control from 80-1600 rpm.

UV spectra were obtained using Shimadzu UV-160 Ultraviolet-Visible Spectrometer. Solvent used was methanol (CH₃OH) while the wavelength in which the spectrum was recorded is 200-700 nm.

IR spectra were obtained with CHCl₃ on a Perkin Elmer Spectrum 2000-FTIR Spectrometer.

Optical rotations were determined on JASCO (Japan) P1000 automatic digital polarimeter.

The mass spectra were measured on a JMS 700 spectrometer using NBA as the

matrix for FAB analysis. The Automass Thermofinnigan was used for HRESI⁺ and ESI⁻ analysis. The EIMS spectra were obtained on Shimadzu GC-MS QP2000A spectrometer 70 eV.

The NMR (¹H, ¹³C and 2D) spectra were recorded in deuterated chloroform on JEOL JNM-FXIOO (400 MHz). Chemical shifts were reported in ppm and the coupling constants were given in Hz.

6.3 Chromatography

6.3.1 Thin Layer Chromatography (TLC)

Aluminum supported silica gel 60F 254 TLC sheets (Merck 1.05554.0001); glass ported silica gel 60F254 TLC plates (Merck 1.05715.0001) were used for TLC. Fractions were monitored by TLC profiling and appropriate fractions were combined and when necessary subjected to further separation by chromatographic technical TLC. TLC was routinely used to detect and separate the various alkaloids. The alkaloid spots were visualized under UV light (254 and 365 nm), followed by spraying with Dragendorff's reagent which gave orange colour.

6.3.2 Column chromatographic

Silica gel 60F, 70-230 mesh ASTM (Merck 7734) and silica gel 60F, 230-400 mesh ASTM (Merck 9385) were used for column chromatography.

A slurry of silica gel 60 (approximately 30:1 silica gel to sample ratio) in solvent was poured into a glass column with gentle tapping to remove the trapped air bubbles. The crude extract was dissolved in a minimum amount of solvent and loaded on the top of packed column. The extract was eluted with appropriate solvent system at a certain flow rate and the fraction was collected using 10 mL test tubes. Fractions with the same TLC profiling were combined and evaporated to dryness.

6.3.3 High Performance Liquid Chromatography (HPLC)

Waters HPLC System was used for HPLC separation, equipped with Binary Gradient Module, System Fluidics Organizer and UV detector set at the range from 200-400 nm. Chromatographic analysis and separations were performed supelco (15 cm x 10 mm x 5µm) HPLC columns. HPLC grade methanol and deionized water were used as mobile phase solvents with HPLC grade formic acid as buffer. All solvents and samples were filtered with 0.45 µm nylon membrane filter (Waters) prior to HPLC analysis. The data were collected and analysed by using MassLynx software.

6.4 Plant Materials

The plant materials were collected and identified by phytochemical team, Chemistry Department, Faculty of Science, University of Malaya. The specimens were deposited at the Chemistry Herbarium, Faculty of Science, University of Malaya. The locality and the times of collection are shown in the (Table 6.1).

Table 6.1: Yield of crude extracted from *Lindera oxyphylla* and *Litsea costalis* (Nees) Kosterm (Lauraceae)

Species	Herbarium Specimen Number	Location and Date of collection	Part of plant	Weight of crude extract (g)	% Yield
<i>Lindera oxyphylla</i> (Lauraceae)	KL5359	Hutan Simpan Ulu Muda, Baling, Kedah 09/02/2007	Leaves (2.00 kg)	N-hexane, 5 g	0.25
				DCM, 2 g	0.1
				MeOH, 1 g	0.05
<i>Lindera oxyphylla</i> (Lauraceae)	KL5359	Hutan Simpan Ulu Muda, Baling, Kedah 09/02/2007	Bark (3.00 kg)	N-hexane, 13 g	0.43
				DCM, 1 g	0.03
				MeOH, 1 g	0.03
<i>Litsea costalis</i> (Nees) Kosterm (Lauraceae)	KL5410	Hutan Simpan Piah Lasah Sg, Siput, Perak 12/04/2007	Leaves (1.5kg)	N-hexane, 3 g	0.2
				DCM, 2 g	0.13
<i>Litsea costalis</i> (Nees) Kosterm (Lauraceae)	KL5410	Hutan Simpan Piah Lasah Sg, Siput, Perak 12/04/2007	Bark (2 kg)	n-Hexane, 5 g	0.25
				DCM, 10 g	0.5
				MeOH, 2 g	0.1

6.5 Reagents

Mayer's and Dragendorff's reagent were used for alkaloid screening and to detect the presence of alkaloids.

6.5.1 Mayer's reagent (Potassium mercuric iodide)

A solution of mercury (II) chloride (1.4 g) in distilled water (60 mL) was mixed into a solution of potassium iodide (5.0 g) in distilled water (10 mL). The mixture was then made up to 150 mL with distilled water. Positive result is indicated by the formation of white cloudy or precipitate.

6.5.2 Dragendorff's reagent (Potassium bismuth iodide)

Solution A: Bismuth (III) nitrate (0.85 g) in a mixture of glacial acid (10 mL) and distilled water (40 mL).

Solution B: Potassium iodide (8.0 g) in distilled water (20 mL) Stock solution:

A mixture of equal volumes of solution A and solution B. The stock solution (20 mL) was diluted in a mixture of acetic acid (20 mL) and distilled water (60 mL)

Dragendorff's test: Positive result is indicated by the formation of orange, yellow or red spots on TLC plate.

6.6 Extraction and Isolation

6.6.1 Extraction and isolation of *Lindera oxyphylla*.

The dried and ground bark of *Lindera oxyphylla* (KL5359), (3.0 kg) was extracted with n-hexane (10.0 L) for 72 hours followed by evaporation of solvent to give crude extract (13.0 g). The crude extracts were subjected to exhaustive column chromatography over silica gel using n-hexane/dichloromethane as a solvent system with ratio 100:0→0:100 to give 30 fractions. Fractions 1 to 4 were combined and the resulted compounds were separated using PTLC Merck KGaA silica gel 60 F₂₅₄; using N-hexane-dichloromethane; 98:2 as a solvent system to afford (+)-onysilin **LOB4** (50.0 mg; 0.4%). linderone **LOB28** (10.0 mg; 7.69%) was obtained from the combination of fraction 20 to 28 using n-hexane-dichloromethane; 80:20) as a solvent system.

The plant residue was dried and left to soak with CH₂Cl₂ (12.0 L) for 4 days followed by filtration and solvent evaporation to give crude extract (1.0 g). The crude extract was subjected to exhaustive column chromatography over silica gel using dichloromethane/ methanol as a solvent system with ratio 100:0→0:100 to give 25 fractions. Fraction 1 to 7 were combined and separated using PTLC Merck KGaA silica gel 60 F₂₅₄; using CH₂Cl₂:MeOH; 98:2 as a solvent system to afford (+)-pinostrobin

LOB7 (5.0 mg; 0.5 %), flavokawain B **LOB15** (5.0 mg, 0.5%) was obtained from fraction 8 to 15 using CH₂Cl₂:MeOH; 95:5 as a solvent system and linderone A **LOB25** (10.0 mg, 1.0%) was obtained from fraction 20 to 25 using CH₂Cl₂:MeOH; 92:8 as a solvent.

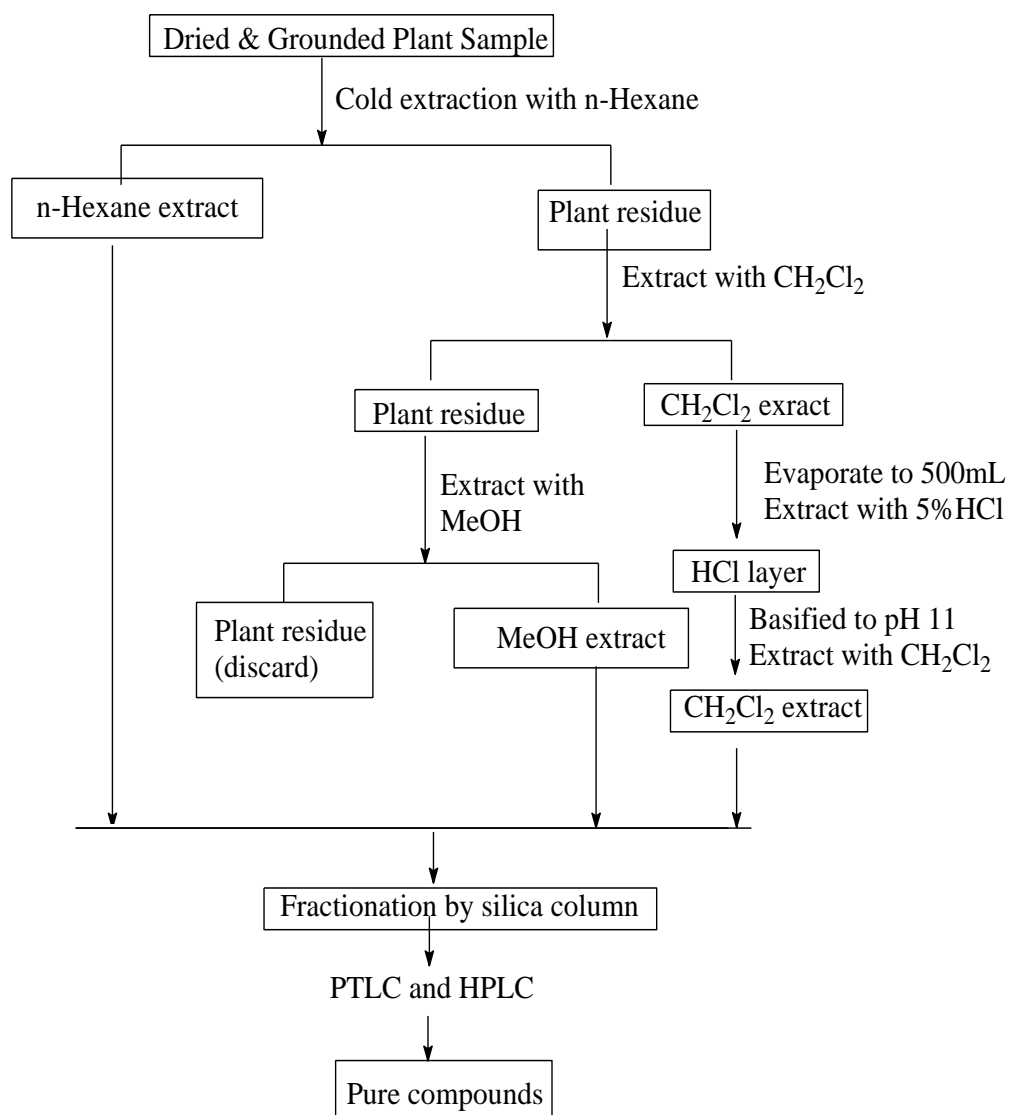
Plant residue was soaked with MeOH (12.0 L) for 4 days. The solvent was filtered and evaporated to give crude extract (1.0 g) . The crude extract was introduced into column chromatography over silica gel using CH₂Cl₂ and gradually enriched with methanol to give 3 fractions. Fraction 2 was further separated using PTLC and CH₂Cl₂:MeOH; 90:10 to afford (+) - pinocembrin **LOB2** (5.0 mg, 0.5%).

The air-dried and ground leaves (2.0 kg) of *Lindera oxyphylla* were extracted with n-hexane (10.0 L) for 72 hours followed by filtration and evaporation of solvent to give crude extract (5.0 g). The crude extract were subjected to exhaustive column chromatography over silica gel using dichloromethane/methanol as a solvent system with ratio 100:0→0:100 to give 35 fractions. Fraction 34 was separated using PTLC Merck KGaA silica gel 60 F₂₅₄; and CH₂Cl₂:MeOH; 98:2 as solvent system to afford methylinderone **LOL 34** (5.0 mg, 0.1%).

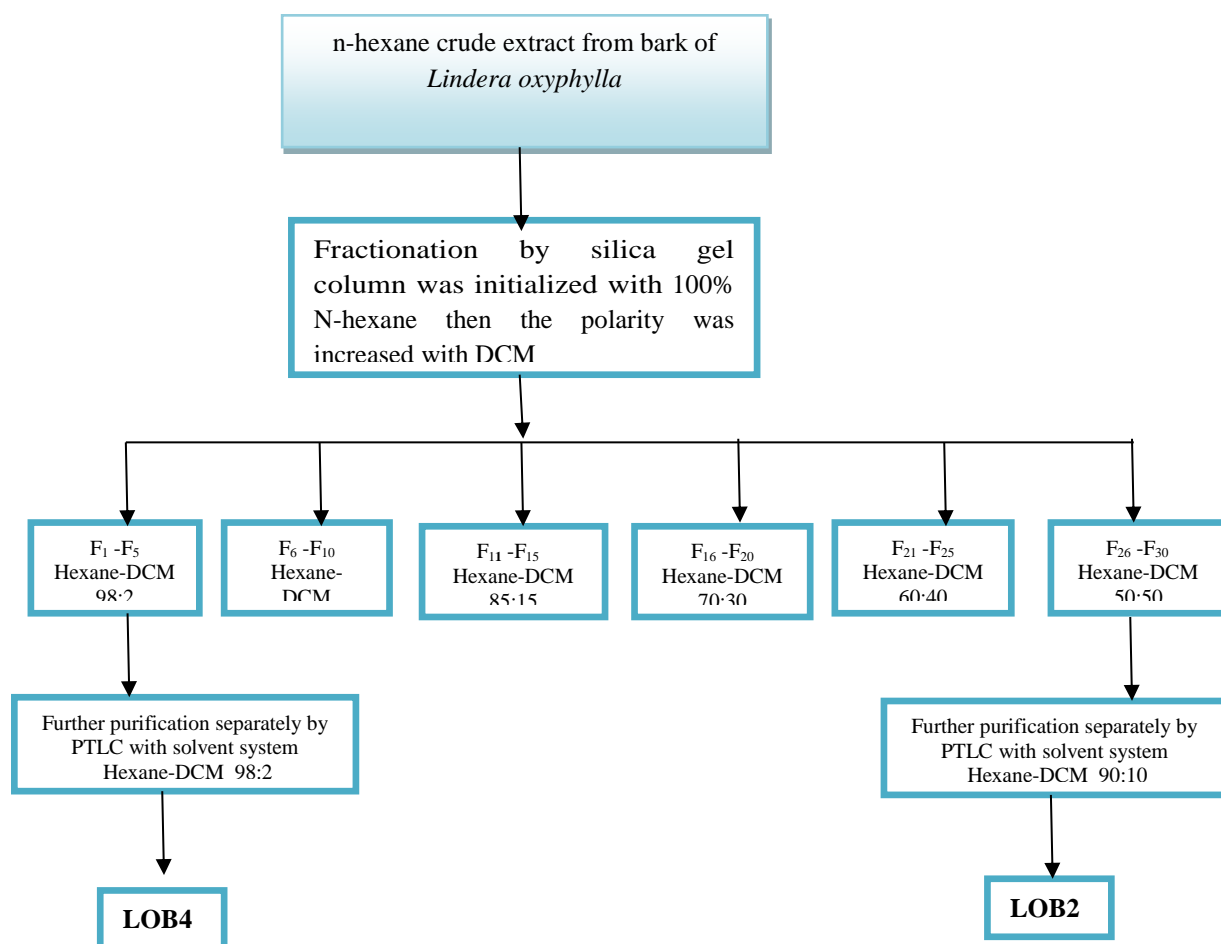
The residual plant material was dried and moistened with 10% NH₄OH and left for 4 hrs. before soaking with CH₂Cl₂ (12.0 L) for 4 days. After filtration, the supernatant was concentrated to 500 mL followed by acidic extraction with 5% HCl until a negative Mayer's test result was obtained. The aqueous solution was basified to pH 11 with NH₄OH and re-extracted with CH₂Cl₂. The CH₂Cl₂ extract was filtered, dried over anhydrous sodium sulphate, and evaporated to give crude alkaloid (2.0 g). The crude extract were subjected to exhaustive column chromatography over silica gel using dichloromethane/methanol as a solvent system with ratio 100:0→0:100 to give 65 fractions. Fraction 15 to 20 were combined and the resulted compounds was separated using PTLC Merck KGaA silica gel 60 F₂₅₄; and CH₂Cl₂-MeOH; 98:2 as a

solvent to afford (+)- laurotetanine **LOL20** (10.0 mg, 0.5%), N-methylaurotetanine **LOL35** (5 mg, 0.25%), was obtained from fraction, 30 to 35 using CH₂Cl₂-MeOH; 97:3 as a solvent and (+)-norboldine **LOL50** (10.0 mg, 0.5%) was obtained from fraction 49 to 50 using CH₂Cl₂-MeOH; 95:5 as a solvent. (+)-10-O-N-methylhernovine (+)-**LOL63** (10.0 mg, 0.5%), was obtained from fraction 62 to 63 using CH₂Cl₂-MeOH; 92:8 as a solvent and (+)-norisoboldine **LOL65** (5.0 mg, 0.025%), was obtained from fraction 64 to 65 using CH₂Cl₂-MeOH; 92:8 as a solvent.

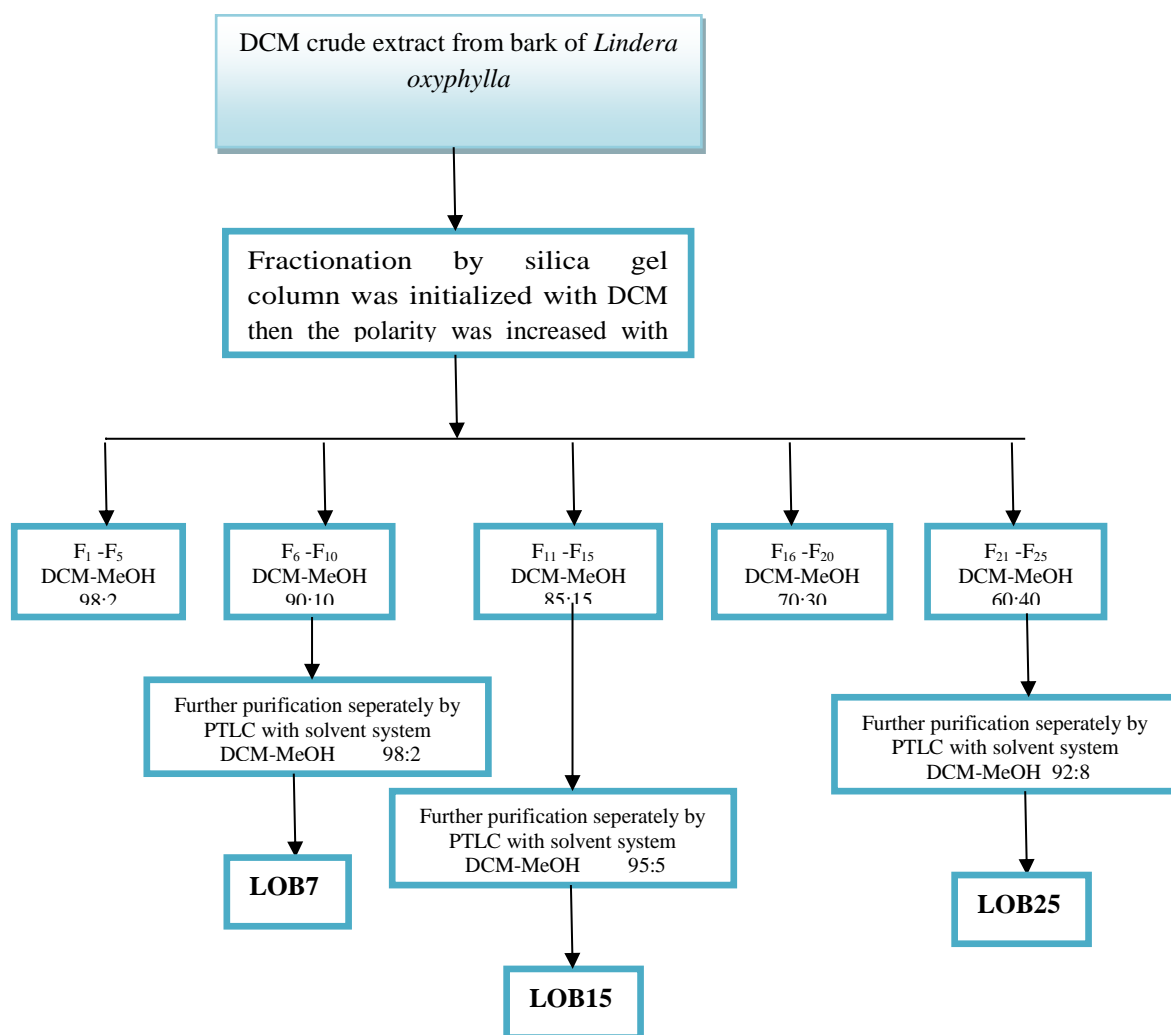
Plant residue was soaked with MeOH (12.0 L) for 4 days. The solvent was filtered and evaporated to give crude extract (1.0 g) . The crude extract was introduced into column chromatography over silica gel using CH₂Cl₂ gradually enriched with methanol to give 18 fractions. Fraction 5 was separated using PTLC and CH₂Cl₂-MeOH; 98:2 to afford kaempferol **LOL5** (1.0 mg, 0.1%).



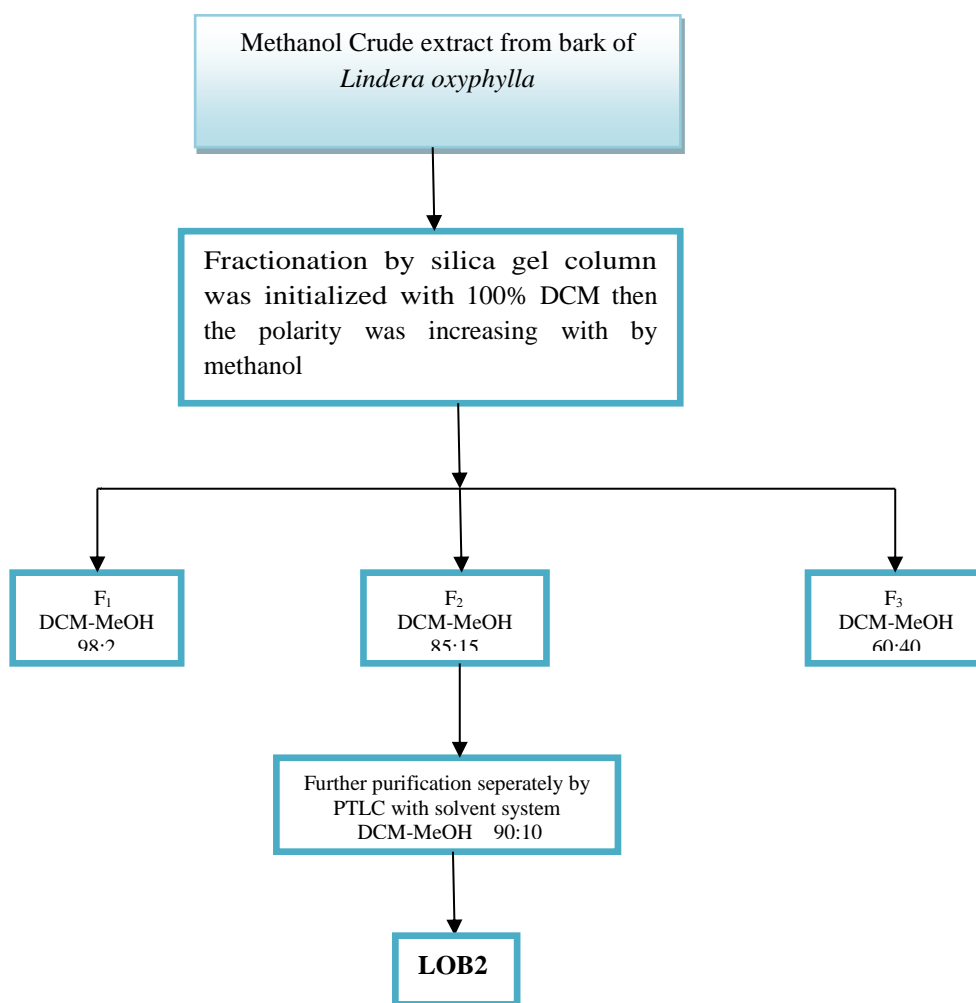
Scheme 6.1: Isolation and purification of chemical constituents from plant



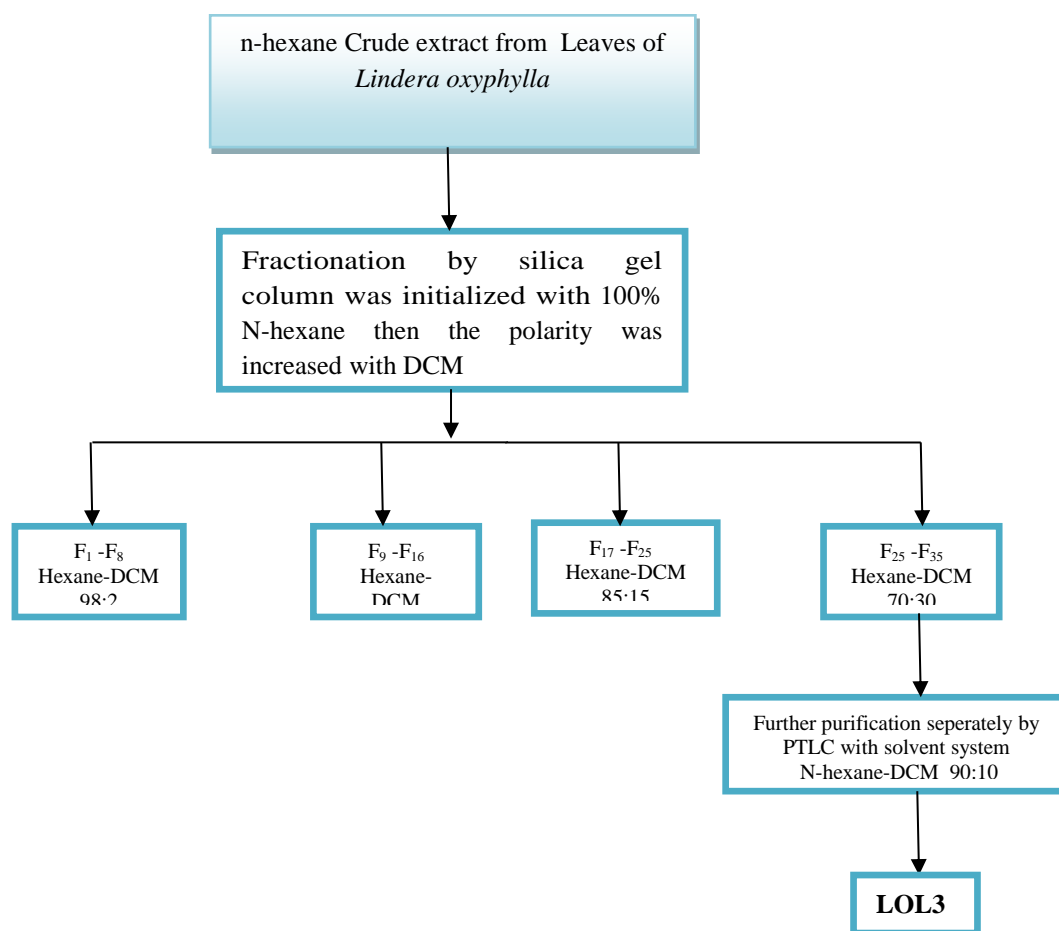
Scheme 6.2: Isolation and purification of chemical constituents from N-hexane crude extract of *Lindera oxyphylla* (bark)



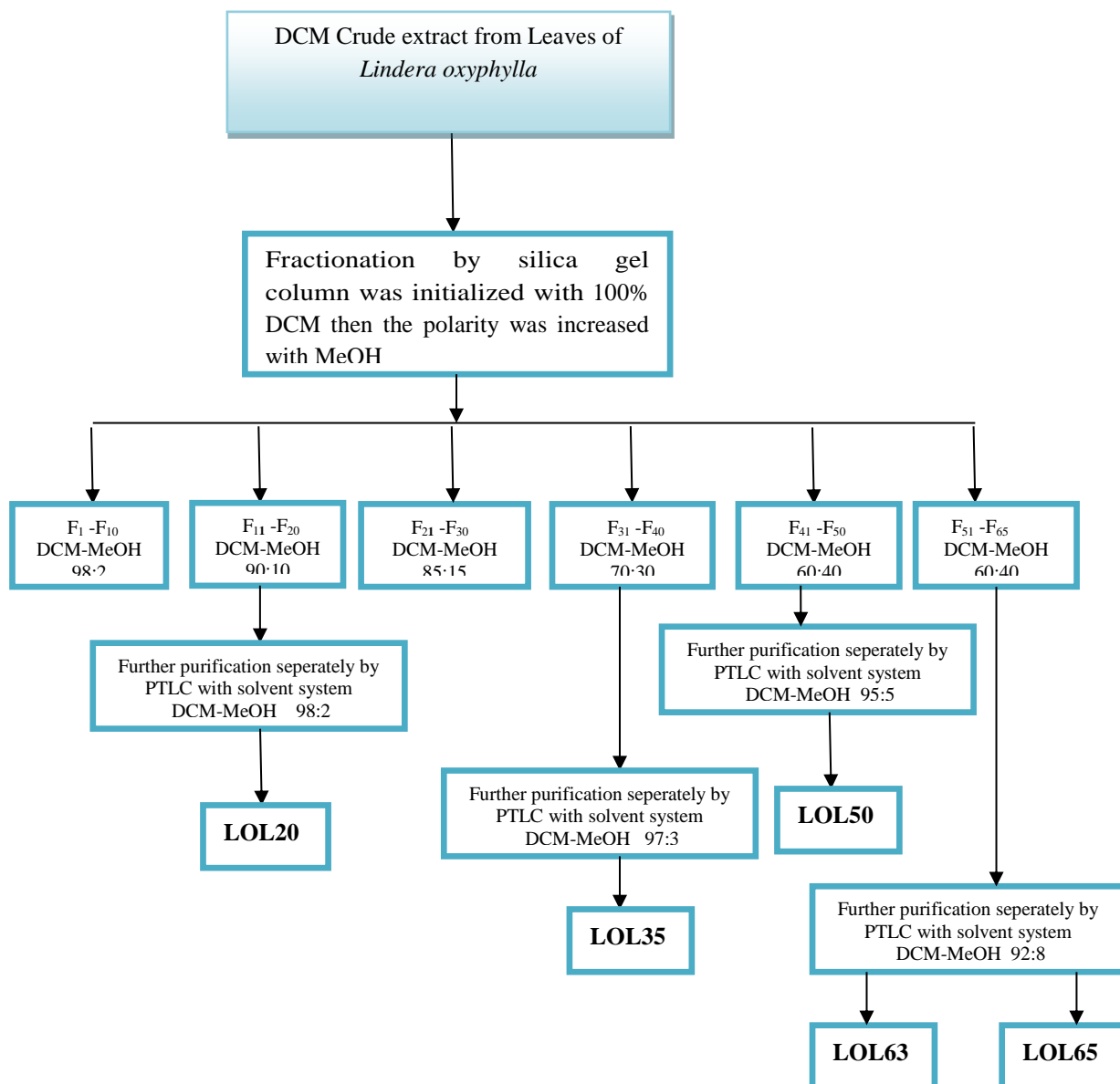
Scheme 6.3: Isolation and purification of chemical constituents from dichloromethane crude extract of *Lindera oxyphylla* (bark)



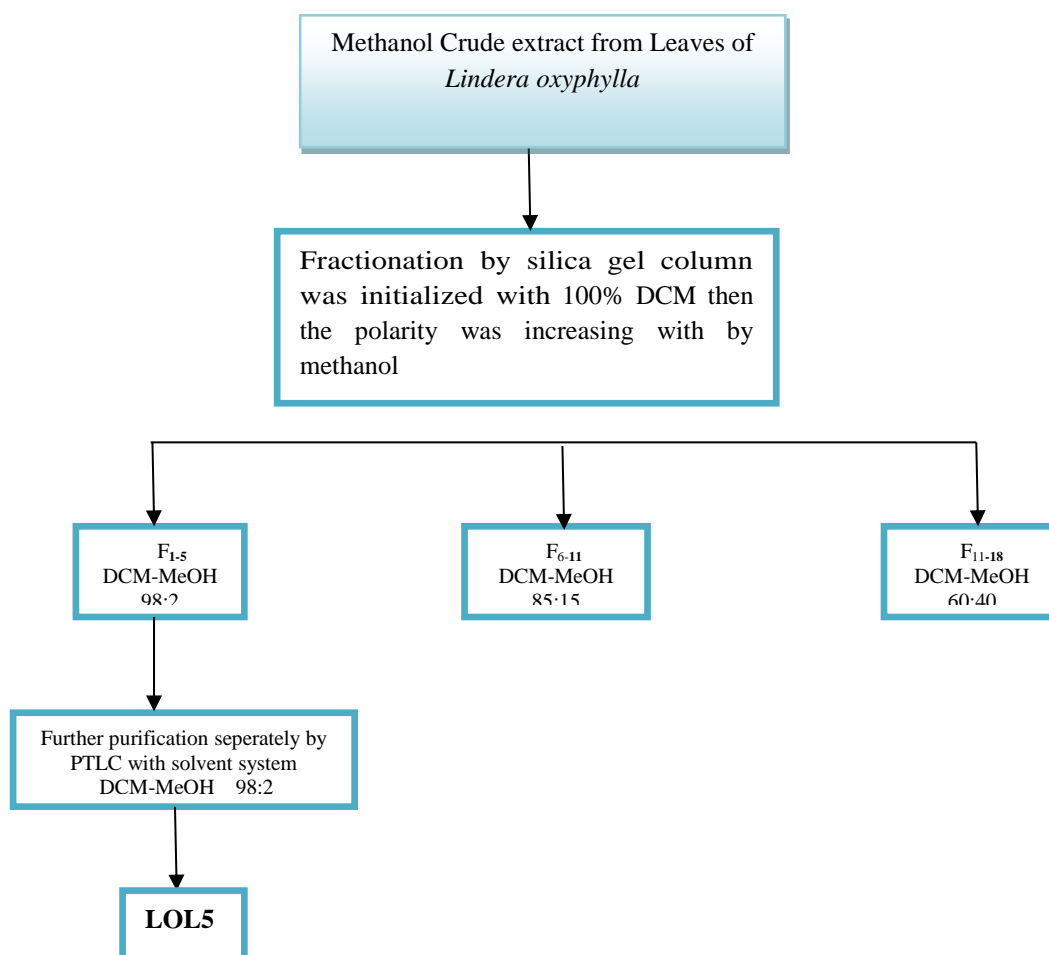
Scheme 6.4: Isolation and purification of chemical constituents from methanol crude extract of *Lindera oxyphylla* (bark)



Scheme 6.5: Isolation and purification of chemical constituents from N-hexane crude extract of *Lindera oxyphylla* (leaves)



Scheme 6.6: Isolation and purification of chemical constituents from dichloromethane crude extract of *Lindera oxyphylla* (leaves)



Scheme 6.7: Isolation and purification of chemical constituents from methanol crude extract of *Lindera oxyphylla* (leaves)

6.6.2 Extraction and isolation of *Litsea costalis* (Nees) Kosterm

The dried and ground bark of *Litsea costalis* (Nees) Kosterm (KL 5410), (2.0 kg) was extracted with n-hexane (10.0 L) for 72 hours followed by solvent evaporation to give crude extract (5.0 g). The crude extract was then subjected to exhaustive column chromatography over silica gel using n-hexane/dichloromethane as a solvent system with ratio 100:0→0:100 to give 15 fractions. Fractions 1 to 5 were combined and were separated using PTLC Merck silica gel 60 F₂₅₄; using N-hexane-dichloromethane; 95:5 as a solvent system to afford cinnamaldehyde **LCB7** (7.0 mg; 0.35 %). 2-Hydroxy-5-methoxybenzaldehyde **LCB11** (2.0 mg; 0.04 %) was obtained from fraction, 6 to 10 using n-hexane;dichloromethane; 90:10 as a solvent system and 2, 5-dimethoxybenzaldehyde **LCB15** (5.0 mg; 0.1 %) was obtained from fraction, 11 to 15 using n-hexane;dichloromethane; 90:10.

The residual plant material was dried and moistened with 10% NH₄OH and left for 4 hours. before soaking with CH₂Cl₂ (12.0 L) for 4 days. After filtration, the supernatant was concentrated to 500 mL followed by acidic extraction with 5% HCl until a negative Mayer's test result was obtained. The aqueous solution was basified to pH 11 with NH₄OH and re-extracted with CH₂Cl₂. The CH₂Cl₂ extract was filtered, dried over anhydrous sodium sulphate, and evaporated to give crude alkaloid (10.0 g). The crude extract were subjected to exhaustive column chromatography over silica gel using dichloromethane/methanol as solvent system with ratio 100:0→0:100 to give 20 fractions. Fraction 1 to 3 were combined separated using PTLC Merck KGaA silica gel 60 F₂₅₄; and CH₂Cl₂;MeOH; 98:2 as a solvent system to afford 4,4'-diallyl-5,5'-dimethoxy-(1,1'-biphenyl)-2,2'-diol or biseugenol A **LCB3** (10.0 mg, 0.5%) was obtained from fractions 10 to 17 and give three mix compounds and were separated using HPLC (70% MeOH and 30% H₂O aqueous with 0.1% formic acid, 3.0 ml/min, 254 nm) to give pure compounds, 4,4'-diallyl-6,6'-dimethoxy-(1,1'-biphenyl)-2,2'-diol

or biseugenol **LCB9** (50 mg, 10.0%), 2,2'-oxybis(4-allyl-1-methoxybenzene), biseugenol B **LCB10** (3000 mg, 30%), and 1,2-bis(2-allyl-6-methoxyphenyl) hydrazine, biseugenol C **LCB17** (3000 mg, 30%).

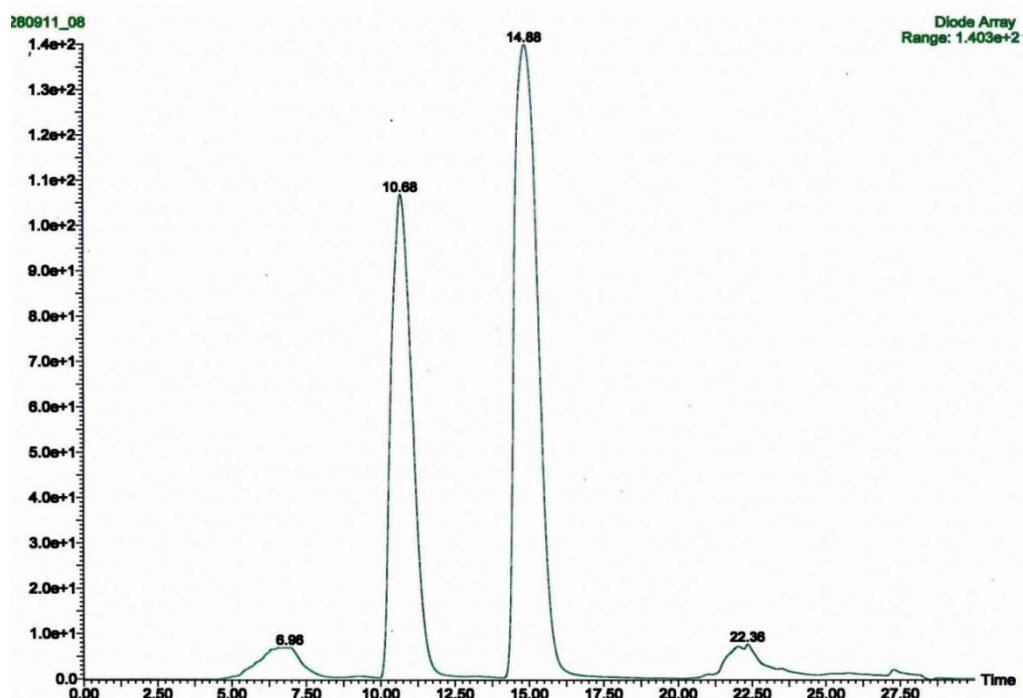


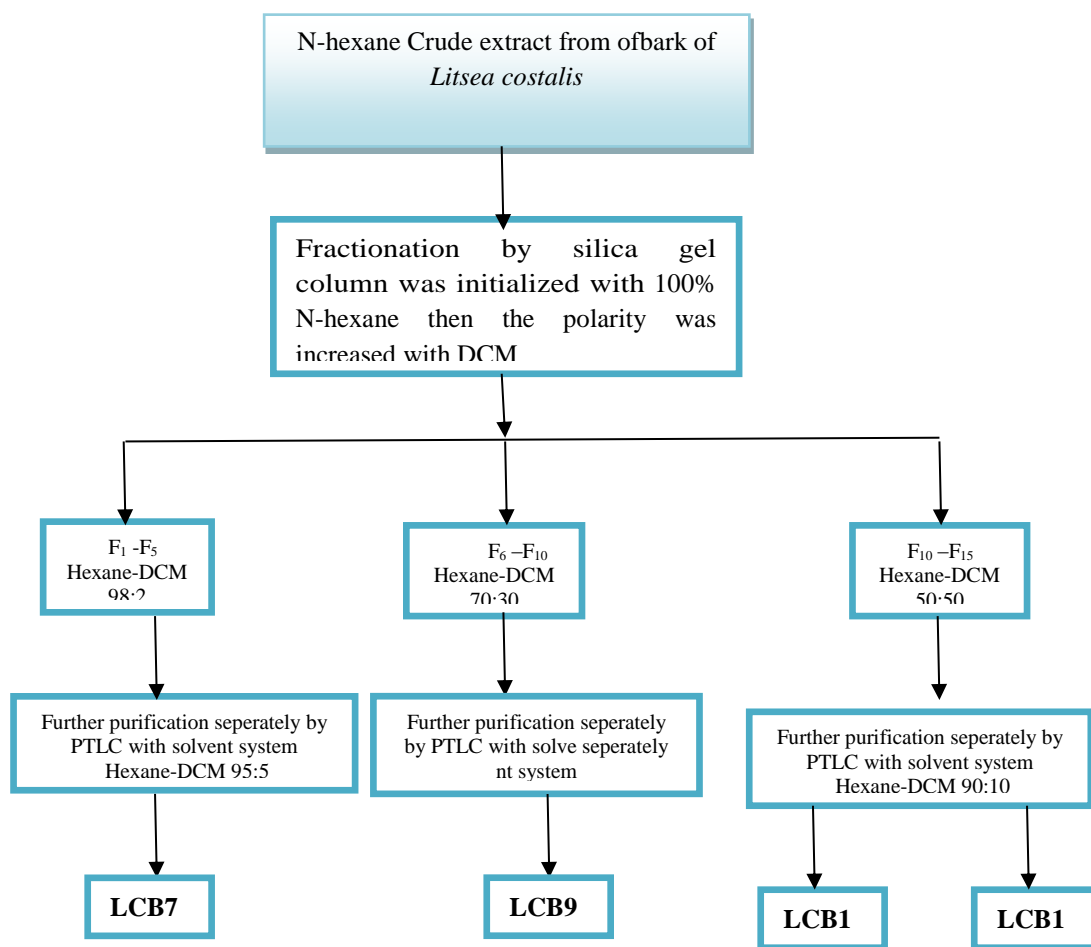
Figure 6.1: HPLC spectrum of **LCB10** and **LCB17**.

Plant residue was soaked with MeOH (12.0 L) for 4 days. The solvent was filtered and evaporated to give crude extract (2.0 g). The crude extract was introduced into column chromatography over silica gel using CH₂Cl₂ gradually enriched with methanol to give 60 fractions. Fractions 1 to 4 were combined and separated using PTLC and CH₂Cl₂;MeOH; 98:2 to afford (*E*)-4(4-hydroxy-1,1-dimethoxybut-2-en-1-yl)benzene-1, 2-diol, litsin **LCB4** (50 mg 0.5%). mean white, (*E*)-4-styrylphenol **LCB58** (5.0 mg, 2.5%) was obtained from fractions 50 to 58 using CH₂Cl₂;MeOH; 90:10 as a solvent system.

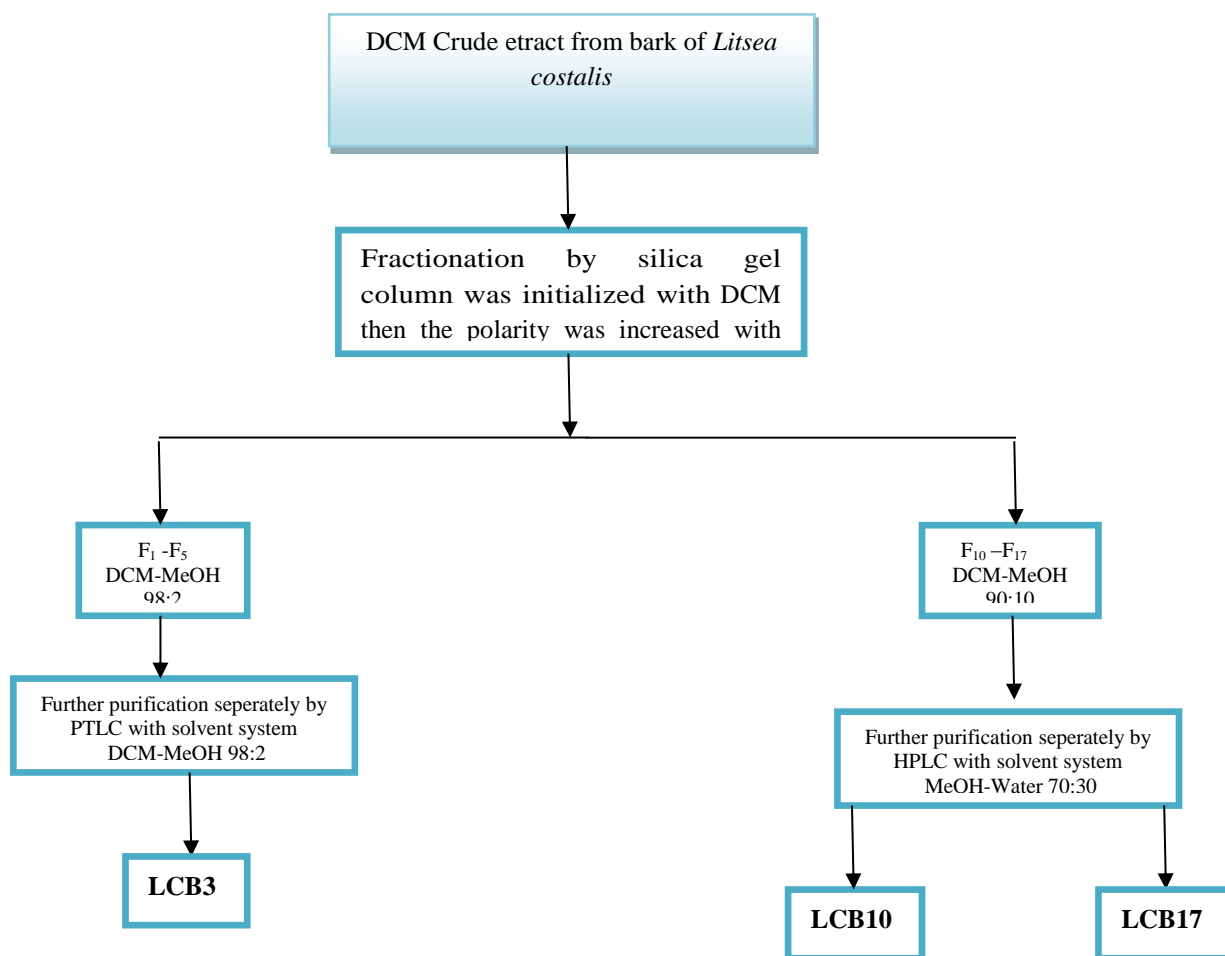
The dried and ground leaves of *Litsea costalis* (Nees) Kosterm (KL 5410), (1.5 kg) was extracted with n-hexane (10.0 L) for 72 hours followed by solvent evaporation to give crude extract (3.0 g). The crude extract was then subjected to exhaustive

column chromatography over silica gel using n-hexane/dichloromethane as a solvent system with ratio 100:0→0:100 to give 5 fractions. Fractions 1 to 2 were combined and separated using PTLC Merck KGaA silica gel 60 F₂₅₄; and n-hexane-dichloromethane; 98:2 as a solvent system to afford 2,4-dimethoxybenzamide **LCL2** (2.0 mg, 0.1%). Cinnamaldehyde **LCL4** (2.0 mg, 0.1%) was obtained from fraction 4 using n-hexane-dichloromethane; 95:5 as eluting solvent system and 3,4-dimethoxybenzamide **LCL5** (2.0 mg, 0.1%) was obtained from fraction 4 to 5 using n-hexane- dichloromethane; 90:10.

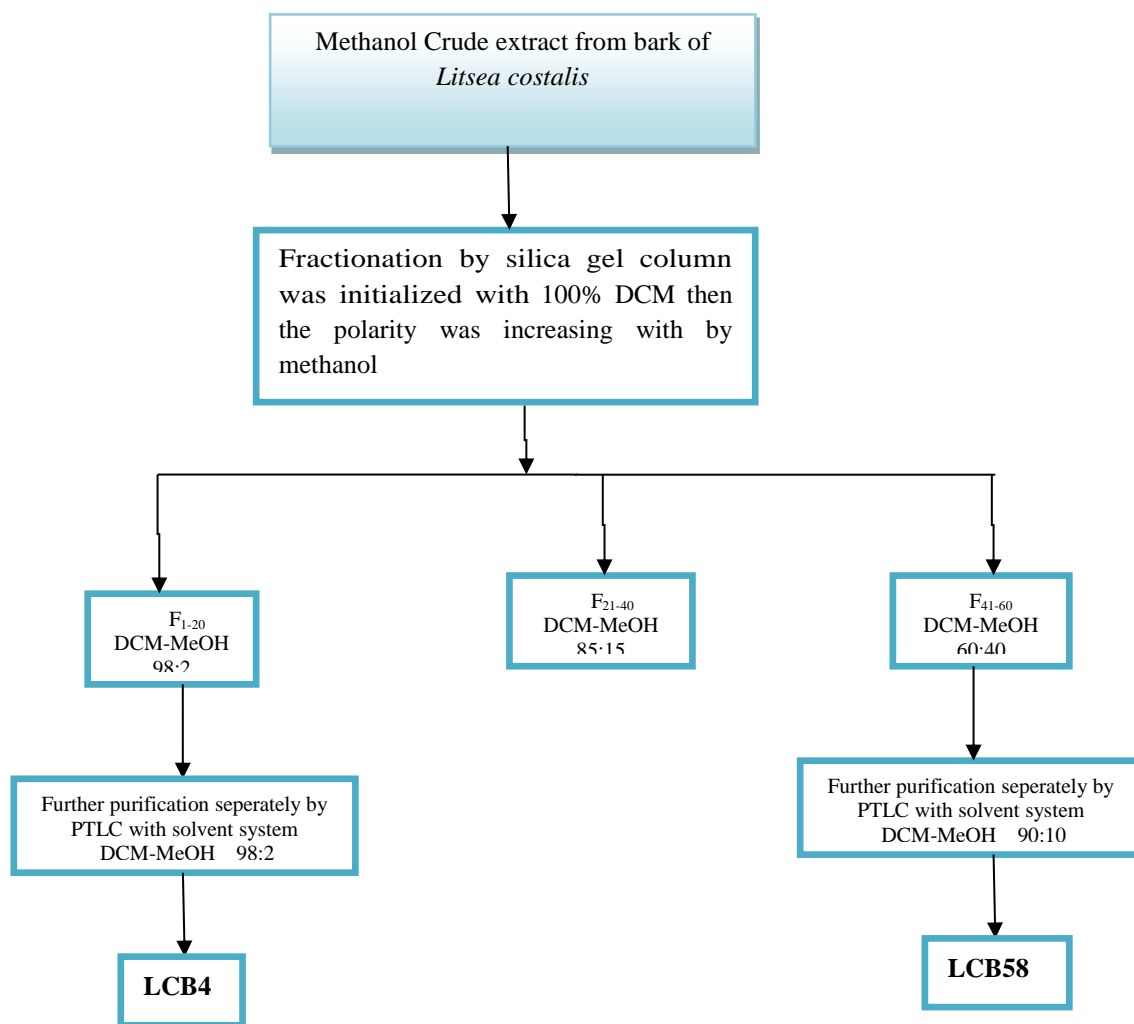
The residual plant soaking CH₂Cl₂ (12.0 L) for 4 days. After filtration re-extracted with CH₂Cl₂. The CH₂Cl₂ extract was filtered, dried over anhydrous sodium sulphate, and evaporated to give crude extract (2.0 g). The crude extract was subjected to column chromatography over silica gel using dichloromethane/ methanol a solvent system with ratio 100:0→0:100 to give 15 fractions. Fractions 5 to 7 were combined and the resulted compounds are separated using PTLC Merck KGaA silica gel 60 F₂₅₄; and CH₂Cl₂-MeOH; 98:2 as eluting solvent system to afford 2*S*,4*S*-(3',4'-methylenedioxyphenyl)-5,7-dimethoxychroman-4-ol, costalin **LCL7** (50 mg, 25%), (+)-pinostrobin **LCL9** (5.0 mg, 0.25%) was obtained from fractions 8 to 9 using CH₂Cl₂;MeOH; 97:3 as a solvent , 4-allyl-1,2-dimethoxybenzane **LCL15** (3.0 mg, 0.15%), (+)-onysilin **LCL13** (3.0 mg; 0.15 %) was obtained from fractions 10 to 13 using CH₂Cl₂;MeOH; 96:4 as a solvent , (+)-pinocembrin **LCL14** (3.0 mg, 0.15%) was obtained from fraction 14 using CH₂Cl₂;MeOH; 95:5 as a solvent and 4-allyl -2-methoxyphenol **LCL17** (3.0 mg, 0.15%) was obtained from fraction 15 using CH₂Cl₂;MeOH; 95:5 as a solvent.



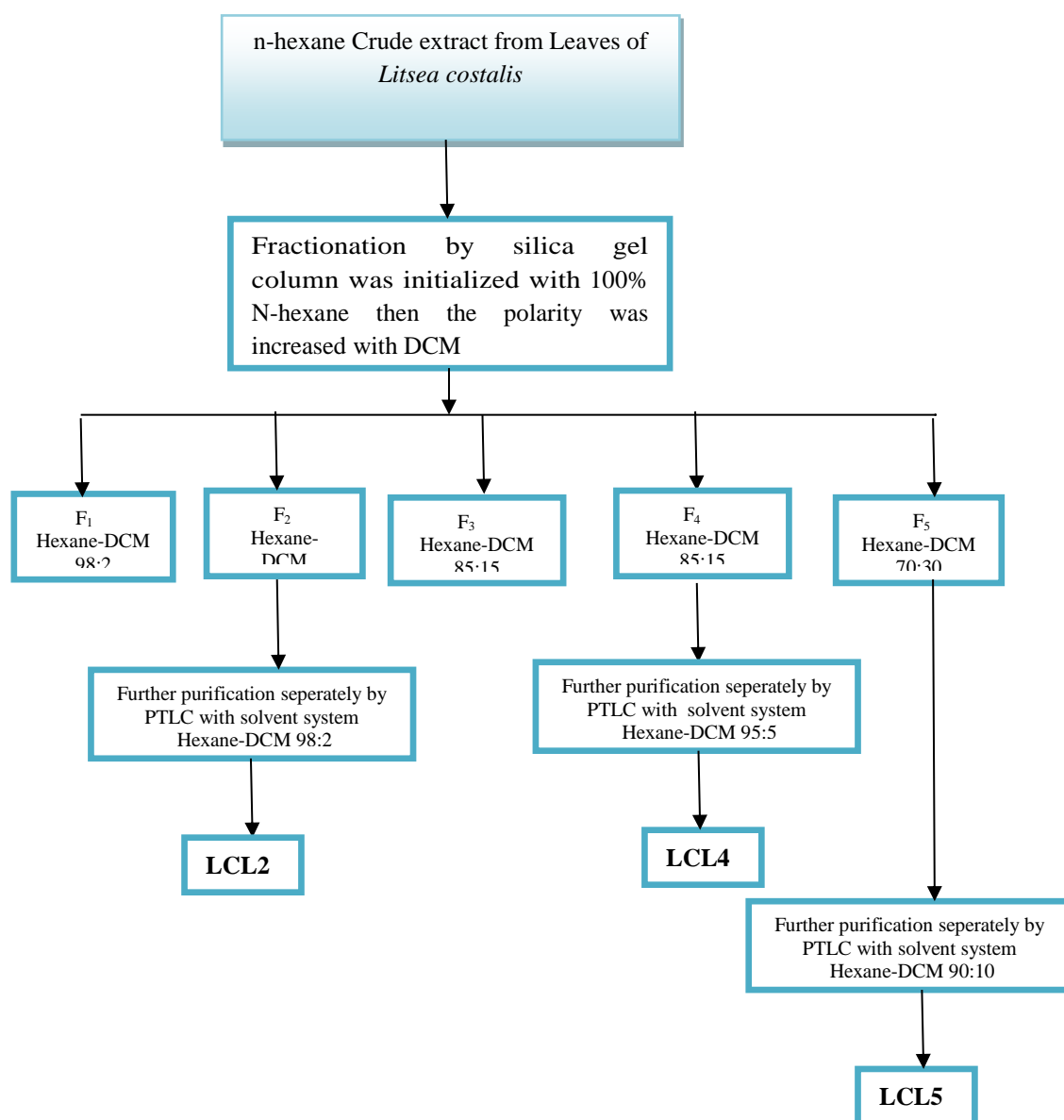
Scheme 6.8: Isolation and purification of chemical constituents from N-hexane crude of *Litsea costalis* (bark)



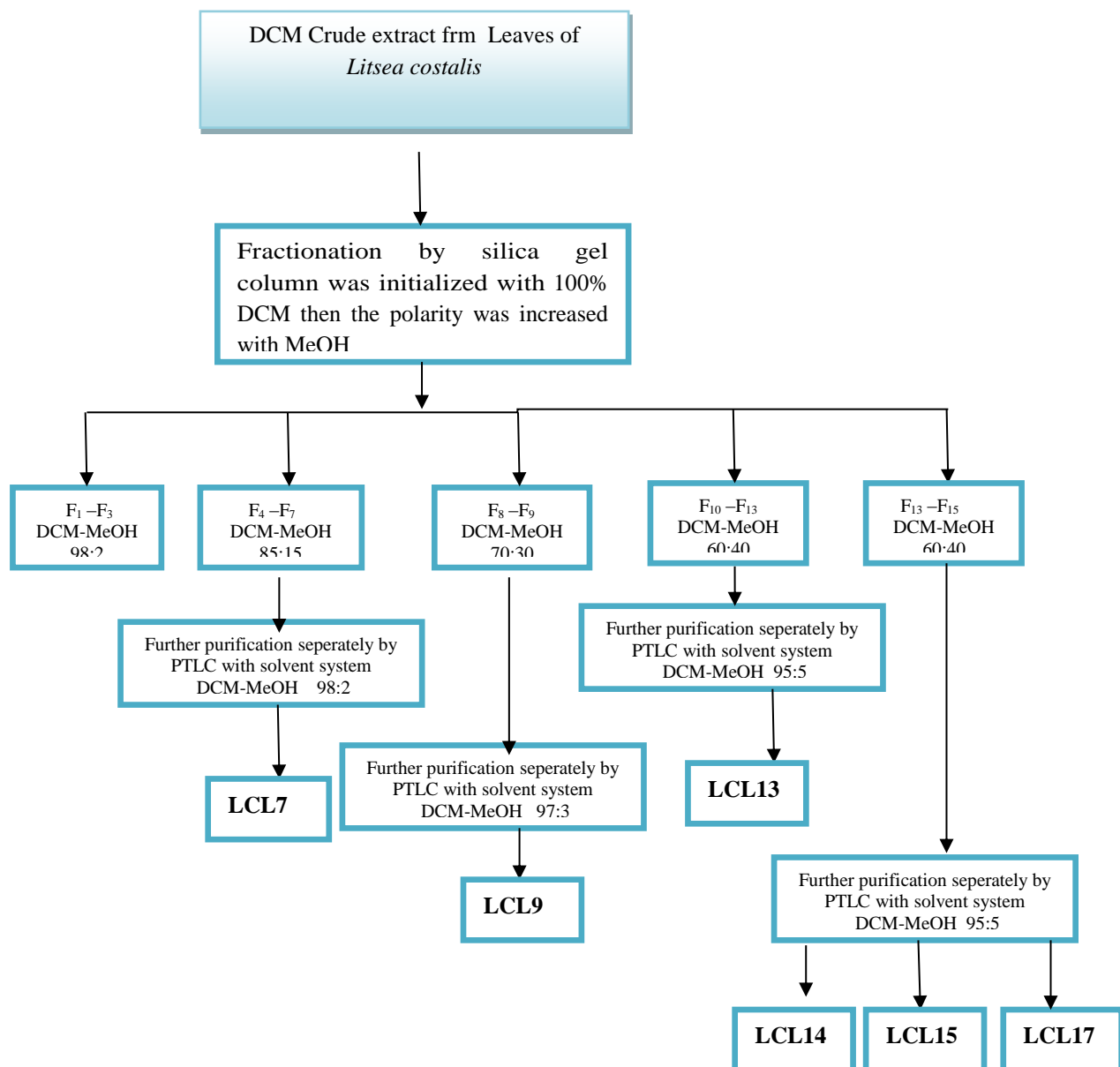
Scheme 6.9: Isolation and purification of chemical constituents from dichloromethane crude of *Litsea costalis* (bark)



Scheme 6.10: Isolation and purification of chemical constituents from methanol crude of *Litsea costalis* (bark)



Scheme 6.11: Isolation and purification of chemical constituents from n-Hexane crude of *Litsea costalis* (leaves)



Scheme 6.12: Isolation and purification of chemical constituents from dichloromethane crude of *Litsea costalis* (leaves)

Table 6.2: Chromatography solvent systems and the yield of compounds isolated from *Lindera oxyphylla* (KL5359)

Part of Plant	Solvent systems	Compounds	Yield (mg)	Yield (%)
Bark of <i>Lindera oxyphylla</i> (KL 5359)	98: 2 (N-hexane)	(+)-Onysilin LOB4	50.00	0.4
	90:10 (N-hexane)	Linderone LOB28	1000	7.69
	98:2 (DCM)	(+)-Pinostrobin LOB7	5.00	0.5
	95:5 (DCM)	Flavokawain B LOB15	5.00	0.5
	92:8 (DCM)	Linderone A LOB25	10.00	1.00
	90:10 (MeOH)	(+)-Pinocembrin LOB2	5.00	0.5
Leaves of <i>Lindera oxyphylla</i> (KL 5359)	90:10 (N-hexane)	Methyllinderone LOL34	5.00	0.1
	98:2 (DCM)	(+)-Laurotetanine LOL20	10.00	0.05
	97:3 (DCM)	N-Methylaurotetanine LOL35	5.00	0.25
	95:5 (DCM)	(+)-Norboldine LOL50	10.00	0.05
	95:5 (DCM)	(+)-010-N-methyl Hernovine LOL63	10.00	0.05
	92:8 (DCM)	(+)-Norisoboldine LOL65	5.00	0.25
	98:2 (MeOH)	Kaempferol LOL5	0.1	0.01

Table 6.3: Chromatography solvent systems and the yield of compounds isolated from *Litsea Costalis* (Nee.)Kosterm (KL5410)

Part of Plant	Solvent systems	Compounds	Yield (mg)	Yield (%)
Bark of <i>Litsea costalis</i> (KL 5410)	95:5 (N-hexane)	3, 4-dimethoxycinnamaldehyde LCB7	7.00	0.35
	90:10 (N-hexane)	2-hydroxy-5-methoxybenzaldehyde LCB11	2.00	0.04
	85:15 (N-hexane)	2, 5-dimethoxybenzaldehyde LCB15	5.00	0.1
	98:2 (DCM)	4,4'-diallyl-5,5'-dimethoxy-(1,1'-biphenyl)-2,2'-diol LCB3	10.00	0.5
	HPLC	4,4'-diallyl-6,6'-dimethoxy-(1,1'-biphenyl)-2,2'-diol LCB9	50.0	10.0
	HPLC	2,2'-oxybis(4-allyl-1-methoxy benzene) LCB10	3000	30
	HPLC	1,2-bis(2-allyl-6-methoxy phenyl)hydrazine LCB17	3000	30
	98:2 (MeOH)	(E)-4(4-hydroxy-1, 1-dimethoxybut-2-en-1-yl) benzene-1, 2-diol LCB4	50.00	0.5
	98:2 (MeOH)	(E)-4-styrylphenol LCB58	5.00	2.5
Leaves of <i>Litsea costalis</i> (KL 5410)	98:2 (N-hexane)	Cinnamide LCL4	2.00	0.1
	98:2(N-Hexane)	2,4-dimethoxybenzamide LCL2	2.00	0.1
	90:10 (N-hexane)	3,4-dimethoxybenzamide LCL5	2.00	0.1
	98:2 (DCM)	2S,4S-2-(3',4'-methylene dioxyphenyl)-5,7-dimethoxy chroman-4-ol LCL7	50.00	25
	98:2 (DCM)	(+)- pinostrobin LCL9	5.00	0.25
	97:3 (DCM)	(+)-Onysilin LCL13	3.00	0.15
	92:8 (DCM)	4-allyl-1,2dimethoxybenzane LCL15	3.00	0.15
	95:5(DCM)	(+)-pinocembrin LCL14	3.00	0.15
		4-allyl-2methoxyphenol LCL17	3.00	0.15

6.7 Physical property and Spectral Data of Isolated compounds

6.7.1 Bark of *Lindera oxyphylla* (KL 5359)

LOB4: (+) – Onysilin	yellow amorphous solid
Molecular Formula	: $C_{17}H_{16}O_5$
$[\alpha]_D^{25}$: $+3.1(2.00 \times 10^{-4} \text{ g/100 mL, MeOH})$
UV _{max} (MeOH), nm	: 293 (4.00) and 349 (1.43) nm
IR (KBr) ν_{max} cm^{-1}	3446 and 1644 cm^{-1}
Mass spectrum m/z $[M+H]^+$: 301.0824
$^1\text{H-NMR}$ (CDCl_3) δ , ppm	: Refer Table 3.3
$^{13}\text{C-NMR}$ (CDCl_3) δ ppm	: Refer Table 3.3
LOB7: (+)-pinostrobin	yellow amorphous solid
Molecular Formula	: $C_{16}H_{14}O_4$
$[\alpha]_D^{25}$: $+1.52 (2.00 \times 10^{-4} \text{ g/100 mL, MeOH})$
UV _{max} (MeOH), nm	: 223 (2.316) and 306 (1.273) nm
IR (KBr) ν_{max} cm^{-1}	3429 and 1642 cm^{-1}
Mass spectrum m/z $[M+H]^+$: 271.088
$^1\text{H-NMR}$ (CDCl_3) δ , ppm	: Refer Table 3.4
$^{13}\text{C-NMR}$ (CDCl_3) δ ppm	: Refer Table 3.4

LOB15: Flavokawain B	Red crystal
Molecular Formula	: $C_{17}H_{16}O_4$
$[\alpha]_D^{25}$: +12.3 (2.00×10^{-4} g/100 mL, MeOH)
UV _{max} (MeOH), nm	: 241 (1.297) and 336 (1.86) nm
IR (KBr) ν_{\max} cm^{-1}	3436 and 1634 cm^{-1}
Mass spectrum m/z $[M-H]^+$: 283.7380
1H -NMR ($CDCl_3$) δ , ppm	: Refer Table 3.5
^{13}C -NMR ($CDCl_3$) δ ppm	: Refer Table 3.5
LOB2: (+)-Pinocembrin	yellow amorphous solid
Molecular Formula	: $C_{15}H_{12}O_4$
$[\alpha]_D^{25}$: +2.81 (2.00×10^{-4} g/100 mL, EtOH).
UV _{max} (MeOH), nm	: 241 (1.519) and 290 (2.783) nm
IR (KBr) ν_{\max} cm^{-1}	3417 and 1640 cm^{-1}
Mass spectrum m/z $[M-H]^+$: 255.0475
1H -NMR ($CDCl_3$) δ , ppm	: Refer Table 3.6
^{13}C -NMR ($CDCl_3$) δ ppm	: Refer Table 3.6

LOB28: Linderone

yellow crystal

Molecular Formula	: $C_{16}H_{14}O_5$
Mp:	$92^{\circ}C$
UV _{max} (MeOH), nm	: 246 (1.529) and 364 (1.631) nm
IR (KBr) ν_{max} cm^{-1}	3435 and 1632 cm^{-1}
Mass spectrum m/z $[M+H]^+$: 287.0677
1H -NMR ($CDCl_3$) δ , ppm	: Refer Table 3.7
^{13}C -NMR ($CDCl_3$) δ ppm	: Refer Table 3.7

LOB25: Linderone

yellow amorphous solid

Molecular Formula	: $C_{16}H_{14}O_5$
UV _{max} (MeOH), nm	: 246 (1.291) and 309 (1.580) nm
IR (KBr) ν_{max} cm^{-1}	3431 and 1639 cm^{-1}
Mass spectrum m/z $[M+H]^+$: 287.0677
1H -NMR ($CDCl_3$) δ , ppm	: Refer Table 3.8
^{13}C -NMR ($CDCl_3$) δ ppm	: Refer Table 3.8

6.7.2 Leaves of *Lindera oxyphylla* (KL 5359)

LOL34: Methyl Linderone yellow amorphous solid

Molecular Formula	:	$C_{17}H_{16}O_5$
UV _{max} (MeOH), nm	:	241 (0.908) and 357 (1.158) nm
IR (KBr) ν_{\max} cm^{-1}		1702 cm^{-1}
Mass spectrum m/z $[M]^+$:	300.88
1H -NMR ($CDCl_3$) δ , ppm	:	Refer Table 3.9
^{13}C -NMR ($CDCl_3$) δ ppm	:	Refer Table 3.9

LOL5: Kaempferol yellow amorphous solid

Molecular Formula	:	$C_{15}H_{10}O_6$
UV _{max} (MeOH), nm	:	253 (0.434) and 364 (0.616) nm
IR(KBr) ν_{\max} cm^{-1}	:	3431 and 1646 cm^{-1}
Mass spectrum m/z $[M-H]^+$:	285.04
1H -NMR ($CDCl_3$) δ , ppm	:	Refer Table 3.10
^{13}C -NMR ($CDCl_3$) δ ppm	:	Refer Table 3.10

LOL20: (+)-laurotetanine	dark brown amorphous solid
Molecular Formula	: C ₁₉ H ₂₁ NO ₄
$[\alpha]_D^{25}$: +29.4° (2.00×10 ⁻⁴ g/100 mL, MeOH)
UV _{max} (MeOH), nm	: 217 (2.345) and 242 (3.098) nm
IR (KBr) ν_{\max} cm ⁻¹	3429 cm ⁻¹
Mass spectrum m/z [M+H] ⁺	: 328.1566
¹ H-NMR (CDCl ₃) δ , ppm	: Refer Table 3.11
¹³ C-NMR (CDCl ₃) δ ppm	: Refer Table 3.11

LOL35: N-methylaurotetanine	brownish amorphous solid
Molecular Formula	: C ₂₄ H ₃₅ NO ₄
$[\alpha]_D^{25}$: +15.0 (2.00×10 ⁻⁴ g/100 mL, MeOH)
UV _{max} (MeOH), nm	: 222 (2.098) and 320 (3.564) nm
IR(KBr) ν_{\max} cm ⁻¹	: 3391 cm ⁻¹
Mass spectrum m/z [M+H] ⁺	: 401.1625
¹ H-NMR (CDCl ₃) δ , ppm	: Refer Table 3.12
¹³ C-NMR (CDCl ₃) δ ppm	: Refer Table 3.12

LOL50: (+)-Norboldine	brown amorphous solid
Molecular Formula	: C ₁₈ H ₁₉ NO ₄
$[\alpha]_D^{25}$: +9.87 (2.00×10 ⁻⁴ g/100 mL, MeOH)
UV _{max} (MeOH), nm	: 276 (3.765) , 317 (2.987) nm
IR (KBr) ν_{\max} cm ⁻¹	3432 cm ⁻¹
Mass spectrum m/z [M+H] ⁺	: 314.1397
¹ H-NMR (CDCl ₃) δ , ppm	: Refer Table 3.13
¹³ C-NMR (CDCl ₃) δ ppm	: Refer Table 3.13

LOL63: (+)-O10-N-methylhernovine	brownish amorphous powder
Molecular Formula	: C ₁₉ H ₂₁ NO ₄
$[\alpha]_D^{25}$: +4.50 (2.00×10 ⁻⁴ g/100 mL, MeOH)
UV _{max} (MeOH), nm	: 244 (1.65) and 276 (2.76) nm
IR (KBr) ν_{\max} cm ⁻¹	3390 cm ⁻¹
Mass spectrum m/z [M+H] ⁺	: 328.20
¹ H-NMR (CDCl ₃) δ , ppm	: Refer Table 3.14
¹³ C-NMR (CDCl ₃) δ ppm	: Refer Table 3.14

LOL65: (+)-norisoboldine

brownish amorphous powder

Molecular Formula	: $C_{18}H_{19}NO_4$
$[\alpha]_D^{25}$: +11.52 (2.00×10^{-4} g/100 mL, MeOH)
UV _{max} (MeOH), nm	: 241 (1.87), 250 (1.98) and 270 (2.98) nm
IR (KBr) ν_{\max} cm^{-1}	3436 cm^{-1}
Mass spectrum m/z $[M+H]^+$: 314.1399
1H -NMR ($CDCl_3$) δ , ppm	: Refer Table 3.15
^{13}C -NMR ($CDCl_3$) δ ppm	: Refer Table 3.15

6.7.3 Bark of *Litsea costalis* (KL5410)**LCB7: Cinnamaldehyde**

brown oil

Molecular Formula	: $C_{11}H_{12}O_3$
UV _{max} (MeOH), nm	: 306 (1.874) and 326 (1.876) nm
IR (KBr) ν_{\max} cm^{-1}	2848 and 1668 cm^{-1}
Mass spectrum m/z $[M+H]^+$: 191.04
1H -NMR ($CDCl_3$) δ , ppm	: Refer Table 3.18
^{13}C -NMR ($CDCl_3$) δ ppm	: Refer Table 3.18

LCB11: salicylaldehyde	light yellow amorphous solid
Molecular Formula	: $C_8H_8O_3$
UV _{max} (MeOH), nm	: 306 (1.845) and 231 (1.723) nm
IR (KBr) ν_{max} cm^{-1}	3431 and 1669 cm^{-1}
Mass spectrum m/z $[M+H]^+$: 153.0504
1H -NMR ($CDCl_3$) δ , ppm	: Refer Table 3.19
^{13}C -NMR ($CDCl_3$) δ ppm	: Refer Table 3.19

LCB15: 2,5-DimethoxyBenzaldehyde	light yellow solid
Molecular Formula	: $C_9H_{10}O_3$
UV _{max} (MeOH), nm	: 306 (2.703) and 234 (2.537) nm
IR (KBr) ν_{max} cm^{-1}	1669 and 2848 cm^{-1}
Mass spectrum m/z $[M+H]^+$: 167.064
1H -NMR ($CDCl_3$) δ , ppm	: Refer Table 3.20
^{13}C -NMR ($CDCl_3$) δ ppm	: Refer Table 3.20

LCB3: Biseugenol A	brown oil
Molecular Formula	: $C_{20}H_{22}O_4$
UV _{max} (MeOH), nm	: 247 (3.121) 291 (2.214) and 3.6 (1.462) nm
IR (KBr) ν_{max} cm^{-1}	3427 and 1642 cm^{-1}

Mass spectrum m/z $[M+H]^+$: 325.1394
^1H -NMR (CDCl_3) δ , ppm	: Refer Table 3.21
^{13}C -NMR (CDCl_3) δ ppm	: Refer Table 3.21
LCB9: Biseugenol	brown oil
Molecular Formula	$\text{C}_{20}\text{H}_{22}\text{O}_4$
UV_{max} (MeOH), nm	2 47 (3.121) 291 (2.214) and 3.6 (1.462)nm
IR (KBr) ν_{max} cm^{-1}	3427 and 1642 cm^{-1}
Mass spectrum m/z $[M+H]^+$	325.1394
^1H -NMR (CDCl_3) δ , ppm	Refer Table 3.22
^{13}C -NMR (CDCl_3) δ ppm	Refer Table 3.22
LCB10: Biseugenol B	brown oil
Molecular Formula	: $\text{C}_{20}\text{H}_{22}\text{O}_3$
UV_{max} (MeOH), nm	: 2 78 (2.337) and 239 (2.767) nm
IR (KBr) ν_{max} cm^{-1}	1591 and 1638 cm^{-1}
Mass spectrum m/z $[M-H]^-$: 309.20
^1H -NMR (CDCl_3) δ , ppm	: Refer Table 3.23
^{13}C -NMR (CDCl_3) δ ppm	: Refer Table 3.23

LCB17: Biseugenole C

yellow oil

Molecular Formula	:	$C_{20}H_{24}N_2O_2$
UV_{\max} (MeOH), nm	:	225 (2.413) and 239 (2.763) nm
IR (KBr) ν_{\max} cm^{-1}		3517 and 1515 cm^{-1}
Mass spectrum m/z $[M]^+$:	324.7967
1H -NMR ($CDCl_3$) δ , ppm	:	Refer Table 3.24
^{13}C -NMR ($CDCl_3$) δ ppm	:	Refer Table 3.24

LCB4: Litsin

white amorphous solid

Molecular Formula	:	$C_{12}H_{16}O_5$
$[\alpha]_D^{25}$:	+ 2.93 (2.00×10^{-4} g/100 mL, MeOH)
UV_{\max} (MeOH), nm	:	261 (2.486) and 223 (2.202) nm
IR (KBr) ν_{\max} cm^{-1}		3434 and 1640 cm^{-1}
Mass spectrum m/z $[M]^+$:	240.72
1H -NMR ($CDCl_3$) δ , ppm	:	Refer Table 3.25
^{13}C -NMR ($CDCl_3$) δ ppm	:	Refer Table 3.25

LCB5: (E)-4-Styrylphenol

brown amorphous solid

Molecular Formula	:	$C_{14}H_{12}O$
$[\alpha]_D^{25}$:	-22.8° (2.00×10^{-4} g/100 mL, MeOH)
UV_{\max} (MeOH), nm	:	306 (0.418) and 213 (0.424) nm

IR (KBr) ν_{\max} cm^{-1}	3425 and 1643 cm^{-1}
Mass spectrum m/z $[\text{M}]^+$: 196.0295
^1H -NMR (CDCl_3) δ , ppm	: Refer Table 3.26
^{13}C -NMR (CDCl_3) δ ppm	: Refer Table 3.26

6.7.4 Leaves of *Litsea costalis* (KL5410)

LCL4: Cinnamide	colorless crystalline needle
Molecular Formula	: $\text{C}_9\text{H}_9\text{NO}$
UV_{\max} (MeOH), nm	: 223 (1.204) and 278 (0.875) nm
IR (KBr) ν_{\max} cm^{-1}	3353 and 1669 cm^{-1}
Mass spectrum m/z $[\text{M}+\text{H}]^+$: 148.30
^1H -NMR (CDCl_3) δ , ppm	: Refer Table 3.27
^{13}C -NMR (CDCl_3) δ ppm	: Refer Table 3.27
LCL2: 2,4-Dimethoxybenzamide	brown oil
Molecular Formula	: $\text{C}_9\text{H}_{11}\text{NO}_3$
UV_{\max} (MeOH), nm	: 261 (2.474) and 258 (2.486) nm
IR (KBr) ν_{\max} cm^{-1}	3353 and 1669 cm^{-1}
Mass spectrum m/z $[\text{M}]^+$: 181.044

$^1\text{H-NMR}$ (CDCl_3) δ , ppm	: Refer Table 3.28
$^{13}\text{C-NMR}$ (CDCl_3) δ ppm	: Refer Table 3.28
LCL5: 3,4-dimethoxyBenzamide	brown oil
Molecular Formula	: $\text{C}_9\text{H}_{11}\text{NO}_3$
UV_{max} (MeOH), nm	: 261(2.474) and 258 (2.486) nm
IR (KBr) ν_{max} cm^{-1}	3448 and 1607 cm^{-1}
Mass spectrum m/z $[\text{M}]^+$: 181.044
$^1\text{H-NMR}$ (CDCl_3) δ , ppm	: Refer Table 3.29
$^{13}\text{C-NMR}$ (CDCl_3) δ ppm	: Refer Table 3.29
LCL7: Costalin	white amorphous solid
Molecular Formula	: $\text{C}_{18}\text{H}_{18}\text{O}_6$
UV_{max} (MeOH), nm	: 293 (4.00) and 349 (1.433) nm
IR (KBr) ν_{max} cm^{-1}	3431, 1576 and 1446 cm^{-1}
Mass spectrum m/z $[\text{M}]^+$: 331.0867
$^1\text{H-NMR}$ (CDCl_3) δ , ppm	: Refer Table 3.30
$^{13}\text{C-NMR}$ (CDCl_3) δ ppm	: Refer Table 3.30

LCL9: (+)-Pinostrobin Yellow amorphous solid

Molecular Formula : C₁₆H₁₄O₄

¹H-NMR (CDCl₃) δ, ppm : Refer Table 3.4

¹³C-NMR (CDCl₃) δ ppm : Refer Table 3.4

LCL14: (+)-Pinocembrin yellow samorphous olid

Molecular Formula : C₁₅H₁₂O₄

¹H-NMR (CDCl₃) δ, ppm : Refer Table 3.10

¹³C-NMR (CDCl₃) δ ppm : Refer Table 3.10

LCL13: (+)-Onysilin Yellow amorphous solid

Molecular Formula : C₁₇H₁₆O₅

¹H-NMR (CDCl₃) δ, ppm : Refer Table 3.3

¹³C-NMR (CDCl₃) δ ppm : Refer Table 3.3

LCL15: 4-allyl-1,2-Dimethoxybenzene :brown oil

Molecular Formula :C₁₁H₁₄O₂

UV_{max} (MeOH), nm :225 (2.413) and 239 (2.763) nm

IR (KBr) ν_{max} cm⁻¹ 3517 and 1515 cm⁻¹

Mass spectrum *m/z* [M-1]⁺ 177.87

$^1\text{H-NMR}$ (CDCl_3) δ , ppm	Refer Table 3.23
$^{13}\text{C-NMR}$ (CDCl_3) δ ppm	Refer Table 3.23
LCL17: 4-allyl-2-methoxyphenol	:yellow oil
Molecular Formula	: $\text{C}_{10}\text{H}_{12}\text{O}_2$
UV_{max} (MeOH), nm	:225 (2.413) and 239 (2.763) nm
IR (KBr) ν_{max} cm^{-1}	3517 and 1515 cm^{-1}
Mass spectrum m/z $[\text{M}-1]^+$	177.87
$^1\text{H-NMR}$ (CDCl_3) δ , ppm	Refer Table 3.23
$^{13}\text{C-NMR}$ (CDCl_3) δ ppm	Refer Table 3.23

Achenbach, H., Renner, C., & Addae-Mensah, I. (1982). Constituents of West African medicinal plants. Study of the constituents of *Hexalobus crispiflorus*. *Liebigs Ann. Chem*, 9, 1623-1633.

Achenbach, H., Renner, C., Wörth, J., Addae-Mensah, I. (1982). Inhaltsstoffe Westafrikanischer Arzneipflanzen, VIII. 3-Hydroxynornuciferin und 3-Hydroxy-6a, 7-dehydronuciferin, Nebenalkaloide in *Hexalobus crispiflorus* Massenspektrometrische Strukturfestlegung an Noraporphinen. *Liebigs Annalen der Chemie*, 6, 1132-1141.

Adedapo, A., Jimoh, F., Afolayan, A., & Masika, P. (2008). Antioxidant activities and phenolic contents of the methanol extracts of the stems of *Acokanthera oppositifolia* and *Adenia gummifera*. *BMC Complementary and Alternative Medicine*, 8(1), 54.

Afzali, D., Karimi-Maleh, H., Khalilzadeh, M. A. (2011). Sensitive and selective determination of phenylhydrazine in the presence of hydrazine at a ferrocene-modified carbon nanotube paste electrode. *Environmental Chemistry Letters*, 9(3), 375.

Bard, A., Faulkner, R. (2001). *Electrochemical Methods: Fundamentals and Applications*, 2nd edition., Wiley, New York, 544–554.

Alarcón, S. H., Olivieri, A. C., & González-Sierra, M. (1994). ¹³ C NMR spectroscopic and AM1 study of the intramolecular proton transfer in anils of salicylaldehyde and 2-hydroxynaphthalene-1-carbaldehyde. *J. Chem. Soc., Perkin Trans. 2*(5), 1067-1070.

Amir, M., Shikha, K. (2004). Synthesis and anti-inflammatory, analgesic, ulcerogenic and lipid peroxidation activities of some new 2-[(2, 6-dichloroanilino) phenyl] acetic acid derivatives. *European Journal of Medicinal Chemistry*, 39(6), 535-545.

Ardestani, A., Yazdanparast, R. (2007). Antioxidant and free radical scavenging potential of *Achillea santolina* extracts. *Food Chemistry*, 104(1), 21-29.

Arfan, M., Amin, H., & Amarowicz, R. (2008). Antioxidant activity of phenolic fractions of *Litsea monopetala* (persimmon-leaved litsea) bark extract. *Polish Journal of Food and Nutrition Sciences*, 58(2), 229-233.

Balasubramanian N. D. B., Devayani, P. (2004). Esters, amides and substituted derivatives of cinnamic acid: synthesis, antimicrobial activity and QSAR investigations. *European Journal of Medicinal Chemistry*, 39, 827-834.

Bannister, J. M., Conran, J. G., Lee, D. E. (2012). Lauraceae from rainforest surrounding an early Miocene maar lake, Otago, Southern New Zealand. *Review of Palaeobotany and Palynology*. 178, 13–34.

Beavis, R. C., Chait, B. T., & Fales, H. (1989). Cinnamic acid derivatives as matrices for ultraviolet laser desorption mass spectrometry of proteins. *Rapid Communications in Mass Spectrometry*, 3(12), 432-435.

- Beitollahi, H., Karimi-Maleh, H., & Khabazadeh, H. (2008). Nanomolar and selective determination of epinephrine in the presence of norepinephrine using carbon paste electrode modified with carbon nanotubes and novel 2-(4-Oxo-3-phenyl-3, 4-dihydro-quinazoliny)-N'-phenyl-hydrazinecarbothioamide. *Analytical Chemistry*, 80(24), 9848-9851.
- Benavente-García, O., Castillo, J., Marin, F. R., Ortuño, A., & José, A. (1997). Uses and properties of citrus flavonoids. *Journal of Agricultural and Food Chemistry*, 45(12), 4505-4515.
- Benowitz, S. (1996). As war on cancer hits 25-year mark, scientists see progress, challenges. *Scientist*, 10, 1-7.
- Berkov, S., Georgieva, L., Kondakova, V., Atanassov, A., Viladomat, F., Bastida, J., & Codina, C. (2009). Plant sources of galanthamine: phytochemical and biotechnological aspects. *Biotechnology and Biotechnological Equipment*, 23(2), 1170-1176.
- Bhakuni, D. S., Labroo, V. M., Singh, A. N., & Kapil, R. S. (1978). Biosynthesis of the bisbenzylisoquinoline alkaloid cocsulin. *J. Chem. Soc., Perkin Trans. 1*(2), 121-125.
- Bhakuni, D. S., Singh, A. N., & Jain, S. (1981). The structure, absolute configuration and biosynthesis of nortiliacorinine A. *Tetrahedron*, 37(15), 2651-2655.
- Bick, I. R. C., Brown, R. B., Hillis, W. E., (1972). Three flavanones from leaves of *Eucalyptus sieberi*. *Australian Journal of chemistry*, 25, 449-451.
- Bohm, B. A. (1998). *Introduction to flavonoids*. Taylor & Francis. (Vol. 2).503.
- Bombardelli, E. M. (1993). The Flavonoids: New Perspectives in Biological Activities and Therapeutics. *Chimicaoggi*, 25-28.
- Buchanan, M., & Dickey, E. (1960). Liriodenine, A Nitrogen-Containing Pigment of Yellow Poplar Heartwood (*Liriodendron tulipifera*, L.). *The Journal of Organic Chemistry*, 25(8), 1389-1391.
- Buchanan, M. S. C., Anthony R. Pass, David, Quinn, Ronald J. (2007). Aporphine alkaloids from the Chinese tree *Neolitsea aurata* var. *paraciculata*. *Natural Product Communications* . 2(3), 255-259.
- Cancer facts and figures. (2002) In American Cancer Society. <http://www.cancure.org/statistics.htm>.420.860-867.
- Carpinella, M. C., Giorda, L. M., Ferrayoli, C. G., and Palacios, S. M. . (2003). Antifungal Effects of Different Organic Extracts from *Melia azedarach* L. on Phytopathogenic Fungi and Their Isolated Active Components. *J. Agric. Food Chem.Pharm.Bull*, 51, 2506-2511.
- Castro, L., & Freeman, A.B. (2001). Reactive Oxygen Species in Human Health and Disease. *Nutrition*, 17, 161-165.

- Cave, A., Leboeuf, M., Waterman, P. G., & Pelletier, S. (1987). Em Alkaloids: Chemical and Biological Perspectives. *Alkaloids: Chemical and Biological Perspectives*, 5, 180-187.
- Chang, H. Y., Ho, Y. L., Sheu, M. J., Lin, Y. H., Tseng, M. C., Wu, S. H., Huang, G. J. Chang, Y. S. (2007). Antioxidant and free radical scavenging activities of *Phellinus merrillii* extracts. *Botanical Studies*, 48, 407-417.
- Chang, S., & Grubbs, R. H. (1998). A highly efficient and practical synthesis of chromene derivatives using ring-closing olefin metathesis. *Journal of Organic Chemistry*, 63(3), 864-866.
- Chantrapromma, K., Seechamnaturakit, V., Ponglimanont, C., Pakawatchai, C., Fun, H. K., & Sivakumar, K. (1997). 2, 3-Dihydro-5-hydroxy-6, 7-dimethoxy-2-phenyl-4*H*-1-benzopyran-4-one (Onysilin). *Acta Crystallographica Section C: Crystal Structure Communications*, 53(6), 734-736.
- Cheah, S.C. A., D. R., Lee, S.T., Lam, M.L., Hadi, A.H.A., Mustafa, M.R. (2011). Panduratin A Inhibits the Growth of A549 Cells through Induction of Apoptosis and Inhibition of NF-KappaB Translocation. *Molecules* 16, 2583-2598.
- Chen, I.S., Lai-Yaun, I. L., Duh, C. Y., Tsai, I. L. (1998). Cytotoxic butanolides from *Litsea akoensis*. *Phytochemistry*, 49(3), 745-750.
- Chen, J. J., Obering, C. (2005). A review of intermittent subcutaneous apomorphine injections for the rescue management of motor fluctuations associated with advanced Parkinson's disease. *Clinical therapeutics*, 27(11), 1710-1724.
- Chew, Y. L., Goh, J. K., Lim, Y. Y. (2009). Assessment of in vitro antioxidant capacity and polyphenolic composition of selected medicinal herbs from Leguminosae family in Peninsular Malaysia. *Food Chemistry*, 116(1), 13-18.
- Cook, N.C., Samman, S. (1996). Flavonoids—chemistry, metabolism, cardioprotective effects, and dietary sources. *The Journal of nutritional biochemistry*, 9, 66-76.
- Cordell, G. (1981). Introduction to alkaloids: a biogenetic approach. *Wiley*. 234-345.
- Cordell, G. A., Southon, I. W., Buckingham, J. (1989). *Dictionary of Alkaloids: Indexes* (Vol. 2): *Chapman and Hall*. 456-487.
- Corner, E. J. H. (1988). *Wayside Trees of Malaya* (3 ed. Vol. 1). Cambridge. 139-154.
- Cragg, G. M., D.J. Newman, . Snader, K.M.. (1997). Natural products in drug discovery and development. *Journal of Natural Products*, 60(1), 52-60.
- Cuong, N. M., Kamperdick, C., Sung, T.V., Adam, G. (1996). Flavonoid and *Carya tonkinensis*. *Die Pharmazie*, 51, 128.
- Cutillo, F., D'Abrosca, B., DellaGreca, M., Fiorentino, A., Zarrelli, A. (2003). Lignans and neolignans from *Brassica fruticulosa*: effects on seed germination and plant growth. *Journal of agricultural and food chemistry*, 51(21), 6165-6172.

- DaRocha, A. B., Lopes, R. M., Schwartzmann, G. (2001). Natural products in anticancer therapy. *Current Opinion in Pharmacology*, 1(4), 364-369.
- Dakternieks, D., Baul, T. S. B., Dutta, S., & Tiekink, E. R. T. (1998). Synthesis, characterization, and X-ray structures of diphenyltin (IV) N-(2-hydroxyacetophenone) glycinate, its 1:1 adduct with triphenyltin (IV) chloride, and related systems. *Organometallics*, 17(14), 3058-3062.
- Dawson, R. M. C., Daphne C. Elliott, William H. Elliott, & Kenneth M. Jones. (1986). pH, buffers, and physiological media *Data for biochemical research*. New York: Oxford University Press (3rd ed., pp. 417-448).
- Dawson, R. M. C., Daphne C. Elliott, William H. Elliott and Kenneth M. Jones. (1986). pH, buffers, and physiological media data for biochemical research. New York: Oxford University Press., 3rd ed., pp. 417-448.
- Delogu, G., Fabbri, D., Antonietta, D. M., Forni, A., Casalone, G., (2004). Enantiopure 2,2-dihydroxy-3,3-dimethoxy-5,5-diallyl-6,6-dibromo-1,1-biphenyl: a conformationally stable C₂-dimer of a eugenol derivative. *Tetrahedron*, 15, 275-282.
- Deng, Z., Zhong, H., Cui, S., Wang, F., Xie, Y., & Yao, Q. (2011). Cytotoxic sesquiterpenoids from the fruits of *Lindera communis*. *Fitoterapia*. 82. 1044-1046.
- Dewick, P. M. (2009). Medicinal natural products: a biosynthetic approach: John Wiley & Sons Inc. 324-789.
- Dinis, T. C. P., Madeira, V.M.C., Almeida, L.M. (1994). Action of phenolic derivatives (acetaminophen, salicylate and 5-aminosalicylate) as inhibitors of membrane lipid peroxidation as peroxyl radical scavenging effects. *chemistry Pharmacy Bulletin*, 36, 2090-2097.
- DHR Barton, K. Nakanishi., O. Meth-Cohn, K. Mori (1999). Comprehensive Natural Products Chemistry. Pergamon-Elsevier, Oxford, 8, 197-373.
- Dorman, G., Prestwich, G. D. (1994). Benzophenone photophores in biochemistry. *Biochemistry*, 33(19), 5661-5673.
- Durtsche, R. D. Thieret, J.W. Johan Linder (Lindestolpe) (2005). Eponym of the generic name *Lindera Thunberg* (Plantae: Lauraceae). *Journal of the Kentucky Academy of Science*. 66(1): 44-49.
- Ensafi, A. A., & Karimi-Maleh, H. (2010). Modified multiwall carbon nanotubes paste electrode as a sensor for simultaneous determination of 6-thioguanine and folic acid using ferrocenedicarboxylic acid as a mediator. *Journal of Electroanalytical Chemistry*, 640(1-2), 75-83.
- Ensafi, A. A., Karimi-Maleh, H., Mallakpour, S., & Hatami, M. (2011). Simultaneous determination of N acetylcysteine and acetaminophen by voltammetric method using N-(3,4-dihydroxyphenethyl)-3,5-dinitrobenzamide modified multiwall carbon nanotubes paste electrode. *Sensors and Actuators B: Chemical*, 155(2), 464-472.
- Fabre, N., Rustan, I., de Hoffmann, E., & Quetin-Leclercq, J. (2001). Determination of flavone, flavonol, and flavanone aglycones by negative ion liquid chromatography

electrospray ion trap mass spectrometry. *Journal of the American Society for Mass Spectrometry*, 12(6), 707-715.

Fischer, D., Gonçalves, M., Oliveira, F., Alvarenga, M. (1999). Constituents from *Siparuna apiosyce*. *Fitoterapia*, 70(3), 322-323.

Friedman, M., Levin, C. E., Lee, S. U., Kim, H.J., Lee, I. S., Byun, J. O. Kozukue N. . (2009). Tomatine-Containing Green Tomato Extracts Inhibit Growth of Human Breast, Colon, Liver, and Stomach Cancer Cells. *Journal Agriculture and Food Chemistry*. , 57, 5727–5573

Fujisawa, S., Kashiwagi, Y., Atsumi, T., Iwakura, I., Ueha, T., Hibino, Y., & Yokoe, I. (1999). Application of bis-eugenol to a zinc oxide eugenol cement. *Journal of Dentistry*, 27(4), 291-295.

Garo, E., Maillard, M., Antus, S., Mavi, S., & Hostettmann, K. (1996). Five flavans from *Mariscus psilostachys*. *Phytochemistry*, 43(6), 1265-1269.

Geoigina N. D., Carpinella, M. C.Palacios, S. M.. (2009). Antifeedant activity of ethanolic extract from *Flourensia oolepis* and isolation of pinocembrin as its active principle compound. *Bioresource Technology*, 100, 3669-3673.

Goodwin, S., Shoodery, J. N., Johnson, L. F. (1958). Significance of the nonequivalence of methylenedioxyhydrogen nuclei in the nuclear magnetic resonance spectra of aporphine alkaloids, . *Proceedings of the Chemical Society London*, 306-307.

Govindachari, T. R. N., K.; Rajeswari, S.; Suguna, H., Pai, B. R. (1977). Studies in protoberberine alkaloids. Photolytic syntheses of dl-laurotetanine, dl-schefferine and dl-corytenchine. *Indian Journal of Chemistry, Section B: Organic Chemistry Including Medicinal Chemistry* 15B(10), 873-875.

Graham, T. L. (1991). Flavonoid and isoflavonoid distribution in developing soybean seedling tissues and in seed and root exudates. *Plant Physiology*, 95(2), 594.

Green, D. R. (2006). At the gates of death. *Cancer Cell*, 9(5), 328-330.

Gu, Q., De Wang, J., Xia, H. H. X., Lin, M. C. M., He, H., Zou, B., Lam, S. K. (2005). Activation of the caspase-8/Bid and Bax pathways in aspirin-induced apoptosis in gastric cancer *Carcinogenesis*, 26(3), 541-546.

Guinaudeau, H., Leboeuf, M., & Cavé, A. (1994). Aporphinoid Alkaloids, V. *Journal of Natural Products*, 57(8), 1033-1135.

Guinaudeau, H., Leboeuf, M., Cavé, A. (1988). Aporphinoid alkaloids, IV. *Journal of Natural Products*, 51(3), 389-474.

Haibo, T. Zheng, C., Liu, Zi., Wang, D.Z. (2011). Biomimetic total syntheses of linderaspirone A and bi-linderone and revisions of their biosynthetic pathways. *Organic Letter*, 13, 2192-2195.

- Heim, K. E., Tagliaferro, A. R., & Bobilya, D. J. (2002). Flavonoid antioxidants: chemistry, metabolism and structure-activity relationships. *The Journal of Nutritional Biochemistry*, 13(10), 572-584.
- Henning, S. M., Niu, Y. Lee, N.H., James, G.D. Minutti, R.R., Wang, H., Go, V.L., Heber, D.(2004). Bioavailability and antioxidant activity of tea flavanols after consumption of green tea, black tea, or a green tea extract supplement. *American Journal Clinical Nutrition*. 80, 1558-1564.
- Anderson, H. T. (1999). Plant Alkaloids: Anmol Publications.876-970.
- Herath, H. M. T. B., Dassanayake, R. S., Priyadarshani, A. M. A., De Silva, S. & Wannigama, G. P., and Jamie (1998). Isoflavonoids and a pterocarpan from *Gliricidia sepium*. *Phytochemistry*, 47, 117-119.
- Hiok-Huang, G. J. B. (1990). ¹³C NMR Study on Linderones and Lucidones. *Magnetic Resonance in Chemistry* . 28, 337-342.
- Ho, C. L., Jie-Pinge, O., Liu, Y. C., Hung, C. P., Tsai, M. C., Liao, P. C., Su, Y. C. (2010). Compositions and in vitro anticancer activities of the leaf and fruit oils of *Litsea cubeba* from Taiwan. *Natural Product Communications*, 5(4), 617.
- Ho, C. L., Lin, C. Y., Wang, E. I., & Su, Y. C. (2011). Composition, antioxidant and antimicrobial activities of leaf and twig essential oils of *Litsea akoensis* from Taiwan. *Natural Product Communications*, 6(6), 901.
- Ho, J. C., & Chen, C. M. (2002). Flavonoids from the aquatic plant *Eriocaulon buergerianum*. *Phytochemistry*, 61(4), 405-408.
- Horowitz, R. M. (1963). Dihydrochalcone derivatives and their: Google Patents.
- Hosseinzadeh, M., Mukhtar, M. R. Khalilzadeh, M. A. Khaledi, H. (2012). A triclinic polymorph of (E)-2-(1-hydroxy-3-phenylprop-2-en-1-ylidene)-4, 5-dimethoxy cyclopent -4-ene-1, 3-dione. *Acta Crystallographica Section E: Structure Reports Online*. 68(2): o453-o453.
- Hosseinzadeh, M., Mukhtar, M. R., Mohamad, J., Awang, K., Ng, S. W. (2011). Whole-molecule disordered (E)-2-(1-hydroxy-3-phenylprop-2-en-1-ylidene)-4, 5-dimethoxycyclopent-4-ene-1, 3-dione isolated from *Lindera oxyphylla* (Lauraceae). *Acta Crystallographica Section E: Structure Reports Online*, 67(6), o1544-o1544.
- Howes, M. J. R., Perry, N. S. L., Houghton, P. J. (2003). Plants with traditional uses and activities, relevant to the management of Alzheimer's disease and other cognitive disorders. *Phytotherapy Research*, 17(1), 1-18.
- Huang, D., Ou, B. Prior, R.L. (2005). The chemistry behind antioxidant capacity assays. *Journal Agriculture and Food Chemistry*, 53(6), 1841-1856.
- Hughes, D. A. (1999). Effects of dietary antioxidants on the immune function of middle-aged adults. *Proceedings of the Nutrition Society*, 58(1), 79-84.

- Hwang, J. K., Choi, E. M., & Lee, J. H. (2005). Antioxidant activity of *Litsea cubeba*. *Fitoterapia*, 76(7), 684-686.
- Hyun, M. O., Choi, S. K., Lee, J.M., Lee, S.K., Kim, H.Y., Han, D. C. Kim, H.M., Son, H.M., Kwon, B.M. (2005). Cyclopentenones, inhibitors of farnesyl protein transferase and anti-tumor compounds, isolated from the fruit of *Lindera erythrocarpa* Makino. *Bioorganic Medicinal Chemistry*, 13, 6182-6187.
- Iio, K., Iida, T., Ichino, K., Tsunozuka, M., Hattori, M., Namba, T. (1982). Obovatal and obovatal novel biphenyl ether lignans from the leaves of *magnolia obovata* Thunb. *Chemistry Pharmace Buletin*, 30(9), 3347-3353.
- Imbert, T. F. (1998). Discovery of podophyllotoxins. *Biochimie*, 80, 207-222.
- Institute of Botany, C. A. S. (1982). *Flora Reipublicae Popularis Sinicae* (Vol. 32): Science Press, Beijing. 102-210.
- Jayaprakasam, B., Damu, A. G., Gunasekar, D., Blond, A., & Bodo, B. (1999). Dihydroechioidinin, a flavanone from *Andrographis echinoides*. *Phytochemistry*, 52(5), 935-937.
- Jemal, A. B., F, Center, MM, Ferlay, J, Ward, E, Forman, D. (2011). Global cancer statistics. *CA: A Cancer Journal for Clinicians*, 61 (2), 69-90.
- Jemal, A. M., Ward, T. E., Samuels, A., Tiwari, R. C., Ghafoor, A., Feuer, E. J., Thun, M. J., (2005). Cancer statistics. *Ca-a Cancer Journal for Clinicians*. 55, 10-30.
- Jensen, S., Hansen, J., Boll, P. M. (1993). Lignans and neolignans from Piperaceae. *Phytochemistry*, 33(3), 523-530.
- Ji, H. F., Zhang, L. W., Zhang, Y., Jin, H. H., Wang, L. Y. Antioxidant Properties of Laoying Tea (*Litsea Coreana* L.) Extracts. *Advanced Materials Research*, 340, 209-214.
- Jin, Z., Li, Y., Pitti, R., Lawrence, D., Pham, V. C., Lill, J. R., Ashkenazi, A. (2009). Cullin 3-based polyubiquitination and p62-dependent aggregation of caspase-8 mediate extrinsic apoptosis signaling. *Cell*, 137(4), 721-735.
- Johns, S., Lamberton, J., Li, C. S., & Sioumis, A. (1970). New alkaloids from a *Popowia species* (Annonaceae). *Australian Journal of Chemistry*, 23(2), 363-368.
- Joshi, S. C., & Mathela, C. S. (2012). Antioxidant and antibacterial activities of the leaf essential oil and its constituents furanodienone and curzerenone from *Lindera pulcherrima* (Nees.). *Pharmacognosy Research*, 4(2), 80.
- Kähkönen, H. A., Vuorela H. J., Rauha J.P, Pihlaja K, Kujala T.S., Heinonen M. (1999). Antioxidant activity of plant extracts containing phenolic compounds. *Journal of Agricultural and Food Chemistry*, 47, 3954-3962.
- Kamperdick, C., Hong Van, N., Van Sung, T. (2002). Constituents from *Miliusa balansae* (Annonaceae). *Phytochemistry*, 61(8), 991-994.

- Kaplan, W. (1942). *Codylamata acuminata*. *New Orleans Medical Surgical Journal*, 94, 388.
- Katayama, T., Davin, L. B., & Lewis, N. G. (1992). An extraordinary accumulation of (–)-pinoresinol in cell-free extracts of *Forsythia intermedia*: evidence for enantiospecific reduction of (+)-pinoresinol. *Phytochemistry*, 31(11), 3875-3881.
- Kawanishi, K., . Hashimoto, Y., (1981). Dehydrodieugenol and its monomethyl ether from *Viola Carinata*. *Phytochemistry*, 20(5), 1166.
- Keng, H. (1978). Orders and Families of Malayan Seed Plants. *Singapore University Press*, 117.
- Keng, H. (1978). Orders and families of Malayan seed plants: synopsis of orders and families of Malayan gymnosperms, dicotyledons, and monocotyledons: Ohio University Press. 543.
- Kim, B. G., Kim, H., Kim, J. H., Lim, Y., & Ahn, J. (2006). Synthesis of ermanin, 5, 7-dihydroxy-3, 4'-dimethoxyflavone from kaempferol, 3, 5, 7, 4'-tetrahydroxyflavone with two *O*-methyltransferases expressed in *E. coli*. *Bulletin Korean Chemical Society*, 27(3), 357.
- Kluck, R. M., Bossy-Wetzel, E., Green, D. R., & Newmeyer, D. D. (1997). The release of cytochrome c from mitochondria: a primary site for Bcl-2 regulation of apoptosis. *Science*, 275(5303), 1132.
- Ko, C. W., Tao, Y. T., Danel, A., Krzeminska, L., & Tomasik, P. (2001). Organic light-emitting diodes based on 2-(stilben-4-yl) benzoxazole derivatives: an implication on the emission mechanism. *Chemistry of Materials*, 13(7), 2441-2446.
- Kochummen, K. M. (1997). *Tree flora of Pasoh forest*: Forest Research Institute Malaysia. 1230.
- Koorbanally, N. A., Randrianarivelojosia, M., Mulholland, D. A., Quarles van Ufford, L., & Van Den Berg, A. J. J. (2003). Chalcones from the seed of *Cedrelopsis grevei* (*Ptaeroxylaceae*). *Phytochemistry*, 62(8), 1225-1229.
- Koumis, T., & Samuel, S. (2005). Tiotropium bromide: a new long-acting bronchodilator for the treatment of chronic obstructive pulmonary disease. *Clinical Therapeutics*, 27(4), 377-392.
- Kulmagambetova, E. A., Yamovoi, V. I., Kusainova, D. D., Pak, R. N., Kulyyasov, A. T., Turdybekov, K. M., Gatilov, Y. V. (2002). Synthesis and structure of pinostrobin oxime and its biological activity. *Chemistry of Natural Compounds*, 38(6), 527-531.
- Kulmagambetova, E. A., Seitembetova, A. G., Kulyjasov, A. T., Raldugin, V. A., Gatilov, Y. V., Shakirov, M. M., Tolstikov, G. A. (2003). Chlorination of tectochrysin and pinostrobin in methanol. *Russian Chemical Bulletin*, 52(3), 752-754.
- Kumara, P. B., Kannana, M. M., Lavanyaa, B., Suthakaranb, R., & Quinec, S. D. GC-MS analysis of methanolic extract of *Litsea decanensis gamble* and its free radical scavenging activity. *Journal of Pharmacy Research*, 4.3, 342-351.

- Kwak, J. H., In, J. K., Lee, M. S., Choi, E. H., Lee, H., Hong, J. T., Suh, Y. G. (2008). Concise synthesis of Obovatol: Chemoselective ortho-bromination of phenol and survey of Cu-catalyzed diaryl ether couplings. *Archives of Pharmacal Research*, 31(12), 1559-1563.
- Kwon, H. C., Choi, S. U., Lee, J. O., Bae, K. H., Zee, O. P., & Lee, K. R. (1999). Two new lignans from *Lindera obtusiloba blume*. *Archives of Pharmacal Research*, 22(4), 417-422.
- Lamola, A. (1967). Lowest π , π triplet state of acetophenone. *The Journal of Chemical Physics*, 47, 4810.
- Lea, P. J., Ireland, R. J. (1999). Nitrogen metabolism in higher plants. *Plant Amino Acids: Biochemistry and Biotechnology*. New York, 1-47.
- Lee, L. S. A., I.J., Watling, R. (1990) .Forest Research Inst. Malaysia, Kepong, Kuala. Kepong. 52109 Kuala Lumpur. Malaysia.32-35..
- Lewington, A. (1993). Medicinal plants and plant extracts: A review of their importation into Europe. *Cambridge, United Kingdom, : Traffic International*.254.
- Li, J., Tanaka, M., Kurasawa, K., Ikeda, T., & Nohara, T. (2005). Lignan and neolignan derivatives from *Magnolia denudata*. *Chemical and Pharmaceutical Bulletin*, 53(2), 235-237.
- Li, L., Zhao, X. T., Luo, Y. P., Zhao, J. F., Yang, X. D., & Zhang, H. B. (2011). Novel Cytotoxic Chalcones from *Litsea rubescens* and *Litsea pedunculata*. *Bioorganic Medicinal Chemistry letters*. 21, 24, 7431–7433
- Li, Z., Jo, J., Jia, J. M., Lo, S. C., Whitcomb, D. J., Jiao, S., Sheng, M. (2010). Caspase-3 activation via mitochondria is required for long-term depression and AMPA receptor internalization. *Cell*, 141(5), 859-871.
- Mukhtar, M., Awang, K., Hadi, A. H.A. (2000). *Malaysian Journal of Science* 19, 67-70
- Mukhtar, M., Awang, K., Hadi, A. H. A. (2000). Chemical Constituents of *Phoebe grandis* (Ness) Merr.(Lauraceae). *Malaysian Journal of Science*, 19, 67-70.
- Ma, Y., Li, Q., Van den Heuvel, H., & Claeys, M. (1997). Characterization of flavone and flavonol aglycones by collision- induced dissociation tandem mass spectrometry. *Rapid Communications in Mass Spectrometry*, 11(12), 1357-1364.
- Manach, C., Mazur, A., & Scalbert, A. (2005). Polyphenols and prevention of cardiovascular diseases. *Current Opinion in Lipidology*, 16(1), 77.
- Manaf, A., Khozirah, S., Zuriati, Z. (1999). Trade and Investment Prospects in Malaysia. Phytochemicals and Biopharmaceutins from the Malaysian Rain Forest. *Medicinal Plants*. 6, 90-98.
- Marsaioli, A. J., de A.M. Reis, F., Magalhães, A. F., Rúveda, E. A., & Kuck, A. M. (1979). ^{13}C NMR analysis of aporphine alkaloids. *Phytochemistry*, 18(1), 165-169.

- Merken, H. M., & Beecher, G. R. (2000). Measurement of food flavonoids by high-performance liquid chromatography: a review. *Journal of Agricultural and Food Chemistry*, 48(3), 577-599.
- Middleton Jr, E., Kandaswami, C., & Theoharides, T. C. (2000). The effects of plant flavonoids on mammalian cells: implications for inflammation, heart disease, and cancer. *Pharmacological Reviews*, 52(4), 673-751.
- Miliauskas, G., Venskutonis, P., & Van Beek, T. (2004). Screening of radical scavenging activity of some medicinal and aromatic plant extracts. *Food Chemistry*, 85(2), 231-237.
- Miller, H. E., Rigelhof, F., Marquart, L., Prakash, A., & Kanter, M. (2000). Antioxidant content of whole grain breakfast cereals, fruits and vegetables. *Journal of the American College of Nutrition*, 19(suppl 3), 312-319.
- Mohan, S., Abdelwahab, S. I., Kamalidehghan, B., Syam, S., May, K. S., Harmal, N. S. M., Rahmani, M. (2012). Involvement of NF- κ B and Bcl2/Bax signaling pathways in the apoptosis of MCF7 cells induced by a xanthone compound Pyranocycloartobiloxanthone A. *Phytomedicine*. 9, 1007–1015
- Mukherjee, R. K., Fujimoto, Y., & Kakinuma, K. (1994). 1-(ω -Hydroxyfattyacyl)glycerols and two flavanols from *Cinnamomum camphora*. *Phytochemistry*, 37 (6), 1641-1643.
- Mulder, T. P., Rietveld, A.G., van Amelsvoort, J.M.. (2005). Consumption of both black tea and green tea results in an increase in the excretion of hippuric acid into urine. *American Journal Clinic Nutrition*. , 81, 256-260.
- Nam, I., Hyeyoung, K., Youhui, L., Jong Dae, P., KyuSang, K., Shin, K, (1992). A new dehydrodieugenol from *Magnolia Officinalis*. *Planta Medica*, 58(6), 566-568.
- Napoli, C., Lemieux, C., & Jorgensen, R. (1990). Introduction of a chimeric chalcone synthase gene into petunia results in reversible co-suppression of homologous genes in trans. *The Plant Cell Online*, 2(4), 279-289.
- Natiello, M., Contreras, R., Facelli, J., & De Kowalewski, D. (1983). Nuclear magnetic resonance and PCILO study of the side-chain conformations in anisaldehyde and 2, 5-dimethoxybenzaldehyde. *The Journal of Physical Chemistry*, 87(14), 2603-2607.
- Neacsu, P.C., Sjöholm, R. E., Pietarinen, S. P., Ahotupa, M. O., Holmbom, B. R., Willfor, S. M., (2007). Antioxidant flavonoids from knotwood of jack pine *European aspen Holz.Roh.Werkst*, 65, 1-6.
- Newman, D. J., Cragg, G. M., Snader, K. M. (2003). Natural products as sources of new drugs over the period 1981-2002. *Journal of Natural Products*, 66(7), 1022-1037.
- Newman, D. J., G. M. Newman, D. J. Cragg, G. M. , (2007). Natural products as sources of new drugs over the last 25 years. *Journal Natural Product*., 70: 461–477.
- Niki, E. N. (2000). Evaluation of Antioxidant Capacity. What Capacity is Being Measured by Which Method? 50, 323-329.

- Odwyer, P. J. L., B.; Alonso, M. T., Marsoni, S., Wittes, R. E. (1985). Etoposide (VP-16-213)- Current status of an active anticancer drug. *Natural England Journal Method.* 312, 692–700.
- Oh, H. M., Choi, S. K., Lee, J. M., Lee, S. K., Kim, H. Y., Han, D. C., Kwon, B. M. (2005). Cyclopentenenediones, inhibitors of farnesyl protein transferase and anti-tumor compounds, isolated from the fruit of *Lindera erythrocarpa* Makino. *Bioorganic Medicinal Chemistry*, 13(22), 6182-6187.
- Okuda, T., Suzuki, M., Adachi, N., Quah, E. S., Hussein, N. A., & Manokaran, N. (2003). Effect of selective logging on canopy and stand structure and tree species composition in a lowland dipterocarp forest in Peninsular Malaysia. *Forest Ecology and Management*, 175(1-3), 297-320.
- Ono, E., Fukuchi-Mizutani, M., Nakamura, N., Fukui, Y., Yonekura-Sakakibara, K., Yamaguchi, M., Tanaka, Y. (2006). Yellow flowers generated by expression of the aurone biosynthetic pathway. *Proceedings of the National Academy of Sciences*, 103(29), 11075-11080.
- Ono, M., Mishima, K., Yamasaki, T., Masuoka, C., Okawa, M., Kinjo, J., Nohara, T. (2009). A new lignan glucoside from the stems of *Callicarpa japonica* Thunb. var. *luxurians* Rehd. *Journal of Natural Medicines*, 63(1), 86-90.
- Onojafe, I. F., Adam, D. R., Simeonov, D. R., Zhang, J., Chan, C. C., Bernardini, I. M., Brilliant, M. H. Nitisinone improves eye and skin pigmentation defects in a mouse model of oculocutaneous albinism. *The Journal of Clinical Investigation*, 121(10), 3914.
- Orito, K., Yorita, K., & Suginome, H. (1991). A new stereo-and regioselective synthesis of (\pm)-sesamin involving a [β]-scission of alkoxyl radicals as the key step1. *Tetrahedron letters*, 32(42), 5999-6002.
- Ozsoy, N., Can, A., Yanardag, R. & Akev, N. (2008). Antioxidant activity of *Smilax excels* L. Leaf extracts. *Food Chemistry*, 110, 571-583.
- Pachler, K. G. R. A., R. R.; Baarschers, W. H. (1965). Nuclear magnetic resonance of aporphine alkaloids. II. Structure of rogersine. *Tetrahedron* 21(8), 2159-2167.
- Passador, E. A. P., das Gf da Silva, M. F., Fo, E. R., Fernandes, J. B., Vieira, P. C., & Pirani, J. R. (1997). A pyrano chalcone and a flavanone from *Neoraputia magnifica*. *Phytochemistry*, 45(7), 1533-1537.
- Pharmacognosie, B. J. (1999). Phytochimie Plantes Medicinal. *Lavoisier* 3, 1078-1079.
- Pietta, P. G. (2000). Flavonoids as antioxidants. *Journal of Natural Products*, 63(7), 1035-1042.
- Piettre, S. Heathcock, C. H. (1990). Biomimetic total synthesis of proto-daphniphylline. *Science*, 248(4962), 1532.

- Qin, J. K., Lan, W. L., Han, L. Y., Tang, H., SU, G. F., Dai, Z. K., & Xu, Q. (2010). Synthesis and Bioactivity of Quaternary Ammonium Salts of Pyridino-xanthone. *Chinese Journal of Applied Chemistry*, 27 (5), 528-532.
- Rahman, A. C., M. I.; Thomsen, W. J. (2003). Bioassay techniques for drug development. 6, 1-3.
- Rahmani, M., Mahmood, M., Sukari, M.A., Lian, G. E. C., Yin, T. Y. Y., Ali, D. A. I. . (2001). Interdisciplinary Approaches in Natural Products Research, Kuala Lumpur. *The Malaysian Natural Products Society*. 6, 211-221.
- Randhir, R., Lin, Y. T., & Shetty, K. (2004). Phenolics, their antioxidant and antimicrobial activity in dark germinated fenugreek sprouts in response to peptide and phytochemical elicitors. *Asia Pacific Journal of Clinical Nutrition*, 13(3), 295-307.
- Ranilla, L. G., Kwon, Y. I., Apostolidis, E., & Shetty, K. (2010). Phenolic compounds, antioxidant activity and in vitro inhibitory potential against key enzymes relevant for hyperglycemia and hypertension of commonly used medicinal plants, herbs and spices in Latin America. *Bioresource technology*, 101(12), 4676-4689.
- Rao, Y. K., Fang, S. H., & Tzeng, Y. M. (2005). Anti-inflammatory activities of flavonoids isolated from *Caesalpinia pulcherrima*. *Journal of Ethnopharmacology*, 100(3), 249-253.
- Raoa, Y. K., Geethangilia, M., Chana, H. S., Wub, W. S., Tzeng, Y. M., (2009). High-performance liquid chromatographic determination of kaempferol glycosides in *Cinnamomum osmophloeum* leaves.8, 654-675.
- Reddy, M. V. B., Reddy, M. K., Gunasekar, D., Caux, C., & Bodo, B. (2003). A flavanone and a dihydrodibenzoxepin from *Bauhinia variegata*. *Phytochemistry*, 64(4), 879-882.
- Rep, R. D. H. A. (1936). Natural resins. *Ann Rep Prog Chem*, 33, 266-279.
- Ridley, H. (1924). *The flora of the Malay peninsula: Apetalae*: Reeve & Co.342-345.
- Robbins, R. J. (2003). Phenolic acids in foods: an overview of analytical methodology. *Journal of Agricultural and Food Chemistry*, 51(10), 2866-2887.
- Sako, M., Hosokawa, H., Ito, T., Iinuma, M. (2004). Regioselective oxidative coupling of 4-hydroxystilbenes: Synthesis of resveratrol and ϵ -viniferin (E)-dehydrodimers. *The Journal of Organic Chemistry*, 69(7), 2598-2600.
- Samman, S., Lyons Wall, P. M., Cook, N. C. (1998). Flavonoids and coronary heart disease: Dietary perspectives.54, 980-987.
- Sanster, A. W. Stuart., K. L. (1965). Ultraviolet spectra of alkaloids. *Chemistry Review.*, 65(1), 69-130.
- Schiff Jr, P. L. (1991). Bisbenzylisoquinoline alkaloids. *Journal Natural Product.*, 54, 645-749.

- Schmidt, A., Habeck, T., Kindermann, M. K., & Nieger, M. (2003). New pyrazolium-carboxylates as structural analogues of the pseudo-cross-conjugated betainic alkaloid nigellidine. *The Journal of Organic Chemistry*, 68(15), 5977-5982.
- Schnyder, A., Beller, M., Mehlretter, G., Nsenda, T., Studer, M., & Indolese, A. F. (2001). Synthesis of primary aromatic amides by aminocarbonylation of aryl halides using formamide as an ammonia synthon. *The Journal of Organic Chemistry*, 66(12), 4311-4315.
- Schroeter, H., Heiss, C., Balzer, J., Kleinbongard, P., Keen, C. L., Hollenberg, N. K., Kelm, M. (2006). (–)-Epicatechin mediates beneficial effects of flavanol-rich cocoa on vascular function in humans. *Proceedings of the National Academy of Sciences of the United States of America*, 103(4), 1024-1029.
- Shamma, M., Slusarchyk, W. A. (1964). The Aporphine Alkaloids. *Chemical Reviews*, 64(1), 59-79.
- Sindrup, S. H., Brøsen, K. (1995). The pharmacogenetics of codeine hypoalgesia. *Pharmacogenetics*, 5(6), 335.
- Soepadmo, E. (1999). Botanical Study of Malaysian Medicinal Plant and Appraisal. Phytochemicals and Biopharmaceutins from the Malaysian Rain Forest. *Forest Research Institute Malaysia, Kuala Lumpur*, 10.
- Song, M., Nigussie, F., Yang, H., & Baek, N. (2007). A new benzophenone from *Lindera fruticosa*. *Bulletin Korean Chemical Society*, 28(7), 1209.
- Song, M. C., Nigussie, F., Jeong, T. S., Lee, C. Y., Regassa, F., Markos, T., & Baek, N. I. (2006). Phenolic Compounds from the Roots of *Lindera fruticosa*. *Journal of Natural Products*, 69(5), 853-855.
- Srivastava, V. N., A. S., Kumar, J. K., Gupta, M. M., Khanuja, S. P. S. (2005). Plant-based anticancer molecules: A chemical and biological profile of some important leads. *Bioorganic Medicine Chemistry*. 13, 5892–5908.
- Suarez, M., Bonlila, J., DeDiaz, Aura M.P., Achenbach, H. (1983). Studies of Colombian Lauraceae, Dehydrodieugenols from *Nectandra Polita*. *Phytochemistry*, 22(2), 609-610.
- Sulaiman, M., Hadi, A. H. A., & Awang, K. (2003). Alkaloids and Flavones from *Desmos dumosus*, Roxb. Salt.(Annonaceae). *Malaysian Journal of Science*, 22(1), 87-93.
- Sulaiman, S. N., Mukhtar, M. R., Hadi, A. H. A., Awang, K., Hazni, H., Zahari, A., Morita, H. (2011). Lancifoliaine, a new bisbenzylisoquinoline from the Bark of *Litsea lancifolia*. *Molecules*, 16(4), 3119-3127.
- Sumioka, H., Harinantenaina, L., Matsunami, K., Otsuka, H., Kawahata, M., & Yamaguchi, K. (2011). Linderolides AF, eudesmane-type sesquiterpene lactones and linderoline, a germacrane-type sesquiterpene from the roots of *Lindera strychnifolia* and their inhibitory activity on NO production in RAW 264.7 cells in vitro. *Phytochemistry*, 6, 987-990.

- Susin, S. A., Lorenzo, H. K., Zamzami, N., Marzo, I., Brenner, C., Larochette, N., Kroemer, G. (1999). *The Journal of Experimental Medicine*, 189(2), 381.
- Suwannarat, P., O'Brien, K., Perry, M. B., Sebring, N., Bernardini, I., Kaiser-Kupfer, M. I., Gahl, W. A. (2005). Use of nitisinone in patients with alkaptonuria. *Metabolism*, 54(6), 719-728.
- Suzuki, K., Nakagawa, H. (1971). Late Pleistocene flora from the Pacific coast of Fukushima Prefecture, Japan. *Sweeney*.357-37.
- Swerdlow, J. L. (2000). Nature's medicine: A chronicle of mankind's search for healing plants through the ages. *National Geographic Society. Washington, DC*. 7, 954-965.
- Tan, G., C., Soejarto, D. (2006). Biodiversity as a source of anticancer drugs. *Current Drug Targets*, 7, 265–277.
- Thomson, R. H. (1993). The chemistry of natural products: *Springer*.231-245.
- Thug, T. T. T. Quan, T. D., Anh, N. T. H., Van Sung, T. (2011). A new Hydrochalcone from *Miliusa Sinensis* *Natural Product Research*, 25, 1361-1365.
- Tsai, S. F., & Lee, S. S. (2011). Flavonoid Composition in the Leaves of Twelve *Litsea* and *Neolitsea* Plants. *Journal of the Chinese Chemical Society*, 58(3), 376-383.
- Van Agtmael, M. A., Eggelte, T. A., Van Boxtel, C. J. (1999). Artemisinin drugs in the treatment of malaria: from medicinal herb to registered medication. *Trends in Pharmacological Sciences*, 20(5), 199-205.
- Van Daele, G. (1991). Novel *N*-(3-hydroxy-4-piperidiny) benzamide derivatives: Google Patents.
- Vaux, D. L., & Korsmeyer, S. J. (1999). Cell death in development. *Cell*, 96(2), 245-254.
- Wang, L., Zhao, J. F., Zeng, X. H., Xie, M. J., Yang, X. D., Zhang, H. B., & Li, L. (2009). A novel aryltetralone lignan from *Litsea pedunculata*. *Journal of Asian Natural Products Research*, 11(12), 1028-1031.
- Wang, Q., & Finn, M. G. (2000). 2H-Chromenes from Salicylaldehydes by a Catalytic Petasis Reaction. *Organic Letters*, 2(25), 4063-4065.
- Weber, J. F. B., J., Pusset, J. (1986). Plants of New Caledonia Part 103. *Alkaloids of Litsea lecardii*. 1, 74-75.
- Wikipedia, T. F. E. (2011). *Lauraceae*. *Wikipedia Foundation Inc. USA*. 8 March 2010.
- Wilson, L. B., Jr., Mizel, SB., Grisham I. M., Creswell, KM. (1974). Session V- Networks and shared facilities- Rapporteurs summary. *Fed. Proc. Fed. Am. Soc. Exp. Biol.* , 33, 158.
- Wood, C. E. J. (1958). The genera of the woody Ranales in the southeastern United States. *Journal Arnold Arboretum.* , 39, 296-346.
- Wu, H., Haig, T., Pratley, J., Lemerle, D., & An, M. (2000). Allelochemicals in Wheat

- (*Triticum Aestivum L*): Variation of Phenolic Acids in Root Tissues. *Journal of Agricultural and Food Chemistry*, 48(11), 5321-5325.
- Wu, W.-N., Beal, J.L and Doskotch, R. W. , (1980). Alkaloids of *Thalictrum* XXXV. Northalcarpine, A New Aporphine-Benzylisoquinoline Dimer, *N*-Methylaurotetanine and Thalflavidine from the Roots of *Thalictrum revolutum*. *Journal of Natural Products*, 43(5), 567-570.
- Xiao, M., Cao, N., Fan, J., Shen, Y., Xu, Q. (2011). Studies on flavonoids from the leaves of *Lindera aggregata*. *Journal of Chinese Medicinal Materials*, 34(1), 62.
- Xin, Z., & Yan-fei, S. L. Z. (2008). Antimutagenic and in vitro anticancer effect of *litsea coreana* levl. var. lanuginisa . *Food Engineering*, 4, 011.
- Yan, R., Peng, X., Zou, G. (2011). Anticancer and Antioxidant Activity of *Lindera strychnifolia* Extracts. *Journal of Wuhan University (Natural Science Edition)*, 3, 017.
- Yang, J. H., Li, L., Wang, Y. S., Zhao, J. F., Zhang, H. B., Luo, S. D. (2005). Two new aporphine alkaloids from *Litsea glutinosa*. *Helvetica Chimica Acta*, 88(9), 2523-2526.
- Yenjai, C., Wanich, S., Pitchuanchom, S., Sripanidkulchai, B. (2009). Structural modification of 5, 7-dimethoxyflavone from *Kaempferia parviflora* and biological activities. *Archives of Pharmacal Research*, 32(9), 1179-1184.
- Yoon, W. J., Ham, Y. M., Yang, W. H., Park, S. Y. (2010). Bioactive Materials: Article; Antioxidative and Anti-inflammatory Activities of *Litsea japonica* Leaves. *Journal of the Korean Society for Applied Biological Chemistry* 53(1), 27-32.
- Yu, L., Zhao, M., Cui, C., Yang, B., Jiang, Y., Zhao, Q. (2008). Antioxidant, immunomodulatory and anti-breast cancer activities of phenolic extract from *pine Pinus massoniana* Lamb bark. *Innovative Food Science & Emerging Technologies*, 9(1), 122-128.
- Zakri, A. H. (1999). The National Policy on Biological Diversity and its Possible Impact on Natural Products Development in Malaysia. *Interdisciplinary in Natural Product Sciences*.6, 123.
- Zhang, C., Nakamura, N., Tewtrakul, S., Hattori, M., Sun, Q., Wang, Z., & Fujiwara, T. (2002). Sesquiterpenes and alkaloids from *Lindera chunii* and their inhibitory activities against HIV-1 integrase. *Chemical and Pharmaceutical Bulletin*, 50(9), 1195-1200.
- Zhang, L., Wang, Sh., Shuangliu Zhou, Sh., Yang, G, and Sheng, E., (2006). Cannizzaro-Type Disproportionation of Aromatic Aldehydes to Amides and Alcohols by Using Either a Stoichiometric Amount or a Catalytic Amount of Lanthanide Compounds. *Journal Organic Chemistry*. 71, 3149-3153.
- Zhang, Z. L., Xiongmin; Ma, Li; Zhou, Haifeng; Liang, Qiuxia. (2010). Preparation of cinnamide from cinnamon slag by biodegradation. *Jingxi Huagong* 27(1), 43-47.
- Zhao, Q., Zhao, Y., & Wang, K. (2006). Antinociceptive and free radical scavenging activities of alkaloids isolated from *Lindera angustifolia* Chen. *Journal of Ethnopharmacology*, 106(3), 408-413.

PUBLICATIONS

1. Masoumeh Hosseinzadeh, Mat Ropi Mukhtar, Jamaludin Mohamad, Khalijah Awang, and Seik Weng Ng. Whole-molecule disordered (*E*)-2-(1-hydroxy-3-phenylprop-2-en-1-ylidene)-4,5-dimethoxycyclopent-4-ene-1,3-dione isolated from *Lindera oxyphylla* (Lauraceae) . **Journal of Acta Crystallogr Sect E.**, **2011**, **Volume 67(Pt 6): o1544.**
2. Masoumeh Hosseinzadeh, Mat Ropi Mukhtar, Mohammad Ali Khalilzadeh, and Hamid Khaledi. A triclinic polymorph of (*E*)-2-(1-hydroxy-3-phenylprop-2-en-1-ylidene)-4,5-dimethoxycyclopent-4-ene-1,3-dione. **Journal of Acta Crystallogr Sect E.**, **2012**, **Volume 68(Pt 2): o453**
3. Masoumeh Hosseinzadeh, A. Hamid A. Hadi, Jamaludin Mohamad, Mohammad A. Khalilzadeh, Shiau-Chuen Cheahd, Mehran Fadaeinasab. Flavonoids and Linderone from *Lindera oxyphylla* and their bioactivities. **Journal Combinatorial Chemistry & High Throughput Screening**, **2013** .
4. Masoumeh Hosseinzadeh, A. Hamid A. Hadi, JamaludinMohamad, Mohammad A. Khalilzadeh, Bioactivity of New Flavonoid from Leaves of *Litsea Costalis* (Lauraceae).(Submitted to **Chemistry of natural products**, **2013**)
5. Masoumeh Hosseinzade^a, A. Hamid A. Hadi, Jamaludin Mohamad, Mohammad A. Khalilzadeh, Mohammad Reza Zardoost Chemical Constituents from the Bark of *Litsea costalis* (Submitted to **Tetrahedron Letters**, **2013**).
6. Masoumeh Hosseinzadeh, Behnam Kamalidehghan, A. Hamid A. Hadi, Jamaludin Mohamad, Mohammad A. Khalilzadeh,,Involvement of Intrinsic and Extrinsic Apoptotic Pathways through Caspase-3/7, 8 and 9 signaling in the apoptosis of MCF-7 cells induced by a New Phenolic Compound, *Litsin 1*, from Bark of *Litsea Costalis* .(Submitted to **Phytochemistry Letters**,**2013**)
7. Masoumeh Hosseinzadeh, A. Hamid A. Hadi, Syam Mohan^b, Jamaludin Mohamad Mohammad A. Khalilzadeh, Hassan Karimi-Maleh, Behnam Kamalidehghan, Suvitha Syam, Pouya Hassandarvish, Mostafa Ghaderian. Biseugenol C, a new hydrazine isolated from *Litsea costalis* (nees) Kosterm (Lauraceae) induces mitochondria mediated apoptosis in MCF-7 cells in conjunction with Bcl2/Bax and NFkB pathways regulation.(Submitted to **Phytomedicine**, **2013**).